Studies in Process Analysis and Control in Batch Reactors

Álvaro Diez-Lázaro BSc (Hons)

March 2002

A thesis submitted to the Department of Pure and Applied Chemistry, University of Strathclyde, Glasgow, in partial fulfilment of the regulations for the degree of Doctor of Philosophy.

March 2002

Abstract

This work is part of a number of projects dealing with the development of novel techniques for better analysis and control of chemical processes carried out in batch reactors. The problems of pH measurement and sampling, linked to the implementation of NMR and HPLC on-line analysers, are presented as key areas in this development work. Also, part of the engineering work summarised in this thesis assisted the work of other researchers who participated in the project.

In the area of sampling, the difficulties associated with the collection of representatives samples from agitated vessels are introduced. Also, the ideas of calibration and modelling of sampling systems are presented. Modelling tests were used to optimise the design and development of a fast sampling loop system to obtain representative samples from stirred vessels. In addition to this, the modelling studies also assisted the work of other researchers in the project who needed the kinetic and heat-exchange parameters for the process of esterification of crotonic acid. The fast sampling loop was shown to be adequate for the implementation of a low-field NMR system for on-line analysis. The development of discrete samplers designed to collect, dilute and deliver representative samples for LC analysis is also covered in this work. A Mark IV prototype of LC sampler was tested and developed to acceptable levels.

In the area of pH measurement the advantages and disadvantages of the use of thermally grown iridium-oxide electrodes are introduced. Their response was compared to that of standard glass electrodes and found to be faster, more stable at high temperatures and no alkaline error was observed. However, the problem of drift of the signals was not fully overcome and it is presented as the limiting factor in the use of the sensors for on-line industrial measurements. Finally, a new type of total iridium-oxide probe is presented.

Abreviations

ADDS	*Adaptative Deferred Standard System*
AIROF	*Anode Iridium Oxide Film*
ANOVA	*Analysis of Variance*
approx.	*Approximately*
atm.	*Atmospheres*
ATR	*Attenuated Reflectance*
CFD	*Computational Fluid Dynamics*
CPACT	*Centre for Process Analytics and Control Technology*
CSTR	*Continuous Stirred Tank Reactor*
DS	*Deferred Standard*
Eq.	*Equation*
FID	*Free Induction Decay*
GC	*Gas Chromatography*
HEL	*Hazard Evaluation Laboratory*
HPLC	*High Performance Liquid Chromatography*
IC	*Ion Chromatography*
ID	*Inside Diameter*
ISFT	*Ion Sensitive Field Effect Transistor*
LC	*Liquid Chromatography*
LDA	*Laser Dopler Anemometry*
NA	*Non Applicable*
NFPA	*National Fire Protection Association*
NIR	*Near Infrared*
NMR	*Nuclear Magnetic Resonance*
NPSH	*Net Positive Suction Head*
OD	*Outside Diameter*
OST	*Office of Science and Technology*
PAC	*Process Analytical Chemistry*
PC	*Personal Computer*
PCA	*Principal Components Analysis*
PFR	*Plug Flow Reactor*
PhD	*Doctor of Philosophy*
PID	*Proportional Integral Derivative*

PLC	*Process Liquid Chromatography*
PLC	*Programmable Logic Controller*
r.p.m.	*Revolutions per minute*
RS	*Radio Spares Components*
RSD	*Relative Standard Deviation*
SB	*SmithKline Beecham*
SPM	*Sample Preparation Module*
TIROF	*Thermal Iridium Oxide Film*
UV	*Ultra Violet*
vol%	*Percentage in volume*
vs.	*Versus*

List of contents

CHAPTER 1

INTRODUCTION

1. Process Analysis and Control: General Aspects

Over the last two decades there has been a dramatic change in the chemical process industries. Industrial processes are now tightly constrained by high product specifications and subject to strict safety and environmental regulations[1,2]. These more stringent operating conditions place new constraints on the operating flexibility of a process and therefore high performance control systems are needed in modern industrial plants. Traditional methods for controlling chemical processes have relied almost exclusively on the measurement of temperature, pressure and flow rate. Nowadays, more information is needed for the safe and optimal operation of a plant and therefore it is necessary to add other types of process analysers. Better process control with the use of detailed, real time chemical measurements has become the key to lowering quality costs in chemical and materials manufacturing (estimated to be ten per cent of sales)[2]. Process Analytical Chemistry (PAC), is the application of analytical science to the monitoring and control of industrial chemical processes[2,3].

The first stage involved in the analysis and control of processes is the measurement of the variable that it is required to control (controlled variable). When dealing with chemical processes, monitoring of chemical composition is of great importance in process control. In a traditional chemical manufacturing plant, samples are taken from reaction areas and analysed in specialised laboratories producing results typically in a few hours to a few days. Implementation of PAC has changed this scene and now analysers are situated either in or immediately next to the manufacturing process. They are designed to withstand the rigours of a manufacturing environment and to give high reliability.

These improvements in the way of monitoring chemical processes has led to the definition of three main types of analysis[2,3]:

- Off-line analysis. Involves manual removal of the sample and transport to a measurement instrument located in a specialised laboratory for analysis.
- At-line analysis. Involves manual sampling but in this case the measurement is carried out on a dedicated analyser situated by the process operative. At-line analysis is not only based on simple transfer of laboratory analysis equipment

from the specialised laboratories to the plant floor, but it is also accompanied by significant method development work and modifications on the measurement techniques to permit the use of more robust and equally reliable instrumentation.

- On-line analysis. The type of analysis that uses fully automated analyser systems. Some authors have subdivided this type further into on-line, in-line and non-invasive analysis[2,3]. The differences between them are that for in-line analysis a sample interface is located in the process line itself eliminating the need for a separate sampling system (e.g. pH probes and infrared ATR probes) whereas for non-invasive analysis no sample contact is required since the analyser obtains a measurement of the process via a sample window (e.g. Raman and ultrasonic analysers).

There are many control strategies that can be applied using the information obtained with the measurement of a specific variable. Among all of them, the most important are the classical techniques of feed-back and feed-forward control[4]. In order to provide a full picture of the methodology used in process analysis and control, the basics of two control strategies will be introduced. This will also indicate the importance of physical and chemical modelling in the design of controllers.

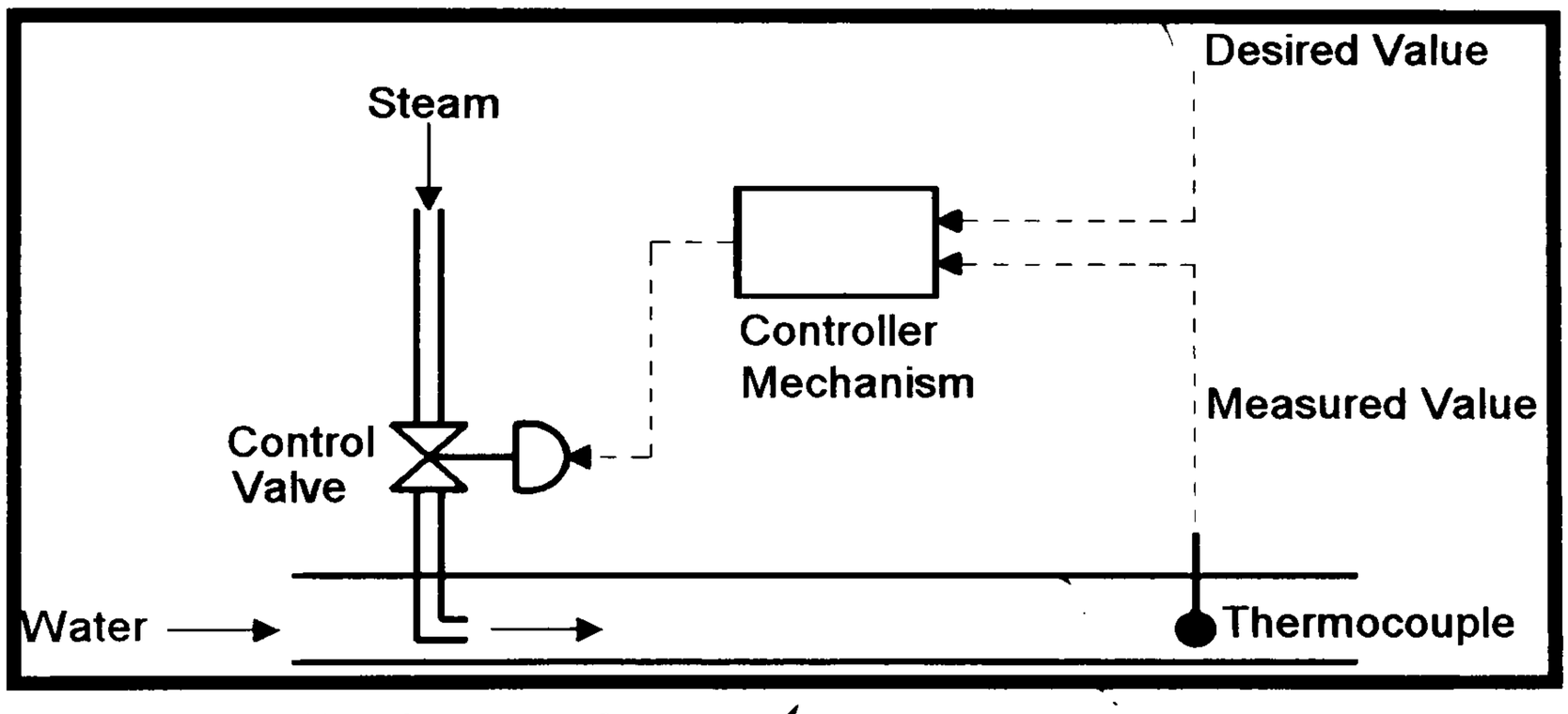

Figure 1.1. Simple feedback control system[4]

In the feed-back type of control, the value obtained from the empirical measurement will be compared with that at which it is desired to maintain the controlled variable (set point). After this, the process controller will adjust some further variable (manipulated value) which has a direct effect on the controlled variable until the desired value or set point is obtained[4-6]. This type of control system or loop is illustrated in *Figure 1.1* where a change in temperature for a water stream is

compensated by adding more or less steam in a controlled manner, in order to achieve a desired stream temperature.

On the other hand, what a forward controller does is, rather than measure the value of the controlled variable, it measures the values of the disturbances over the process and then calculates the manipulation required to balance exactly the disturbing effects and to keep the variable under control[4-6]. The operation of this type of control is shown in *Figure 1.2* where a disturbance in the flow inside the line, which will produce a change in temperature, is compensated by adding more or less steam in a controlled manner, in order to maintain the stream temperature under control. Forward controllers do not need empirical measurements of the variable to be controlled. Therefore, this control system is preferred when the analysis time is high for the monitoring of a particular process[7,8]. There are even variations of this type of controller that learn about the process and are used when the analysis response time is longer than the residence time in the reactor[9,10].

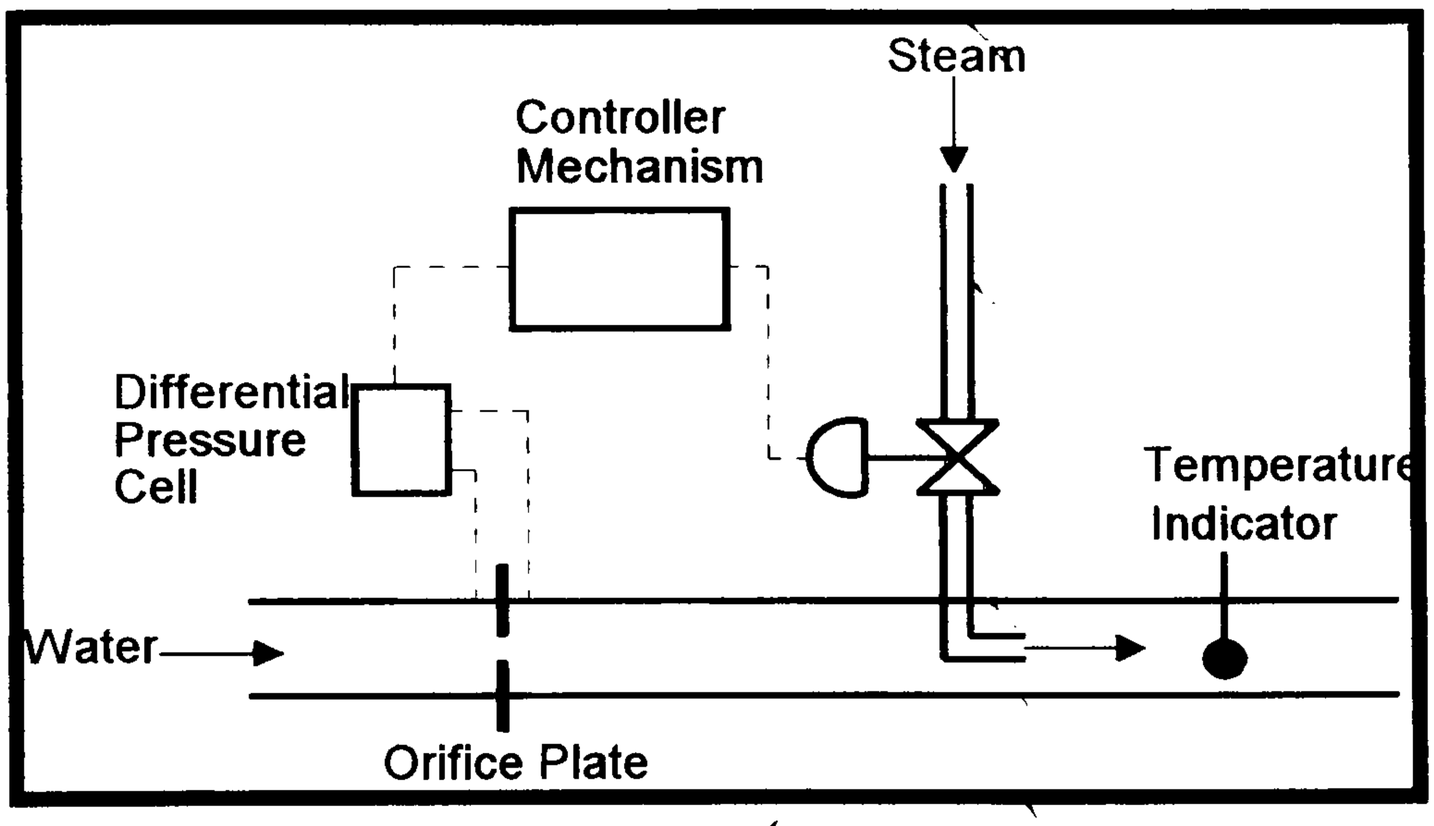

Figure 1.2. Simple feed-forward control system[4]

Modelling plays a key role in the design of control strategies. For a feed-back controller, a model that relates the effect of the manipulated parameter over the controlled variable is needed to design the control system. Similarly, a feed-forward controller has to contain models of how the process will respond to both the disturbances and to the manipulation. In addition to this, modern software packages can assist in the resolution of complicated mathematical models[11].

Sometimes the set point or desired value (or control recipe in the case of batch reactors[12]) is not totally constant but depends upon the value of other variables that affect the process. In this more complicated case, the mathematical model of the

system relates the changing set point value or model prediction with the process variables.

Therefore, the model of the process is important in order to design control algorithms needed to get a determined response. To obtain a model, detailed and complete information about the process is needed. Modelling is based on the study of mass, component and energy balances together with the kinetics of the process when dealing with chemical reactions. Therefore, preliminary quantitative chemical analysis is very important within the control loop in order to define the kinetics of the process needed for the model.

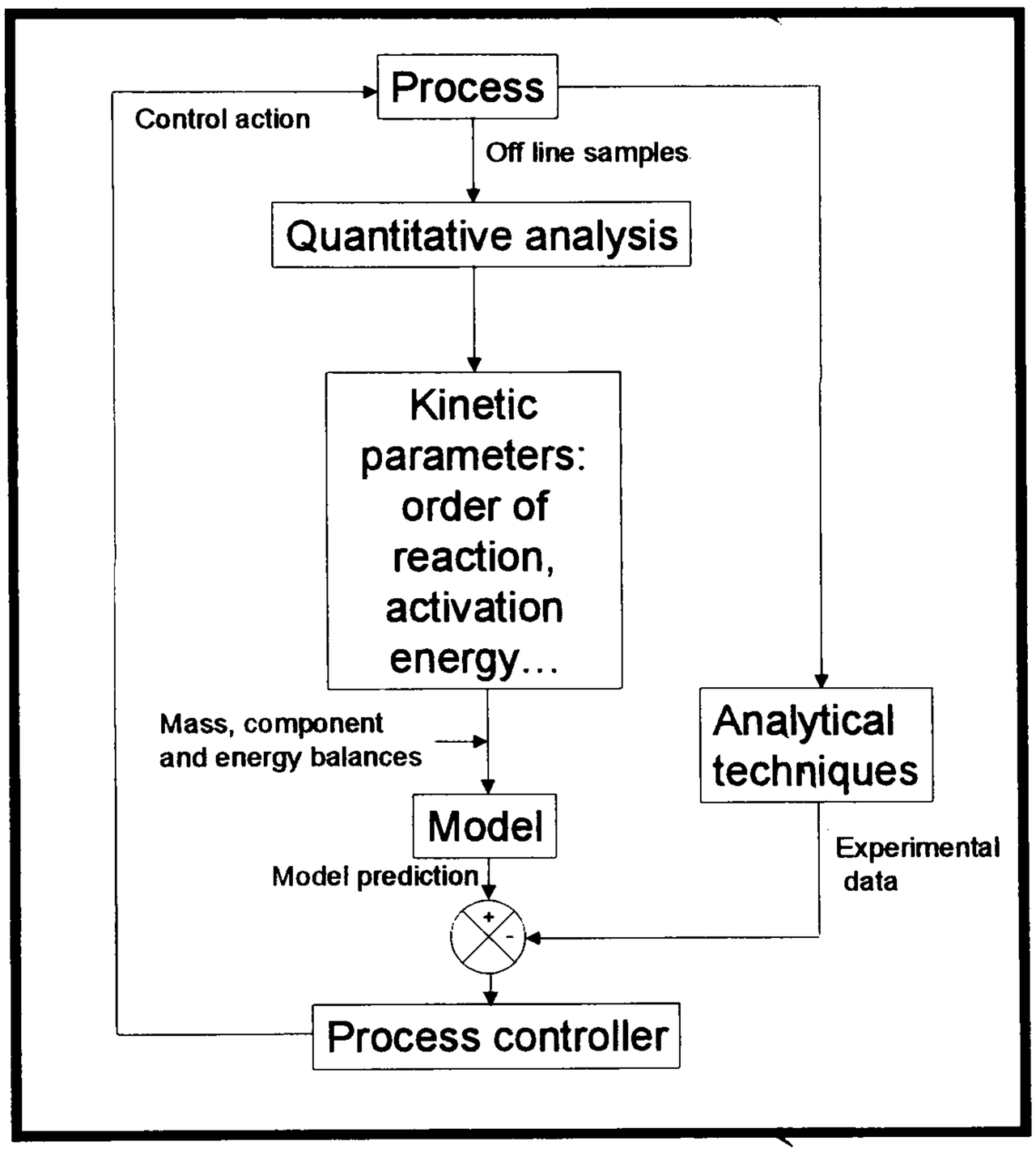

Figure 1.3. Stages involved in feedback control of chemical processes

Empirical modelling is sometimes very useful when the mathematical model of the process is very complicated. In these cases, models are formulated from measurements made on the plant. They assume that the real process dynamics can be represented by more simplified expressions (frequently as simple as first order equations) that closely fit the response. Experimental modelling is of particular interest with complicated systems that do not behave ideally, such as semibatch reactors[13] and multi-chamber tank reactors[14]. If success in process control is desired, the difficulties encountered in the development of a model must be kept to a

minimum. As Lee *et al.* say, a complete and perfect model is not only technically impossible but it is not even necessary[15].

In some way, theoretical models of relatively new chemical processes can be considered as half-empirical since the purely mathematical model is fed with kinetic information obtained after analysis of experimental results and responses of the process that are fitted to mathematical expressions for the kinetics, such as the Arrhenius equation[16]. All these stages involved in the analysis and control of chemical processes are shown in the block diagram in *Figure 1.3*. This figure shows how a half-empirical model of the chemical process determines the set point for a feed-back control loop. Measurements in the process will be compared with this set point in order to apply the adequate control action to the process.

In most industrial chemical processes the controlled process variables cannot be measured as frequently as would be desired and these measurements are not free of noise. Moreover, the manipulated variables of a process cannot be adjusted to implement control action as often as would be required and such adjustments are not 'cost-free'. Because of all these reasons, a detailed analysis of the variability of the measurements is of great importance in order to assess whether a change in a certain variable is only due to inherent measurement 'variability' (e.g. due to noise effects) or such a change needs a corrective action in order to keep the process under control[1].

This is where statistical analysis of data is required and statistical process control and dynamic modelling becomes a more practical approach. Chemometrics is the science of relating measurements made on a chemical system to the state of the system via application of mathematical or statistical methods[3,17]. Chemometrics applied to the acquired data is very important at the monitoring stage to avoid overloading of data and to get rid of unnecessary or redundant information. Data might also be in the presence of large amounts of noise and it would be desirable to take advantage of some sort of signal averaging techniques.

Adequate design of experiments is also needed in order to get the maximum information about a chemical industrial process in the most time and cost efficient manner (i.e. with the least possible number of experiments)[17,18]. This is of great importance for modelling, when the best set of experiments is required to ensure that

statistical procedures[19].

Improving the performance of batch reactors can be achieved by better control. However, this presents a difficult problem for a number of reasons[20,21]. Firstly, information on product quality and process performance is often delayed until a batch is completed. Secondly, key measurements of variables which value changes with time (e.g. conversion, size distributions, compositions) are often scarce and delayed. Finally, the final outcome of a batch process run is very difficult to predict using a first-principles model and thus it is necessary to deal with the problem of imperfect modelling.

Paying attention to the challenges from the control point of view, Berber[21] provides a good overview of control techniques to overcoming the problem of non-linearity and modelling inadequacies in batch reactors. Attending to the analytical limitations, there is a need for fast and frequent on-line measurements during the process and not only when the batch has been completed. These provide valuable empirical information that can be used to define more accurate models of the process. The measurements also offer fast information about the system that can be compared with the model prediction in order to take an adequate control action. Time and cost savings can be achieved by using on-line monitoring since one becomes aware of problems early and a remedial action to bring the process back to normal can be taken. Also, in case of failure the reaction can be stopped if it is not worth taking any remedial action[25].

The research presented in this thesis will deal with studies in process analysis and control of processes carried out in chemical reactors. Kinetic modelling, sampling issues and the development of new on-line analytical techniques for use in batch reactors will be discussed using esterification reactions as model processes.

2.1. Challenging problems in process analysis and control in batch reactors

The PhD work presented in this report is part of the work carried out in some of the projects within CPACT phase I. CPACT (Centre for Process Analytics and Control Technology) is a partnership funded by industry and the OST (Office of Science and Technology), involving three universities and many leading chemical and instrumentation companies[26]. CPACT phase I was divided into seven projects

aiming at the development of different techniques within the area of process analysis and control. The research presented in this thesis deals with chemical reactors and ways to improve monitoring and control in these systems. Due to the author's applied chemistry background and as part of the Chemical Technology section of the department of Pure and Applied Chemistry at Strathclyde, this work provided assistance to some of the projects in the area of chemical engineering. For example, the design of sampling systems for use in chemical reactors was one of the tasks. This not only allowed the collection of representative samples for off-line analysis and empirical modelling of batch chemical processes but it also assisted in the implementation of on-line analysers.

Besides the design and testing of sampling systems for NMR or HPLC on-line analysis, some of the work described here dealt with the development of new solid-state pH sensors. This project began as a way to overcome some of the difficulties encountered while monitoring pH in other projects. It soon attracted interest from the industrial partners in the project who encouraged a great deal of research in this area. Finally, kinetic studies were used to assess the effect of sampling devices on the rate of the chemical processes. Furthermore, the kinetic work also assisted the empirical needs of control engineers in the development of a general model of the process.

2.1.1. Problem of sampling

Within the stages involved in process analysis and control of industrial processes, the problem of getting a representative sample from the system is a key aspect, especially when dealing with chemical processes and monitoring chemical composition. In the last decade there has been a continuing growth in the use of process analytical instruments whose performance clearly depend on that of the sampling system. Unfortunately, developments in analyser technology have outpaced those in sampling[27].

A sampling system is an assembly of components and equipment with the function of taking an adequately representative sample from the process, conditioning (or processing) the sample in such a way as to render it suitable for direct input to the process analyser, transporting it in that state to the analyser, presenting it to the analyser, and finally disposing of the sample[28].

The main issues to consider when designing sampling systems for process analysis are[3,28]:

- Representativeness: The sample does not necessarily have to be representative, but adequately representative of the process. This means that, the sampled material must be adequately representative for the analytical information required. For example, it does not matter sometimes if the time representativeness of the sampled material is destroyed via preconditioning or purposely non-representative sampling as long as it does not affect the validity of the information supplied by the analyser.
- Compatibility: Sample has to be compatible with the analyser. In order to achieve this, sample conditioning might be required.
- Timeliness: Sampling systems have to provide timely information about the process which will depend very much on the response time of the analyser.
- Safety and environmental concerns: They are of great importance, especially when considering the final disposing stage involved in a sampling system.
- Reliability: Sampling systems have to be reliable in order to get samples whenever it is required for adequate monitoring and therefore control of the process. In fact, as much as 90% of all process analyser problems are ultimately attributable to problems with the sampling system[2].
- Cost: Is very important at an industrial plant scale.

Typically a sampling system for a gas or liquid consists of a sampling point or probe, pipelines, filters, pressure regulators, valves, pumps, flow meters, condensers or vaporisers, pressure gauges and other components. Selection of these parts, design of the components and adaptation to the system have to be carefully considered.

The importance of getting a representative sample to get a true response from the analysers is clear. Poor sampling will lead to erroneous results even with the most sophisticated instruments of analysis. For batch reactors, sampling seems to be quite straightforward as in theory any point inside the vessel possesses the same properties if the mixture is well stirred. However, in real industrial processes this is not the case and further aspects must be considered in order to get a representative sample,

specially from heterogeneous processes[28]. The effect of the flow-patterns inside the reactor, the stirring speed, the velocity in the sampling line, the shape, size and angle of the sampling probe are some of the factors that must be carefully considered when designing sampling systems for chemical reactors.

The importance of these and other factors over the representativeness of the off-line sample obtained via the sampling loop can be assessed for a particular sampling system, which may have not necessarily been well designed. This information can be used for the so called modelling of sampling system, which can correct the data from analysers implemented using sampling systems that have not been optimally designed.

2.1.2. Implementation of on-line analysers

Except with in-line and non-invasive analysers, where no sample transport and conditioning is required, the implementation of any analyser system for use on-line requires the design of a specific type of sampling system[28]. Some on-line analytical techniques such as GC or NIR have been extensively studied and are present in numerous applications in chemical plants. However, others like NMR or HPLC are still at the development stage and trying to make their way out of laboratories into the industrial plants[29,30].

In fact, two of the CPACT projects within phase I dealt with the implementation of nuclear magnetic resonance spectrometry and liquid chromatography for on-line analysis. In both cases, sampling has proven to be a key aspect. The work described in this thesis also covers the sampling issues affecting these two projects, where multidisciplinary teams intended to develop the techniques of NMR and HPLC for use on-line.

a) Implementation of NMR spectrometry for on-line analysis

NMR is one of the most powerful laboratory analytical tools, which is slowly moving into the area of process control. Early observations in 1951 showed a linear increase in signal amplitude with an increase in flow-rate as an aqueous solution passed through a simple NMR device[31]. In the 1980s, two companies tried to bring NMR to the field of on-line analysers[27]. They, however, were not successful and did not survive. Early in 1997, Foxboro purchased a company that had made some

progress in NMR and put its first application into the field for analysis of a sulphuric-acid alkylation process[27,32].

Early flow-NMR work was time consuming and sometimes tedious. The greater computing power of workstations and personal computers today have made it possible to reduce substantially the time between data collection and data reporting[32] which commonly need chemometrics and statistical treatment[33]. In addition to this, the constant evolution and miniaturization of electronic components has also facilitated the use of NMR technology in process environments. Magnet technology has produced smaller powerful systems that have in turn reduced the size and weight problems associated with laboratory systems.

Despite all these advances, NMR is still most commonly used for at-line measurements[2]. However, it is relatively easy to adapt the instrument to a flow cell for measurements on-line. With the use of flow cells for monitoring process streams and due to the non-invasive character of NMR, these systems overcome many problems with probe fouling typical of other techniques. Besides, the technique of low-field NMR offers a very fast, non-destructive, flexible and relatively cheap analysis[34]. In fact, in the past few years low-field NMR has been used extensively in a variety of industries including those involving the manufacture of food, pharmaceuticals and petrochemicals. Example applications include the determination of moisture content, fat content, hydrogen content and fluorine content[33].

When the sample is flowed through the magnetic field, the magnetic nucleus of the sample adopt one of a small number of allowed orientations with different energy. The transition between the few energy levels that are permissible generates a radio frequency signal that is transformed into a spectrum showing chemical species and their concentrations. In addition to chemical composition information, physical properties can also be correlated to the spectrum[32].

The introduction of a sample from the process stream to the analyser can be the Achilles' heel of any on-line analytical technique. The viscosity and flowing properties of the process stream will determine the type of sampling system to use for NMR analysis[31]. If the technique of NMR spectrometry is to be implemented for on-line monitoring in batch reactors, the development work will be closely linked to the

problem of sampling in this type of vessel. Furthermore, suitable sampling conditioning to adequately render the sample to the process analyser has to be considered. A "fast-loop" is the most sensible strategy to transport rapidly a representative sample from the process reactor to the sampling conditioning system, for final delivery of the sample to the NMR spectrometer. However, in its design there is the need to consider carefully factors like sampling velocity, flow-rate, temperature conditioning and the already mentioned sampling considerations to obtain good samples from batch reactors.

This thesis reports on the sampling considerations needed for the implementation of a low-field NMR analyser for on-line monitoring of batch processes. Preliminary experiments showed the success in the use of this technique in monitoring heterogeneous processes.

b) Implementation of HPLC for on-line analysis

Liquid chromatography is a very widely used laboratory analytical technique. However, unlike gas chromatography, it has not successfully made the transition from laboratory to the manufacturing plant. As part of one of the projects in CPACT phase I, H. Vandenburg was asked to produce a literature review[30] to understand the reasons for the current low use of on-line LC. These main reasons were found to be as follows:

- Poor reliability and high cost of the sampling systems.
- The use of flammable and expensive solvents.
- The complexity of the instrument and therefore the need for qualified staff for calibration and maintenance.

However, there are several incentives that encouraged the work in this project to try to overcome these problems. For example, on-line HPLC offers significant advantages over other methods such as spectroscopic and flow-injection analysis, as complex mixtures can be simultaneously analysed for a number of components over a wide concentration range, with relatively simple calibration. Also, there are many analyses where LC is the only reliable method available. These include situations where trace and bulk materials need to be determined, and mixtures that are too

complex for spectrometric methods.

There have already been developments in LC which could reduce the running costs and safety hazards involved in HPLC analysis. Narrow bore columns, small diameter packing materials and the possibility of water only mobile phases remove some of the problems related with the implementation of LC for on-line analysis. Better data processing and the use of chemometrics in fast liquid chromatography have reduced run times to a few minutes, making LC available for fast processes. Also, pumps and detectors are now robust and stable, requiring low service. However, sampling and sample preparation still remain as the most difficult stage to overcome for LC to become more widely accepted as a process technique. Whilst sampling solutions exists, these can be complex and therefore expensive. Complexity also leads to a decrease in reliability. Therefore, the problem of the implementation of HPLC for on-line analysis is reduced to the development of simple, cheap and reliable sampling systems for LC. In fact, one chapter of this thesis will be dedicated to the testing and development work carried out with different prototypes of discrete samplers in order to overcome the sampling problems affecting HPLC. Furthermore, these discrete sampling prototypes can also be used for the on-line implementation of other analytical techniques in other CPACT projects.

2.1.3. Problem of pH measurement

The measurement of pH at high temperature solutions (over 100°C) possess a difficult problem. The maximum useful temperature for glass electrodes is in the 100°C range, as higher temperatures lead to excessive drift related to sodium ion diffussion[35]. In addition to this, fragility is the major drawback of pH sensing glass electrodes[36,37].

In particular, the current interest in alternative ways of pH sensing within this project came about due to the fact that the pH glass electrodes failed to monitor the concentration of protons during the esterification of crotonic acid. In *Figure 1.4* it can be observed how the pH probe fails after holding a high temperature of 105°C in the esterification process (a mixture of toluene, butanol and crotonic acid) for more than 155 minutes.

Solid state sensors in general and metal-metal oxide electrodes in particular, have proved to give acceptable responses when measuring pH under high temperature and pressure conditions[35]. Among those, iridium oxide films have shown the best performance. There are various ways to produce these metal-metal oxide films but thermally grown iridium oxide electrodes represent a good compromise between quality of response and ease of construction.

Several applications of various types of iridium oxide sensors have been reported, mainly biological applications such as pH measurements in biofilms[36] and animal tissues[38]. However, no industrial scale uses have been found to the best of our knowledge. Therefore, the study of the performance in monitoring and control of pilot scale industrial processes appears to be a good challenge and an attractive focus for a good part of the research presented in this thesis.

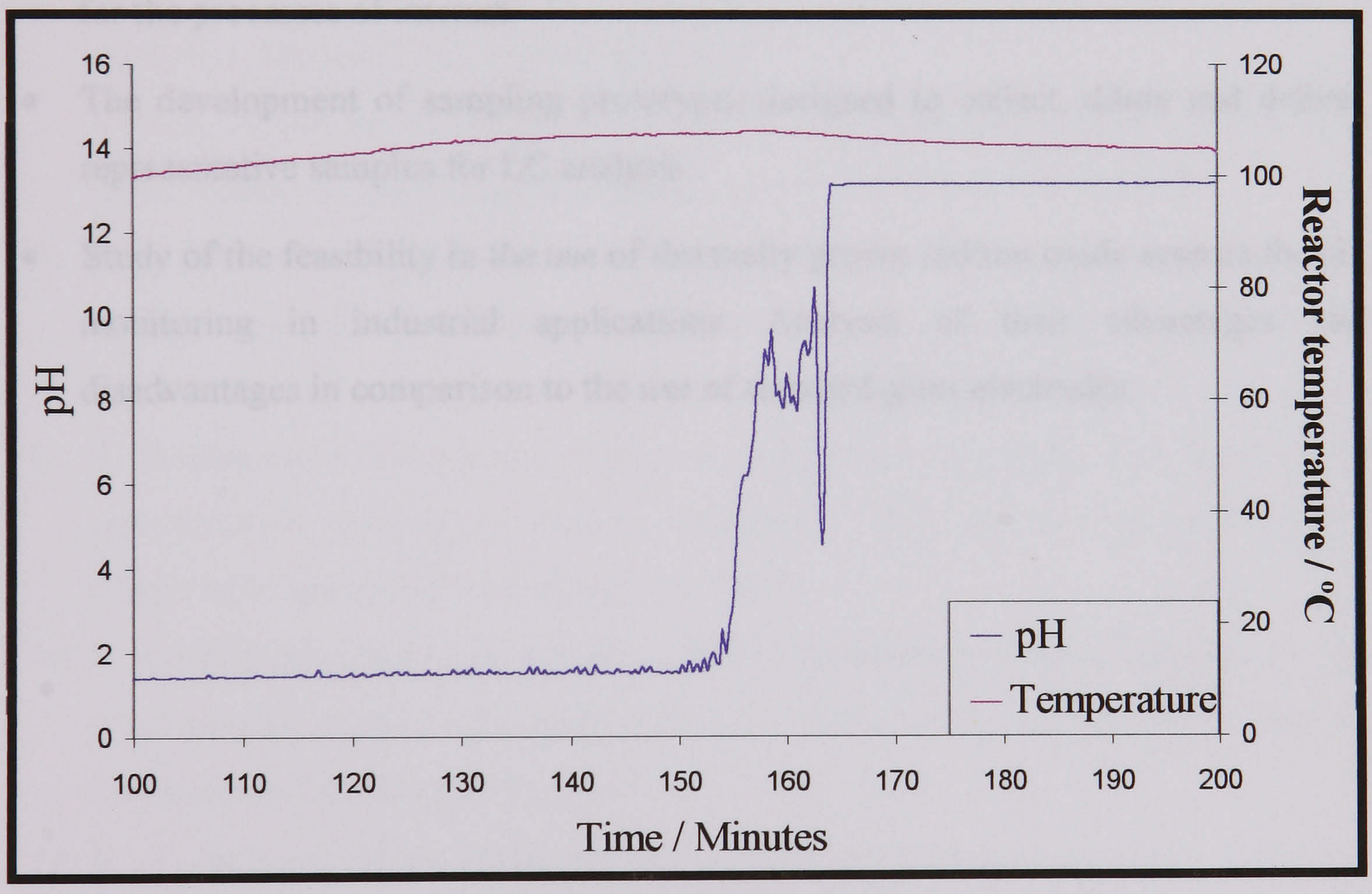

Figure 1.4. pH probe fouling during the process of monitoring crotonic acid esterification at 100°C

3. Aims

As pointed out in the previous sections, this work was focussed in some of the relevant aspects in the monitoring and control of batch reactors. The aims of the research could be outlined as follows:

- The design and development of a fast sampling loop system to obtain representatives samples from stirred vessels. The difficulties associated with the collection of representative samples from heterogeneous processes in agitated reactors will be reviewed in the design. The implementation of a low-field NMR spectrometer in the loop for on-line analysis will be the final aim for such a design.

- The sampling work should also assist other researchers in the project with the kinetic and heat-exchange parameters needed for the definition of a general model for the processes of interest.

- The development of sampling prototypes designed to collect, dilute and deliver representative samples for LC analysis.

- Study of the feasibility in the use of thermally grown iridium oxide sensors for pH monitoring in industrial applications. Analysis of their advantages and disadvantages in comparison to the use of standard glass electrodes.

4. References

1. B. A. Ogunnaike and W. H. Ray, 1994, *Process dynamics, modelling and control*, Oxford University Press, New York, USA.
2. C. Hassell and E. M. Bowman, 1998, *Process analytical chemistry for spectroscopists,* Applied Spectroscopy, Vol. 52 No. 1, 18A-29A.
3. F. McLennan and B. R. Kowalski, 1995, *Process analytical chemistry*, Blackie Academic and Professional, London, UK.
4. J. F. Richardson and D. G. Peacock, 1994, *Chemical Engineering, Volume 3: Chemical Reactor Design, Biochemical Reaction Engineering Including Computational Techniques and Control*, Pergamon, Oxford, UK.
5. F. G. Shinskey, 1988, *Process control systems: application, design, and tuning*, McGraw-Hill, New York, USA.
6. W. L. Luyben, 1990, *Process modelling, simulation, and control for chemical engineers*, McGraw-Hill, New York, USA.
7. J. Broll, A. Rix and H. Gelbe, 1995, *Nonlinear model-based feedforward control of distillation columns*, Chemical Engineering Technology, 18, 178-182.
8. K. Schnitzlein, K. Bolze and A. Löwe, 1993, *A learning fedforward control strategy for the concentration control of recycle reactors – Part III: Implementation and operation*, Chemical Engineering Technology, 16, 376-382.
9. K. Schnitzlein and A. Löwe, 1993, *A learning fedforward control strategy for the concentration control of recycle reactors – Part II: Disturbance control*, Chemical Engineering Technology, 16, 26-34.
10. K. Schnitzlein and A. Löwe, 1992, *A learning fedforward control strategy for the concentration control of recycle reactors – Part 1: Set-point control*, Chemical Engineering Technology, 15, 26-34.
11. B. A. Horwitz, 1996, *Avoid nausea when solving dynamic problems*, Chemical Engineering Progress, March, 44-51.
12. ANSI/ISA-S88.01-1995, 1995, *Batch control – Part 1: Models and terminology*, The International Society for Measurement and Control.
13. F. Stoessel, 1995, *Design thermally safe semibatch reactors*, Chemical Engineering Progress, September, 46-53.
14. P. Shain, 1997, *Correctly calculate conversion in multichamber tank reactors*,

Chemical Engineering Progress, September, 76-80.

15. W. Lee and V. W. Weekman, 1976, *Advanced control practice in the chemical process industry: a view from industry,* AIChE Journal, Vol. 22 No. 1, 27-38.
16. M. Weerasinghe, J. Wilkie, D. A. Mamman, A. Diez-Lazaro and M. L. Hitchman, 2000, *Modelling and simulation of a laboratory scale esterification process,* ADCHEM 2000 – International Symposium on Advanced Control of Chemical Processes, 1073-1078.
17. R. G. Brereton, 1990, *Chemometrics: applications of mathematics and statistics to laboratory systems*, E. Horwood, New York, USA.
18. W. P. Gardiner, 1997, *Statistical methods for chemists: a software based approach*, The Royal Society of Chemistry Information Services, Cambridge, UK.
19. P. Nomikos and J. F. MacGregor, 1994, *Monitoring batch processes using multiway principal components analysis,* AIChE Journal, Vol. 40 No. 8, 1361-1375.
20. E. C. Martinez, R. A. Pulley and J. A. Wilson, 1998, *Learning to control the performance of batch processes,* Transactions of Institution of Chemical Engineers, Vol. 76, Part A, 711-722.
21. R. Berber, 1996, *Control of batch processes: a review,* Institution of chemical engineers, Chemical Engineering Research and Design: Transactions of Institution of Chemical Engineers, Part A, 74 A1, 3-20.
22. J. P. Kennedy, 1976, *Impact of computers on process design: batch vs continuous processing*, Chemical process control, AIChE symposium series, Vol. 72 No. 159, 77-79.
23. R. C. Ashley, 1996, *Real-time control – Time to reap some rewards*, ICHEME Advances in Process Control, 39-47.
24. A. Kumar, P. D. Christofides and P. Daoutidis, 1998, *Singular perturbation modelling of nonlinear processes with nonexplicit time-scale multiplicity,* Chemical Engineering Science, Vol. 53 No. 8, 1491-1504.
25. M. Cabassud, M. V. Le Lann, B. Ettedgui and G. Casamatta, 1994, *A general simulation model of batch chemical reactors for thermal control investigations*, Chemical Engineering Technology, 17, 225-268.
26. Centre for Process Analytics and Control Technology (CPACT), Internet web

page, 2001, http://www.strath.ac.uk/Other/cpact/

27. D. E. Podkulski, 1997, *How do new process analysers measure up?*, Chemical Engineering Progress, October, 33-46.
28. K. G. Carr-Brion and J. R. P. Clarke, 1996, *Sampling systems for process analysers*, Butterworth-Heinemann, Oxford, UK.
29. J. F. Haw and T. W. Skloss, 1993, *Early experiences with NMR in process analysis*, Spectroscopy, 8(9), 22-27.
30. H. Vanderburg, 1999, *On-line liquid chromatography*, CPACT IMB internal report (Ref:99/P7/1), Centre for Process Analytics and Control Technology, CPACT/University of Strathclyde, Glasgow, UK.
31. M. L. Snoddy, 1993, *The potential of process NMR on flowing streams,* Spectroscopy, 8(3), 41-47.
32. Foxboro, 1998, *I/A series NMR. On-line, real time strategic analytical measurement. For the first* time, Commercial leaflet
33. A. Nordon, C. A. McGill and D. Littlejohn, 2001, *Process NMR spectrometry,* Analyst, 126, 260-272.
34. Sintef group, Internet web page, 2001, *At-line/On-line NMR of porous materials*, http://www.sintef.no/units/unimed/mr/Material/At_on_line.htm
35. K. G. Kreider, M. J. Tarlov and J. P. Cline, 1995, *Sputtered thin-film pH electrodes of platinum, palladium, ruthenium, and iridium oxides*, Sensors and Actuators B, 28, 167-172.
36. P. VanHoudt, Z. Lewandowski and B. Little, 1992, *Iridium oxide pH microelectrode*, Biotechnology and Bioengineering, 5, 601-608.
37. M. J. Tarlov, S. Semancik and K. G. Kreider, 1990, *Mechanistic and response studies of iridium oxide pH sensors*, Sensors and Actuators B, 1, 293-297.
38. S. A. M. Marzouk, S. Ufer, R. P. Buck, T. A. Johnson, L. A. Dunlap and W. E. Cascio, 1998, *Electrodeposited iridium oxide pH electrode for measurement of extracellular myocardial acidosis during acute ischemia*, Analytical Chemistry, 70, 5054-5061.

CHAPTER 2

REACTOR FACILITIES AND SYSTEMS OF INTEREST

1. Reactor Facilities and Systems of Interest

The purpose of this chapter is that of describing the experimental facilities available for the project. The main model reactions and processes used in the research will also be described. The CPACT reactor facility at the University of Strathclyde is available to academic and industrial users to experiment with advanced control and instrumentation techniques. The reactors are used by a consortium of researchers for studies into the optimisation and improved control of batch systems as well as the study of the use of analytical instrumentation in an on-line capability[1].

One of the objectives of CPACT project 1 was to set up a facility, which could be used to compare existing and new approaches to 'on-line' chemical analysis as well as evaluate improved calibration methods and test novel control procedures[2]. The works on the reactor facility started in late 1998 and continued up to mid 1999, including improvements to the facility and tests which ensured that the system was satisfactory before the commissioning of the facility. This took a great amount of researcher's time so the work on the projects could not start until the facility was finished. In addition to this, a new control program in a LabVIEW environment was developed and tested along with the reactors[1,3]. This control software is more flexible than the one provided with the reactors, and allows any information derived from analytical data to be used for control. The analytical instrumentation needed for the projects was also obtained during the course of the project. This included a Bomem MB155 FTIR/NIR spectrometer, a Kaiser HoloPROBE Raman spectrometer, a Zeiss MCS UV-visible spectrometer, a Foss NIRSystems on-line 6000 NIR spectrometer, and a Resonance Instruments low-field NMR spectrometer to be implemented on-line[2].

Two main esterification reactions were chosen as model processes to be used for achieving the objectives of comparing on-line analytical techniques and testing novel analytical and control procedures[2,4-6]. One of the reactions was a homogeneous reaction and constituted a simple model reaction to be used for initial experiments before moving on to more complicated processes. The second reaction possessed more challenges as it was a heterogeneous reaction and led to the formation of two different compounds where one was the preferred product. More details about these

processes are described later (section *1.2*).

1.1. Reactor system

As mentioned earlier, the development of advances in the area of monitoring and control of chemical processes in reactor systems were the main goals within the projects described in this thesis[2]. Therefore, it is worth spending a little bit of time describing the reactor facilities before progressing any further in this report. The reactor system available at Strathclyde University can be considered as a pilot scale device formed by two vessels. These are two 5 litre stirred reactors that can be used either in a batch mode or in a continuous manner. The latter is achieved by operating on a virtual CSTR system transferring by gravity the contents of one vessel from the bottom of one reactor to the top of a second reactor. The processed material is then recycled from second reactor to the first by using a diaphragm pump as shown in *Figure 2.1*.

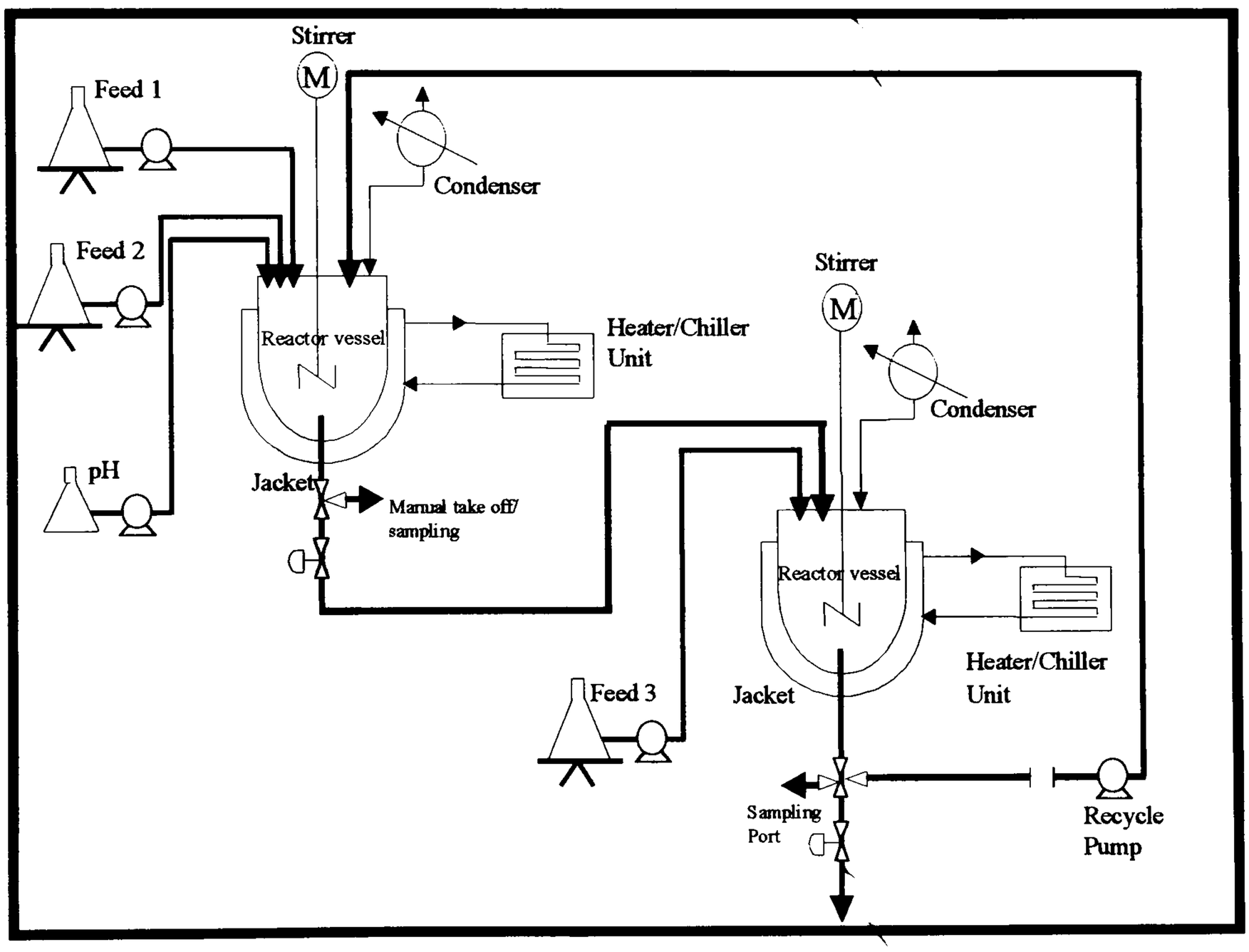

Figure 2.1. Diagram of the continuous reactor system

The vessels can also be used as two independent batch reactors. In fact, the batch mode was not only more challenging from the analysis and control point of view[7,8], but it also showed to be more attractive for the industrial partners involved in the projects[2]. Initially, only one control unit was available and the two batch reactors

could not be used simultaneously. Currently, an upgrading process is taking place so that the two vessels can be used in a batch mode at the same time[9]. *Figure 2.2* shows the batch reactor diagram valid for each of the two vessels.

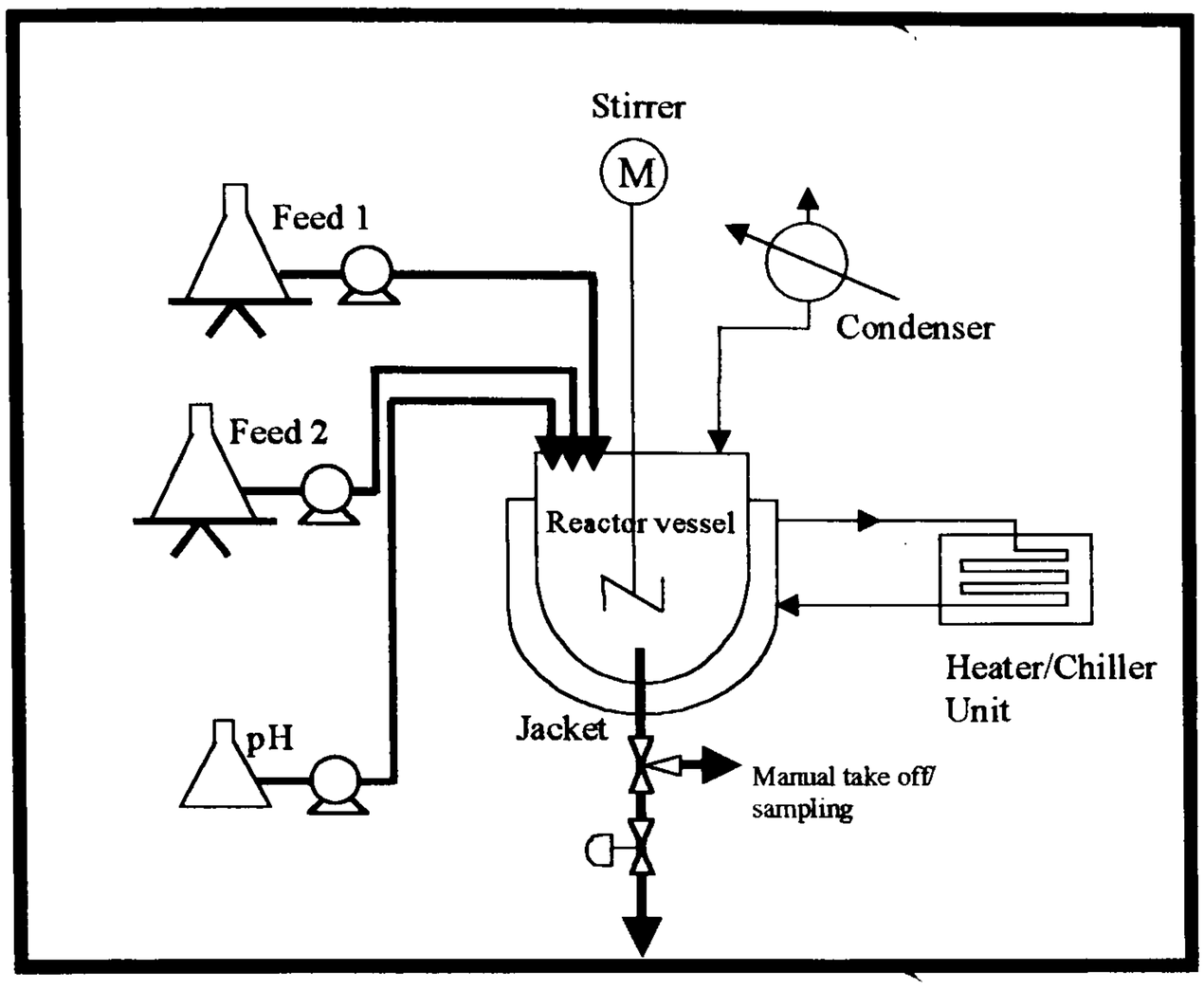

Figure 2.2. Diagram of the batch reactor system

The vessels are made of glass with an inner heating jacket and an outer vacuum jacket. Both are made of glass to permit visual observation of the reaction. The inner jacket serves as a heat exchanger to maintain the reaction at the desired temperature. The heat is transferred to the reactor using silicon oil circulated through the inner jacket and temperature controlled by a heater/chiller unit. The outer vacuum jacket serves to minimise heat losses to the surroundings and avoid the risk of personnel injuries by contact with hot surfaces[9,10]. The reactor vessel and the jackets have two side measurement ports used to insert NIR and temperature probes into the reactor. Both reactors have a top lid with nine ports for use of further on-line probes for temperature, pH, infrared and Raman analysis.

Three feed vessels (normally used for solvent, liquid reactants and catalyst) are available in the system. Two weighing scales are used to weigh the feed and dosing vessels giving signals used to calculate the flow of chemicals going into the reactors. A condenser is used to condense and reflux the vaporised reactants and products back into the reactor. It can also be used to vent steam out of the system by switching off the condensing facility[11].

The signals coming from the different sensors in the system are transferred to a PC where they are monitored and recorded. WINISO is the name of the software provided by the manufacturer to achieve this as well as to control the system using standard PID control. Examples of some of the measured and monitored signals are: liquid levels in the vessels (important for filling and emptying processes), temperature in the reactor (to control the temperature of reaction), oil temperature in the inlet and outlet port of the jacket (to monitor the temperature of the fluid in the jacket used to regulate the temperature in the reactor), flow of water through the condenser (to verify the good functioning of the condensers), stirrer speed (important for kinetic and sampling modelling), pH (especially interesting with acid catalysed chemical reactions), weight on the balances (to monitor and control the feed of chemicals into the reactor) and feed and recycling flows (to monitor and control the pumping rate). *Figure 2.3* shows a general view of the reactor facility.

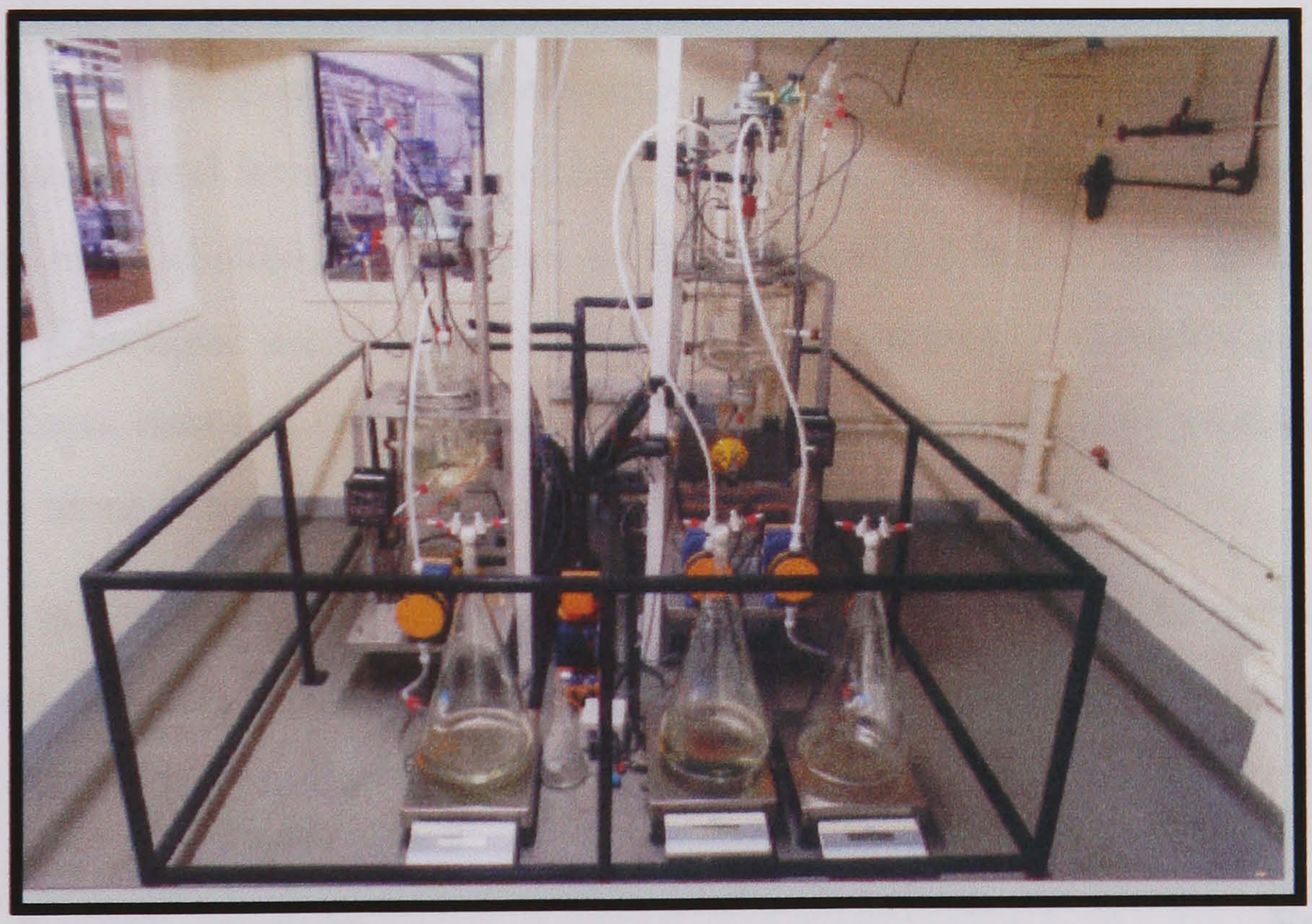

Figure 2.3. General view of the two 5-L reactor system

For smaller scale experiments a 1-L reactor vessel with a single jacket was used (see *Figure 2.4*). This reactor has a small heater/chiller unit to maintain the reaction temperature. It also provides a reading of the temperature for the oil inside the jacket. The vessel has a lid with 3 ports, one used for the condenser, one for monitoring the temperature with a small mercury thermometer and the last one normally used to feed in reactants and catalyst.

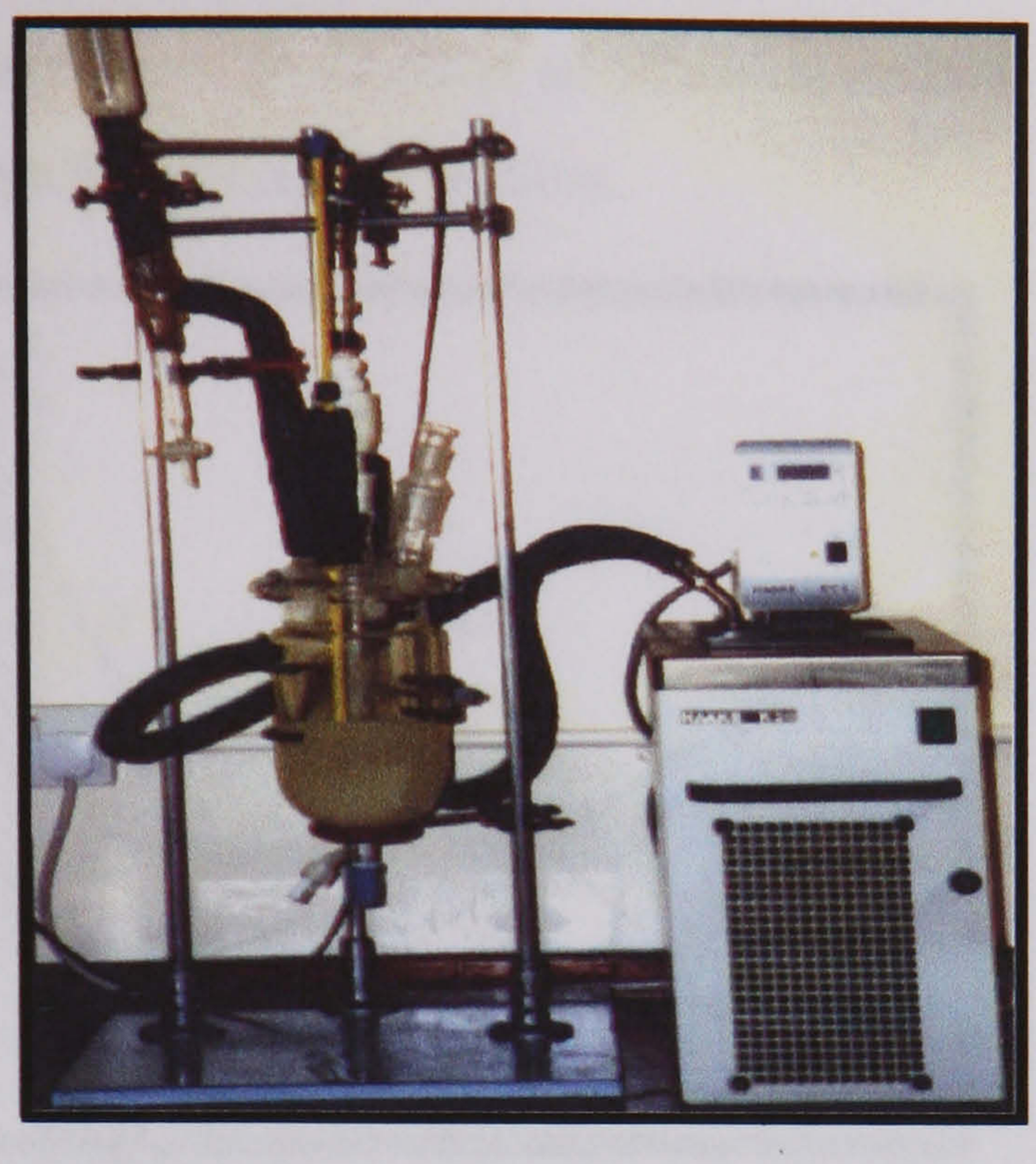

Figure 2.4. General view of the 1-L reactor system[12]

1.2. Process esterification reactions

As mentioned earlier, analysis and control studies in chemical reactors are of great challenge and interest[7,8]. In addition to this, the use of certain types of reactions add some extra challenging features to those described before for batch processes. 'Complex Reactions' are examples of this type of processes. A complex system is one in which more than one reaction occurs[13]. They can lead to multiple products some of which are more desirable than others from a practical standpoint.

It is therefore the challenge in controlling the reaction to yield optimum production of a desirable product which makes these types of processes of interest for analysis and control studies[2]. The two main types of complex reactions are[13]:

- Simultaneous reactions:

$$A \xrightarrow{k_1} B$$
$$A \xrightarrow{k_2} C \qquad \text{Eq. 2.1}$$

- Consecutive reactions:

$$A \xrightarrow{k_1} B \xrightarrow{k_3} D \qquad \text{Eq. 2.2}$$

A typical concentration versus time plot for a simultaneous reaction would show a decrease in the concentration of reactant while the product concentration increases until they both eventually reach the equilibrium. On the other hand, a typical concentration versus time plot for consecutive-reactions would look like that shown in *Figure 2.5*. Therefore, the consecutive-reaction system is more interesting from the

control point of view as there is an optimum production of B product. Maintaining the conditions needed for maximum production of the intermediate component B will frequently be the challenge for the control system.

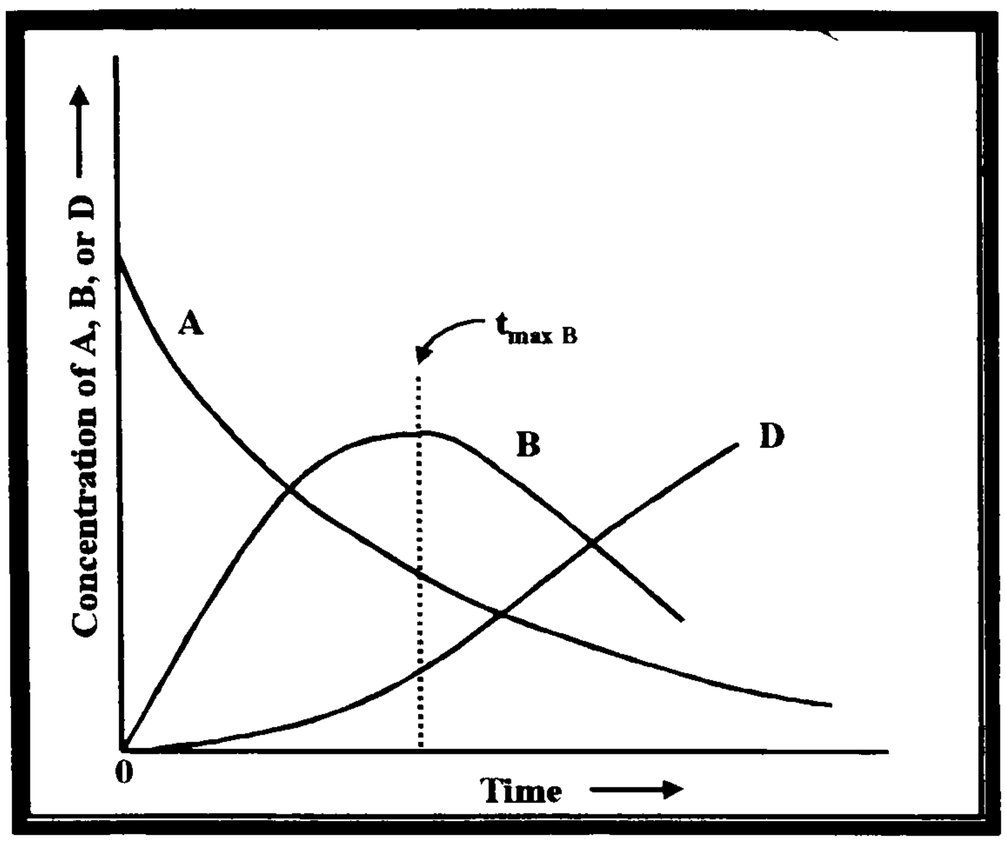

Figure 2.5. Typical concentration-time plot a consecutive-reaction system

In addition to all the kinetic demands, a good process for our studies should also have some kind of industrial interest due to the applied character of this research[4-6]. Furthermore, the process also has to be feasible to carry out in the reactor system available for the research, considering not only the operating conditions and specifications of the reactors and analysers, but also aspects such as safety regulations and running costs of the process. Therefore, control interest, industrial applicability and feasibility of the process were the criteria to follow at the time of selecting a reactive process for our studies.

Industrial partners involved in these projects proposed a number of reactions of interest for analysis and control studies in batch reactors[2]. Initially, the feasibility of nitration of anthraquinone was studied[14]. However, problems with a broad variety of by-product forming during the reaction and poor amenability of monitoring with certain types of on-line analytical techniques, made this process not recommended for further investigation.

The esterification of itaconic acid was another proposed reaction that seemed to satisfy all the criteria stated above for a good process reaction[4-6]. From the analysis and control point of view, esterification of itaconic acid was an interesting and challenging complex process that could lead to two different products[15]. Since itaconic acid is a dicarboxylic acid, the esterification process can produce mixtures

of monoester and diester species.

Dicarboxylic acid + Alcohol ↔ Monoester + Diester + Water Eq. 2.3

Figure 2.6 shows the itaconic esterification reaction scheme as well as the formulas of the compounds involved in the process.

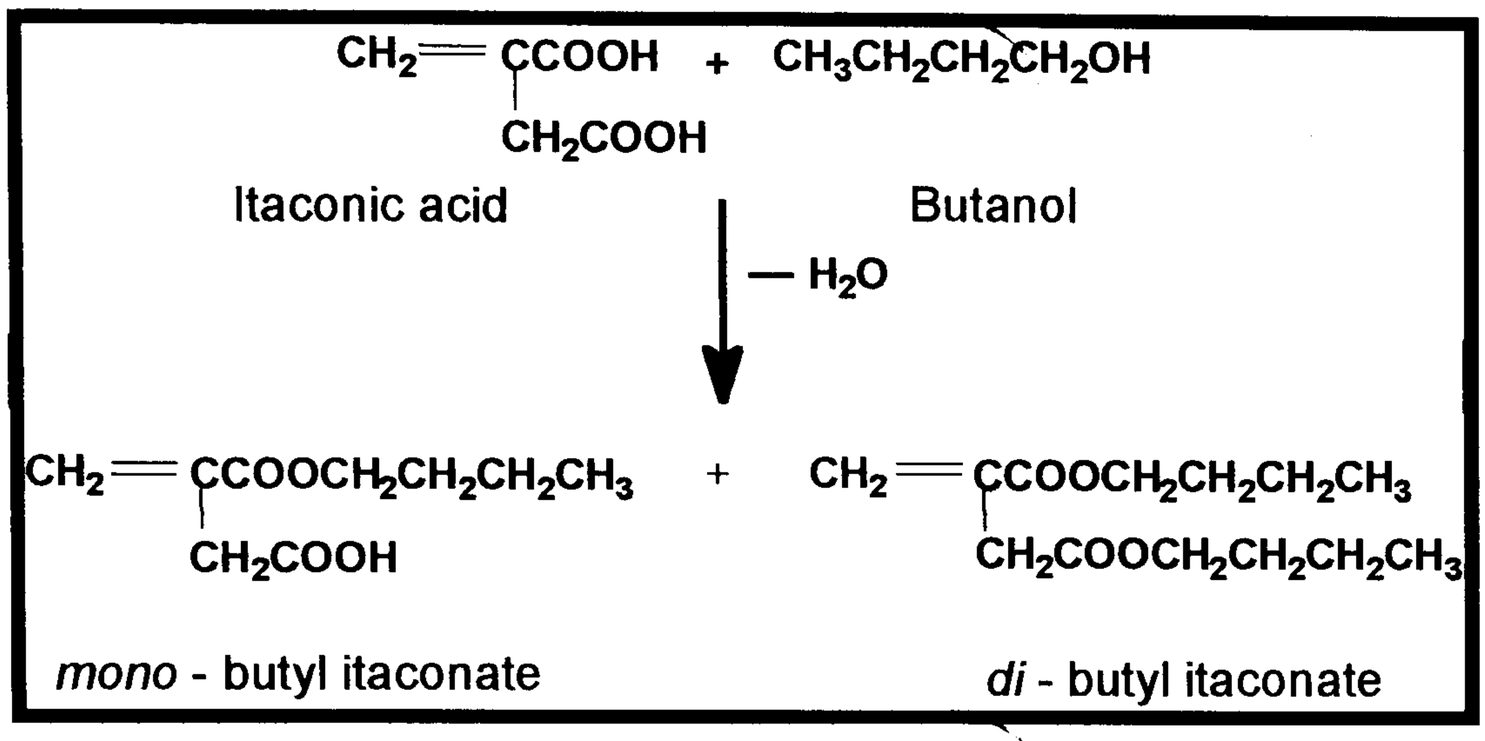

Figure 2.6. Itaconic esterification reaction scheme and compound formulas

This reaction is acid catalysed. Baker and co-workers[15] have demonstrated that with limited amounts of alcohol, the acid catalysed esterification of itaconic acid or its anhydride produces mixtures of acid, diester and monoester. The latter can be separated from the diester by extraction procedures[4,16]. The melting point of the monoester decreases as the chain length of the alcohol increases. Therefore, in order to avoid very low melting point products, a short chain length must be used. For safety reasons, butanol was used as an alcohol in our experiments[4]. From the industrial point of view, mono and di-itaconate esters are of increasing interest. They readily undergo polymerisation, copolymerisation with other monomers and condensation polymerisation of both ester and amide derivatives can be made[15]. Although a great variety of polymers incorporating the itaconates have been reported in the patent literature, many of these have not been produced commercially.

Considering the feasibility of carrying out this process in our system it should be mentioned that itaconic compounds are relatively innocuous materials that can be handled without special precautions[4,15,17]. Reaction conditions are normally not excessively harsh. Initially, a maximum temperature of 35°C (close to the monoester melting point)[16] was used in the process in order to avoid the formation of polymers of both the acid and the ester[5]. However, later experiments showed that higher

temperatures could be used with no formation of side-products[18]. Atmospheric pressure conditions were used and relatively small amounts of acetyl chloride were added as a catalyst. In addition to this, the cost of the reactants is relatively low[19]. The reaction was carried out in toluene producing a complicated heterogeneous mixture with organic phase (toluene, butanol and diester), aqueous phase and solids in suspension (itaconic acid is sparingly soluble)[4,16,20]. These features made the process also challenging from a sampling point of view.

However, despite all these favourable features for the reaction, some initial problems were faced which forced the use of a simpler process until more was known about the itaconic esterification. Problems with the development of a good off-line calibration method for GC and HPLC were encountered[16,20]. Besides, it was not clear whether the formation of diester was a simultaneous process or a consecutive process. Preliminary experiments on the kinetics of this process did not clarify whether the monobutyl itaconate was formed first and continued to form dibutyl itaconate or if the diester was formed concurrently[16,18,20].

After all these problems with the itaconic acid reaction, the esterification of crotonic acid was suggested as an alternative process for the project[2]. This is a simpler esterification reaction that produces a single ester product starting from a monocarboxylic acid. It can be described by the reaction scheme[12] showed in *Figure 2.7*. The fact that it is also an esterification process is useful when transferring information (acquired with experimental experience in the study of this process) to the more complicated case of itaconic acid esterification.

It is true that this new process is not as challenging as the itaconic reaction from the control point of view. It is not a consecutive process and does not produce two esters. Furthermore, crotonic acid is soluble in the solvent and the small heterogeneity in the process comes from the small production of water during the esterification reaction[12]. It is, therefore, not as challenging as the itaconic process from the sampling point of view either. However, it is a simpler process that has been more extensively studied in the literature than the itaconic acid esterification. Moreover, it has been also proposed before for on-line monitoring purposes and control studies[21]. The simplicity of the process was very useful in order to focus the

initial stages of the research more in the control of pure batch processes rather than in problems derived by the complexity of the reaction.

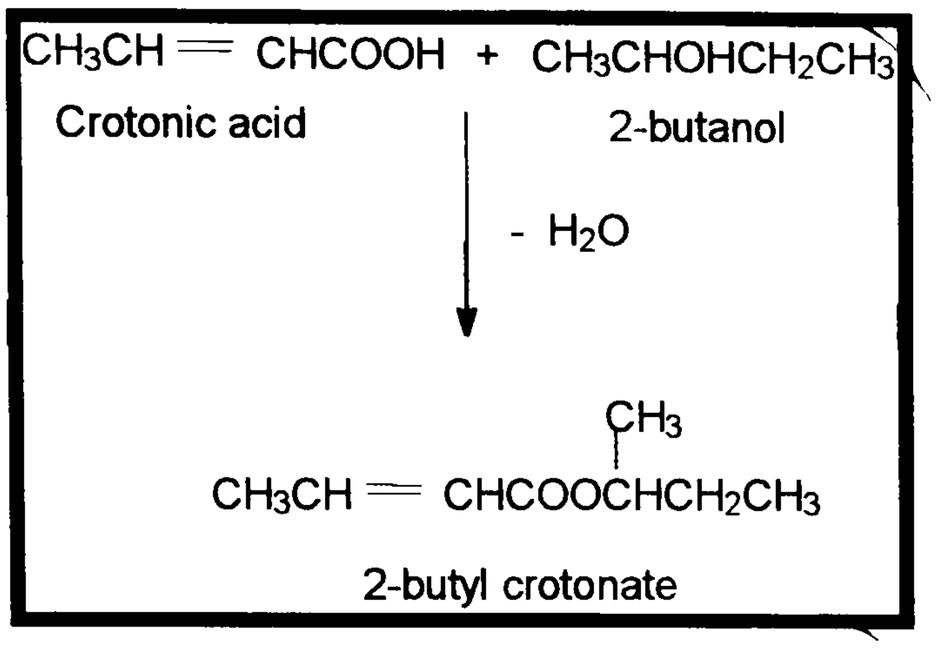

Figure 2.7. Crotonic esterification reaction scheme and compound formulae

Therefore, the esterification of crotonic acid was the process of interest in the project when the use of reactive systems was needed. For pure physical sampling studies, where process reactions were not important, the use of non-reactive heterogeneous mixtures was used.

1.3. Other process of interest

Apart from the esterification processes described above, there were other reactive and non-reactive processes that were used in the experimental work carried out in this thesis. Examples of these non-reactive processes are suspensions of inorganic salts in water[22], glass beads in water and non-miscible mixtures of solvents such as heating oil, toluene and water. Examples of other reactive processes are mainly titrations and step changes in acidity both in aqueous and non-aqueous environments. Detailed information on these systems and the reasons why they were needed are described in later chapters dealing with the experimental part of this thesis.

2. References

1. M. Weerasinghe, J. Wilkie, D. A. Mamman, A. Diez-Lazaro and M. L. Hitchman, 2000, *Modelling and simulation of a laboratory scale esterification process*, ADCHEM 2000 – International symposium on advanced control of chemical processes, 1073-1078.
2. CPACT Centre for Process Analytics and Control Technology, Internet web page, 1999, http://www.strath.ac.uk/Other/cpact/
3. M. Weerasinghe, 2000, *LabVIEW Monitoring and Control System for the CPACT Batch Reactor Process*, CPACT IMB internal report (Ref:00/P1/2), Centre for Process Analytics and Control Technology, CPACT/University of Strathclyde, Glasgow, UK.
4. D. Mamman, 1998, *Esterification of Itaconic acid: a review*, Internal report, Department of Pure and Applied Chemistry, University of Strathclyde, Glasgow, UK.
5. D. Mamman, 1999, *Partial esterification of Itaconic acid*, Internal report, Department of Pure and Applied Chemistry, University of Strathclyde, Glasgow, UK.
6. D. Mamman, 2000, *Esterification of Itaconic Acid: A Report*, CPACT IMB internal report (Ref:00/P1/3), Centre for Process Analytics and Control Technology, CPACT/University of Strathclyde, Glasgow, UK.
7. E. C. Martinez, R. A. Pulley and J. A. Wilson, 1998, *Learning to control the performance of batch processes,* Trans IchemE, Vol. 76, Part A, 711-722.
8. R. Berber, 1996, *Control of batch processes: a review,* Institution of chemical engineers, Chemical Engineering Research and Design: Transactions of Institution of Chemical Engineers, Part A, 74 A1, 3-20.
9. D. A. Mamman, M. Weerasinghe and A. Diez-Lazaro, 2000, *Strathclyde Reactor Systems*, CPACT IMB internal report (Ref:00/P1/5), Centre for Process Analytics and Control Technology, CPACT/University of Strathclyde, Glasgow, UK.
10. M. Weerasinghe, J. Wilkie and M. Johnson, 1988, *Preliminary report on monitoring and control aspects*, ICC/147/June, Internal report, Industrial Control Centre, University of Strathclyde, Glasgow, UK.
11. J. Wilkie, M. Weerasinghe and D. A. Mamman, 1998, *Development of a model*

process system for analysis of control and instrumentation techniques, Internal report, Industrial Control Centre, University of Strathclyde, Glasgow, UK.

12. F. Clark, 1999, *The development of process near infrared spectroscopy for batch reactor analysis*, 4th year project, Department of Pure and Applied Chemistry, University of Strathclyde, Glasgow, UK.
13. J. M. Smith, 1970, *Chemical Engineering kinetics*, McGraw Hill, New York, USA.
14. D. A. Mamman, 1998, *Nitration of Anthraquinone*, Internal report, Department of Pure and Applied Chemistry, University of Strathclyde, Glasgow, UK.
15. E. C. Leonard, 1970, *Vinyl and diene monomers*, Part1, Wiley, New York, USA.
16. N. Khaliq, 1999, *Investigation of the kinetics of partial esterification of Itaconic acid by NIR spectroscopy*, 4th year project, Department of Pure and Applied Chemistry, University of Strathclyde, Glasgow, UK.
17. S. Patai, 1969, *The chemistry of carboxylic acids and esters*, Wiley, New York, USA.
18. Alison Nordon, 2000, *Personal communications (further tests on the reaction conditions for the esterification of itaconic acid)*, Department of Pure and Applied Chemistry, University of Strathclyde, Glasgow, UK.
19. Aldrich, 1999, *Catalogue handbook of fine chemicals*, UK.
20. N. McSporran, 2000, *Investigation of the kinetics of the partial esterification of itaconic acid*, 4th year project, Department of Pure and Applied Chemistry, University of Strathclyde, Glasgow, UK.
21. P. MacLaurin, N. Crabb, I. Wells, P.J. Worsfold and D. Coombs, 1996, *Quantitative in-situ monitoring of an elevated temperature reaction using a water-cooled mid-infrared fibre-optic probe*, Analytical Chemistry, Volume 68, No. 7, 1116-1123.
22. C. Wong, 2001, *Development of sampling procedures for process analysis and control*, 4th year project, Department of Pure and Applied Chemistry, University of Strathclyde, Glasgow, UK.

CHAPTER 3

SAMPLING STUDIES IN BATCH REACTORS

1. Literature Review and Background Theory on Sampling

This section presents the essential concepts of sampling that are relevant in the design of a sampling system to be used in stirred batch reactors. Also, a literature review of other work related with sampling from stirred vessels is presented. Some of the basic features of some of the commercial devices available for sampling in reactors are also covered in this chapter. The information extracted from these reviews was used in the design work presented here. In addition to this, the ideas of modelling of sampling systems are introduced and used later for the development work with the sampling designs. Finally, some theory on NMR is overviewed towards the implementation of a low-field NMR spectrometer for on-line analysis of batch processes.

1.1. Introduction: general concepts of sampling

There are many measurement situations in which a sample conditioning system is required to deliver the sample to the process analyser. In these cases, it is common strategy to use a "fast loop" to transport rapidly a representative sample from the process stream to the sample conditioning system with the use of a pumping device. The conditioning system then conditions this sample for the temperature, flow, pressure, etc., that can be tolerated by the analyser. The term "slow loop" is commonly used at the delivery stage because of the frequently lower flow rate of the resulting secondary sample stream that takes the sample to the analyser[1].

There are other sampling alternative to the use of fast loops that can be taken, as will be described in the chapter about HPLC samplers later Chapter 4. However, if the implementation of NMR for on-line analysis is desired, the sampling loop is more compatible with the requirements of a continuous flow through the NMR cell[2]. Therefore, the purpose of a bypass or fast loop would be to provide a continuous sample stream at a convenient point where it would be analysed or sampled and collected with a minimum dead volume. The point where the sample is collected in the reactor vessel is called the sampling point. The device that collects the sample at the sampling point is called the sampling probe[3].

Probe shape, orientation and dimensions affect very much the quality of the sample and therefore must be designed carefully[2]. This is due to the fact that, with heterogeneous processes, there are two main factors that affect the particle collection[4]:

- Particle inertia: This is observed when the trajectory of the heavy phase deviates from the light fluid streamlines in a heterogeneous mixture. The magnitude of this effect depends upon factors like the size of particles in solution, their density, the viscosity of the solvent and the local velocity[5,6]. It is represented by the dimensionless group called the Stokes number which represents the dependence of the particle inertia over these and other variables of interest. The Stokes number (k) for solid particles immersed in a fluid is given by the following expression[6]:

$$k = \frac{\rho_p d_p^2 U_0}{18 \mu_L (\phi/2)} \qquad \text{Eq. 3.1}$$

where:

d_p = *Particle size diameter (m)*
ρ_p = *Particle density (kg m^{-3})*
U_0 = *Local velocity (m s^{-1})*
ϕ = *Sample tube inside diameter (m)*
μ_L = *Liquid viscosity (kg m^{-1} s^{-1})*

Similarly, when using two liquid phases the expression for k can also be used to quantify the inertia[2] but with parameters showing the average size of the droplets of the heavy phase instead of d_p. However, this average size is sometimes difficult to predict and is highly dependent on stirring speed, and the viscosity of the fluids, and may even change with time[7]. A high value for k obtained with Eq. 3a means that the particles have very high inertia and do not follow the fluid streamlines. These particles tend to travel in straight lines resulting in serious sampling errors. These errors arise when the particle and fluid velocity are not collinear.

- Particle bouncing effect: This occurs when a particle moving in the fluid strikes a surface and loses some of its inertia. If this happens near a sample tube opening, then the reduction of particle inertia can be enough to allow particles to be extracted where they otherwise would have not been.

Therefore, the flow streamlines in stirred tank reactors must be considered to deal with the problem of particle inertia[4-6,8]. Also, the dimensional and shape

features of the probe must be carefully designed in order to minimise the particle bouncing effect at the desired sampling point[2].

In a fast sampling system, the loop length must be as short as possible and the loop velocity as fast as practicable in order to reduce any associated lag time and improve timeliness[5]. Some authors consider negligible the evolution of the reactive mixture inside the sampling system when the dead time, i.e. the time to run the distance from the sample point to the analyser, is less[9] than 30 s.

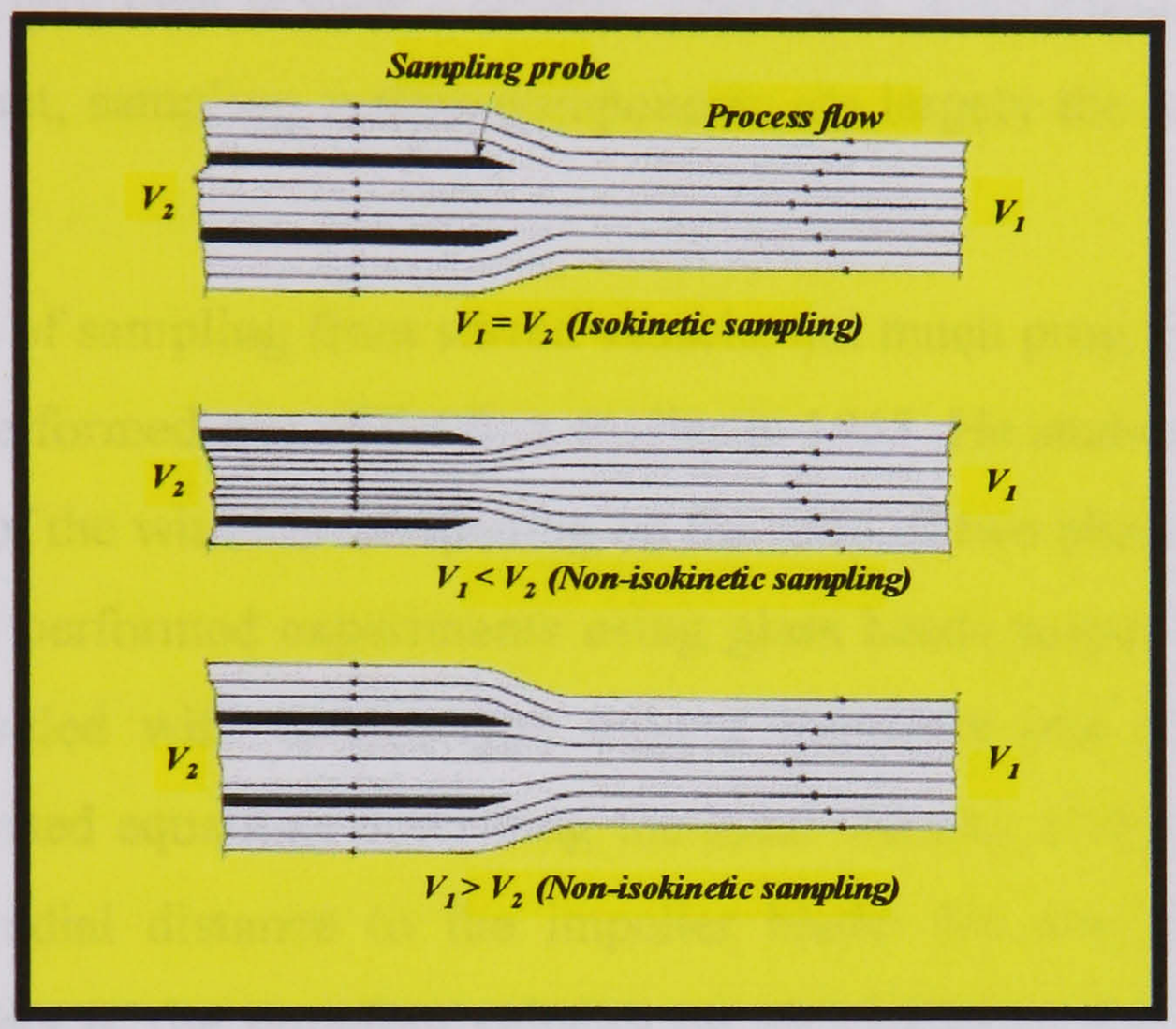

Figure 3.1. Types of sampling depending on the sampling velocity

Besides, sampling velocity is found to affect the performance of the sampling system[6,8,10]. This effect is more important in heterogeneous mixtures of solids or liquids in gases than in mixtures of immiscible liquids. However, several studies have shown how the wrong choice of sampling velocity leads to the collection of samples that are non-representative of the process involving suspensions of solids in liquids[4,6,11,12]. Isokinetic sampling is achieved when the sampling velocity equals the local system velocity at the point of sampling. This type of sampling must be used in order to ensure representative sampling from heterogeneous processes[5,13,14]. If the sampling velocity is higher than the isokinetic value, superisokinetic sampling is achieved and an excessive amount of lighter particles enters the probe. However, under subisokinetic sampling conditions, portions of the light phase stream are deflected, the lighter particles follow the deflected stream and are not collected, while the heavier particles continue into the probe due to their inertia[13]. In both super and

subisokinetic conditions, a non-representative sample of the process is obtained[5]. These three types of sampling are ilustrated in *Figure 3.1*.

1.2. Previous studies on sampling from stirred vessels

Unfortunately, developments in analyser technology clearly have outpaced those in sampling. There are two main reasons for this. First, there are more analyser than sample system manufacturers. Second, analysers always have been more important components of analyser projects than sample systems. The analyser is usually the largest cost item in such a project. Therefore, more attention is given to its performance. In fact, sampling system components are largely the same as they were 20 years ago[15].

In the area of sampling from stirred vessels, not much progress has been made since Rushton[11] performed one of the first studies in 1965. He studied the effect of the position and size of the withdrawal opening on the ratio of two phased being mixed in a stirred tank. He performed experiments using glass beads suspended in water in a baffled tank provided with turbine-type mixing impellers (the so called Rushton turbine). He proposed equations describing the local velocity at the stirrer plane as a function of the radial distance to the impeller blade. He also defined equations describing the effect of the sampling velocity on the quality of the sample collected. More attention will be paid to these findings later in this thesis (section *1.3.3*).

At the end of the seventies, Sharma *et al.*[14] considered Rushton's work and proposed the stirrer plane as the best place to withdraw samples in stirred vessels. They analysed the data obtained when sampling from a point at the stirrer plane and at different sampling velocities. They also defined a model that relates the quality of the sample with the sampling velocity at those sampling conditions.

At the start of the eighties, Baldi *et al.* defined some examples of concentration profiles in stirred vessels with solids in suspension[16]. They proved that a representative sample can only be obtained from the region that goes from the stirrer plane to the point that determines 60% of the total volume in the reactor. Above this region the local concentration is lower than the bulk concentration. Below it, the local concentration is higher than the bulk value. These concentration profiles were found to be dependent upon the size and density of the particles in suspension. They also

depended upon the stirring speed. However, the profiles were found to be independent of the particle concentration provide that the stirring speed was high enough to obtain complete suspension of the particles.

In 1984, Nasr-El-Din *et al.* successfully developed a mathematical model to study the errors arising in sampling through probes projecting into the flow[12]. However, the model was developed and tested in a straight pipe where the flow-streamlines are well defined. This is not the case with the complicated patterns that are present in stirred reactors.

In 1986 Buurman *et al.*[17] defined the scaling-up rules for stirred vessels with respect to solids in suspension. They found similar profiles for the suspended solids to those of Baldi *et al.*, with higher homogeneity for large scale vessels. In their experiments the samples were drawn by gravity, i.e. no pumping system was used. At the low withdrawal velocities that they used, the concentration of solids in the samples were found not to be sensitive to the sampling velocity. This caused great controversy at the time and such a statement was criticized by Nasr-El-Din[8] who claimed that in Buurman's work an inadequate choice of sampling points led the author to obtain his results. Buurman replied[10] that in the conditions he used, the orientation of the probe and sampling velocity did not have a big influence, but was aware of the fact that in other conditions their effect on sampling might be important.

At the start of the nineties, Nasr-El-Din *et al.*[18] proved the importance of sampling in the direction of the flow. They showed how a side port perpendicular to the direction of the flow in a pipe line led to erroneous sampling. Moreover, the quality of the sample depended on many factors such as the particle size, particle density, fluid viscosity, solid concentration and main pipe velocity. However, they also proved that it is possible to define a model that is able to predict the sample efficiency (i.e. the quality of the sample) depending on the conditions used in the process. Again, this was only applicable to a straight pipe line where the flow patterns are simple and well defined. However, useful ideas can be extracted from this work for our studies in stirred vessels. These findings are included in the design part of this chapter.

In 1993, MacTaggart *et al.*[4] published the most complete work on sampling from stirred vessels. They studied the effect of location and sample tube geometry on the sample obtained from a suspension of sand in water. They also studied the effect of sampling velocity, stirring speed and size and concentration of solids on the reactor. They used a 4-baffled reactor with a Rushton-type impeller. The authors proved how sampling velocity and sample tube diameter significantly affect the sample solids concentration. The sampled solids concentration was also found to be a strong function of the particle size and bulk solids concentration in the tank. Finally, it was found that the shape of the sample tube also influenced the sample collection, although to a lesser extent. Hence, they concluded that representative sampling in a slurry mixing tank, stirred by a radial flow impeller, can be obtained at the impeller plane with a sample tube tapered to 18° or less, operating at isokinetic velocity, when the solids concentration does not display a strong dependence in the vertical direction.

A few years later, the same authors used a conductivity probe to measure the local concentration in different points of a mixing tank[6]. They also compared these results with those obtained via the sample withdrawal procedure reported in their previous work. The operation of the conductivity probe relied on the variation of the slurry resistance as the concentration of non-conducting solids changes. With this study they proved that the flow at the stirrer plane is three dimensional and the local concentration at this point is different from that obtained by withdrawing samples at this point. MacTaggart *et al.* showed how the samples withdrawn at the stirrer plane are representative of the bulk concentration in the reactor[4] but not of the local concentration at the sampling point[6].

Other less detailed studies highlight the importance of sampling velocity and the design of the sampler in particle collection when defining concentration profiles for solids in fluidised beds[19,21], when measuring droplet size in two-phase flows[21], or for sampling in separation devices such as cascade impactors or cyclones[22].

Searching through journals and information that different companies have on the Internet, some designs of samplers and sampling systems for reactor vessels were found. However, only a few of them take into consideration the ideas and findings obtained by the researchers mentioned above. One of the few examples that verify

this is the new sampling device that Freitas *et al.* developed for measuring solids hold-up in fluidised three-phase reactors[23]. The sampler consisted of a cylinder with two valves, one at each end. The cylinder was connected to a long rod that permitted sampling at different depths in the reactor. For sampling, the cylinder was introduced into the reactor in the direction of the flow and with the valves opened. The valves were closed simultaneously for sample collection. This study highlights the importance of sampling in the direction of the flow and the erroneous measurements obtained with sidewall sampling.

Other designs of samplers for reactors like the Neotecha PV system[24-29] (see *Figure 3.2*) are reported to allow the customer to place the suction hose in the exact spot where it is wanted to draw the sample from the reactor. However, features regarding the orientation of the sampling port or the sampling velocity, which affect the representativeness of the sample, are not specified. This happens also in other sampling devices like the Technova system[30], and the ASI Applied Systems design[31], where a sample is pneumatically retrieved, analysed and collected. The non-used sample is then returned to the vessel via a dip pipe. Other mechanical samplers like the Giba-Geigy system[32], which uses a retractable plunger that is inserted into the process vessel, also pay little attention to the orientation of the probe and the sampling velocity.

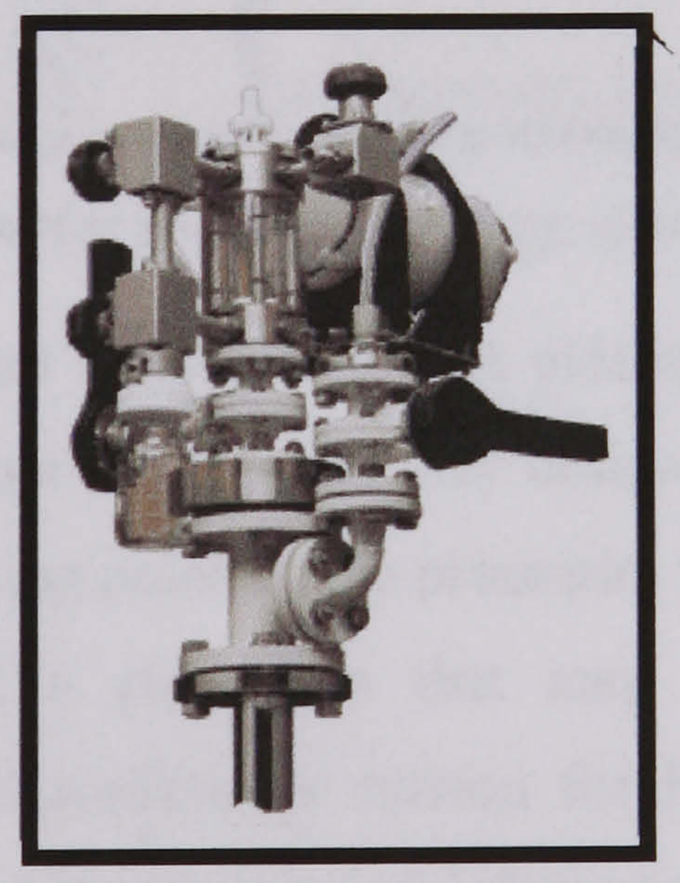

Figure 3.2. Detail of the Neotecha PV reactor sampling system[26]

Prosys Sampling Systems Ltd. have three different designs for the sampling of liquids from reactors[33]: an overflow top reactor sampler, a recirculation reactor sampler and the bottom reactor sampler. The overflow reactor sampler extracts a

liquid sample from the top of the reactor via a dip pipe that is purged using nitrogen. Vacuum is applied to the system and the sample is drawn through the standpipe, which overflows and fills the sample chamber. The bottom reactor sampler operates via a piston that retracts and the sample fills the sample chamber and sample bottle by gravity. The recirculation top reactor sampler pumps the sample through a recirculation loop for a short period using a double diaphragm pump. This is reported to guarantee a representative sample and allows accurate pH readings to be taken. Again, none of these designs refer to the orientation of the probe or the sampling velocity.

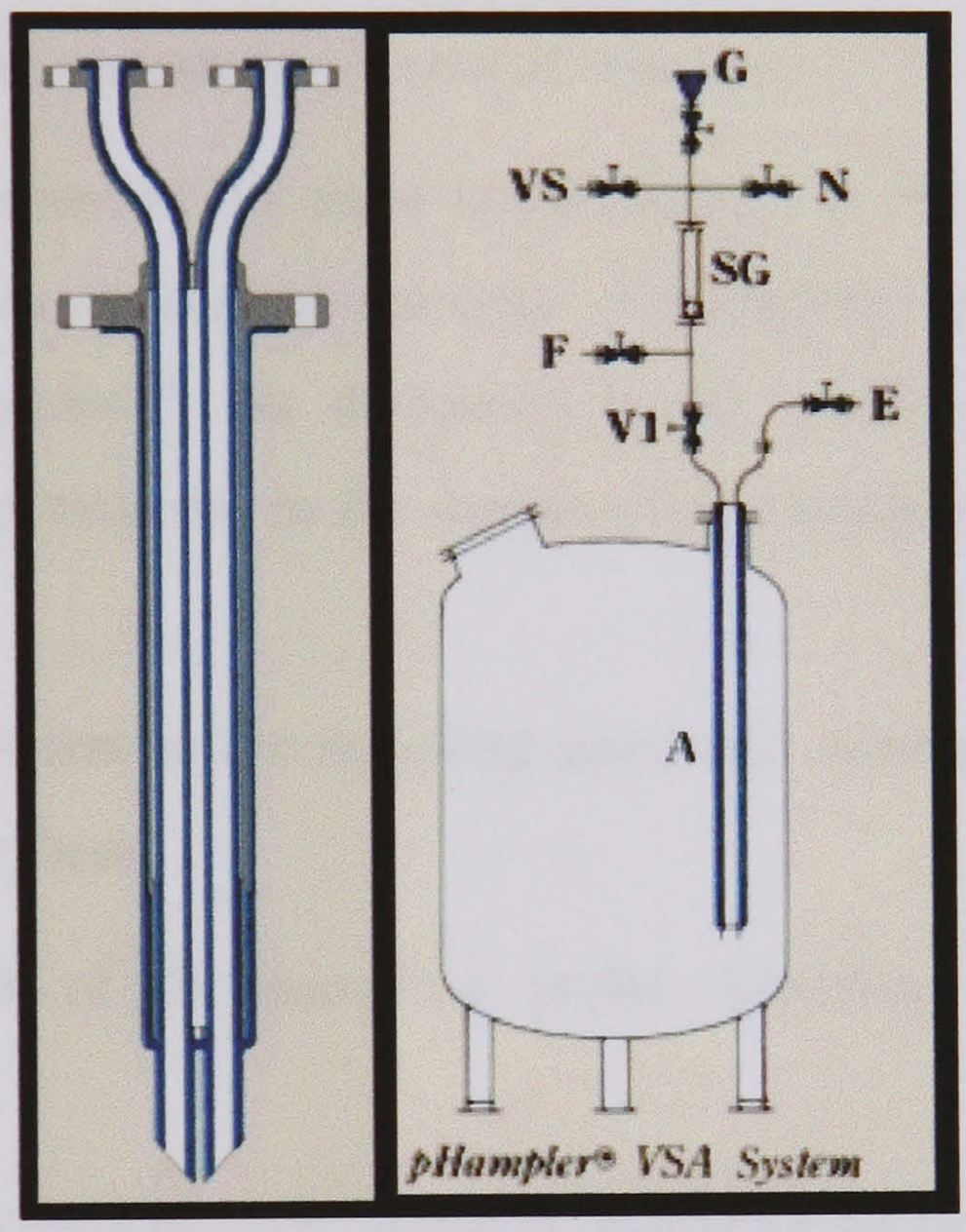

Figure 3.3. Detail of the pHampler reactor sampling system[34]

To the best of the author's knowledge, the pHampler reactor sampler by the Ethylene Corporation[34] (see *Figure 3.3*) is the only design in the market that refers to a specific location of the sampling point. In the pHampler the liquid is pulled from the reactor and pumped through a pipe loop that may include various analytical equipment. There is also a discontinuous version for liquid addition and manual sampling of reactors. In both of the designs it is advised to locate the sampling point just above the agitator blade in order to achieve representative sampling. This is due to the fact that the return point is located exactly beside the sampling point and therefore good mixing is needed to avoid the collection of part of the returned sample. However, the design does not pay any attention to the position and orientation of

the probe with respect to the flow-streamlines inside the vessel. The sampling velocity to be used during the sampling is not considered either.

In conclusion, not much work has been undertaken in the area of sampling from stirred vessels. Moreover, the few ideas proposed and achievements obtained in the field have not been considered significantly at the time of designing sampling systems for chemical reactors. The goal of this project was the design of a fast loop sampling system to implement NMR for on-line analysis which would consider the findings obtained from previous research. Further studies within the project were performed in order to test and optimise the design of the sampling system.

1.3. Design of a sampling system for chemical reactors

This section summarises the main considerations found in the literature and that have been taken into account at the time of designing an optimised sampling system for chemical reactors[2]. As discussed in the previous section, the most important factors to be considered in the design of any sampling device for flowing systems are:

- The flow patterns present at the sampling point and orientation of the sampling probe with respect to them.
- Engineering features of the sampling probe regarding its size, shape and dimensions.
- Sampling velocity to be used. This factor is related to the design of the pump that is needed for the sampling loop.

Other important considerations, regarding the safety aspects related with the design as well as the materials needed to build the sampling prototype, are also considered in this section.

1.3.1. Flow patterns and sampling point

A review of previous studies concluded that the flow streamlines must be carefully considered for the design of sampling systems in stirred tank reactors[2]. Also, the sample probe must be orientated parallel to them to overcome the problem of particle inertia[4,6,8]. There have been many studies[35-41] trying to define the streamlines in stirred reactors. They have used experimental techniques such as LDA (Laser

Doppler Anemometry) or mathematical simulations like CFD (Computational Fluid Dynamics) predictions. Both methods have been shown to agree very well and describe similar flowpatterns[35,37,40].

The shape of the streamlines and effectiveness of mixing in a vessel depends upon the dimensions of the vessel, the type, shape and dimensions of the stirrer and the presence of baffles in the reactor[42-44]. However, for any configuration, one of the few regions where the flow field is best defined is at the stirrer plane[11]. For efficient stirrers (e.g. Rushton type, the most efficient and studied stirrer)[39,43], well defined radial streamlines are found at the stirrer plane (see *Figure 3.4*) where a parallel orientation of the sampling probe with respect to the flow lines is more feasible than at any other point in the vessel. Several authors have tried to define the concentration profile of solids suspended in stirred reactors[16-17]. They found that a representative sample can only be obtained from the region that goes from the stirrer plane to 60% of full volume of the tank[16]. Outside of this region, the concentration of particles is different compared with the bulk concentration, due to sedimentation factors and particle bouncing at the bottom. In fact, some withdrawal studies in stirrer vessels have shown that the best place to locate a sampling probe in order to obtain a representative sample of the bulk phase is the stirrer plane[4]. The sample probe should be orientated parallel to the flow lines, which are normally radial in the proximities of the stirrer.

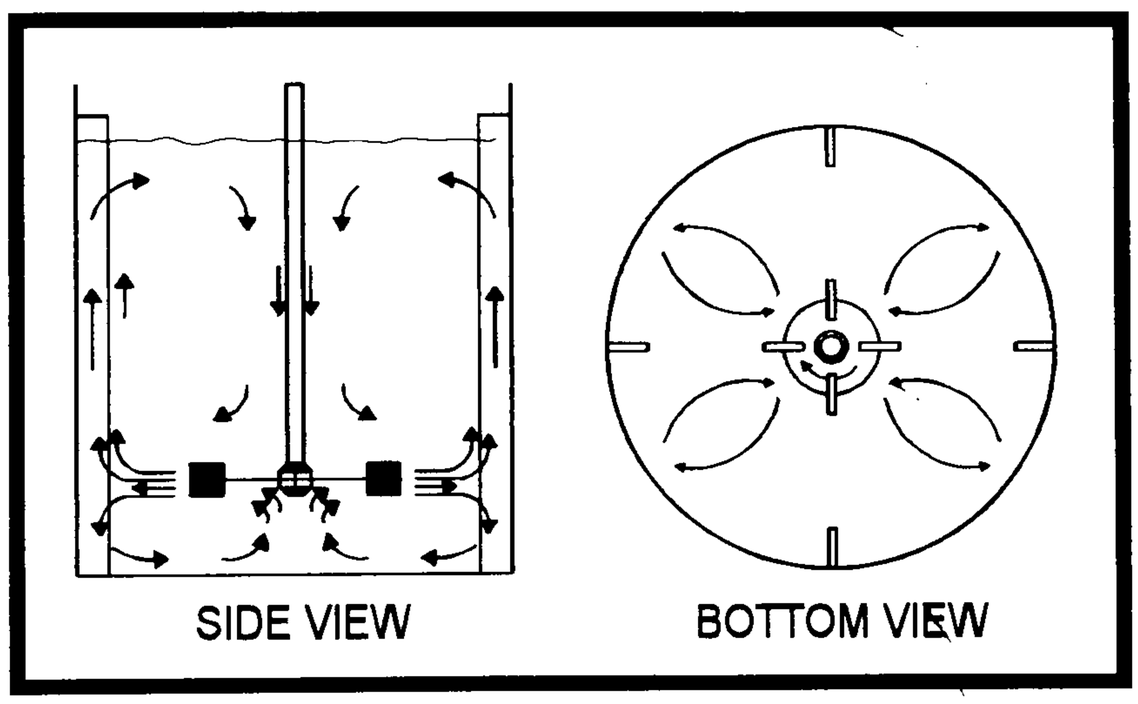

Figure 3.4. Flow streamlines in a stirred reactor with a Rushton type stirrer and four baffles[11]

1.3.2. Features of the sampling probe

The dimensional and shape features of the probe must be carefully designed in order to minimise the particle bouncing effect at the desired sampling point[2], although the final shape of the probe is usually a matter of intuitive design[45]. Different types of probe-ends have been tested in some of the published work in the field as illustrated in *Figure 3.5*. It has been showed that the probe must be tapered to minimise particle bouncing, although the type of edge has proven not to affect excessively the quality of the sample when sampling at the stirrer plane[6].

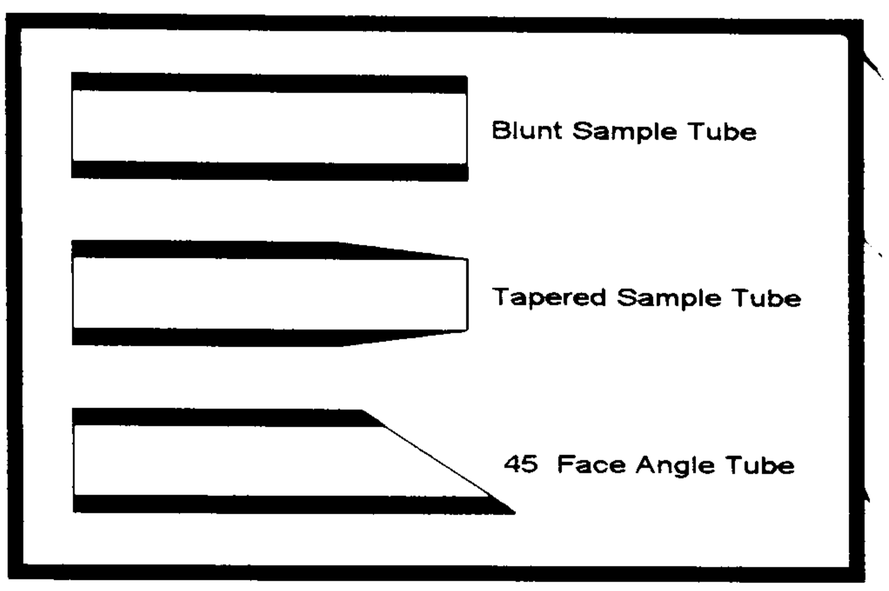

Figure 3.5. Schematic of the three main types of sample tubes [6]

The sample tube diameter can have a large impact on sampling when sampling is normal to the flow direction. The effect gets less important when sampling is almost parallel to the flow, as when sampling from a point within the impeller plane[4]. When sampling normal to the flow, it is desirable to sample with as large a sample tube as possible[6]. This is obvious since the larger the tube diameter the easier the flow lines are modified in order to get into the sample tube. Again, the significance is much less at the stirrer plane where the particle inertia factor is not so important[4]. Considering the particle bouncing effect, the diameter of the sampling tube must also be as large as possible since the larger the diameter of the tube the lower percentage of sampled particles are affected by particle bouncing and therefore, the sample is more representative[22]. Also, risk of blockage occurring decreases with larger diameters. In the literature, it is recommended that the inlet orifice should be at least ten times bigger than the maximum size of particle or droplet size and never less[45] than 6 mm, although the use of smaller sampling probes have been reported with solid suspensions[19,46-47].

Generally, a proper sampling probe design should avoid any undesired disturbances of the flow. However, this is only of importance when sampling in pipelines and not in stirred reactors[2]. This is due to the fact that in stirred vessels the disturbance of flow is desirable in order to improve mixing. Therefore, the design of probes for sampling in reactors does not need to be very careful in terms of flow disturbances, as long as the flow patterns do not change dramatically.

The probe should also be of sufficient strength to withstand the bending moments imposed by the maximum velocity conditions [45]. The maximum permissible length of any probe from its support, required to avoid the stresses created by the stream velocity conditions, can be determined from the following expression[9]:

$$L_{\max} = K_x \left[\frac{\varepsilon d_0^2 \, (d_0^2 + d^2)}{U_{\max}^2 \rho} \right]^{0.25} \qquad \text{Eq. 3.2}$$

where ε and ρ are the modulus of elasticity and density of the probe material respectively, d_0 and d are the outside and inside diameter of the probe tube, U_{max} is the maximum possible velocity of the process fluid at the sampling point and K_x is a dimensionless constant ($\approx$3.4) . Finally, some authors advise the use of tubes with a bend radius equal to or greater than five times the diameter of the sampling line[48]. This should be borne in mind if the sampling probe is to be bent to reach the desired sampling point.

1.3.3. Sampling velocity

Once the features, position, and orientation of the probe are chosen, sampling velocity has been found to affect the performance of the sampling system[6,8,10]. This effect is more important in heterogeneous mixtures of solids or liquids in gases than in mixtures of liquids in different phases[5]. However, several studies have shown how the wrong choice of sampling velocity leads to the collection of samples that are non-representative of the process in suspensions of solids in liquids[4,6,11,12]. Isokinetic sampling is achieved when the sampling velocity equals the local system velocity at the point of sampling. Therefore, this type of sampling is preferable in order to get representative samples from heterogeneous processes[5,13,14]. If super or subisokinetic

conditions are used, a non-representative sample of the process is likely to be obtained.

a) Design of the pump

There are two important aspects to be considered in the design of a pumping system for any sampling system. First, the type of pump to be used should be the initial consideration. Once this is selected, the requirements needed from the device should be considered in terms of head and flow-rate[2].

When selecting the type of pump for any service, it is necessary to specify carefully all the features of the system such as the liquid to be handled, total dynamic head, suction and discharge heads and, in most cases, the temperature, viscosity, vapour pressure and specific gravity of the fluid to be pumped. There exist graphs which helps in pump selection depending on the conditions and range of operation. At a pilot scale, i.e. when working with low head and capacity values, centrifugal pumps are the most suitable type[49]. The primary advantages of a centrifugal pump are simplicity, low initial cost, small space, low maintenance expenses, quiet operation and uniform (non-pulsating) flow. The latter is very important when pumping in a pipe system for continuous sampling purposes, especially when a constant sampling velocity is to be maintained. However, in some cases when there are large solids in suspension, a different type of pump must be used.

Regarding the requirement for the pumping system, it is important to realise that the testing of sampling systems is linked to the analysis of the effect of sampling velocity on the representativeness of the sample. Therefore, the pump to be used in the sampling loop must be capable of reaching at least isokinetic conditions at the sampling probe. Hence, it is clear that the specifications of the pump needed for our loop depended upon the local velocity at the sampling point which is mainly a function of the stirring speed[2]. In the design of the pump, the range of stirring speeds most commonly used in the system were considered. Also, the equation described by Rushton to describe the local velocity at the stirrer plane was used in our design, bearing in mind that this mathematical expression is only applicable to a particular type of stirrer and vessel configuration[11]. Nevertheless, the equation provides a good estimation of the conditions at the sampling point that can be included in the standard

equations for pump design[49,50,51] and gives an idea of the pumping requirement for the current research. The Rushton equation[11] relates the local velocity with the impeller rotational speed, the impeller diameter and the radial distance from the centre of the impeller[1], and can be represented as:

$$U_0 = \frac{B_1 N D^2}{r} \qquad \text{Eq 3.3.}$$

U_0 = *Sampling velocity (ft/s)*
B_1 = *Constant dependent upon the number of impeller blades and the ratio of the impeller to tank diameter (1/rev)*
N = *Impeller rotational speed (rev/s)*
D = *Impeller diameter (ft)*
r = *Radial distance measured from the centre of the impeller (ft)*

This expression is applicable only in the plane of a radial flow impeller between the impeller blade tip (r/R=D/2R) and near the tank wall (r/R≈0.95) where D is the diameter of the impeller and R is the radius of the vessel. In our case, with given values for B_1, D and N, r can be varied between r/R≈0.95 and r/R=D/2R. Therefore, in the design, the isokinetic sampling velocity was in the range between the local velocity at the edge of the impeller blade and the local velocity at the proximity of the wall[2]. In addition, sometimes it may be useful to work at sampling velocities greater than the isokinetic conditions in order to decrease the dead time and increase the effectiveness of the fast sampling loop. This is feasible only if the sampling error is not very high under these conditions, which depends upon the sampling system to be used.

The isokinetic conditions normally give the minimum limit of velocity that can be used when sampling heterogeneous mixtures. This is due to the fact that the sampling error is normally higher at subisokinetic conditions[4]. When sampling from homogeneous mixtures the sampling velocity does not affect the representativeness and the velocity would usually be superisokinetic in order to reduce the dead time in the sampling system[2].

Detailed information on the calculations and specifications involved in the design of the pump are outlined in Appendix 1. They are based on the considerations stated above.

1.3.4. Safety considerations in the design

Considering the high velocities at which the sample flows through the loop at isokinetic conditions, it is necessary to take special precautions regarding the safety aspects in the case of leaks. The extent of any safety action to be taken always depends upon the risk associated with the chemicals used in the process. A summary of the main features needed for risk assessment of the principal chemicals used in this project are described in the following table[52].

Table 3.1. Analysis of the risk for the chemicals used in the esterification of crotonic acid

	P_{vapor} *(mBar at 20°C)*	*Flash Point (°C)*	*NFPA code of toxicity (1-4)*
Toluene	29	4	2
2-Butanol	17.3	14	1
Crotonic acid	0.25	88	3

As can be observed from the table, these compounds are not extremely volatile and therefore the risk of flammability is moderate. In fact, this was the reason why butanol and not methanol was chosen for the esterification reactions used in this project. However, the flash points are quite low for both butanol and toluene[53]. This requires precautions in the system, especially regarding electrical connections that can produce sparks. The high value of NFPA (National Fire Protection Association, USA) for crotonic acid comes from the fact that it is a highly corrosive substance[52]. The main risk associated with these chemicals occurs because some of the experiments are carried out at temperatures about 100°C. Under these conditions, the reactive mixture becomes extremely corrosive as well as volatile. Therefore, any potential risk of leakage must be identified, assessed, and carefully controlled or mitigated.

As outlined in the specifications of the pump, the maximum pressure that the pump provides in the sampling system (less than 0.3 atm.)[2] has to be lower than the pressure that the connections between fittings are able to withstand. This is the reason

why threaded connections are preferred to quick-fit fittings that might pop off if the pressure builds up. Nevertheless, any pressure building up in the system due to, for instance, blocking of flow-meters, control valves, etc., can be prevented by installing a pressure relief valve in a bypass line between the outlet of the pump and the reactor[5]. This is shown in the example of the sampling system sketched in *Figure 3.6.*

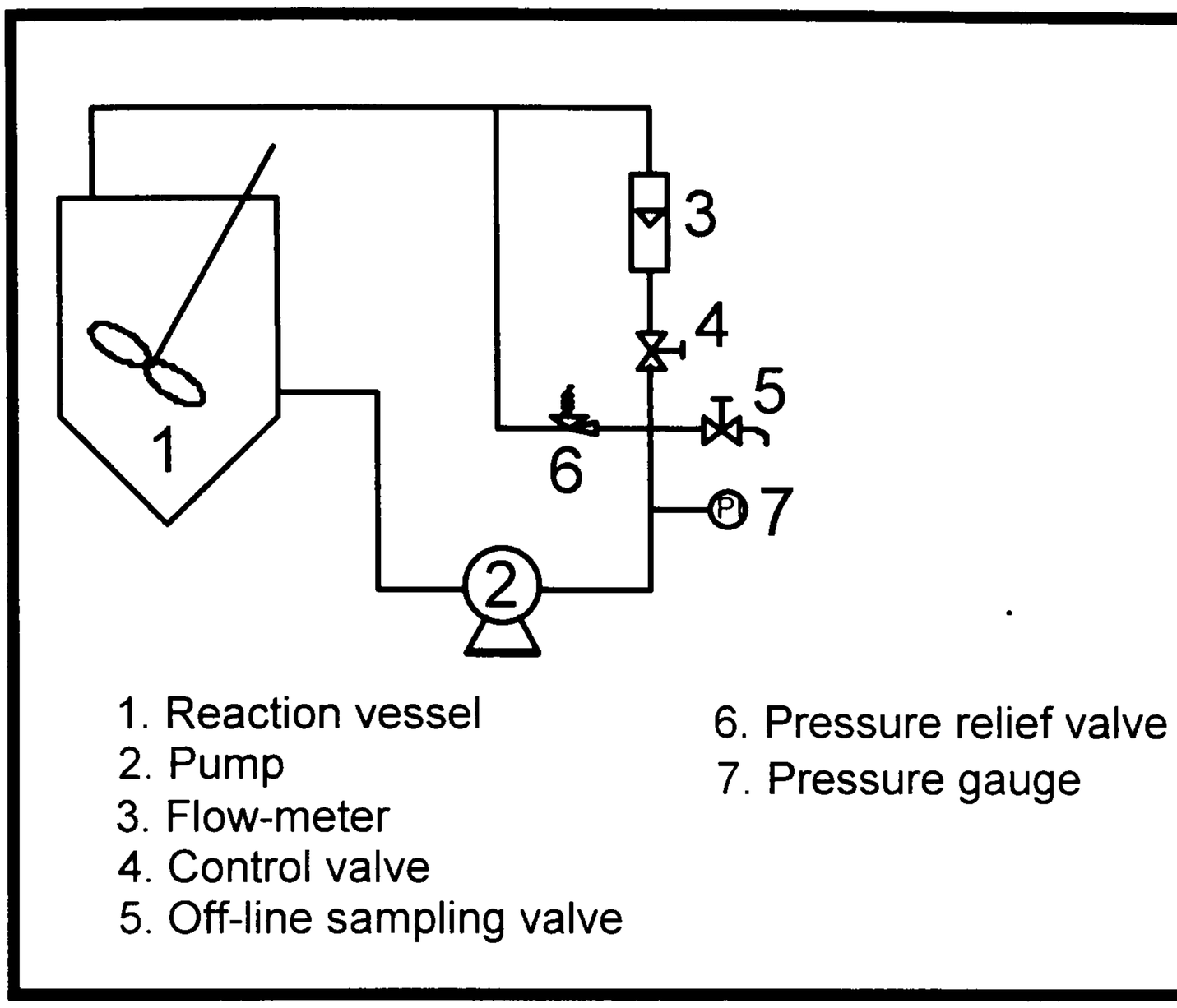

Figure 3.6. Sketch of sampling loop with pressure relief line

Other safety actions that help to mitigate the effect of leaks in the system are strategically located drains in the proximity of the system. In fact, the sampling loop could be cased in a second protective layer that would contain any spillage of chemicals and lead any leaking liquid to an adequate drain. This would reduce the damage until the operators detect the leak and stop the experiment. Another way to stop the process in the event of leaks would be the installation of leak detectors in the loop. Two different approaches can be considered for this purpose[54]. One is the installation of a case with two parallel conductive wires in all the lines and fittings in the loop. As the reactive mixture is conductive due to the acid in solution, any leak would short-circuit the two wires, trigger an alarm system and stop the pump in the loop. This alternative is not only very tedious to implement but it could also be open to many interferences producing false alarms. The second option for the installation of leak detectors is much simpler. It assumes that the loop is protected with a second

layer (as described above) leading any possible fluid leaking from the process to a specific point where a single leak detector would be located.

For the purpose of the research described in this thesis only the type of connections between fittings and the use of trays with absorbent pads to contain any possible spillages were considered. The other alternatives, which are more sophisticated and expensive to implement, can be taken into consideration for future needs. Finally, the protection of the analysers used in the experiments was also carefully assessed following the standard guidelines for best practice[55-57].

1.3.5. Other considerations

Taking into account all the features described already concerning the characteristics of reactors and the sampling probe, the structure or final shape of the sampling system could be designed. As can be seen in *Figure 3.7*, the reactor provided from HEL has a suitable hole for a probe slightly under the impeller plane. This goes very well with the already justified need of sampling at the stirrer plane in order to get representative samples from reactor vessels.

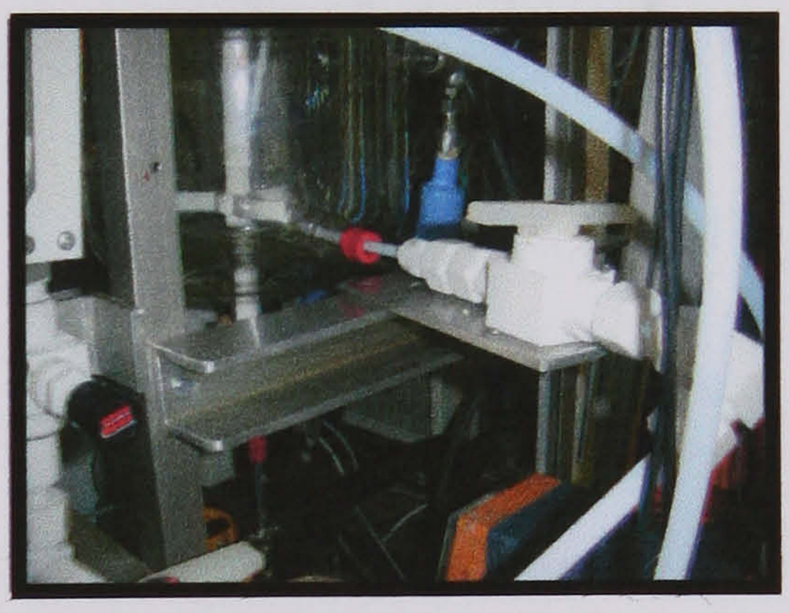

Figure 3.7. Detail of the reactor port used for the sample collection

When designing the returning point of the sampling loop back to the reactor, several circumstances had to be taken into account[2]:

1. - The returning point had to be quite a way from the sampling point in order to avoid immediate "resampling" of the mixture already extracted. Designs such as found in some references[24-34] did not take this factor into consideration and are only appropiate if the mixing speed is high enough to provide an almost instantaneous mixing of the sample returned back to the reactor.

2. - The jet of fluid back to the reactor had to modify the flow streamlines as little as possible. This is very important in the proximity of the sample probe. Therefore, it is of interest to place the returning point as far as possible from the sampling point.

Considering these points and the fact that spare ports for probes were placed on the top of the reactor[58], it was convenient to use one of these holes as the returning point. This port had to be the one furthest away from the sampling point, i.e. the one diagonally opposite. The orientation of the returning jet was towards the reactor wall (see *Figure 3.8*) since this makes the returning stream lose its kinetic energy[2]. This avoids the power of the jet modifying the flow features of the reactor. It also makes the stream fall down nearer the wall where the flow streamlines have the same vertical direction. The flow-patterns are then almost unchanged and the streamlines in the point of sampling keep their typical horizontal orientation.

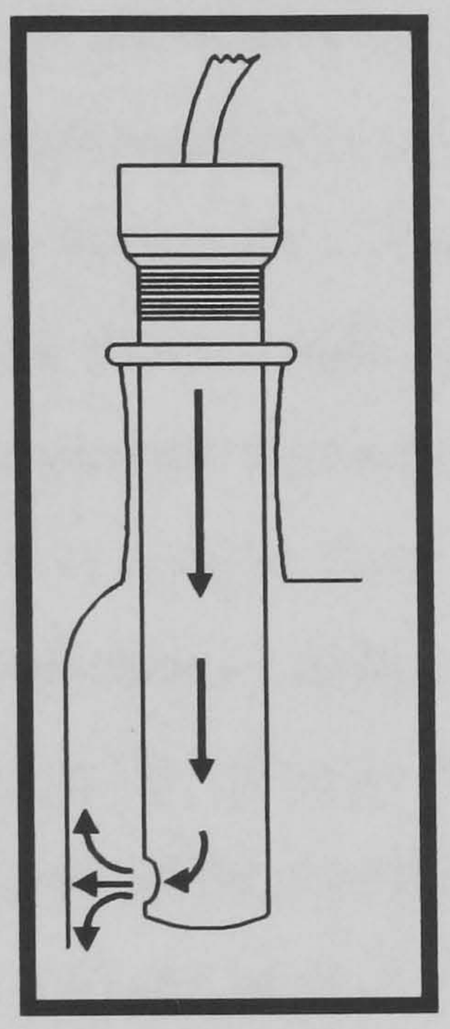

Figure 3.8. Detail of the returning point configuration

Insulation of the loop also had to be considered in order to minimise heat loses in the loop and return the unused sample back to the reactor at a similar temperature to the rest of the content of the reactor[2]. This was of particular importance as most of the processes carried out in the reactor system were isothermal, i.e. they operated at constant temperature[59]. Therefore, it was important to return the unused sample from the loop to the reactor at a similar temperature to that which it had when the sample was extracted. The theoretical design of a insulation system basically consists of working out the radius and heat conductivity features of the material to be used as an

insulator[2]. Another consideration at the time of designing the thickness of the insulator is the cost of the insulator. There exist graphs which show how the total costs varies with the insulation thickness in order to determine the most economically favourable thickness and then the optimum insulation thickness[60]. However, these kind of economical aspects were not considered in this design since the aim was to avoid changes in temperature and not to decrease costs via reducing heat energy losses. This criterion would, though, be of great importance when designing industrial installations.

The theoretical calculations related to the design of the insulation system are described in the Appendix 2. They were based on heat balances[60,61] and showed that the drop in temperature was minimal and could be neglected[2]. In addition to these theoretical considerations, the capacity of response of the heater/chiller system was another important factor to consider. It automatically controls the temperature in the reactor system. The performance of experimental tests is the best way to evaluate the importance of this effect and analyse how such a control device can cope with the decrease in temperature as the sample flows inside the loop. In other words, it was necessary to carry out experiments to see how the automated temperature controller in the reactor helped to avoid the effect of a mass flow coming into the reactor with a temperature slightly less than the temperature inside the vessels. The tests performed for this evaluation are described later on this chapter. The results obtained in the tests proved that any drop in the temperature of the sample when it was returned back to the system could be successfully compensated by the heater/chiller unit which controls the temperature of the jacket in the reactor. Therefore, a lack of insulation did not affect greatly the ability of the system to keep the reactor mixture at a desired constant temperature.

Finally, the sampling loop had to be constructed with materials that withstand the conditions of operation and the flow of corrosive chemicals inside them. 316 stainless steel is the most popular material used in the construction of sampling systems if non-corrosive materials are used[33]. Teflon and PTFE encased materials, together with special alloys such as hastalloy, are the choice when more reactive chemicals are employed.

Detailed drawings and information on the final design of the sampling system can be seen in Appendix 3.

1.4. Modelling of sampling systems

As shown earlier, even if a sampling system is optimally designed to get representative samples, factors such as sampling velocity can affect the performance of the system[4,5]. Therefore, a sampling system can be modelled and used to analyse how parameters such as the sampling velocity, density of the different phases in the mixture and temperature affect the representativeness of the samples collected with the sampling device[2]. Provided this modelling is feasible and the model is robust enough, no need for careful control of isokinetic conditions would be necessary, as any non-representative sample collected at non-isokinetic conditions could be related to a representative sample by using the model. This modelling of sampling systems has many potential useful applications. In fact, similar calibration procedures for non-isokinetic probes have been used for solid flux measurements in fluidised beds[19,20]. In process analysis, this is interesting because not all of the sampling systems that exist in industry have been optimally designed in terms of shape, dimensions and orientation of the probe for good sampling from heterogeneous processes. Some examples are the commercial systems for sampling from chemical reactors mentioned in the introduction of this chapter[24-34]. Also, replacing sampling devices in a chemical plant by others more optimally designed could be a highly costly process, requiring major modifications to the reactor vessels and some other existing infrastructure. If modelling of any of the already existing sampling systems is feasible, any non-representative sample that they provide from heterogeneous systems could be related to a more representative value by using the model. Therefore, the final analysis of data can be corrected.

Another interesting application of the modelling of sampling systems is the implementation of analysers for on-line monitoring. In some cases (as will be seen in the case of NMR) the analyser requires special conditions for the sample that differ from the isokinetic conditions needed to obtain representative samples[2]. The delivery of non-representative samples to this particular analyser would not be a problem if a robust model of the sampling system is applied for correction of the analytical data.

Apart from physical modelling, a chemical modelling of the loop might also be needed to account for the differences between the reactive evolution of the sample in the loop and that of the mixture that remains in the reactor. This chemical model can usually be obtained by comparing the kinetics of a particular process both using and not using the sampling system[2,9].

1.4.1. Physical modelling of the loop

The physical model of a sampling system relates the quality of the sample with the physical parameters that affect the sample collection. In reactor vessels, the quality of the sample is usually measured as the withdrawal-bulk concentration ratio, which is commonly known as sampling efficiency. There have been some studies trying to define robust physical models of sampling systems in stirred vessels[4,11,14,16] and in more simple systems such as straight pipelines[12,18].

Rushton[11] was the first in defining a relationship, which shows the effects of withdrawal velocity on the concentration in the extracted sample. He studied suspensions of sand and glass beads (specific gravity 2.41) ranging in size from 100 to 250 μm diameter and for concentrations between 1 and 20 vol%. In these conditions he found that:

- At subisokinetic conditions (i.e. $u_w/u_I<1$):

$$\frac{C_W}{C_T} = K\left(\frac{u_W}{u_I}\right)^{-0.14} \qquad \text{Eq 3.4.}$$

- At superisokinetic conditions (i.e. $u_w/u_I>1$):

$$\frac{C_W}{C_T} = K\left(\frac{u_W}{u_I}\right)^{-0.087} \qquad \text{Eq 3.5.}$$

where:

C_w = *Withdrawal sample concentration (g/ml)*
C_T = *Bulk concentration in the tank (g/ml)*
u_w = *Withdrawal sampling velocity (m/s)*
u_I = *Isokinetic sampling velocity (m/s)*

The parameter K in the equations was found to be dependent on the type of opening. Rushton found that K=1.25 for flush openings in the wall and K=1 with

openings one-fortieth of tank diameter in from the wall. He also found that K vary with different densities of solids or liquids. For example, he found that when alumina particles were used (specific gravity 1.6) the K values were 90% of those for sand and glass. Particle size also affected the equations. Smaller particles resulted in smaller values of the exponents whereas larger particles produced larger concentration ratios, and the exponents in the equations should be larger.

Almost 15 year later, Sharma *et al.*[14] performed a careful analysis of more data in a great variety of suspensions. They obtained more detailed expressions that considered the effect of changes in density and location of the sampling probe on the quality of the sample. They concluded that:

$$(\phi - 1) = C(\frac{\Delta\rho}{\rho_1})(\frac{Z}{D_e})^{0.5}[(\frac{u_e}{u_i})^{-1.} - 1] \qquad \text{Eq 3.6}$$

where:

ϕ = *Separation coefficient* C_W/C_T
ρ = *Liquid density* (g/cm^3)
ρ_l = *Density of the solid particles* (g/cm^3)
Z = *Insertion length (cm)*
D_e = *Diameter of the outlet (cm)*
u_e = *Velocity of suspension in the outlet (cm/s)*
u_i = *Velocity of suspension inside the vessel in the vicinity of the outlet at isokinetic withdrawal (cm/s)*

C is a constant dependent on the particle size. The equation was valid for $Z>T/36$ where T is the diameter of the tank. The relationships shown above were obtained in baffled tanks using turbine-type impellers. Baldi *et al.*[16] also studied these systems but they defined the profiles of suspended solids, i.e. a relationship between the withdrawal-bulk concentration ratio and the stirring speed. Their most important conclusion was that this ratio is $C_{os}/C_o = 1$ (where C_{os} is the concentration of the withdrawn sample and C_o is the bulk concentration in the vessel) when L = 0.25-0.55 (where L is the normalised distance from the vessel bottom). This relationship was only valid when the stirring speed was greater than the minimum stirrer velocity for complete suspension (N_e). Other relationships for the case of $N<N_e$ were also found but they are not relevant to this work as $N>N_e$ was always be used in our experiments.

Other work was performed in simpler systems such as slurry pipelines where the flow-patterns are better defined. For example, Nasr-El-Din *et al.*[12] proved the relationship $C/C_o = (r_o/R)^2(u_o/u)$ as valid for a probe projecting into the flow. In this relationship C/C_o is again the withdrawal-bulk concentration ratio, r_o determines the undisturbed upstream portion, R is the sample radius, u_o the isokinetic velocity and u is the sampling velocity.

A few years later, the same group of researchers proved that in the same system but with the sampling port in the wall, the following correlation was able to predict the sampling efficiency[18]:

$$\frac{C_W}{C_o} = \exp[-A(1-\alpha_o)^a K^b] \qquad \text{Eq 3.7}$$

$$K = k\frac{\rho_s - \rho_f}{\rho_s} \qquad \text{Eq 3.8}$$

where:

C_W = *Sample solids concentration (vol%)*
C_o = *Solids concentration in the main pipe (vol%)*
A = *Constant in the semi-empirical correlation*
α_o = *Solids volume fraction in the main pipe = C_o/100*
K = *Modified particle inertia parameter*
k = *Particle inertia parameter*
ρ_s = *Solids density (kg/m^3)*
ρ_f = *Fluid density (kg/m^3)*

(They obtained the best fit when A = 0.46, a = 1.0 and b = 0.5)

Finally, MacTaggart *et al.*[4], in the most recent work using baffled turbine stirred vessels, proved that Rushton and Sharma were right in their predictions. However, their equations were found applicable only for the particular conditions for which they were developed. MacTaggart *et al.* showed that there are many factors that affect the particle collection, and it is almost impossible to define a simple set of equations to define all of them. MacTaggart *et al.* only outlined general conclusions that can be extracted from their studies such as the preferable use of isokinetic sampling in order to obtain a sampling efficiency (C_W/C_o) close to unity (i.e. representative sampling).

1.4.2. Chemical modelling of the loop

So far, only physical modelling of the loop has been referred to, based on physical variables such as sampling velocity, density or particle size. However, the reactive evolution of the sample in the sampling loop system can be different to that of the mixture that remains in the reactor[2]. If this is the case, chemical modelling of the loop is needed to account for these differences. This chemical model can be experimentally obtained by comparing the kinetics of a particular process both using and not using the loop. *Table 3.2* summarises how the kinetics of the process affect the design equations for the three types of ideal reactors[62,63].

Table 3.2. Equations of design for ideal chemical reactors[62,63]

$\theta = N_{A0}\int_{x_{A0}}^{x_{Af}} \frac{dx_A}{Vr_A} \xrightarrow{V=cons\ tan\ t} \theta = C_{A0}\int_{x_{A0}}^{x_{Af}} \frac{dx_A}{r_A}$	*BATCH REACTOR*
$\tau = \frac{V}{q} = C_{A0}\int_{x_{A0}}^{x_{Af}} \frac{dx_A}{r_A}$	*PLUG FLOW REACTOR*
$\tau = \frac{V}{q} = C_{A0}\frac{x_A - x_{A0}}{r_A}$	*CSTR SYSTEM*

where:

θ	=	*Time of reaction in a batch process (s)*
τ	=	*Mean residence time in a continuous reactor (s)*
V	=	*Reactor volume (m^3)*
q	=	*Flow-rate of chemicals in a continuous system (m^3/s)*
N_{A0}	=	*Initial number of moles for reactant A*
C_{A0}	=	*Initial molar concentration for reactant A*
x_A	=	*Fractional conversion for reactant A*
x_{A0}	=	*Initial fractional conversion for reactant A*
r_A	=	*Kinetic equation as a function of reactant A*

In real reactive systems (i.e. with non-ideal mixing patterns) and systems formed by devices with different flowing properties, the chemical model is generally obtained by dividing the system into more simple ideal reactors[63]. Hence, a system like the batch reactor plus sampling loop could be considered as formed by the main reactor itself, considered as an ideal reactor, and the loop, which is equivalent to a

plug reactor whose longitude is given by the dimensions of the sampling loop. Finally, the equations in the model will depend upon whether the reactor is a batch system or a CSTR (Continuous Stirred Tank Reactor)[2].

a) Batch reactors

With batch reactors, the differences between the reactive evolution of the mixture that remains in the reactor and the sample that flows in the sampling loop system are likely to be negligible. This is due to the fact that, in theory, the chemistry in the vessel (described by the design equation of a batch reactor) is equal to that of the sample flowing through the loop (described by the design equation of a plug flow reactor)[62,63]. This is only true if the mixing inside the reactor and the plug flow properties in the loop are close to ideal[63]. In the case of CSTR, even in theory and considering ideal reactors, the evolution of the reactive mixture is different to that of the sample flowing through the loop. Therefore, chemical modelling is more crucial for CSTR systems than for batch systems[2].

b) CSTR reactors

As mentioned above, in a CSTR plus sampling loop systems the reactive evolution of the sample in the sampling loop system is always different to that of the mixture that remains in the reactor[62,63]. Therefore, if this difference in evolution is wanted to be minimised, the volume of the tubular sampling system should be as low as possible and the flow-rate as fast as practicable, provided that the superisokinetic conditions do not affect the sampling collection in the particular design of sampling device[2]. These conditions mean that the sample is collected with a minimun dead time and is more representative of the content in the reactor at the time of sampling. Some studies[9] have proposed a maximum dead time of 30 s for sampling systems in reactors in order to obtain highly representative samples.

The particular features of CSTRs force the engineer to take special considerations for the design of sampling systems. The ideal model for CSTR postulates that the feed mixture gets the final conditions as soon as it gets into the reactor. This assumes that ideal flow patterns of perfect mixing are present[63]. However, there are cases that cannot be handled by these assumptions since the flow patterns are not close to these extreme limits. This can be caused by such aspects of

real equipment at corners, baffles, and so on, that can lead to stagnant regions, or non-uniform flow paths that can lead to bypassing of fluid[62,63]. A sketch of the abnormalities in the flow inside the reactor due to bypassing is shown in *Figure 3.9*. This modifications of the flow patterns due to the bypass flow of certain elements of fluid may alter the required paralleling of the flow streamlines and the sample probe at the point of sampling[2]. However, these bypass flow pathways are usually forced to run near the wall at the impeller plane[63]. Keeping our sample probe carefully away from the wall should be enough to overcome the problem[2].

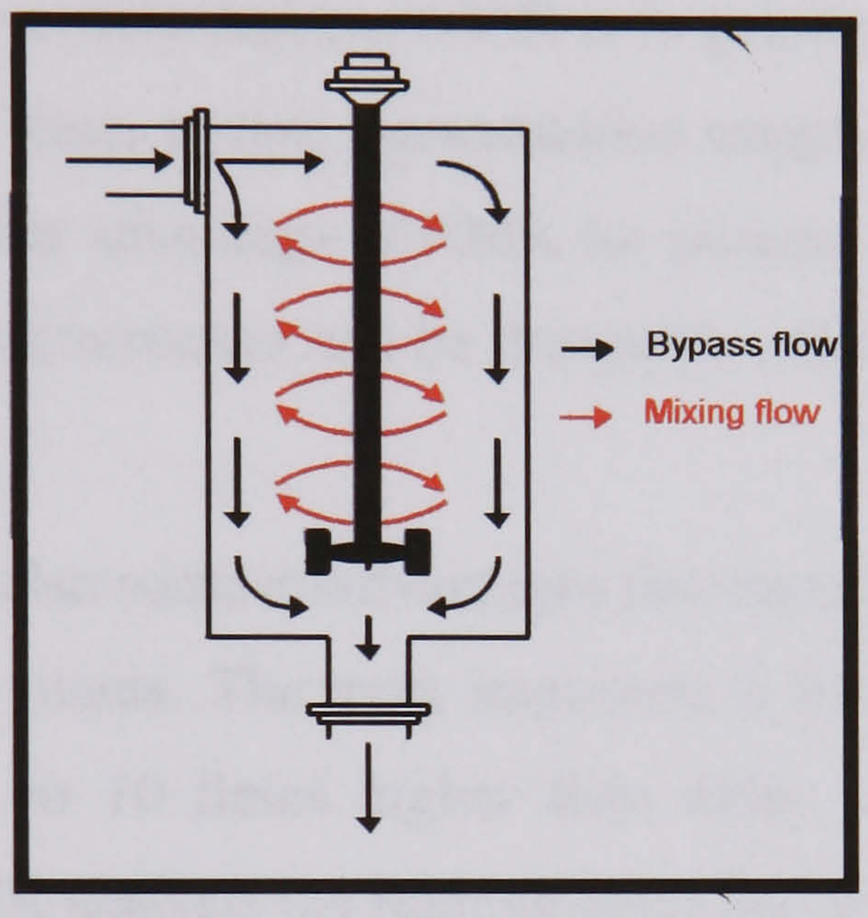

Figure 3.9. Non-ideal flow patterns due to bypassing in CSTR systems

1.5. Implementation of a NMR spectrometer for on-line analysis

In the NMR technique the magnetic moment (nuclear spin) present in e.g. the hydrogen nuclei are aligned in a magnetic field. Application of it promotes nuclei to an excited state. The excited nuclei generate a small and oscillating magnetic field which induces an alternating voltage in a detection coil[64]. The area of this signal is a direct measure of how many nuclei of any specific type are present in the sample.

NMR is well suited to a variety of process control and quality control applications. Its capabilities for chemical selectivity and its non-destructive character have attracted interest for process and quality control applications since the 1950's and 1960's[65]. The non-destructive character of NMR renders it specially attractive from the point of view of having the NMR sample available for other subsequent tests or returning it to the main production line[2,65].

The fact that NMR experiments are usually performed at or near room temperature (although much higher or lower temperatures can be used if desired) is an advantage with respect to GC methods for monitoring thermally sensitive components. Another good point of the NMR technique is that, unlike chromatographic methods, it does not use dangerous solvents as no dilution is needed[64]. However, the greatest advantage of NMR over gas chromatography is the much lower analysis time[66]. In fact, the time of analysis is within an acceptable time scale (seconds or minutes) depending on the sample.

Besides all of these considerations, NMR is in principle applicable to a wide range of sample forms and sizes, so that representative samples of most processes can be examined. Finally, another advantage of NMR for process control is that relatively trouble-free and rugged spectrometers can be designed, which do not require highly specialized personnel[65,67].

However, there are also some disadvantages that have limited the popularity of this technique in chemical plants. The most important is the high cost of the NMR instruments, sometimes 5 to 10 times higher than other techniques available for process analysis[65]. For NMR analysis the running costs are low, though[68]. Finally, the NMR technique is much less sensitive than others such as IR spectroscopy[69].

Although the use of NMR for control applications is scientifically still in its infancy in many respects, the literature in this area is already voluminous, although much of the most successful work is highly proprietary and therefore not published[65].

1.5.1. Features of a NMR system for on-line analysis

There are essentially two different types of modern NMR strategies for use in process control[65,67]:

- Time-domain strategies, which distinguish one component from another by means of differences in behaviour in the time domain and do not require high-resolution magnets, typically using low-field permanent magnets.
- Frequency-domain strategies that depend on distinguishing resonances according to chemical shifts and require high-resolution magnets, often based on high-field superconducting magnets.

Some authors divide this latter alternative into two types depending on whether the high resolution instrument is used in a laboratory in the plant for at-line tests or the spectrometer is specifically designed for on-line analysis[66].

High resolution instruments are more expensive and less rugged, although they are sometimes demanded for at-line applications. They also require more specialized personnel. These reasons have made low-resolution spectrometers have more potential than the high resolution models (either high-field or low-field) for on-line analysis[65,67]. In process applications a permanent magnet operating at less than 100 MHz is preferred over cryogenic magnets[70].

One obstacle to the potential growth of time-domain process NMR is the tendency for some of the instrument manufacturers to expect the applications to fit their instruments, rather than developing instruments to match the potential applications. The most specific aspects of process NMR instruments are related with the probe design and the sampling requirements[65,66]. In fact the sampling system is the most important modification that a NMR spectrometer has to undergo for use in on-line analysis. There are two main approaches to achieve this:

- Either the NMR probe is filled with the material to analyse and the flow is stopped for analysis[71-73].
- Or the sample flowing at a slow rate is analysed using flow NMR with cells provided with premagnetisation regions and ways of averaging the spectra obtained at different time intervals[65,67].

Flow NMR presents an advantage over stopped flow measurements as the NMR result represents the average signal of a large amount of sample from the flow across the probe during the time of the measurement. Therefore, flow NMR partially resolves the problem of sampling in heterogeneous materials and could avoid the necessity to construct large sample probes, which also require costly magnet modifications[67]. However, if the sample is heterogeneous, both the first and the second alternative could allow the different phases to separate out if the flow-rate is very low thus affecting the analysis. Neudert *et al.*[73] applied the stopped flow technique successfully for heterogeneous systems although they noticed a high

variability in the results. However, they did not give clear indications of how heterogeneous the system that they used was.

The work in flow NMR started in the early 1950s. In 1951, Suryan showed a linear increase in signal amplitude with an increase in flow rate as an aqueous solution passed through a simple NMR device[70]. McIvor[74] presented in 1969 one of the first designs of NMR flow cell and highlighted that the technique had advantages over the use of static samples. He observed that flow NMR enables higher radio frequency power to be used without fear of saturation. This leads to an increased accuracy in quantitative analysis. However, he noticed some disadvantages, the most important being the loss of resolution which made the observation of small couplings difficult to resolve at that time due to the lack of statistical techniques that are now available.

In flow-NMR analysis, a sample stream flows through the magnetic field. The magnetic nucleus of the sample "line up" with the magnetic field direction. Once aligned, they are pulsed with radio frequency waves to move them off their aligned axis[75-76]. The amount of the deflection and the time to return to alignment are determined by the sample's molecular structure. The resulting realignment of the molecules in the magnetic field sends a radio frequency signal back. This signal is transformed into a spectrum showing chemical species and their concentrations. Multiple pulses are averaged and the analysis is available within minutes or even seconds[76].

Early flow NMR work was time-consuming and tedious, in part because of the absence of high-speed data processing capabilities. The greater computing power of workstations and PCs today have made it possible to substantially reduce the time between data collection and data reporting[70]. This has been crucial in the implementation of NMR for on-line analysis. Also, chemometric techniques can be used to extract the desired information from the often convoluted spectra provided by low-field flow NMR spectrometers. These techniques use mathematical and statistical methods to enhance the productivity of chemical experimentation[66,69].

There are numerous instrument vendors that manufacture and sell instruments designed for control applications. All of these instruments have been based on low-field magnets (20-60 MHz proton resonance frequency) with most of them not

capable of high-resolution performance[65]. For many years Bruker Instrument company has been the worldwide leader in vending control NMR spectrometers with its Minispec series[65,77] (see *Figure 3.10*). Other important manufacturers are Foxboro[76], Resonance Instruments, Process Control Technology and Oxford Instruments[69].

Figure 3.10. Low field NMR from the Minispec series[77]

Low field NMR spectrometry has been used extensively in a variety of industries, mainly in those involving the manufacture of food, pharmaceuticals and petrochemicals. Examples of applications include the determination of moisture content, fat content, hydrogen content and fluorine content[69]. Polymer manufacturers can use low-field NMR measurements for determining viscosity[70]. NMR can also be used to determine flow rates and study other related phenomena such as velocity distributions and profiles[69,78]. Finally, high-field NMR combined with HPLC has been extensively used in the pharmaceutical industry[69].

1.5.2. Problems: flow-rate, probe design and temperature conditioning

A NMR system enclosing the production line would offer the best performance as it would avoid the use of special sampling devices. However, this is not suitable for physically large samples which would require a large and expensive magnet. In these cases, a side-stream solution diverted from the main line through a smaller magnet is normally used[67]. This approach (adopted in our sampling loop system)[2] assumes that the sample has the same characteristics as in the main stream, which is usually valid for liquids or solids with low viscosity. With viscous samples laminar flow can be produced due to the low flow rate used in the line. This may lead to separation of phases and therefore affecting the NMR results. If this occurs, the concentration obtained with the NMR measurement would change continuously with time.

Many probe designs incorporate a premagnetization region that enables the spins to be completely polarised prior to reaching the detection region. This produces a larger signal[69]. In a continuous or a stopped flow experiment premagnetization of the sample occurs as the sample flows through the magnet before the detection flow. For quantitative measurements, all sample nuclei must be completely premagnetized prior to observation[67]. The faster the flow rate the lower is the magnetization time producing lower intensities and poorer quality spectra. However, the faster the flow rate the less saturation effects are observed and the intensity is higher. Therefore, there is an optimum value for the flow rate where the intensity reaches a maximum level. This is shown in *Figure 3.11*.

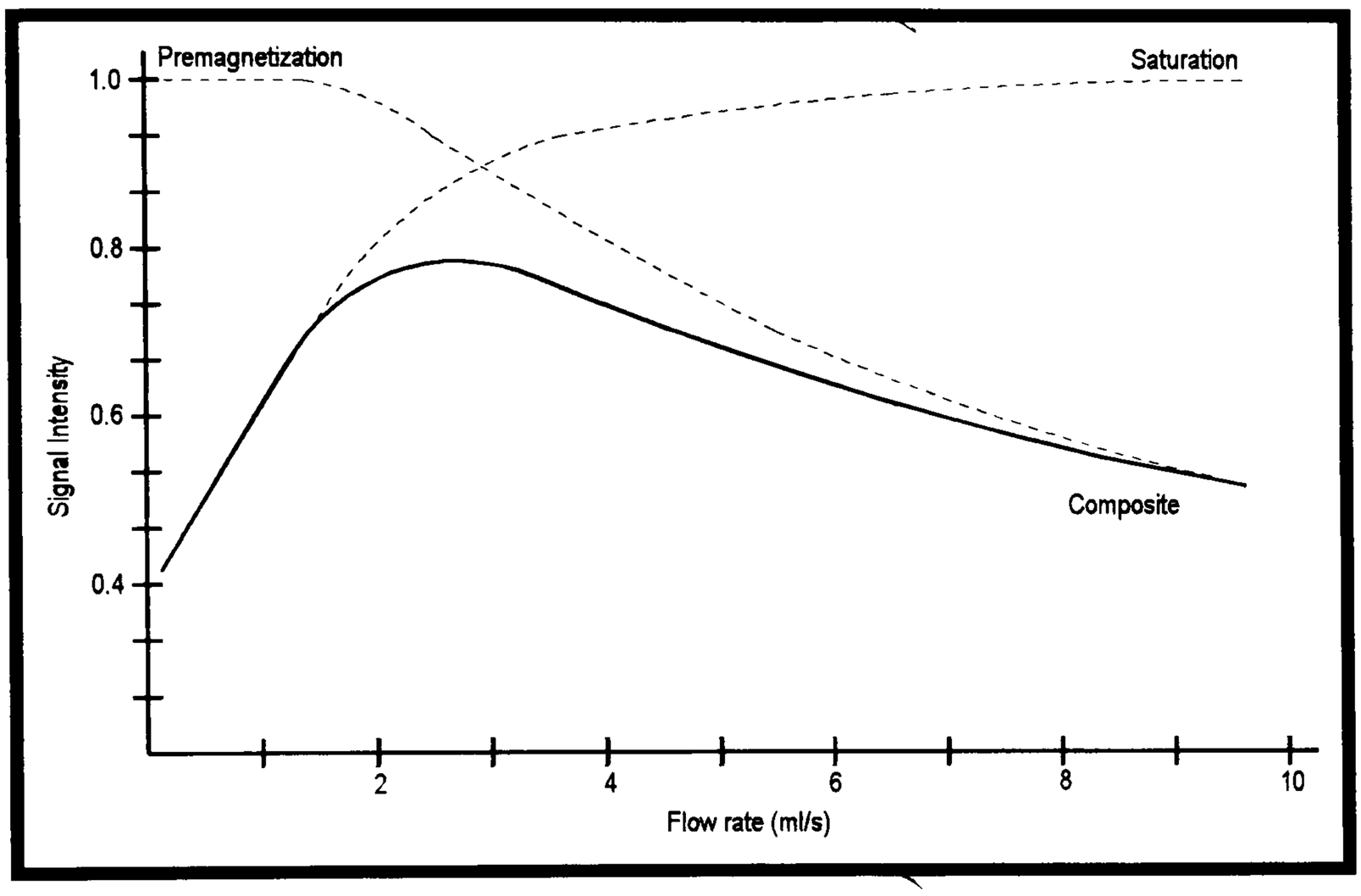

Figure 3.11. Intensity of the NMR signals as a function of the flow-rate[67]

The NMR cell is the conduit through which the process stream flows, and therefore it must be able to withstand temperatures and pressures, some of which are extreme. The standard glass-lined cells are suitable in low-pressure, low-temperature applications, but as the pressure and temperature increase, materials such as Teflon, Kel-F, or other nonhydrogen-bearing non-metallic materials must be used[70].

The physical properties of the stream are a factor in determining the diameter of the cell. Standard 5-mm-diameter NMR tubes are suitable for low viscosity liquids containing a significant number of protons. Larger diameters 6-25 mm are used for streams of high-viscosity materials or solids as they allow easier passage as well as assist in providing larger sample volumes for an enhanced signal-to-noise ratio[70]. In

addition, the flow-cell material must not react with the chemical process and must be resistant to fouling, corrosion or adherence by chemicals.

In the design of continuous-flow NMR probes the geometry of the cell is important. The flow cell should enable laminar flow and wall (memory) effects must be avoided. To aid laminar flow the cell should be held vertically and with the flow going against gravity to avoid the presence of air bubbles[69]. It is said[67] that the sample flowing through the NMR instrument must be in equilibrium with its environment. These equilibrium conditions involve a regular laminar flow for liquids, no thermal or concentration gradient, and a constant packing for solid samples. If the NMR cell is broader than the connecting line, then a gradual tapering of the NMR cell helps to avoid the formation of eddy flows and therefore turbulences[69].

The low-field magnets are usually constructed of rare-earth materials and can be affected by temperature variations that produce frequency drift, making temperature control of the magnet critical. To avoid this, a system "lock" to a specific frequency (either by software routines or by hardware design) is normally used[70]. The low-field NMR produced by Foxboro is reported not to affect the results when the sample temperature fluctuates[76]. However, while the effect of the variation in the temperature of the magnet can be reduced with the use of lock channels, that due to the variation in the sample temperature can not easily be eliminated[79]. In fact, some authors have reported difficulties due to the lack of temperature control that led to erroneous results in the case of heterogeneous or strongly exothermic reactions[73].

Regardless of sample type, one precaution that is essential for maintaining the integrity of the magnet-probe assembly is the removal of any ferromagnetic contaminants from the sample before it enters the NMR probe. Otherwise, the homogeneity of the permanent field is destroyed, thereby rendering the NMR analyser useless[70]. The use of in-line self cleaning filters that are capable of working continuously can be implemented in the sampling line if required[80].

All of these flow, probe design and temperature factors must be carefully considered when the NMR system is to be implemented in the sampling loop for on-line NMR analysis of the processes carried out in the reactor system. Therefore, the implementation requires sample conditioning to deliver the sample at the conditions

of temperature and flow-rate needed for NMR analysis[2]. The adjustment of the temperature is not covered in this work since the analysis of the effect of temperature in the response of the low field NMR instrument was one of the aims of other projects[2,79].

In terms of flow-rate, a low flow-rate (0-100 ml/min depending on the heterogeneity of the sample) through the NMR cell[79] is needed in order to get an acceptable response from the system and retain an appropriate retention time of the sample in the magnetic field. These flow rates are considerably smaller than those used to achieve the isokinetic conditions needed to get representative samples from the process[2].

A flow-cell was already designed[79] according to the requirements highlighted above. A sketched of the glass (4 mm OD) flow-cell with premagnetisation region used in the experiments carried out in this work is shown in *Figure 3.12*.

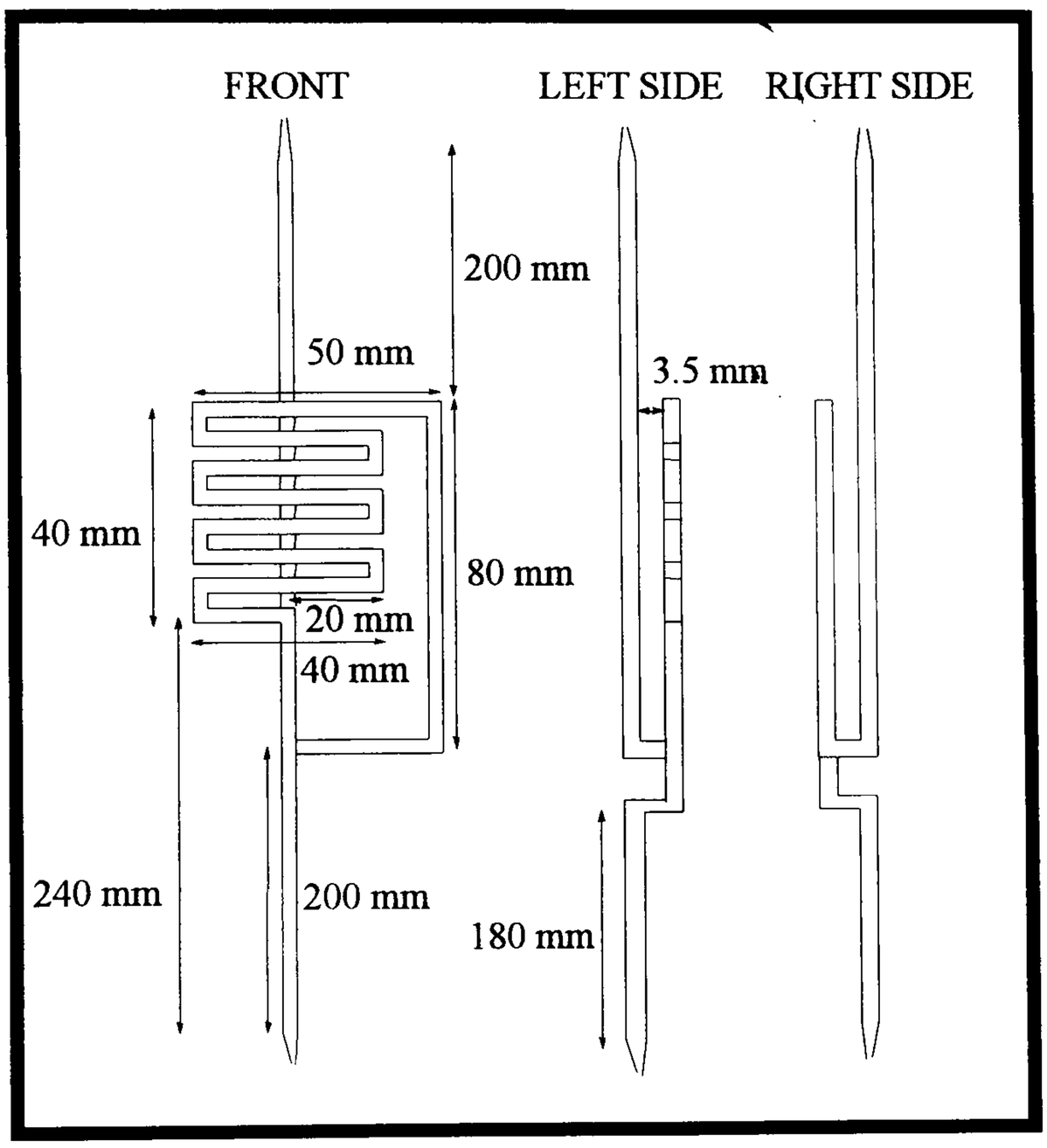

Figure 3.12. Glass NMR flow-cell used in the low-field NMR experiments[79]

1.5.3. Solutions: subsampling and modelling of sampling systems

There are two alternatives to solving the problem of flow conditioning for the implementation of on-line NMR spectrometry[2]. One is to change the flow-cell for one with a considerably larger diameter so that the flow-rate decreases as the sample

flows through the NMR instrument and remains long enough in the magnetic field. This alternative implies substantial modifications of the hardware of the NMR spectrometer and therefore was found not to be viable[79]. The other possibility is to get a subsample from the sampling loop (that is assumed to contain a representative sample) at a lower flow-rate. Similar strategies are used with isokinetic probes used in particle size measurements that need a particular flow-rate through the instrument[22].

Sample collection from pipes is simpler than from chemical reactors as the flow-patterns are better defined[6,12]. Besides, isokinetic sampling is not as important as in sampling from reactors as the orientation of the sampling probe parallel to the streamlines is more feasible. An example of a probe configuration parallel to the direction of the flow is the fitting sketched in *Figure 3.13*. This second alternative to sort out the problem of flow conditioning was the one that was chosen for application in this project and is sketched in the *Figure3.14*.

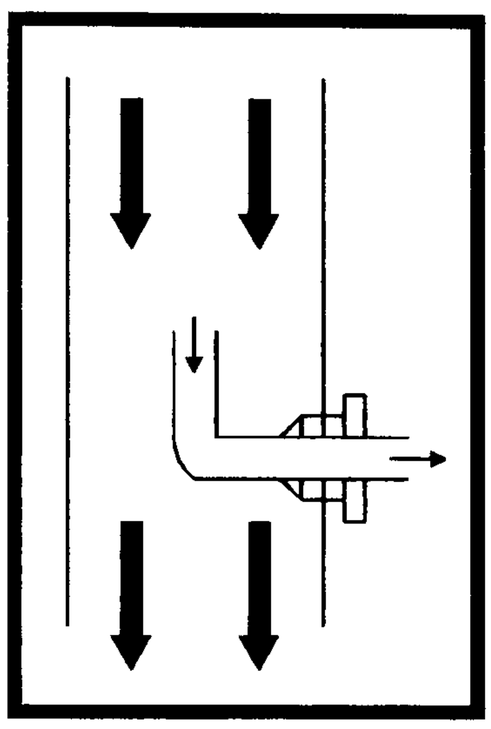

Figure 3.13. Connection fitting to extract a representative sample from a straight pipe-line in a direction parallel to the flow-streamlines

In any case, as mentioned in the previous section, modelling of the sampling loop system can sometimes get away with problems of the non-optimum orientation of the sampling probe[2]. If a robust model of the loop is produced, the NMR loop system could be connected and samples could be collected straight from the reactor at a low flow-rate. These samples, obtained at non-isokinetic conditions, would not be representative of the process but their analysis could be corrected by using the sampling model. A study of the feasibility of using the model for this purpose is one of the aims of the study in the implementation of the NMR system for on-line analysis.

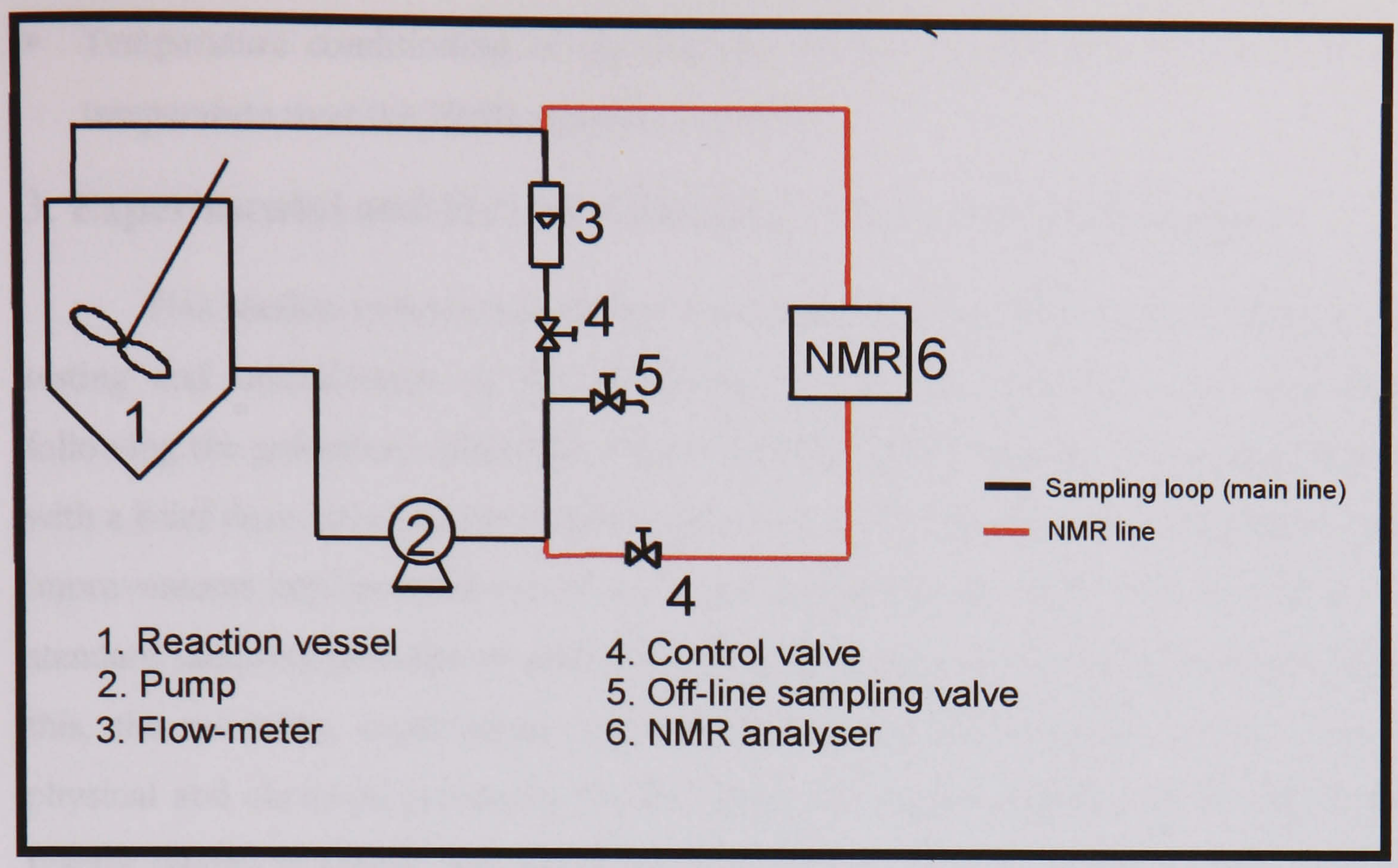

Figure 3.14. Sketch of sampling loop plus NMR line

1.6. Technical features of the fast sampling loop for chemical reactors

The theory reviewed in the previous sections within this chapter constituted the basis for the design of the sampling loop for our batch reactor system[2]. Full details of the final design are attached as an Appendix with calculations and sketches included (see Appendices 1-3). The following points summarise the main conclusions extracted from the literature review outlined above:

- The stirrer plane is the area where the flow patterns are better defined and the probe can be better orientated for representative sampling.
- The inside diameter of the sampling probe should be greater than 6 mm and it should be orientated horizontal between the stirrer blade and the reactor wall.
- The pump should be able to provide a flow rate at least equal to that which determines the isokinetic sampling conditions. This depends on the stirring speed used in the process.
- A secondary loop will take a sample from the main sampling line (where the flow patterns are simple and well defined) and render it to the NMR system at a flow-rate within the range 0-100 ml/min.

- Temperature conditioning of the sample can be covered after the effect of the temperature over the NMR signals is assessed.

3. Experimental and Results Obtained in the Area of Sampling

This section summarizes all the experimental work and results obtained in the testing and optimization of the sampling system. The sampling loop was built following the guidelines described at the beginning of the chapter. The section begins with a brief description of the problems faced in the initial stages of construction. The improvements implemented over the original design are also described, as well as the standard sampling procedures needed for the correct use of the sampling system. After this, the modeling experiments and calibration tests are outlined for the case of physical and chemical processes. At this stage, the results obtained in the use of the reactor facility in kinetic and thermodynamic experiments are also described. Finally, the results obtained in the implementation of the low-field NMR system using the loop are covered at the end of the chapter.

3.1. Construction of a fast sampling loop and initial tests

Three different versions of the loop were built. The first prototype was constructed using 316 stainless steel pipe work with an air driven pump made of the same material. Problems with corrosion were detected in the 316 stainless steel alloy when crotonic acid was used as reactant and concentrated sulphuric acid was added as the catalyst. Therefore, the tubing was substituted by corrosion resistant PTFE lines connected by glass fittings. The pump was replaced by a Ritchie & Mackenzie PTFE cased centrifugal pump (Reference number B25-A0)[81]. Its technical specifications meet the requirements listed in Appendix 2. In addition, the stainless steel stirrer inside the reactor had to be replaced by a home-made PTFE stirrer[82].

The use of glass fittings with quick-fit connections caused great concern about safety in case pressure built-up in the system caused the fittings to pop-off[83]. Therefore, these connections were replaced by PTFE fittings with compression ferrule-type connections that withstand pressure conditions[84] 100 psig, higher than the maximum pressure that can be reached in the system (less than 5 psig)[2]. The much higher cost of these new fittings was the reason why the glass connections were

installed first and their performance was carefully analysed. The high quality of the new connectors and their capacity to withstand relatively high pressure conditions led to the decision of not using the high pressure relief valve initially designed. The high cost of this element also contributed to taking this decision of not building the pressure relief line. Instead, other safety measures were adopted. For instance, collecting trays with absorbent pads were installed underneath each of the reactors and the pump in the loop[85]. Furthermore, a ball-valve to isolate the loop in case of leaks and a safety switch were installed to disconnect the pump in case of material failure in the connections[83].

Finally, the use of pressure indicators in the lines was avoided for economic reasons and due to the fact that this element was found not to be essential for the initial versions of the sampling system. The use of a flow-meter in the NMR loop was also avoided as the flow-rates in this line were fairly low (in the range of 0-100 ml/min) and could be easily measured manually (i.e. measuring the volume flowing in the loop in a certain period of time). The final version of the sampling loop is sketched in *Figure 3.15*.

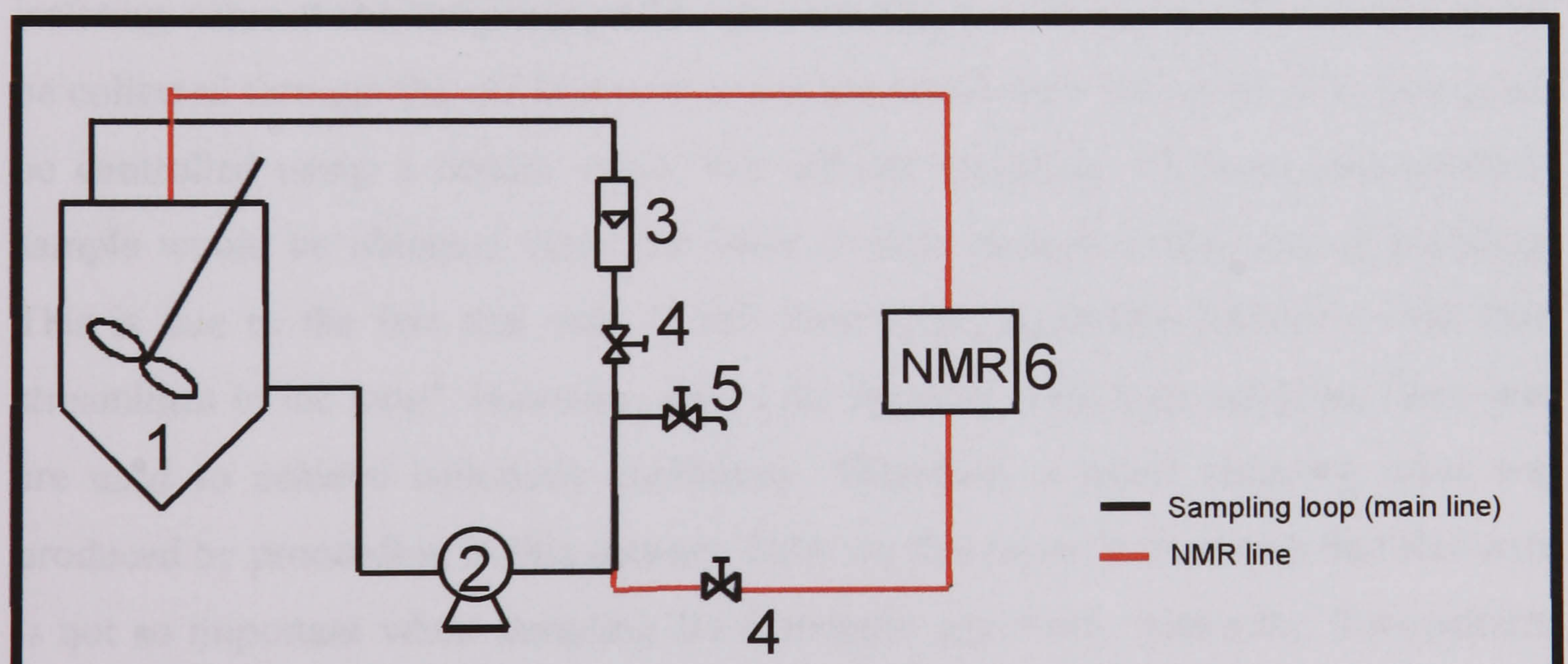

Figure 3.15. Sketch of sampling loop without pressure relief line

3.1.1. Dead volume and sampling procedures

The dead volume was determined by adding water to the loop and measuring its volume. The results and the precision obtained in the replicates of this experiment are summarised in *Table 3.3*. As can be observed, the total dead volume constituted 11.6% of the total volume inside the 5-L reactor system (normally 4 litres). It should be mentioned that the sampling system was designed regardless of the volume of the reactor. Therefore, this dead volume would be the same if the device were to be used in bigger industrial reactors.

Table 3.3. Dead volume for the different parts of the sampling loop system

Element in the loop	*Volume of water (ml)*	*Precision (ml)*
Pump	150	± 5
Needle valve	12	± 1
Flow-meter	80	± 3
Main loop pipe-work	121	± 4
NMR loop pipe-work	85	±3
NMR flow-cell	15	±1
Total sampling loop system	463	± 8

The standard protocol for the use of the loop started off by opening the isolating valve at the sampling probe and switching on the pump. The samples could be collected through the off-line port or via the NMR loop where the flow-rate could be controlled using a needle valve. For off-line sampling, the most representative sample would be obtained when the valve is fully opened at the time of sampling. This is due to the fact that only in this case is the collection parallel to the flow streamlines in the loop[2]. However, this is not feasible when high sampling flow-rates are used to achieve isokinetic conditions. Therefore, a small sampling error was produced by proceeding in this manner. Later on this report it is proved that this error is not so important when sampling from straight pipe-lines, where the flow-patterns are well defined. When sampling from agitated vessels the orientation of the sampling probe is more crucial as the flow-patterns are not well defined and the turbulences in the system may even produce a change of patterns with time[2]. Results in the literature confirmed these facts[4,6].

The sampling experiments were stopped by switching off the pump before closing the isolating valve. Part of the content remaining inside the loop was

drained out through the off-line port and NMR loop. The rest of the liquid still in the loop was located inside the pumping chamber. This could be drained by opening a hole (normally blocked with a screwed-on stopper) at the bottom of the casing of the pump[81]. As this orifice was difficult to access, it was found to be easier to disconnect the pump from the loop and drain the content of the loop and pumping chamber into the collecting tray with absorbent pads. The little dead volume remaining inside the pump was removed by turning the pump upside down. The loop had to be carefully cleaned with acetone before it was assembled and used again.

As the continuous assembling and dissembling of the loop might have damaged the connections in the loop[82] the system had to be tested periodically for leaks using water. Those connections that were damaged during the cleaning stage had to be replaced to avoid material failure in the lines. This undesired effect was the consequence of using soft PTFE in the loop and could be avoided by improving the access to the bottom draining hole in the pump so that can be used for draining instead of dismantling the loop.

3.1.2. Calibration of the flow-meter

It has been mentioned previously that one of the most interesting sampling experiments is the study of the effect of sampling velocity on the quality of the off-line samples[2]. This study is one of the most important analyses leading to the development of a reliable sampling system. In order to know the flow-rate (related to the sampling velocity) in the loop, a prior calibration of the rotameter implemented in the line was needed. The stainless steel float in the original flow-meter was replaced by a PTFE float to avoid corrosion problems. As Teflon is lighter than steel, the new float had to have a smaller diameter in order to be used in the rotameter to measure a similar range of flows[82]. Therefore, after this replacement, the flow-meter needed to be recalibrated. The new PTFE float had to be constructed with the faces well machined to avoid air bubbles getting attached to the float and therefore modifying the reading obtained on the meter. Moreover, the symmetry of the float had to be maintained since the smaller diameter of the PTFE float would have made the float oscillate too much, affecting the reading. Another way to sort out this symmetry and oscillation problems would be to construct a float with a larger diameter and make it

heavier by using a steel float covered in PTFE[82].

The easiest and safest way to carry out the calibration of the flow-meter was to perform a direct measure of the volume being delivered in a certain period of time for the different marks of the scale of the meter. This had to be carried out with water as the flow-rates within the isokinetic range were fairly large (normally in the range 0-10 l/min) and splashes of liquid were likely to occur with these conditions. Calibration information for other liquids that are more hazardous can be obtained in two ways. Either by using in-line clean non-invasive measurement systems to measure the flow-rate (e.g. hot wire anemometers or magnetic meters)[86] or from results obtained with water are extrapolated to the new substances. This latter method was the one adopted in this work and is described in the following section where the results obtained for water and other mixtures are presented.

a) Calibration with other liquids and mixtures

When hazardous mixtures are used it is advisable to avoid the direct calibration of the flow-meter and correct the parameters obtained for water using the density of the new system. In the most common rotameters or variable-area flow-meters, a float, moving vertically within a linearly tapered tube, exposes a variable area to the flow. At design conditions the differential pressure remains constant across the float, because buoyant and weight forces are constant and the float height changes to expose the area that satisfies Bernoulli's equation[87]:

$$P_{f1} - P_{f2} = \frac{\rho_f}{2g}(v_{f2}^2 - v_{f1}^2) \qquad \text{Eq. 3.9}$$

where (see *Figure 3.16*):

P_{f1} = *Pressure at the inlet of the meter (kg/m^2)*
P_{f2} = *Pressure at the equilibrium point (kg/m^2)*
ρ_f = *Density of the fluid flowing in the meter (kg/m^3)*
v_{f1} = *Fluid velocity at the inlet of the meter (m/s)*
v_{f2} = *Fluid velocity at the equilibrium point (m/s)*
g = *Acceleration of gravity (m/s^2)*

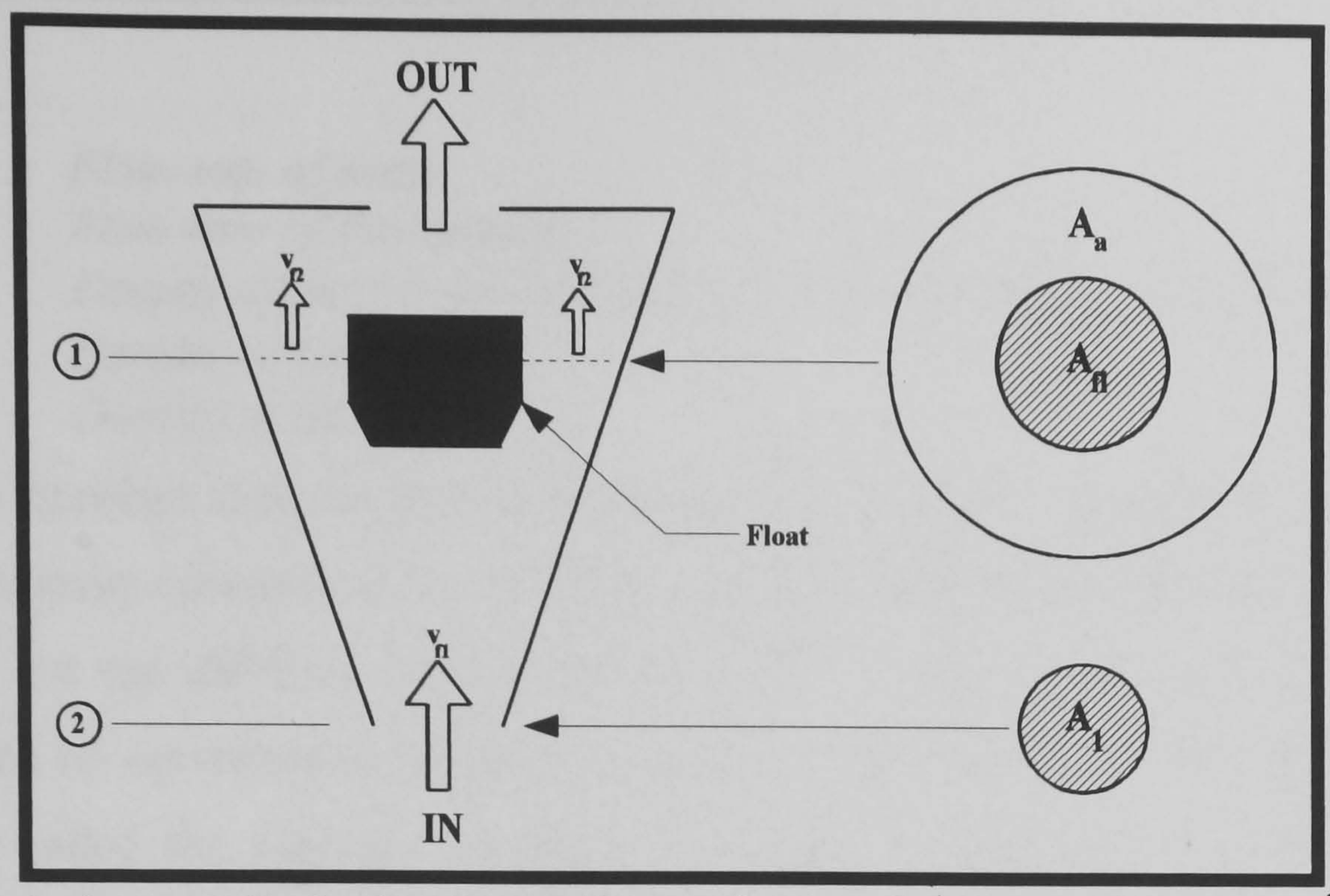

Figure 3.16. Area and velocity nomenclature in a variable-area flow-meter[87]

The flow area between the tube and the float is then an indication of the flow-rate. Since the float height is a linear function of the flow area, visual observation allows the flow-rate to be observed. Using Bernouilli's equation and considering the static pressure acting downwards, the total pressure acting upwards and the variable flowing area, the following equation can be obtained for the flow-rate across the meter[86-88]:

$$q_f = \left[K_{VA} \sqrt{\frac{2 g_l V_{fl}}{A_{fl}}} \right] \sqrt{\frac{\rho_{fl}}{\rho_f} - 1}\; A_a \qquad \text{Eq. 3.10}$$

where:

q_f = *Flow-rate for a particular fluid (m^3/s)*
K_{VA} = *Flow coefficient to correct for the factors not included in the analysis*
g = *Acceleration of gravity (m/s^2)*
V_{fl} = *Float volume (m^3)*
A_{fl} = *Float area (m^2)*
ρ_{fl} = *Density of the float (kg/m^3)*
ρ_f = *Density of the particular fluid (kg/m^3)*
A_a = *Annular area between the float and the tube wall (m^2)*

If this mathematical expression for water is divided by the same equation when another mixture is used, the following equation can be obtained which relates the flow of any fluid with the calibrated flow-rate of water[89].

$$\frac{q_w}{q_m} = \sqrt{\frac{(\rho_{fl} - \rho_w)}{\rho_w} \cdot \frac{\rho_m}{(\rho_{fl} - \rho_m)}} \qquad \text{Eq.3.11}$$

where:

q_w = *Flow-rate of water*
q_m = *Flow-rate of the mixture*
ρ_f = *Density of the rotameter float (ρ_f = 1.984 g/cm^3 for the PTFE float)*
ρ_w = *Density of water*
ρ_m = *Density of the mixture*

It is therefore clear that there is a density correction associated with the change of fluid. Viscosity corrections are difficult to calculate and can be neglected when the values are not too different for the two fluids[86,87]. Usually, the value of viscosity below which no correction is required, is provided for a particular float design. This number is called the viscosity immunity ceiling[87]. It could not be found in the literature for the float design used in this project.

The experimental results obtained for the flow-meter calibration with water are presented in *Figure 3.17* along with the theoretical calculations for toluene (density = 0.867 Kg/m^3), saturated sodium carbonate in water at 30°C (density = 1.375 Kg/m^3) and a 1% weight/weight suspension of glass beads in water (density = 1.013 Kg/m^3).

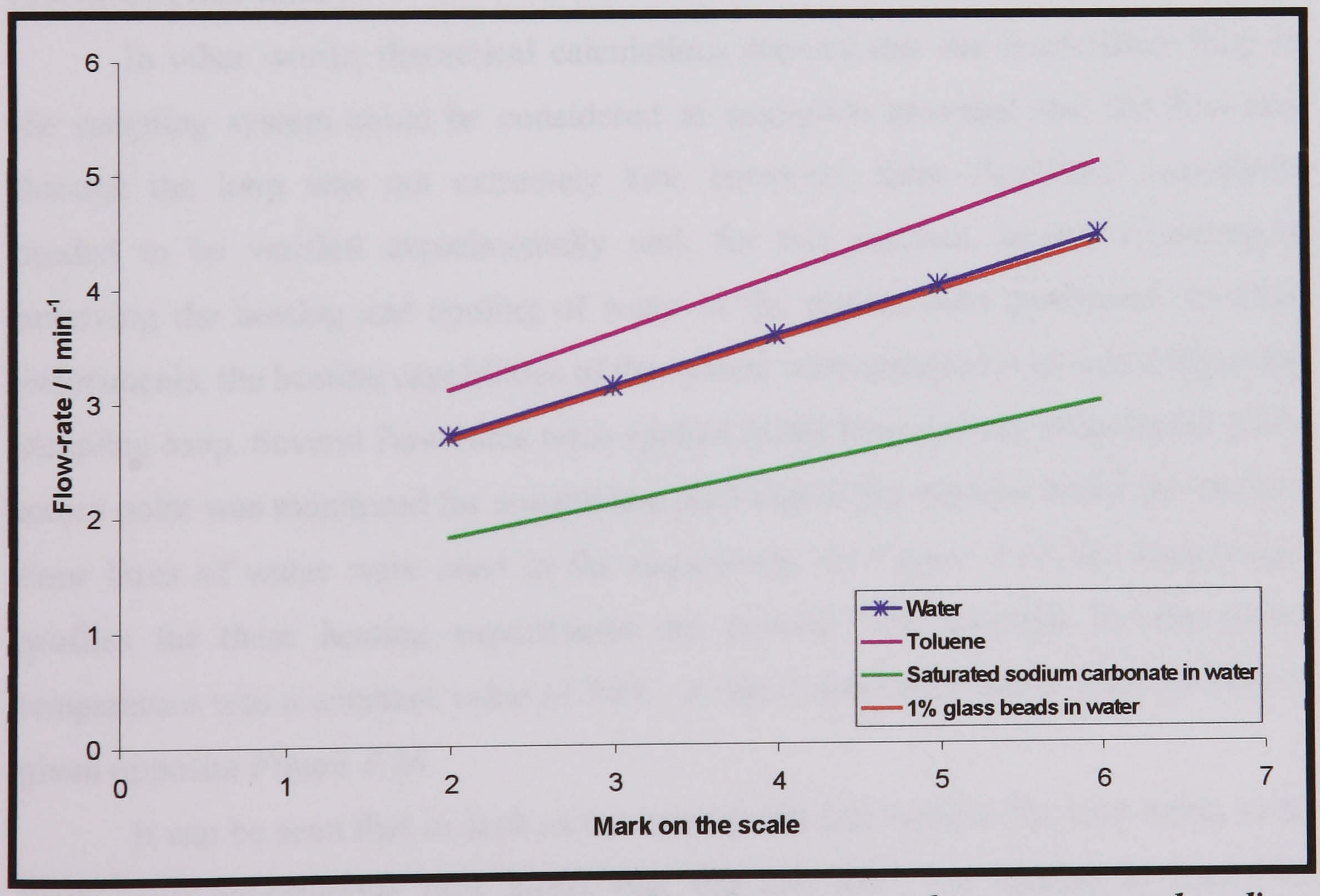

Figure 3.17. Flow-meter calibration plots for water, toluene, saturated sodium carbonate in water and 1% glass beads in water

3.1.3. Heat transfer in the loop

The majority of the processes carried out in the reactor system were isothermal[58]. Therefore, it was of interest to return the unused sample from the loop to the reactor at a similar temperature to that which it had when the sample was extracted from the vessel. In order to achieve this, an insulation system had to be designed (if needed) to avoid the heat losses in the loop. This design basically consisted in working out the radius and heat conductivity features of the material to be used as an insulator[2]. Another important consideration at the time of designing the thickness of the insulator can also be the cost of the insulator[60].

With a simple energy balance between the two ends of the sampling system, it could be worked out how the heat losses in the loop produced a decrease in the temperature in the fluid flowing through the pipe. The basic chemical engineering equations and calculations for the design of the insulation are described in Appendix 2. The results showed that even with a very small thickness of insulation the temperature at the return point was very similar in value to that at the sampling point (99.99% of this value)[2].

In other words, theoretical calculations showed that the temperature drop in the sampling system could be considered as negligible provided that the flow-rate through the loop was not extremely low. However, these theoretical hypothesis needed to be verified experimentally and, for this purpose, several experiments involving the heating and cooling of water in the system were performed. In these experiments, the heating capabilities of the system were analysed with and without the sampling loop. Several flow-rates were applied in the loop and the temperature at the return point was monitored for comparison with that of the mixture inside the reactor. Four litres of water were used in the experiment. In *Figure 3.18* the temperature profiles for these heating experiments are plotted. The set-point for the jacket temperature was a constant value of 90°C. A short discussion about these profiles is given opposite *Figure 3.18*.

It can be seen that in both of the cases (with and without the loop being used) there were considerable heat losses that did not allow the system to reach the temperature set for the jacket. Also, the heat losses in the loop were not found to vary with the flow-rate of the sample through the loop.

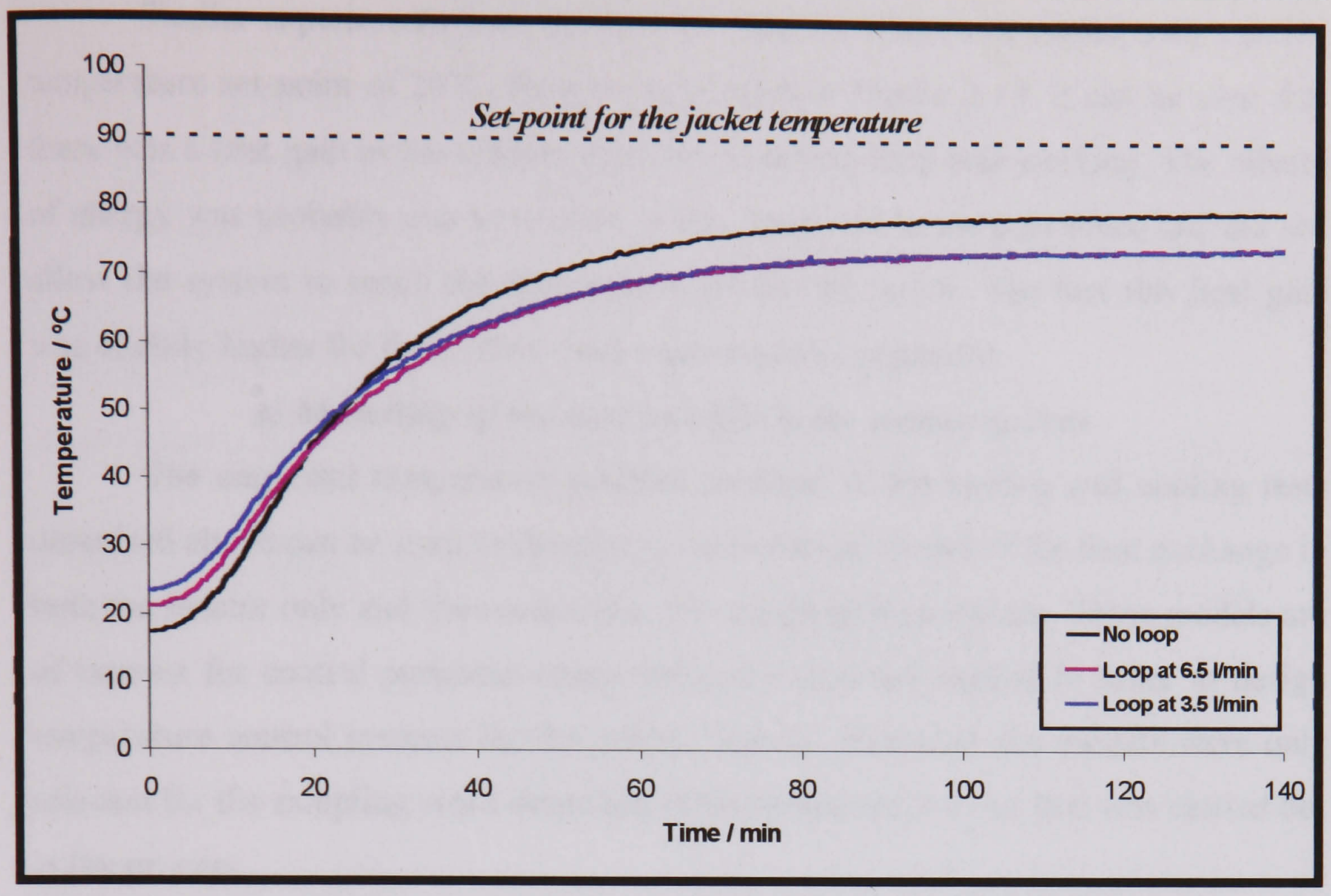

Figure 3.18. Temperature profiles for a heating experiment (set-point for jacket temperature 90°C) with and without the main sampling loop

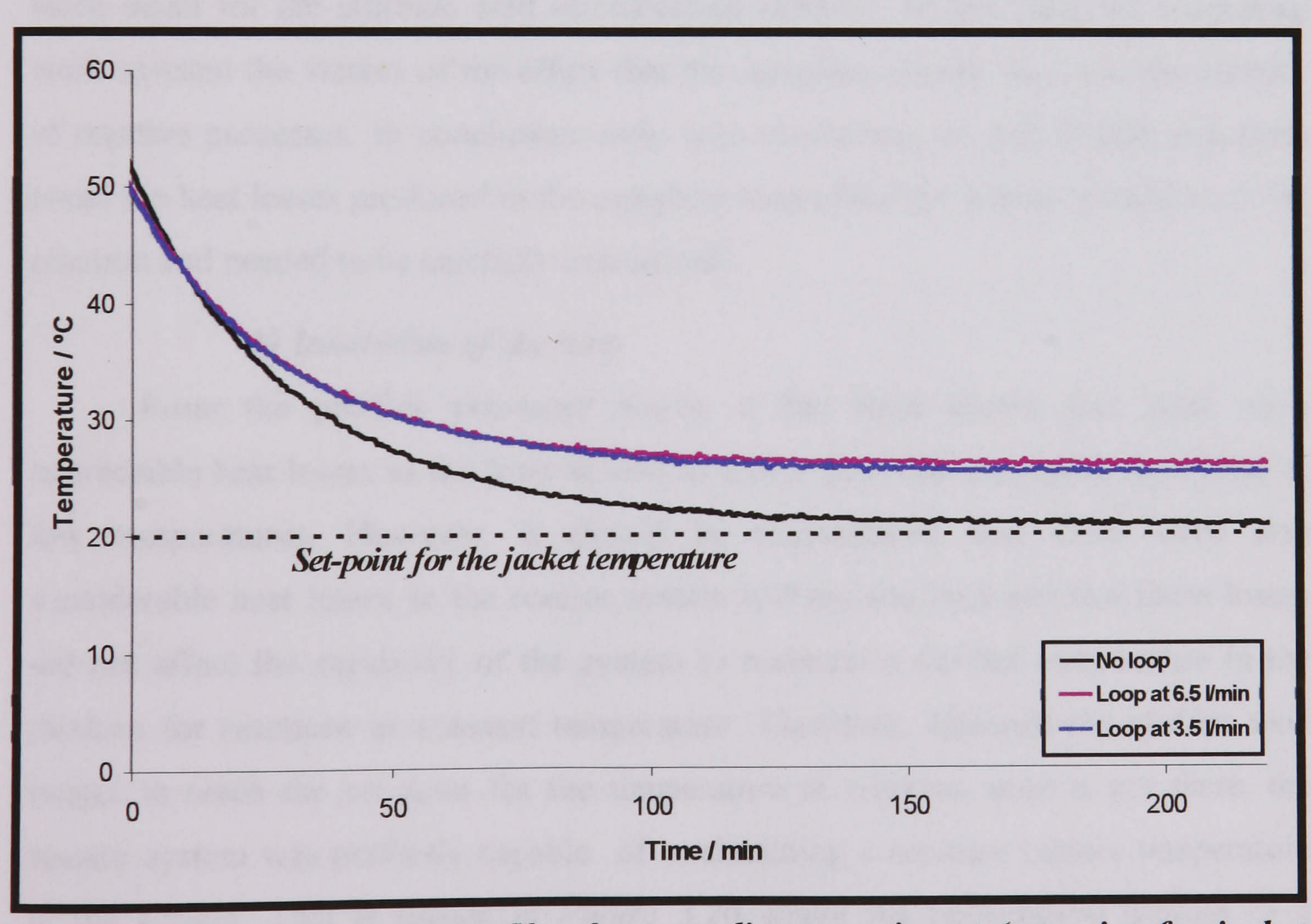

Figure 3.19. Temperature profiles for a cooling experiment (set-point for jacket temperature 20°C) both using and not using the main sampling loop

Similar experiments were performed when the water was cooled with a jacket temperature set-point of 20°C. Results are plotted in *Figure 3.19*. It can be seen that there was a heat gain in the system when the sampling loop was working. The release of energy was probably due to friction in the pump and in the pipe-work and did not allow the system to reach the temperature set for the jacket. The fact this heat gain was slightly higher for faster flow-rates supported this argument.

a) Modelling of the heat transfer in the reactor system

The empirical temperature profiles obtained in the heating and cooling tests described above can be used to develop a mathematical model of the heat exchange in both the reactor only and the reactor plus the sampling loop system. These models are of interest for control purposes where the heat losses are needed in order to design temperature control systems for the reactor facility. However, the models were only relevant for the sampling work described in this thesis when a reaction was carried out in the process.

In fact, later in this chapter, an example of this type of modelling is covered in more detail for the crotonic acid esterification reaction. In this case, the modelling work assisted the studies of the effect that the sampling system had over the kinetics of reactive processes. In conclusion, only with exothermic or endothermic reactions could the heat losses produced in the sampling loop affect the normal evolution of the reaction and needed to be carefully considered[2].

b) Insulation of the loop

From the profiles presented above, it has been shown that there were appreciable heat losses in the loop as well as a heat gain that was more significant at low temperatures. However, it should be remembered that there were also considerable heat losses in the reactor system without the loop and that these losses did not affect the capability of the system to maintain a desired temperature in the mixture for reactions at constant temperature. Therefore, although the system took longer to reach the set-point for the temperature of reaction, once it got there, the reactor system was perfectly capable of maintaining a constant reactor temperature in the system. This is shown in *Figure 3.20* where the temperature profiles of a heating experiment with water (set-point: 95°C) are compared with and without the loop. In both cases the system was capable of reaching the set point, although the

heating rate was slightly lower when the sampling loop was working. Similarly, for experiments at low temperature, the fact that a heat gain existed did not imply that temperatures below 26°C could not be set for the reactor mixture when the loop was working. This temperature set-point could be perfectly reachable but, to achieve this purpose, the control system would need to set a lower temperature for the oil in the jacket than in the case where the sampling system was not working.

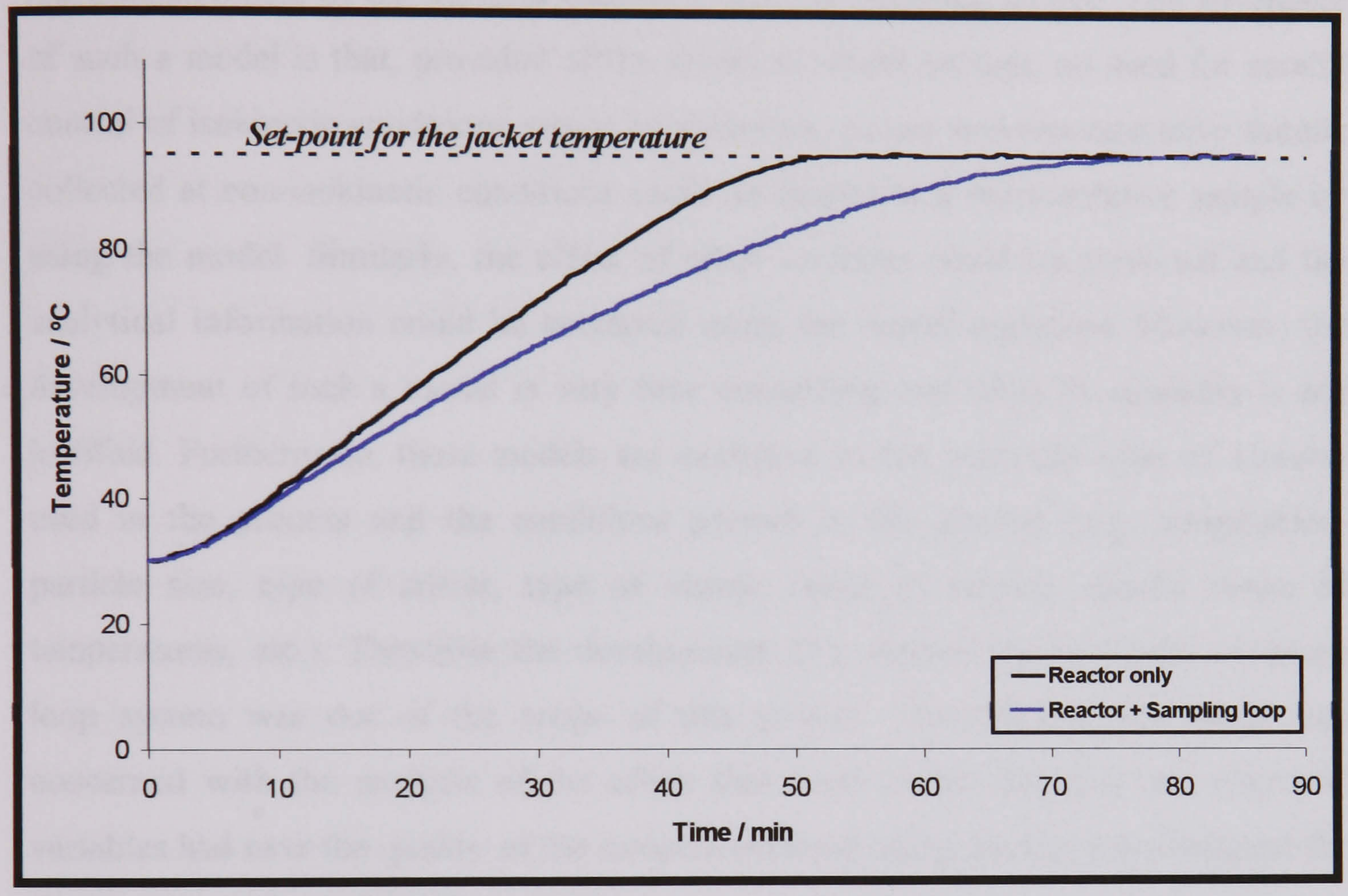

Figure 3.20. Temperature profile for a heating experiment (set-point for reactor temperature 95°C) using and not using the loop

In conclusion, both the reactor only and the reactor plus the sampling loop system produce heat losses that made it impossible to reach a temperature inside the reactor similar to that set in the jacket. However, the processes of interest for this project were carried out at a constant temperature set-point for the contents in the reactor and this could be achieved regardless of the heat losses reported above. Therefore, no insulation was implemented in the reactor system or the reactor plus the sampling loop system at this stage. Should the insulation be needed for future experiments, the guidelines and key points outlined in this thesis should be followed[2].

3.2. Evaluation and modelling of the sampling system

It has been already been mentioned that even if a sampling system is optimally designed to get representative samples, factors such as sampling velocity can affect the performance of the system. An interesting exercise can be the modelling of the particular sampling system to define how parameters such as the sampling velocity, density of the different phases in the mixture and temperature affect the representativeness of the samples collected with the sampling device. The advantage of such a model is that, provided of the model is robust enough, no need for careful control of isokinetic conditions would be necessary, as any non-representative sample collected at non-isokinetic conditions could be related to a representative sample by using the model. Similarly, the effect of other variables could be predicted and the analytical information could be corrected using the model equations. However, the development of such a model is very time consuming and often its necessity is not justified. Furthermore, these models are exclusive to the particular type of sampler used in the process and the conditions present in the process (e.g. composition, particle size, type of stirrer, type of vessel, range of stirring speeds, range of temperatures, etc.). Therefore the development of a general model of the sampling loop system was out of the scope of this project. Nevertheless, this work was concerned with the analysis of the effect that some of the physical and chemical variables had over the quality of the samples obtained using the fast loop designed for the implementation of NMR analysers.

This simplified modelling work was therefore focussed on the testing of the designed sampling system. This design was based in the reviewed work on sampling and information collected about other sampling prototypes in the market. If during the modelling experiments a specific variable is found to affect considerably the sample collection, an univariable model could developed to correct its effect. Finally, the ultimate goal in the project was to ensure that an adequate sample was being delivered to the NMR instrument implemented in the sampling system.

3.2.1. Physical modelling

The physical model of a sampling system relates the quality of the sample with the physical parameters that affect the sample collection. As already mentioned there

are many physical variables that affect sampling, such as sampling velocity, stirring speed, sampling point and orientation of the sampling probe, shape of the sampling probe, type of mixture, ratio of the different phases, particle size, type of stirrer, type of vessel, and range of temperatures used in the process. It is therefore clear that a complete modelling study considering all these factors is complicated, time-consuming and of little industrial interest. Hence, this work was focussed on the effect of the two most important variables affecting the particle collection: sampling velocity and stirring speed. The rest of the variables were normally fixed by the conditions in the process (e.g. temperature, type of stirrer, type of mixture etc.) or by the parameters of design (e.g. location of sampling point, orientation and shape of the sampling probe, etc.). Nevertheless, some attention was also paid to some of the other parameters such as the location of the sampling point, type of the stirrer, type of vessel (i.e. use of baffles) and type of mixture, to check the effect of them on the sample collection.

In this work, the experiments to study the quality of the samples were carried out in two different systems. It should be mentioned that in reactor vessels, the quality of the sample was usually measured as the withdrawal-bulk concentration ratio, which is commonly known as sampling efficiency. Initially, some tests were performed in the 5-L reactor system. However, this facility did not offer the flexibility that was expected in terms of variable speed for the stirrer or interchange ability for different types of agitators. In fact, mechanical problems in the stirrer motor led to failures that forced us to look for alternative devices to carry out the experiments. Therefore, the majority of the experiments were performed in a 5-L beaker (see *Figure 3.21*) that was intended to simulate the conditions in the reactor. A flexible Heidolph RZR1 stirrer head motor was used for varying the stirrer speed and trying different types of stirrers. A complete description of the features of this alternative system are listed in Appendix 4. The conclusions extracted from the work with this vessel were extrapolated to the usual sampling and reactor system where some improvements were implemented.

Figure 3.21. General view of the two 5-L beaker system and its two sampling ports

a) Isokinetic velocity at different stirring speeds

As stated above, the most interesting modelling experiments were those that give information on how the sampling and stirring velocities affect the sample collection. However, prior to their performance, it was necessary to define the iso-, sub- and super-isokinetic sampling conditions that were present in the system. In other words, the local velocities at the sampling point had to be defined for different values of stirring speed. In these experiments two different sampling locations were used: one at the stirrer plane (which is the optimally designed location according to the literature that has been reviewed) and another considerably above that region. Only one sampling probe orientation (horizontal) was used in both cases, as preliminary tests[89] and literature reviews[2] showed that vertical probes are not good for sampling from stirred vessels. Two different vessel configurations were used to analyse the effect of baffles (which improve mixing) over the sample collection. The choice of the two sampling points was made for the following reasons:

- First, it was intended to prove that the stirrer plane was a better region for sample collection, especially when the horizontal orientation was chosen for the sampling probe.
- Second, the feasibility of modelling the sample collection at points where the sample representativeness is not good (e.g. at the point above the stirrer plane) could be studied. If this is found to be feasible, the idea of using these models to

correct the final analyser data in plants where poor designs of sampler are used, would be demonstrated. This is related to the fact that any non-representative sample that the non-optimised sampling system provides from heterogeneous systems could be related to a more representative value by using the model.

Similar to the case of flow-meter calibration, a safer approach for the local velocity measurements was to measure the performance in water first. Subsequently, the results obtained in water could be extrapolated to other fluids and mixtures using simple mathematical expressions and neglecting the compressibility of the fluids.

i. Experiments with water

As the local velocity can be related to the pressure at the sampling point by a simple mechanical energy balance, measurements of pressure at the sampling point were performed for different stirrers (see *Figure 3.22*) and stirring speeds. The effect of the presence and absence of baffles in the system were also studied. The relationship between the pressure (called impact pressure and measured with a simple manometer at the particular point)[86] and the local velocity at the sampling point is given by Eq. 3.12.

$$v = \sqrt{2g\Delta h} \qquad \text{Eq.3.12}$$

where:

v = *Local velocity at the sampling point (m/s)*
g = *Gravitational constant (m/s^2)*
Δh = *Difference in height of the liquid in the manometer (m)*

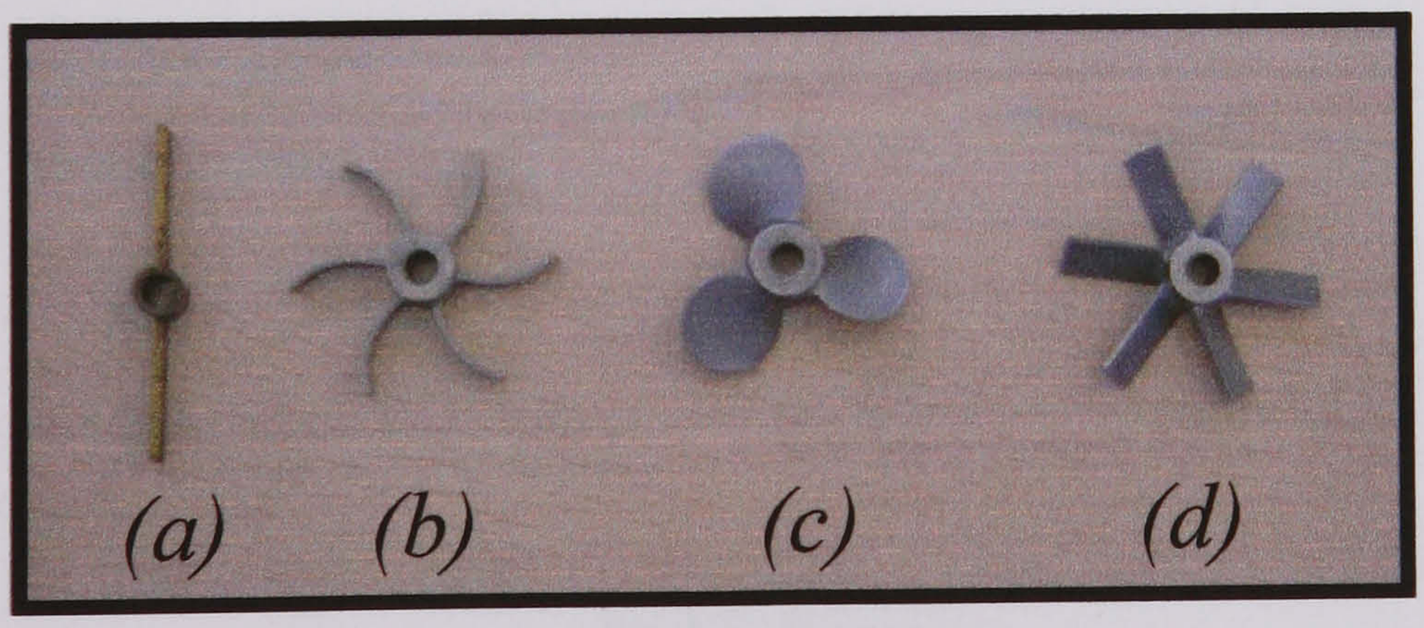

Figure 3.22. Different types of stirrers used in the experiments (a) Flat 2-blade (b) Curved 6-blade (c) FloMor 3-blade (d) Pitched 6-blade

Preliminary experiments were successfully performed in the 5-L reactor system[89] before moving to the 5-L beaker system. The manometer used for the measurements was a simple graduated L-shaped tube connected to the sampling port. In the absence of stirring the level of liquid in the tube was the same as that of the 3 litres of water in the reactor. With stirring, the pressure at the sampling point produced an increase Δh in the level of liquid in the L-shaped tube. The results obtained in this system can be observed in *Figure 3.23* (sampling point at the stirrer plane, no baffles), *Figure 3.24* (sampling point above the stirrer plane, no baffles), *Figure 3.25* (sampling point at the stirrer plane, with baffles), *Figure 3.26* (sampling point above the stirrer plane, with baffles).

Not only could the pressure measurements be used to calculate local velocities but they also gave an indication of the flow patterns that the different stirrer blades produced in the mixing vessels. For example, in the experiments with no baffles it could be observed that *Stirrer (c)* was the type that produced the lowest

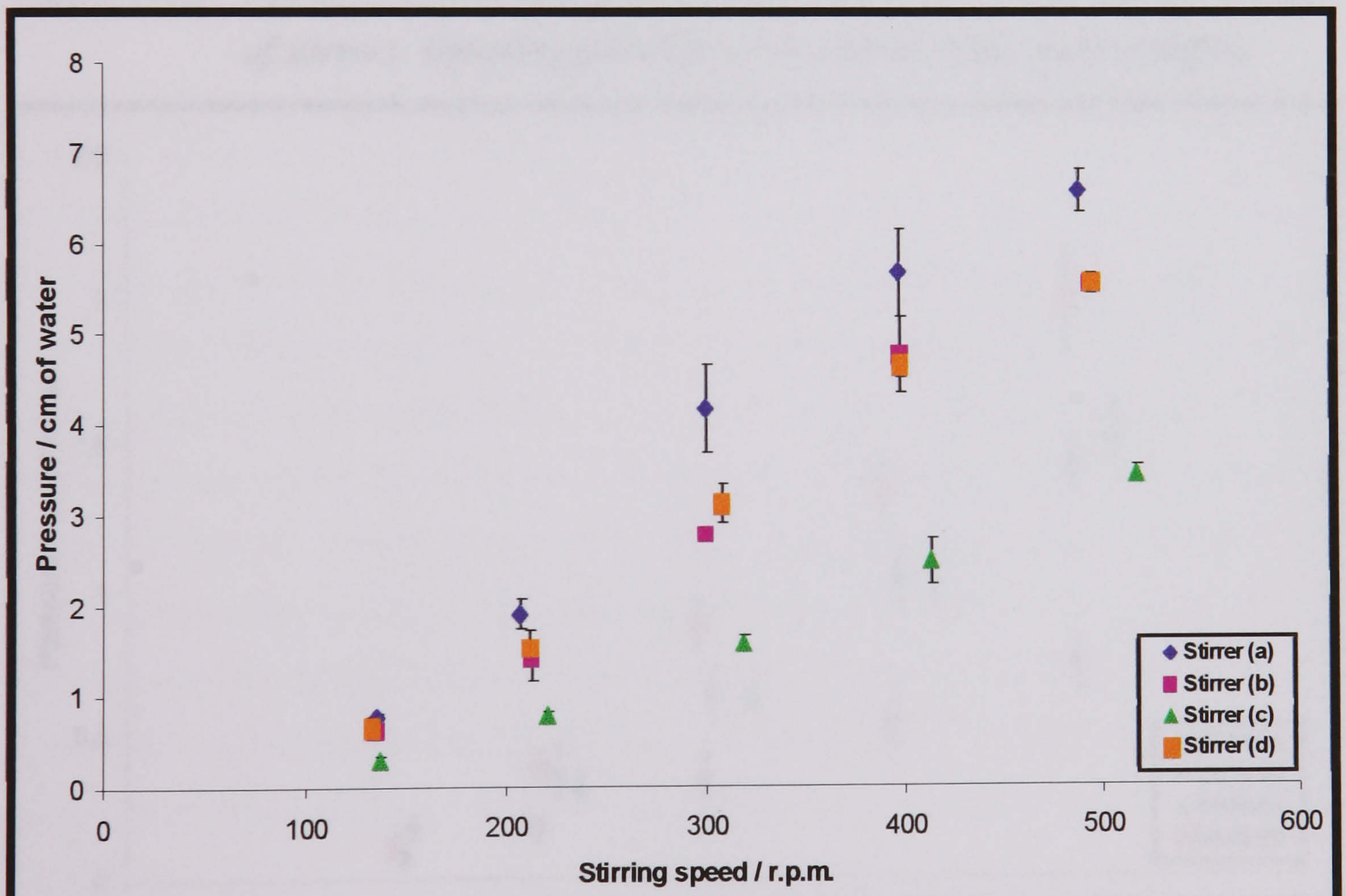

Figure 3.23. ***Pressure at the sampling point for different stirring speeds and type of stirrers: sampling point at the stirrer plane and no baffles***

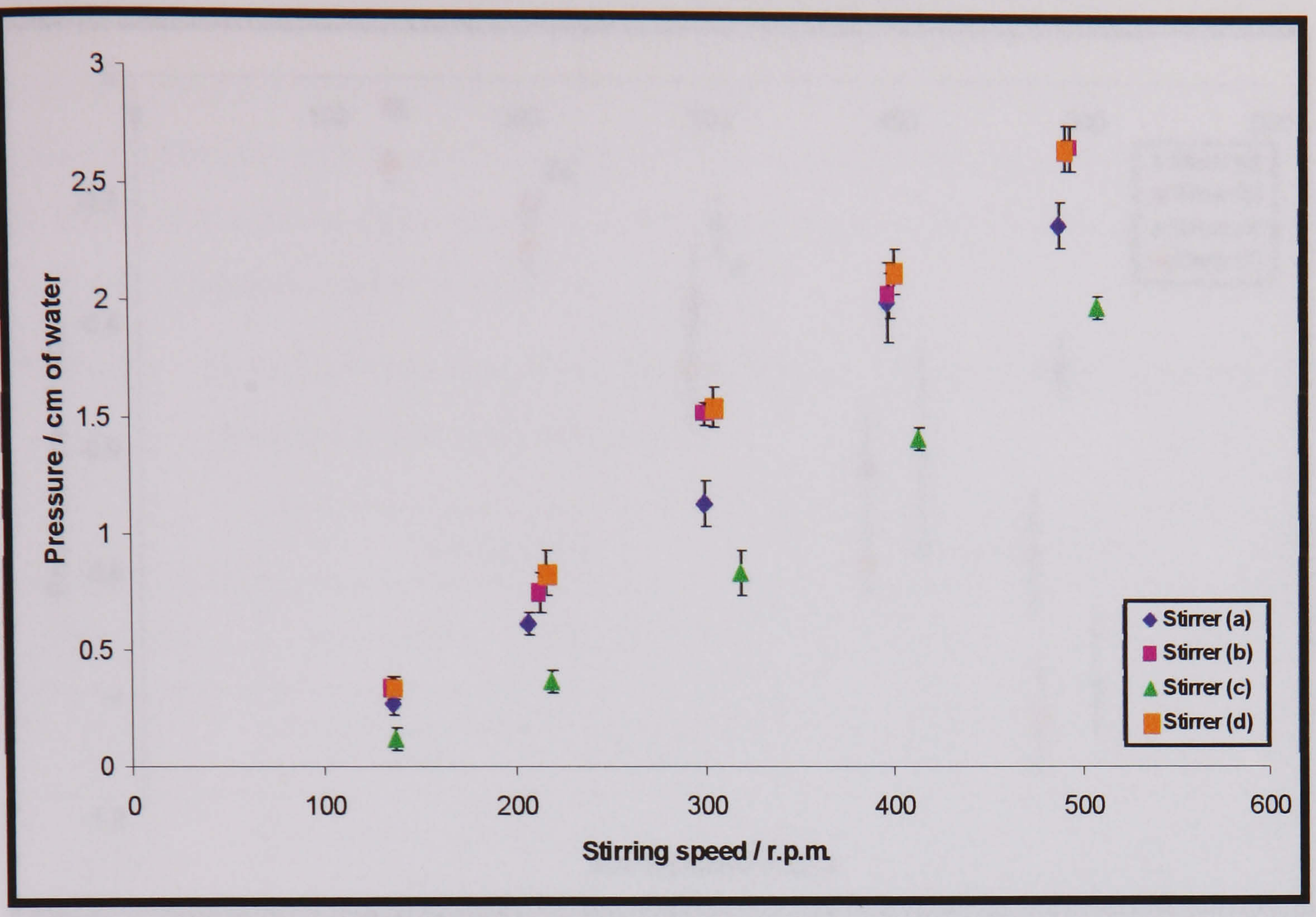

Figure 3.24. Pressure at the sampling point for different stirring speeds and type of stirrers: sampling point above the stirrer plane and no baffles

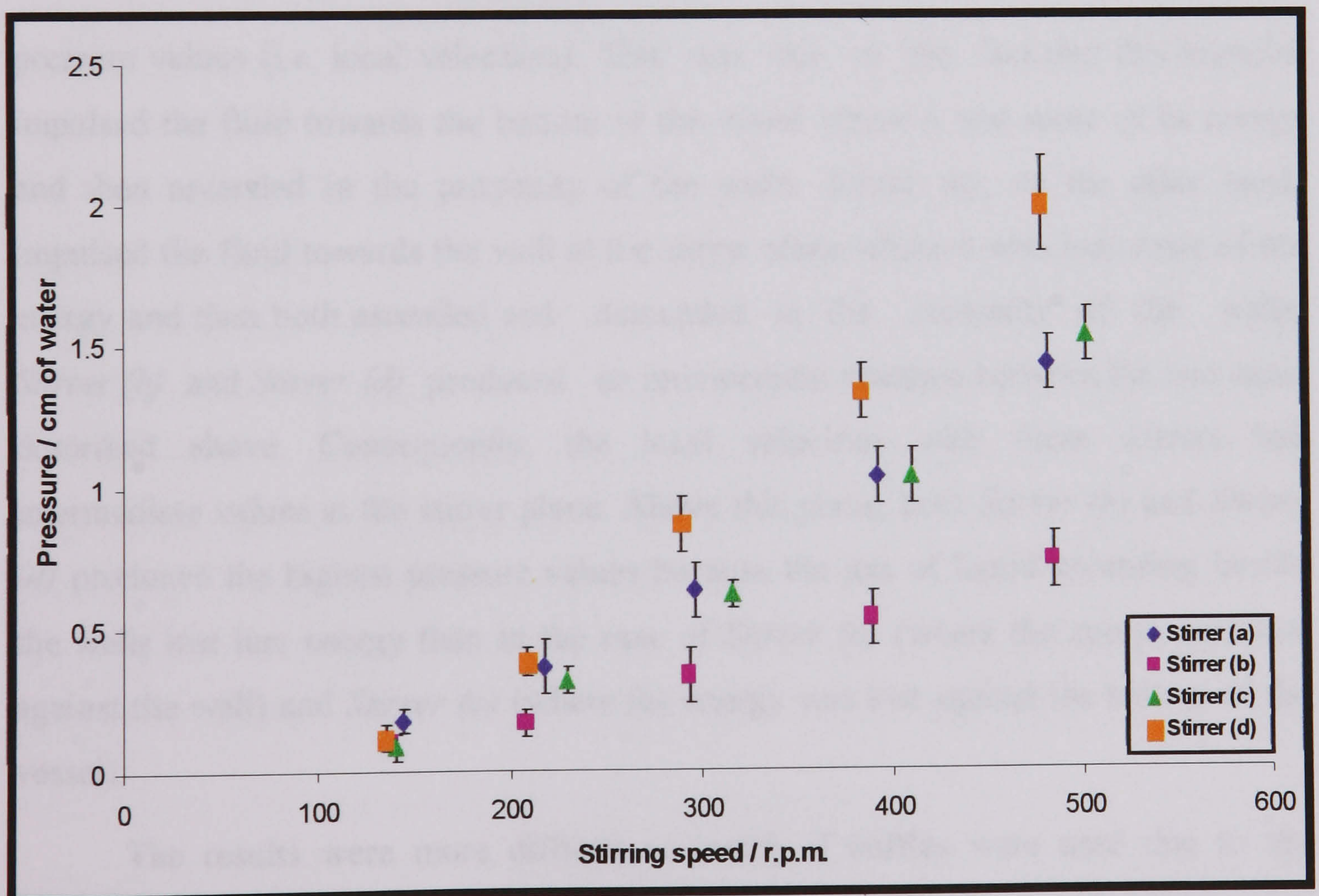

Figure 3.25. Pressure at the sampling point for different stirring speeds and type of stirrers: sampling point at the stirrer plane and with baffles

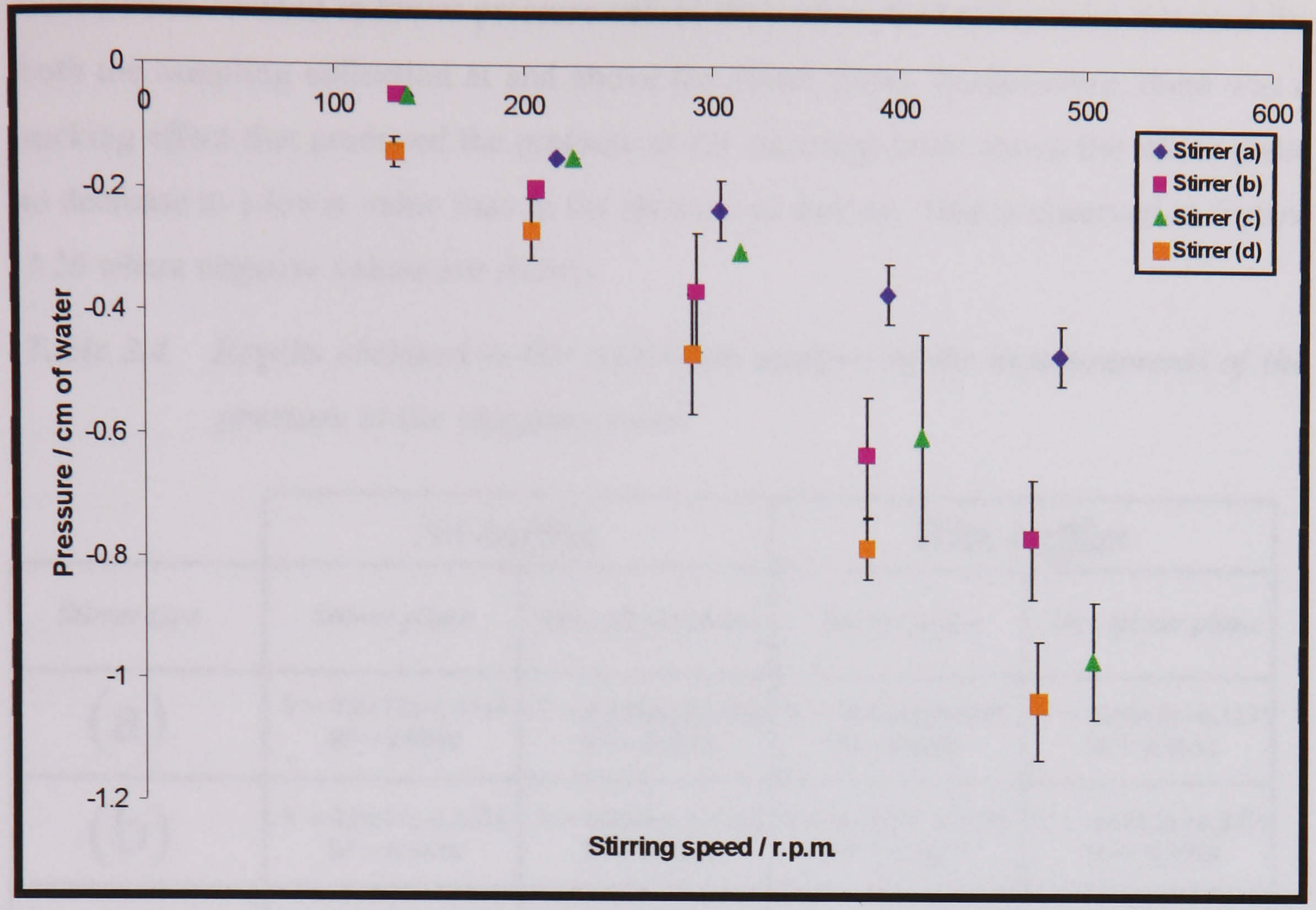

Figure 3.26. Pressure at the sampling point for different stirring speeds and type of stirrers: sampling point above the stirrer plane and with baffles

pressure values (i.e. local velocities). This was due to the fact that this impeller impulsed the fluid towards the bottom of the vessel where it lost some of its energy and then ascended in the proximity of the walls. *Stirrer (a)*, on the other hand, impulsed the fluid towards the wall at the stirrer plane where it also lost some of the energy and then both ascended and descended in the proximity of the walls. *Stirrer (b)* and *Stirrer (d)* produced an intermediate situation between the two cases described above. Consequently, the local velocities with these stirrers had intermediate values at the stirrer plane. Above this plane, both *Stirrer (b)* and *Stirrer (d)* produced the highest pressure values because the jets of liquid ascending beside the walls lost less energy than in the case of *Stirrer (a)* (where the energy was lost against the wall) and *Stirrer (c)* (where the energy was lost against the bottom of the vessel).

The results were more difficult to justify if baffles were used due to the unpredictable turbulences produced in the system. Baffles improved mixing with these variable turbulences that had the side effect of decreasing the reproducibility of the results (i.e. larger error bars). It should also be highlighted that the experiments

with baffles resulted in lower pressure values than when the baffles were not used for both the sampling collection at and above the stirrer plane. Furthermore, there was a sucking effect that produced the pressure at the sampling point above the stirrer plane to decrease to a lower value than in the absence of stirring. This is observed in *Figure 3.26* where negative values are shown.

Table 3.4. Results obtained in the regression analysis of the measurements of the pressure at the sampling point

	No baffles		***With baffles***	
Stirrer type	***Stirrer plane***	***Abv. stirrer plane***	***Stirrer plane***	***Abv. stirrer plane***
(a)	**Y = 0.0172x-1.4449 R^2 = 0.9802**	**Y = 0.0062x-0.6238 R^2 = 0.9853**	**Y = 0.0038x-0.4285 R^2 = 0.9908**	**Y = -0.0012x+0.1175 R^2 = 0.9966**
(b)	**Y = 0.0147x-1.5321 R^2 = 0.9826**	**Y = 0.0066x-0.5743 R^2 = 0.9944**	**Y = 0.0019x-0.1944 R^2 = 0.9887**	**Y = -0.0022x+0.2479 R^2 = 0.9920**
(c)	**Y = 0.0084x-1.0012 R^2 = 0.9935**	**Y = 0.0051x-0.6948 R^2 = 0.9862**	**Y = 0.0040x-0.5647 R^2 = 0.9812**	**Y = -0.0025x+0.3862 R^2 = 0.9469**
(d)	**Y = 0.0142x-1.3012 R^2 = 0.9912**	**Y = 0.0067x-0.5657 R^2 = 0.9967**	**Y = 0.0055x-0.7058 R^2 = 0.9912**	**Y = -0.0027x+0.2535 R^2 = 0.9895**

Finally, it can be mentioned that in all of the cases the pressure at the sampling point (or equivalently, the local velocity) varied linearly with the stirring speed. The mathematical expressions obtained in the linear regression analysis carried out over the results are summarised in *Table 3.4*. This table also shows the regression coefficients (R^2) obtained in the statistical analysis, which were greater than 0.98 in most of the cases. The equations in *Table 3.4* show the relationship ($\Delta h=f(r.p.m.)$) between the pressure at the sampling point and the stirring speed for each one of the conditions used in the experiments. Therefore, using these expressions the local velocity could be calculated as $v = \sqrt{2g\Delta h}$. When the velocity values were multiplied by the cross sectional area of the sampling probe (diameter = 6 mm), the sampling flow-rate conditions could be determined. When analysing the results obtained in the sampling tests, it was preferable to work with isokinetic flow-rates instead of velocities as the former is usually a control variable being monitored with a

specific type of flow-meter. *Figures 3.27* and *3.28* show how the isokinetic sampling flow-rate changed with the stirring speed when different stirrers, vessel configurations and sample locations were used.

In *Figures 3.27* and *3.28* it can be observed that at the stirrer plane almost all the data showed positive values for the flow-rate and a continuous increase when the stirring speed was incremented. However, this did not occur when sampling was produced above the stirrer plane when negative values were observed, although the absolute values always increased with the stirring speed. A positive value of the flow-rate means that the direction of the flow is towards the sampling probe. When a negative value was obtained, a suction effect was produced and the direction of the flow was opposite to the flow in the sampling probe (i.e. towards the centre of the vessel) which did not help sampling. The fact that negative values were obtained above the stirrer plane supports the configuration of the flow-streamlines

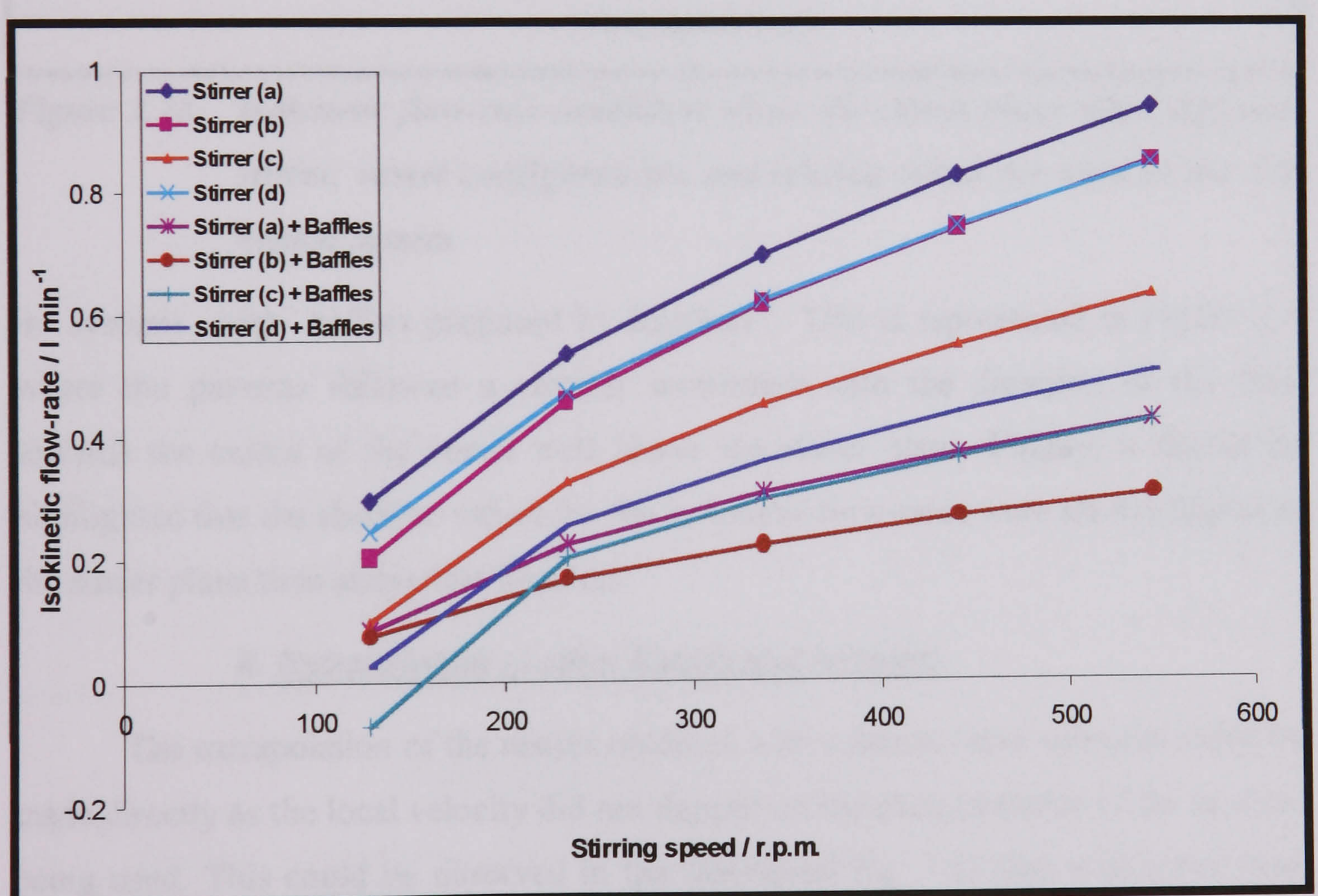

Figure 3.27. ***Isokinetic flow-rate conditions at the stirrer plane when different stirrer, vessel configurations and stirring speed are used in the 5-L beaker system***

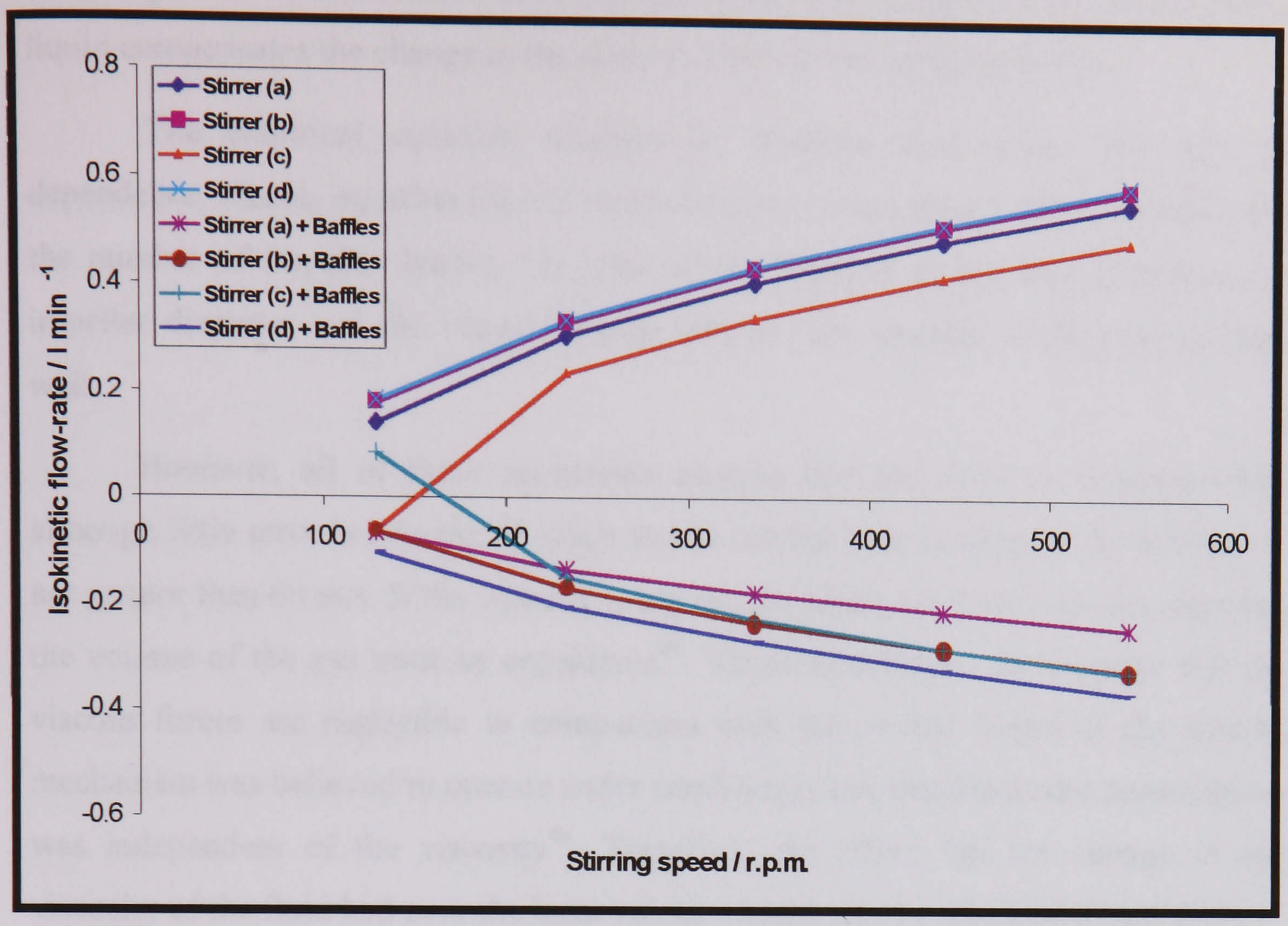

Figure 3.28. Isokinetic flow-rate conditions above the stirrer plane when different stirrer, vessel configurations and stirring speed are used in the 5-L beaker system

in systems with baffles proposed by Rushton[11]. This is represented in *Figure 3.4* where the patterns followed a circular movement with the direction of the flow towards the centre of the vessel well above the stirrer plane. Finally, it should be highlighted that the absolute values for the isokinetic flow-rates were always higher at the stirrer plane than above this location.

ii. Extrapolation to other liquids and mixtures

The extrapolation of the results obtained with water to other mixtures could be made directly as the local velocity did not depend on the characteristics of the mixture being used. This could be observed in the theoretical Eq. 3.12 that relates the local velocity with only the gravity and the reading in the manometer. If a different fluid is used, the pressure at the sampling point changes as the weight of the liquid above this point also changes. However, the kinetic energy at this point does not vary as it only depends upon the stirring speed and the stirrer configuration. Therefore, the local velocity remains unchanged with the new fluid. Also, Δh, the difference in height

of the liquid in the manometer, does not vary either as the change in the weight of the liquid compensates the change in the static pressure at the sampling point.

The empirical equation obtained by Rushton also proves this lack of dependence. Hence, equation Eq. 3.3 shows how the local velocity only depends upon the number of impeller blades, the ratio of the impeller to the tank diameter, the impeller diameter and the radial distance between the impeller blade and the tank wall.

However, all of these arguments assume that the fluid is incompressible although little error is introduced when this is not the case so long as the velocity is not greater than 60 m/s. If the velocity is higher, the relation between the pressure and the volume of the gas must be considered[86]. These conclusions also assume that the viscous forces are negligible in comparison with the inertial forces as the stirring mechanism was believed to operate under conditions such that the power consumption was independent of the viscosity[44]. Therefore, the effect that the change of the viscosity of the fluid had over the local velocity could also be considered negligible.

b) Sampling at different stirring speeds, different sampling velocities

At this stage the flows delivered by the pump in the sampling systems were defined and the isokinetic conditions were also known for the different stirring speeds. Therefore, the interesting experiments of studying how the quality of the sample varies with both the stirring speed and the sampling velocity could be carried out. The experiments were performed in the two systems mentioned above: 5-L reactor facility (preliminary tests) and 5-L beaker system (a more flexible device that allowed us to study a wider range of parameters). Besides, two different processes were analysed: systems with solids in suspension and liquid mixtures of two immiscible phases.

i. <u>Systems with solids in suspension</u>

Initially, a saturated solution of sodium carbonate in water was used for preliminary experiments in the reactor[89]. Good temperature control was crucial in these experiment as the solubility of the salt varied significantly with the temperature. The advantages of such a system were that blockages of salt in the lines were easily removable with hot water and the samples were easy to analyse by simple titration methods[89,90]. However, several disadvantages were found that led to no further use

of this process. Deposits of salt were found to block rotameters and valves very frequently as the solution touched cold surfaces while flowing in the loop. In addition to this, the grow of crystals in small cavities present at the bottom and side ports in the reactor was a potential cause of breaks in the glass surface.

A process was chosen using a low concentration suspension of small glass beads in water. The results obtained in some preliminary tests in the reactor system[89] are shown in *Figure 3.29*. In this test, the sampling velocity was varied using the same constant stirring speed. The mixture was a 0.75 % (weight/weight) suspension of glass beads (425-600 μm diameter) in water. Three replicate experiments were performed at identical conditions. The scattering in the results was found to be due to the presence of dead volumes and changes in the direction of the flow inside the sampling loop. When some of the changes in direction (two elbows and one tee) and dead volumes (in the sampling port being the samples collected at the return point) were removed from the sampling line, the results plotted in *Figure 3.30* were

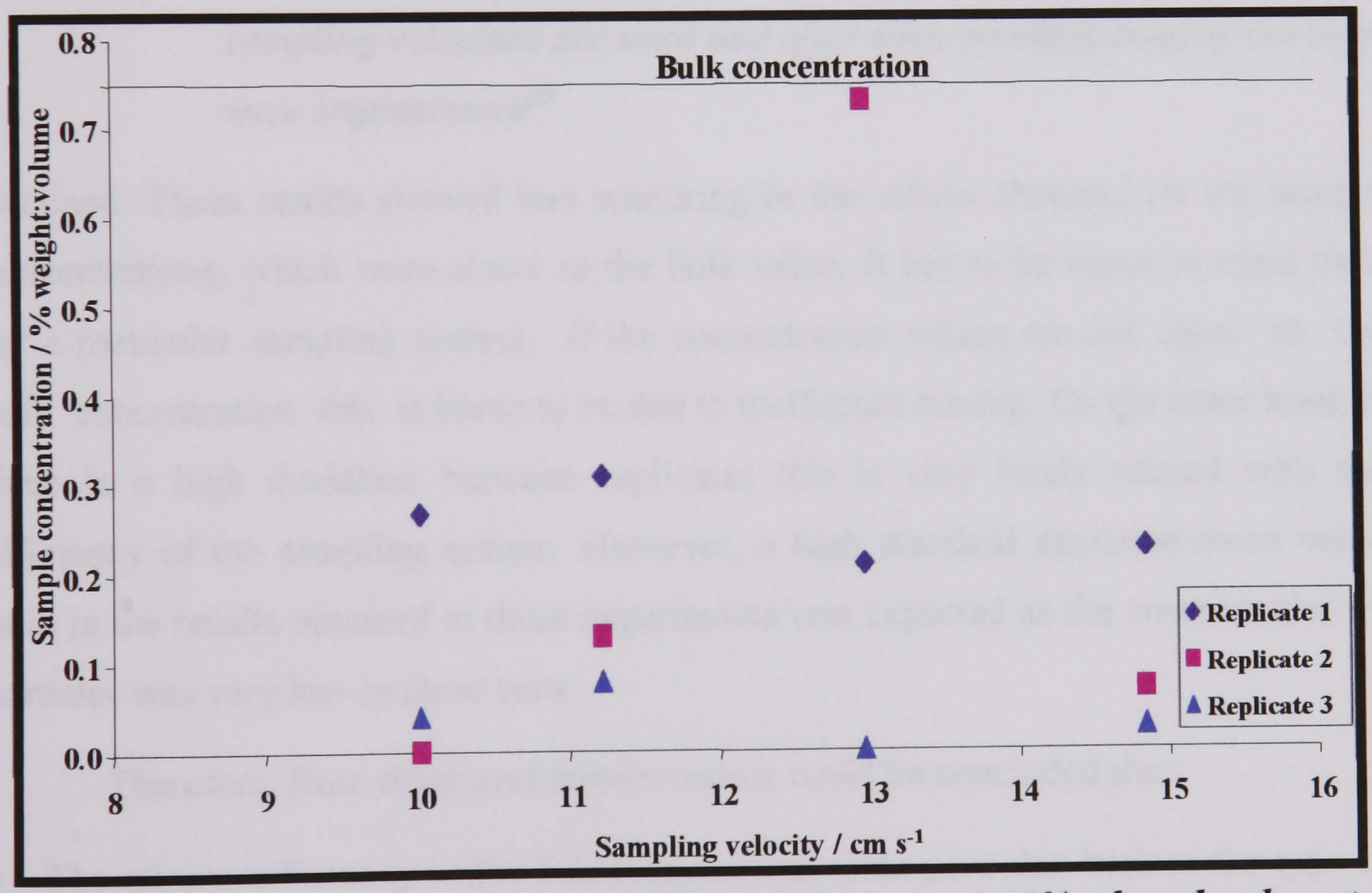

Figure 3.29. Percentage recovery of glass beads for a 0.75% glass beads-water mixture for three replicates of the same experiment when different sampling velocities are used[89]

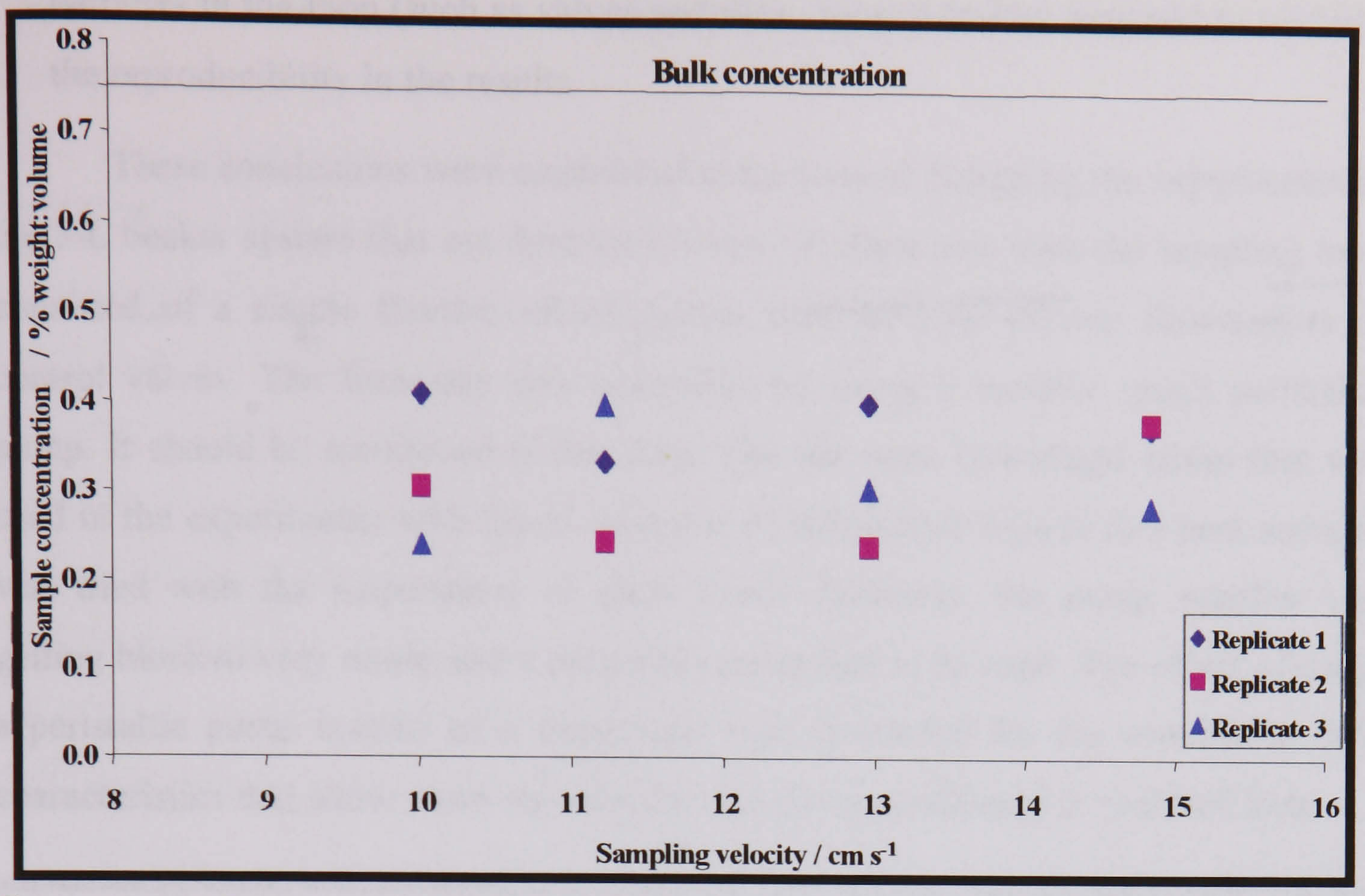

Figure 3.30. Percentage recovery of glass beads for a 0.75% glass beads-water mixture for three replicates of the same experiment when different sampling velocities are used and after some modifications in the loop were implemented[89]

obtained. These results showed less scattering in the values obtained for the sample concentrations, which were closer to the bulk value. It has to be borne in mind that, for a particular sampling system, if the concentration values are not equal to the bulk concentration this is likely to be due to inefficient mixing. On the other hand, if there is a high deviation between replicates this is very likely related with the efficiency of the sampling system. However, a high standard deviation-mean value ratio in the results obtained in these experiments was expected as the concentration of particles was very low in these tests.

Therefore, from these preliminary tests it could be concluded that:

- The mixing efficiency in the 5-L reactors was quite poor due both to the type of stirrer used in the experiment (type flat 2-blade) and to the configuration of the vessels (with no baffles).
- The design of the sampling loop had to be improved in order to enhance the precision in the sampling experiments. Any unneeded obstacles to the free flow of

particles in the loop (such as valves and flow-meters) had be removed to increase the reproducibility in the results.

These conclusions were considered at the time of designing the experiments in the 5-L beaker system that are described below. In these new tests the sampling loop consisted of a simple flexible silicon rubber tube with no elbows, flow-meters or control valves. The flow-rate was controlled by using a variable speed peristaltic pump. It should be mentioned at this stage that the same centrifugal pump that was used in the experiments with liquid mixtures of immiscible liquids (see next section) was tried with the suspensions of glass beads. However, the pump impeller was getting blocked very easily and a peristaltic pump had to be used. The effect of using a peristaltic pump instead of a centrifugal type (preferred for the continuous flow characteristics that allow more reproducible sampling conditions) is analysed later.

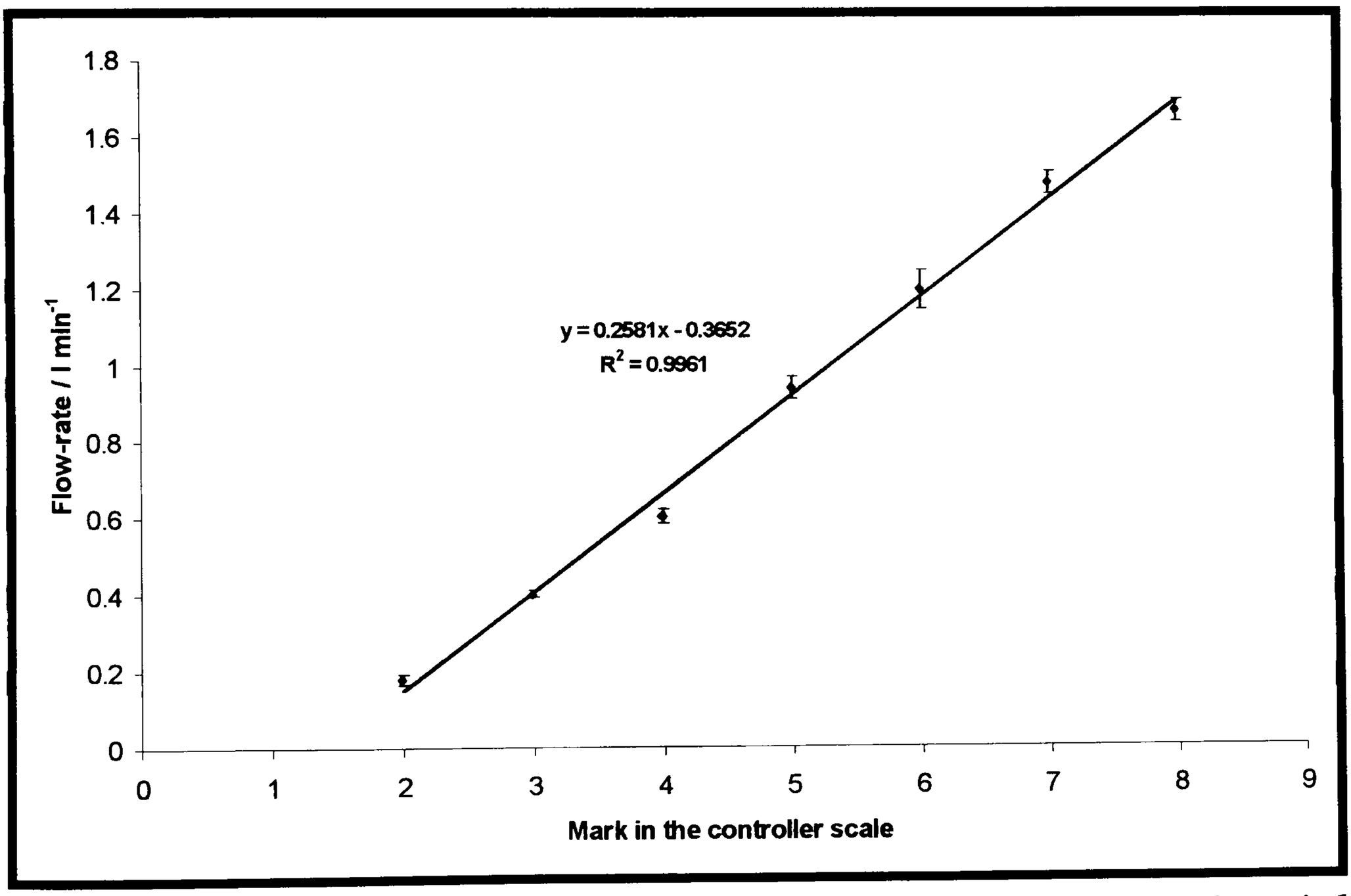

Figure 3.31. Calibration relationship for water only when the flow-rate is varied using the different marked positions in the peristaltic pump speed controller

The first stage in the tests related with the physical modelling of the sampling system is always the calibration of the device in terms of flow-rate. In other words, as the use of a flow-meter was avoided in the line, the way the flow-rate varied with

position of the flow regulator in the pump needed to be defined. By doing this, the sampling velocity was known for each condition used in the experiments. In these calibration experiments, the flow-rates delivered by the pump were measured (as volume in a certain period of time) for the different marks in the flow regulator. This was performed using 3 litres of water only as the presence of glass beads was not found to affect the flow-rate controlled by the regulator. Furthermore, the stirrer speed was varied in these experiments to analyse its effect in the control of the flow-rate. Also, the effect of different stirrers and the presence and absence of baffles was also studied. However, neither the stirrer, nor the stirrer speed and the presence of baffles were found to affect the results obtained in the calibration experiment and therefore the intrinsic capability of the system to control the flow-rate. *Figure 3.31* shows the calibration results and how the flow-rate (i.e. the sampling velocity considering the diameter of the sampling line used in the system) changed with the mark position in the flow regulator.

Once the conditions for the sampling experiments were perfectly defined, the tests related with the physical modelling of the sampling system could be performed. In these experiments, the quality of the samples obtained using the sampling line were studied for different concentration of beads and values of the sampling velocity. First, a set of experiments were performed at different sampling velocities, stirring conditions and stirrer configurations in order to assess the best conditions for reproducible sampling. This was carried out using 3 litres of a 1% glass beads-water mixture and sampling from the two points, at the stirrer plane and above the stirrer plane. *Stirrer (a)* and *Stirrer (c)* with and without baffles were used as they produced the best mixing conditions, as will be shown later with the experiments with mixtures of immiscible liquids. Using the conclusions extracted from these experiments, another test was performed at the optimum conditions determined for the calibration of the sampling system. Different concentrations of mixtures glass beads-water were used in this experiment.

The results of the preliminary experiments to define the best sampling conditions are shown in *Figures 3.32* and *3.34*. The analysis of the precision in the results is shown in *Figures 3.33* and *3.35* where the %RSD is plotted for the triplicate experiments carried out in different conditions.

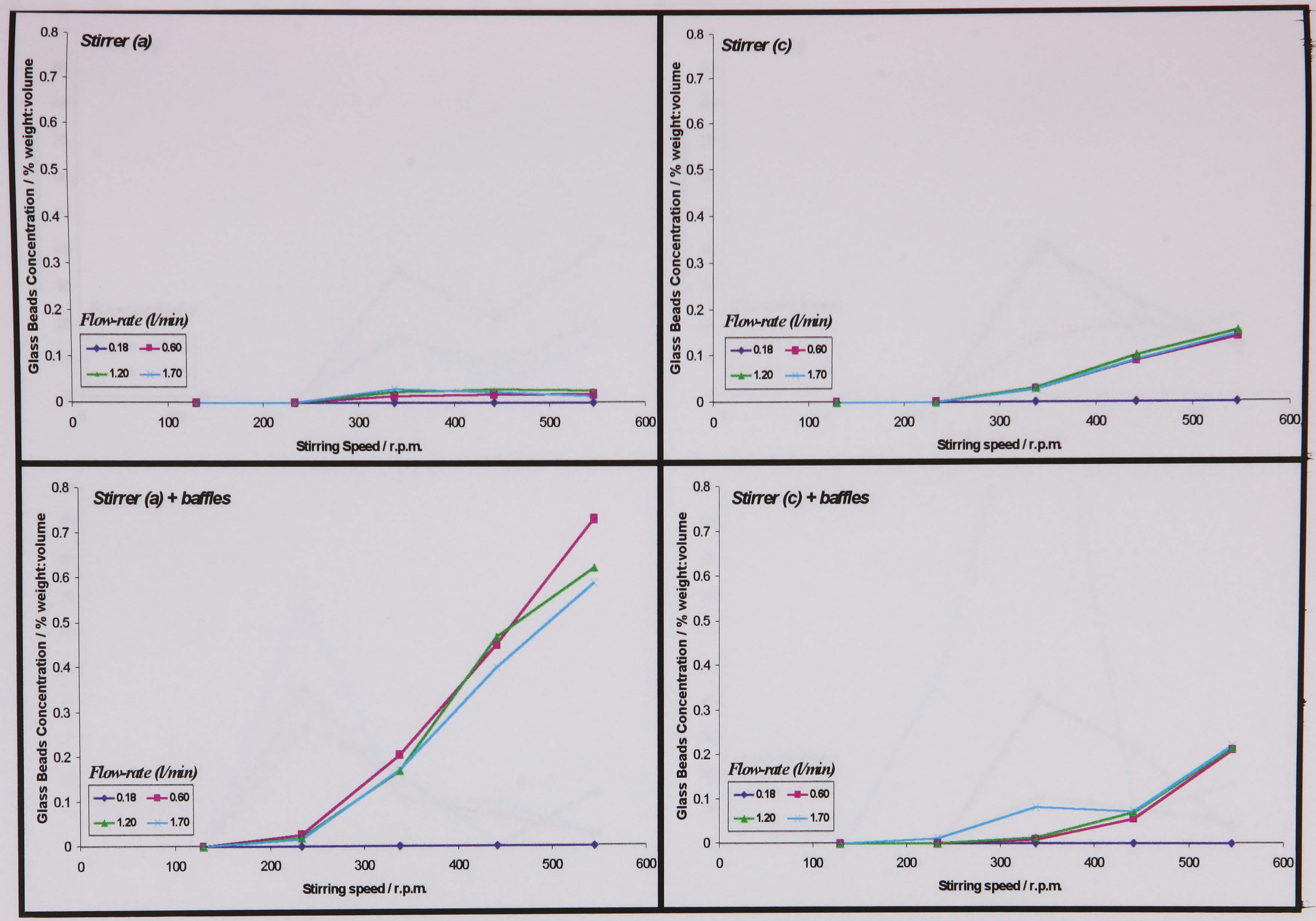

Figure 3.32. Quality of the samples (1% glass beads in water) collected at the stirrer plane and at different stirring speeds when different stirrers, vessel configurations and sampling flow-rates were used

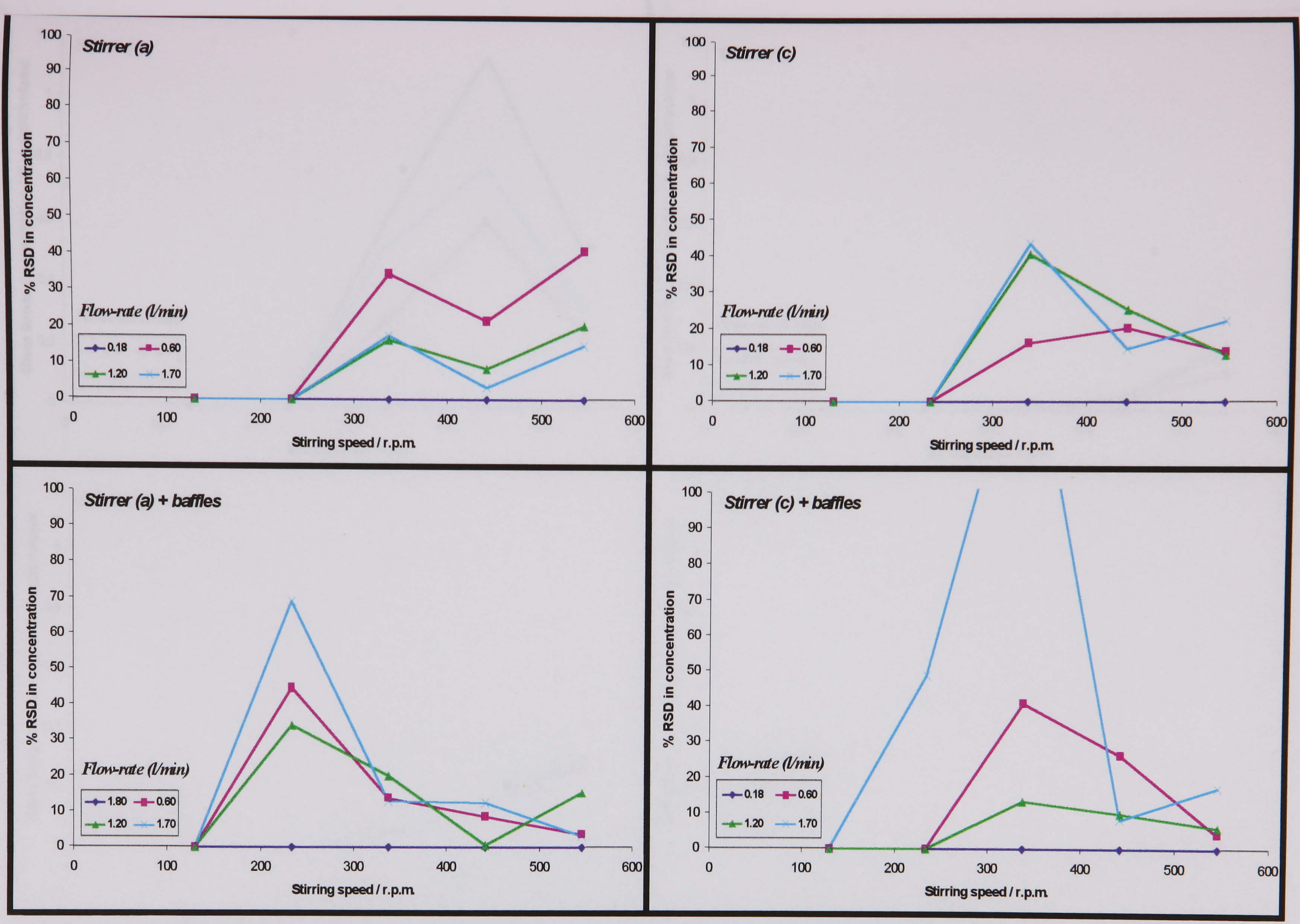

Figure 3.33. %RSD in the sample collection (1% glass beads in water) at the stirrer plane and at different stirring speeds ***when*** *different stirrers, vessel configurations and sampling flow-rates were used*

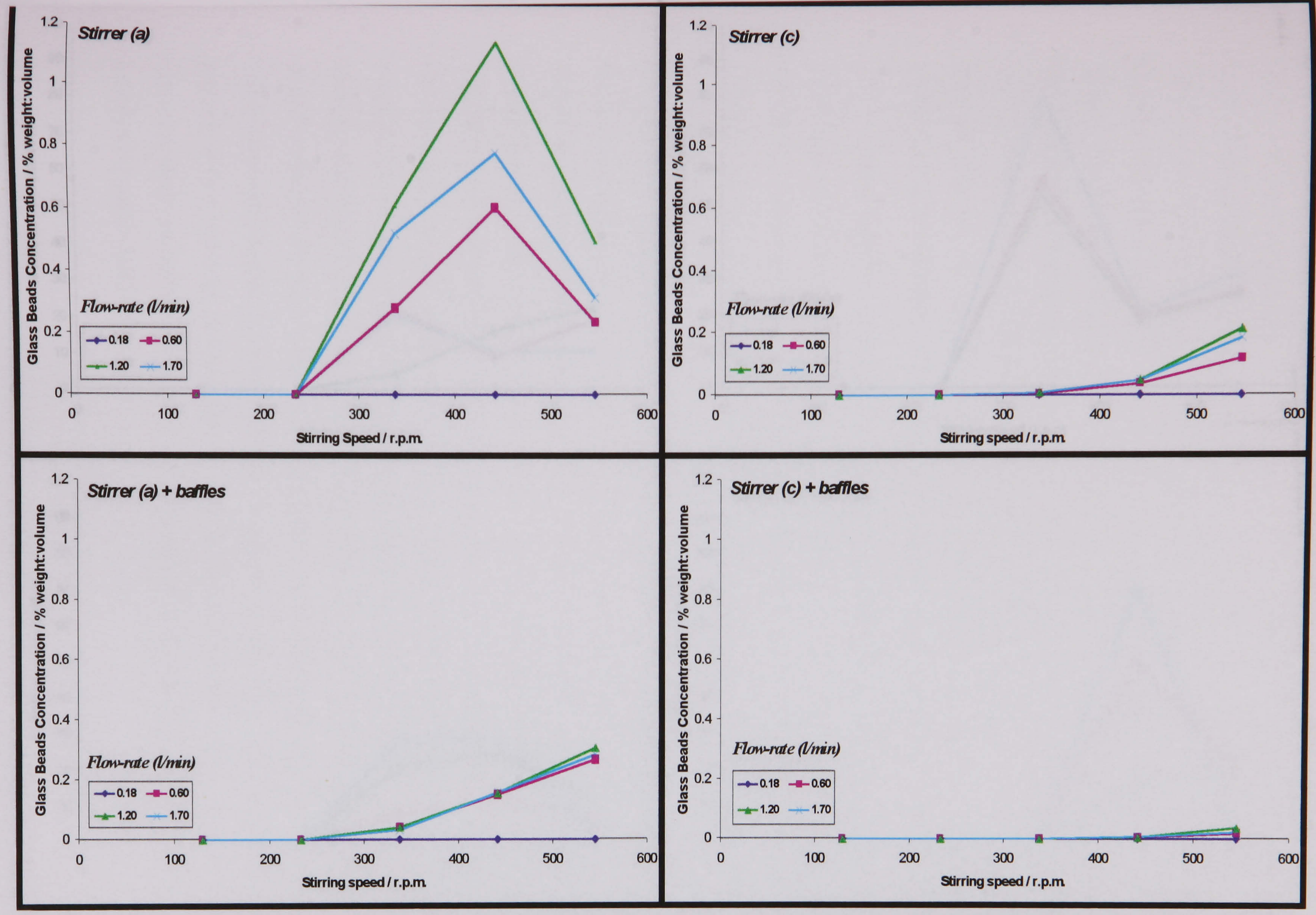

Figure 3.34. Quality of the samples (1% glass beads in water) collected above the stirrer plane and at different stirring speeds when different stirrers, vessel configurations and sampling flow-rates were used

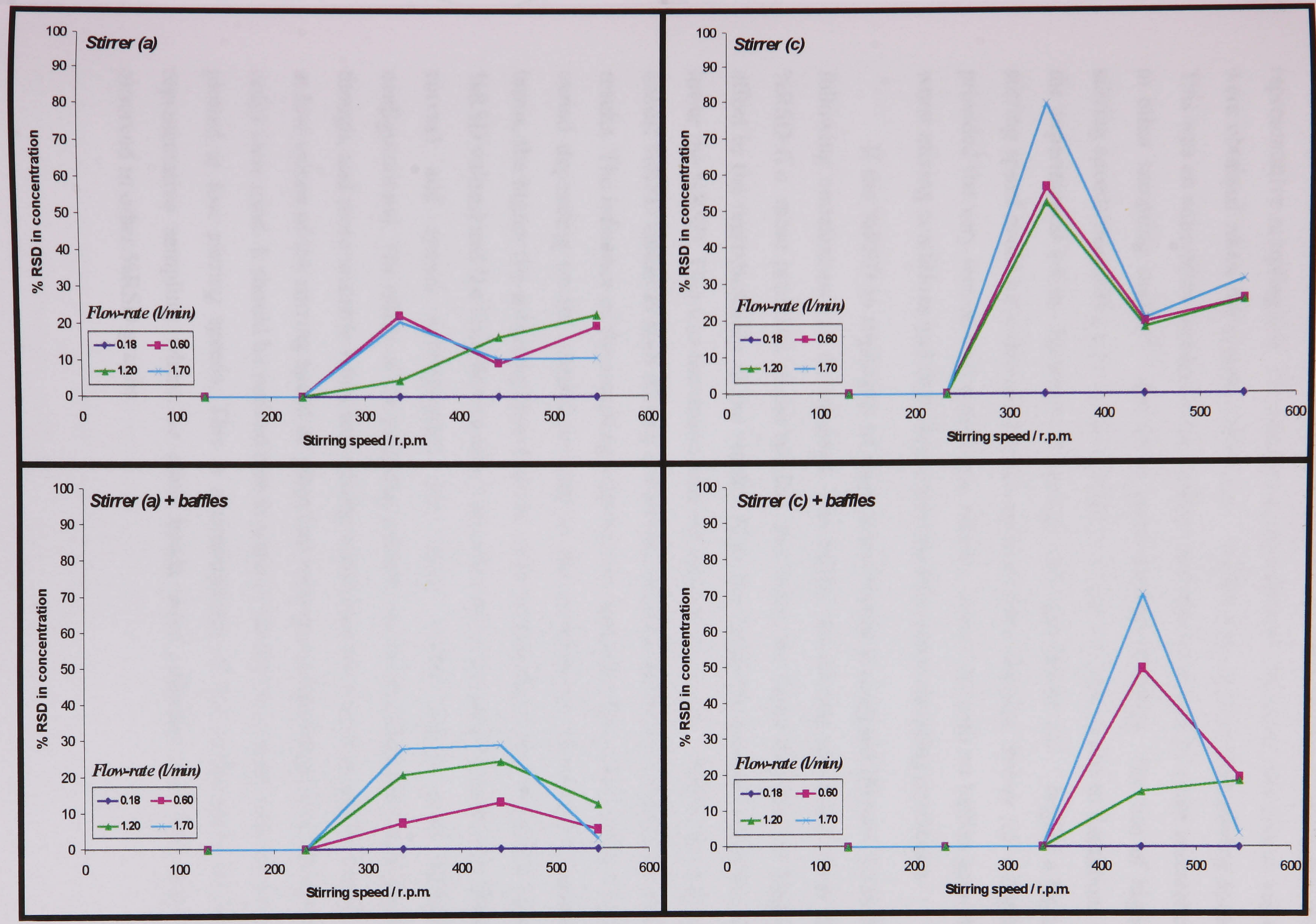

Figure 3.35. %RSD in the sample collection (1% glass beads in water) above the stirrer plane and at different stirring speeds when different stirrers, vessel configurations and sampling flow-rates were used

In *Figure 3.32* it can be observed that the type of stirrer and vessel configuration had a more important effect on the sample collection than the sampling flow-rate. In none of the situations and conditions used in the experiments, was representative sampling (i.e. 1% concentration) achieved. However, the closest values were obtained when the system *Stirrer (a)* + *baffles* was used at high stirring speed. This was an equivalent system to the Rushton impeller type used by other researchers in other sampling studies[4,11] due to its good mixing efficiency. The use of higher stirring speeds than 600 r.p.m. was not feasible in our 5-L system due to limitations in the experimental set-up. However, it appears that with *Stirrer (a)* + *baffles* a higher stirring speed could have delivered more representative samples. *Stirrer (c)* + *baffles* provided the very second best conditions. Finally, *Stirrer (a)* with no baffles gave the worst mixing conditions and therefore it provided the worst sampling conditions.

If the %RSD in triplicates of these experiments is analysed (*Figure 3.33*) the following conclusions can be reported. The higher the stirring speed the lower the %RSD (i.e. more precision in the results), this being the factor that has the biggest effect in the reproducibility of the results. Also, the better the mixing conditions the lower the %RSD. This was the reason why the system *Stirrer (a)* + *baffles* showed the lowest %RSD values at high stirring conditions whereas *Stirrer (a)* showed the worst results. The influence of the sampling velocity (i.e. sampling flow-rate) on the %RSD varied depending on the conditions used in the experiments. However, in general terms, the higher the sampling flow-rate the more precise the results were (i.e. lower %RSD values) and the less these results were affected by the stirring speed (i.e. flatter curves) and system configuration (i.e. more similar values with different configurations). The effect of the sampling velocity on the reproducibility was greater though, and more unstable when bad mixing conditions were used as can be observed at low values of the stirring speed or when bad mixing configurations (e.g. *Stirrer (a)* only) were used. It should be noticed that in some of the %RSD results zero values are plotted at low stirring speeds. This is a consequence of the reproduction of non-representative sampling where no glass beads were collected and will also be observed in other %RSD graphs.

When the samples were collected from the port above the stirrer plane similar conclusions were obtained (see *Figure 3.34*). *Stirrer (a)* + *baffles* provided the most stable conditions in terms of variation with the flow-rate and representativeness of the sample. It must be highlighted that the system with only *Stirrer (a)* provided concentration values higher than expected showing that its capacity to lift the glass beads was high. These values also show a parabolic trend that varies greatly with the sampling flow-rate. This shows that the agitation with *Stirrer (a)* showed an optimum value at around 450 r.p.m. At higher values of the stirring speed the glass beads possibly lost some kinetic energy by impacting against the walls and were not lifted as much. This would therefore explain the decrease in the concentration values above 450 r.p.m.

If the %RSD values are studied (*Figure 3.35*), the most stable conditions with respect to the stirring speed and also the lowest %RSD values were observed with the system *Stirrer (a)* + *baffles*. *Stirrer (a)* also showed quite a flat curve with relatively low %RSD values. However, as has been previously mentioned, this system was not as stable as *Stirrer (a)* + *baffles* when the sampling flow-rate was varied.

Therefore, these results led to the conclusion that the system *Stirrer (a)* + *baffles* was the one that provided the most balanced conditions in terms of representativeness, mixing and reproducibility in the results. So, this was the system of choice for the analysis of the calibration of the sampling system, where different concentrations of glass beads-water mixtures were used. The results have also shown agreement with the results obtained by previous researchers in the sense that the Rushton turbine was found to be the best system to provide good suspensions for sampling experiments[4,11]. However, no representative sampling (i.e. sample concentration = 1 %) was obtained at sub-, super- or isokinetic conditions. Indications that very high stirring speeds should be used in order to achieve this has been shown. The result also showed that, although the sampling velocity had an effect on sampling, the mixing conditions (i.e. type of stirrer and configuration of the vessel) played a more important role in sampling. Therefore, when designing sampling systems, great attention must be paid to the configuration of the system. Once the good mixing properties were ensured, the sample location and orientation of the probe had the second biggest influence on sampling. Finally, sampling velocity had the least

important effect and superisokinetic conditions usually guaranteed high reproducibility and representativeness in the results.

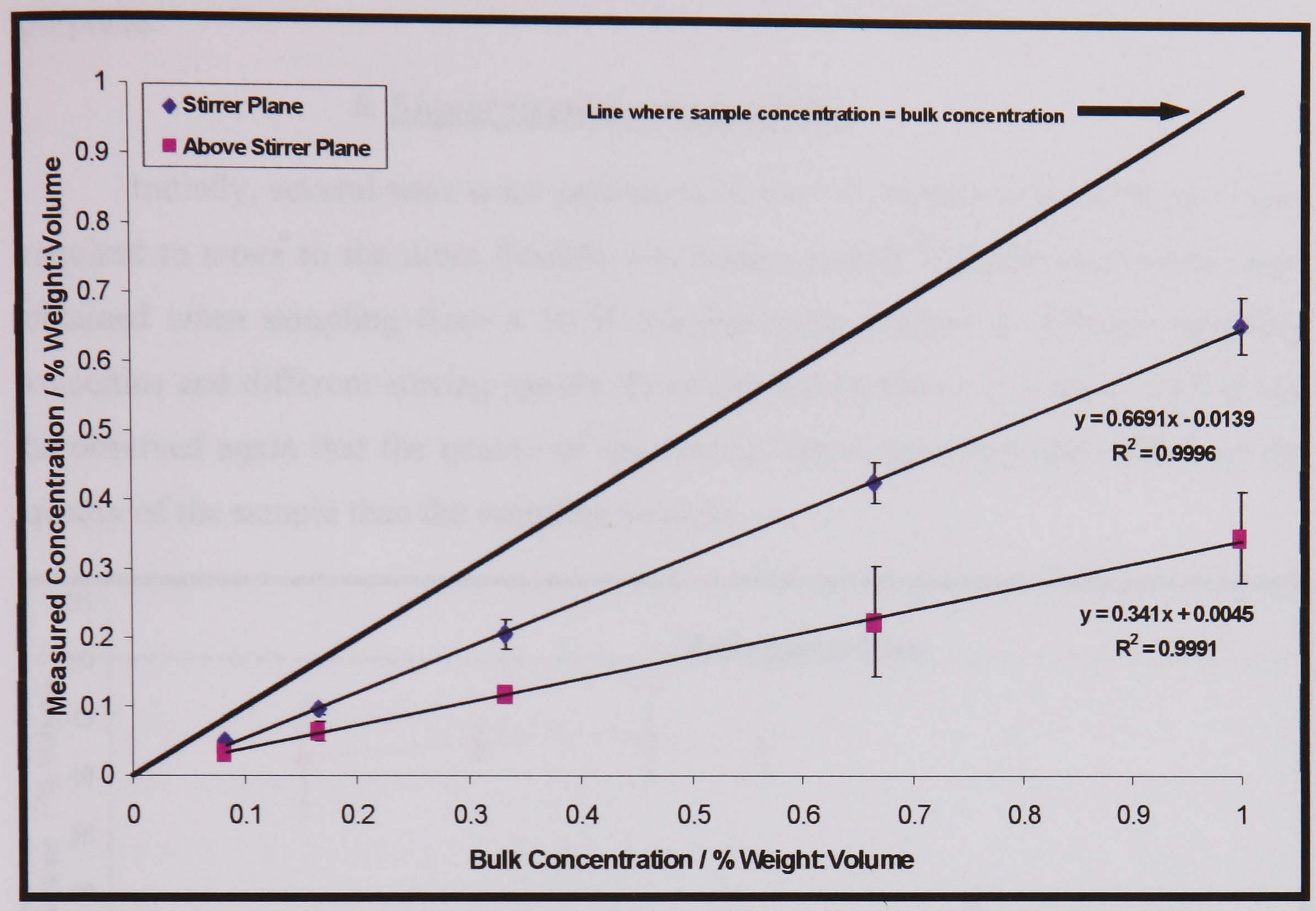

Figure 3.36. Sample concentration values for sampling experiment at and above the stirrer plane, in the stirrer (a) + baffles system and for different bulk concentrations of glass beads in water between 0 and 1 % weight:volume

Based on these considerations, the calibration experiment was performed at 1.70 l/min (highest sampling flow-rate used in the experiments) from 3-L of a mixture of glass-beads and water in different concentrations. The system used was *Stirrer (a) + baffles*. The results obtained in the calibration test are plotted in *Figure 3.36*. The results showed that, although representative sampling was not achieved in any of the sampling conditions, a robust calibration was possible for both sampling at and above the stirrer plane. It is also observed that in both cases the sample concentration values were lower than the true value or bulk concentration. When sampling above the stirrer plane, the concentration values were lower due to the patterns of the streamlines, directed towards the centre of the vessel opposite to the sampling direction[11]. Moreover, the local concentration of solids tended to decrease as the height increased due to the weight of the particles. This agreed with the concentration profiles reported

by other authors[16]. Finally, the error bars were bigger when sampling above the stirrer plane. This also showed that the port at the stirrer plane was preferable for sampling purposes.

ii. Liquid mixtures of two phases

Initially, several tests were performed in the 5-L reactor system before it was required to move to the more flexible 5-L beaker system[89]. Interesting results were obtained when sampling from a 50:50 toluene-water mixture at different sampling velocities and different stirring speeds. From the results shown in *Figure 3.37*, it can be observed again that the quality of the stirring had a more important effect on the quality of the sample than the sampling velocity.

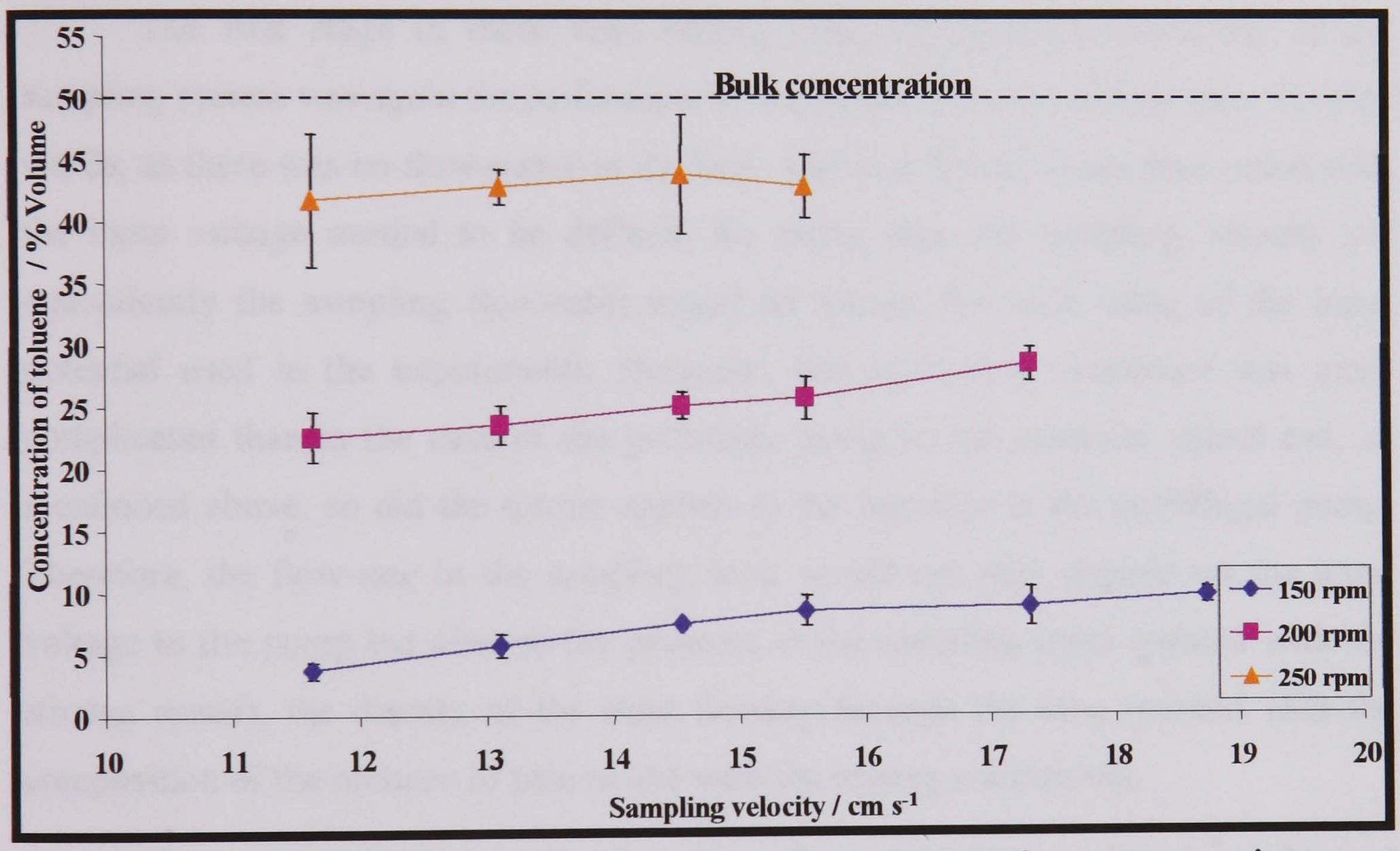

Figure 3.37. Percentage recovery of toluene for a 50:50 toluene-water mixture at 60°C when different sampling velocities and stirring speeds were used[89]

Similar experiments to those described above with glass beads were performed in the 5-L beaker system for different mixtures of immiscible oil (oil for heat transfer, from Across Organics, Cat. No. 26877-0025) in water. The oil (with a similar density to toluene) was used instead of toluene to avoid any toxic smells in the beaker which, unlike the 5-L system, was an open system. Initially, a centrifugal pump (see Appendix 4 for details) was used in the sampling loop implemented in this system.

However, in later experiments, the same centrifugal pump as used in the test with the glass beads was used for comparison in the results. The flow-rate in the system with the centrifugal pump was controlled by varying the input potential to the pump via a home-made voltage regulator (within the range 0-220 V). The main advantage of this method is that it avoided the use of needle valves in the line that are obstacles to the free flow of the heterogeneous mixture and can easily block the lines. The disadvantage of this way of controlling the flow-rate was that the change in voltage not only produced a variation in the speed of the pump impeller but it also varied its torque[91]. Therefore, this may mean that, at low voltages, the torque being delivered would not be sufficient to achieve the flow of highly viscous fluids. In fact, this was observed in some of the results presented below as will be seen later.

The first stage in these tests related with the physical modelling of the sampling system was again the calibration of the device in terms of flow-rate. In other words, as there was no flow-meter in the line, the way the flow-rate was varied with the input voltage needed to be defined. By doing this, the sampling velocity (or equivalently the sampling flow-rate) would be known for each value of the input potential used in the experiments. However, this calibration procedure was more complicated than in the case of the peristaltic pump as the potential varied and, as mentioned above, so did the torque applied to the impeller in the centrifugal pump. Therefore, the flow-rate in the sampling loop would not only depend on the input voltage to the pump but also on the pressure at the sampling point (related with the stirring speed), the density of the fluid flowing through the loop (related with the composition of the mixture of phases and with the mixing conditions).

Figure 3.38 shows how the flow-rate of water in the sampling loop changed when the input voltage was varied in the centrifugal pump and when different stirring speeds and system configurations were used. It therefore reflects the effect that the pressure conditions at the sampling point had over the flow-rate delivered by the pump. It can be observed that as the stirring speed increased, the flow-rate tended to decrease for all of the configurations except *Stirrer (c) + baffles*. However, this was believed to be due to air bubbles entering into the sampling probe through the deep vortices that was formed at high stirring speeds rather than to the change in pressure

conditions. Visual observations confirmed this and agreed with the fact that the system *Stirrer (c)* + *baffles* did not show any vortices during mixing.

Figure 3.39 shows how the flow-rate of a 50% oil-water mixture in the sampling loop changed when the input voltage was varied in the centrifugal pump and when different stirring speeds and system configurations were used. Therefore, the effect of using a heterogeneous mixture and the quality of the mixing of the two phases over the flow-rate delivered by the pump were analysed. In fact, the mixing conditions make a change in the density of the fluid that flows through the loop and hence the flow-rate being delivered by the centrifugal pump. Again, it was observed that as the stirring speed increased, which increased the ratio of oil (lighter phase) in the mixture, the flow-rate tended to decrease in all of the configurations. Similar to the case of water being mixed with trapped air, increasing the amount of oil entering the loop changed the density and viscosity of the mixture inside the sampling device. This affected the flow-rate as the results show in all of the plots represented in *Figure 3.39*.

Figure 3.40 shows how the flow-rate of different oil-water mixtures in the sampling loop changed when the input voltage was varied in the centrifugal pump and when different system configurations were used. Therefore, the effect of using different heterogeneous mixtures over the flow-rate delivered by the pump was analysed in this test. The stirring speed used was 550 r.p.m. in all of the tests. As can be observed, this had a similar effect to the mixing conditions factor mentioned above. In fact, the change in composition also produced a variation in the density of the fluid that flowed through the loop and therefore the flow-rate being delivered by the centrifugal pump. Again, increasing the amount of oil entering the loop changed the density and viscosity of the mixture in the sampling device in such a way that the flow-rate decreased.

The information extracted from these results could be used to determine the flow-rate present in the loop when the input potential to the pump was changed and depending on the stirrer and vessel configuration used in the experiment. However, it should be highlighted that these tests were performed at the stirrer plane and no

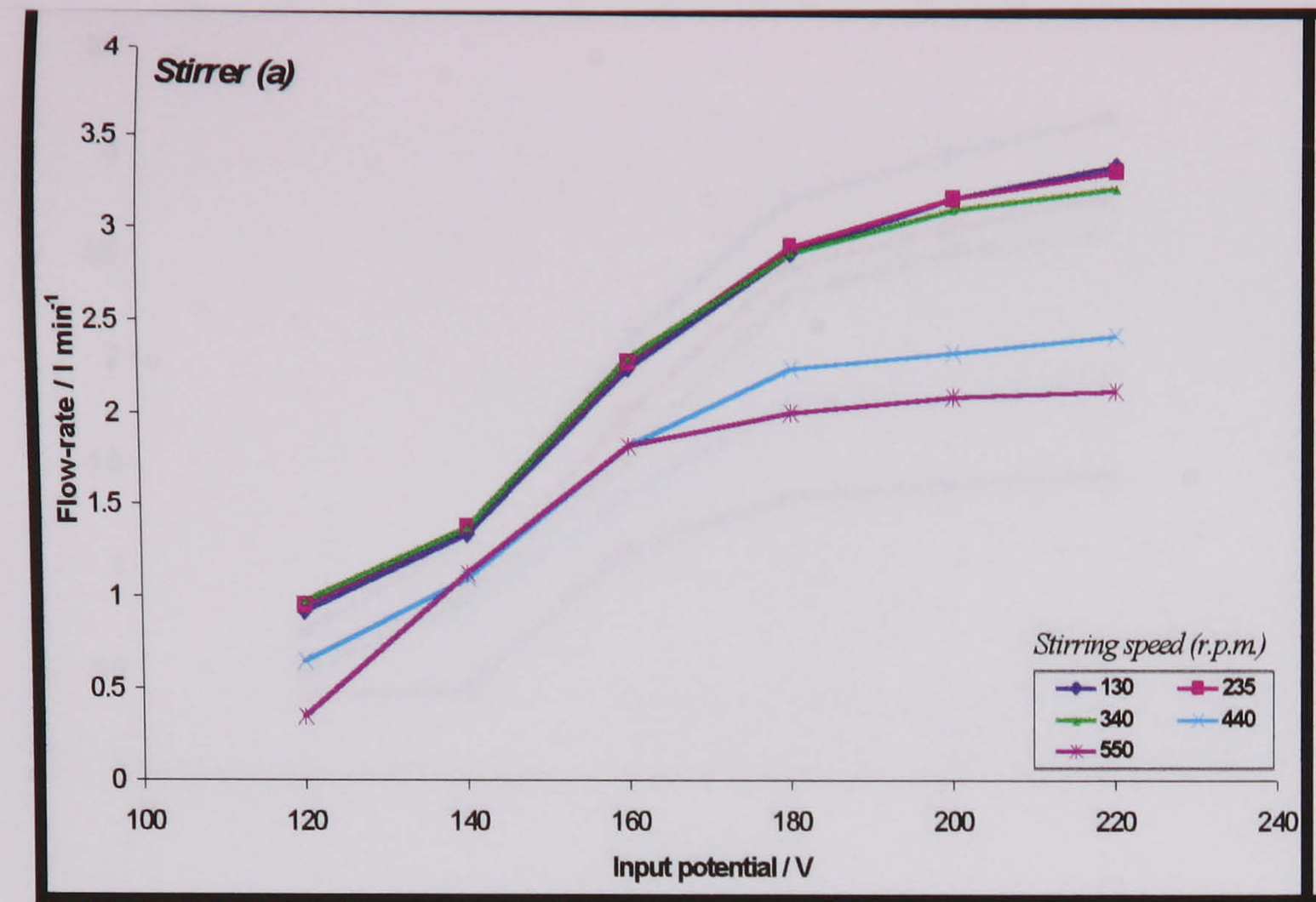

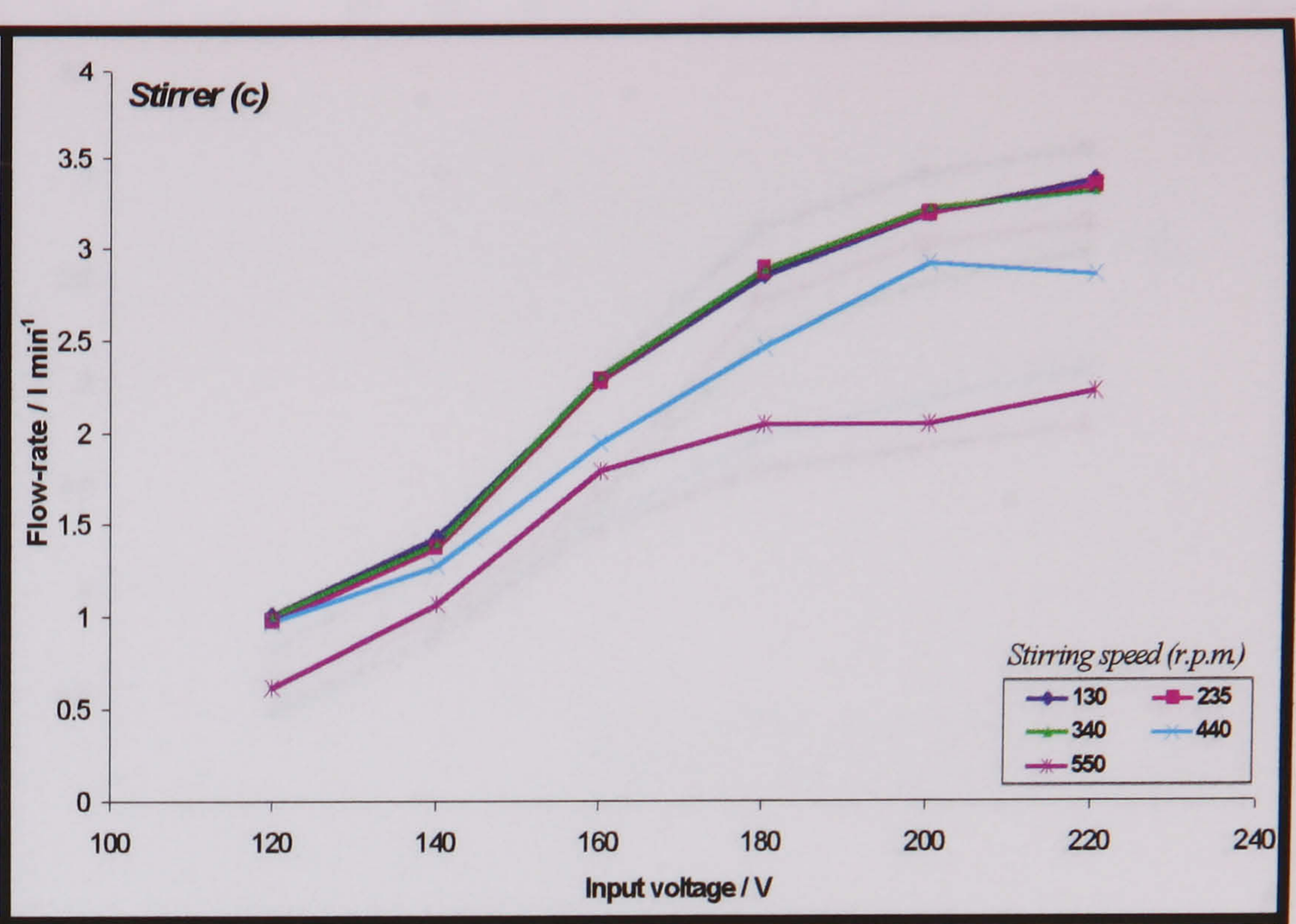

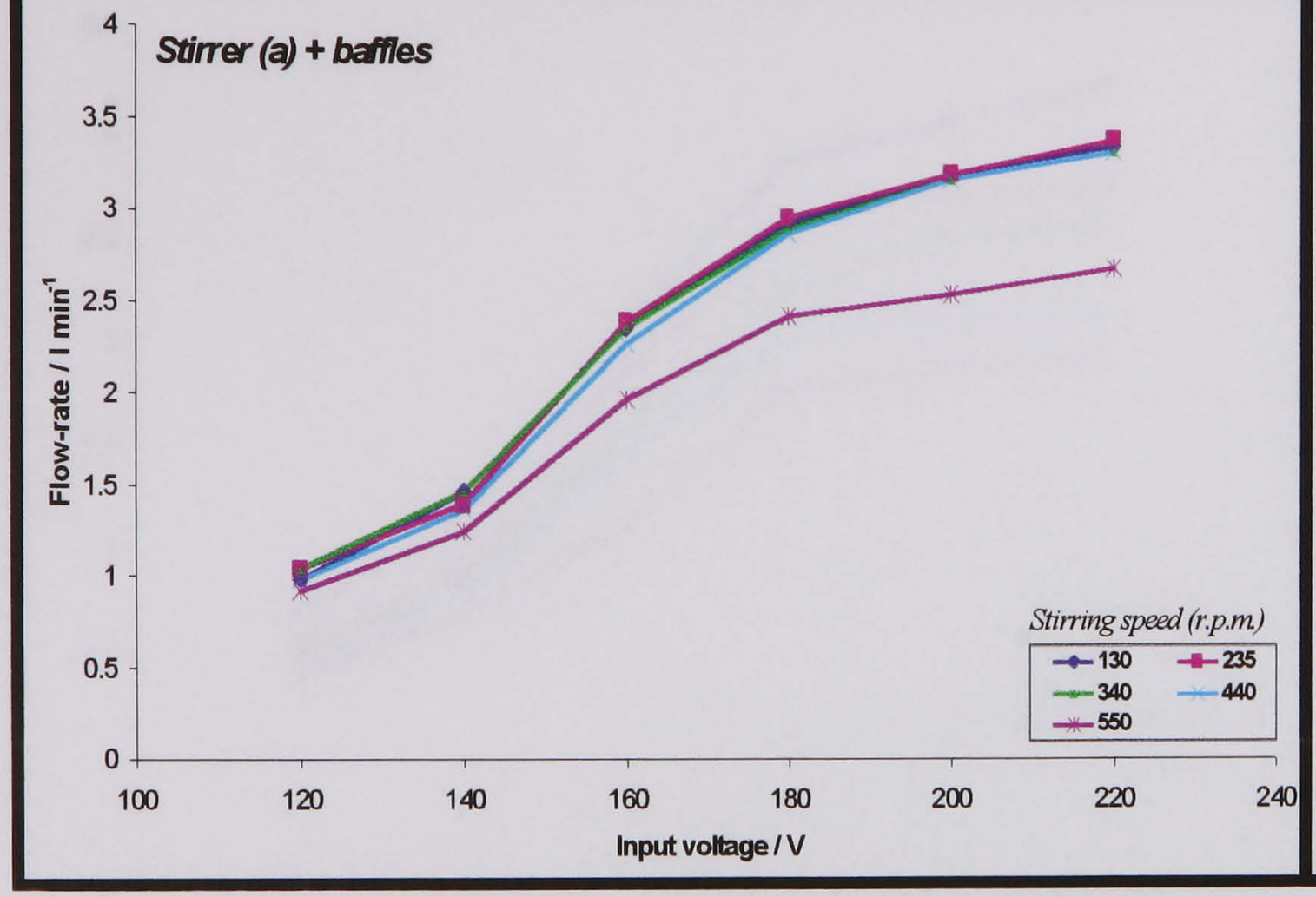

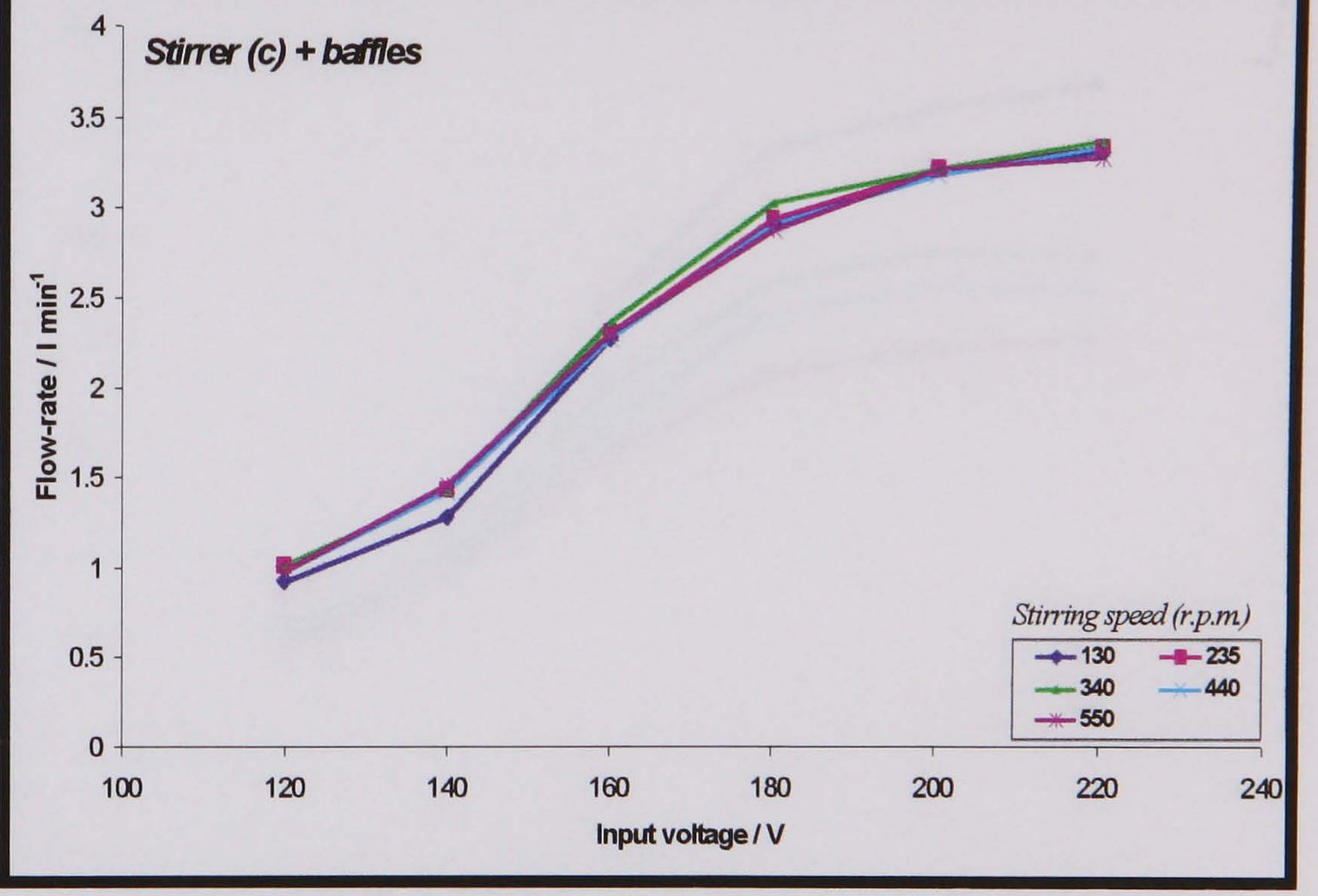

Figure 3.38. Flow-rate of water in the sampling loop when the input voltage is varied in the centrifugal pump used in the 5-L beaker system when different stirring speeds and system configurations were used

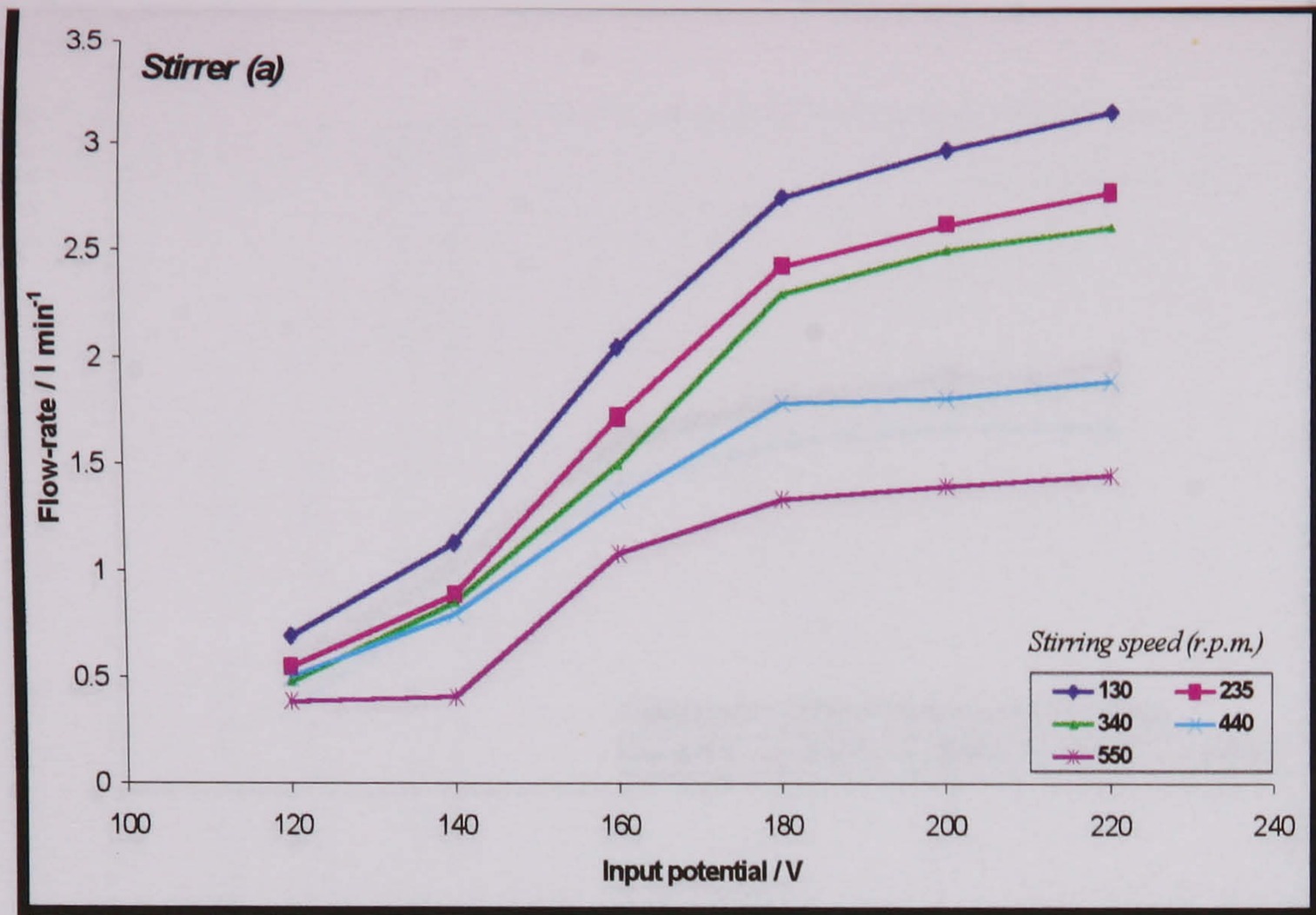

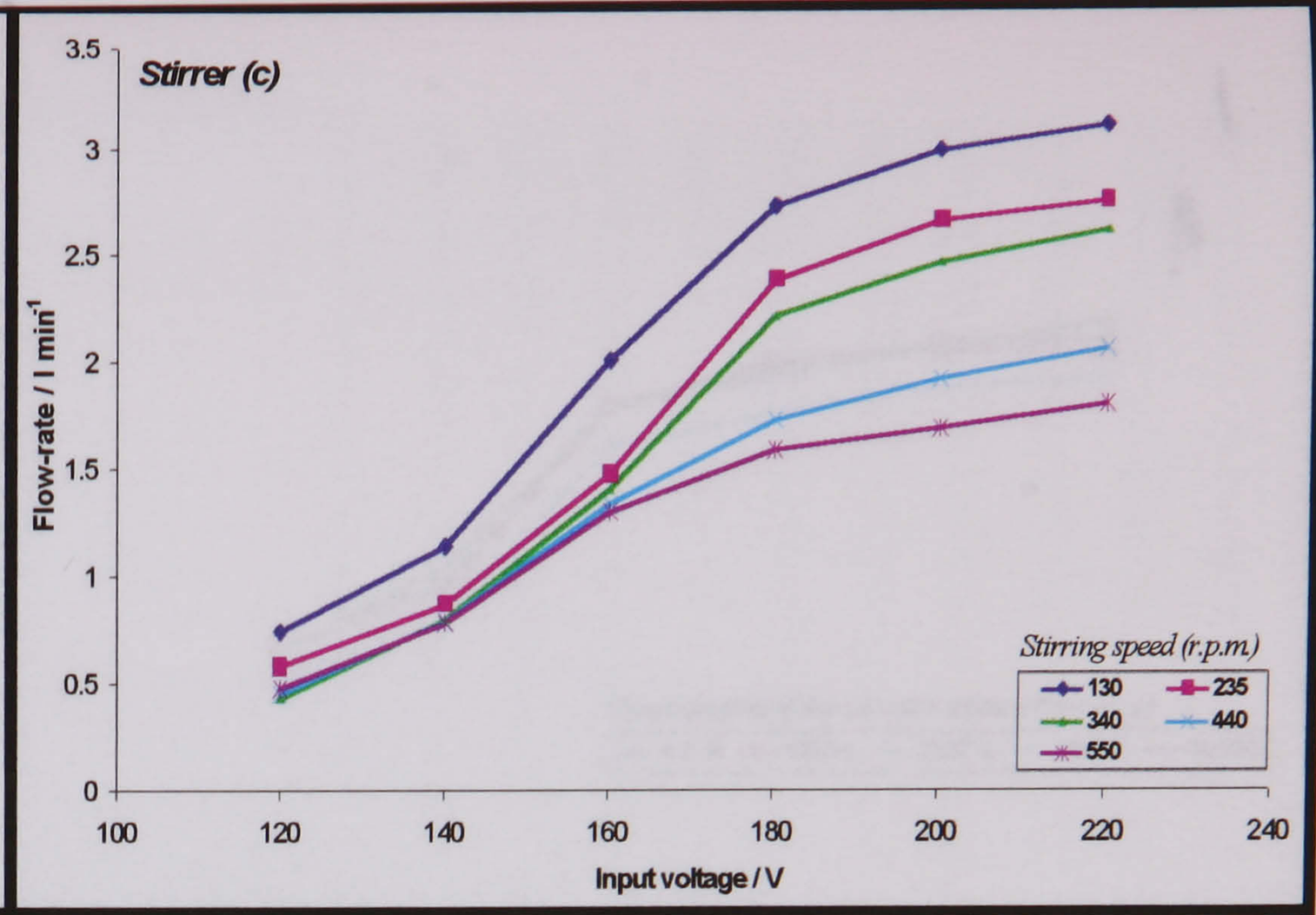

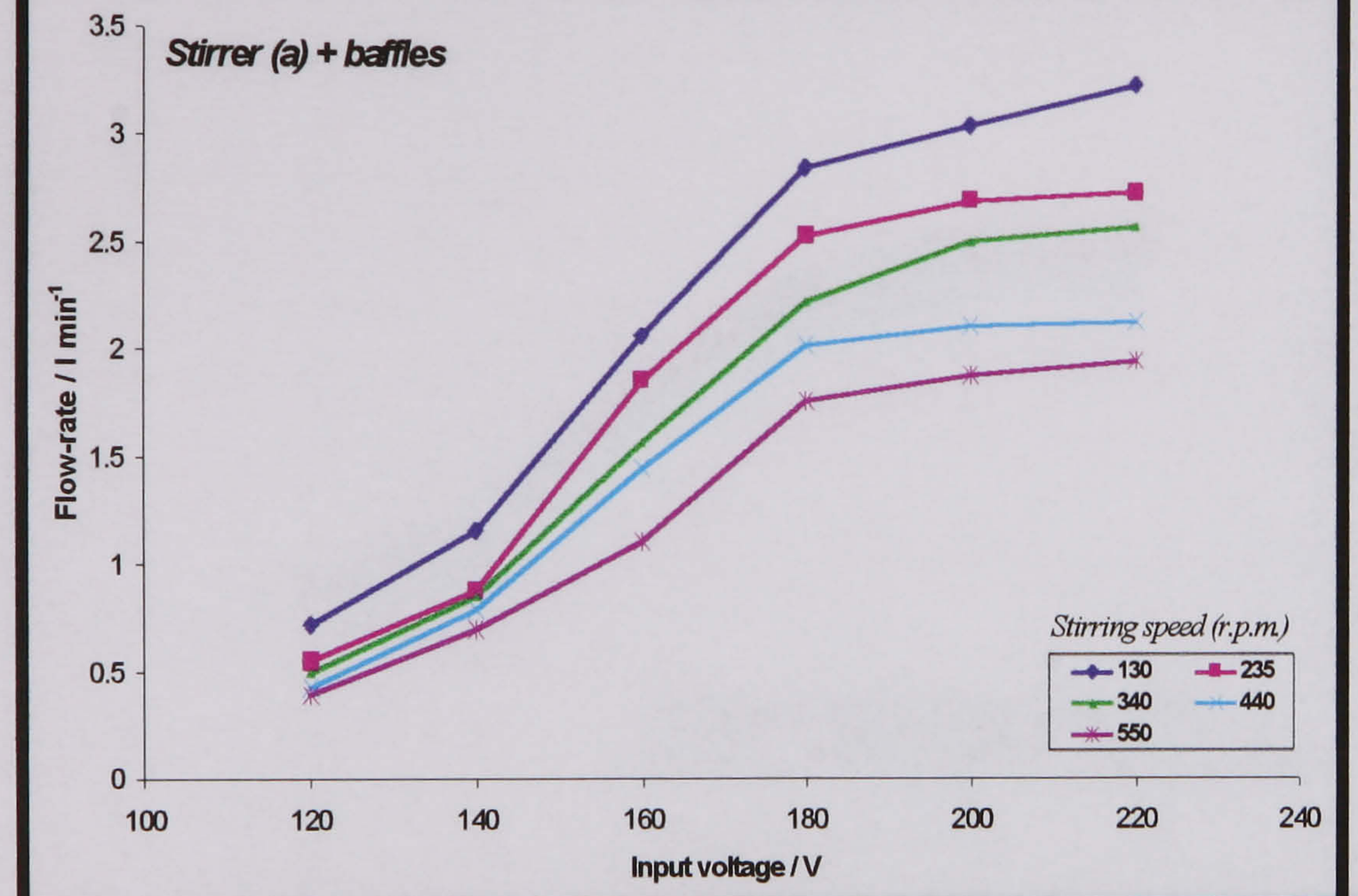

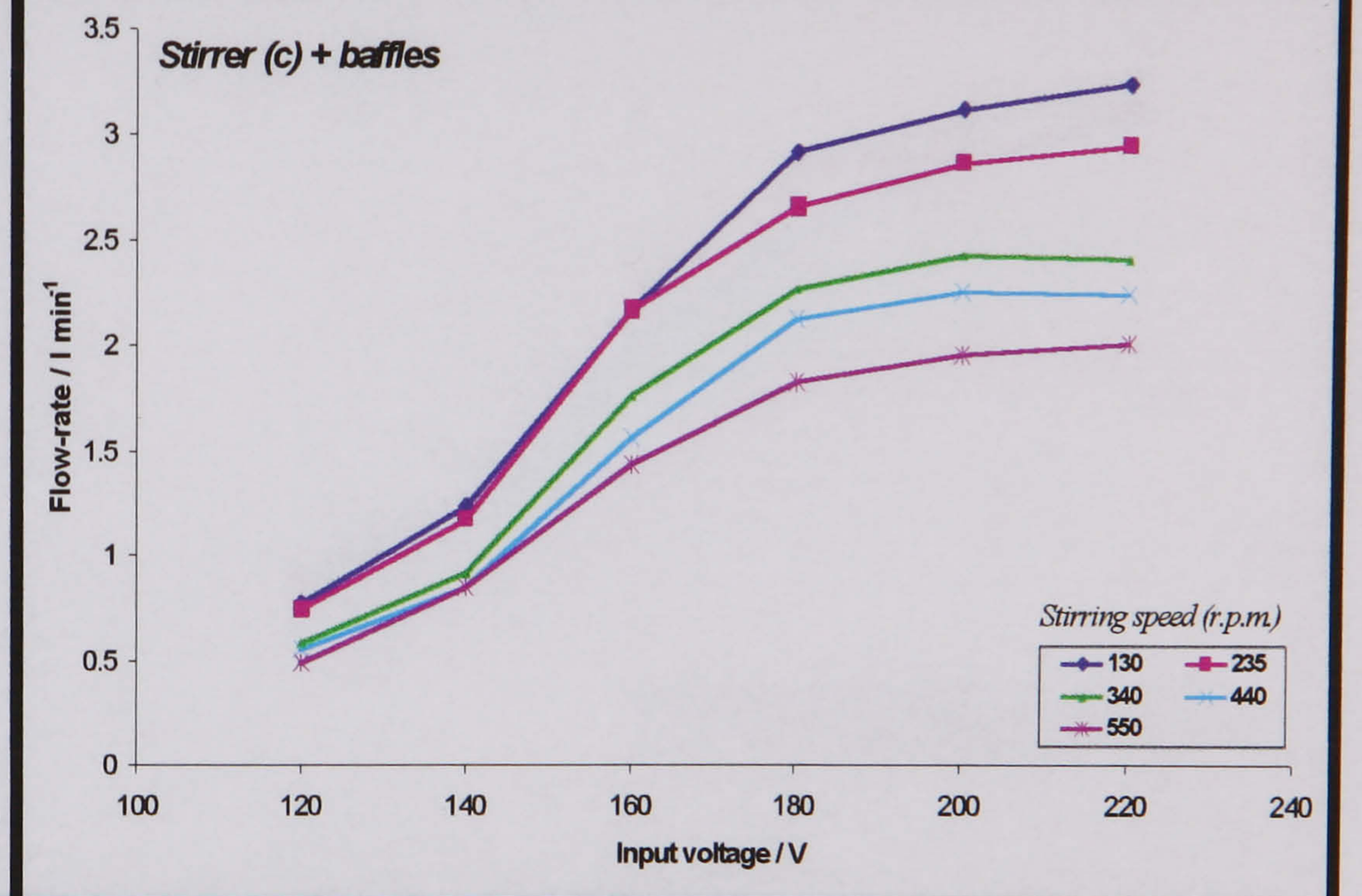

Figure 3.39. Flow-rate of a 50 % oil-water mixture in the sampling loop when the input voltage was varied in the centrifugal pump used in the 5-L beaker system when different stirring speeds and system configurations were used

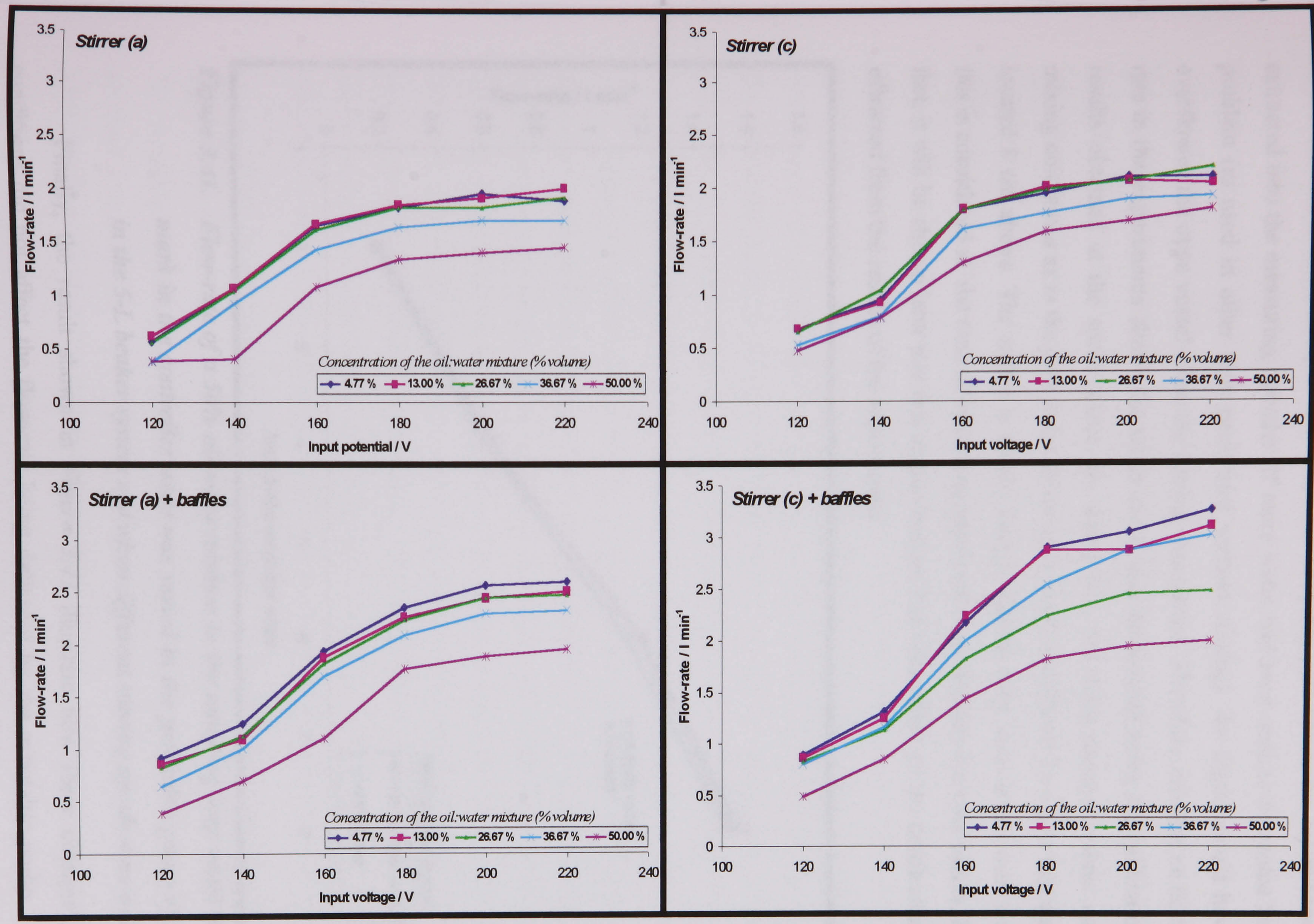

Figure 3.40. Flow-rate of different oil-water mixtures in the sampling loop when the input voltage was varied in the centrifugal pump used in the 5-L beaker system when different system configurations were used

experiments using the port above the stirrer plane were carried out. This was due to the fact that if the tests were performed above the stirrer plane, during the flow-rate measurement the level of liquid fell below the sampling port due to the liquid being extracted into the measuring cylinder. If more water had been used to overcome this problem (as used in other tests performed without stirring), the liquid would have overflowed the open vessel when the stirring was started. Therefore, the data on flow-rate in the experiments above the stirrer plane was determined using the calibration results obtained at the stirrer plane. By doing this, the same pressure values and mixing conditions as in the port at the stirrer plane were considered for a port that was located 8 cm above. The author is aware though, that an error was carried over and this is considered at the time of extracting appropriate conclusions from the results. In fact, it will be shown later that this approximation had little effect on the conclusions extracted from the results of the experiments.

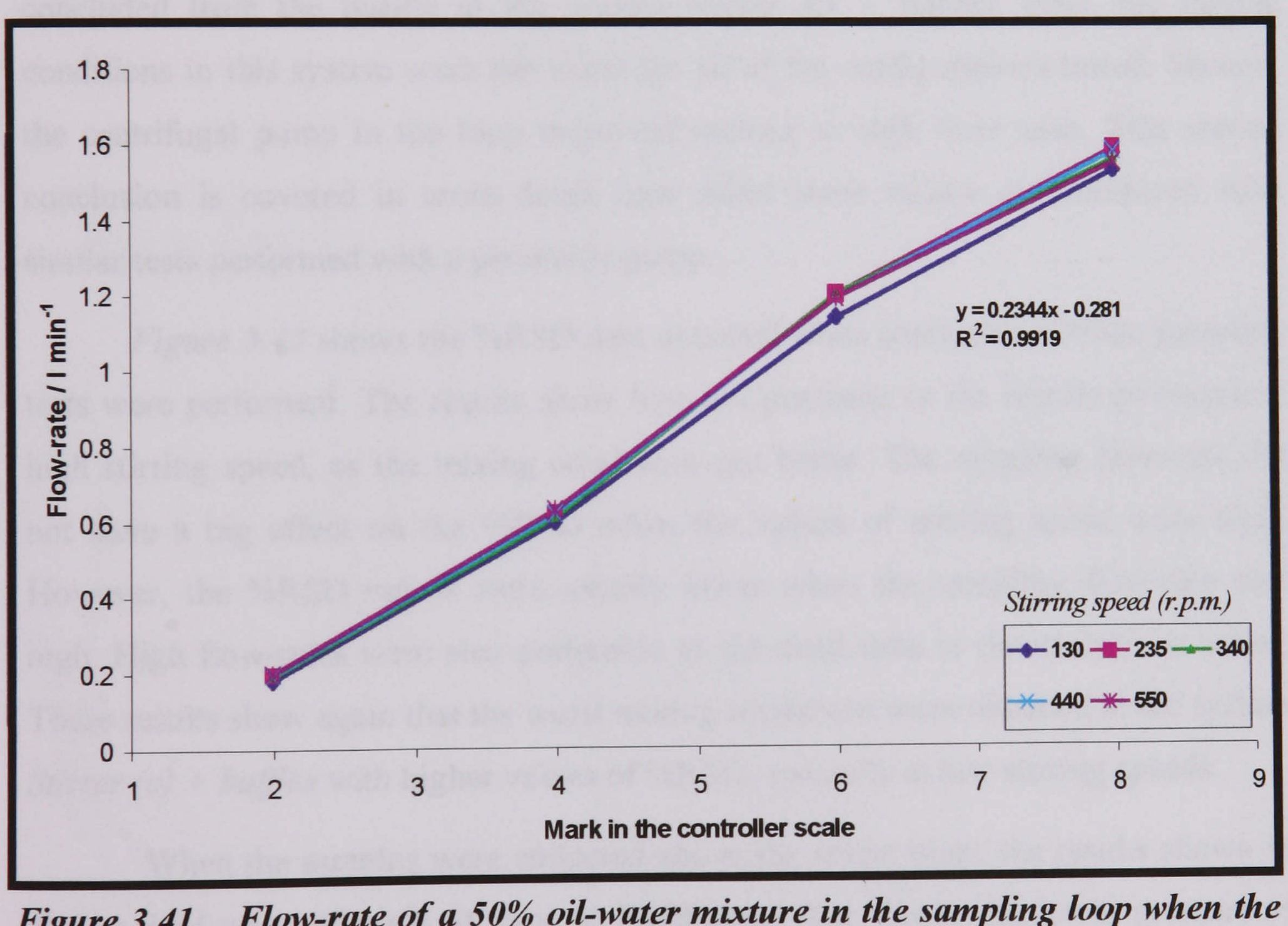

Figure 3.41. Flow-rate of a 50% oil-water mixture in the sampling loop when the mark in the controller scale was varied in the peristaltic pump used in the 5-L beaker system and when different stirring speeds were used

Finally, the result shown in *Figure 3.41* illustrate how these changes in conditions did not affect the flow-rate being delivered by the peristaltic pump.

This was due to the fact that the flow in the peristaltic pump was varied by actuating a controller intrinsic to the pump. This built-in control system has been designed to actuate the rotational speed of the impeller and keep a constant torque in the system.

Figure 3.42 shows how the quality of the samples collected at the stirrer plane changed when both the stirring speed and the sampling flow-rate were varied for different vessel and stirrer configurations. It can be observed that at high stirring rates the sampling was more representative and less dependent on factors such as sampling flow-rate, stirrer type or vessel configuration. In fact, above 300 r.p.m. a good mixing was achieved, the curves became flatter and sampling did not depend on the stirring speed. Only the system *Stirrer (c)* + *baffles* differed slightly from this general tendency. In this particular system, the dependence upon the sampling flow-rate was larger and only if the flow in the loop was very fast were good mixing conditions above 300 r.p.m. (i.e. flat curve) achieved. Two important conclusions can be concluded from the results in the system *Stirrer (c)* + *baffles*. First, the mixing conditions in this system were the worst for all of the configurations tested. Second, the centrifugal pump in the loop improved mixing at high flow-rates. This second conclusion is covered in more detail later when these results are compared with similar tests performed with a peristaltic pump.

Figure 3.43 shows the %RSD data obtained when triplicates of these sampling tests were performed. The results show how the precision in the results increased at high stirring speed, as the mixing conditions got better. The sampling flow-rate did not have a big effect on the %RSD when the values of stirring speed were high. However, the %RSD values were usually lower when the sampling flow-rate was high. High flow-rates were also preferable as the dead time in the analysis is lower. These results show again that the worst mixing conditions were obtained in the system *Stirrer (c)* + *baffles* with higher values of %RSD, specially at low stirring speeds.

When the samples were collected above the stirrer plane the results shown in *Figure 3.44* were obtained. It must be highlighted that, due to the lower pressure at the sampling point, higher input potentials to the pump were needed in order to produce a considerable flow in the loop. This is the reason why the results at low sampling flow-rates (i.e. low input voltages) are not shown in the plots. Furthermore,

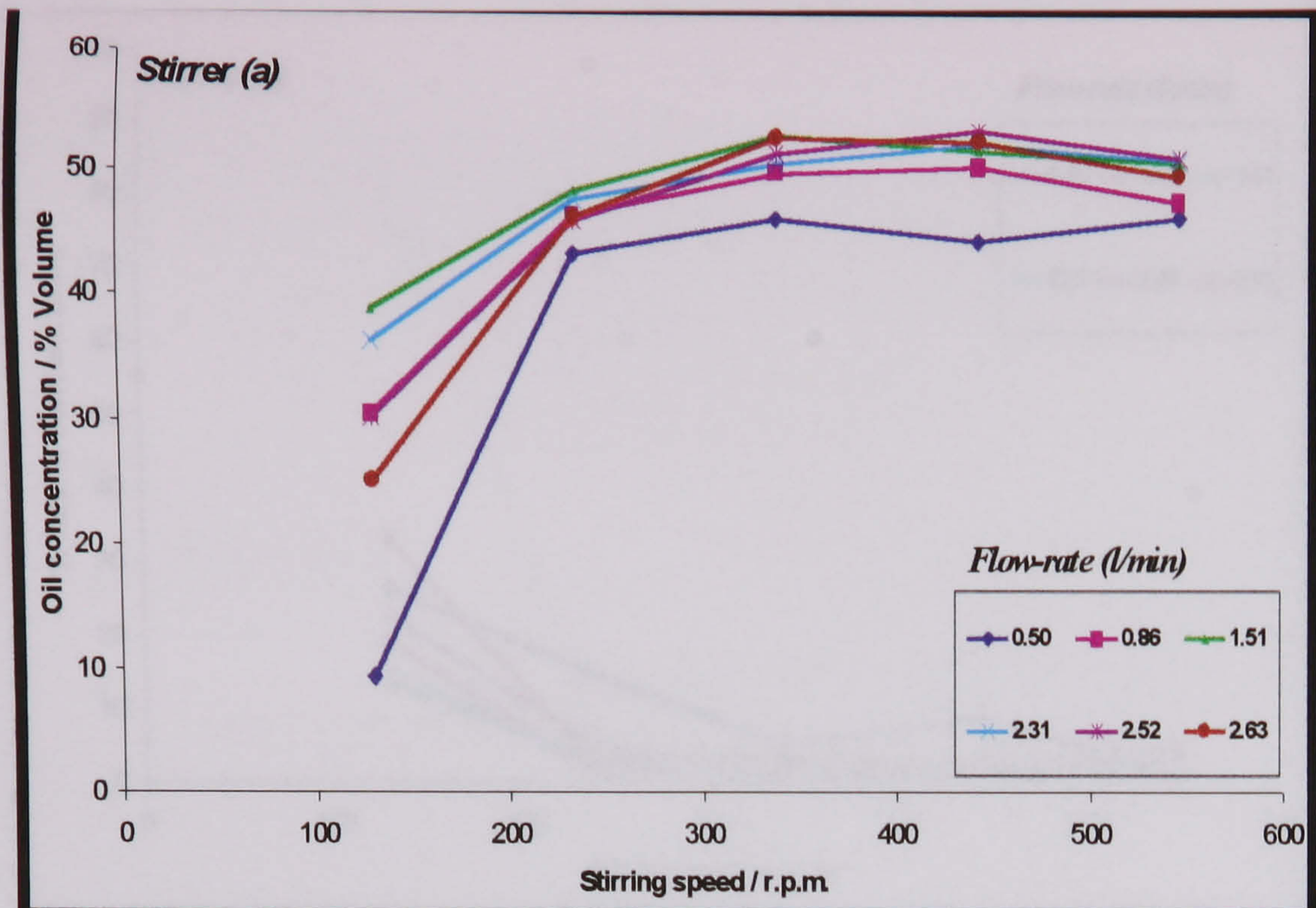

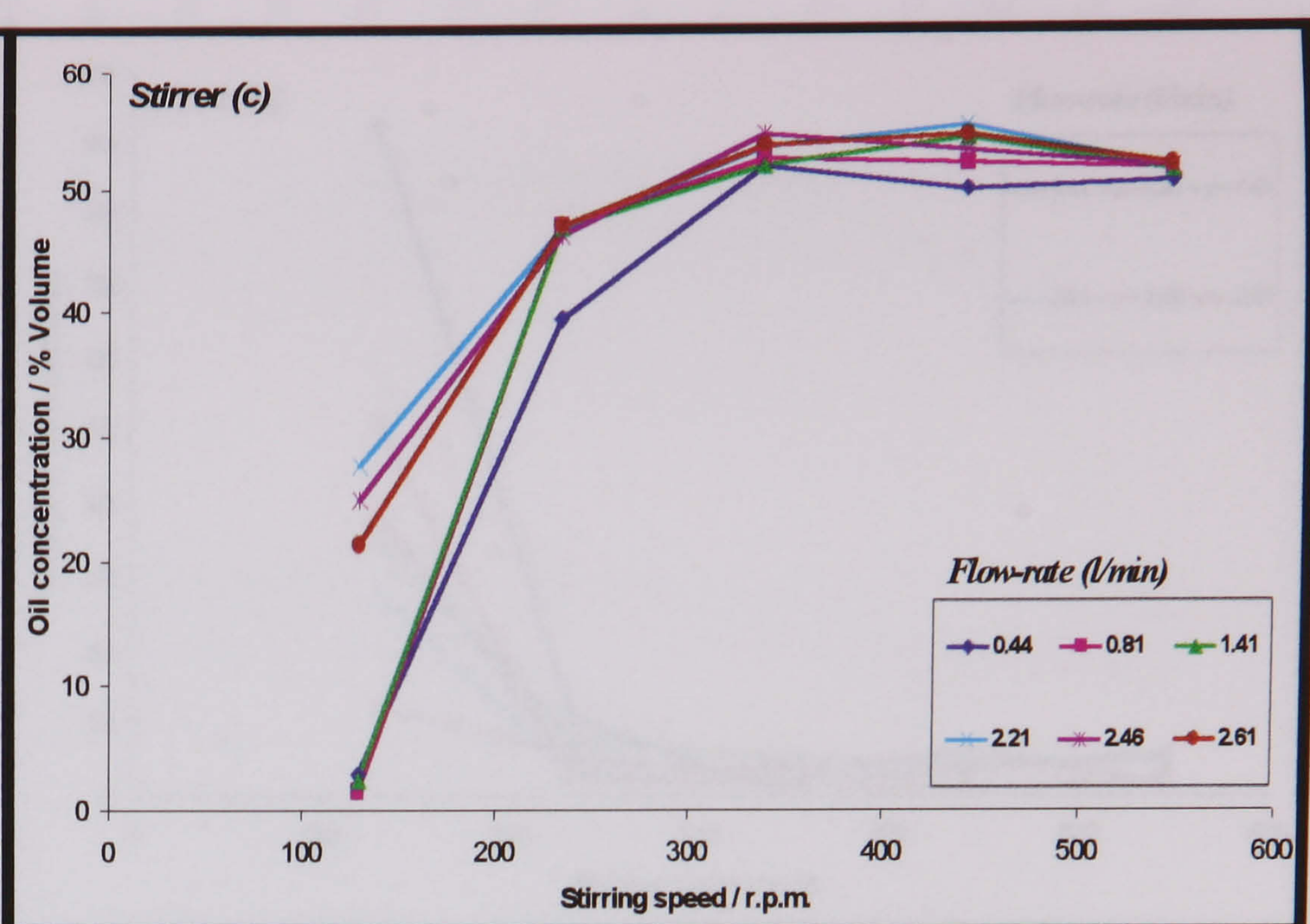

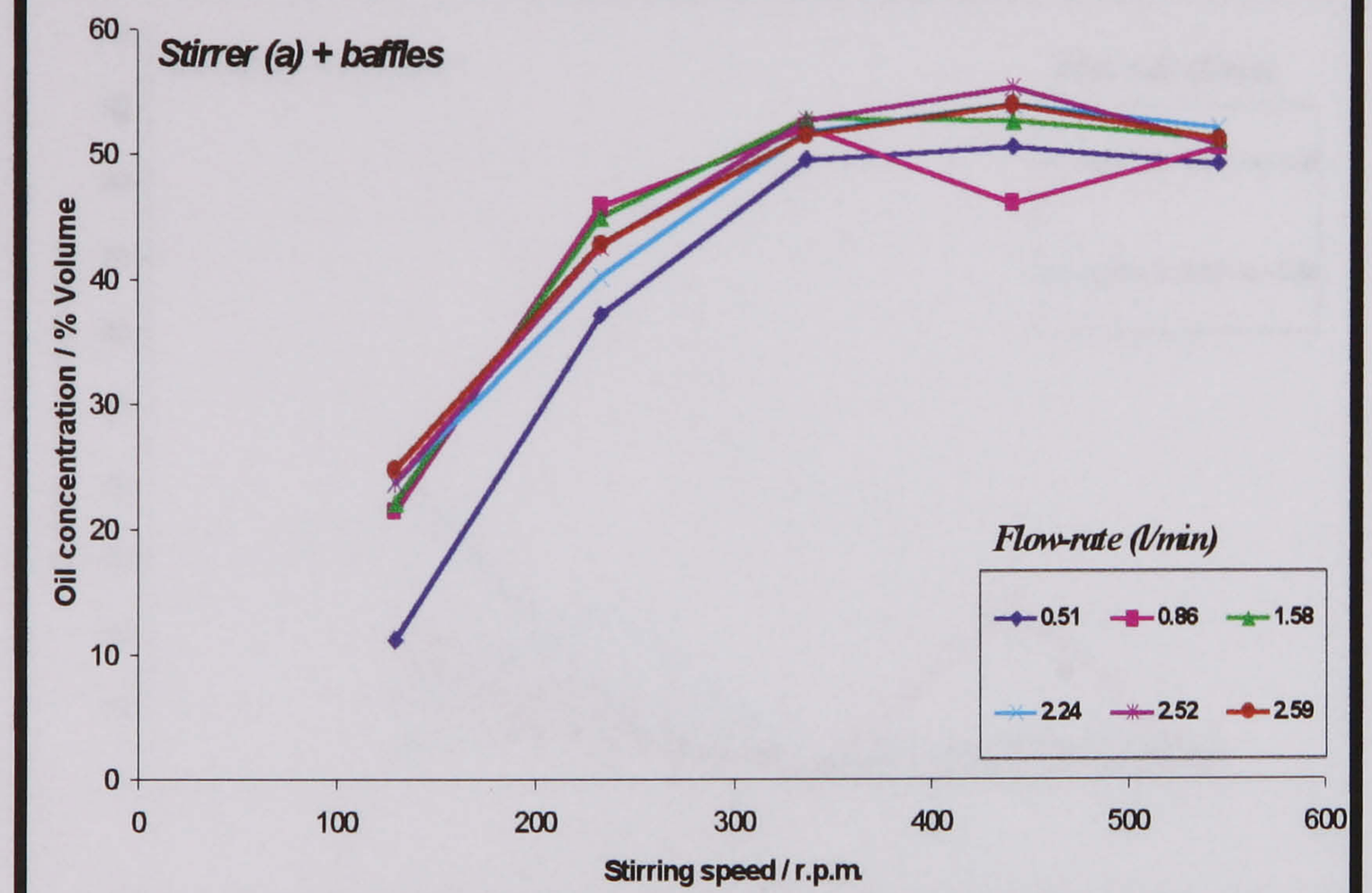

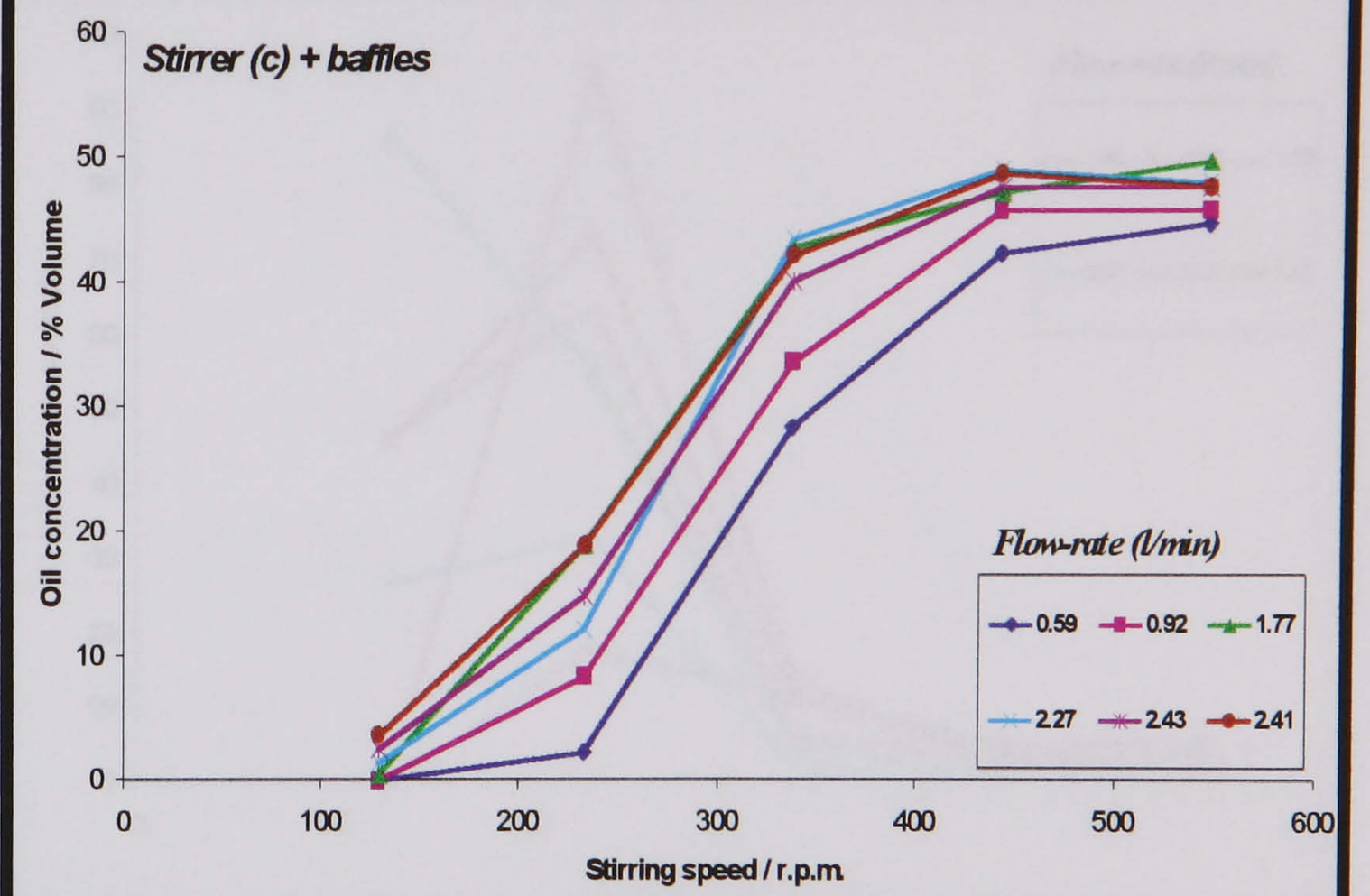

Figure 3.42. Quality of the samples (50% volume oil-water mixture) collected at the stirrer plane and at different stirring speeds when different stirrers, vessel configurations and sampling flow-rates were used

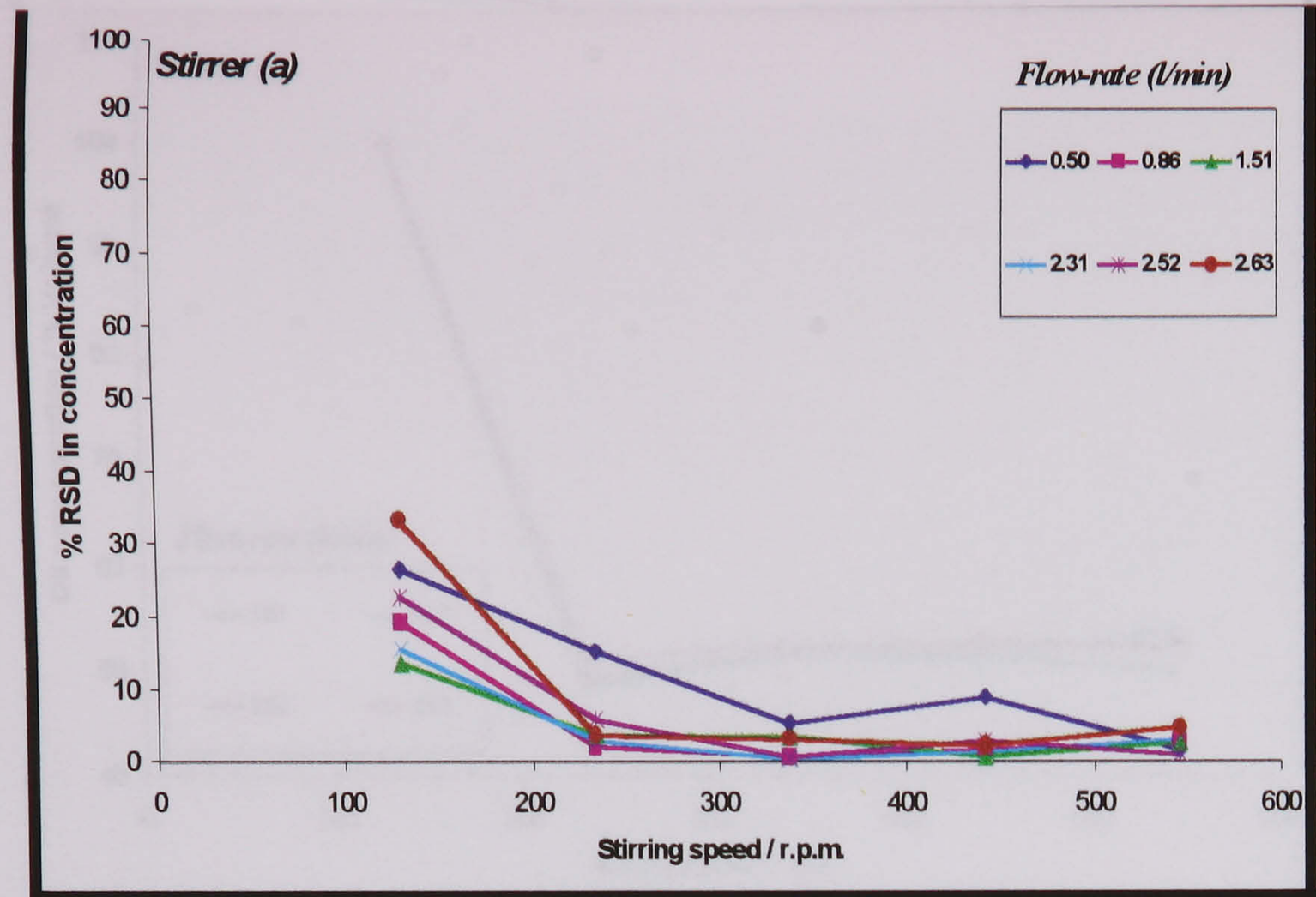

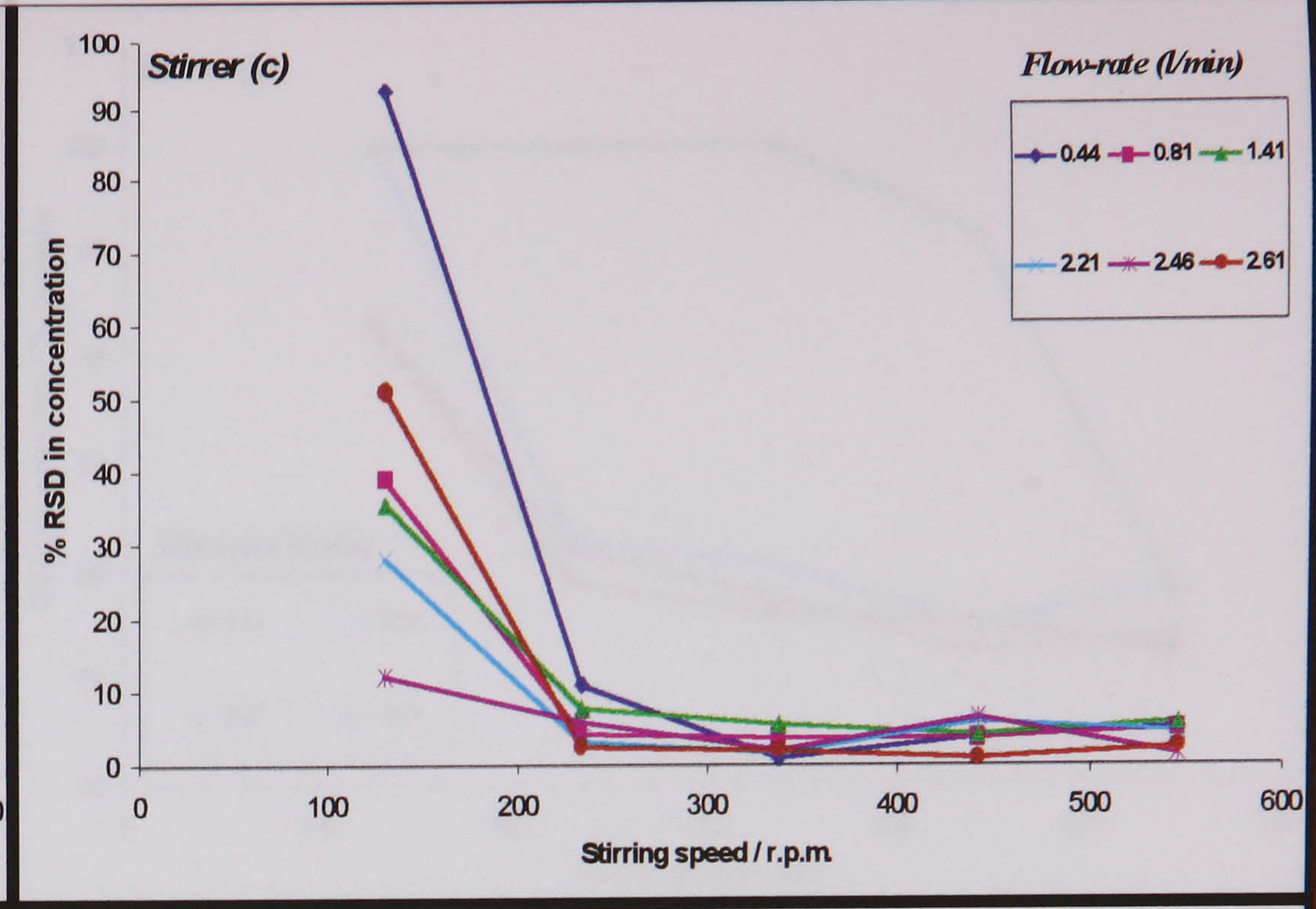

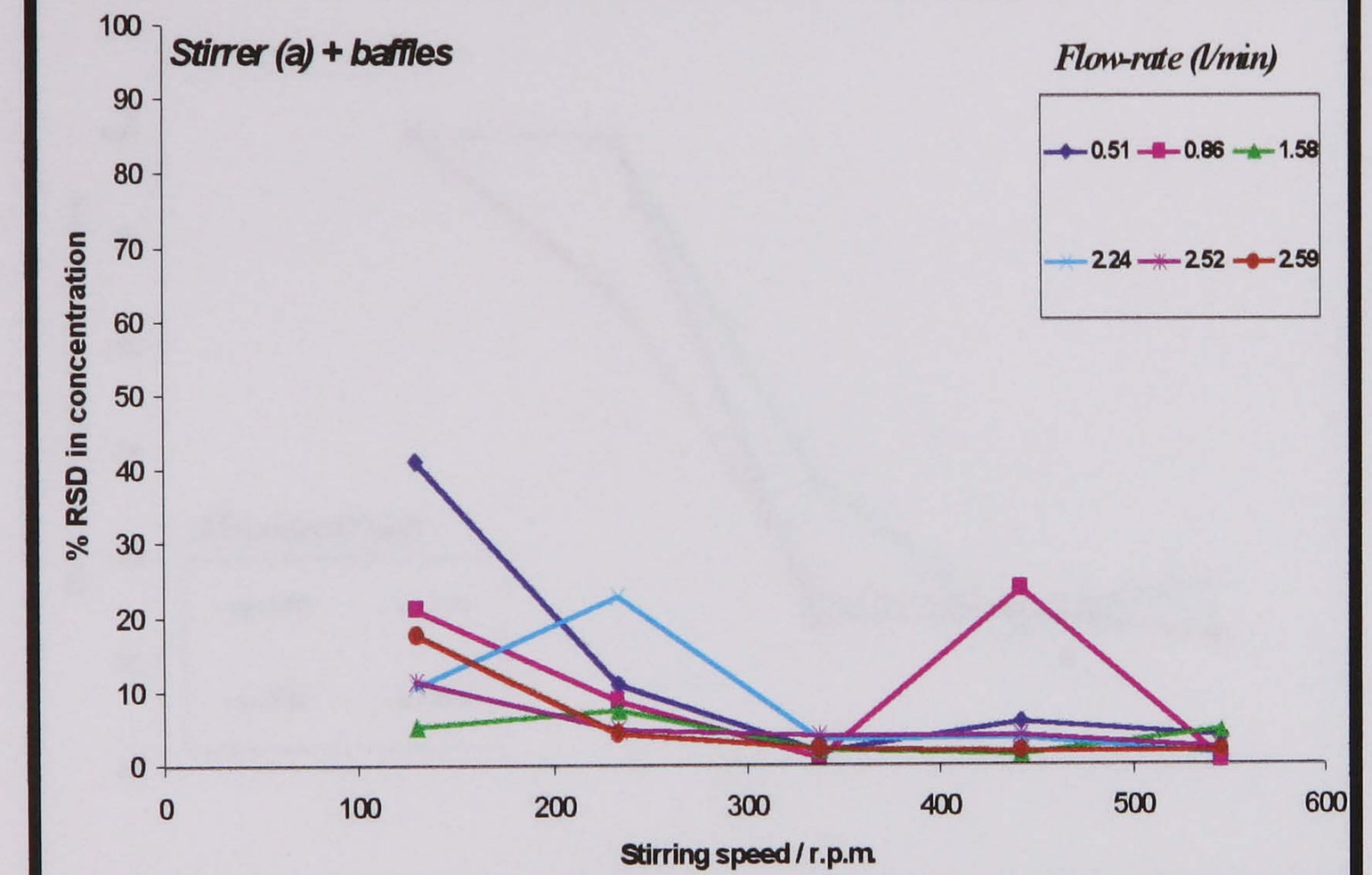

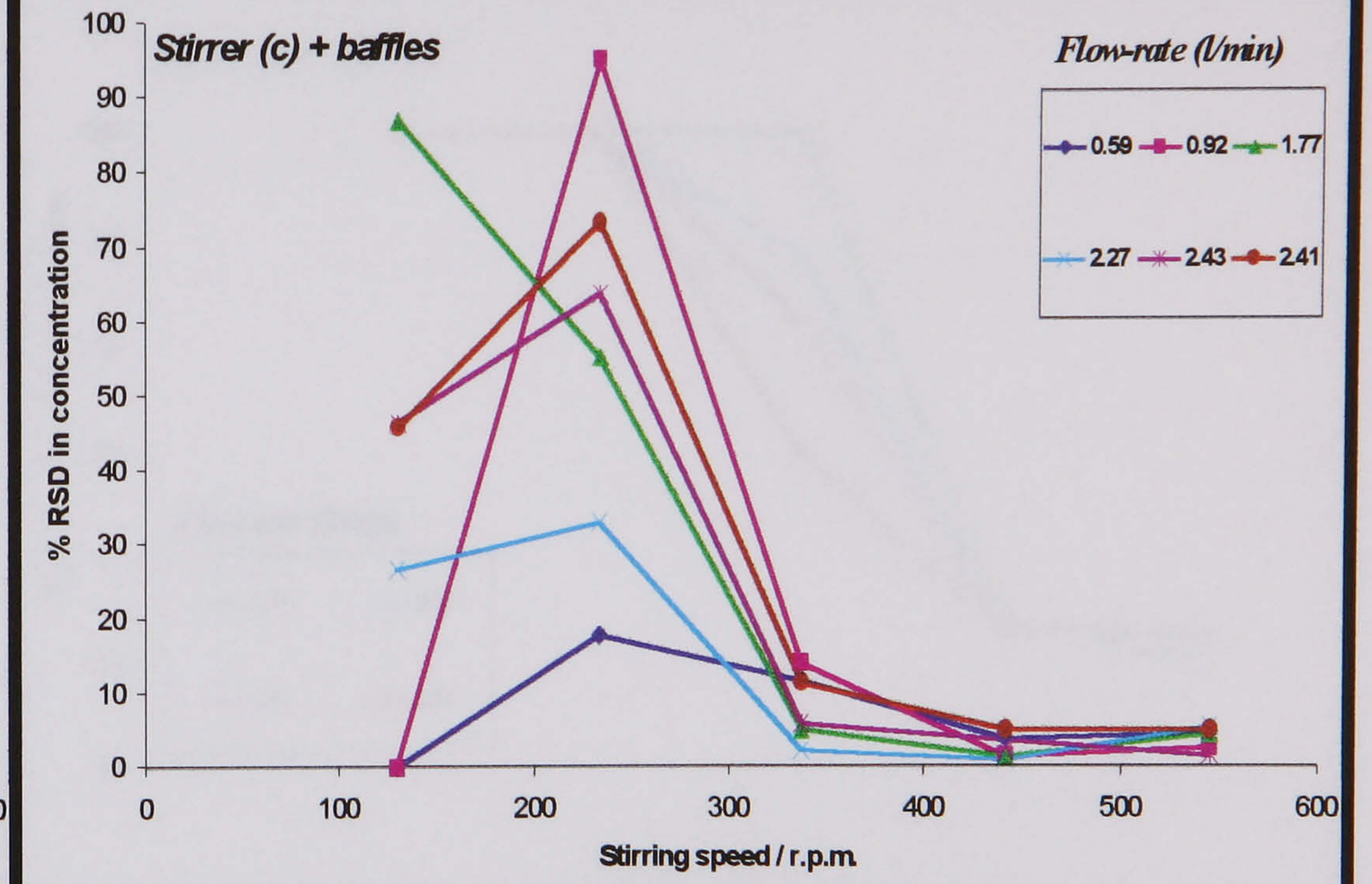

Figure 3.43. %RSD in the sample collection (50% volume oil-water mixture) at the stirrer plane and at different stirring speeds when different stirrers, vessel configurations and sampling flow-rates were used

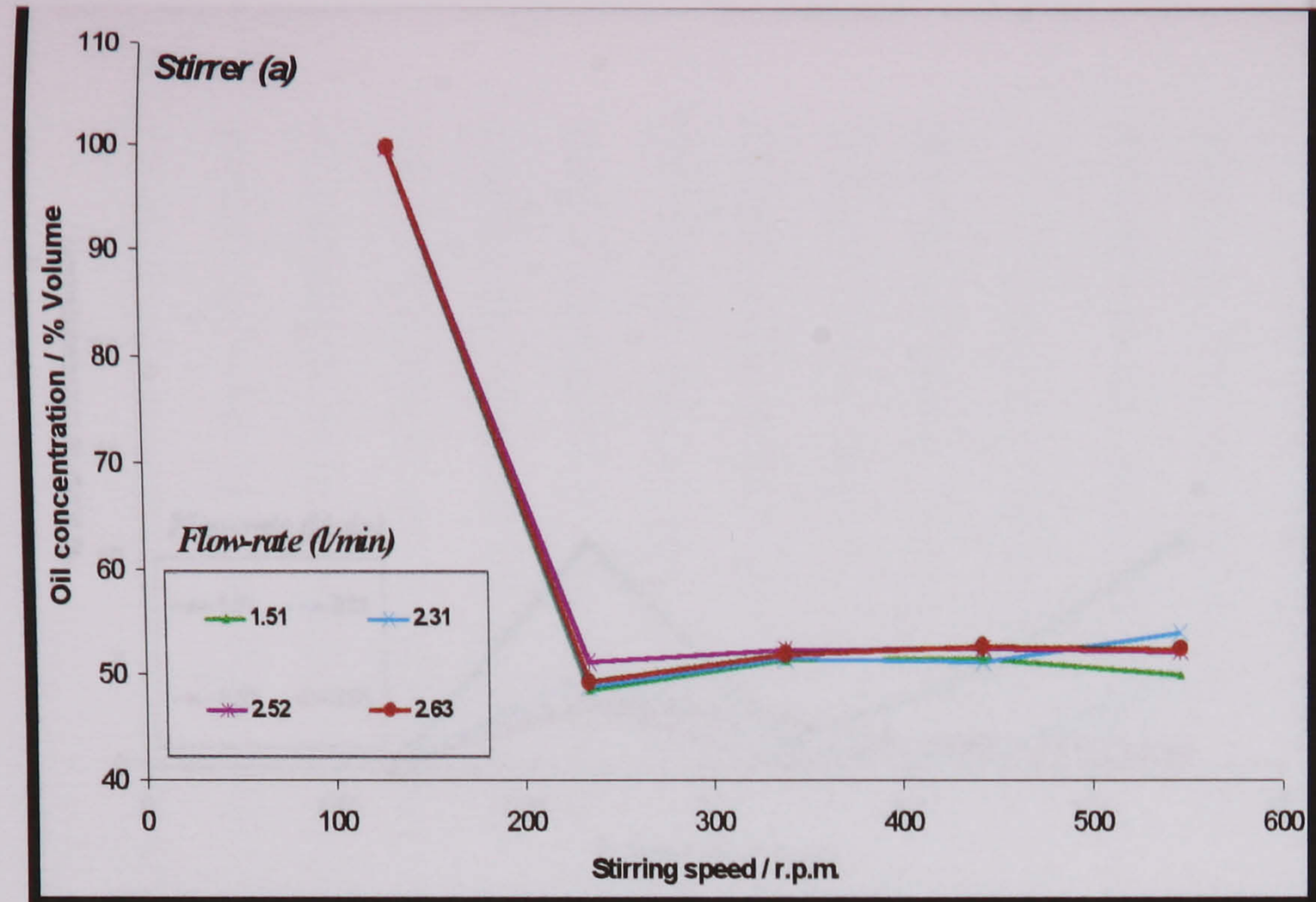

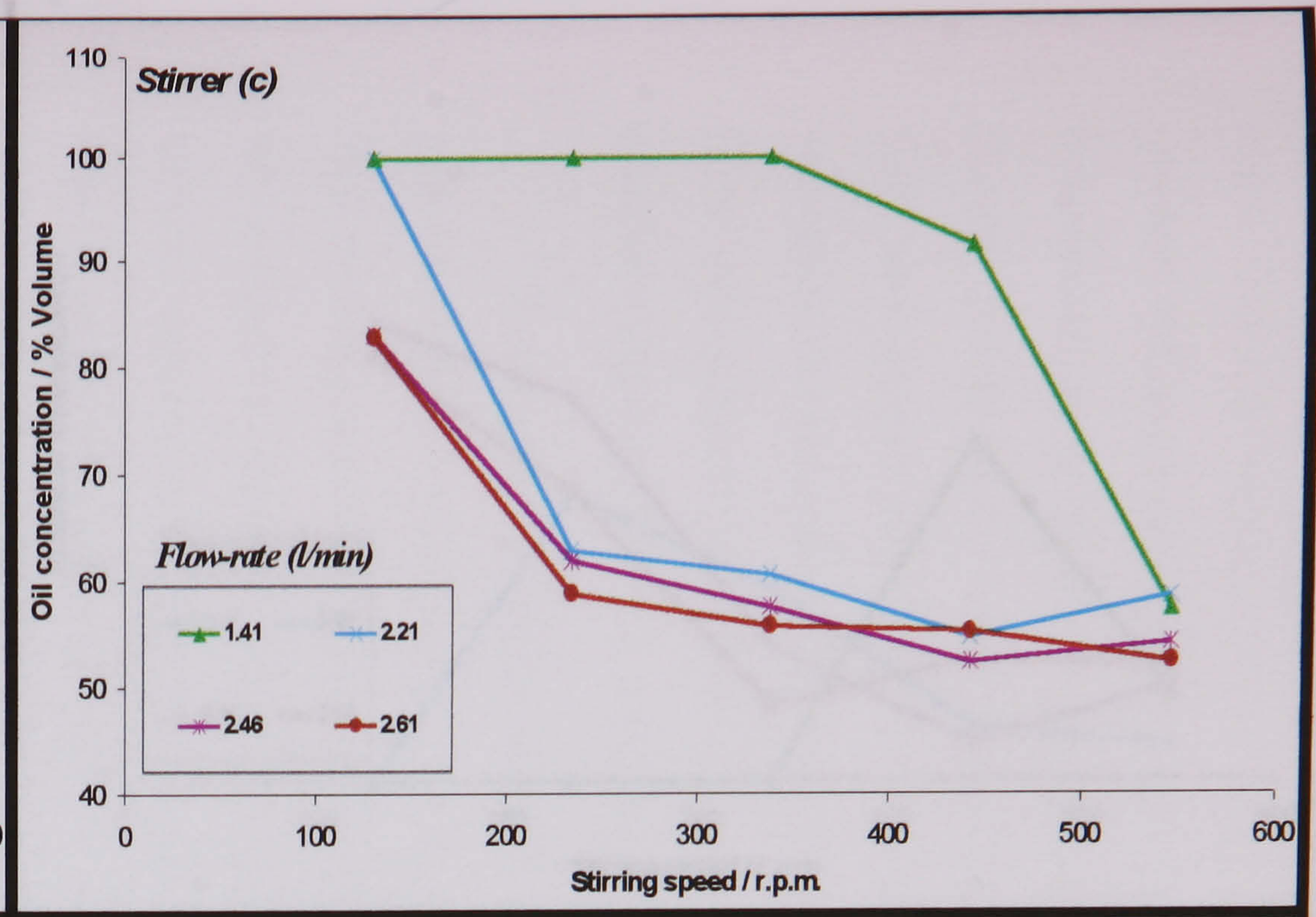

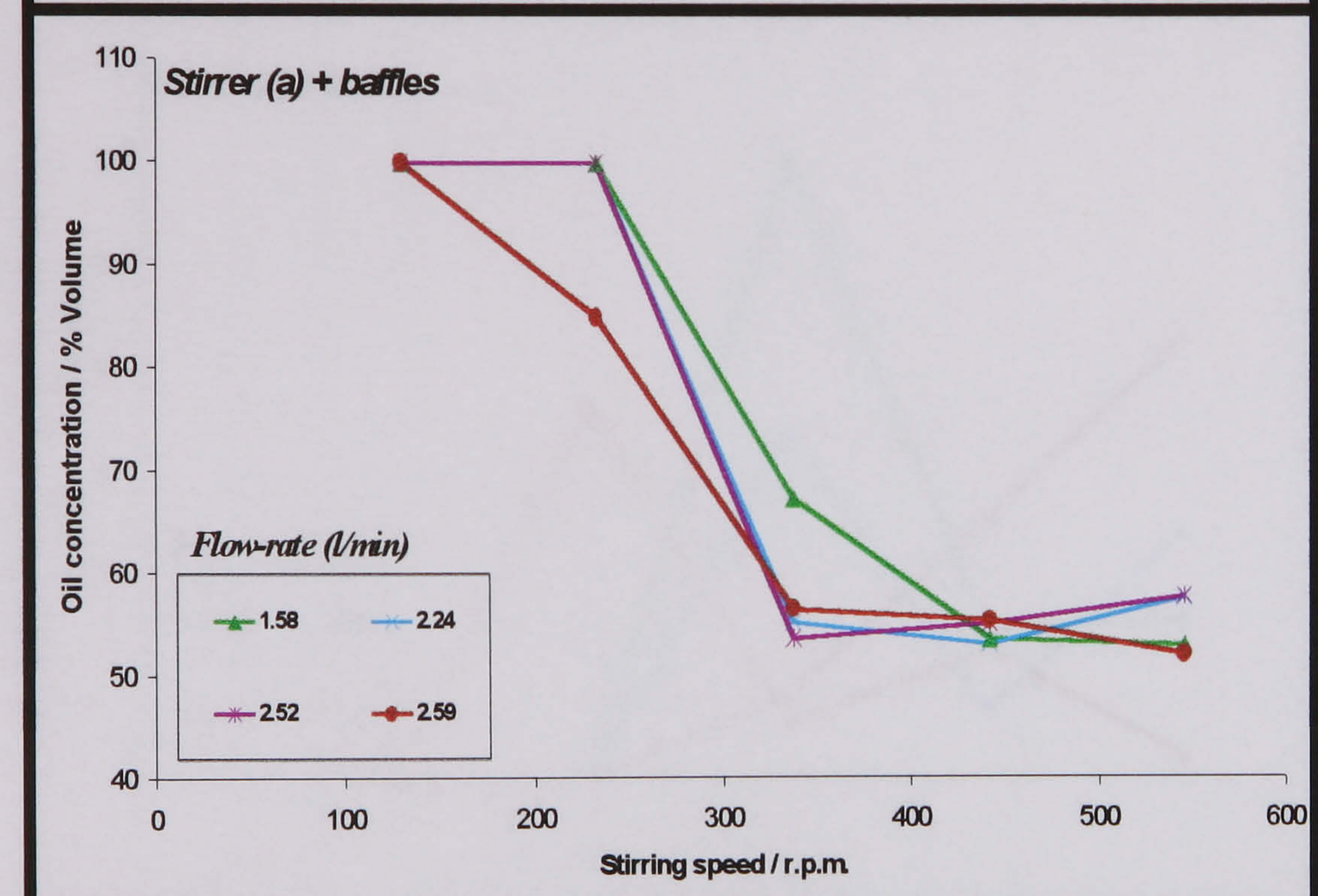

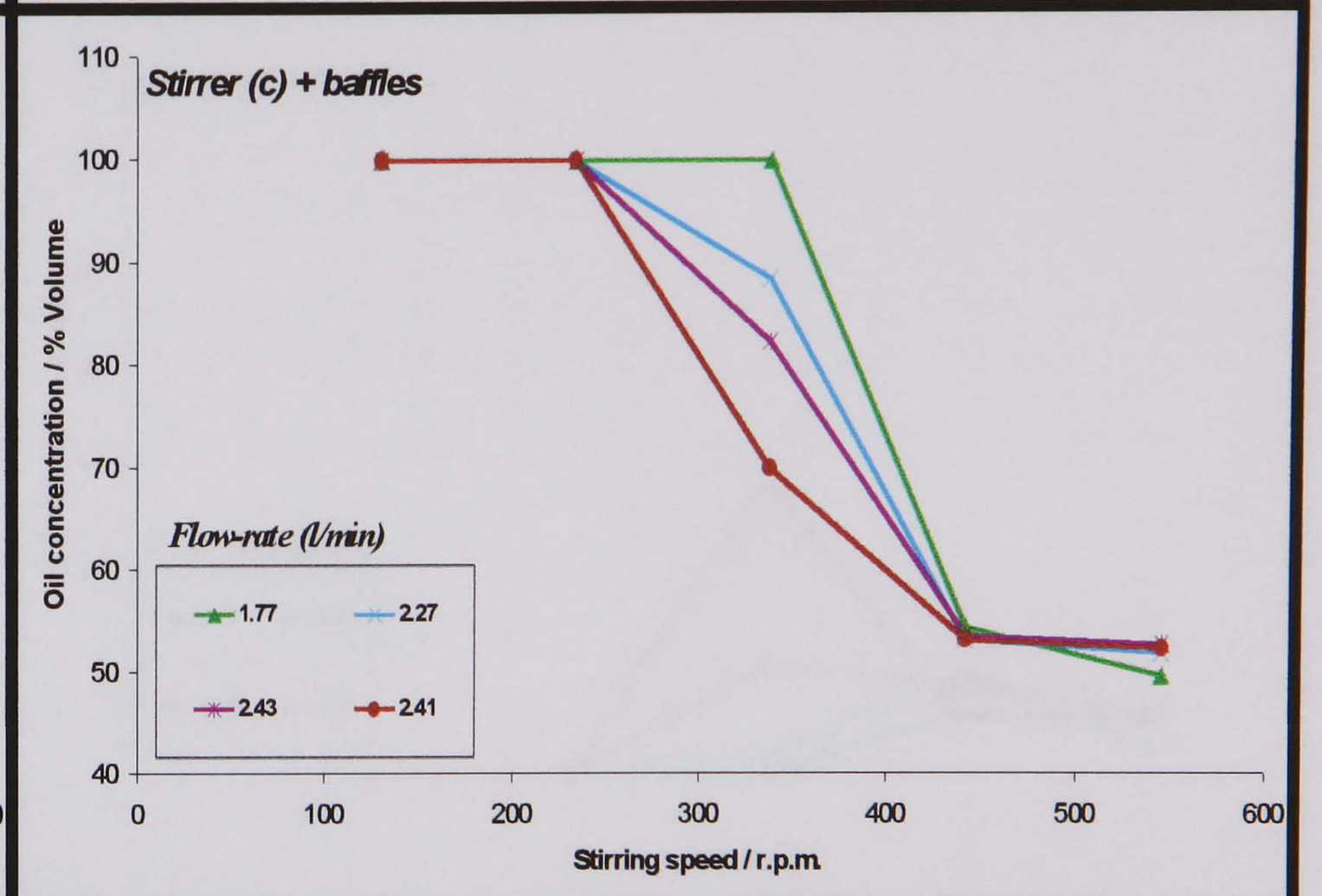

Figure 3.44. Quality of the samples (50% volume oil-water mixture) collected above the stirrer plane and at different stirring speeds when different stirrers, vessel configurations and sampling flow-rates were used

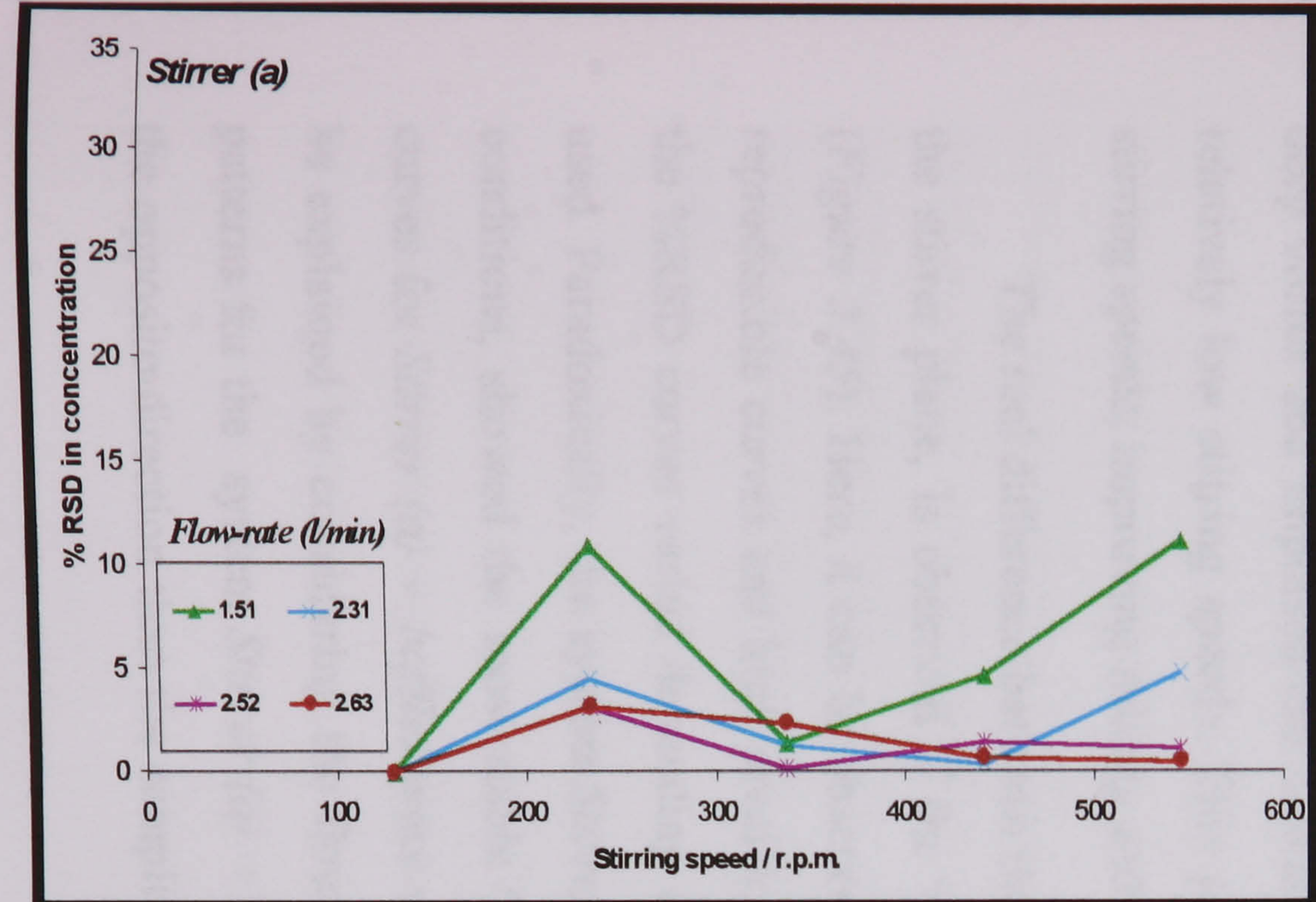

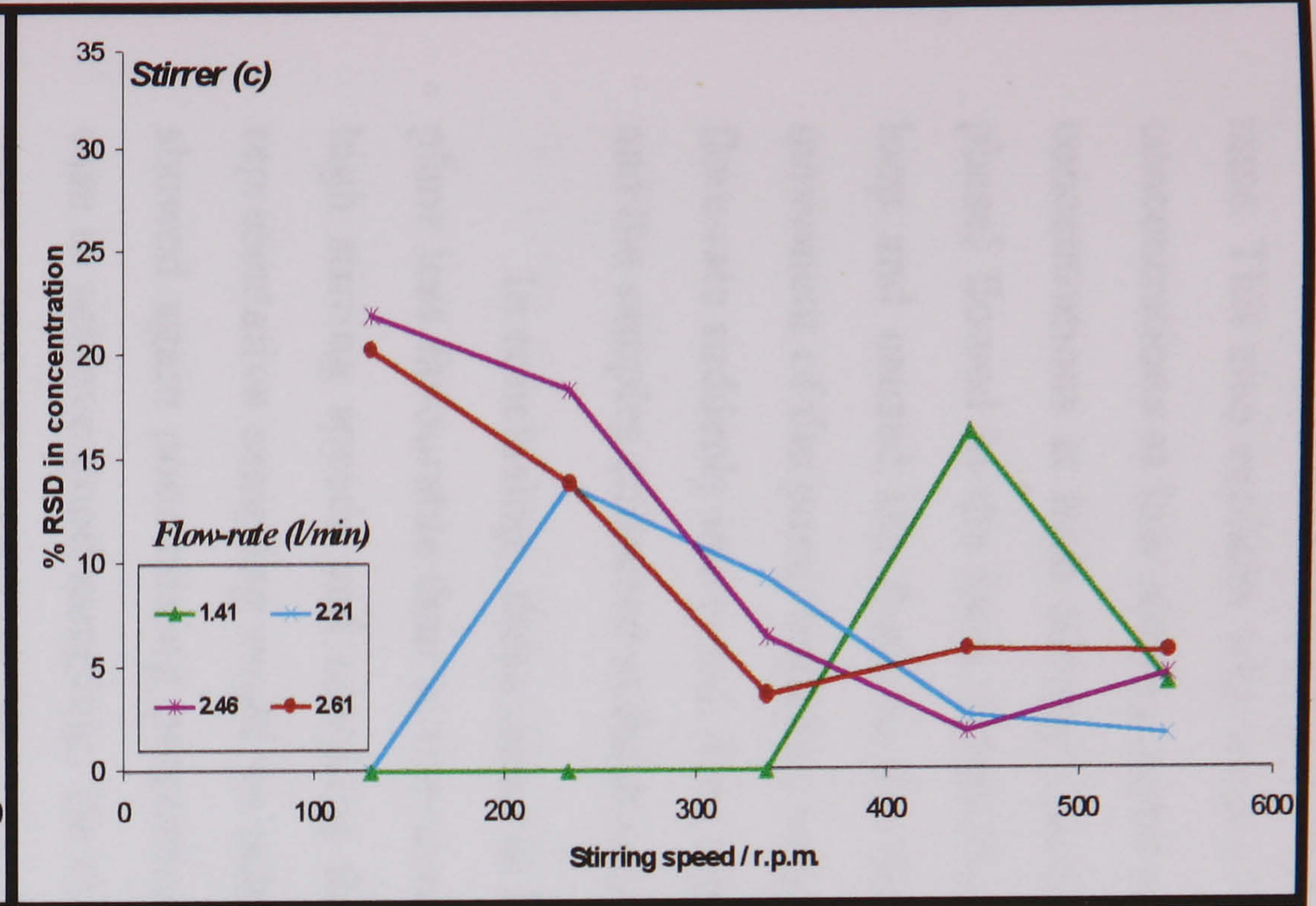

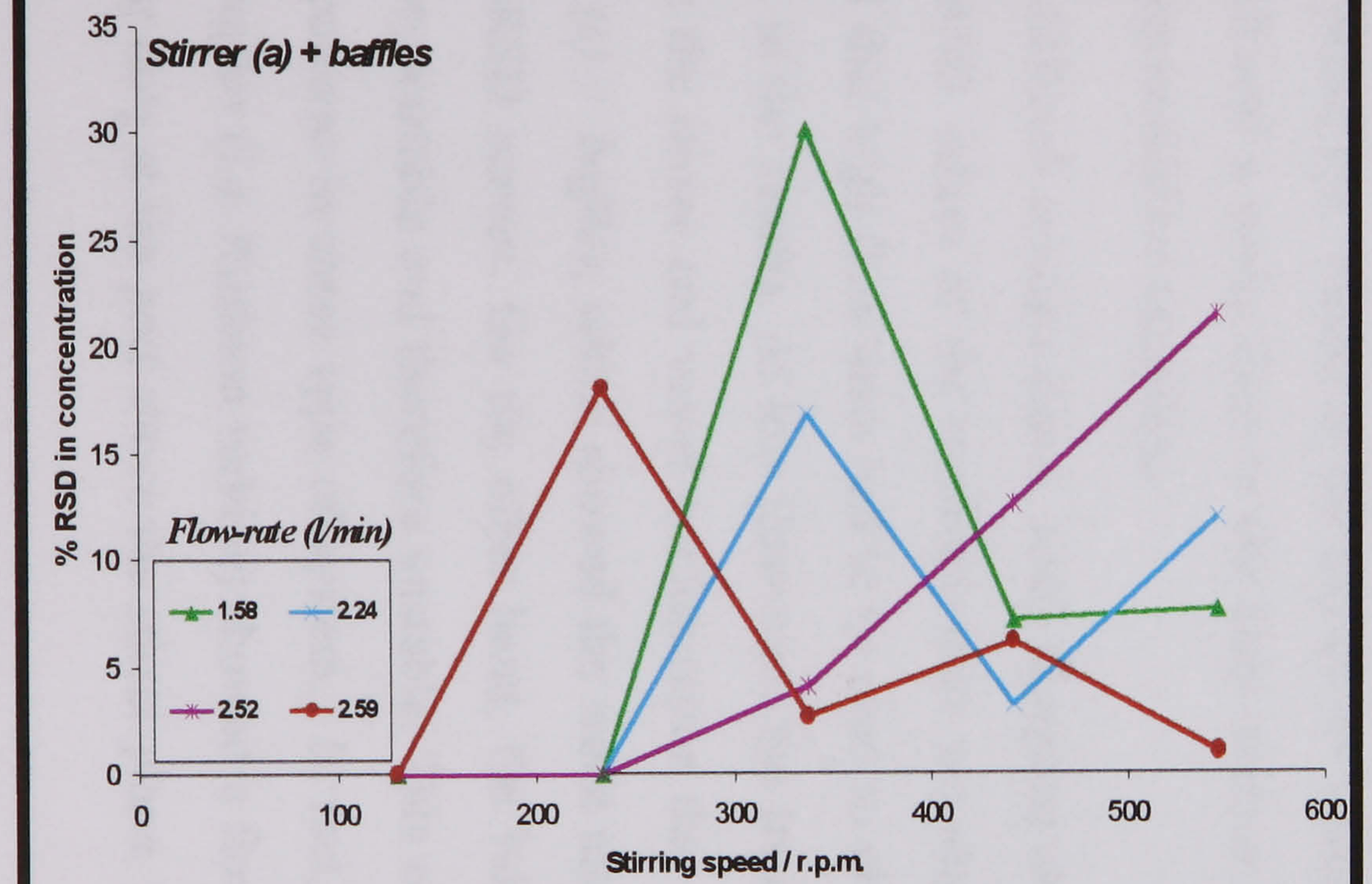

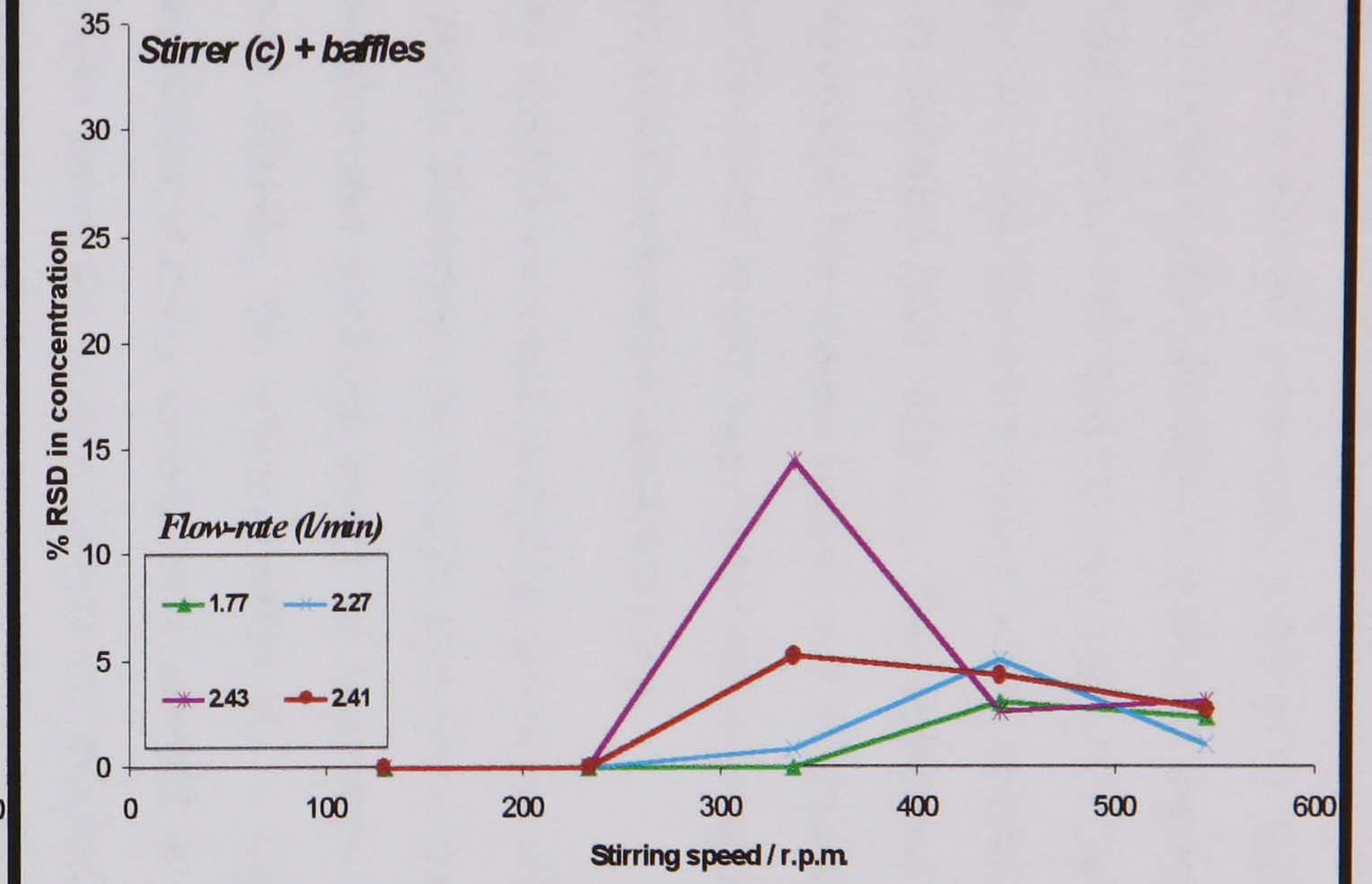

Figure 3.45. %RSD in the sample collection (50% volume oil-water mixture) at the stirrer plane and at different stirring speeds when different stirrers, vessel configurations and sampling flow-rates were used

PAGE NUMBERING AS ORIGINAL

in some of the experiments the flow in the loop was unstable due to the low torque and large plugs of water flowing between the oil in the loop when the mixing conditions were not good. Thus *Stirrer (c)* showed an unusual behaviour at low flow-rates. This also explains why most of the plots showed a common trend with high oil concentrations at low stirring speed and a sudden step change to high representative concentrations at high stirring speeds. Therefore, with bad mixing only oil (lighter phase) flowed in the loop. When the mixing was improved some water entered the loop and caused the fluid in the line to become less viscous. This enhanced the movement of the pump impeller, which turned at low torque values, and therefore the flow-rate suddenly increased. This higher flow-rate in the loop improved mixing itself and the samples collected at these conditions became more representative.

In conclusion, these unstable flow conditions made sampling above the stirrer plane less favourable than at the stirrer plane. However, the results also show that at high stirring speeds and sampling flow-rates this problem could be overcome and representative sampling could be achieved. Finally, the system *Stirrer (c)* + *baffles* showed again poor mixing properties as higher stirring speeds were needed in this case to achieve good sampling. On the other hand, the system *Stirrer (a)* produced a deep vortex and impulsed the heavier phase (i.e. water) to the top of the vessel at relatively low stirring speeds. This produced a stable flow in the loop even at low stirring speeds, improving mixing and representative sampling.

The real difference between the different configurations, when sampling above the stirrer plane, is observed if the %RSD values of the triplicate tests are studied (*Figure 3.45*). Here, it can be observed that high flow-rates had to be used to obtain reproducible curves and high precision in the results. At low flow-rates the trend in the %RSD curves varied depending on the stirrer and vessel configuration that was used. Paradoxically, the system *Stirrer (c)* + *baffles*, which showed the worst mixing conditions, showed the most stable %RSD curves. On the other hand, the %RSD curves for *Stirrer (a)* + *baffles* were very variable and therefore unstable. This could be explained by considering the flow-patterns in these type of system. In fact, the patterns for the system *Stirrer (a)* + *baffles* (i.e. Rushton turbine) showed a flow in the opposite direction than the sampling flow at the port above the stirrer plane. This

could be the reason for the high variability in the results obtained in this system. On the other hand, in the system *Stirrer (c) + baffles* the flow at the sampling port was not fast and could be more easily changed in direction as the fluid (being pushed to the bottom of the vessel) lost most of its kinetic energy.

As mentioned before, the flow in the loop and through the centrifugal pump was believed to improve mixing in the system. In order to demonstrate this, experiments were performed with a peristaltic pump for comparison. This type of pump produced a plug flow that did not improve mixing as much as the centrifugal type, where the impeller reduced the size of the droplets of the phase in suspension. With the purpose of showing more clearly the differences in mixing enhancement between the two pumps, the comparison was performed in the system which showed the worst mixing conditions (i.e. *Stirrer (c) + baffles*).

Therefore, similar experiments to those performed with the centrifugal pump and the *Stirrer (c) + baffles* were carried out using a peristaltic pump in the sampling line. The results and %RSD obtained in the experiments with the peristaltic pump are represented in *Figure 3.46* both at and above the stirrer plane. These results were compared with those obtained when a centrifugal pump was used in the line (shown in *Figures 3.42* and *3.44*, and *Figures 3.43* and *3.45* for the %RSD). It can be observed that there was less variation between the curves when the flow-rate was changed for the case with the peristaltic pump. Therefore, the effect of sampling flow-rate was less important for the sample collection when using the peristaltic pump. As mixing was found to be the most important factor affecting the sample collection, this showed how the centrifugal pump improved mixing in the line. Finally, the %RSD values showed similar trends for both sampling with the peristaltic and the centrifugal pumps.

From all the results shown above, it was concluded that at high stirring speed and sampling flow-rates, representative sampling was obtained from both the sampling port at the stirrer plane and above. Furthermore, there was usually a value of the stirring speed above which representativeness reached a maximum. These conclusions are shown with the results given in *Figure 3.47* where representative sampling is seen at any value of bulk oil concentration (between 0-50% volume),

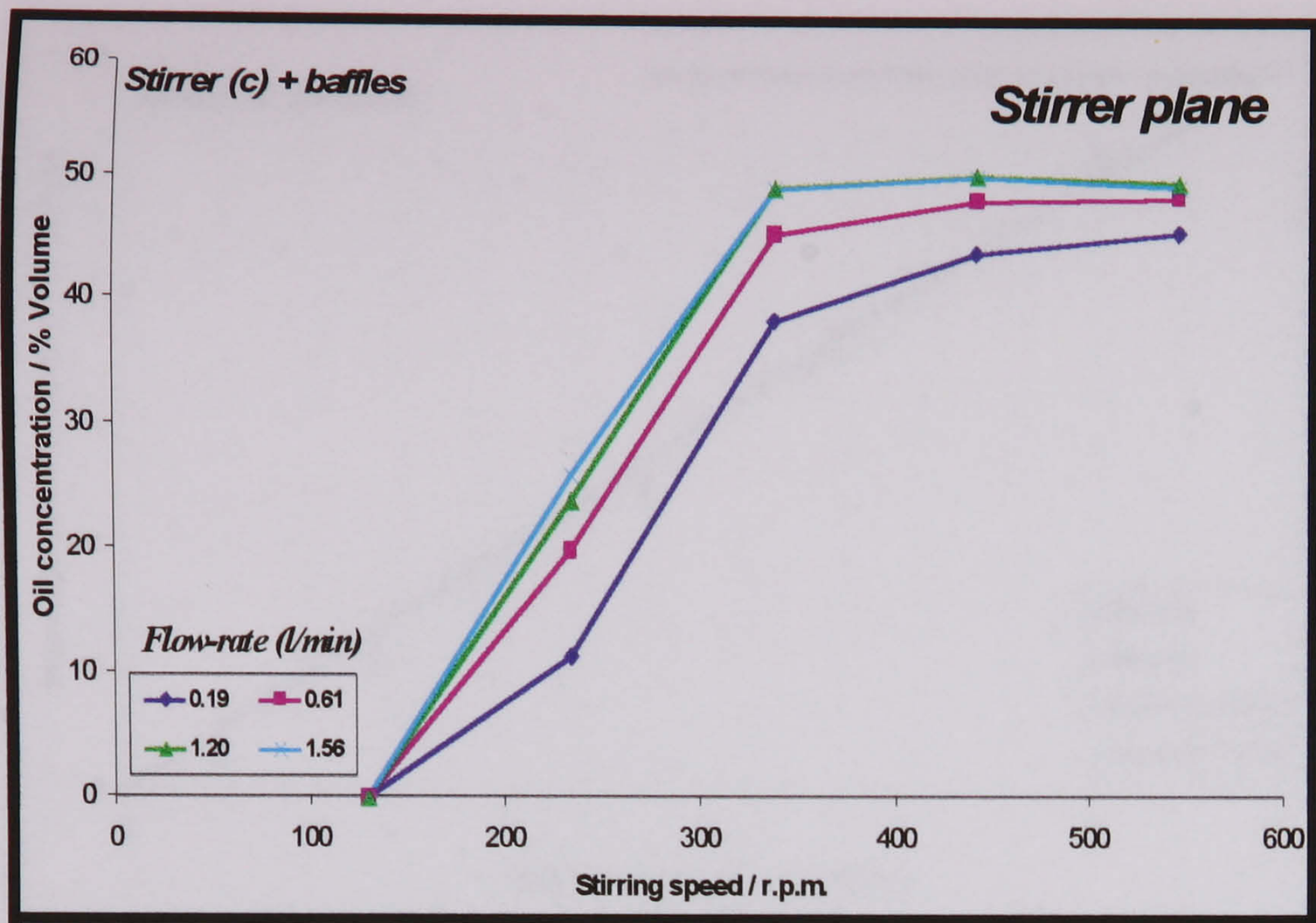

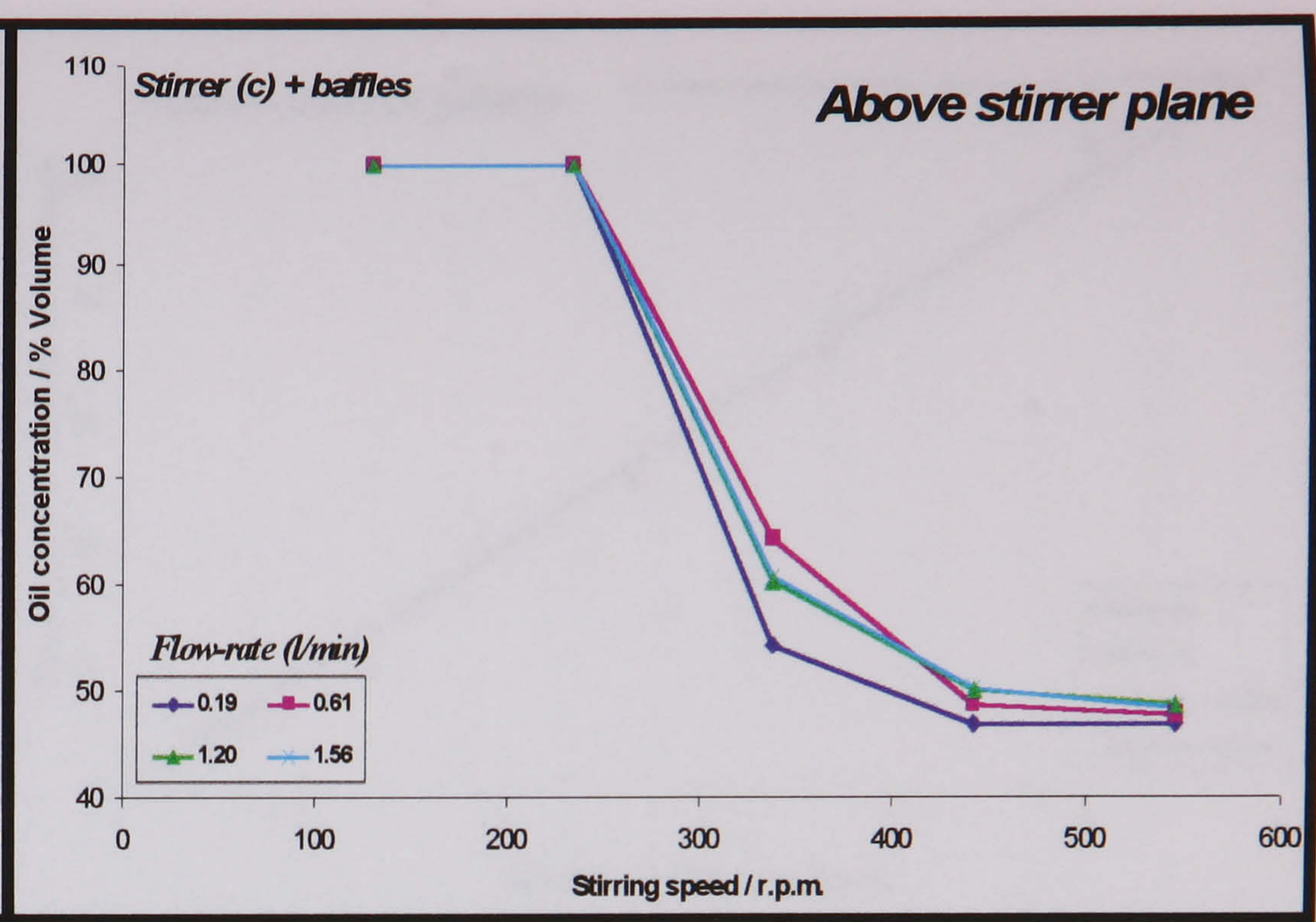

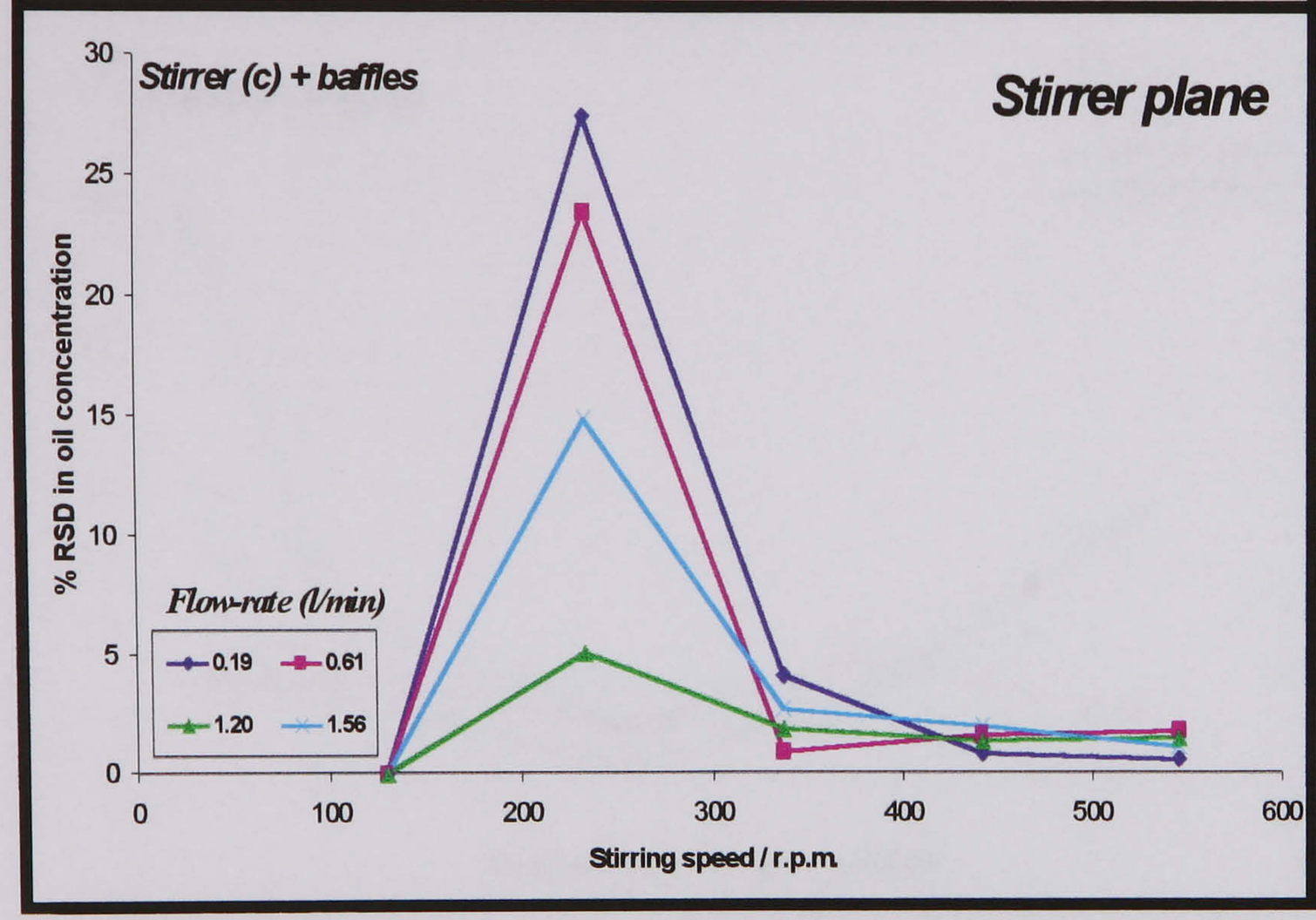

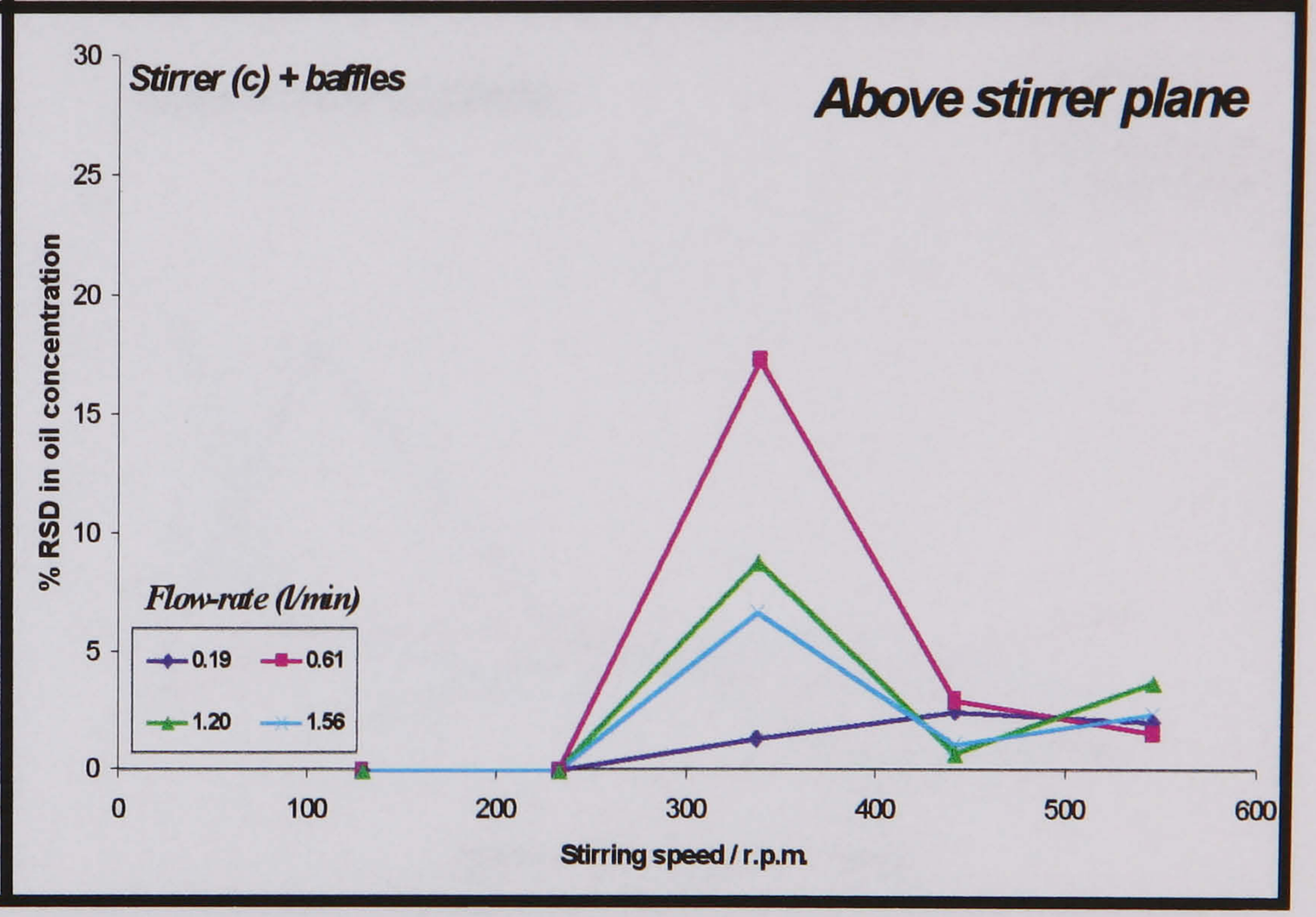

Figure 3.46. Concentration and %RSD in the sample collection (50% volume oil-water mixture) at and above the stirrer plane and at different stirring speeds when stirrer (c)+ baffles and different sampling flow-rates were set up with a peristaltic pump

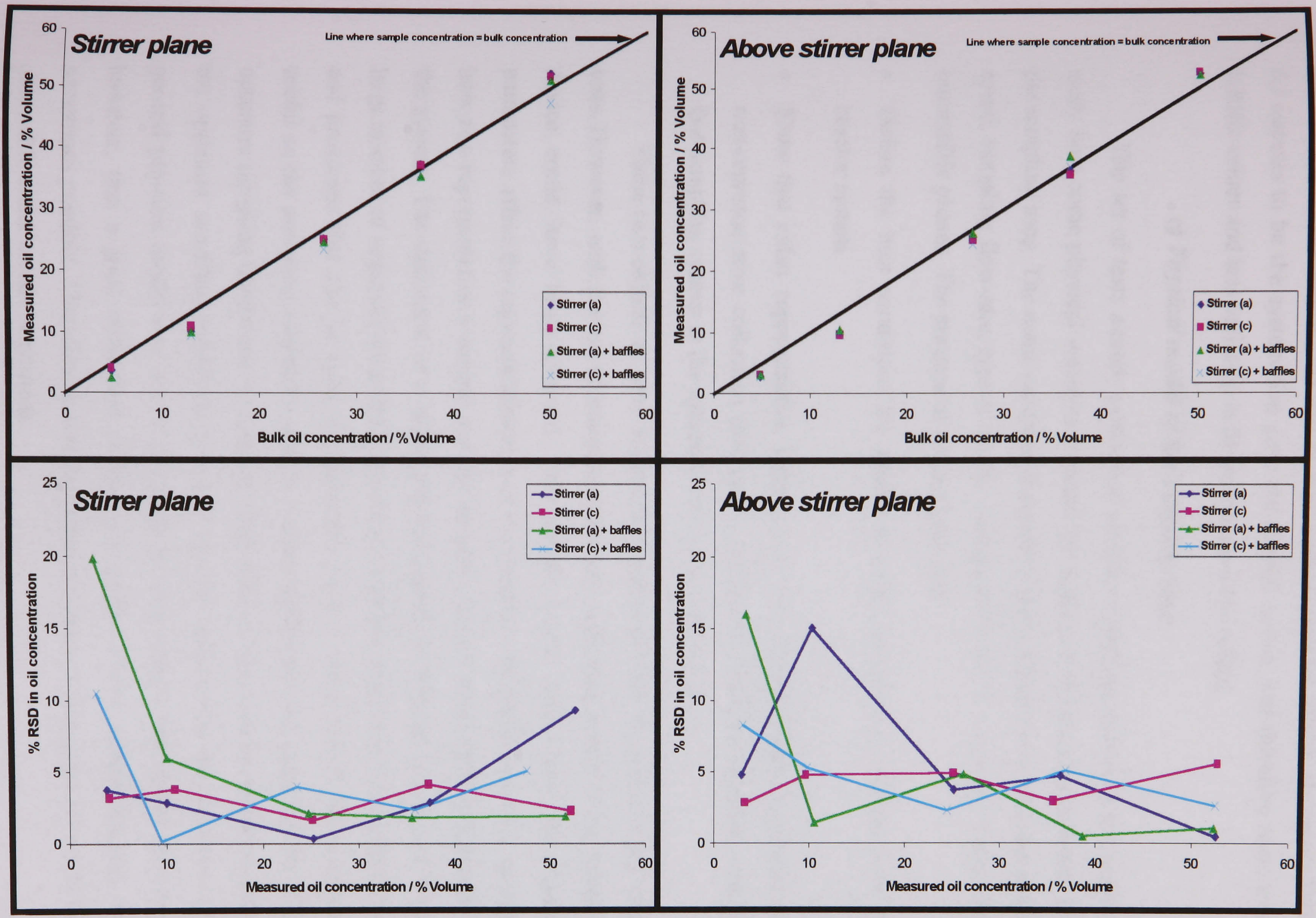

Figure 3.47. Sample concentration and %RSD values for sampling experiments at and above the stirrer plane, for different stirrers and vessel configurations and for different bulk concentrations of oil in an oil-water mixture between 0 and 50 % volume

for any stirrer and vessel configuration and when sampling at and above the stirrer plane. Looking at the %RSD values it is observed that most of the configurations showed acceptable values, specially at high bulk oil concentrations. However, *Stirrer (c)* appears to be the system that gave the flattest curves, and therefore more stable %RSD values and less variation in the precision of the results.

c) Physical model of the sampling loop

The set of tests already performed with the sampling systems were useful to study how some physical variables affected the quality of the samples collected with the sampling loop. The main variables analysed in those experiments were the stirring speed, sampling flow-rate, type of stirrer, configuration of the vessel and ratio of the immiscible phases. The purpose of this analysis was:

- Define the best conditions for sampling using the fast-loop designed for the reactor system.
- Show that either representative sampling or reproducible sample collection (i.e. non-representative collection that can be calibrated) could be obtained with the fast sampling system at the optimum conditions defined above.

These two objectives were successfully achieved after the performance of the tests. However, with the use of statistical treatment, a physical model of the sampling device could have been obtained. This model would define how the physical parameters affect the representativeness of the samples and could be used to quantify how non-representative a sample was for the particular physical conditions present in the system. The definition of a robust physical model would though, require a very large number of experiments as there are many variables, many reactor configurations and processes that can be used. Furthermore, such a model would not always be useful as the sampling conditions usually remain unchanged and good control of the optimum sampling conditions is preferred. Therefore, it was more interesting to define the optimum sampling conditions and this was the reason why the definition of a general physical model was out of the scope of this project. The results did prove, however, that a good calibration of how the quality of the sample changed was sometimes possible. Therefore, it was demonstrated that a robust physical model was obtainable under certain conditions.

3.2.2. Chemical modelling of the sampling system

The chemical modelling of the sampling loop accounts for the differences in the reactive evolution of the sample in the sampling loop system and that of the mixture in the reactor. This chemical model could be experimentally obtained by comparing the kinetics of a particular process both using and not using the loop[2]. In this section, the kinetics of the reaction used in the tests (i.e. esterification of crotonic acid) are defined. Also, the analytical procedures used in these kinetic studies are presented. Later in the section, the new kinetics when the loop was used are defined in order to analyse how the sampling conditions affected the chemistry of the process. Finally, the information collected in these experiments was used to define the chemical model of the system.

a) Kinetics of the process

For the determination of the kinetic parameters for the reaction of crotonic acid the 5-L reactor system was used, although preliminary tests were also performed in the 1-L reactor system. In the 1-L reactor, off-line samples were obtained during the reaction at regular intervals by sampling from the bottom port. Before sampling, the dead volume of liquid in the port was removed and put back in the reactor to ensure representativeness. In the 5-L system the samples were taken at regular intervals from the sampling port at the stirrer plane and after removing and feeding-back to the reactor the small dead volume of liquid present in the line. The sampling system was a simple 8 cm glass tube (ID 6 mm) inserted in the reactor port and with an open-close glass valve in one of the ends. Several experiments were carried out at different temperatures and the samples obtained were analysed by gas chromatography (GC) following the procedure described below.

i. GC analysis

The GC method of analysis used for the off-line monitoring of the esterification process was adapted from that reported by MacLaurin *et al.*[92]. Wells of Avecia provided the parameters used in this method, which were used as a starting point[93]. The capillary column that they used was a 25 m Chrompack Cp-Sil-5 CB of 0.25 mm ID. Since a slightly different column was available to us (a 25 m Chrompack Cp-Sil-5 CB 0.32 mm ID capillary column) some changes in the original method

were needed. The parameters used in the new GC method of analysis are summarised in *Table 3.5*. A Carlo Erba 8000 GC instrument with Chrom-Card acquisition software was used for the analysis.

Table 3.5. Parameters of the GC method of analysis used to monitor the esterification of crotonic acid

Column	CP Sil 5 CB 25m ID 0.32mm
Carrier gas	He
Detector	Flame ionization detector
Temperature program	$75^{o}C\,(3\,\text{min}) \xrightarrow{30^{o}C/\text{min}} 150^{o}C\,(5\,\text{min})$
Temperature at injector and detector	$250\ ^{0}$ C
Flow-rate carrier gas	1.5 ml/min.
Split ratio	40:1
Peak width	0.1
Peak threshold	1
Minimum area	100
Internal Standard	Undecane
Solvent	Dichloromethane
Dilution of samples	8×10^{-3} % w/w sample 7×10^{-5} % w/w Internal Standard

A typical chromatogram observed in the GC analysis of the samples extracted from the crotonic acid esterification process is shown in *Figure 3.48*. In the chromatogram it is seen how the peaks for both the butanol and the toluene could not be resolved and these two compounds were eluted together with the solvent. The monitoring of the concentration of butanol had to be sacrificed with the use of this new column. The concentration of toluene was not of interest as toluene was used only as a solvent for the reaction. The peak for crotonic acid showed to be fronting. No better results were obtained when parameters such as the flow-rate for the carrier gas or the temperature program were varied. The resolution for the ester peak was improved by increasing the split ratio and the dilution of the samples injected into the column. This avoided overloading of the column, which was observed when the initial parameters from the method reported by Wells were used with the new column[93]. Finally, the resolution for the internal standard (i.e. undecane) was good for quantitative analysis. Therefore, the ester peak was used for the off-line monitoring and kinetic studies for the esterification of crotonic acid.

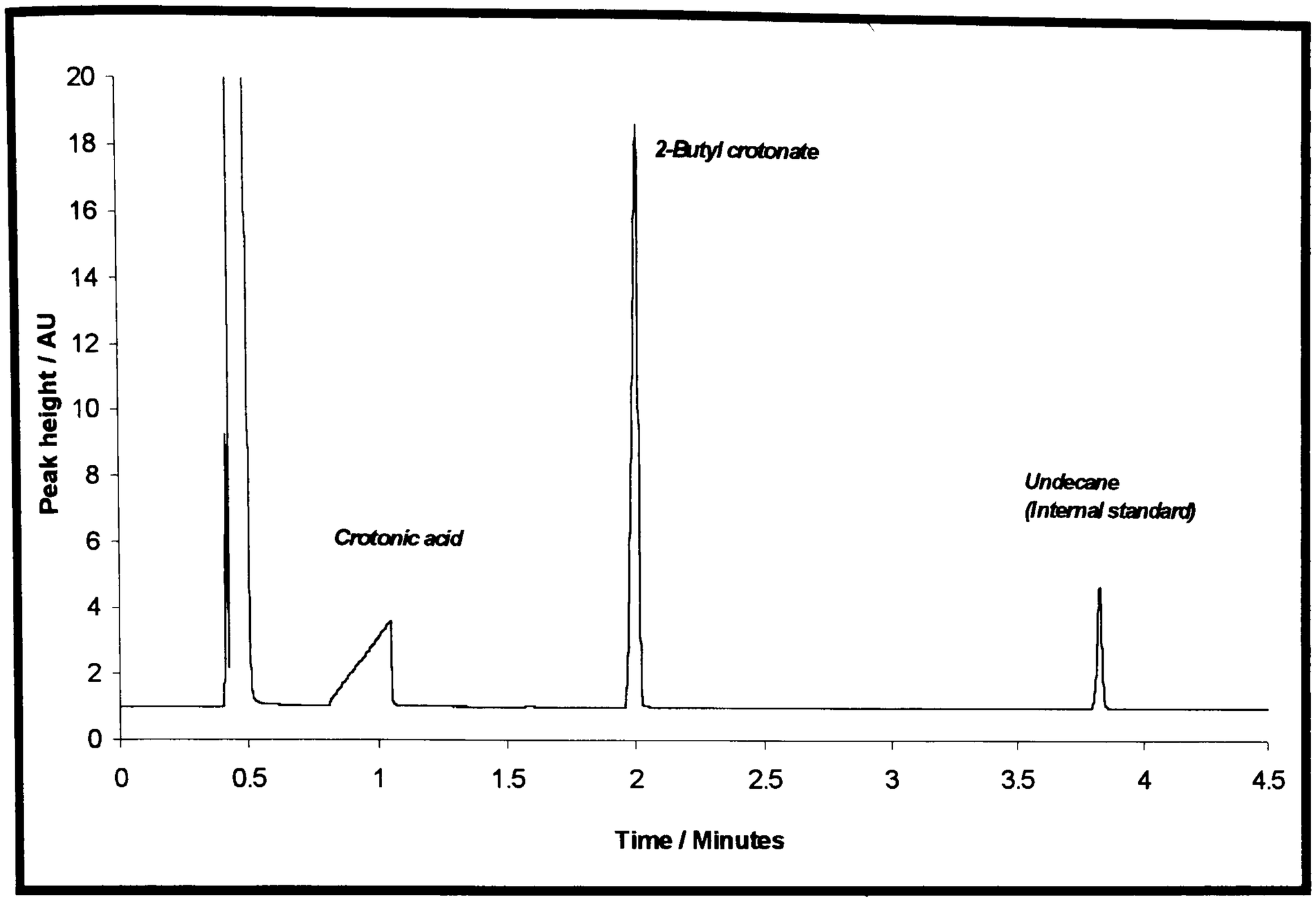

Figure 3.48. Typical chromatogram of one of the samples extracted from the esterification of crotonic acid

ii. Analysis of the kinetics of the esterification of crotonic acid

The reactions in the 1-L system were carried out by adding 86 g (1 mole) of crotonic acid (Aldrich 11,301-8) and 154 ml (1.7 moles) of 2-butanol (Aldrich B8,591-9) to 500 ml of toluene (Merck 28676,468) following the procedure described by MacLaurin *et al.*[92,94-96]. Toluene was used as a solvent to help the removal of water, and hence to improve yields[94]. After a sample at time zero was taken, the reaction was initiated by adding 2 ml of sulphuric acid. Paratoluene sulphonic acid was also studied as a catalyst since it has similar catalytic effects but it has the benefit of causing lower side reactions[94-95]. Another advantage of this acid is that it is not as strong as sulphuric acid and, in theory, it does not tend so much to protonate back the acid favouring the reverse reaction. However, no notable differences were observed between the reactions when the two acids were used. After initiating the reaction, samples were taken for off-line analysis and quenched in an ice bath.

From the preliminary experiments carried out in the 1-L system, two conclusions were obtained that affected the kinetic studies later with the 5-L system:

- A problem with the quenching procedure employed was detected. Only putting the samples overnight in an ice bath straight after sampling and keeping them at room temperature until analysis did not seem to be enough to stop the reaction. The reaction was observed to proceed further. This was confirmed by comparison of the results obtained by HPLC just after the reaction was concluded and the GC results obtained one week later[97].

- The conclusions obtained from the kinetic studies performed with the results obtained in the 1-L system were satisfactory. The tests could be used to obtain a good kinetic model provided the results were corrected to overcome the problem of quenching[98]. Therefore, the kinetic model showed some promising predictions that could be considered for the studies in the 5-L reactor.

The results shown in this section focus on the work using the 5-L reactor system. A comparison between the kinetic parameters obtained in the studies with both of the reactor systems is shown later. In the reactions carried out in the 5-L system, 516 g (6 mole) of crotonic acid (Aldrich 11,301-8) and 924 ml (10.2 moles) of 2-butanol (Aldrich B8,591-9) were added to 3000 ml of toluene (Merck 28676,468)[95-96]. A stirring speed of 250 r.p.m. was used in all of the reactions. By using the GC method described above, the analysis of the samples taken at regular intervals during the esterification process was carried out. This was done for the same esterification reaction at three different temperatures in order to acquire data to work out the activation energy of the process. The results obtained are shown in *Figure 3.49*. In the figure it can be observed that the reaction rate diminished as temperature decreased. This was expected for an endothermic process. Similarly, the time to achieve the value of conversion at equilibrium increased when the temperature decreased.

A rigorous kinetic study of reversible reactions with stoichiometry $A+B \leftrightarrow C+D$ is usually quite complicated[99]. Normally trial-and-error methods must be used. They require the choice of different values for the rate constant and the comparison of the concentration-time data with the suggested integrated kinetic

equation for each value in order to establish the best value. However, this analysis can be simplified as is shown below.

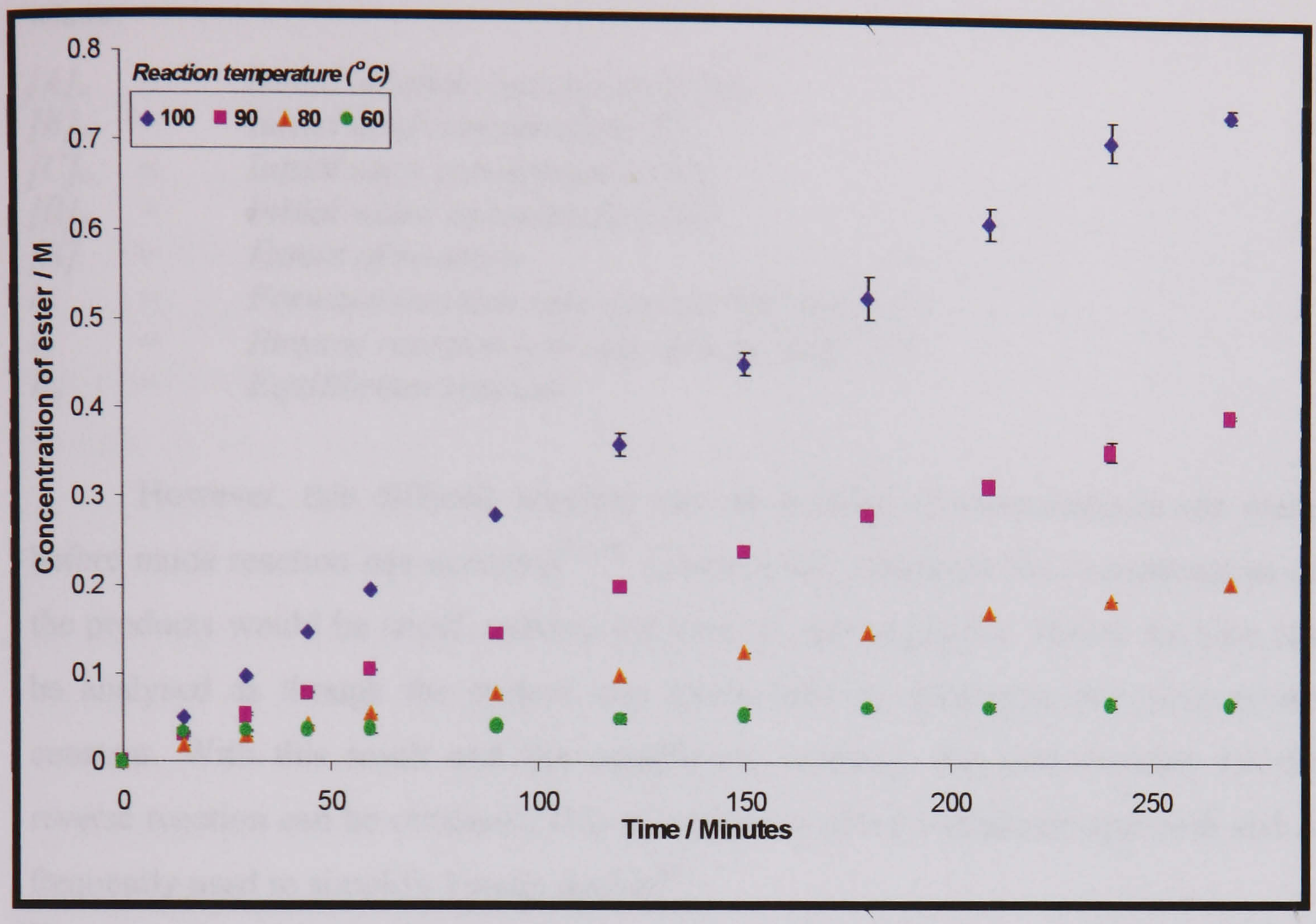

Figure 3.49. Monitoring of the crotonic acid esterification at three different temperatures in the 5-L reactor system

The kinetics would be defined by the following equation[59,99,100]:

$$-\frac{d[A]}{dt} == k_f [A][B] - k_r [C][D] \qquad \text{Eq. 3.13}$$

that can be integrated giving the following relationship[99]:

$$q^{1/2}\, t = \ln \frac{\{2\gamma [X]/(\beta - q^{1/2})\}+1}{\{2\gamma [X]/(\beta + q^{1/2})\}+1} \qquad \text{Eq. 3.14}$$

where:

$$[X] = [A]_o - [A] \qquad \text{Eq. 3.15}$$

$$\beta = -k_f \{([A]_o + [B]_o) + \frac{1}{K_e}([C]_o + [D]_o)\} \qquad \text{Eq. 3.16}$$

$$\gamma = k_f (1 - \frac{1}{K_e}) \qquad \text{Eq. 3.17}$$

$$q = \beta^2 - 4\alpha\gamma \qquad \text{Eq. 3.18}$$

$$\alpha = k_f\{[A]_o[B]_o - \frac{1}{K_e}[C]_o[D]_o\} \qquad \text{Eq. 3.19}$$

where:

$[A]_o$ = *Initial alcohol concentration (M)*
$[B]_o$ = *Initial acid concentration (M)*
$[C]_o$ = *Initial ester concentration (M)*
$[B]_o$ = *Initial water concentration (M)*
$[X]$ = *Extent of reaction*
k_f = *Forward reaction rate constant ($m^3\ mol^{-1}\ s^{-1}$)*
k_r = *Reverse reaction rate constant ($m^3\ mol^{-1}\ s^{-1}$)*
K_e = *Equilibrium constant*

However, this difficult analysis can be avoided if measurements are made before much reaction has occurred[99,100]. Under these conditions the concentrations of the products would be small, making the reverse rate negligible. Hence the data can be analysed as though the system was irreversible to determine the forward-rate constant. With this result and the equilibrium constant, the rate constant for the reverse reaction can be obtained. This procedure is called initial-rate approach and is frequently used to simplify kinetic studies[99].

The kinetic studies for the data obtained using integration methods and the initial-rate approach showed a good fit to an irreversible second order reaction model. Such a model predicts that for a reaction aA + bB → P the concentration changes according to:

$$-\frac{d[A]}{dt} = k_R\,[A][B] \qquad \text{Eq. 3.20}$$

and, therefore, using the integration method[99,100]:

$$\ln\frac{[A]}{[B]} = \ln\frac{[A]_o - [X]}{[B]_o - \frac{b}{a}[X]} = \frac{b[A]_o - a[B]_o}{a}k_R\,t + \ln\frac{[A]_o}{[B]_o} \qquad \text{Eq. 3.21}$$

where:

$[A]_o$ = *Initial alcohol concentration (M)*
$[B]_o$ = *Initial acid concentration (M)*
$[X]$ = *Ester concentration (M)*
k_R = *Reaction rate constant ($m^3\ mol^{-1}\ s^{-1}$)*
a = *b=1 = Stoichiometric coefficients for crotonic acid esterification*

It should be noticed that the water concentration has not been considered in the kinetics rate expression as a product concentration since the water was separated from the non-aqueous mixture where the reaction occurs because it was not soluble in toluene[100]. This was one of the reasons why the toluene improves the yield in the process and was chosen as the solvent for the reaction[94].

The tests for second order of reaction are plotted in *Figures 3.50*, *3.51* and *3.52* for the results obtained at the three different temperatures. It should be mentioned that in one of the preliminary experiments in the 1-L reactor the reaction was carried out at 110°C, the boiling point of the toluene[53]. However, the samples obtained at these conditions were highly heterogeneous with a clear separation between the toluene and the water being produced during the reaction. This caused problems of reproducibility in the results obtained with the GC analysis. This sampling problem was confirmed by the detection of outliers in both the GC results and the NIR monitoring of the process[94]. Finally, to model the dependence of k_R with the temperature T, the Arrhenius equation was used[100]. Plotting $ln(k_R)$ versus $1/T$, the E_a/R value was obtained as the slope of a straight line (see *Figure 3.53*).

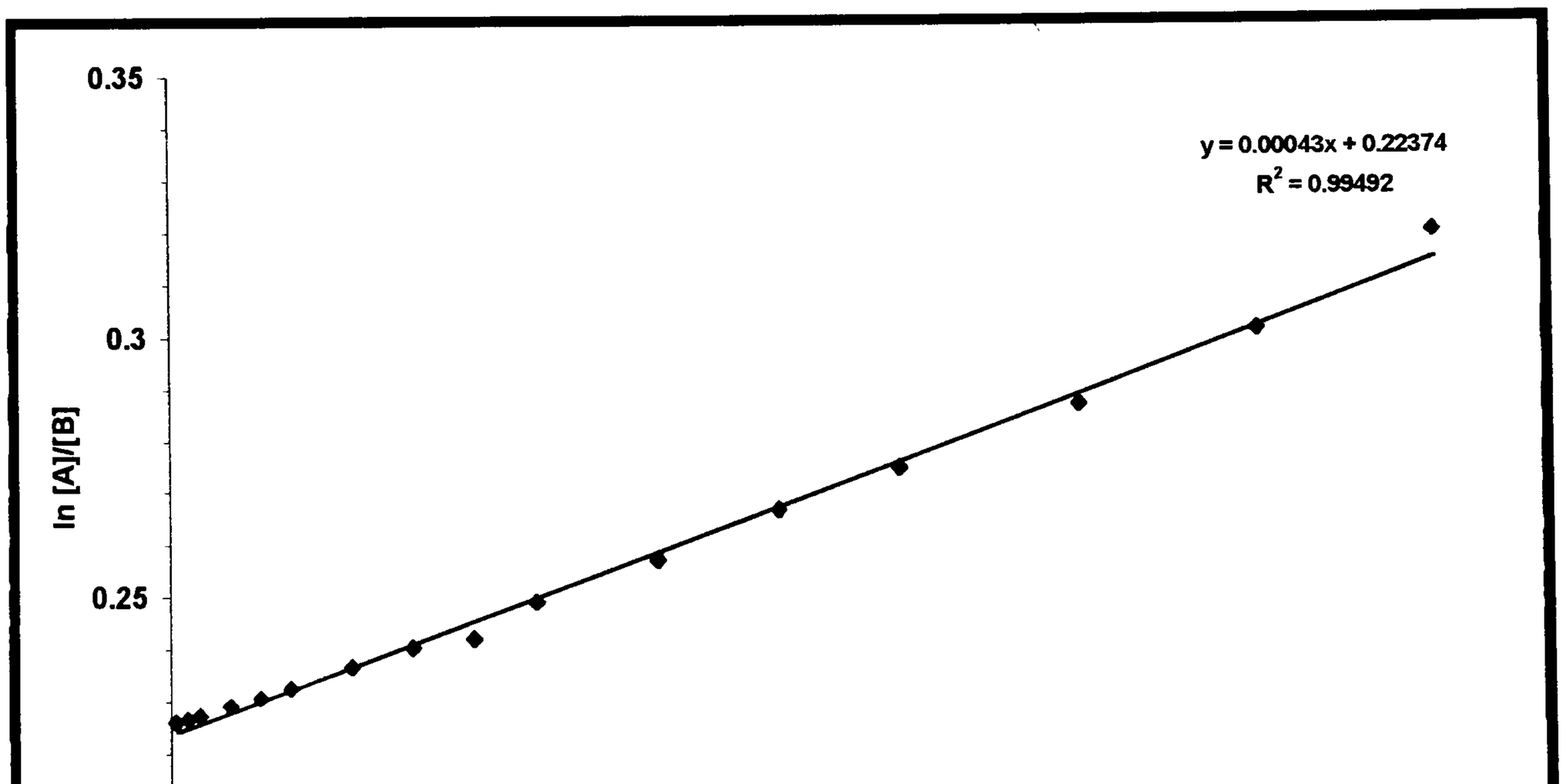

Figure 3.50. Test for second order kinetics for the crotonic acid esterification reaction carried out at 100°C

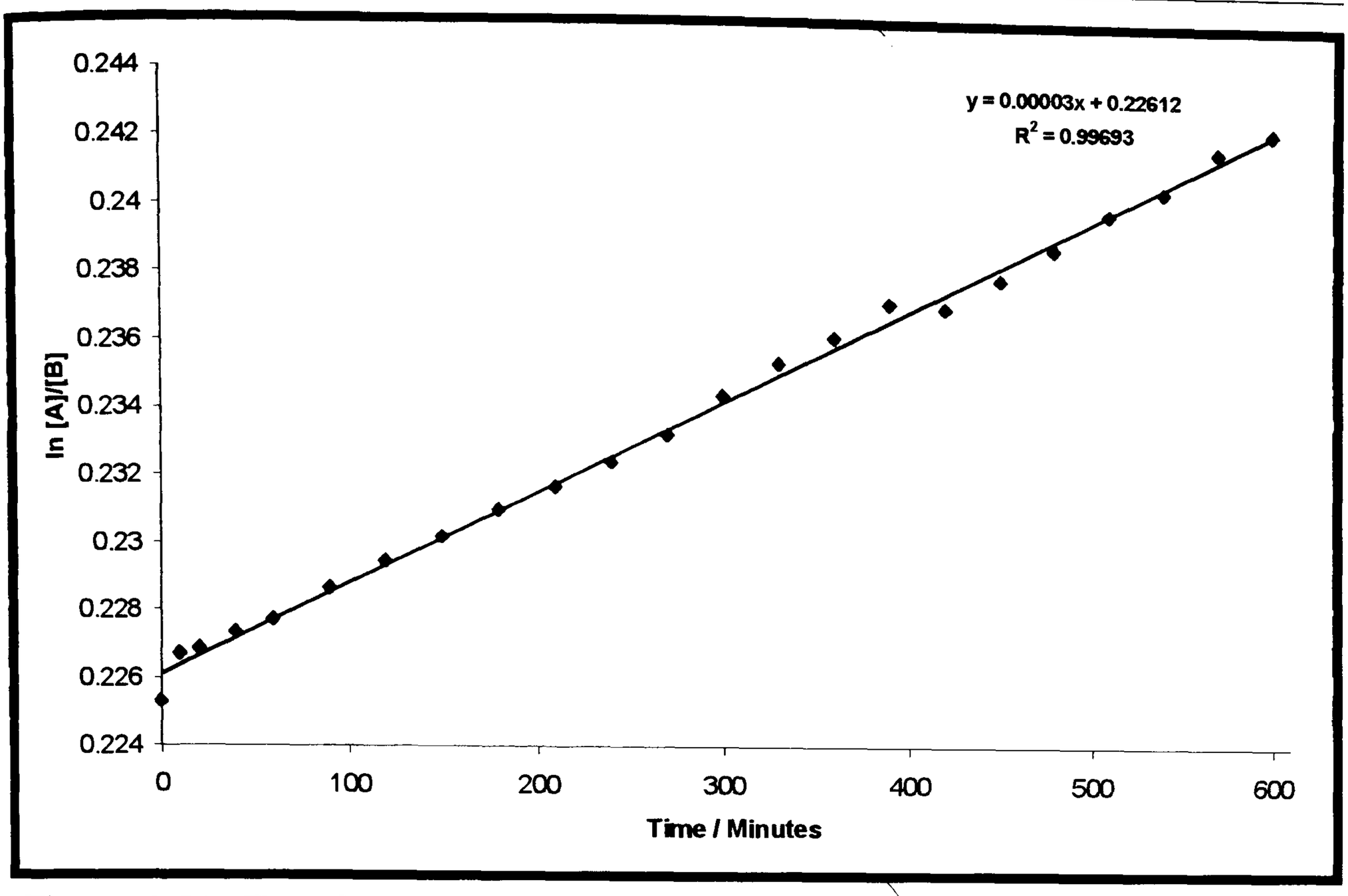

Figure 3.51. Test for second order kinetics for the crotonic acid esterification reaction carried out at 80°C

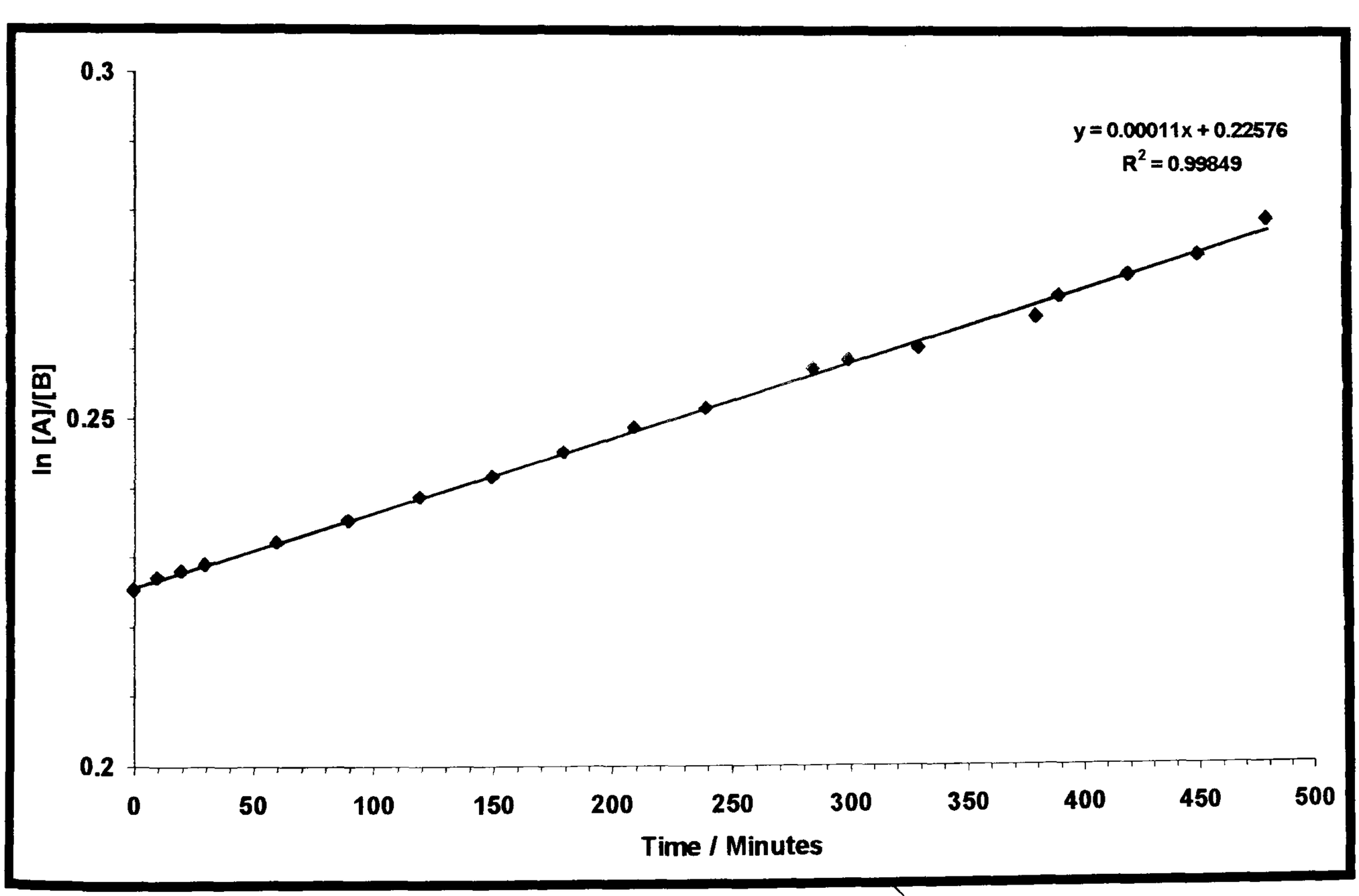

Figure 3.52. Test for second order kinetics for the crotonic acid esterification reaction carried out at 60°C

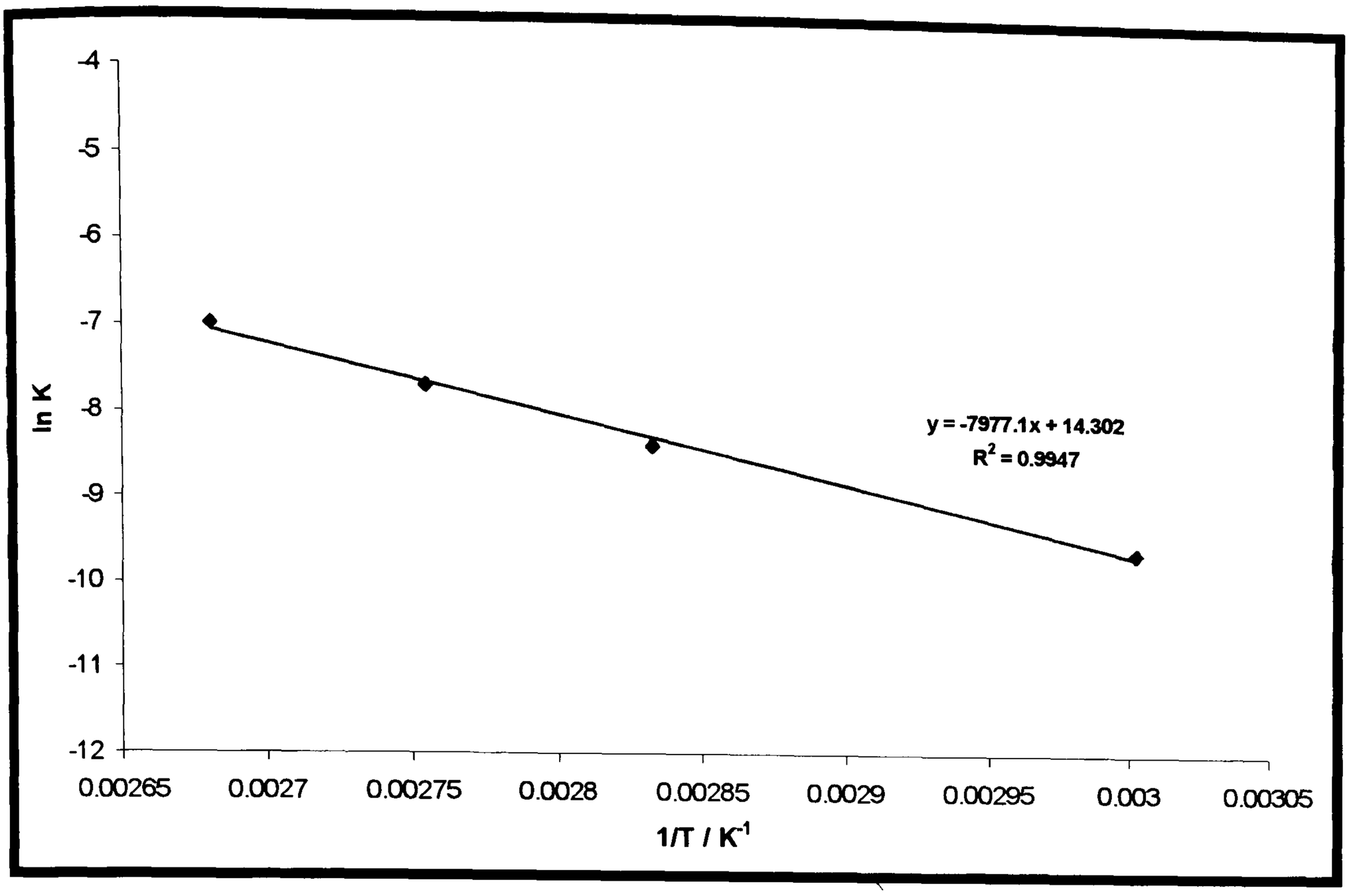

Figure 3.53. Temperature dependence of rate constant for the crotonic acid esterification reaction

Therefore, the following second order reversible reaction model was proposed for the esterification of crotonic acid:

$$-\frac{d[X]}{dt}=k_R[A][B]-\frac{k_R}{K}[X] \qquad \text{Eq. 3.22}$$

This model was used in numerical dynamic simulations of the process and analysis of how the ester concentration varied with time under certain conditions. In order to validate the kinetic model, a fourth reaction was carried at 90°C and the GC analysis of the off-line samples from the process were compared with the model prediction[59,100]. This is shown in *Figure 3.54* where the validity of the model is demonstrated. The development of the pure empirical model without constraints due to balances and the necessity to fit the data to specific kinetic model equations could also be analysed. A simple polynomial fitting could be performed to model how the ester production varies with the variables it depends upon. However, this would need a greater number of experiments and a wider range of conditions in order to get a reasonably robust model.

Table 3.6 summarises the difference between the kinetic parameters obtained in the experiments performed in the 1-L and the 5-L reactor systems. Initially factors like the type of sampling (from the bottom port in the 1-L reactor and at the stirrer plane in the 5-L system) or the accumulation of water in the bottom ports of the reactors were believed to be the reason behind the difference in the kinetic parameters obtained at high temperatures. However, some experiments performed after removing the dead volume at the bottom of the 5-L system showed good agreement with the previous results. Therefore, only the difference in the mixing properties between the two systems was found as the reason behind the different kinetic parameters. Later kinetic experiments using the fast sampling loop proved that changes in the mixing properties have a significant effect on the kinetics of the esterification of crotonic acid.

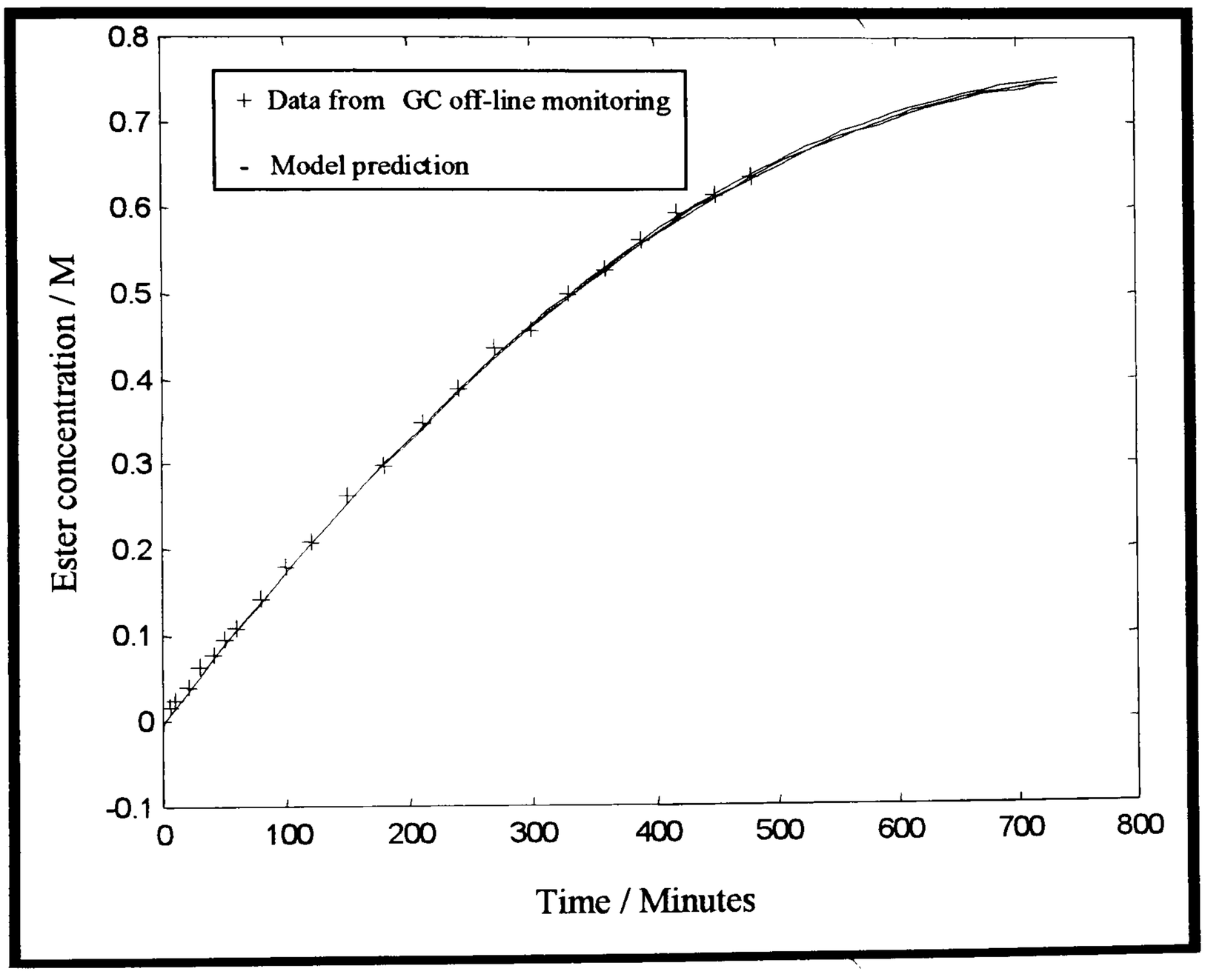

Figure 3.54. Comparison between model prediction and GC analysis of the samples[100]

*Table 3.6. Values for the kinetic constant k ([m^3 mol^{-1} s^{-1}] * 10^5) obtained in the kinetic studies with the 1-L and the 5-L reactor system*

System	*100°C*	*80°C*	*60°C*
1-L reactor	67.70	22.60	6.77
5-L reactor	90.31	22.57	6.77

b) Effect of the sampling loop on the kinetics

In order to prove that the use of the sampling system had an effect on the kinetics of the process, the esterification of crotonic acid was also followed when the sampling loop was continuously used. A detailed study of the kinetics of the process using the loop was carried out in a similar way to that described above when the sampling system was not used. The kinetic study described above assisted the modelling work carried out by the control engineers working in the project. On the other hand, the kinetic study using the loop described in this section had only the purpose of proving that there was an effect and therefore was not so detailed. Therefore, instead of repeating the same experiments at three different temperatures, and working out the new kinetic parameters and comparing them to those obtained when the loop was not used, only one experiment at high temperature was performed. By comparing the results obtained in this experiment with those obtained without the loop, the procedure for the kinetic modelling was introduced. This procedure is applicable to any particular process carried out in the reactor system.

i. GC analysis

The same GC method introduced previously was used to analyse the samples obtained under the new conditions using the loop. The samples were now obtained from the off-line port in the sampling loop. The sampling system used in this experiment was the version developed after the development tests carried out in the 5-L reactor system and the 5-L beaker system. Therefore, the maximum possible sampling flow-rate was used in a loop where the fittings and changes in the direction of the flow were kept to a minimum.

ii. Analysis of the kinetics of the esterification of crotonic acid

A single experiment was performed at 80°C with the loop working at the maximum flow-rate with no control valve or flow-metering systems in the sampling line. This flow-rate was manually determined and found to be 9 l/min for water. The operation of the esterification reaction at a temperature above 90°C produced some unusual noises in the pump. This was believed to be associated with cavitation, although the specifications of the pump guaranteed a satisfactory functioning at the conditions applied. Tests with water showed that the cavitation of the pump occurred at conditions very close to the boiling point of the solvent (97°C). When toluene (lighter but with higher boiling point than water) was used in the tests, the cavitation was observed close to 90°C, limiting the temperature conditions that could be used in the kinetic experiments using the loop.

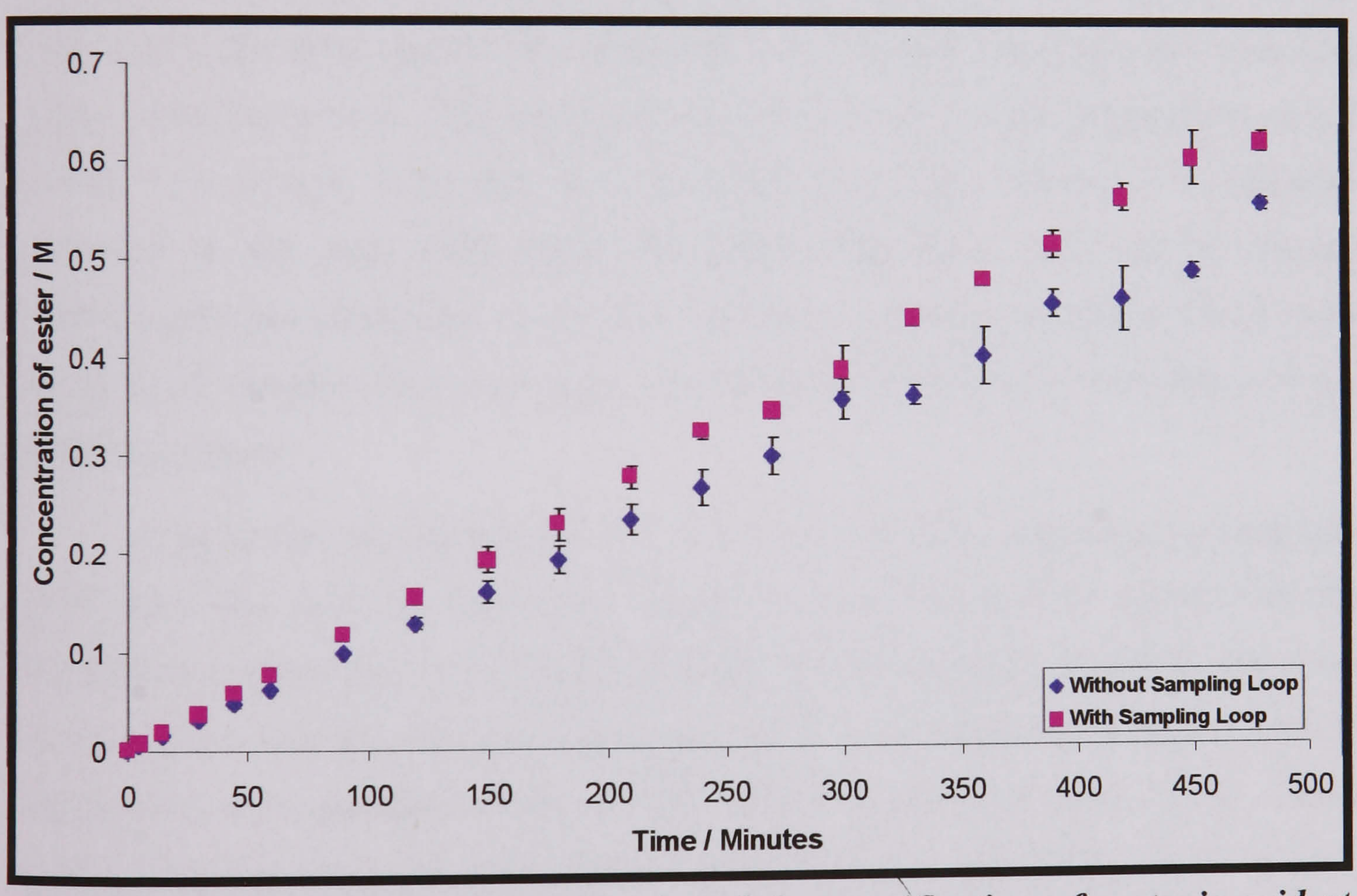

Figure 3.55. Comparison of the kinetics of the esterification of crotonic acid at 80°C with and without the sampling loop

The results obtained for the GC off-line monitoring of the process at 80°C and using the loop are shown in *Figure 3.55*. In the figure, the results with the loop are compared with those determined without the loop. The differences between the kinetics of the two processes were believed to be due to the mixing enhancement

produced by the centrifugal pump, which enables a better contact between the chemical species. This improvement in the mixing conditions was already shown when the results obtained with the peristaltic and centrifugal pumps were compared after the sampling experiments. This was also later confirmed by results obtained by near infrared (NIR) spectrometry obtained with and without the loop in the NMR experiments using heterogeneous mixtures. Later on this chapter, it will also be described how these chemical differences due to the mixing properties can be modelled.

c) Heat of reaction

Another parameter needed for the complete definition of the chemical modelling of a sampling system is the heat of reaction. In fact, this parameter affects the heat exchange properties of the process, which determines the design of the insulation and temperature conditioning systems needed for a sampling device. Fortunately, the importance of this parameter was minimal in the chemical modelling of our particular system. This was due to the fact that our reactor temperature control system was proved to be able to cope rapidly with any change in temperature produced in the loop. Only when the jacket temperature (and not the reactor temperature) was controlled, or the flow-rate in the loop was extremely slow, could the heat of reaction have any great relevance on the chemical modelling of the sampling system.

Despite the negligible effect that the heat of reaction may have on sampling, some time was spent in the project trying to define the heat of reaction for the esterification of crotonic acid. This had the purpose of assisting the control engineers in the project with the chemical information needed to develop the general model of the process, as no published data was found in the literature for this reaction. There are two experimental approaches that can be taken for the determination of the heat of reaction. One is the analysis of the concentration of the substances involved in the process at the equilibrium point at different temperatures. Once the values of the equilibrium constants are defined for three or more different temperatures, the application of the Van't Hoff equation provides a good estimation of the heat of reaction for the process. The Van't hoff equation is given by[99,101]:

$$\frac{d(\ln K_e)}{dT} = \frac{\Delta H^0}{RT^2} \qquad \text{Eq. 3.23}$$

where

ΔH^0 = *Standard-state enthalpy change for the reaction (J mol^{-1})*
T = *Temperature of reaction (K)*
R = *Ideal gas constant (J K^{-1} mol^{-1})*

The value for ΔH^0 varies with temperature depending on how much the heat capacity for the reactive substances vary with temperature. However, it is a common assumption with liquids to consider that the values for the heat capacity are more or less constant[101]. Therefore, the Van't Hoff equation is commonly integrated considering that ΔH^0 does not vary with temperature. As mentioned above, the use of the Van't Hoff equation for the definition of the heat of reaction assumes that the equilibrium constants at different temperatures are known. In the case of the esterification of crotonic acid, it was estimated that a minimum period of 10-12 hours was needed in order to achieve equilibrium at a temperature close to the boiling point[94,100]. Therefore, a longer period of time would be needed if a lower temperature of reaction was used. On the other hand, for safety reasons it was decided to avoid the overnight use of the reactor facility at Strathclyde University. Consequently, it was decided to look for another way to define the heat of the process instead of using the Van't Hoff equation.

Another way to find the value of heat of reaction is by calorimetric studies on the process[101]. In any calorimetric experiment, the thermal change in a particular mixture when the substances undergo a process can be related to the thermodynamics of the process, which are to be defined. There are different designs of apparatus that can be used in calorimetric studies, but the common feature is that they all look for ways of reducing the heat losses[102]. This is due to the fact that the larger the value of the heat losses, the less accurate is the definition of the thermodynamics of the process. However, a small thermal leakage, typical of any calorimeter, is often determined experimentally in order to calibrate the system and obtain a more accurate definition of the thermodynamics.

One of the simplest systems used in calorimetric studies is the Dewar flask, which is a vacuum-walled type of calorimeter[102,103]. It consists of a vacuum-jacketed vessel where the vacuum diminishes the tendency toward thermal leakage. It also has an inner reflective layer to avoid heat losses due to radiation. The equation that describes the thermodynamics of experiments in a Dewar flask and how the temperature of the content of the flask varies with time is[61,103]:

$$Mc_P \frac{dT}{dt} = \overline{\Delta H}_{Process} - Heat\ losses \qquad \text{Eq. 3.24}$$

where:

M = *Mass of solution (kg)*
c_p = *Specific heat of solution ($J\ kg^{-1}\ K^{-1}$)*
T = *Temperature in the flask (K)*
$\overline{\Delta H}_{Process}$ = *Energy per unit of time absorbed/released in the process ($J\ s^{-1}$)*

In some other calorimeters, the temperature of the jacket is controlled while the temperature of the content of the vessel is monitored. The equation that relates how the temperature of the process mixture changes with time for a specific jacket temperature is described below[103]:

$$Mc_P \frac{dT}{dt} = UA(T_J - T) + \overline{\Delta H}_{Process} - Heat\ losses \qquad \text{Eq. 3.25}$$

where:

U = *Overall heat transfer coefficient between the fluid in the jacket and the reactive mixture ($J\ m^{-2} K^{-1} s^{-1}$)*
A = *Internal surface of the reactor wall (m^2)*
T_J = *Temperature of the fluid flowing through the jacket (K)*

As the reactor facilities in this project allowed the control of the jacket temperature surrounding a reactor vessel, the feasibility of the use of such facilities for calorimetry was studied and the results obtained are presented in the next section of this chapter. Finally, it should be mentioned that in both of the cases mentioned above, Dewar flasks and more sophisticated calorimeters, the heat losses are normally

dependent on the difference in temperature between the content of the vessel and the environment. Therefore, the term due to the heat losses should be substituted by $U^*A^*(T-T_e)$ before the equations are integrated for analysis of the data[60,61,103]. Here, T_e is the temperature of the environment whereas U^* is the overall heat transfer coefficient between the environment and the reactive mixture. U^* is defined with respect to the area of the vessel, A^*.

i. Calorimetric studies performed in the Dewar flask

A commercial thermo-flask with a volume of approximately 500 ml was used as a vacuum-walled calorimeter following the procedure invented by Dewar in the last century[102]. The drop in temperature with time was monitored using a thermocouple. Several experiments were performed with and without the reaction in order to quantify the heat of reaction and the heat losses in the system. The experiments were performed at the conditions obtained by scaling down the parameters used in the 5-L reactors. In a normal test the following quantities of reactants and solvent were added to the Dewar flask: 300 ml toluene, 92.4 ml butanol, 51.6 g crotonic acid. After this, 1.2 ml of H_2SO_4 (catalyst) was added to initiate the reaction. Manual agitation of the mixture using a metallic bar and monitoring of the temperature using a digital thermocouple were carried out during 15 min.

A first experiment at room temperature showed that the reaction proceeds slowly at low temperatures. This experiment did not show a decrease of temperature in the mixture as the reaction proceeded, typical of an endothermic reaction such as the esterification of crotonic acid. This showed that, at low temperatures, the extent of reaction was so small that the release of energy due to the dilution of the catalyst predominated. Therefore, only an increase in the temperature of the mixture was detected in the experiment when the catalyst was added. The conclusion reached from this experiment was that another experiment at a higher temperature was needed in order to try to determine the heat of reaction.

In a new test, the mixture was heated to approximately 55°C. It was observed that, after the addition of the catalyst, the temperature of the mixture increased. After approximately 1 minute the temperature started to drop due to both the endothermic character of the reaction and the heat losses in the calorimeter. Additional experiments

were performed to define both the heat losses in the system and the heat of dilution released after the addition of the concentrated sulphuric acid to the mixture. No clear differences between the results with and without reaction were observed. Therefore, it was concluded that the heat of reaction in the conditions of the experiment was very small compared with the heat losses in the flask. In other words, these experiments with a simple Dewar flask would have never led to an accurate value for the heat of reaction for the process of esterification of crotonic acid and some other empirical method had to be used.

ii. Calorimetric studies in the 5-L reactor system

With the experiments above, it was concluded that the Dewar flask was not useful for the determination of the heat of reaction for the esterification process carried out in this project. In this section another way of studying the thermodynamics of the process is assessed. As the reactor facility in this project allowed a good control of the jacket temperature, the feasibility of the use of such a facility for calorimetric studies was analysed. As seen above, the equation that describes the thermal evolution of a reactive mixture is[103]:

$$Mc_P \frac{dT}{dt} = UA(T_J - T) + \overline{\Delta H}_{Process} - U^* A^* (T - T_e) \qquad \text{Eq.3.26}$$

where the term $U^* A^* (T - T_e)$ represents the heat losses in the system[60,61,103].

Prior to the use of the system for the determination of $\overline{\Delta H}_{Process}$, the rest of the terms in the equation must be fully defined by modelling the thermal behaviour of the jacketed reactor system. Therefore, the heat transfer parameters between the reactor and the jacket, and between the reactor and the environment had to be defined. A single heat transfer coefficient between the reactor and the environment was not considered due to the fact that most of the heat losses were produced in the unjacketed areas of the system. In other words, the reactor system can be divided in two regions (unjacketed and jacketed region) where the heat exchange properties were very different.

The easiest way to define the parameters U, A, U^* and A^* would be to perform an experiment without reaction that would provide the data to model the system. 3

litres of toluene, 924 ml of butanol and 516 g of crotonic acid were introduced into the reactor and the temperature of the mixture was monitored during a heating experiment with a constant jacket temperature of 90°C. Once the reactor temperature got to a steady value, a similar experiment was performed but when the mixture was cooled down. The set point for the temperature of the jacket was 20°C this time. These experiments were repeated three times for the analysis of the precision in the parameters obtained in the modelling. The temperature profiles for both the heating and the cooling experiment are plotted in *Figures 3.56* and *3.57*.

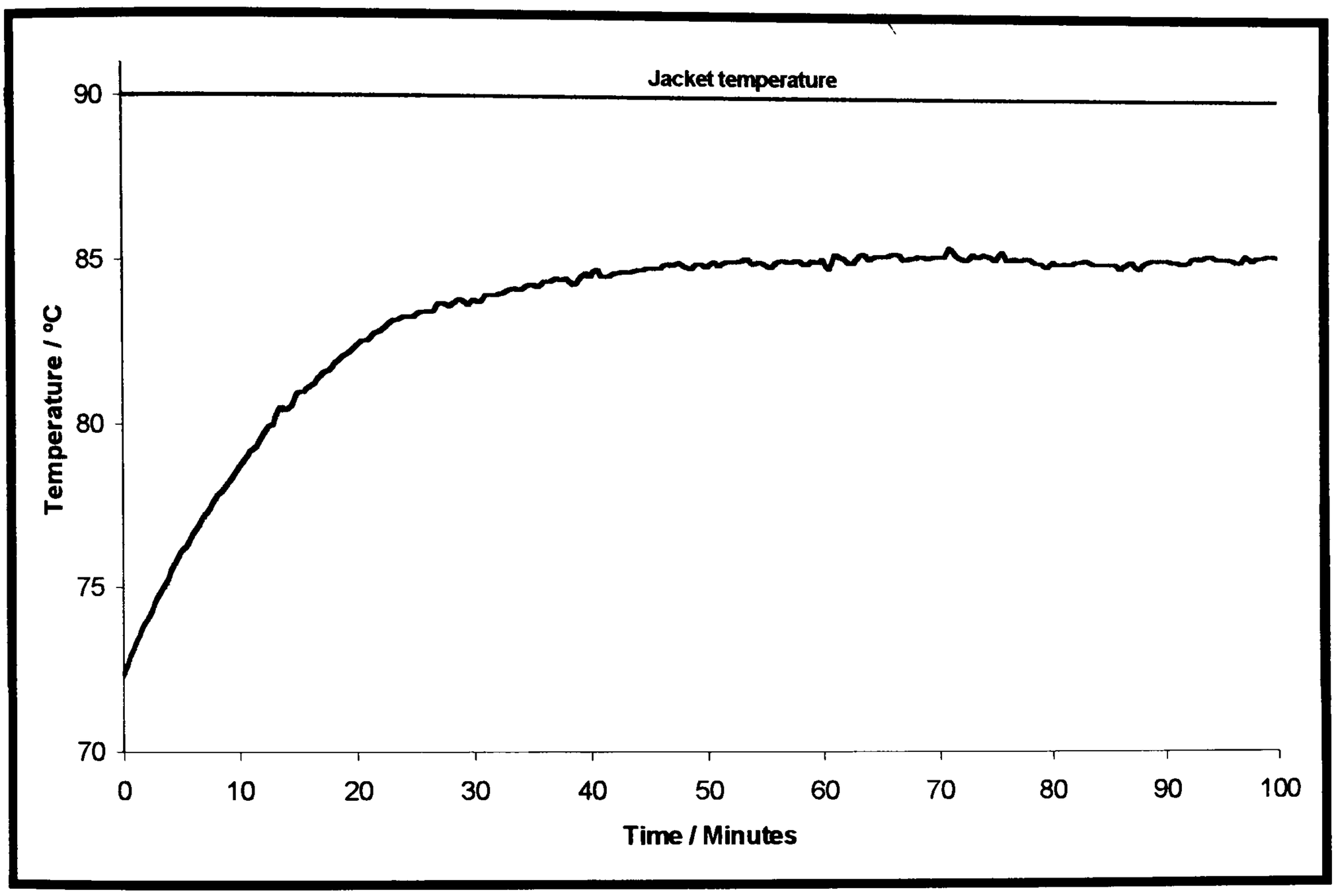

Figure 3.56. Temperature profile obtained during the heating experiment (jacket temperature 90°C) performed with the reactive mixture in the 5-L reactor

It should be noticed that, although the heating experiment was initiated with the mixture at room temperature, time zero was taken when the jacket temperature reached its set point. At this moment, the temperature of the mixture in the reactor was already considerably high (or low in the cooling experiment). More data could have been obtained if the set point for the reactor temperature was reached with the reactor empty and therefore without having any chemicals in the system. At this point, when the jacket reached the set-point, the reactive mixture at room temperature could have been added. However, this was not possible to perform in our reactor facility

as the vessels are made of glass and a big difference between the temperature of the reactor and the temperature of the jacket could have caused a thermal shock and breakage of the reactor.

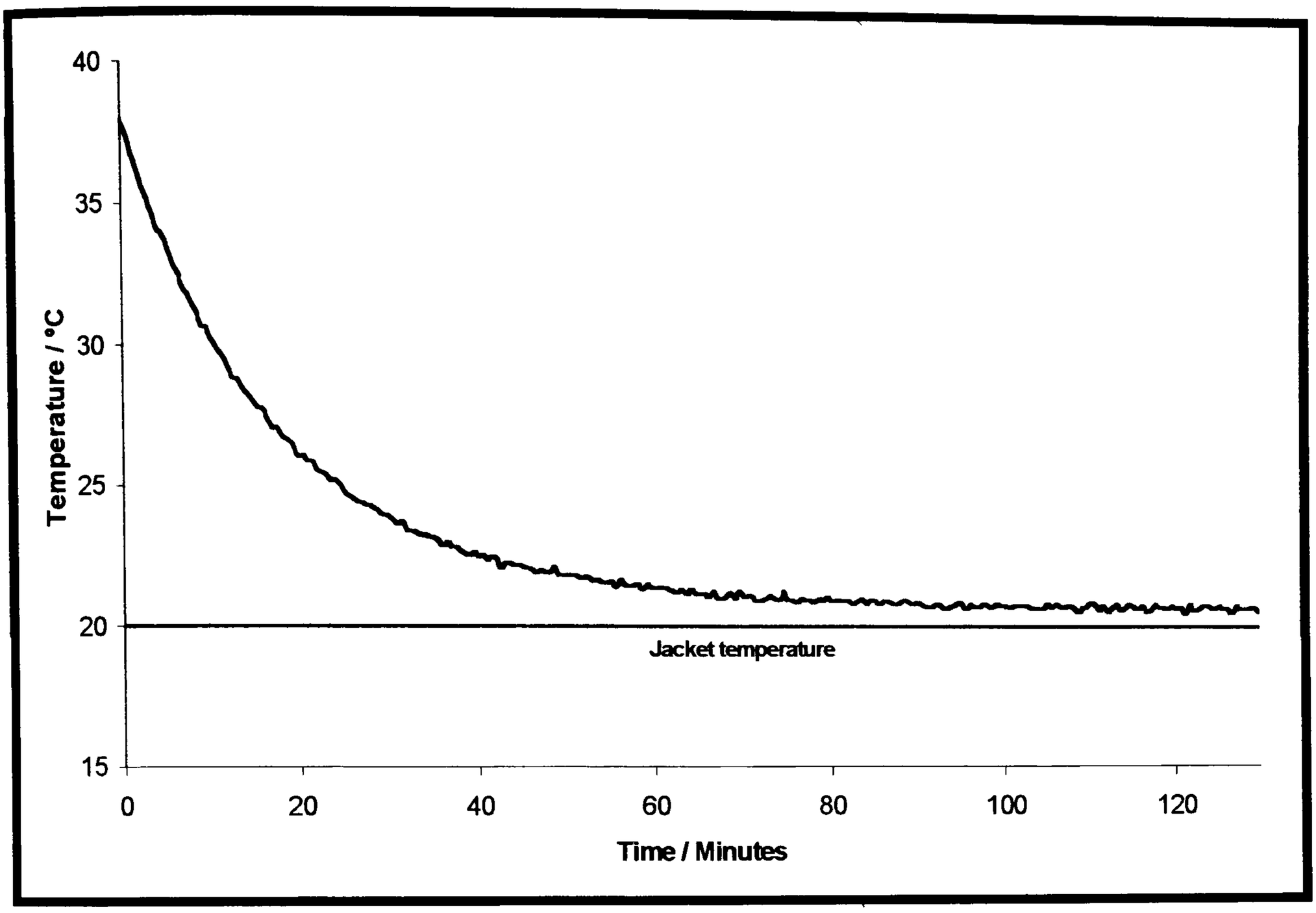

Figure 3.57. Temperature profile obtained during the cooling experiment (jacket temperature 20°C) performed with the reactive mixture in the 5-L reactor

The simplest way to analyse the data obtained from these heating and cooling experiments was by dividing the whole experiment into two stages. One stage was the period where the reactor temperature varied until it reached a steady value. The second was the steady state when the temperature of the reactor reached a constant value. During the first period, the term due to the heat losses is less important than that due to the exchange of energy between the jacket and the reactor and thus can be neglected[103]. Therefore,

$$Mc_P \frac{dT}{dt} = UA(T_J - T) \qquad \text{Eq. 3.27}$$

and so,

$$\ln(T_J - T) = \frac{UA}{Mc_P}t + C \qquad \text{Eq. 3.28}$$

Hence, if $ln(T_J\text{-}T)$ is plotted versus time, the heat transfer parameters for the jacket-reactor system can be obtained from the slope. *Figure 3.58* shows this type of representation for our heating experiment.

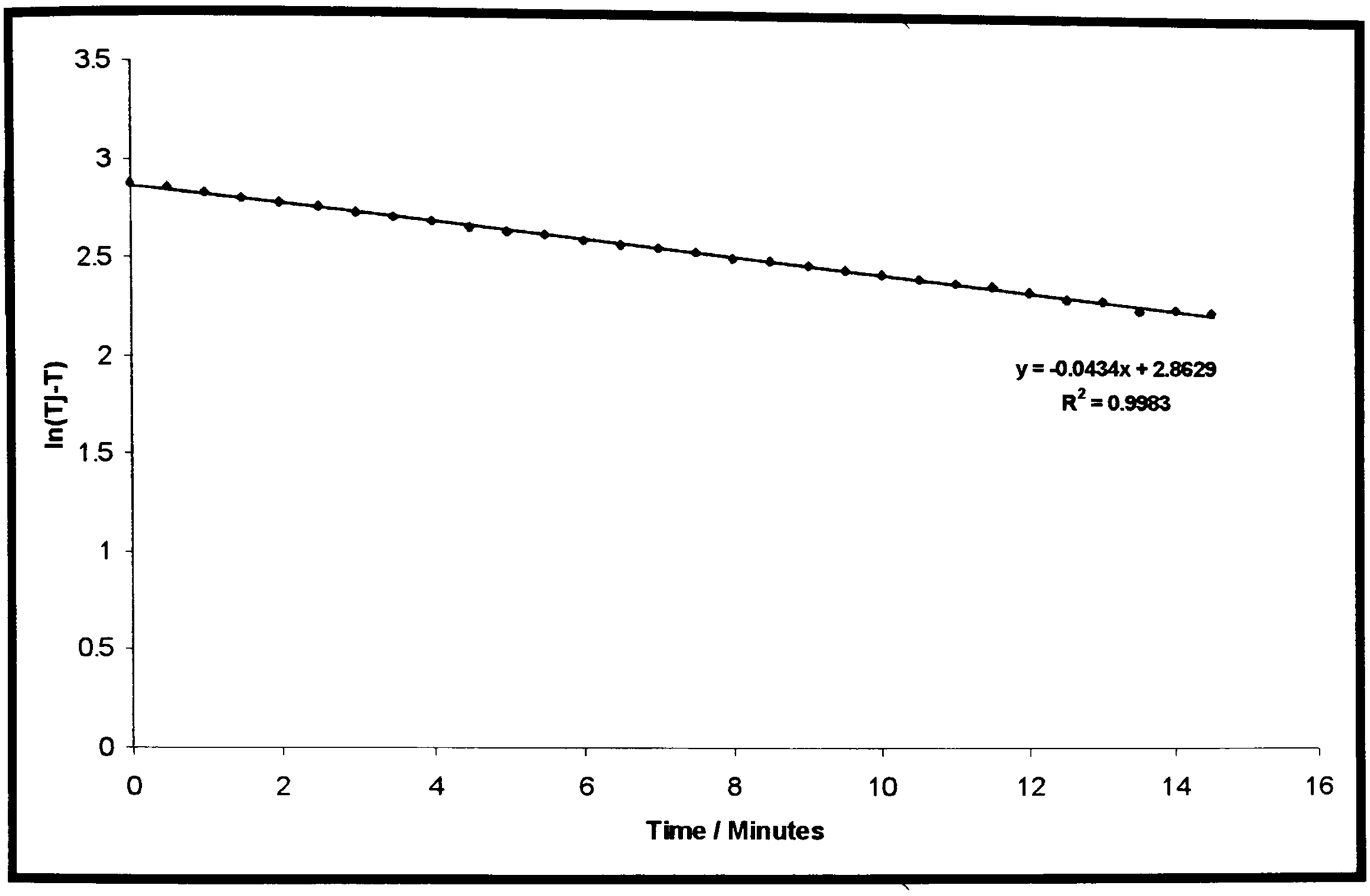

Figure 3.58. Analysis of the data for the initial period of the heating experiment (jacket temperature 90°C) performed with the reactive mixture in the 5-L reactor

A similar analysis can be carried out over the initial period for the cooling experiment. In this case, a better result should be obtained for the slope UA/Mc_p as the heat losses were more negligible during the cooling experiment due to the driving force $(T - T_e)$ being smaller at low temperatures. The values for UA/Mc_p obtained for both the heating (Heat.) and cooling (Cool.) experiments are represented in *Table 3.7*.

Table 3.7. Heat transfer parameters for the jacket-reactor system

	EXP.1 (HEAT.)	*EXP.2 (HEAT.)*	*EXP.3 (HEAT.)*	*EXP.1 (COOL.)*	*EXP.2 (COOL.)*	*EXP.3 (COOL.)*
UA/Mc_p	0.0402	0.0455	0.0434	0.0474	0.0515	0.0520

It can be observed that the heat transfer parameters between the jacket and the reactor obtained in the cooling experiment were slightly larger. This was due to the heat losses being less important than for the heating experiment. In our studies an average value of $UA/Mc_p = 0.0467 \pm 0.0138$ was used.

The second period in which the experiments were divided for data analysis was that when the temperature reached a steady value. During this stage $dT/dt = 0$ and therefore the equation for the energy balance becomes[103]:

$$\frac{UA}{Mc_P}(T_J - T') = \frac{U^* A^*}{Mc_P}(T' - T_e) \qquad \text{Eq. 3.29}$$

and so,

$$\frac{U^* A^*}{Mc_P} = \frac{(T_J - T')}{(T' - T_e)} * \frac{UA}{Mc_P} \qquad \text{Eq. 3.30}$$

where T' is the reactor temperature at the steady state. With the results obtained in these experiments the heat transfer parameters, and consequently the heat losses, were quantified. In order to use as many data points as possible in the calculation of the heat transfer parameters, the ratio $(T_J\text{-}T')/(T'\text{-}T_e)$ was worked out for different time intervals and an average value for $(U^*A^*/Mc_p)/(UA/Mc_p)$ was used. It should be mentioned that this type of data analysis could only be applied to the data obtained in the heating experiment, where the heat losses did not let the reactor mixture get to the temperature set for the jacket. On the other hand, at the end of the cooling experiment, $T' \cong T_e$ (i.e. no heat losses) as well as $T' \cong T_J$. The values obtained for the heat transfer parameters that define the heat losses in the system are summarised in *Table 3.8*. Using an average value of these results and including them into the heat exchange modelling equations, the following heat balance expression was obtained, which

describes the thermal behaviour of the reactor system:

$$\frac{dT}{dt} = 0.0467(T_J - T) - 0.0038(T - T_e) \qquad \text{Eq. 3.31}$$

Table 3.8. Heat transfer parameters for the system reactor-environment

	EXP.1 (HEAT.)	***EXP.2 (HEAT.)***	***EXP.3 (HEAT.)***
$(U^*A^*/Mc_p)/(UA/Mc_p)$	0.0860	0.0930	0.0840
$U^*A^*/Mc_p\ (min^{-1})$	0.0035	0.0042	0.0037

By integrating this equation, the model prediction of how the temperature of the reactor (T) changed with time was obtained. Thus, the following equation predicted the temperature profile for a heating experiment when T_J = 90°C and T_e = 20°C, the example that was used for the validation of the model:

$$\mathrm{T} = \frac{4.279 - \exp(-(0.0505\mathrm{t} + \mathrm{C}))}{0.0505} \qquad \text{Eq. 3.32}$$

where C is an integration constant that depends upon the initial conditions in the experiment, i.e. T at t = 0. If the temperature is predicted with this equation and the results are compared with the empirical data, an idea of the performance of the model can be obtained. This comparison is plotted in *Figure 3.59*. From this figure, it is observed that the model predicted relatively well the thermal behaviour of the system with a maximum difference between the actual and predicted value of ±1°C.

The next step in the calorimetric studies using the 5-L reactor system was the performance of the same type of experiment but now with the addition of the catalyst and, therefore with a reaction in the process. Again, the jacket temperature was kept constant at 90°C. When a steady value was achieved for the reactive mixture, the catalyst was added and therefore the reaction was initiated. Any change in temperature due to the progress of the reaction had to verify the equation that describes the model of the system:

$$\frac{dT}{dt} = 0.0467(T_J - T) + \frac{\overline{\Delta H}_{\mathrm{Process}}}{Mc_P} - 0.0038(T - T_e) \qquad \text{Eq. 3.33}$$

where $\overline{\Delta H}_{Process}$ varies with time depending on the kinetics of the process. Therefore:

$$\overline{\Delta H}_{Process} = \Delta H_{Process} \frac{d[Products]}{dt} \qquad \text{Eq. 3.34}$$

where $\Delta H_{Process}$ is now the energy per mol (usual units for the heat of reaction) and does not vary with time.

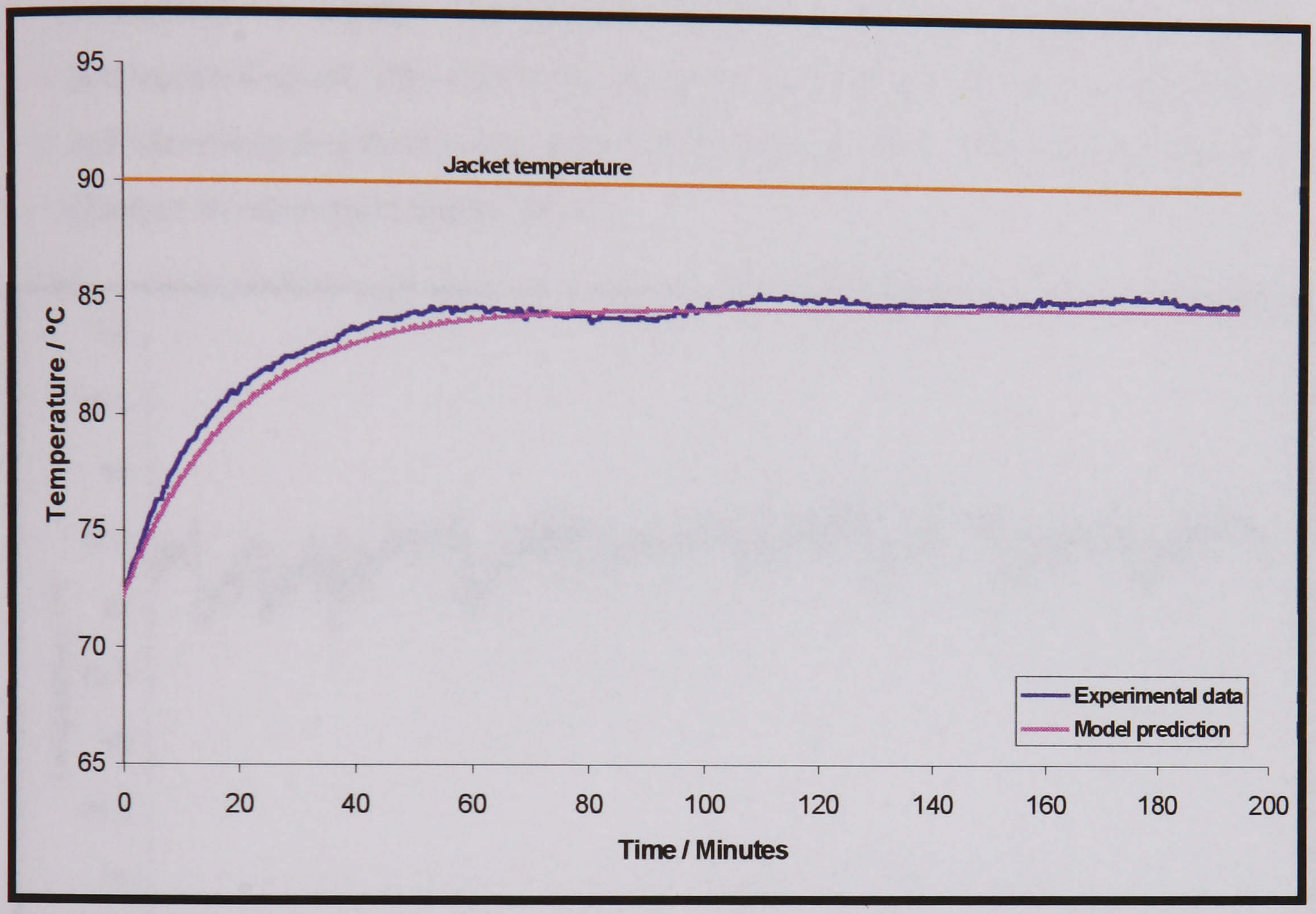

Figure 3.59. Comparison of the model prediction and the empirical data for a heating experiment (jacket temperature 90°C) performed with the reactive mixture in the 5-L reactor

When the experiment with the reaction described above was performed, the temperature profile observed in *Figure 3.60* was obtained. Here, it is seen that the temperature in the system did not vary appreciably with time as the reaction proceeded. Only minor changes in the temperature, due to noise in the measurement, were detected. Also, the returning of the dead volume extracted from the sampling system for the collection of off-line samples caused the small step changes observed in the figure. These results led to the following conclusions:

- The heat absorbed during the reaction at the temperature set for the experiment was very small compared to the heat losses or heat exchange between the

jacket and the reactor. A further experiment at a higher temperature would have probably led to the same conclusion, as a very high temperature was already used in these experiments.

- The response of the temperature control system is very fast and any change in the temperature of the system (that also modifies slightly the jacket temperature that is controlled) is rapidly compensated by increasing the temperature of the heating/cooling oil. This fact was verified by monitoring the temperature of the oil and observing that there were small changes to correct for the variation due to the changes in the reactor temperature.

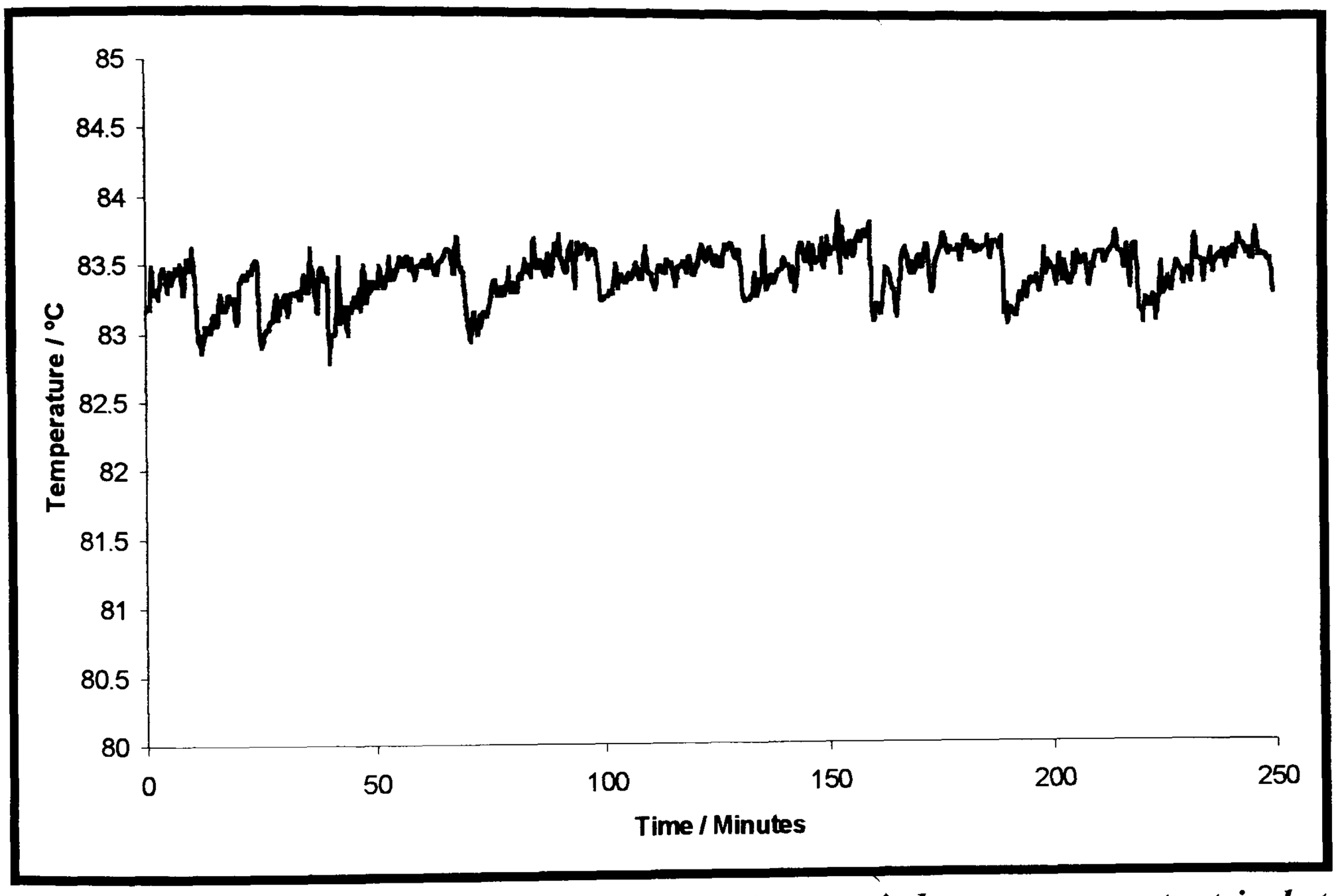

Figure 3.60. Temperature profile for a reaction carried out at a constant jacket temperature of 90°C

These two reasons limited the use of the reactor facility for the calorimetric studies of this particular reaction. Therefore, a more sophisticated calorimetric system had to be used in order to try to determine the heat of reaction for the esterification of crotonic acid.

iii. Calorimetric studies in more sophisticated facilities

Due to the problems that were experienced in the empirical determination of the heat of reaction for the esterification of crotonic acid, the assistance of the industrial members in the project was requested. John E. Richardson (SmithKline Beecham) very kindly took the responsibility of carrying out new calorimetric studies in the specialised facilities that SB had in one of their laboratories. The experiments were performed as follows[104]. Crotonic acid (50g, 0.58mol), 2-butanol (72.34g) and toluene (251.45g) were charged into a calorimetric reactor vessel. The mixture was heated to 75°C. The system was then ramped from 75 to 80°C, before being calibrated over 10 min. Sulphuric acid (2.24g) was added to the mixture in one portion and the resulting clear yellow solution was left to stir overnight at 80°C. The mixture was calibrated and ramped from 80 to 75°C and the experiment was then terminated. In the test, it was observed that the addition of sulphuric acid to the mixture produced a mild exotherm[104] (i.e. low released of energy). The total heat output in this addition process was -0.58 kJ. No significant heat release was associated with the 20 hours stir-out period that followed. The effective heat output for the addition of the acid was -1kJ/mole with respect to crotonic acid and the effective adiabatic temperature rise was 0.6°C (Cp=2576 J/kgK).

It should be highlighted that the parameters used in this experiment were generally obtained by scaling down the values normally used in a esterification process in the 5-L reactor. This was true for all of the species but not for the sulphuric acid that was added in excess. However, since sulphuric acid is only the catalyst for the reaction, this extra addition was not expected to affect the results obtained in the experiment for the heat of reaction in the esterification process. This excess of catalyst was only expected to affect the value of the heat output for the acid addition per mol of crotonic acid. It could also have produced some sulphonation (responsible for the yellow colour) in the toluene. However, neither toluene (inert solvent), nor its sulphonated form were expected to affect the normal progress of the reaction.

In conclusion, even with the more sophisticated calorimetric equipment at SB, no temperature change during the esterification process was observed. Therefore, the heat of reaction in the esterification of crotonic acid was considered as negligible.

However, the heat transfer studies reported earlier in the chapter were not a waste of time as they provided valuable information regarding the heat-exchange parameters for the 5-L reactor system. In fact, these parameters were used by the control engineers in the project in the general model of the system that they developed. Furthermore, these studies and the definition of the heat-exchange parameters can be used in the future for calorimetric studies carried out in the 5-L reactor. This is only possible though, if the processes being used have a heat of reaction that is not very small compared to the heat losses in the system.

d) Chemical model of the sampling loop

There are numerous models that can describe how a particular reactor system differs from the ideal conditions[105]. The ideal models for chemical reactors assume that ideal flow patterns of perfect mixing are present. However, there are cases that cannot be handled by these assumptions due to the presence of corners and baffles that can lead to stagnant regions, or due to non-uniform flow paths that can lead to bypassing of fluid. This non-ideal features are more typical from flowing systems such as Continuous Stirrer Tank Reactor (CSTR) and Plug Flow Reactor (PFR) systems than from batch processes[62,105]. Also, these alterations in the flow affect far more to the continuous processes where the deviations from the ideal situation alter the age distribution of the elements of the fluid in the reactor. This means that only a few of those elements stay the theoretical residence time inside the reactor. However, in batch processes all of the elements of fluid stay the same period of time inside the reactor but there are zones where the mixing of the chemicals is different than in other regions. This does not affect the final yield and production in the reactor as much as the variations in age distribution typical of continuous processes.

Since chemical modelling is more important in continuous reactors, these studies are more extensively covered in the literature for CSTR and PFR systems[105]. In the analysis of non-ideal features and age distribution dispersion in reactors, the use of tracers is one of the most popular tests. These experiments are performed by introducing tracers, which are marked fluid elements, in the process vessel at a certain instant of time. The observation of the sequence of particles in the outlet gives an idea about the dispersion in residence times. *Figure 3.61* shows the typical age

distributions for different continuous reactor systems[62]. The plots obtained in the experiments with tracers are normally compared with the typical graphs for ideal systems in order to model the non-ideal features of the real system[62,105].

Although these types of studies in batch reactors are less common, there exist methods to perform this kind of analysis in discontinuous systems and define real models for the reactors. However, there are alternative methods that can be used as an easier approach to solve the problem. For example, empirical methods such as LDA or mathematical simulations like CFD are better to study the flow-patterns of stirred vessels and therefore study the stagnant regions and mixing abnormalities in the system[35-41]. In our case, the easiest approach was to compare the kinetics of the process with and without the loop to analyse the effect that the change in the mixing properties had over the chemistry in the system. This method is of special interest when the kinetics of the process are not published in the literature and therefore only an idea of the kinetic parameters can be empirically obtained using non-ideal reactors. This was the case of our process, where the real kinetic values for the esterification of crotonic acid were initially unknown and only approximated experimental values were obtained in the 5-L reactor.

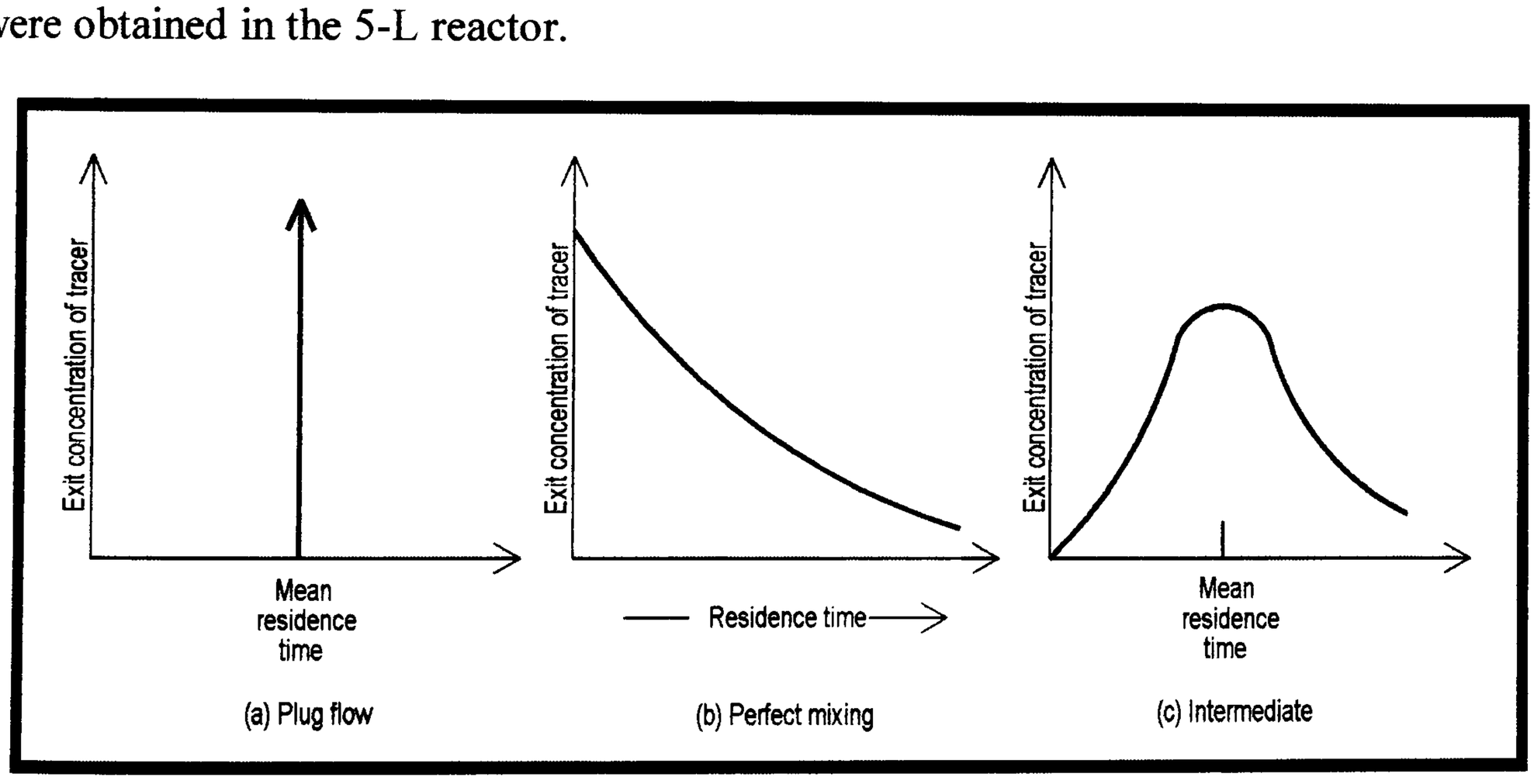

Figure 3.61. Exit concentration of tracers observed in several kind of systems when input stream is tagged at time zero[62]

Therefore, only two experiments were performed to study the effect of the sampling loop in the process. One reaction was carried out at 80°C using the standard procedure described for the kinetic experiments without the loop and sampling at the stirrer plane. A second experiment was performed at the same temperature and

continuously using the loop to get off-line samples. The results obtained in these experiments have been shown before (*Figure 3.55*). These were the only tests considered in the study of the effect of the loop on the chemistry of the process, as the heat of reaction was concluded to be negligible in this particular esterification reaction. It should be mention that, although the experiment at 80°C without the loop was already performed in the kinetic experiments described earlier, the test was repeated as a different reactor and PTFE impeller were used and this was expected to affect the mixing properties in the system. In fact, the results obtained in this new experiment showed a higher conversion than the ones obtained in previous tests. This confirmed that the mixing conditions affected the kinetics of the process and was the reason why the kinetic experiments gave different results in the 1-L and the 5-L reactors.

Figure 3.55 shows how the esterification process was slightly faster when the loop was used due to an enhancement in the mixing of the chemicals obtained with the use of the centrifugal pump. This improvement in mixing was corroborated in later experiments (see section *3.3.1*) when the NIR results obtained in tests with a non-reactive heterogeneous mixture, with and without the loop, were compared. *Table 3.9* shows the different values obtained for the kinetic rate constant at 80°C. A short additional discussion about these values is given opposite.

Table 3.9. Comparison of the values for the kinetic rate constant at 80°C when the loop is used and when it is not

Conditions	***k ([m^3 mol^{-1} s^{-1}] * 10^5) first 75 min.***	***k ([m^3 mol^{-1} s^{-1}] * 10^5) first 240 min.***
With no sampling loop	313	406
With sampling loop	327	587

Another approach that can be followed to model the effect of the loop on the chemistry in a batch process is to try to find a trend in the difference between the results obtained with and without the loop. Eq. 3.35 presents *f(t)* as the function that represents how this difference changes with time:

$$C_A' = C_A + f(t) \qquad \text{Eq. 3.35}$$

where:

C_A' = *Concentration of reactant A in the non-ideal conditions (M)*
C_A = *Concentration of reactant A in the ideal conditions (M)*
$f(t)$ = *Time dependant function that describes how C_A' differs from C_A (M)*

The value of concentration for the reactor under the ideal conditions (i.e. C_A) comes from the integration of the equation of design of the batch reactor (Eq. 3.36) for a particular function r_A that describes the kinetics of the process.

$$\theta = N_{A0}\int_{x_{A0}}^{x_{Af}} \frac{dx_A}{Vr_A} \xrightarrow{V=cons\tan t} \theta = C_{A0}\int_{x_{A0}}^{x_{Af}} \frac{dx_A}{r_A} \qquad \text{Eq. 3.36}$$

where:

θ = *Time of reaction in a batch process (s)*
τ = *Mean residence time in a continuous reactor (s)*
V = *Reactor volume (l)*
q = *Flow-rate of chemicals in a continuous system (l/s)*
N_{A0} = *Initial number of moles for reactant A (mol)*
C_{A0} = *Initial molar concentration for reactant A (M)*
x_A = *Fractional conversion for reactant A*
x_{A0} = *Initial fractional conversion for reactant A*
r_A = *Kinetic equation as a function of reactant A (M/s)*

However, this method was not successfully used in our case for the following reasons:

- The real kinetics (i.e. published values) for the esterification of crotonic acid were unknown and the results obtained in our 5-L reactor system were found to depend very highly on the mixing properties of the system. Therefore, the real kinetic values, which affect the concentration term under ideal conditions (C_A), were not well defined in our particular case.

- *Figure 3.62* shows that only at low ester productions was there a clear trend for the difference in the values obtained with and without the loop. As the ester concentration reached higher values, the trend was less clear and the precision in the results also decreased. Therefore, it was not possible to obtain a reliable *f(t)* for high values of the reaction time.

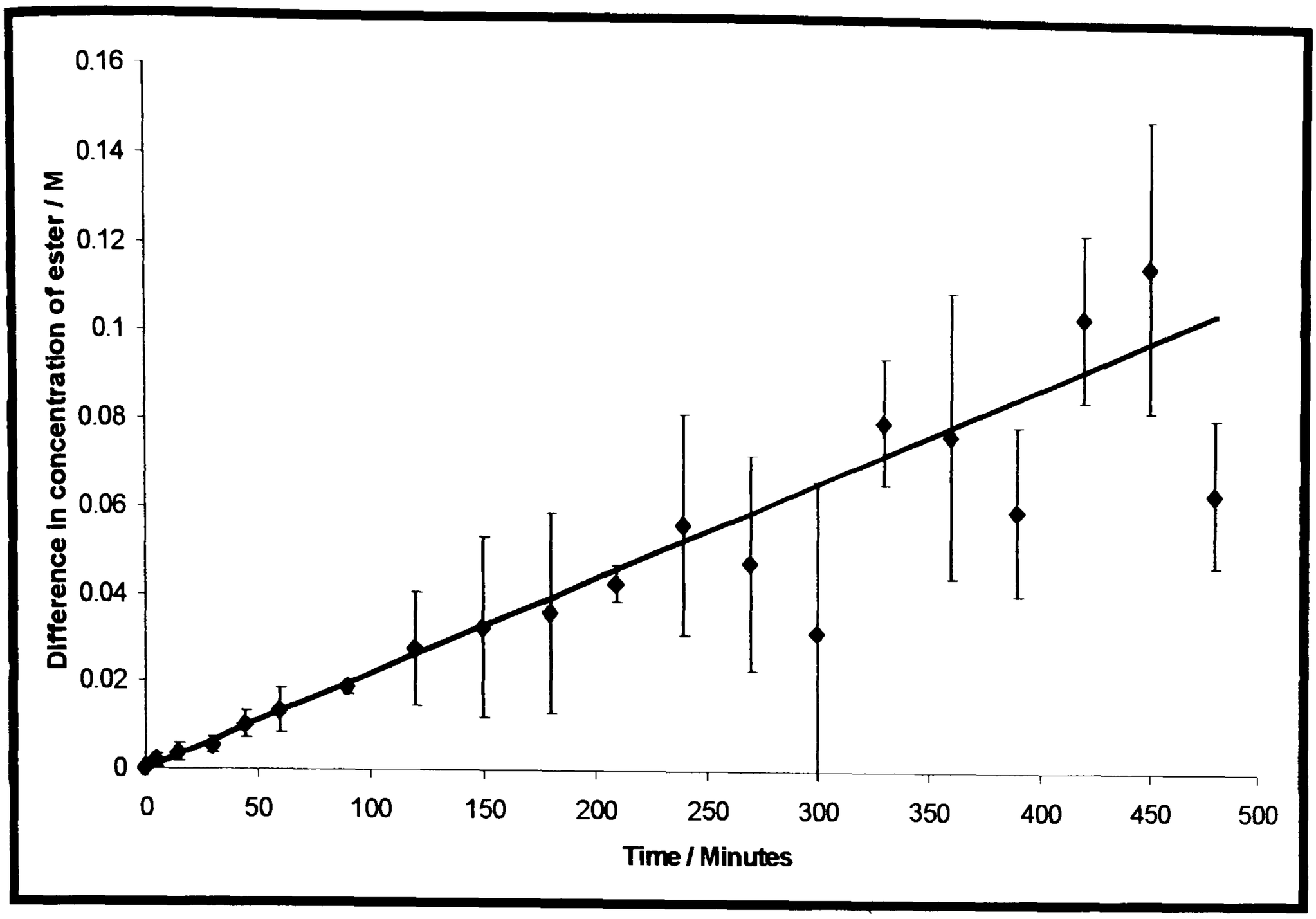

Figure 3.62. Change with time of the difference of the ester concentration with and without the loop for the esterification of crotonic acid at 80°C

3.2.3. Total model of the loop

It has been shown that the definition of a good model that describes the quality of the samples obtained with the fast loop is rather complicated and very time consuming. This modelling requires many experiments to define both the physical and chemical part of the model. Furthermore, some variables such as the mixing speed have been shown to affect both the physical collection of the sample and the chemistry of the process. Therefore, a long experimentation process and the use of statistics are needed to define a robust model that contains the effect of every variable affecting sampling. Furthermore, the model developed in this manner would be very specific and only applicable to the particular system that has been studied. However, the work carried out in this thesis showed how simple physical and chemical experiments typical of the modelling studies are needed, as they lead to the optimisation of sampling devices. The analysis of the effect of some variables on the sample collection and the chemistry of the process has also been shown to give promising results that can be used to correct the information derived from non-representative sampling. For example, it has been shown how representative

sampling of suspensions of solids was difficult to achieve but a robust calibration of the sample collection could be performed and used to correct for non-representative sampling. On the other hand, with heterogeneous mixtures of immiscible liquids representative sampling was easier to achieve and the calibration model and correction of the data was not needed. Finally, the performance of modelling tests provides valuable information on what variables affect sample collection the most. In our process, the quality of mixing and the stirring speed were found to be the variables that most affected the sample collection using the fast loop.

3.3. Experimental and results obtained in the area of on-line NMR

It has been mentioned earlier that the final aim in the design of the fast loop for representative sampling from batch reactors was the implementation of a low field NMR spectrometer for on-line measurements. The need for a secondary loop with a lower flow-rate has also been already justified. In this section, the experiments where the NMR instrument was implemented and tested in the line are described, allowing the achievement of one of the goals in the project. The experiments covered here focussed on the engineering side of the project from the sampling point of view. Analytical chemists within CPACT were involved in the development of the NMR instrument as well as a more detailed study of how it behaved under different conditions[79,95]. Therefore, the tests performed in this work concerned heterogeneous processes where the quality of the samples collected in the NMR line was compared with the spectral information being acquired on-line with the NMR instrument. It should be mentioned that no experiments with reactive processes where used in these tests. This was mainly due to the fact that the esterification of crotonic acid was a homogeneous processes and therefore it did not represent a challenging system from the sampling point of view. At-line monitoring of the esterification of crotonic acid carried out by Dr. Alison Nordon in another CPACT project demonstrated the capacity of the instrument to follow this process[79,95,96]. Other more interesting reactions from the engineering point of view, such as the heterogeneous esterification of itaconic acid, was not fully defined from the analytical point of view. Therefore, the lack of a robust reference method for the esterification of itaconic acid made impossible its use in the on-line NMR studies.

The low-field NMR measurements in this project were carried out using a Fourier transform development spectrometer manufactured by Resonance Instruments. The instrument employed a permanent magnet and was capable of observing ^{1}H, ^{19}F or ^{31}P nuclei. The magnet was enclosed within a temperature controller container, and was maintained at a temperature of 35°C. The operating frequency of the instrument was 29.1 MHz for ^{1}H. The instrument had a lock channel that monitored the variation in frequency of a lock sample located in the probe. A 5 mm ^{1}H probe was employed with a $\pi/2$ pulse duration of 3.7 μs. The ^{1}H probe contained a sample of hexafluorobenzene (C_6F_6) and the ^{19}F NMR signal from this lock sample was used to monitor and adjust the magnetic field and so improve the precision of replicate scans of ^{1}H spectra[79,95].

3.3.1. On-line NMR measurements with heterogeneous mixtures

The low field NMR instrument was implemented in the fast loop using a secondary line as described in Appendix 3. The spectra acquired by the NMR spectrometer were compared with the quality of the samples obtained via the off-line port in the main loop and the return point in the NMR line. This was performed for five different heterogeneous mixtures of toluene and water. The parameters used for the acquisition of NMR spectra are summarised in the *Table 3.10*. The flow-rate used in the NMR loop for these experiments was 60 ml/min. These conditions were chosen after preliminary experiments with the parameters optimised in homogeneous experiments at a lower flow-rate gave unsatisfactory results with low precision. These settings used in the preliminary tests had a longer delay (1s), a lower number of scans (128) and a longer acquisition time (1s). Therefore, the collection of a larger number of scans was adopted in order to improve the precision via the averaging of more spectra. A shorter delay between the end of the FID and the start of the next pulse allowed the collection of a larger number of scans in a reasonable period of time for analysis. This was also achieved by reducing the acquisition time, i.e. the period of time that the FID was observed for. The optimum NMR conditions used in the experiments were also chosen considering the results obtained in preliminary tests, changing the number of scans being acquired, and the flow-rate in the NMR line.

Table 3.10. Parameters used in the NMR experiments

Recycle delay (s)	*Number of scans*	*Acquisition time (s)*
0.1	512	0.5

Figure 3.63 shows how the NMR spectra changed with the composition of the heterogeneous mixture and *Figure 3.64* shows the results obtained when the spectra for five replicates of these experiments were studied. This figure represents the average toluene-water ratio in terms of both the peak areas and the peak intensities. For comparison, the toluene concentration measured in the samples obtained from the off-line sampling port and the NMR line are also plotted in *Figure 3.64*. The determination of the quality of these samples was done by measuring the volume of each one of the phases after separating out the two solvents with a separation funnel.

The results in *Figure 3.64* show how the quality of the samples collected from the NMR line varied linearly with the bulk concentration of the mixture inside the vessel. This means that, although these samples were not fully representative of the bulk concentration, they could be easily calibrated for data correction. On the other hand, the quality of the samples collected from the sampling port were not as good and showed a less linear change with the bulk concentration. This could have been due to the use of a ball valve that could not be opened fully for sampling, and the port would have delivered too high a flow-rate (approx. 9 l/min) for manual sample collection. The NMR results in the same *Figure 3.64* showed a similar trend for both the peak area and the peak intensity ratio. This was expected as a similar flow-rate (approx. 60 ml/min) was reset before each one of the measurements. This procedure avoided the slow change in flow-rate with time that was noticed in the experiments. When the flow-rate is kept constant, the line-width is also constant and the results derived from the peak areas should be similar to those obtained from the peak intensities, as shown in the figure. *Figure 3.64* also shows that both the change in peak area and intensity ratio were reasonably linear (i.e. they could be calibrated) at bulk concentrations of toluene higher than 15%. Below this value, the intensity of the toluene peak was poorer and therefore the precision of the results was low, which

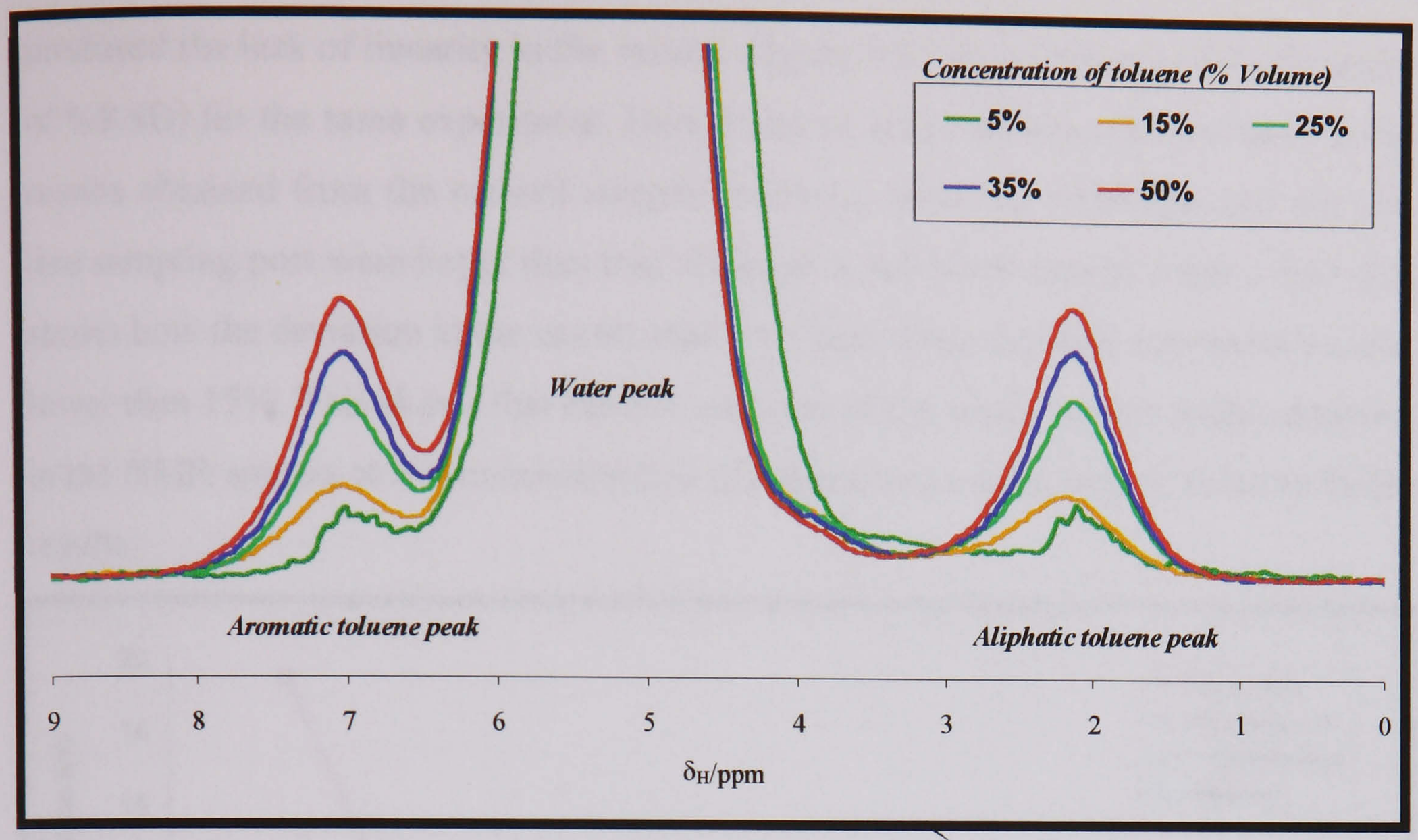

Figure 3.63. Average NMR spectra for five replicate measurements in different mixtures of toluene in water

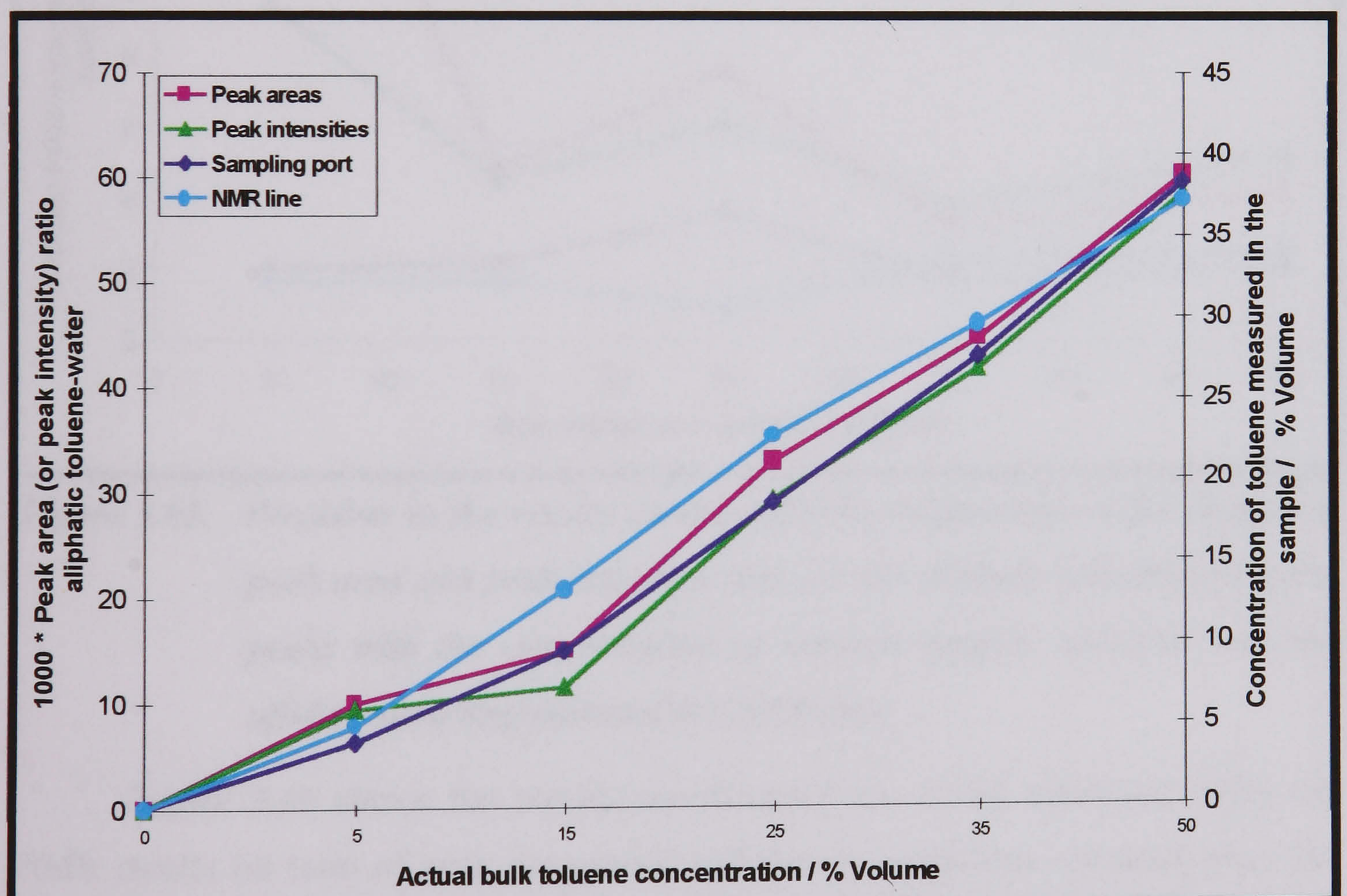

Figure 3.64. Comparison of the change of peak area and peak intensity ratio for the aliphatic toluene and water peaks with the concentration of manual samples collected from the off-line sampling port and the NMR line

produced the lack of linearity in the results. *Figure 3.65* shows the precision (in terms of %RSD) for the same experiment. Here it can be observed how the precision in the results obtained from the manual sample collection from the NMR line and the off-line sampling port were better than that obtained in the NMR results. *Figure 3.65* also shows how the deviation in the results was very high when the bulk concentration was lower than 15%. This shows that the low intensity of the small toluene peaks observed in the NMR spectra at low concentrations of toluene caused the lack of linearity in the results.

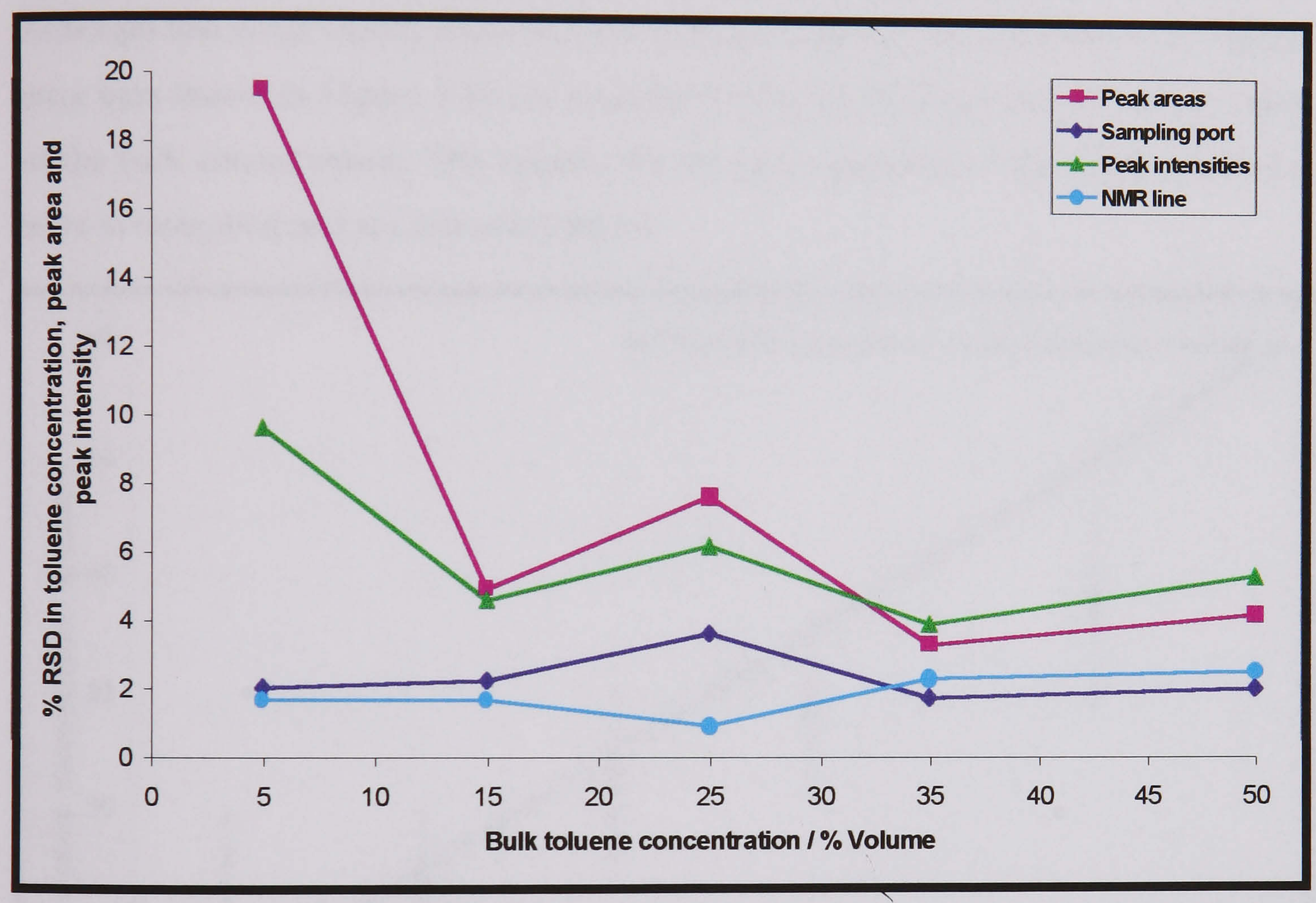

Figure 3.65. Precision in the results obtained for the comparison of the change of peak area and peak intensity ratio for the aliphatic toluene and water peaks with the concentration of manual samples collected from the off-line sampling port and the NMR line

Figure 3.66 shows the comparison between the model prediction using the NMR results (in term of peak intensities) and the measurements obtained when the samples were collected manually from the off-line port and the NMR line. This model was obtained using the data of NMR peak intensity ratios for different values of concentration of the sample that actually passed through the NMR flow-cell (i.e. concentration of the samples collected in the NMR line). Only the data collected for

concentrations of the mixture equal to or greater than 15% were used in the model. *Figure 3.66* shows that a model prediction using the NMR results was feasible provided that the signal to noise ratio of the peak was good (i.e. at bulk toluene concentration greater than 15% in our system). Therefore, the validity of the sampling loop system for the implementation of the NMR spectrometer for on-line monitoring of toluene-water mixtures has been demonstrated with these promising results. However, the precision in the NMR prediction was found to be quite poor with highly heterogeneous systems, as it is shown by the big error bars represented in *Figure 3.66*. Although this is not clearly observed in the figure, it should be highlighted the biggest error bars shown in *Figure 3.66* are associated with the NMR prediction for any value of the bulk concentration. The reasons for the poor precision of the NMR prediction were investigated and are discussed below.

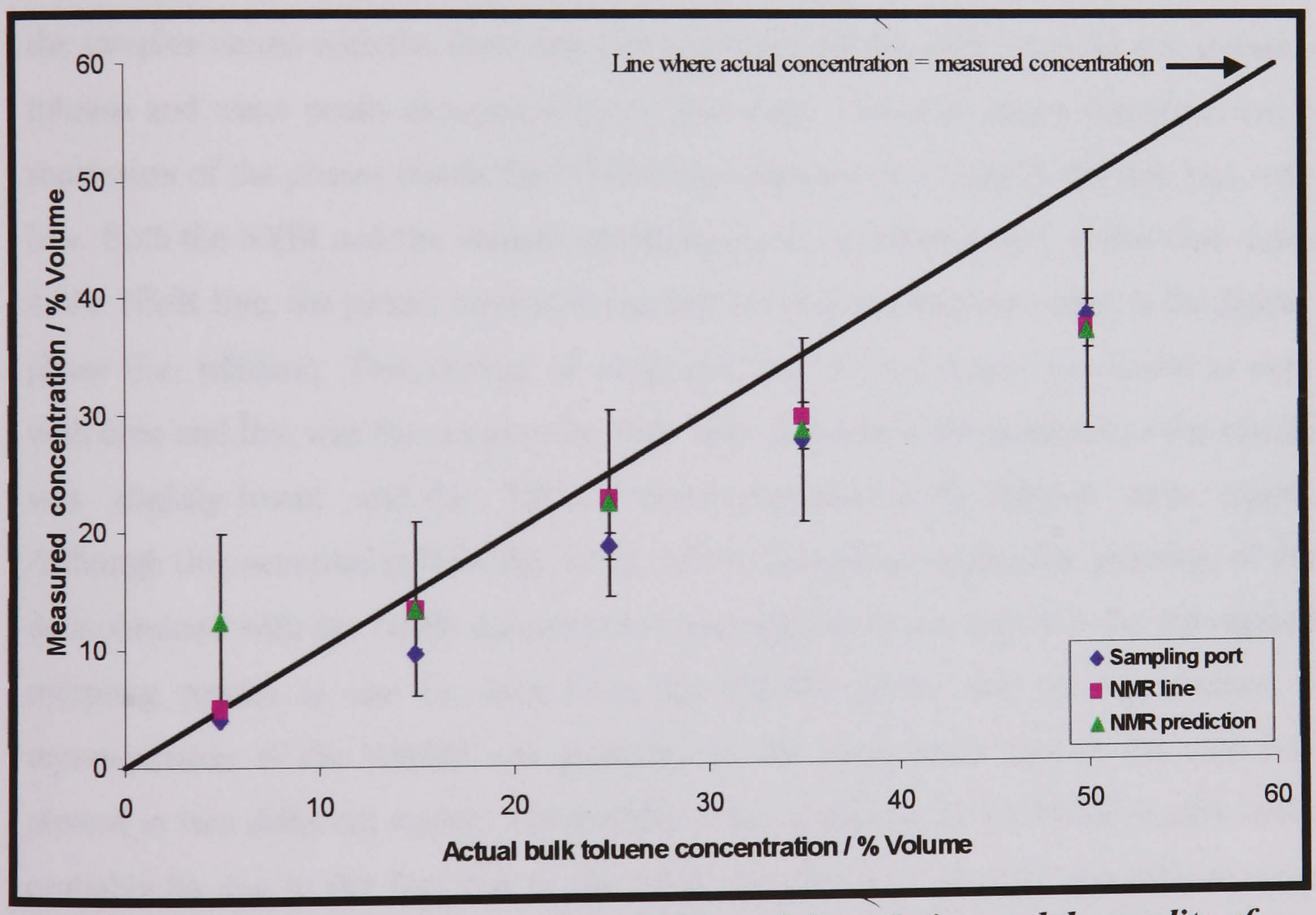

Figure 3.66. Comparison between the NMR model prediction and the quality of the samples collected manually from the off-line port and the NMR line

a) Effect of the flow-rate on the NMR signals

Due to the low precision obtained in some of the NMR results, it was believed that a separation of the two phases inside the NMR line could have occurred during the experiments. Therefore, the effect of the flow-rate in the quality of the samples was studied, as the slower the flow the more likely the separation of phases may occur. For this, a mixture of 50% toluene in water was added to the reactor vessel. The flow-rate in the NMR loop was varied between 20 and 95 ml/min and both NMR spectra and samples from the NMR line were collected with the same conditions used in the experiments described previously. *Figure 3.67* shows how the averaged spectra obtained in the five replicate experiments changed with the flow-rate. The expected increase in the line-width with the flow-rate was obtained in the experiments.

Figure 3.68 shows a comparison between how the concentration measured in the samples varied with the flow-rate and how the peak intensity ratio for the aliphatic toluene and water peaks changed with the flow-rate. This plot shows that there was a separation of the phases inside the NMR loop when the flow-rate in the line was very low. Both the NMR and the manual sampling results confirmed that, at low flow-rates in the NMR line, the phases separated out and the mixture became richer in the lighter phase (i.e. toluene). This change of properties at low flow-rates was found to vary with time and this was the reason why with slow flow-rates the precision in the results was slightly lower and the %RSD values (represented the figure) were larger. Although this occurred in both the NMR and the sampling results, the precision of the data obtained with the NMR spectrometer was slightly better than that for the manual sampling results as can be seen from the %RSD values. For the comparison, a representation of the %RSD was preferred to the usual error bars as the data was plotted in two different scales. The slightly better precision in the NMR results could probably be due to the fact that in the NMR data the 512 spectral acquisitions were co-added in a period longer than 5 minutes whereas in the manual sampling the samples were collected in 1 minute. Also, 5 replicate measurements were performed in the NMR experiment whereas only 3 replicate sample collections were made in the sampling tests.

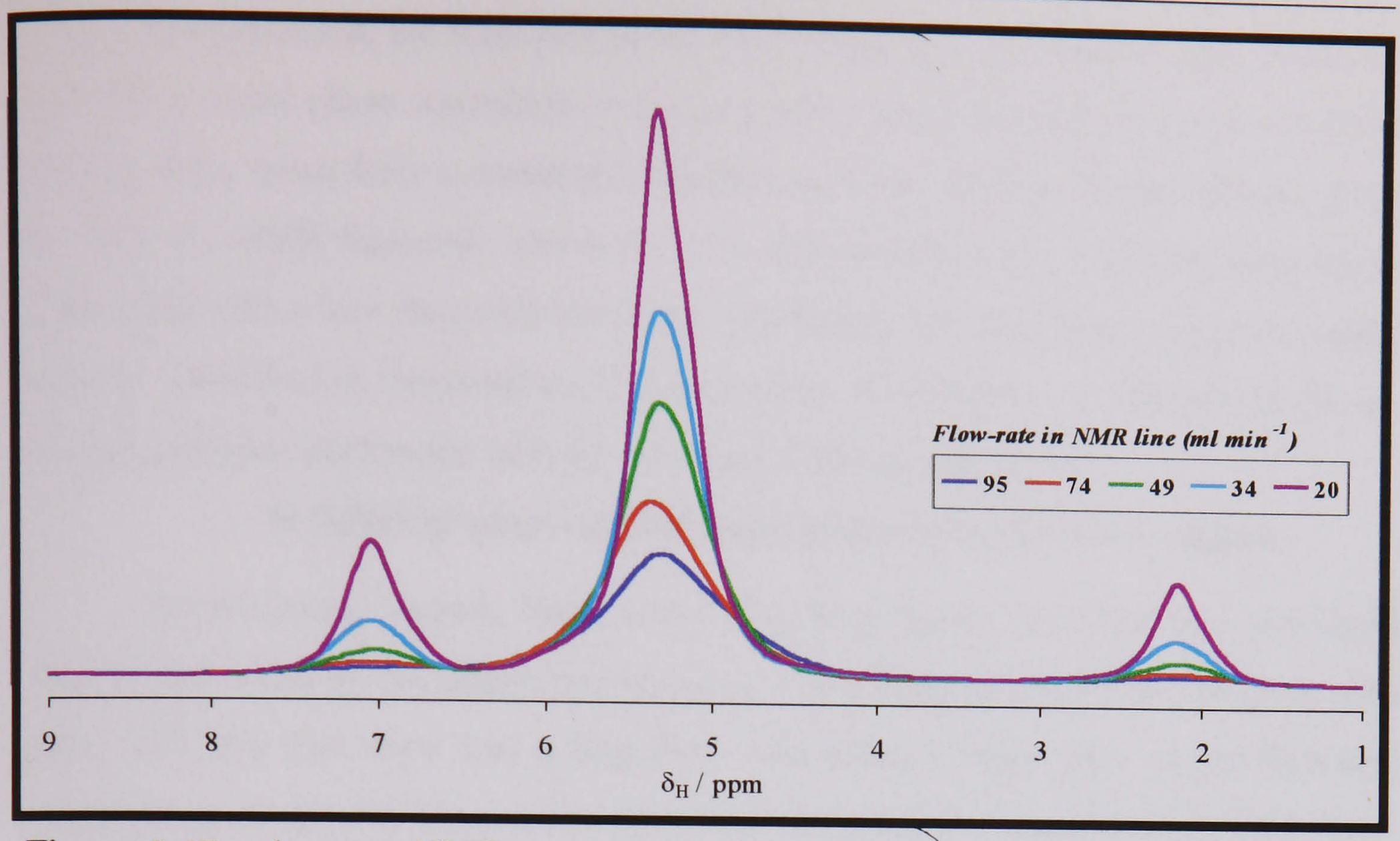

Figure 3.67. Average NMR spectra for five replicate measurements in the 50% toluene-water mixture when the flow-rate in the NMR line is varied

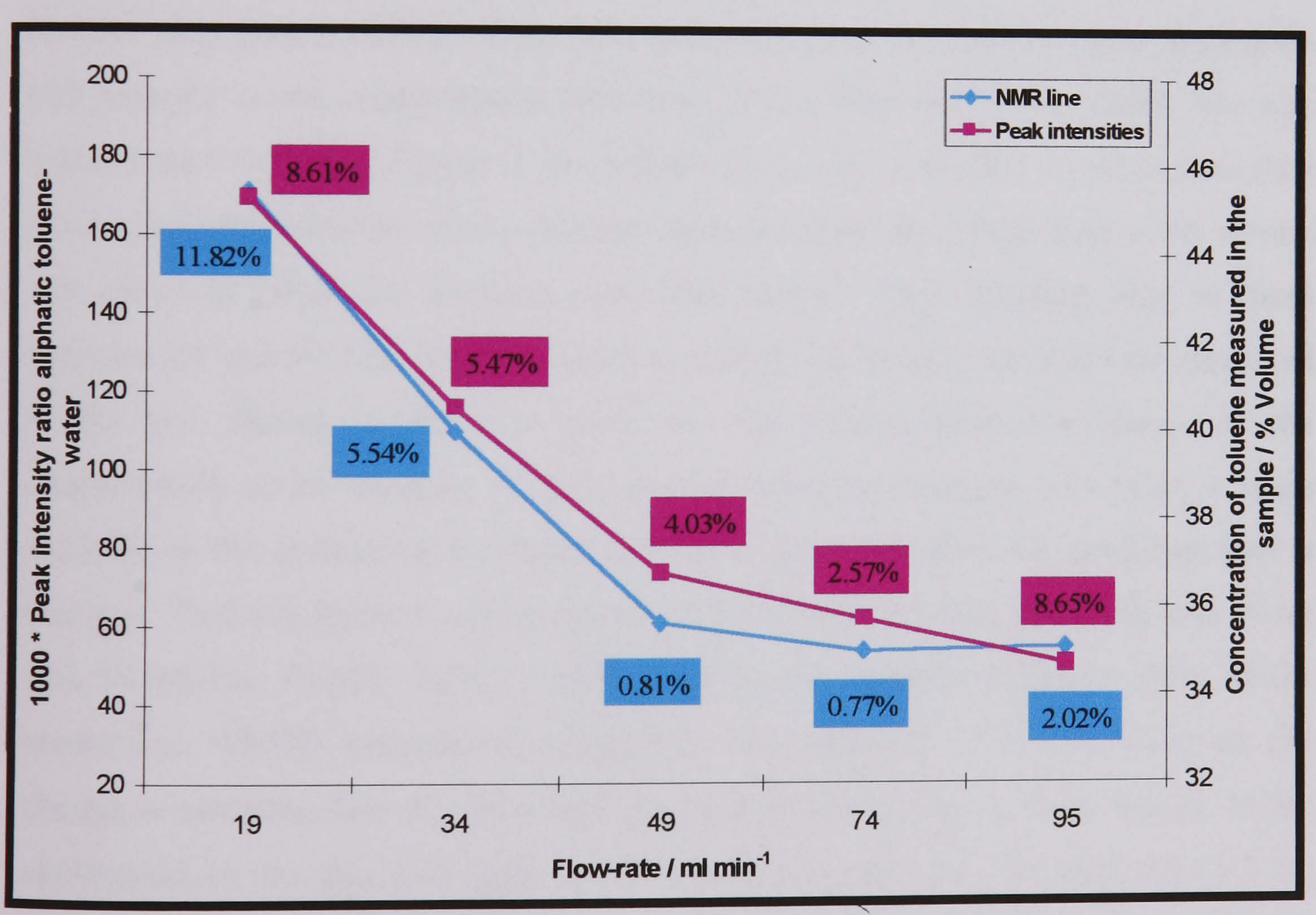

Figure 3.68. Comparison of the change of peak intensity ratio for the aliphatic toluene and water peaks with the concentration of manual samples collected from the NMR loop (50% toluene-water mixture in the vessel) when the flow-rate in the loop is varied

In conclusion, the flow-rate in the NMR loop had to be higher than 50 ml/min in order to avoid phase separation in the loop and a degradation in the precision of the results. Also, a fast flow avoided the saturation effects observed in the mixture going through the NMR flow-cell. However, it is also known that a very fast flow-rate is associated with a low magnetization time, producing low intensities and poor quality spectra. Therefore an intermediate flow-rate value of 60ml/min was chosen for the on-line experiments performed with the low-field NMR spectrometer.

b) Effect of sampling time and number of scans on the signals

As previously shown, there was a plug-flow inside the NMR line that could lead to separation of the phases and changes in the concentration of the mixture with time. The fact that there was a plug-flow was visually observable in the flow-cell where plugs of toluene were observed in between blocks of water flowing in the line. This was due to the small inside diameter of the NMR line and flow-cell system, together with the low flow-rates used in the line. However, it has been shown above that the plug characteristics of the flow did not lead to a complete phase separation and changes in the concentration with time if the flow-rate in the NMR line was higher than 50 ml/min. *Figure 3.69* verifies this as only a slightly increase (less than 2%) in the concentration of the samples collected from the NMR loop at 60 ml/min was observed when the sampling time was varied. The sampling time in these experiments was the time that was taken to collect the sample that was later separated in the two phases in order to work out the concentration of toluene. If the concentration of the mixture flowing through the loop changes with time, a large variation in the concentration results should be observed when the sampling time is changed. This was found to occur only when the flow-rate in the NMR line was lower than 50 ml/min. Finally, *Figure 3.69* also shows the variation in the precision of the results (i.e. %RSD) when the sampling time was changed. As can be observed, the change in sampling time did not affect significantly the precision in the results, as the distribution of the data was random and the values were always lower than 3.5 %. Again, this would not be the case if the concentration in the NMR line changes with time, where a trend with the %RSD descending as the sampling time increases would be observed.

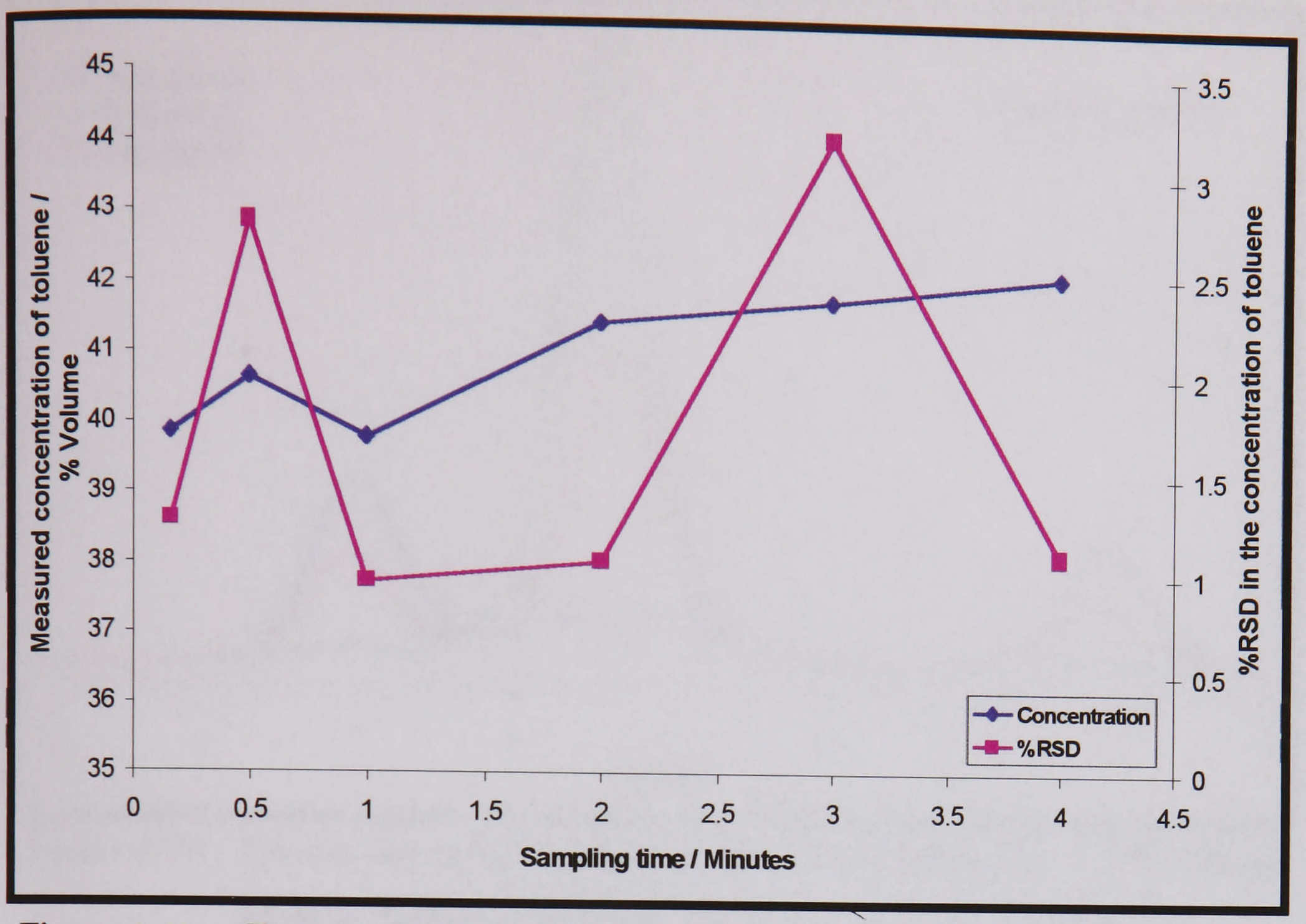

Figure 3.69. Change of the concentration of manual samples collected from the NMR line (50% toluene-water mixture in the vessel) when the sampling time was varied

It is therefore concluded that the use of 60 ml/min in the system guaranteed that no change of the properties with time was produced in the line. However, this was only true provided that the time interval was relatively high (higher than 10 seconds, minimum sampling time used in the experiment). This comes from the fact that at 60 ml/min there was still plug-flow in the line and at some very short time intervals all of the mixture passing through a certain point in the flow-cell might have been toluene or water in the form of plugs. The way to overcome the problem of the plug flow in the NMR acquisition was to co-add a large number of scans in order to improve the precision in the results. *Figures 3.70* and *3.71* show the comparison between the co-addition of 4 scans and 512 scans for three replicate NMR measurements over a 50% toluene mixture flowing at 60ml/min. When only 4 scans were acquired, the results show how in some replicates the average spectra saw only toluene in the flow-cell whereas in some others only water was detected. Only replicate 3 with 4 scans being averaged showed the presence of toluene and water in a similar ratio. On the other hand, the results obtained co-adding 512 scans showed essentially the same

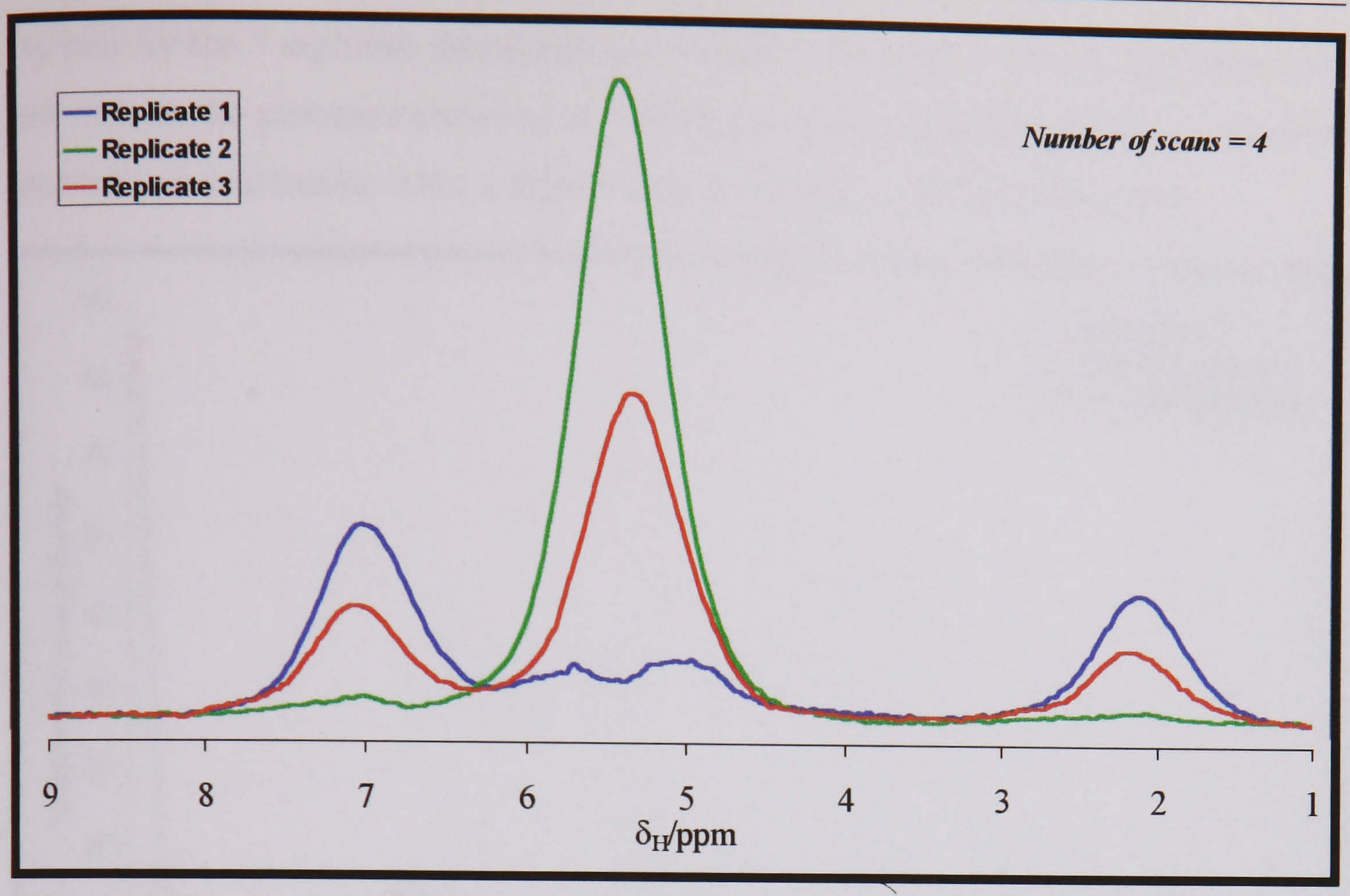

Figure 3.70. Spectra for three replicate NMR measurements for a 50% toluene mixture flowing at 60ml/min where 4 scans were co-added

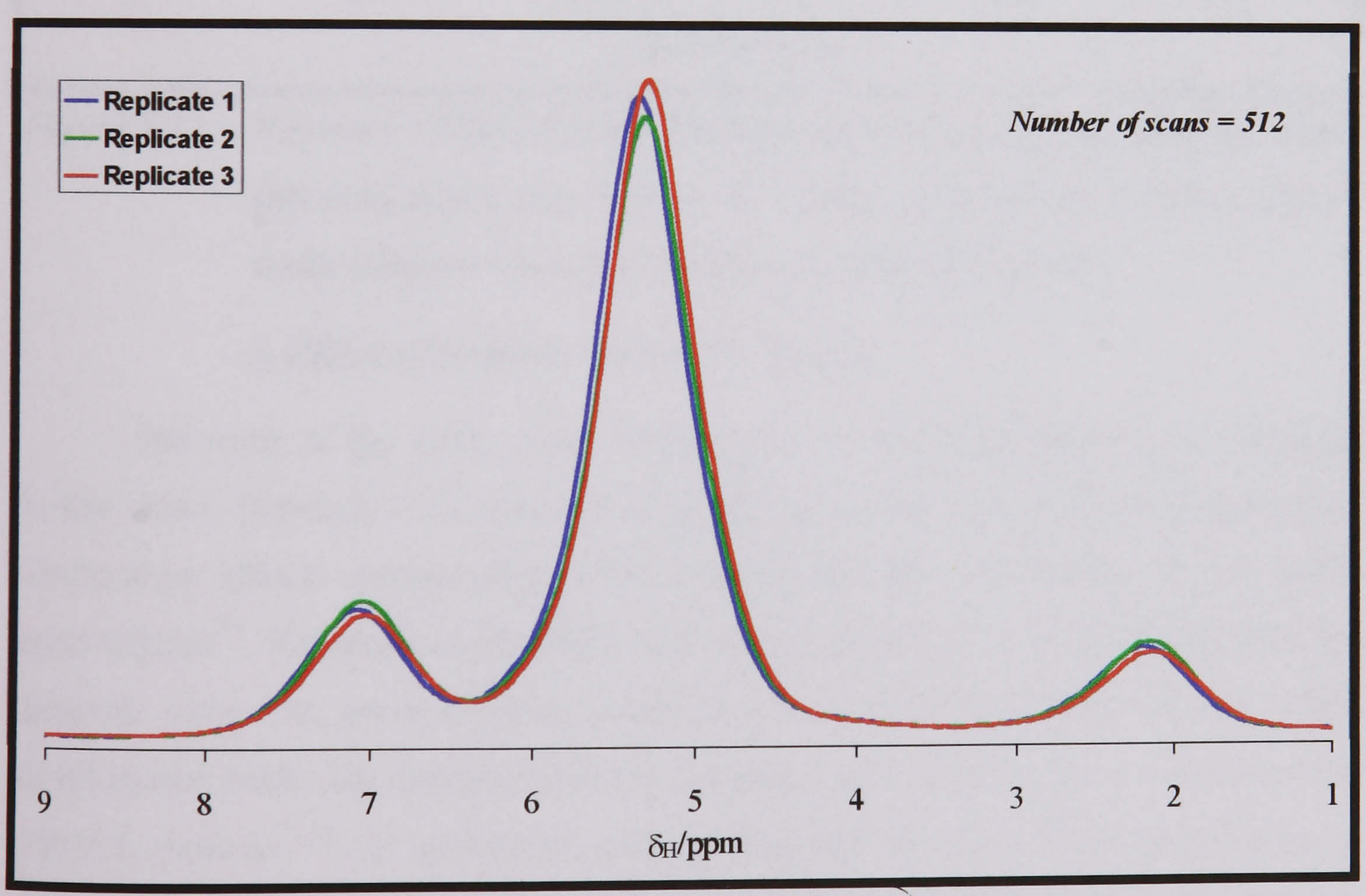

Figure 3.71. Spectra for three replicate NMR measurements for a 50% toluene mixture flowing at 60 ml/min where 512 scans were co-added

spectra for the 3 replicate measurements. *Figure 3.72* verifies these conclusions as it shows how the precision (in terms of %RSD) improved considerably for all the peak intensity measurements when a higher number of scans were being acquired.

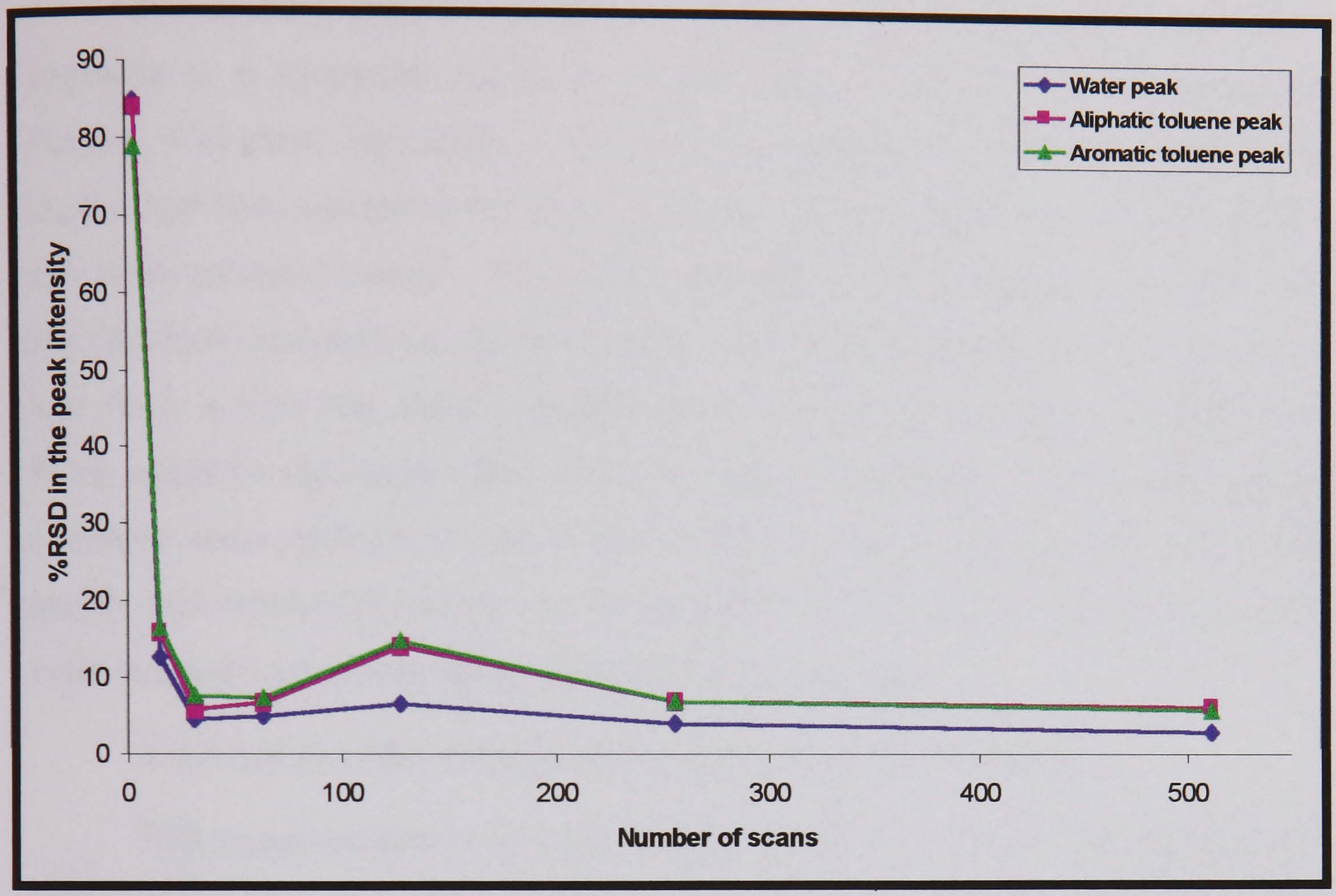

Figure 3.72. Precision obtained in the determination of the average intensity of the different peaks observed in the NMR spectrum for a 50% toluene-water mixture when the number of scans was varied

c) Effect of temperature on the signals

The study of the effect of the temperature on the NMR signals is not covered in this thesis. However, this aspect is of great importance and cannot be forgotten as temperature affects considerably NMR spectra and the performance of the NMR spectrometer[79]. The study of the effect that the temperature has on the NMR analysis depends upon the process being considered and constituted part of the NMR development work that several analytical chemists were carrying out in another of the CPACT projects[79,95]. In preliminary experiments they observed[79] that an increase in the sample temperature generally produced a decrease in the signal area. Also, the use of low temperatures improved the signal to noise ratio, bearing in mind that very low temperatures could produce the undesired crystallisation of the sample. Once the optimum temperature conditions for the NMR monitoring of a particular process are

determined, the conditioning system for the NMR line can be designed. This is the construction of a heating, cooling or isolating device designed to render the sample at a suitable temperature for analysis as it passes through the flow-cell[2].

For sampling and the modelling of sampling systems the temperature effect is important as it varies the miscibility of the different phases in the heterogeneous mixture. Therefore, depending on the reactor temperature the difference between the sample and bulk concentration varies as the solubility of one phase in another (in a two phase mixture) changes. This affects the quality of the sample, i.e. how far it is from the bulk concentration. It also modifies the representativeness of the sample, i.e. how far it is from the actual concentration of the mixture inside the reactor. Chris Wong noticed a significant effect of temperature on the quality of the sampling using a toluene-water mixture as part of the CPACT work in this project[89]. Thus, both quality and representativeness can be modelled with respect to the temperature in order to correct any errors being produced during sampling.

3.3.2. Study of the mixing enhancement produced in the loop

NIR measurements were acquired simultaneously to on-line NMR experiments with different toluene-water mixtures, using and not using the loop. A Bomem MB155 NIR spectrometer and a Hellma transmission probe with 1 mm path length were used in the tests. The NIR probe was placed in one of the port on the reactor lid, with the tip located approximately 6 cm above the stirrer plane. The purpose of this monitoring was to prove with the NIR data that the use of the loop produced an improvement in the mixing properties in the system. This enhancement was believed to affect the different kinetic parameters for the esterification of crotonic acid when the loop was used and when it was not. Five different heterogeneous mixtures of toluene and water were used in the experiment. For each one, five different NIR measurements were acquired both with the loop recycling at approximately 9 l/min and without the loop. The stirring speed in the vessel was kept to a constant value of 250 r.p.m. The average values for those five NIR measurements are plotted in *Figure 3.73* for three out of the five mixtures (for a better appreciation) and under the different mixing conditions. The spectra are shown in the form of the first derivative as this shows more clearly the change of the spectra observed for the different

conditions. Only the region between 5700 and 8200 cm^{-1} was used in the data analysis as the rest of the spectrum was dominated by the water signals. The signal at approx. 7000 cm^{-1} was associated with the water whereas the signals at approx. 6000 cm^{-1} were due to the toluene present in the samples[79].

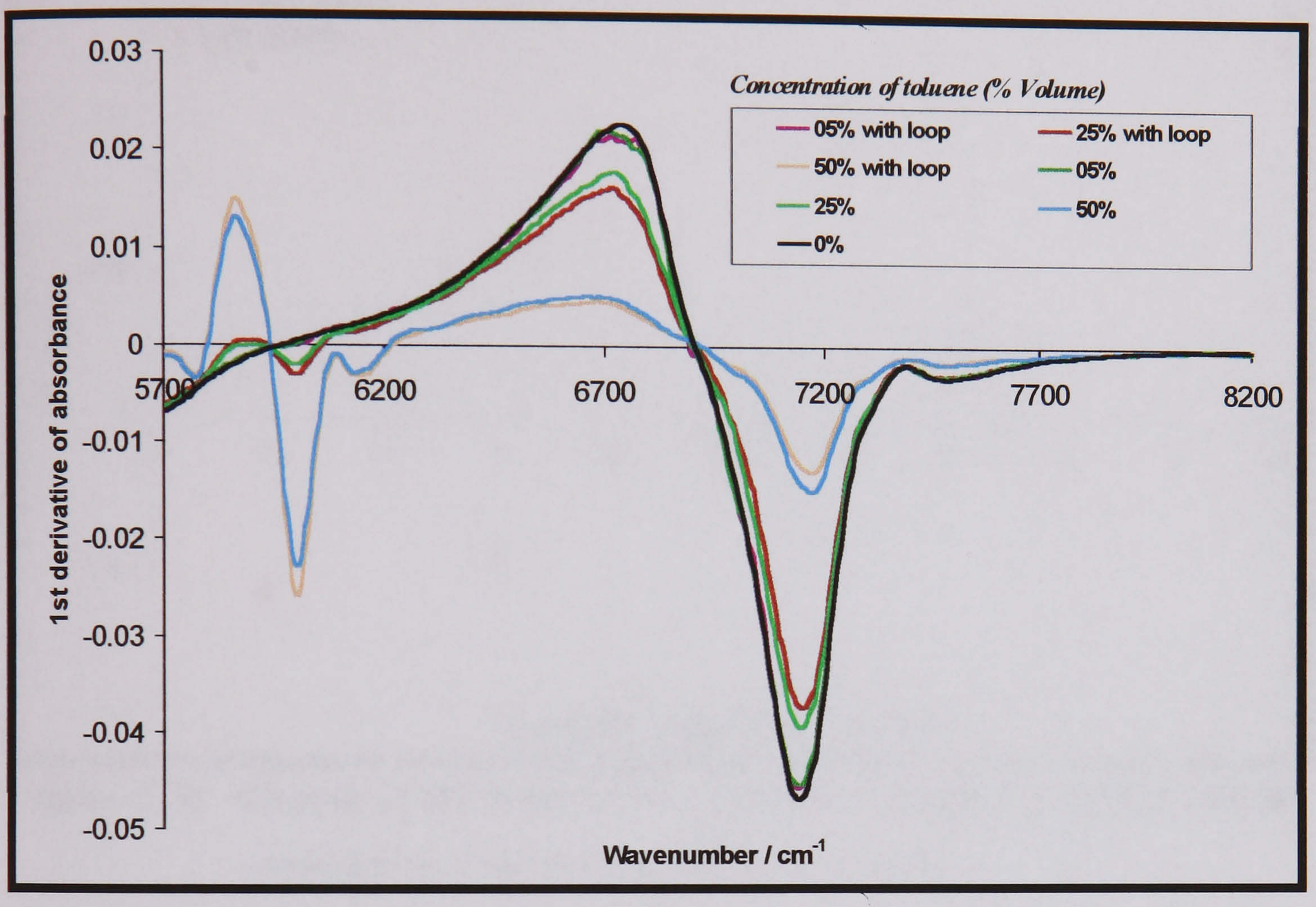

Figure 3.73. First derivative of the NIR spectra acquired with and without the sampling loop for different toluene-water mixtures and between the region 5700 – 8200 cm^{-1}

Principal component analysis was carried out using the NIR data shown in *Figure 3.73* in order to show more clear by the effect of the sampling loop on the mixing conditions. *Figure 3.74* shows how the score for one of the principal components originating in the statistical analysis changed with the composition of the mixture inside the reactor. It can be observed that there was a similar trend but with differences in the values of PC1 at high concentrations of toluene in the mixture between the case when the sampling loop was used and when it was not. This proved that, provided there was enough toluene in the water to produce a heterogeneous mixture, the use of the loop produced different mixing conditions in the system that could be distinguished by NIR measurements. This was the reason why in *Figure 3.73* and for the 50% mixture it can be clearly observed how the NIR measurements

detected more toluene when the sampling loop was used. As the tip of the NIR probe was inserted below the interphase toluene-water where the water was the heavy phase, the results show that the use of the loop enhanced the mixing in the system.

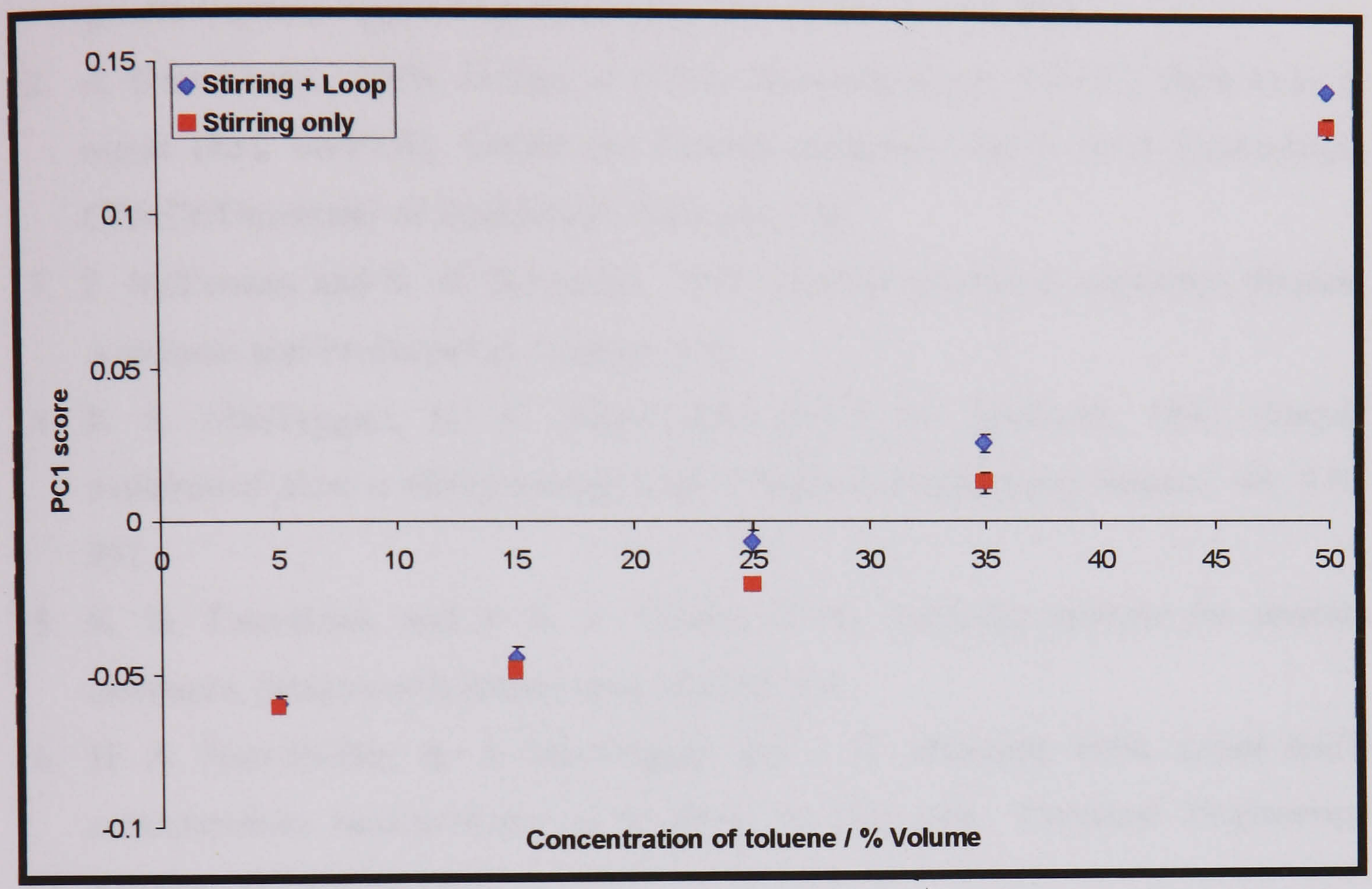

Figure 3.74. Change of the score for the Principal Component 1 (PC1) with the composition of the mixture inside the reactor

4. References

1. C. Hassell and E. M. Bowman, 1998, *Process analytical chemistry for spectroscopists,* Applied Spectroscopy, Vol. 52 No. 1, 18A-29A.
2. A. Diez-Lázaro, 2000, *Design of a Fast Sampling Loop,* CPACT IMB Internal report (Ref: 00/P1/4), Centre for Process Analytics and Control Technology, CPACT/University of Strathclyde, Glasgow, UK.
3. F. McLennan and B. R. Kowalski, 1995, *Process analytical chemistry,* Blackie Academic and Professional, London, UK.
4. R. S. MacTaggart, H. A. Nasr-El-Din and J. H. Masliyah, 1993, *Sample withdrawal from a slurry mixing tank*, Chemical Engineering Science, 48, 921-931.
5. K. G. Carr-Brion and J. R. P. Clarke, 1996, *Sampling systems for process analysers,* Butterworth-Heinemann, Oxford, UK.
6. H. A. Nasr-El-Din, R. S. MacTaggart and J. H. Masliyah, 1996, *Local solids concentration measurement in a slurry mixing tank*, Chemical Engineering Science, 51, 1209-1220.
7. M. Kuriyama, M. Ono, H. Tokanai and H. Cono, 1996, *Correlation of transient sizes of highly viscous drops in dispersion process in liquid-liquid agitation,* Trans IchemE, Vol. 74 A, 431-437.
8. H. A. Nasr-El-Din, 1987, *Comments on scaling-up rules for solids suspension in stirred vessels*, Chemical Engineering Science, 42, 2986.
9. J. F. Richardson and D. G. Peacock, 1994, *Chemical Engineering, Volume 3: Chemical Reactor Design, Biochemical Reaction Engineering Including Computational Techniques and Control*, Pergamon, Oxford, UK.
10. C. Buurman, 1987, *Author's reply to comments by Nasr-El-Din*, Chemical Engineering Science, 42, 2987.
11. J. H. Rushton, 1965, *The continuous removal of mixed phases from a mixing tank.* A.I.Ch.E.-I.Chem.E. Symposium Series, 10, 3-7.
12. H. A. Nasr-El-Din, C. A. Shook and M. N. Esmail, 1984, *Isokinetic probe sampling from slurry pipelines,* The Canadian Journal of Chemical Engineering, 62, 179-185.

13. B. G. Lipták, 1994, *Analytical Instrumentation*, Chilton Book Company, Pennsylvania, USA.

14. R. N. Sharma and H. C. L. Das, 1980, *Effect of withdrawal flow velocity on the composition of a two phase system in a mixing tank*, Collections of Czechoslovak Chemical Communications, 45, 3293-3301.

15. D. E. Podkulski, 1997, *How do new process analysers measure up?*, Chemical Engineering Progress, October, 33-46.

16. G. Baldi, R. Conti, and A. Gianetto, 1981, *Concentration profiles for solids suspended in a continuous agitated reactor*, A.I.Ch.E. Journal, 27, 1017-1020.

17. C. Buurman, G. Resoort and A. Plaschkes, 1986, *Scaling-up rules for solids suspension in stirred vessels*, Chemical Engineering Science, 41, 2865-2871.

18. H. A. Nasr-El-Din, A. Afacanand and J. H. Masliyah, 1991, *Particle collection from vertical slurry flow throughout a small side port*, Trans. IChemE., 69, 374-380.

19. M. J. Rhodes and P. Laussmann, 1992, *A simple non-isokinetic sampling probe for dense suspensions*, Powder Technology, 70, 141-151.

20. J. Aguillón, K. Shakourzadeh and P. Guigon, 1995, *Comparative study of non-isokinetic sampling probes for solids flux measurement in circulating fluidised beds*, Powder Technology, 83, 79-84.

21. G. J. Zhang and M. Ishii, 1995, *Isokinetic sampling probe and image processing system for droplet size measurement in two-phase flow*, International Journal of Heat and Mass Transfer, 38, 2019-2027.

22. A. Williemson, R. S. Martin, B. Harris and T. E. Ward, 1987, *Design and Characterization of an isokinetic sampling train for particle measurements using emission gas recycle*, JAPCA Journal of Air Pollution Control Association, 37, 249-253.

23. C. Freitas, A. A. Vicente, M. Mota and J. A. Teixeira, 1997, *A new sampling device for measuring solids hold-up in a three-phase system*, Biotechnology Techniques, Vol. 11 No. 7, 489-492.

24. Tyco valves and control, Internet web page, 2001, *Neotecha solves hazardous sampling problems*, http://www.tycovalves-na.com/news1.asp

25. Grinnell Corporation, Internet web page, 1998, http://www.grinnell.com/

news/gp1297172.asp

26. Tyco Valves, Internet web page, 2001, *PV reactors sampling system*, http://www.tycovalves.com/pages/valves/neotecha/neotech1.html
27. Tyco Valves, Internet web page, 2001, *Tyco válvulas, actuadores y controles* and *Tyco valves, actuators and controls*, http://www.tycokeystone.com.mx/Cat/General/grale2.pdf and http://www.tyco-valves.com/literature/PDF/1000tvc.pdf
28. Tyco Valves, Internet web page, 2001, *Reactor sampling: Type PV* and *Toma de muestras en reactor: Tipo PV*, http://www.tycovalvespc.com/literature/brands/Neotecha/datasheets/NEOCS-0005-EN.pdf and http://www.tycovalves-na.com/literature/brands/Neotecha/datasheets/NEOCS-0005-ES.pdf
29. Tyco Valves, Internet web page, 2001, *Neotecha lined butterfly valves*, http://www.tyco-valves.com/literature/PDF/215_1309.pdf
30. Hanlon-O'Grady & Co. Ltd., Internet web page, 2001, *Technova reactor sampling systems*, http://www.hanlonogrady.ie/Technova.html
31. ASI applied systems, Internet web page, 2001, *Sampling technology for FTIR chemical monitoring and process analysis*, http://www.asirxn.com/images/technology/compsamp/samplbro.pdf
32. S. Shelley, 1996, *Mechanical sampling enhances ongoing process analysis*, Chemical Engineering, May, 143.
33. ProSys sampling systems Ltd., Internet web page, 2001, *Engineered sampling solutions*, http://www.prosys.ie
34. Sermatech-Ethylene corporation, Internet web page, 1998, *Phampler reactor sampling*, http://www.ethylenecorp.com/phamplers.htm
35. J. C. Middleton, F. Pierce and P. M. Lynch, 1986, *Computations of flow fields and complex reaction yield in turbulent stirred reactors, and comparision with experimental data,* Chemical Engineering Research and Design, 64, 18-22.
36. S. Komori and Y. Murakami, 1988, *Turbulent mixing in baffled stirred tanks with vertical-blade impellers.* A.I.Ch.E. Journal, 34, 932-937.
37. Y. Xu and G. McGrath, 1996, *CFD predictions of stirred tank flows*, Trans. IChemE., 74a, 471-475.
38. A. Bakker, K. J. Myers, R. W. Ward and C. K. Lee, 1996, *The laminar and turbulent flow pattern of a pitched blade turbine*, Trans. IChemE., 74a, 485-491.

39. P. Mavros, C. Xuereb and J. Bertrand, 1996, *Determination of 3-D flow fields in agitated vessels by Laser-Doppler Velocimetry: Effect of impeller type and liquid viscosity on liquid flow patterns*, Trans. IchemE. Part A, 74, 658-668.

40. K. NaG, N. J. Fentiman, K. C. Lee and M. Yianneskis, 1998, *Assessment of sliding mesh CFD predictions and LDA measurements of the flow in a tank stirred stirred by a Rushton impeller*, Trans. IchemE. Part A, 76, 658-668.

41. S. M. Kresta and P. E. Wood, 1991, *Prediction of the three-dimensional turbulent flow in stirred tanks,* AIChE Journal, Vol. 37 No. 3, 448-460.

42. S. Ibrahim and A. W. Nienow, 1996, *Particle suspension in the turbulent regime: the effect of impeller type and impeller/vessel configuration*, Trans. IchemE. Part A, 74, 679-688.

43. K. Rutherford, S. M. S. Mahmoudi, K. C. Lee and M. Yianneskis, 1996, *The influence of Rushton impeller blade and disk thickness on the mixing characterictics of stirred vessels*, Trans. IchemE. Part A, 74, 369-378.

44. G. Zhou and S. M. Kresta, 1996, *Distribution of energy between convective and turbulent flow for three frequently used impellers*, Trans. IChemE. Part A, 74, 379-389.

45. Institute of Petroleum, 1987, *Petroleum Measurement Manual: Part VI. Section 2: Guide to Automatic Sampling of Liquids from Pipelines,* Chichester, New York, USA.

46. P. M. Armenante and E. A. Abu-Hakmeh, 1994, *A novel method for the experimental determination of the minimal agitation speed for complete liquid-liquid dispersion in agitated liquid-liquid-gas systems*, Trans. IchemE. Part A, 72, 677-685.

47. P. M. Armenante and Yu-Tsang Huang, 1992, *Experimental determination of the minimum agitation speed for complete liquid-liquid dispersion in mechanically agitated vessels*, Industrial and Engineering Chemistry Research, 31, 1398-1406.

48. United States Nuclear Regulatory Commission, Internet web page, 1998, *Particulate sampling line bend radii*, http://www.nrc.gov/NRC/FEDWORLD/NRC-HPOS/hppos006.txt

49. R. H. Perry and C. H. Chilton, 1973, *Chemical Engineers' Handbook,* McGraw-Hill, New York, USA.

50. South African Pump Manufactures Association (SAPMA), 1991, *Pumps: Principles & Practice,* K. Myles and Associates, Northcliff, South Africa.

51. Cole-Parmer Instruments Company, 1997, *Cole-Parmer Catalogue of Pumps,* UK.

52. B. Martel, 2000, *Chemical Risk Analysis, A practical handbook*, Prenton Press, London, UK.

53. Aldrich, 1999, *Catalogue handbook of fine chemicals*, UK.

54. M. L. Hitchman, 2000, *Personal communications (safety actions in the design of the sampling loop system)*, Department of Pure and Applied Chemistry, University of Strathclyde, Glasgow, UK.

55. International Standard IEC 1285, 1994, *Industrial-process control - Safety of analyser houses*, First edition.

56. Measurementation group, Internet web page, 2001, *Hazardous areas and analysers*, http://www.measurementation.com.au/papers/analyser.htm

57. Measurementation group, Internet web page, 2001, *Interfacing sample handling systems for on-line process analysers*, http://www.measurementation.com.au/tp-1.htm

58. J. Wilkie, M. Weerasinghe and D. A. Mamman, 1998, *Development of a model process system for analysis of control and instrumentation techniques*, Internal report, Industrial Control Centre, University of Strathclyde, Glasgow, UK.

59. M. Weerasinghe, J. Wilkie, D. A. Mamman, A. Diez-Lazaro and M. L. Hitchman, 2000, *Modelling and simulation of a laboratory scale esterification process*, ADCHEM 2000 – International symposium on advanced control of chemical processes, 1073-1078.

60. J. J. McKetta, 1992, *Heat Transfer Design Methods*, M. Dekker, New York, USA.

61. F. M. White, 1984, *Heat Transfer*, Addison-Wesley, London, UK.

62. G. F. Froment and K. B. Bischoff, 1979, *Chemical Reactors: Analysis and Design,* Wiley, New York, USA.

63. O. Levenspiel, 1966, *Chemical Reaction Engineering: an Introduction to the Design of Chemical Reactors,* Wiley, New York, USA.

64. Sintef group, Internet web page, 2001, *Advanced technique for fast determination of oil content in fish feed by low field NMR*, http://www.sintef.no/units/unimed/mr/Material/Newsletter.htm

65. G. E. Maciel, 1994, *NMR in industrial process control and quality control, Nuclear magnetic resonance in modern technology*, ed. G. E. Maciel, Kluwer Academic, Netherlands, 225-275.

66. J. F. Haw and T. W. Skloss, 1993, *Early experiences with NMR in process analysis*, Spectroscopy, 8(9), 22-27.

67. C. Tellier and F. Mariette, 1995, *On-line applications in food science*, Annual Reports on NMR Spectroscospy, 31, 105-121.

68. Sintef group, Internet web page, 2001, *At-line/On-line NMR of porous materials*, http://www.sintef.no/units/unimed/mr/Material/At_on_line.htm

69. A. Nordon, C. A. McGill and D. Littlejohn, 2001, *Process NMR spectrometry,* The Analyst, 126, 260-272.

70. M. L. Snoddy, 1993, *The potential of process NMR on flowing streams,* Spectroscopy, 8(3), 41-47.

71. R. M. Pearson, L. R. Ream, C. Job and J. Adams, 1987, *The use of small nuclear magnetic resonance spectrometers for on-line process control,* Cereal Foods World, Vol. 32 No. 11, 822-826.

72. L. Andersson, 1971, *The PAT-20 Varian's new NMR process analyser*, Journal of the American Oil Chemists' Society, Vol. 48, 47-49.

73. R. Neudert, E. Ströfer and W. Bremser, 1986, *On-line NMR in Process Engineering*, Magnetic Resonance in Chemistry, Vol. 24, 1089-1092.

74. M. C. McIvor, 1969, *A flow probe for nuclear magnetic resonance spectroscopy,* Journal of scientific instruments (Journal of Physics E), Series 2 Vol.2, 292-293.

75. P. J. Hore, 1995, *Nuclear magnetic resonance*, Oxford University Press, Oxford, UK.

76. Foxboro leaflet, 1998, *I/A series NMR. On-line, real time strategic analytical measurement. For the first time,* UK.

77. Bruker group, Internet web page, 2001, *The Mimispec: NMR analysers for process and quality control as well as R&D in industries and universities,* http://www.bruker.de/wwwesr/minispec/mq-series/

78. S. J. Gibbs, D. E. Haycock, W. J. Frith, S. Ablett and L. D. Hall, 1997, *Strategies for rapid NMR rheometry by magnetic resonance imaging velocimetry,* Journal of Magnetic Resonance, 125, 43-51.

79. A. Nordon, 2001, *Personal Communications (on-line NMR and at-line NMR work at CPACT)*, Department of Pure and Applied Chemistry, University of Strathclyde, Glasgow, UK.

80. Global FIA Inc., Internet web page, 2001, *In-line filter probe*, http://www.globalfia.com/whatsnew/fprobe.htm

81. Crest Pumps, 1999, *Installation, Operation and Maintenance Manual: Pump Type: PP17, Serial No. PS5639*, Bournemouth, UK (Provided by T. Kennedy, Ritchie Mackenzie Co. Ltd, Glasgow, UK).

82. A. Kennedy, 2000, *Personal communications (design and construction of the fast loop sampling system for chemical reactors)*, Department of Pure and Applied Chemistry, University of Strathclyde, Glasgow, UK.

83. M. L. Hitchman and D. Littlejohn, 2000, *Personal communications* (safety actions in the design of the sampling loop system for chemical reactors), Department of Pure and Applied Chemistry, University of Strathclyde, Glasgow, UK.

84. Production Techniques Ltd., 2000, *Catalogue Chemcon PTFE Components*, Hampshire, UK.

85. William Tracey Ltd. Total Waste Managements, 2001, Catalogue of Products, Ayrshire, UK.

86. J. M. Coulson, J. F. Richardson, J. R. Backhurst and J. H. Harker, 1988, *Chemical Engineering, Volume 1: Fluid Flow, Heat Transfer and Mass Transfer*, Pergamon, Exeter, UK.

87. R. W. Miller, 1996, *Flow measurement engineering handbook*, McGraw Hill, USA.

88. C. J. Benard, 1988, *Handbook of fluid flowmetering*, The trade and technical press limited, England, UK.

89. C. Wong, 2001, *Development of sampling procedures for process analysis and control*, 4th year project, Department of Pure and Applied Chemistry, University of Strathclyde, Glasgow, UK.

90. D. C. Harris, 1998, *Quantitative Chemical Analysis*, W. H. Freeman and Company, USA.

91. Steward Tannoch, 2000, *Personal communications (use of a voltage regulator to control the flow-rate of centrifugal pumps)*, Department of Pure and Applied

Chemistry, University of Strathclyde, Glasgow, UK.

92. P. MacLaurin, N. Crabb, I. Wells, P.J. Worsfold and D. Coombs, 1996, *Quantitative in-situ monitoring of an elevated temperature reaction using a water-cooled mid-infrared fiber-optic probe*, Analytical Chemistry, Volume 68, No. 7, 1116-1123.

93. I. Wells, *Personal communications (gas chromatography method for the off-line monitoring of the esterification of crotonic acid)*, Avecia, Grangemouth, UK.

94. F. Clark, 1999, *The development of process near infrared spectroscopy for batch reactor analysis*, 4th year project, Department of Pure and Applied Chemistry, University of Strathclyde, Glasgow, UK.

95. C. A. McGill, 2000, *Studies of low-field nuclear magnetic resonance and Raman spectrometries for process analytical chemistry*, PhD thesis, Department of Pure and Applied Chemistry, University of Strathclyde, Glasgow, UK.

96. C. A. McGill, A. Nordon and D. Littlejohn, 2002, *Comparison of in-line NIR, Raman and UV-visible spectrometries, and at-line NMR spectrometry for the monitoring of an esterification reaction*, The Analyst, 127, 287-292.

97. H. Vanderburg, 1999, *Personal communications (HPLC monitoring of the esterification of crotonic acid)*, Centre for Process Analytics and Control Technology, CPACT/University of Strathclyde, Glasgow, UK.

98. M. Weerasinghe, 2000, *Personal communications (model prediction for the esterification of crotonic acid)*, Industrial Control Centre, University of Strathclyde, Glasgow, UK.

99. J. M. Smith, 1970, *Chemical Engineering Kinetics*, McGraw Hill, New York, USA.

100. M. Weerasinghe, 2000, *LabVIEW Monitoring and Control System for the CPACT Batch Reactor Process*, CPACT IMB internal report (Ref:00/P1/2), Centre for Process Analytics and Control Technology, CPACT/University of Strathclyde, Glasgow, UK.

101. W. F. Sheehan, 1970, *Physical Chemistry*, Allyn and Bacon, New York, USA.

102. W. P. White, 1928, *The modern calorimeter*, The Chemical Catalog Company, New York, USA.

103. G. F. Hewitt, G. L. Shires and T. R. Bott, 1994, *Process Heat Transfer*, CRC

Press, Florida, USA.

104. J. Richardson, 2000, *Personal communications (calorimetry studies at SB for the esterification of crotonic acid)*, SmithKline Beecham, UK.

105. O. Levenspiel, 1986, *Ingeniería de las reacciones químicas*, Reverté, Barcelona, Spain.

CHAPTER 4

DISCRETE SAMPLERS:

DEVELOPMENT OF A SAMPLING PROBE FOR ON-LINE HPLC

1. Background Theory on Discrete Samplers

Liquid chromatography (LC) is a powerful analytical technique used in laboratories. Unlike gas chromatography (GC), the most used on-line analytical technique, LC has not successfully been fully developed for use in industrial processes[1]. One of the CPACT projects in phase I employed an HPLC expert, H. Vandenburg, to study and clarify why LC has still not made a fully successful transition from the laboratory to the manufacturing plant[2]. There are several advantages and disadvantages of LC for on-line applications that are discussed later on this chapter. However, in many situations, sampling and sample preparation remain the most difficult stages[1]. Therefore, the LC study gradually became a sampling project where different prototypes of automated samplers had to be tested and developed[2-4]. The final aim was the development of a simple, inexpensive, robust and reliable sampling system that could be successfully used to implement LC and other analyser equipment for on-line analysis.

1.1. Problems in the implementation of HPLC for on-line analysis

On-line HPLC can offers significant advantages over the methods such as spectroscopic and flow injection analysis, as complex mixtures can be analysed for a number of components over a wide concentration range, with relatively simple calibration[1,5,6]. Also, process liquid chromatography is specifically suitable for separation of high boiling materials, molecular size distribution of heavy hydrocarbon oils and polymers, and the separation of organic materials that cannot be analysed by GC because they are involatile or would be degraded during vaporisation[7-11]. This is why several companies such as Applied Automation and Millipore started commercialising process LC instruments for industrial applications, mainly in the pharmaceutical industry[1]. However, there are also disadvantages in the use of LC in process analysis[1,8] which forced some LC analyser companies to withdraw from the market[1] in the 1980's. This is why other techniques such as flow injection analysis are preferable in some applications as they could be cheaper, faster and more reliable than LC[12]. There exist four main reasons that complicate the use of LC in the process environment[8,13,14]:

- The sampling requirements are demanding as the sample often needs to be filtered and diluted with an adequate solvent. This makes the sampling systems complex, expensive and often not very reliable.
- LC instruments often use liquid carriers that are normally flammable solvents at high pressures. Also, the purchase and disposal costs of the solvents are very significant.
- The separation of components take many minutes, reducing the frequency of sampling and increasing the dead time of analysis[15].
- LC requires technical specialists with higher knowledge of analytical chemistry than required for typical GC applications.

From this consideration of disadvantages it can be seen that the most difficult problems to overcome are those related with sample and sample preparation[1]. The use of flammable solvents in HPLC separations can be eliminated by using water as the mobile phase in some cases[1,8]. However, most lab based HPLC applications involve organic modifiers in the mobile phase[1]. To adapt this to water only chromatography, either the stationary phase or the aqueous mobile phase can be altered[1,8]. The addition of modifiers to the aqueous mobile phase change its polarity while the additives added to the stationary phase change its activity[8]. The high use of expensive solvents (when water is not used) can be solved by recycling the used solvent. However, this can lead to the analytes building up in the solvent and increasing the background level at the detector[1]. Alternatively, narrow bore columns operating at lower flow-rates can reduce the volume of solvent used dramatically[1,14].

There have been many hardware modifications to make the HPLC instruments more reliable and robust[1]. Guillemin presented the most interesting approach with a new probe-PLC (i.e. Process Liquid Chromatograph) design that simplifies the construction of the process chromatograph system and makes it more reliable[8,13,14]. This approach uses a single module incorporating sample handling, the sampling line, sampling conditioning and the chromatographic systems. It avoids the use of temperature controlled systems as changes in temperature affect the peak shape and retention times but not the peak area and concentration. Changes in retention times can be corrected with an appropriate software (ADDS, i.e. ADaptative Deferred

Standard System), data processing and the use of the Deferred Standard (DS) concept. This method includes the injection of a pure compound within each analytical sequence. This injection is delayed with regard to the sample so that it does not interfere with the sample to be analysed. The DS concept can be used to calibrate and check the proper functioning of the chromatograph[8,14]. Not only does this design improve the reliability of the instrument, but it also reduces the response time and maintenance problems as the sampling lines are shortened[13].

The high response time of the analyser relative to the time constant of the process is sometimes not admissible for the use of LC in analysis and control[15]. The long analysis times typical of LC analysis can be minimised using automated on-line systems instead of manual sampling complemented with off-line analysis[16]. Also, the analysis time can be reduced by using smaller size particles with high specific surface area in the HPLC columns[1,14]. This allows the use of shorter columns with the same velocity and pressure drop for the mobile phase while the resolution is maintained. The same flow-rate and shorter columns means a faster separation. There is a limit in the size of particles, though, which can be reliably produced[1]. Smaller particles tend to have a proportionally wider size distribution, which reduces column packing efficiency. Once this limit is reached, the resolution is sacrificed when the analysis time is reduced. However, new statistical chemometric techniques that are now available, make loss of resolution acceptable in the attempt to reduce the analysis time, as the procedures are able to extract quantitative information from poor quality chromatograms[1,17]. An increase in temperature can also be used to reduce the analysis time by lowering the viscosities of the solvents and therefore increasing the flow velocities without increasing the pressure[1]. Moreover, mass transfer kinetics are faster at high temperatures, which also improves resolution at faster rates.

As a result of all these problems which sometimes can only be partially solved and because of the challenges in sampling, HPLC remains a last resort for on-line analysis[1,7]. In fact, there is only one manufacturer currently selling on-line HPLC equipment, Dionex Corporation with the DX-800 process analyser (see *Figure 4.1*)[1,9,18,19]. Moreover, this equipment has principally been used for ion chromatography (IC) applications where, unlike other LC methods, the mobile phases are aqueous[20,21,22]. Another advantage of IC is that temperatures need to be neither

elevated nor well controlled because ion exchange distribution coefficients are relatively insensitive to this variable[11]. Further, low pump pressures are satisfactory because column packings are large and porous so plugging and leaks are unlikely[11,18].

In spite of the difficulties of on-line HPLC, developments for on-line applications has taken place especially in the areas of biotechnology[5,6,15,16,23], environmental analysis[1], wastewater treatment[20,24] and the petrochemical industry[7,11]. Its use is also being extended to the semiconductor industry[25] and pharmaceutical industry[1,26]. In some of these applications the use of on-line LC has already proved significant control payouts that have compensated the high costs of the analytical instrumentation[11].

Figure 4.1. Dionex DX-800 process analyser

1.2. Problem of sampling in on-line HPLC

The use of fully automated sampling systems has been found to reduce the analysis time and sometimes increase the reproducibility of many industrial processes, especially in the areas of biotechnology, environmental analysis and wastewater treatment[5,6,16,24]. The requirements of a sampling system vary depending on the application, but flexibility, robustness, reliability and fast response are usually the major concerns[5,7,15]. Asepticity is also a very important sampling demand in biotechnological processes[15]. One of the most important sampling needs for LC analysis is the removal of particulates[1,8], which is more demanding than for other techniques such as flow-injection analysis[5,6]. For example, in environmental analysis, filtration of suspended solids and pre-concentration of analytes are required[1]. However, simple filtration before analysis can also remove any analyte associated

with the particulates due to absorption onto particulate matter or precipitates. The precipitation of analytes as the sample cools in the transfer line is another sampling problem associate with the removal of particulates necessary for LC analysis[1,8]. There have been numerous designs developed to try to overcome the filtering problems associated with sampling for LC analysis. Most of them have been applied to the areas of biotechnology and environmental analysis where the information obtained via LC analysis is crucial, specially for analytes at low concentration[1].

There exist three main technical solutions to the problem of sampling for LC[8]:

- The use of dissolution loops, fully automated, between the chemical reactor and the analyser[1,10,11]. The dissolution loop is equipped with a fast circulating pump. By means of the fast flow and the mixing of the sample with a heated solvent, a homogeneous mixture is obtained. An aliquot of this solution is then injected into the chromatograph.

- A precolumn-column assembly using a "guard column" to remove solid materials before the sample reaches the separating column. The precolumn may also be used as a concentrating system for enhancing the limit of detection of the process analyser.

- Filtration is the use of inorganic or organic filtering membranes to remove the undesired particles from the sample that is going to be injected into the chromatographic column. The filtration technique is very popular in biotechnological applications.

Two main approaches can be distinguished in the sampling designs involving only filtration technology[1,14]: simple filtration and membrane extraction via dialysis or ultrafiltration. Simple filtration using porous materials has been modified and adapted for LC analysis. A method called solid phase extraction uses solid porous cartridges that are fed on a bandoleer in turn into the sample line[1]. Each solid phase extraction cartridge is relatively cheap and disposable. This technique is widely used for water analysis of organics in rivers. Blocking of the filters and mechanical failure of the sampling device are the biggest problems associated with this type of design.

The use of membrane based sampling devices for on-line monitoring started[15] in the mid-1980s. Membrane based sampling systems can be categorised according to two points of view: dialysis and ultra- or microfiltration[1,15]. In dialysis a concentration gradient is the only driving force for transport through the membrane from the sample to an acceptor phase. In microfiltration, a pressure is applied to force the analyte molecules as well as the solvent through the membrane pores and, consequently, no acceptor phase is necessary[15].

Membrane extraction via dialysis is based on the use of non-porous membranes sampling devices. The principle of operation is that organic molecules in the effluent are soluble in the membrane, and hence diffuse into it[1]. The recipient solvent is selected such that the molecules required are soluble in it, and therefore diffuse into it from the membrane. With the flowing of the recipient solvent, a steady state concentration gradient is rapidly established. The concentration in the flowing recipient solvent is then constant and directly proportional to that in the donor solvent, and can be readily calibrated[1,15]. Internal standards selected to have similar transfer properties as the main analyte are chosen for calibration. Automated on-line dialysis LC has been developed and used for analysis of biological solutions, particularly drugs in plasma[1].

Ultrafiltration is used in fermentation monitoring when dissolved proteins have to be removed as they bind to column packings and degrade the column performance[5,6,16]. The ultrafiltration units are usually connected to a recycle loop where the broth is circulated with a peristaltic pump[5,6]. The slow flows needed in the loop to achieve the ultrafiltration (around[1,5,6]100 ml/min) are associated to relatively large dead times ranging from 5 to 12 minutes depending on the substance passing the membrane[1]. Other ultrafiltration sampling devices avoid the use of recycle loops, which are sometimes the source of infection in fermentation processes[15] if sterile barriers are not used in the loop[5,6]. The system is an internal sampling probe that is immersed in the vessel. The filtrate is sucked by vacuum with a peristaltic pump and into the injection valve of a HPLC system[15,24].

Polarisation and membrane fouling are the major problems associated with the method of membrane extractions, leading to longer dead times[1,5,6]. The phenomenon

of concentration polarisation is reversible and can be controlled by optimising the sample flow[5,6], choosing a sufficiently low pressure or enhancing the turbulence of the sample flow[6,13,14]. However, membrane fouling is irreversible and can only be reduced by back-flushing or by-flushing with acid, alkaline or detergent solutions[5] or by removing the pressure difference over the membrane as frequently as possible[6]. Blocking of the membrane occurs to a lesser degree if the pore size of the membrane is increased[15] and a high turbulence in the vicinity of the membrane is maintained[27]. Dialysis membranes are not very susceptible to fouling. Therefore, membrane fouling is a bigger problem in filtration, because compounds larger than the pores are, reversibly or irreversibly, force against the membrane[15]. In fact, in ultrapurification sampling devices the membrane usually has to be replaced after every run in batch processes or periods of around 5-8 days in monitoring of effluents[1]. New designs of rotating filtration modules have proved to decrease the membrane fouling as the centrifugal force created in these devices removes fouling substances from the membrane surface[15,28]. The use of semi-rigid porous films as a membrane support is another alternative to help minimise the problem of membrane fouling[24].

Apart from the removal of particulates necessary for LC analysis, the quenching and dilution of the samples constitutes another big challenge in the design of samplers for on-line HPLC[22]. The dilution is necessary to keep the analyte concentration in the linear range of the detector and can be a serious source of errors in sampling[27]. Normally, intermediate dissolution loops are used where the sample is dissolved in an appropriate solvent[1]. In biotechnology it is common to use compounds that inhibit the metabolic activity of the microorganisms[15]. In reaction monitoring a sample is normally passed from the reactor through a sample loop from where it is injected into a diluter, usually provided with stirring[1,8]. The commercial Dionex DX-800 on-line IC system is provided with a dilution module (SPM, i.e. Sample Preparation Module) that can be directly connected to a recycling loop and used to quench reactive mixtures[1,20].

In summary, there are engineering solutions capable of solving the most difficult sampling problems. However, the greatest concerns remain in the reliability and cost of the designs. This project concerns the testing and development of new

prototypes of sampling probes designed and built to overcome the reliability and cost problems typically associated with LC samplers.

1.3. Previous prototype samplers: Zeneca Mark I and Mark II

Zeneca developed an analytical system that consists of three main parts: a sampling probe, a control unit and a laboratory analyser[29-32]. Here, interest will focus on the sampling probe and the features of the control unit that regulate the functioning of the sampling device. Two different versions of the sampling probe were initially developed and tested before the start of the work included in this thesis: the Mark I and Mark II probes[30,31,33].

The Mark I probe relies upon the natural circulation in the process vessel to fill an aperture in the body of the probe[29,32]. This fluid is then displaced by a piston and transferred to the analyser. A sequence of events involving valves, pumps and pneumatic actuators is controlled by the control unit (see *Figure 4.2*) in three main steps: purging, sampling and delivering. This allows the lines to be cleaned and purged before sampling and the sample to be mixed with a diluent before delivering the diluted mixture into the analyser. The three steps involved in the functioning of the sampling system can be summarised as follows[31,32]:

- Priming. Any impurities in the lines, the probe and a mixing chamber inside the control unit are flushed out with diluent.
- Sampling. The probe captures a volume of the sample solution that is then flushed to a mixing chamber by a metered volume of diluent. The sample volume and diluent are then mixed by recycling the mixture in a loop through the sampling probe and around the mixing chamber.
- Delivering. A defined volume of diluted sample is metered to the sampling outlet for collection. At the end of this step the sample lines are purged once again to remove any excess sample before the cycle of steps runs again.

Table 4.1 shows the typical sequence of events and their duration[31], which can be varied and optimised in the PLC (Programmable Logic Controller) unit[34] in order to optimise the sampling probe. *Figure 4.3* shows a picture and sketch of the Mark I sampling probe[29]. The probe is normally left in its retracted position where the sample

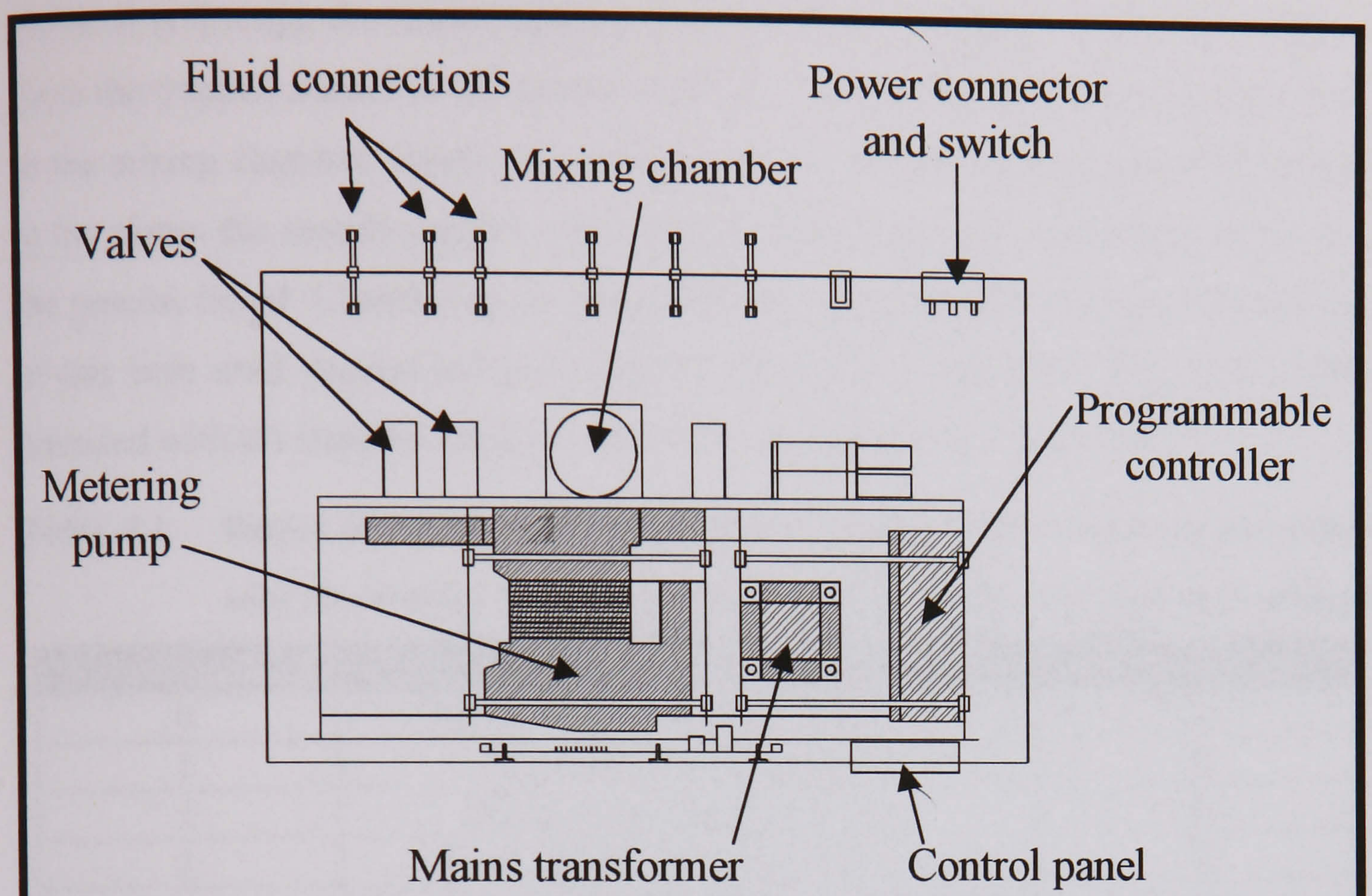

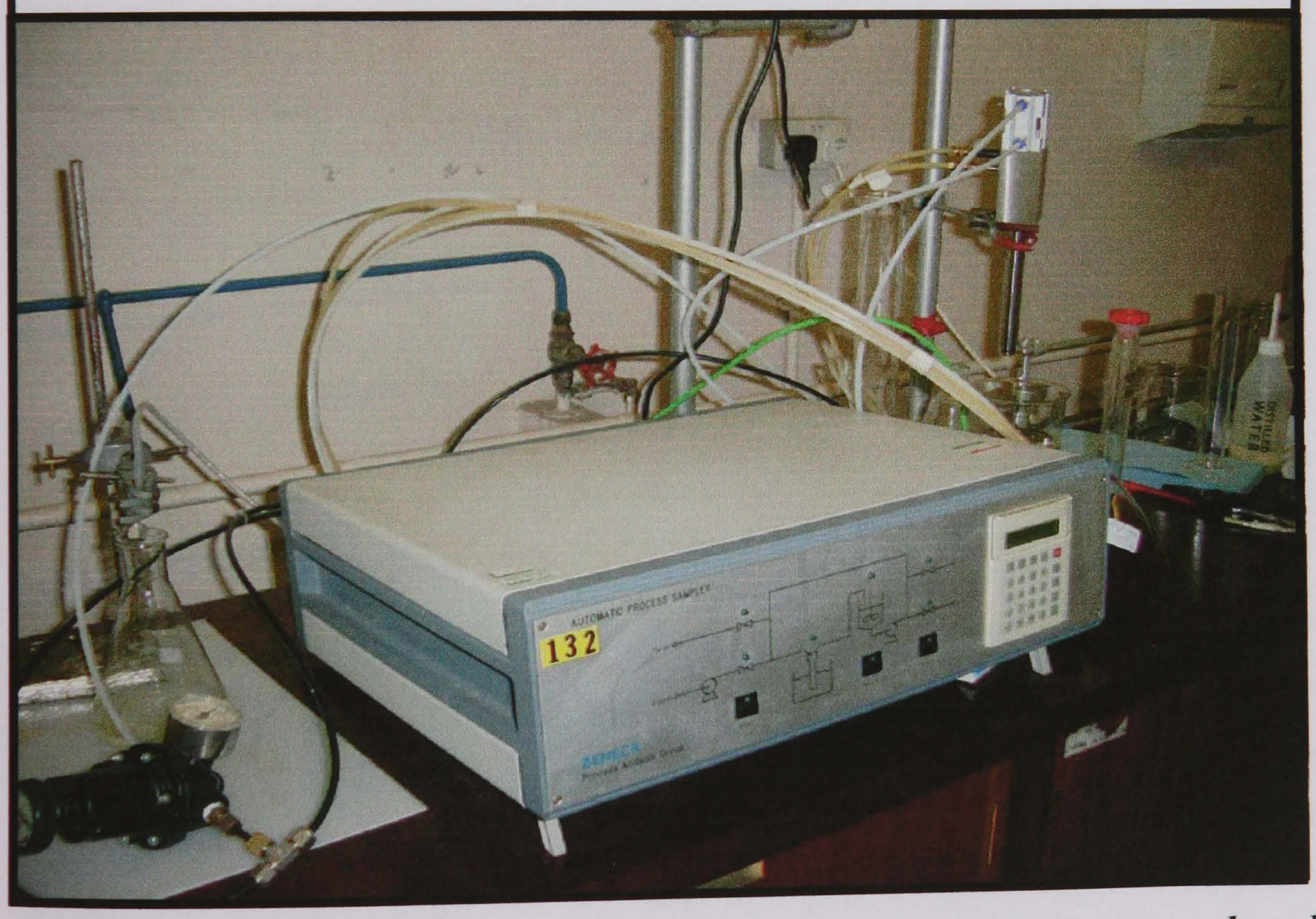

Figure 4.2. Top view and picture of the control unit designed by Zeneca and used with the Mark prototypes

capture valve is open to the feed and return capillaries running along the sides of the probe. It is through the lower capillary that the diluent is fed to the valve in order to force the trapped aliquot of the process fluid out through the upper capillary and back to the mixing chamber inside the control unit. On application of a pneumatic supply to the piston the sample capture valve is forced down and its central hole exposed to the process liquid. Chamfering on the probe body then funnels the liquid into and out of this hole until pressurised gas is fed to the piston return port. The valve is then retracted with the trapped sample open to the feed and return capillaries[29,32].

Table 4.1. Stages involved in the three steps involved in the sampling procedure with the Mark I sampler and the optimised values for the timer settings

Timer number	Description	Timer setting (s)
0	Purge mixer and mixer drain line	20
1	Wash diluent-pump mixer	40
2	Wash mixer-pump-drain line	20
3	Wash and purge probe-drain line	15
4	Purge mixer and purge mixer-drain line	15
10	Insert probe and take sample	5
11	Pump sample through probe	5
12	Meter diluent via probe	75
13	Mix sample and diluent via probe	100
20	Meter diluted sample to analyser	15
21	Purge mixer and purge mixer-drain line	20
22	Purge mixer-probe-drain line	30
23	Purge mixer line and purge analyser line	1
24	Wash diluent-pump-analyser line	40
25	Purge mixer-analyser line	1

Different evaluation tests were performed using this probe and the control unit[30,31,33]. Although the precision of the results was acceptable in most of the cases (i.e. %RSD<5%), the automated sampling system always showed higher deviations in the results than when manual sampling was used. However, the main problems encountered with this design were the large size of the probe for use in the standard vessel ports and the presence of air bubbles in the orifice of the probe[32]. This latter problem was affected by the inclination of the probe and the agitation of the test sample in the vessel[31].

The design of the Mark II sampling probe was intended to overcome the problems observed in the Mark I prototype[32,35]. In the new design the probe diameter was reduced[35] to 57% of the Mark I probe, i.e. 20 mm. Also, the Mark II probe incorporated a small positive displacement pump that actively forces the process liquor through the sample capture valve[32,35]. This was meant to overcome the dependence of the probe orientation and stirring on the sample collection that was observed with the Mark I prototype. However, preliminary tests carried out with the Mark II probe showed leaks occurred owing to air bubbles caused by the vacuum produced with the pumping system[30,32]. Also, the precision of the results was unacceptable (%RSD>10%) and the sealing o-rings used in the probe had a short lifetime[30]. These complications prompted the development of new designs that were used in this work[4]. The prototype Mark I will be the reference prototype used in this thesis for the comparison and analysis of the results obtained with the new designs presented in the next section.

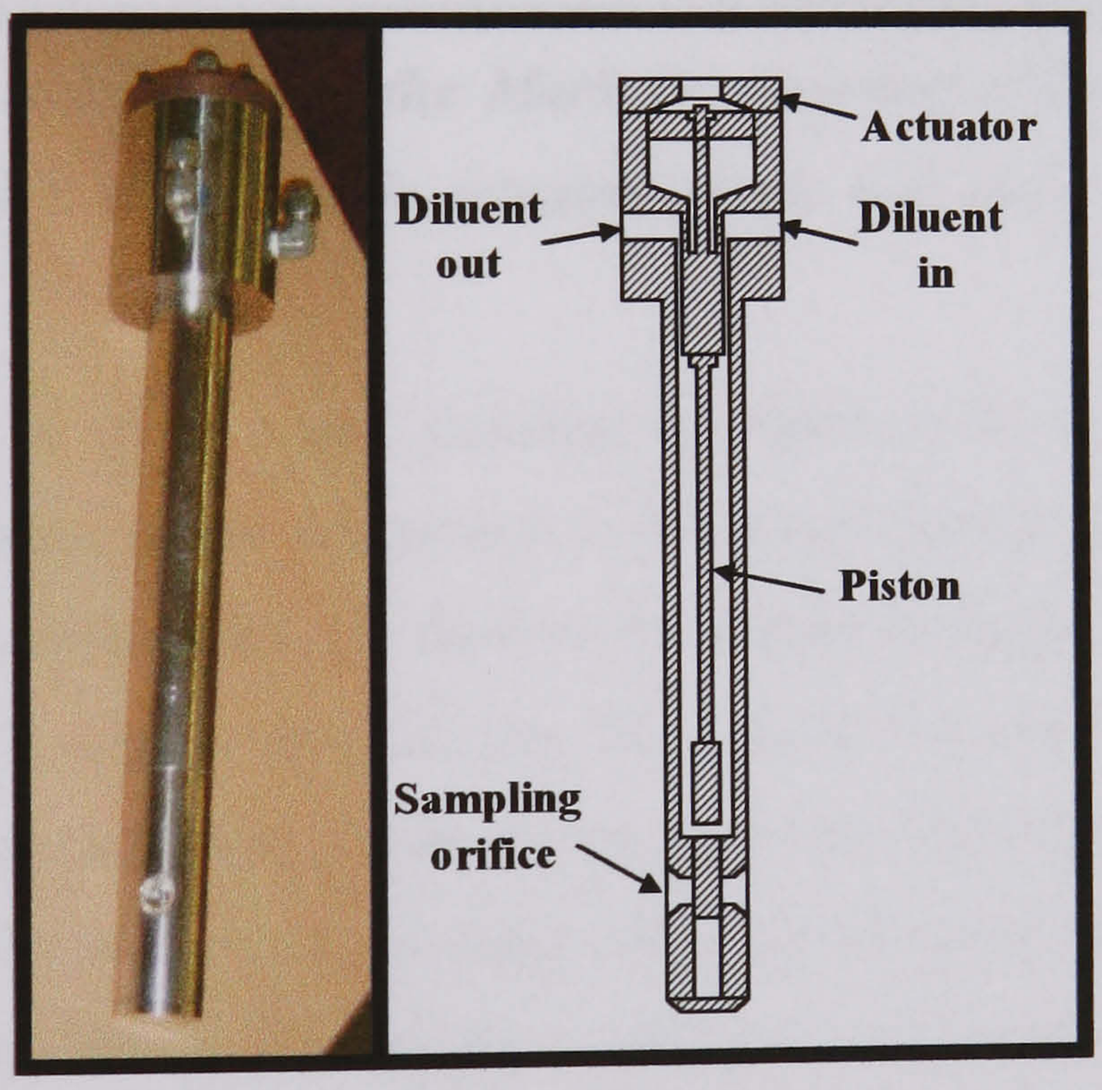

Figure 4.3. Picture and sketch of the Mark I sampling probe

2. Experimental System: Samplers Mark III and Mark IV

In an attempt to improve the unsuccessful Mark II probe two new prototypes were designed named Mark III and Mark IV[32]. The Mark III prototype is the more complicated of the two designs and uses a pumping system to pull in the fluid in the sampling probe where a non-return valve retains the sample. The Mark IV prototype was simpler and was the design built and tested in this PhD development work as

the Mark III design was not fully assembled and ready for testing when this work was carried out[4]. The Mark IV prototype functions in a similar manner to that of the successful Mark I design although the sample is now taken from the bottom of the probe and the size of the system is considerably smaller[32].

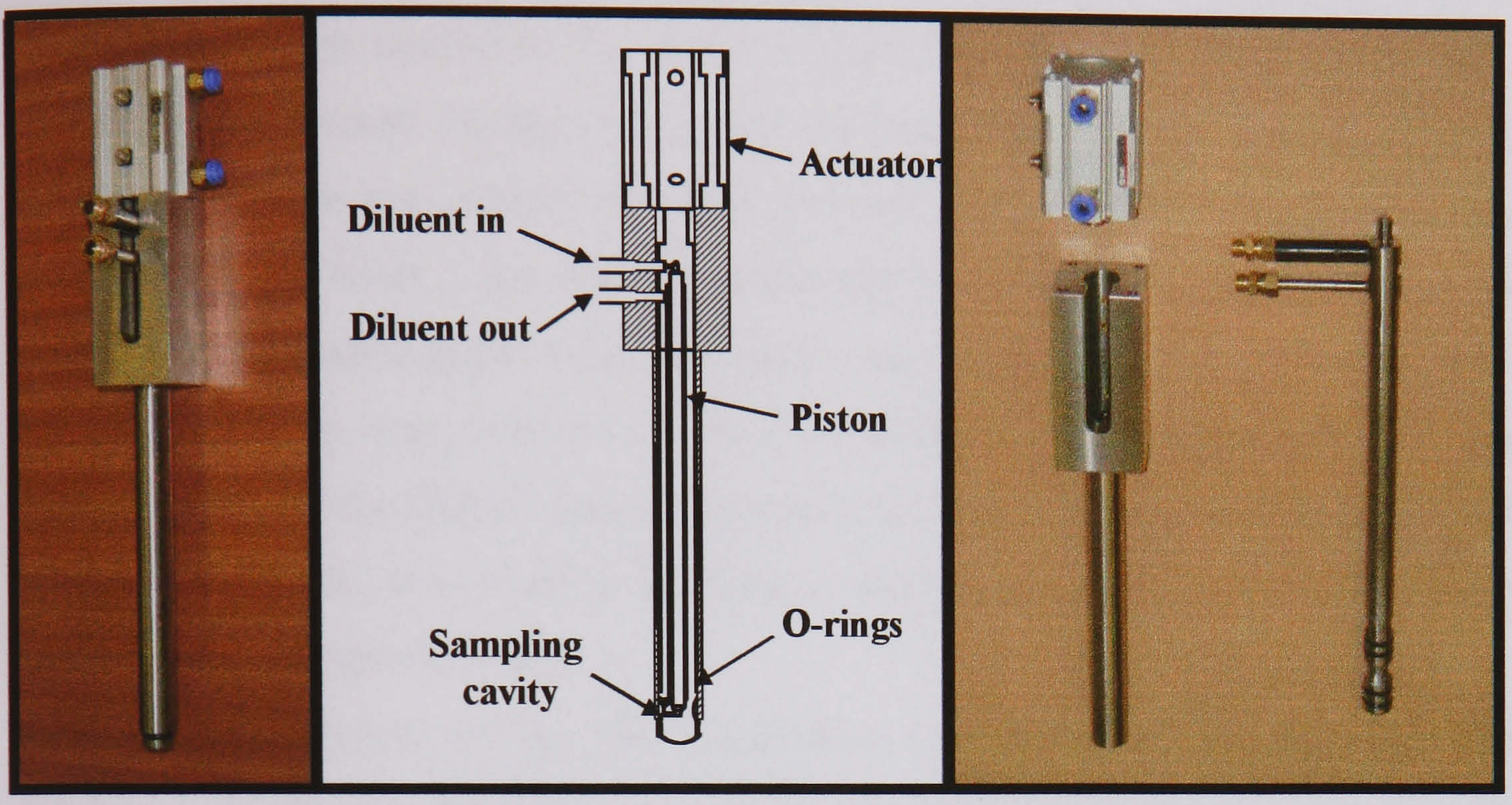

Figure 4.4. Picture and sketch of the Mark IV sampling probe, assembled and dissembled in pneumatic actuator, piston and main body with outside tube

In the Mark IV (shown and sketched in *Figure 4.4*) a grooved piston is immersed in the solution where the groove is filled with liquid. When the piston is pulled back into the outside tube, the fluid in the groove is trapped inside the probe. At this time, diluent is ejected into the inlet tube where it is mixed with the sample and leaves through the outlet tube to the mixing chamber. The bottom of the probe is rounded in the Mark IV probe to avoid unnecessary disturbances in the process. Also, the edges of the space where the sample is collected are smoothed to avoid sharp corners, where bubbles or solid material might be trapped. In addition to this, the inlet and outlet drillings are at an angle to prevent air in the holes (remaining after the purging process) from bubbling out and affecting the volume of sample being captured. According to the design, the volume[32] being trapped in the probe is 1.20 ml. With this design, the same stages in the program of the PLC controller as used with the Mark I prototype were reported to be applicable with no changes. However, modifications to the program, as described in the next section, were required for

optimum performance.

3. Evaluation and Developments on the Discrete Sampler Mark IV

Preliminary tests using the sampling probe[33] resulted in poor sampling with very poor precision in the range 2.1-69.8% RSD. These results indicated that further developments were needed in the probe in order to solve the problem of the large variation in the sample volumes taken with the Mark IV prototype. The development experimental work was initially based on the tests previously performed[30,31,33] in the assessment of the Mark I and Mark II probes and preliminary tests with the Mark IV probe. A concentrated aqueous solution with 1.5 g of methyl orange (Aldrich 23,410-9) in 1 L of water was used as a stock solution for the sampling experiments. The reproducibility of the diluted aqueous samples obtained using the sampling unit with the Mark IV probe was assessed by doing a wavelength scan using an UV-Visible spectrometer (Philips PU 8720).

The calibration of the UV instrument was performed by measuring the maximum absorbance (at 464.8 ± 1 nm) of six calibration samples prepared in the range 1.4-8.5 x 10^{-5} M. This range of concentrations was chosen based on the linear range observed in previous experiments[31] and considering the range of dilutions applied to the theoretical volume of sample being trapped with the probe. Triplicate measurements with the calibration sample set showed very good reproducibility in the results and perfect linearity in the change of absorbance with the concentration. However, a little variation (less than 3.4%) in the calibration results (typically around Absorbance = (26511 ± 884.09) x Concentration (M)) was observed if the sample set was analysed again after a period longer than a day. This reproducibility problem was believed to be due to the UV instrument (used daily in a teaching lab) and was tackled by always performing the calibration before the diluted samples were analysed. Finally, no indication of change in the spectroscopic properties of the dye solutions was observed after the samples were stored for a period shorter than 2 weeks after the sampling experiments and before the UV analysis was performed.

3.1.1. Initial tests

For the initial experiments with the probe new viton seals were assembled in the probe and the quality of the sealing was assessed. For this, the pneumatic actuator was removed from the sampler and compressed air was injected through both the inlet and outlet diluent lines in the probe[36,37]. No leaking was observed when the piston of the probe was exposed up to 11 mm in the sample. It should be highlighted that the probe, in its normal closed position, was exposed 7 mm into the sample. Although one of the O-rings (placed at 4 mm from the tip of the probe) had no sealing effect, no leaking was observed in the probe when using the new viton O-rings. As one of the O-rings was not sealing as expected on the basis of the design specifications[32], the test above was performed periodically to ensure that no leaks were occurring.

Once the quality of the probe sealing was assured, similar experiments to those described by N. Peters[33] were performed. The time settings used in the control unit were the same as specified in *Table 4.1*, which were the optimum values determined by previous researchers. Timer 12 was set to the lowest value that the system was capable of with an acceptable accuracy according to the results obtained by K. Meney[30]. This provided the highest possible concentration values for the diluted samples obtained in the experiments, which should be associated with a higher reproducibility and low %RSD values. Timer 13 was set to the lowest possible value in order to obtain good mixing and also make the initial experiments as short as possible.

The results showed that manual and automatic sampling were not comparable, with high and variable %RSD values (in the range 4.81-13.56% RSD) observed with automatic sampling using the new Mark IV probe. Further experiments were performed to check the quality of the sealing in the probe. Now, timer 10 was set to 0 while timer 11 was varied from 0 to 5 s to see if there were any leaks in the system that produced the pumping of stock solution through the probe even when the tip of the sampling probe was not immersed in the solution. Also, tests were performed keeping timer 11 at a constant value of zero and varying timer 10. The results showed no problems with sealing as no sample was pumped when both timer 10 and 11 were set to 0 seconds. Also, the experiments showed how the use of both timers 10 and 11

were redundant and with this design of probe only one of the two timers was needed. Therefore in later experiments only timer 10 was used in the sampling experiments with stage 11 set at 0 s.

3.1.2. Modifications in the pre-sampling stage

As the preliminary tests concluded that the lack of reproducibility in the performance of the probe was not due to imperfect sealing, new modifications in the functioning of the sampling device were studied. Initially, it was believed that the poor sampling results could be due to an undesired effect that the empty diluent inlet and outlet lines might have produced during the sampling stage[37]. Therefore, it was proposed to change the sequence of steps in the PLC program and fill those lines with diluent before, instead of after, the sampling stage[4,37]. The programming code[38-40] before and after the changes is shown in Appendix 5. *Table 4.2* summarises the new sequence of stages and the timer settings used in the experiments after the changes were made.

Table 4.2. Stages involved in the sampling procedure with the Mark IV probe after the changes in the PLC program to fill the lines with diluent before sampling

Timer number	Description	Timer setting (s)
0	Purge mixer and mixer drain line	20
1	Wash diluent-pump mixer	40
2	Wash mixer-pump-drain line	20
3	Wash and purge probe-drain line	15
4	Purge mixer and purge mixer-drain line	15
5	Meter diluent via probe	Varied
10	Insert probe and take sample	5
11	Pump sample through probe	0
13	Mix sample and diluent via probe	100
20	Meter diluted sample to analyser	15
21	Purge mixer and purge mixer-drain line	20
22	Purge mixer-probe-drain line	30
23	Purge mixer line and purge analyser line	1
24	Wash diluent-pump-analyser line	40
25	Purge mixer-analyser line	1

New experiments were performed to assess the quality of the sampling using the probe and this new sequence. Unlike the Mark II design, and as shown before, this probe did not require pumping of the sample through the probe and therefore timer 11 was set to zero for all of the experiments. In the initial tests several dilutions were studied by changing timer 5 setting when sampling from the methyl orange stock solution. Five replicate sample collections were performed when varying the setting for timer 5, which determined the dilution of the samples. Again, timer 13 was set to the lowest possible value that gives acceptable mixing, in order to make the experiments as short as possible. The results obtained are plotted in *Figure 4.5* (with %RSD values given in brackets) and lead to the following conclusions:

- A reduction of the %RSD was observed with the change in the sequence of events. RSD values lower than 7.71% were observed in all the cases. However, the %RSD values were still too high and poor linearity of response was observed in the results.

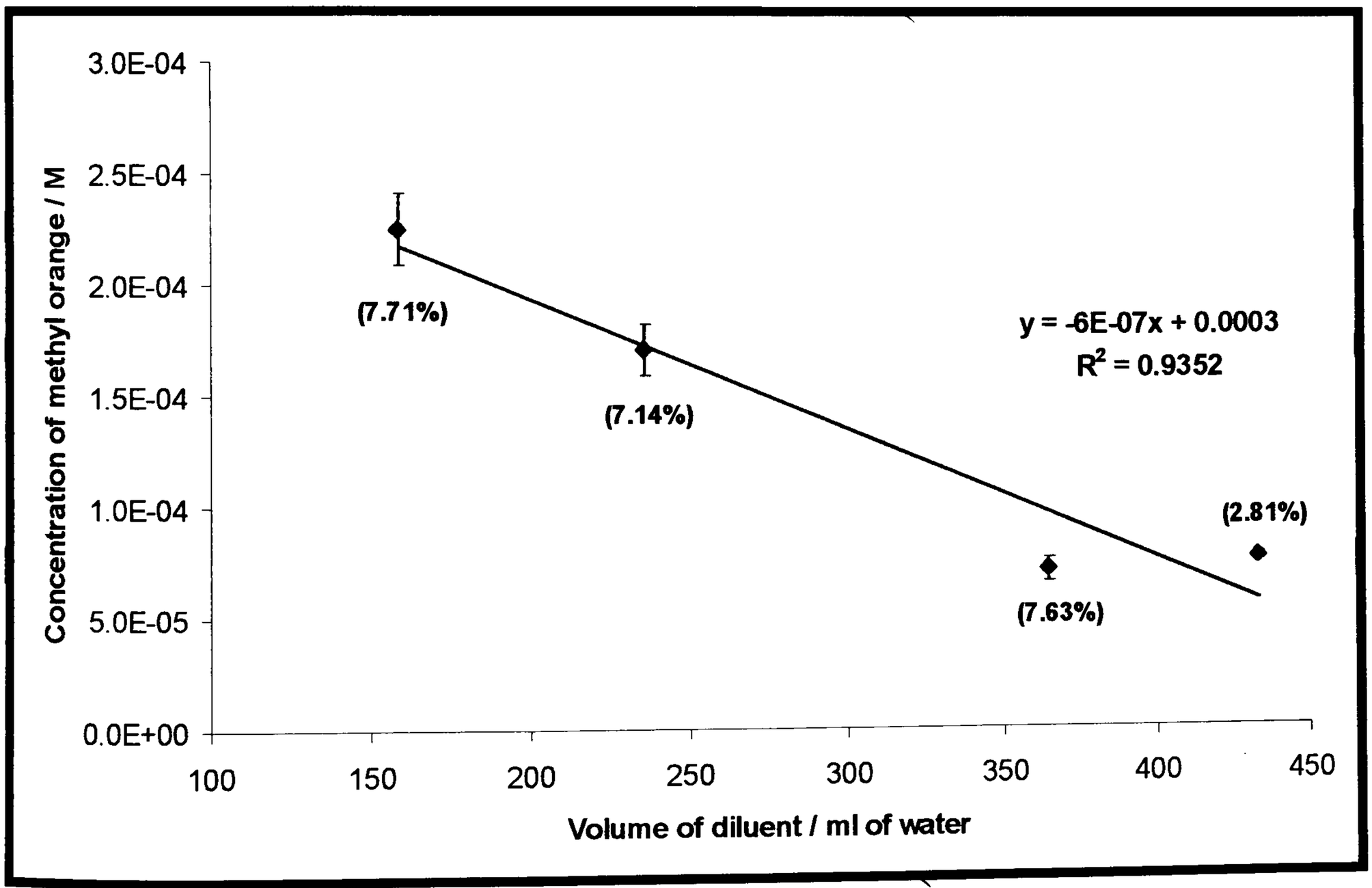

Figure 4.5. ***Concentration of the samples obtained when different volumes of diluent were added and the lines were filled with diluent before sampling***

- The change in the program also produced an increase in the final concentration of the sample. This was probably due to diffusion of the dye into the diluent that filled the lines, while the probe was immersed in the solution.

These results suggested that the change in the program to fill the lines with diluent before sampling could be a good approach that would lead to a better performance of the probe. However, some further changes would have to be implemented to improve the reproducibility in sampling up to acceptable levels (i.e. %RSD values lower than 5%) and to solve the problem of dye diffusion into the diluent.

3.1.3. Use of non-return valves in the system

A non-return valve (South Scotland Valves and Fittings Ltd., ¼ inch OD tube, SS-4C-1/3) in the outlet diluent line was used in order to improve further the performance of the probe. This valve together with the valve already present in the inlet line would help to trap the diluent inside the probe and avoid the variable flow of diluent by gravity into the mixing chamber[37]. Preliminary tests with the non-return valve showed a decrease in the flow-rate provided by the metering pump, possibly due to the incremented friction in the lines caused by the new valve. Also, it was noticed that the non-return valve altered the normal functioning of the control unit during stages 3 and 22, where air should be flowed in counter-current to wash and purge the lines. A manual by-pass line was used in conjunction with the non-return valve to allow the correct functioning of stages 3 and 22. The new valve was opened manually before the delivery stages (20-24) were activated and closed before the lines in the probe were filled (at stage 4). This allowed the counter-current of air in stages 3 and 22 to flow correctly and therefore the effect that the non-return (operating only in the sampling stages) had on the performance of the probe could be assessed. However, this arrangement did not show any improvement in the reproducibility of the results obtained with the probe. Furthermore, the problem of diffusion of the dye in the diluent was still observed and caused great concern about the possibilities of the new PLC program.

To study the problem of diffusion, the timer 10 setting was varied while timer 5 was kept constant at a value of 75 s. This variable controls the time that the probe is

immersed in the dyed solution during sampling. *Figure 4.6* shows how the existence of diffusion in the system was clear as the concentration of methyl orange in the sample increased as the time that the probe was immersed in the solution was incremented. Moreover, this effect was more important when the non-return valve was not used as can be observed from the higher slope observed in the change of concentration with the timer 10 setting. This was primarily due to the drop of diluent by gravity into the mixing chamber, which was the reason why the non-return valve was implemented to try to avoid this effect. The sligh decrease in the flow-rate, provided by the metering pump when the non-return valve was used, also contributed to the difference in the concentration values for the two experiments. However, this should have not affected the value of the slope in the representation as this depends only upon the diffusion when the system is static during sampling.

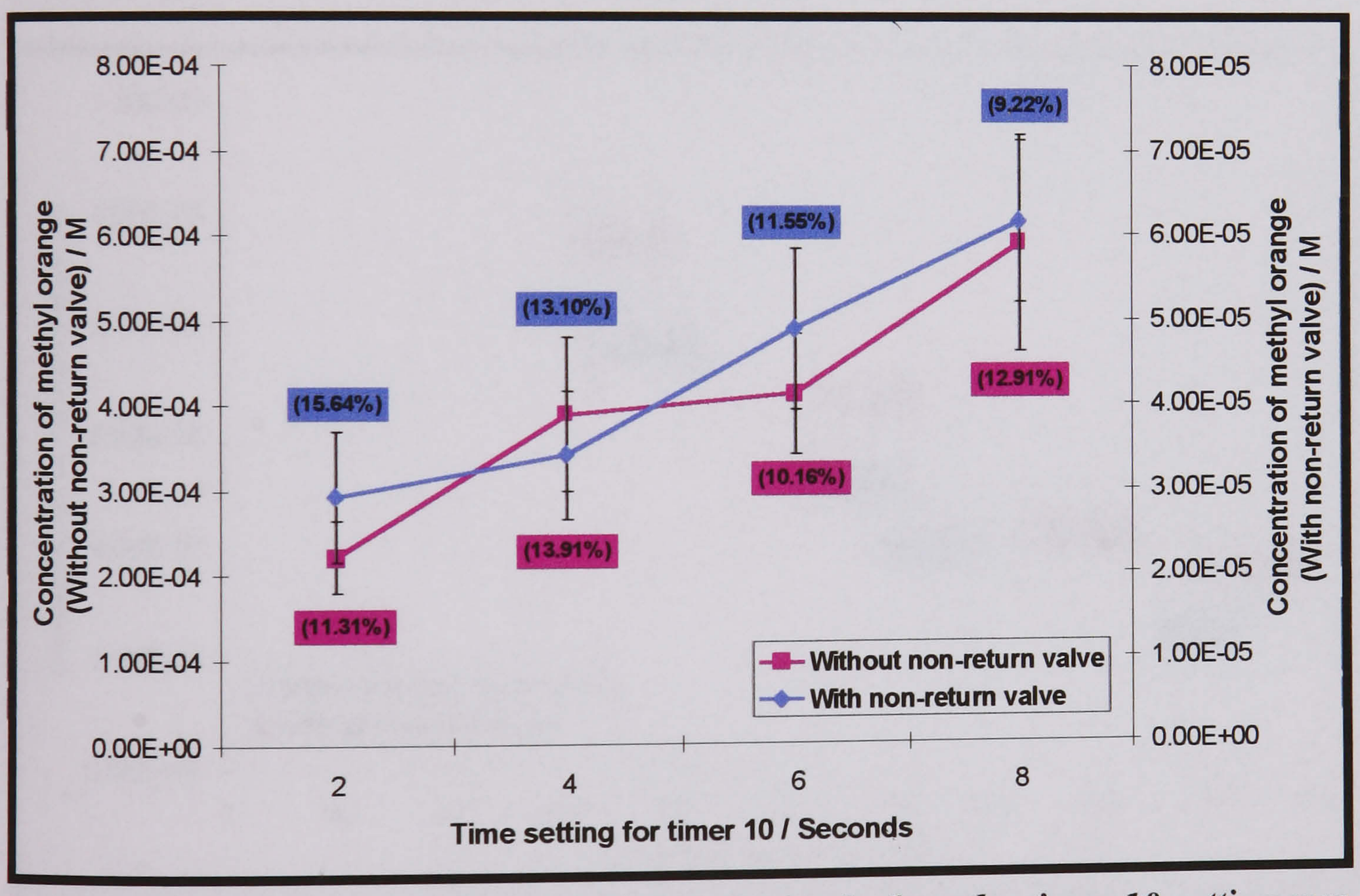

Figure 4.6. Concentration of the samples obtained when the timer 10 setting was varied and the lines were filled with diluent before sampling

Finally, the %RSD results showed that the problem of reproducibility still remained. Moreover, the precision in the results was variable as the %RSD values in these experiments without the non-return valve were much higher than those observed in previous experiments, which were lower than 8%. All these problems of diffusion

and reproducibility in the results made us reconsider the strategy of filling the lines with diluent before sampling.

3.1.4. Use of air-flow restrictors

As filling the lines with diluent before sampling fouled to improve the use of the Mark IV probe, the original PLC program was inserted again in the controller. In order to improve the performance of the prototype, it was suggested that restrictors should be used in the air-lines that drive the actuator[41,42]. This would slow down the vigorous movements of the piston at the sampling stage. The use of the air-flow restrictors was expected to minimise the turbulence at the tip of the probe during sampling, which could affect the sample collection in the grooves of the piston. The use of the restrictors was therefore expected to have a great effect in the performance of the sampler.

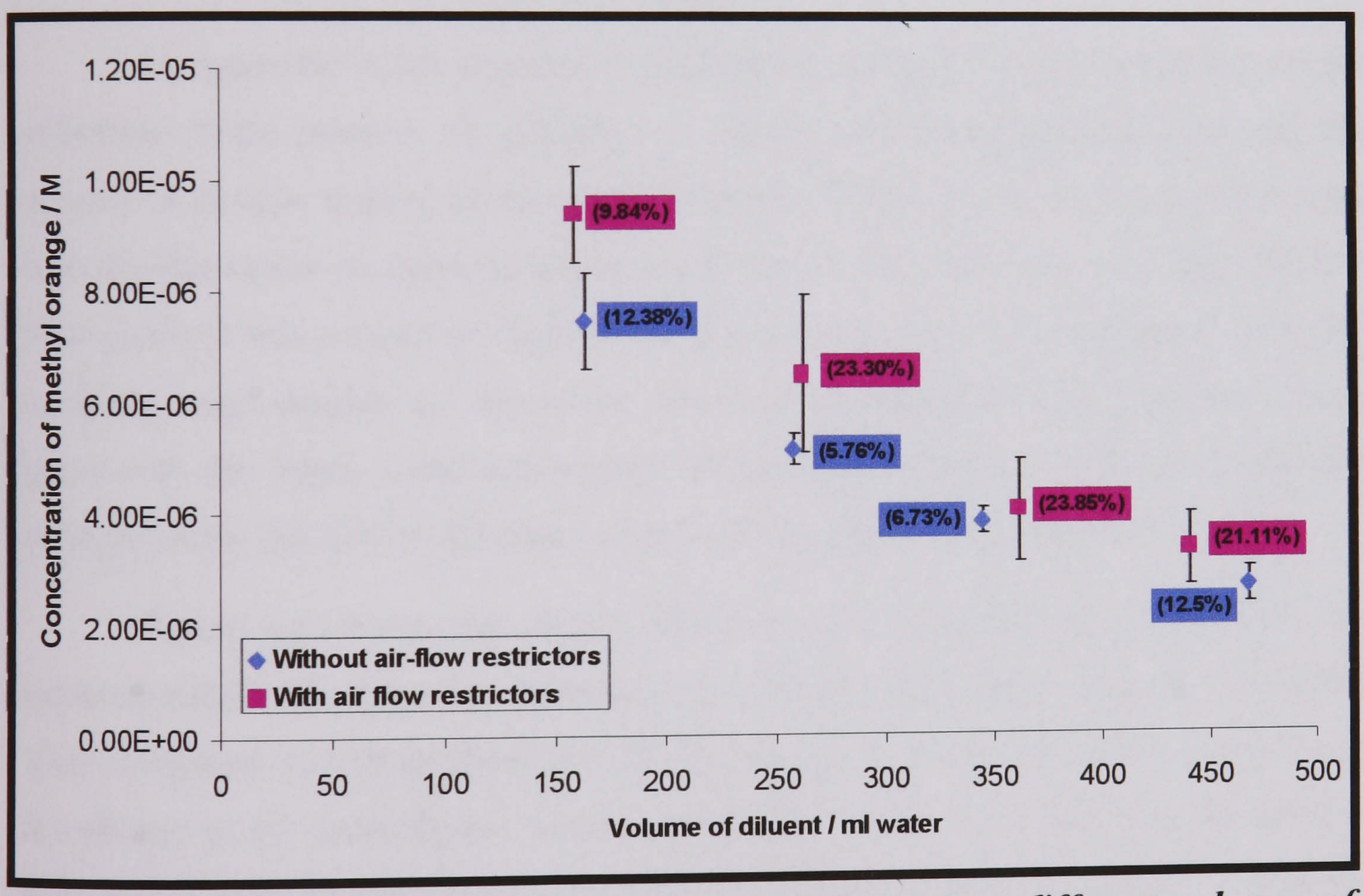

Figure 4.7. Concentration of the samples obtained when different volumes of diluent were added with and without the use of air-flow restrictors in the lines

Figure 4.7 shows the results obtained before and after two air-flow restrictors (RS 192-9182) were implemented in the compressed air lines. One of the restrictors was implemented in the air-inlet line to slow down the speed at which the piston

descended and therefore avoid undesirable turbulences in the system. The second restrictor slowed down the movement of the piston on the way up to ensure reproducible sample collection. Also, timer 10 had to be set to a higher value than 2 s to allow the piston to descend completely before sampling. The figure shows how the precision was not improved with the use of the restrictors, with large error bars and non-linear changes of the concentration with the volume of diluent added in both of the experiments. However, these experiments were very useful for the future development of the probe as the slow movement of the piston allowed for the observation of air bubbles coming out of the probe. This proved that, with this design of probe, there was pumping of solvent in the lines before the piston was actually fully retracted. This did not happened with the Mark I design as the use of timer 11 allowed a dead time between sampling and pumping of diluent.

3.1.5. Dead time in the sampling stage

As suggested in the previous section, the pumping of diluent during the sample collection could produce an alteration in the normal sampling procedure and the volume of sample trapped in the probe. This could have been the reason why good reproducible values in some experiments alternated with bad results with high %RSD. This problem was solved by implementing a delaying timer in the program after the sampling stage number 10. Therefore, timer 11 was adapted from a pumping stage (used with the Mark I and redundant with the Mark IV) to a dead time stage by changing lines 206-217 in the code of the PLC program (see Appendix 5).

Figure 4.8 shows the results obtained with the Mark IV probe after the implementation of a dead time between sampling and pumping of diluent. The results were compared with those obtained with the manual dilution of the stock solution and are plotted in the same figure. In this manual dilution 0.65 ml of the stock solution were mixed with the volume of water indicated on the x-axis of the figure. The results show how with the new program good reproducibility in the samples was obtained with %RSD values lower than 5%. It is also shown how the non-linearity in the change of concentration with the volume of diluent was also observed with the manual dilution. Therefore, this non-linearity of the results had nothing to do with the poor functioning of the probe and was typical for the spectrophotometric detection of

the methyl orange in the range of concentrations used in the experiment. The reason why the non-linearity was not observed in other manual dilutions used in comparison tests carried out previously is very simple. In previous experiments 1 ml of the stock solution was used in the preparation of manually diluted samples, which gave mixtures within a range of concentration where the absorbance varied linearly. The 1 ml was used in accordance with the design specifications of the probe[32] and the development experiments performed by previous researchers[31,33].

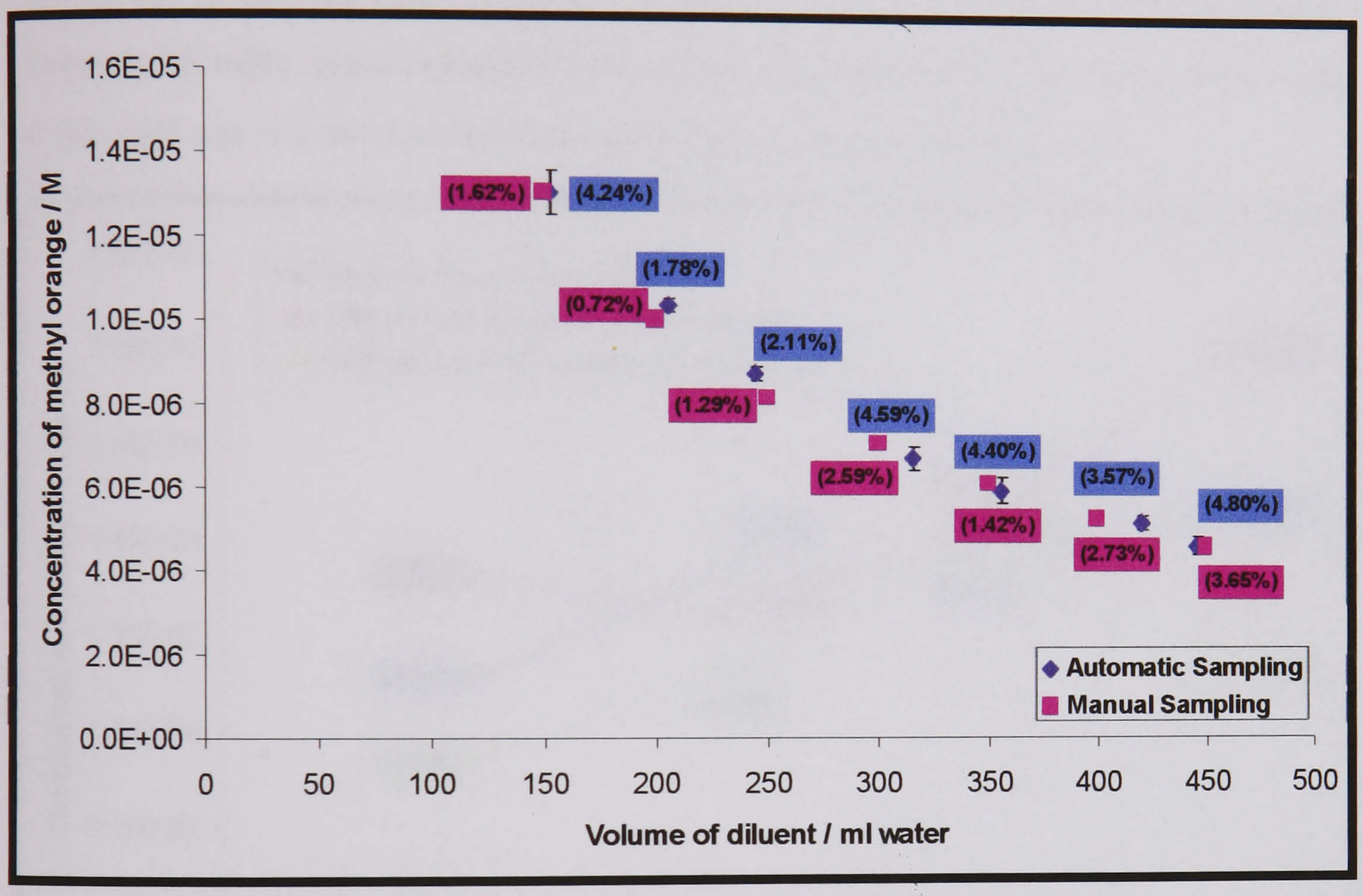

Figure 4.8. Comparison of the concentration in manually diluted samples and the samples obtained when different volumes of diluent were added and a dead-time was used between sampling and pumping of the diluent

3.1.6. Further development tests

Different tests using the restrictors, non-return valves and by-pass lines were performed with the sampling system using the dead time after sampling. However, no further improvements were observed in the performance of the Mark IV prototype. The combined use of the dead time and the filling of the lines with diluent before sampling was not assessed. The reason for this was that it was preferable not to have solvent in the lines before sampling as otherwise the diluent in the sampling groove could contaminate the test solution during sampling. Also, the existence of diffusion

of substances in the solvent made preferable the use of empty lines before sampling as the system showed good results operating in this manner. *Figure 4.9* shows how the concentration of the sample varied less than 10% when the time that the probe was immersed in the solution was varied. This small variation was observed with a dead time of 3 s before pumping of diluent and in all three variations tested: with non-return valve, without non-return valve and with the by-pass line always opened. Due to diffusion problems, variations of sample concentration of up to 200% with timer 10 setting were observed (see *Figure 4.6*) when the lines where filled with diluent before sampling. Finally, good reproducibility of the results was also observed with the lines empty and use of a dead time before sampling, as shown in *Figure 4.9*.

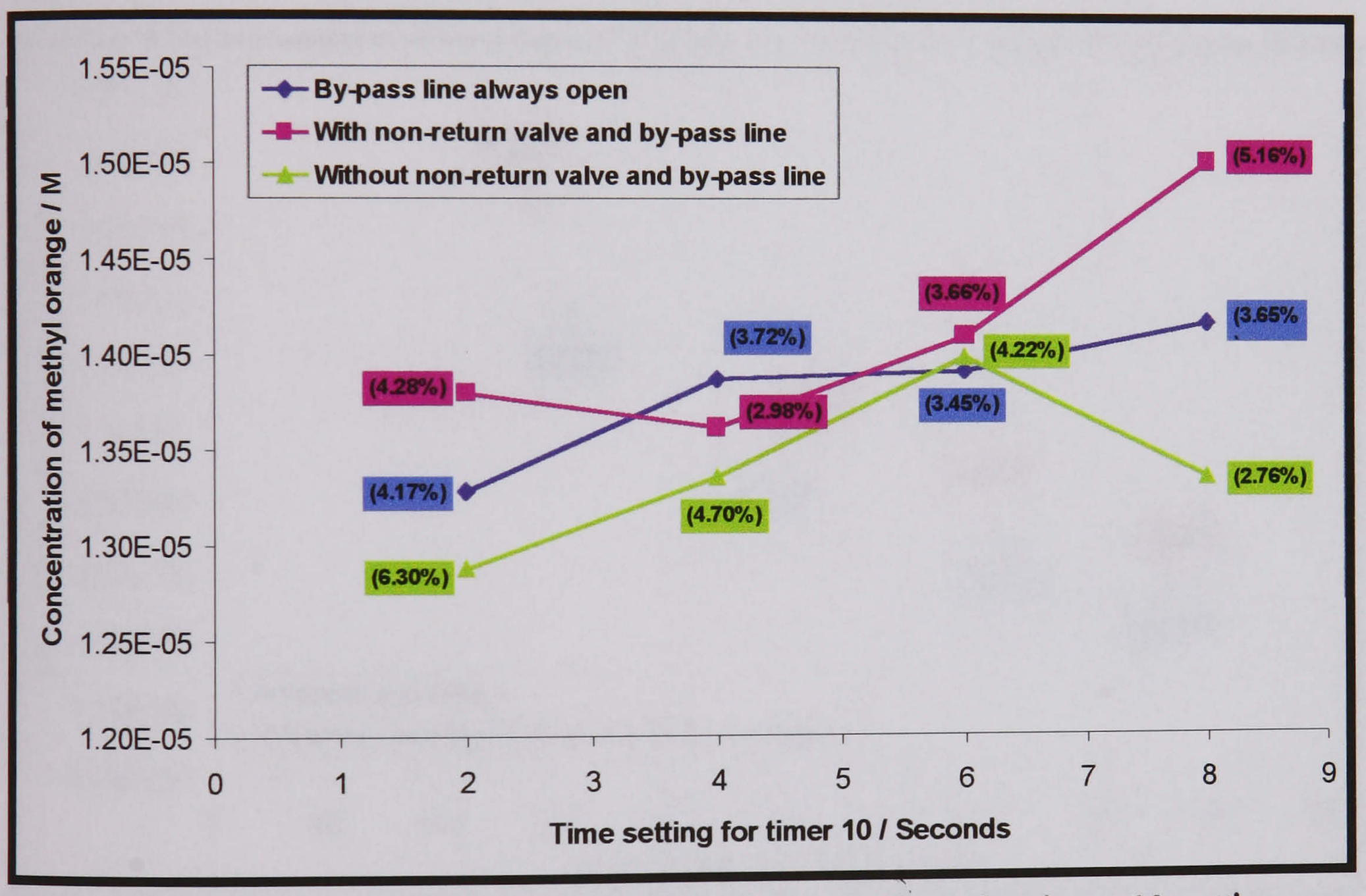

Figure 4.9. Concentration of the samples obtained when the timer 10 setting was varied, and a dead time and no diluent in the lines were used before sampling

In an attempt to discover additional sources of error in the performance of the probe, new experiments were performed. The most interesting experiment derived from the visual observation of some diluent trapped in the sampling gap when the piston was moved down after the priming step and before the sampling stages. In this experiment the effect that this small volume had on the quality of the samples obtained with the Mark IV prototype was assessed. In the test the piston was

manually cleaned and any dead volume of solvent was removed before sampling from the methyl orange stock solution. *Figure 4.10* shows the comparison between the concentrations obtained in this experiment and those measured when no-cleaning was used. In the figure it is shown how the little drops of solvent trapped in the sampling groove produced further dilution of the sample. This made the concentration of the mixtures obtained with manual cleaning of the probe to than that when the samples were collected during the normal automated operation. Also, slightly better precision was obtained when the remains of diluent in the probe were removed. The conclusions obtained from this experiment can be used for future designs where the efficiency of cleaning and flushing of the probe should be improved.

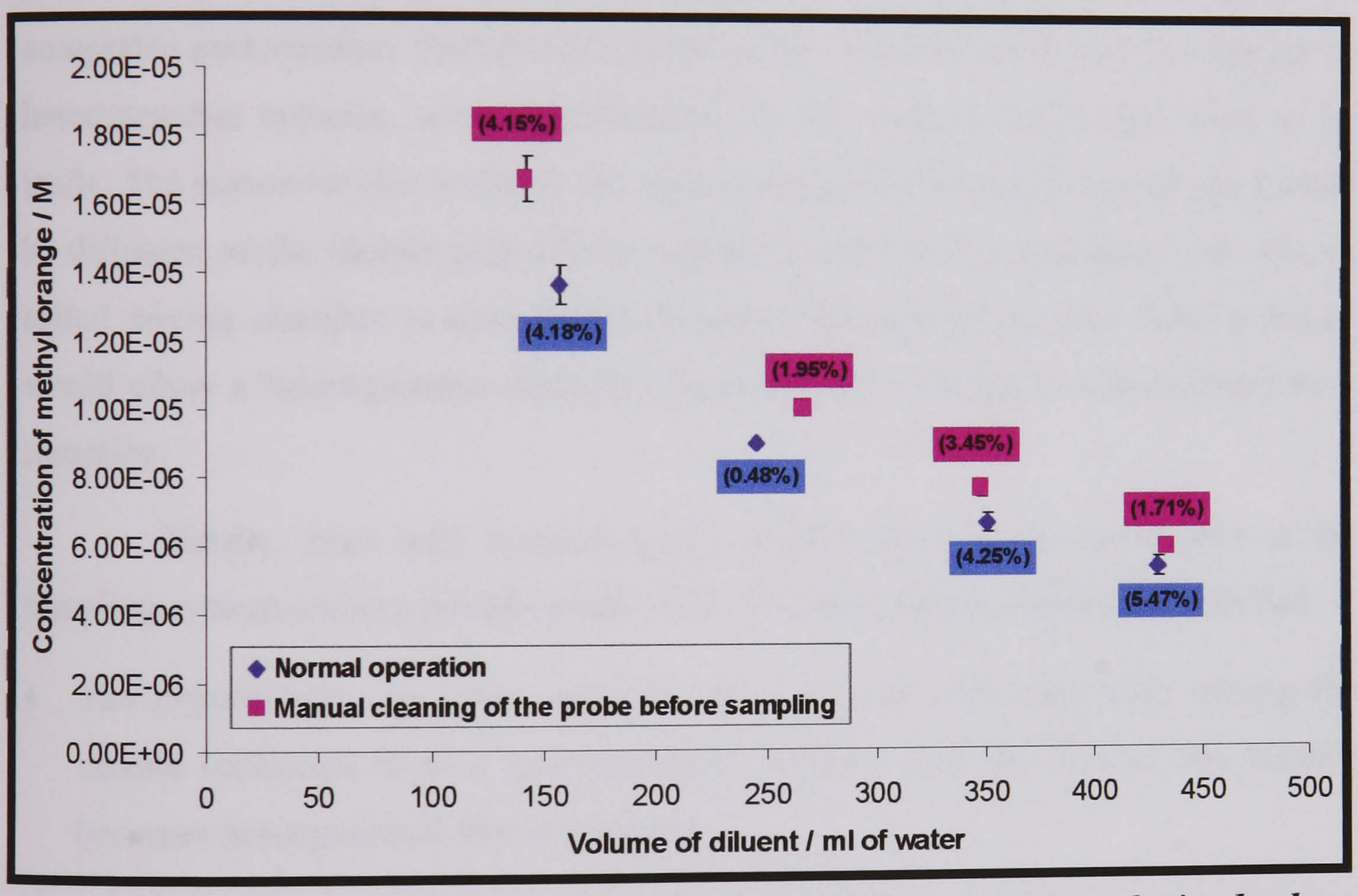

Figure 4.10. Comparison of the concentration of the samples obtained when different volumes of diluent were added to the mixtures with and without manual cleaning of the probe before sampling

4. Problems to Solve for Use in Heterogeneous Systems

In Chapter 3 the requirements of a good sampling system for stirred vessels were reviewed and outlined. None of these considerations were taken into account at the time of designing the sampling probe prototypes towards the implementation of HPLC for on-line monitoring of processes carried out in reactor systems.

Important factors that affect the sample collection, such as the orientation of the probe with respect to the flow-streamlines in the vessel and the sampling velocity, were not considered. More importantly, the small diameter of the sampling orifices (1.5 mm) in the sampling probe can very likely lead to blocking if the Mark IV prototype is used with heterogeneous systems. It must be remembered that the literature recommends[43] inlet probe sizes at least ten times bigger than the maximum particle or droplet size and never less than 6 mm. Also, the slow and discontinuous pumping system in the Mark IV prototype can easily allow the separation of the phases inside the sampling device if the sample is not instantly dissolved in the diluent.

It is therefore clear that, if the probe is to be used in heterogeneous processes, some changes in the original design have to be made in order to achieve an acceptable performance. Furthermore, if the probe is to be tested with no changes in heterogeneous systems, some modifications in the control unit would need to be made. The reason for this is that in the current design the mixing is mainly performed by diffusion as the sample plus diluent circulates inside of the sampling line. The so called mixing chamber is also used to enhance the mixing process. Such a design would allow a heterogeneous mixture to separate out, leading to non-representative sampling.

Finally, tests with heterogeneous systems can only be performed in the sampling system without modifications if the following two conditions are fulfilled:

- The experiments use a test solution and a solvent such that, after mixing the sample (collected from a heterogeneous mixture) with the diluent, the mixture becomes homogeneous almost instantly.
- The experiments use the sampling probe but deliver the sample somewhere else for collection and analysis, avoiding the use of the mixing chamber in the control unit.

In both cases the purpose of the research would be to assess the performance of the probe only (but not the whole of the sampling system!) for use with heterogeneous mixtures. Unfortunately, due to the lack of time, it was impossible to perform further experiments with the Mark IV prototype and systems that verified the conditions mentioned above.

5. References

1. H. Vanderburg, 1999, *On-line liquid chromatography*, CPACT IMB internal report (Ref:99/P7/1), Centre for Process Analytics and Control Technology, CPACT/University of Strathclyde, Glasgow, UK.
2. CPACT Centre for Process Analytics and Control Technology, 1999. Internet web page, http://www.cpact.com
3. H. Vanderburg, 1999, *Personal communications*, (*discussions on sampling for on-line liquid chromatography*), Centre for Process Analytics and Control Technology, CPACT/University of Strathclyde, Glasgow, UK.
4. D. Littlejohn, 1999, *Personal communications*, (*evaluation of the Mark prototypes for on-line liquid chromatography*), Department of Pure and Applied Chemistry, University of Strathclyde, Glasgow, UK.
5. N. C. Vandemerbel, L. M. Kool, H. Lingeman, U. A. Th. Brinkman, A. Kolhorn and L. C. Derijke, 1992, *On-line monitoring of fermentation processes by ultrafiltration and column liquid chromatography*, Chromatographia, 33, 525-532.
6. N. C. Vandemerbel, H. Lingeman, U. A. Th. Brinkman, A. Kolhorn and L. C. Derijke, 1993, *Automated monitoring of biotechnological processes using on-line ultrafiltration and column liquid-chromatography*, Analytica Chimica Acta, 279, 39-50.
7. R. A. Mowery Jr., 1981, *Online process liquid chromatography*, Chemical Engineering, 18, 145-152.
8. C. L. Guillemin, 1990, *Problems and proposed solutions for on-line process liquid chromatography: The software driven chromatograph*, Process Control and Quality, 1, 23-39.
9. Dionex Corporation, Internet web page 2001, *Catalogue of products*, http://www.dionex.com/app/tree.taf?asset_id=7287
10. T. G. Layne, 1984, *Process liquid chromatography: Proving its worth*, InTech, 9, 91-92.
11. T. E. Miller Jr., 1981, *Process liquid chromatography: Next step in on-stream analysis*, InTech, 9, 77-79.
12. M. Carlsen, C. Johansen, R. W. Min, J. Nielsen, H. Meier and F. Lantreibecq, 1993, *Online monitoring of penicillin-V during penicillin fermentations: a*

comparison of two different methods based on flow-injection analysis, Analytica Chimica Acta, 279, 51-58.

13. C. L. Guillemin, 1988, *New concept in chromatographic instrumentation – The probe-process liquid chromatograph*, Journal of Chromatography, 441, 1-12.
14. C. L. Guillemin, 1990, Progress and prospects in on-line process gas and liquid chromatograph, Analytica Chimica Acta, 238, 17-33.
15. N. C. Van de Merbel, H. Lingeman and U. A. Th. Brinkman, 1996, *Sampling and analytical strategies in on-line bioprocess monitoring and control*, Journal of Chromatography A, 725, 13-27.
16. X. Monseur and J. C. Motte, 1988, *On-line monitoring during fermentation of whey based on ultrafiltration and liquid chromatography*, Analytica Chimica Acta, 204, 127-134.
17. R. E. Synovec, 2001, *Process gas chromatography with chemometrics*, Oral presentation at the fifteenth international forum of process analytical chemistry IFPAC-2001, Amelia Island, Florida, USA.
18. H. Small and B. Bowman, 1998, *Ion chromatography: A historical perspective*, http://www.iscpubs.com/pubs/al/articles/a9810/a9810hsm.pdf
19. LGC Investigative Analysis Group, 2002, *Advances in analytical technology resources*, http://www.anamap.co.uk/pdf/te_tech.pdf
20. E. M. Hodge, 2000, *On-line process monitoring in a liquid waste treatment facility using ion chromatography*, http://www.wmsym.org/wm2000/pdf/21/21-13.pdf
21. R. Stevenson, 1997, *American environmental laboratory*, http://www.iscpubs.com/pubs/ael/articles/e9709/e9709st2.pdf
22. École Polytechniqu Fédérale de Lausanne, Internet Web Page 2001, *Lecture notes on sample preparation*, http://dcwww.epfl.ch/icp/ICP-3/ICP3-Lecture_notes/Separation_Methods/Dionex_2.pdf
23. T. M. Larson, 2001, *On-line HPLC monitoring and control of metabolism in mammalian cell cultures*, Oral presentation at the fifteenth international forum of process analytical chemistry IFPAC-2001, Amelia Island, Florida, USA.
24. D. Guang, D. E. Wiley, M. Hlavacek and A. G. Fane, 1996, *On-line automatic sampling for real time monitoring of wastewaters*, Water Research, 30, 2651-

2654.

25. M. Doyle, 2001, *On-line analysis of copper plating baths used in the semiconductor industry*, Oral presentation at the fifteenth international forum of process analytical chemistry IFPAC-2001, Amelia Island, Florida, USA.
26. C. Cicchetti, D. Song, D. Nadkarni and V. Sekhar, 2001, *Monitoring of chemical reaction completion by on-line HPLC in drug substance manufacturing*, Oral presentation at the fifteenth international forum of process analytical chemistry IFPAC-2001, Amelia Island, Florida, USA.
27. K. Schugerl and G. Seidel, 1998, *Monitoring of the concentration of β-lactam antibiotics and their precursors in complex cultivation media by high-performance liquid chromatography*, Journal of Chromatography A, 812, 179-189.
28. D. Picque and G. Corrieu, 1992, *Performances of aseptic sampling devices for on-line monitoring of fermentation processes*, Biotechnology and Bioengineering, 40, 919-924.
29. Process technology department, 1994, *High resolution on-line analysis in process development: interim report*, Internal progress reports derived from the No. E14384B design report, Zeneca, Huddersfield, UK.
30. K. Meney, 1998, *Progress report on the evaluation of Mk I and Mk II sample probes*, Internal report, Zeneca, Huddersfield, UK.
31. R. Waddell, 1999, *Evaluation of Mark I probe*, Internal report summer project, Department of Pure and Applied Chemistry, University of Strathclyde, Glasgow, UK.
32. F. Schnitzlein and A. A. Grant, 1999, *Design assessment and improvement of a pneumatic sampling probe*, Project for exchange students, Department of Mechanical Engineering, University of Strathclyde, Glasgow, UK.
33. N. Peters, 2000, *Evaluation of Mark I and Mark IV sampling probes*, Internal report summer project, Department of Pure and Applied Chemistry, University of Strathclyde, Glasgow, UK.
34. Mitsubishi electric corporation, 1993, *FX-10DU-E operation manual*, Himeji, Japan.
35. Process technology department, 1996, *Mk II automatic process sample extraction*

probe description of construction and operation, Internal report, Zeneca, Huddersfield, UK.

36. K. Meney, 2000, *Personal communications*, (*evaluation of the Mark prototypes for on-line liquid chromatography*), Avecia, Grangemouth, UK.
37. N. Holmes, 2000, *Personal communications*, (*evaluation of the Mark prototypes for on-line liquid chromatography*), BP Chemicals, Grangemouth, UK.
38. B. Grieve, 2001, *Personal communications*, (*evaluation of the Mark prototypes for on-line liquid chromatography*), Syngenta, Grangemouth, UK.
39. Mitsubishi electric corporation, 1992, *FX-10P-E operation manual*, Himeji, Japan.
40. Mitsubishi electric corporation, 1999, *Programming manual: the FX series of programmable controller*, Himeji, Japan.
41. A. A. Grant, 2001, *Personal communications*, (*evaluation of the Mark prototypes for on-line liquid chromatography*), Department of Mechanical Engineering, University of Strathclyde, Glasgow, UK.
42. A. Kennedy, 2001, *Personal communications*, (*evaluation of the Mark prototypes for on-line liquid chromatography*), Department of Pure and Applied Chemistry, University of Strathclyde, Glasgow, UK.
43. Institute of Petroleum, 1987, *Petroleum Measurement Manual: Part VI. Section 2: Guide to Automatic Sampling of Liquids from Pipelines,* Chichester, New York, USA.

CHAPTER 5

DEVELOPMENT OF IRIDIUM OXIDE ELECTRODES FOR PROCESS pH MEASUREMENT

1. Solid State Sensors: an Alternative to Glass Electrodes for pH Monitoring in Industrial Processes

The glass electrode is the sensor of choice for measurement of pH in industrial process control applications. Its popularity can be attributed to its simplicity, relatively rapid and stable Nernstian response to pH and insensibility to redox interferences. On the other hand, glass electrodes also present several sources of error and disadvantages such as acid and alkaline error, sensitivity to monovalent cations, high impedance, mechanical fragility and instability at high temperatures[1,2]. Although there have been some modifications proposed to overcome these disadvantages, fragility is still a major drawback of these sensors for pH sensing in harsh environments. As shown in Chapter 1, the current interest in alternative ways of pH sensing within this project came about due to the fact that a combination pH glass electrode failed to monitor the concentration of protons during the esterification of crotonic acid.

Metal-metal oxide electrodes have been proposed as the most promising candidates for monitoring of pH under harsh conditions, being defined as "the sensors of the future"[3]. The first metal-metal oxide developed and the most commonly used was the antimony electrode[3-6]. However, the response of this electrode was not very linear, reproducible or stable[3] and interference by oxygen has also been reported[4,5]. Numerous other metal-metal oxide systems have been studied[7-10] but only some gave an acceptable response. Among these, iridium-iridium oxide electrodes have proved to be the metal oxide system that gives the most stable response, with low redox interference and small drifts[11-13]. Its good chemical stability in aqueous solutions[11,12], fast response, low impedance[12,14], insensitivity to stirring[11,15] and low sensitivity to irreversible redox interferences[11] make this electrode the best alternative to glass electrodes for pH sensing at high temperatures[1,2]. Besides, iridium has been reported as one of the most corrosion resistant metal known[4].

There are three main ways of preparing iridium oxide electrodes[16]: anodic electrodeposition, plasma reactive sputtering and thermal oxidation. The first method produces so called anodic iridium oxide films (AIROF) that are highly hydrated with poor film adhesion and with a response very much dependent upon the pH of the

solution used during the preparation of the electrode[4,17]. Their response also depends upon the anions used in the process of formation[1,6,17,18]. Reactive sputtered oxides are more complicated to prepare[16], although their response is more stable than that of the AIROFs[19-21]. On the other hand, thermally grown oxide electrodes are easy to prepare and regenerate[14]. This method produces a unhydrated oxide with microcracks[13,22-25] more stable than that of the AIROFs[16,21,23,26,27,28] and are more promising for pH monitoring[17]. AIROF electrodes normally show a super-Nernstian response whereas thermally grown and sputtered generally show a near to Nernstian response[26]. Therefore, thermally grown iridium oxide electrodes will be the focus of interest in the study carried out in this thesis.

This chapter deals with the studies carried out with thermally grown iridium oxide electrodes as part of this PhD thesis. The research aimed at the development of the sensors for industrial applications, with an analysis of their advantages and disadvantages with respect to the glass electrode. The potential use of thermally grown iridium oxide sensors at high temperatures and in non-aqueous solvents possessed a special interest. The chapter begins with an introduction where the chemistry of the sensors is described together with the applications, advantages and disadvantages of the iridium oxide electrodes that have been found in the literature. Brief remarks about the need of robust reference systems and the measurement of acidity in non-aqueous environments are also introduced in those aspects that are relevant for the project. After the introduction, the experimental systems used in the practical work are described as well as the technology involved in the production of the sensors. Further to this, the experimental and results part is presented, starting with simple aqueous systems and moving gradually to more complicated non-aqueous environment. The tests here described were mainly focussed in the calibration of the response to changes in acidity, analysis of the response time and stability of the sensors. Finally, a new design of a total iridium oxide probe is presented and studied at the end of the chapter.

1.1. Chemistry of thermally grown iridium oxide sensors

Pourbaix gives three possible equilibria involving iridium oxide and protons[29]:

(a) $Ir_2O_3 + 6\,H^+ + 6\,e^- \leftrightarrow 2\,Ir + 3\,H_2O$ Eq. 5.1

(b) $IrO_2 + 4\,H^+ + 4\,e^- \leftrightarrow Ir + 2\,H_2O$ Eq. 5.2

(c) $IrO_2 + 2\,H^+ + 2\,e^- \leftrightarrow Ir_2O_3 + H_2O$ Eq. 5.3

Each of these three reactions give a Nernstian slope of 59 mV/pH at room temperature. However, considering the features of the thermally grown IrO_2 films in a thick overlayer[24], it was suggested that no underlying metal takes place in the process and therefore, the third reaction is considered as the predominant process[14,30-32]. The dependence of the equilibrium potential on the activities of the various species in the process can be presented as[14,30]:

$$E = E^o + \frac{2.303RT}{2F}\log_{10}\frac{[IrO_2]^2}{[Ir_2O_3]} - 0.0591pH = E^{o'} - 0.0591pH \qquad \text{Eq. 5.4}$$

Numerous studies[4,7,10-12,14-16,31-33] on iridium oxide electrodes have been performed to obtain results that fit this model. However, little deviations have been observed in both the slope and the offset ($E^{o'}$), that make necessary a frequent calibration of these sensors. The changes in the offset are explained from the fact that $E^{o'}$ for thermally grown iridium oxide depends upon the relative mole fractions of Ir(IV) and Ir(III) oxides. This was not only found with AIROFs[30] but also with other electrochromic oxides such as hydrogen tungsten bronzes[34]. Because in the production of thermally grown iridium oxide electrodes there is not a careful control over the degree of oxidation, there exists an adjustment in solution of the ratio of the two oxides to achieve an equilibrium value, as IrO_2 is the only iridium oxide stable at room temperature[35]. This is the reason why the changes in the offset decrease with time of immersion of the electrodes in solution[30]. This is also why it is convenient to keep the electrodes immersed in distilled water when not in use, although good response of the electrodes kept in dry conditions has also been reported[36]. Carbon contamination of the oxide is pointed out by some authors as one cause of drift in these sensors[1,12].

Any deviations in the Nernstian slope are more likely to happen in hydrated oxides where amphoteric sites are formed due to hydroxylation of the oxide[16]. The take-up or release of protons by these amphoteric sites consume or produce H^+ that affect the true reading of the pH. Several authors have proposed different ways to overcome the problem of the shift of the response of iridium oxide sensors. Some researchers[32] tried to attenuate any possible redox interference responsible for the drift by coating the sensor with a permselective membrane. The downside of this method for pH monitoring with applications to process control is that this membrane increases the response time of the sensors. Some other authors used a field effect transistor to measure the difference of potential between the AIROF electrodes and the solution[4]. Finally, Hitchman *et al.* worked intensively with thermally grown iridium oxide electrodes. They proposed[30] a field induced poising technique by which they reached the equilibrium relative mole fraction of Ir(IV) and Ir(III) oxides in the sensors by using a charge injection/ejection procedure.

1.2. Pros and cons in the use of thermally grown iridium oxide sensors

As mentioned earlier, iridium oxide is the most promising candidate as a pH sensor in harsh environments. The following nine points outline the main reasons that support this statement:

1. Iridium oxide has good chemical resistance and stability over a wide range of pH and temperature in aqueous solutions[37].
2. Iridium oxide exhibits low impedance and therefore high sensitivity of response to changes in pH in environments with low conductivity[12,14,15,36].
3. There are many methods available for preparing iridium oxide[16].
4. Thermally oxidised electrodes are easy to prepare and regenerate[14,38].
5. The electrodes are small, flexible and cheap[36].
6. Iridium oxide electrodes do not present sensitivity to monovalent cations, or acidic and alkaline error (unlike glass electrodes)[1].
7. Iridium oxide electrodes present a fast response comparable, if not faster, than the response for glass electrodes[11].
8. Iridium oxide electrodes are reported to be insensitive to stirring[11,15].
9. Although iridium oxide electrodes are affected by some redox couples they

present low sensitivity to very common redox interferences caused by O_2, CO_2 or phosphates in solution[15,17,36].

The major disadvantages of these systems are that they present drifts in the response and their response can also be affected by some redox couples[1,19,39]. The problem of drift was covered before where several strategies to solve this problem were described. The problem of the redox interference is obvious since the chemistry of these sensors is based on an electrochemical process. Therefore, some redox couple present in the solution can affect the response of these sensors. Several examples of redox interferences have been reported with I^- and the $Fe(CN)^{-3/-4}$ system[1]. Bisulphites and thiosulphates have also been shown to affect the response of the iridium oxide sensors[40]. It has also been proven that this effect does not kill the electrodes as they still keep a good Nernstian response to pH when used in other systems after being affected by redox interference[1]. However, as mentioned above, the most common redox couples present in almost any system (i.e. O_2 and CO_2) do not affect the response of these electrodes[15,17,36].

As mentioned earlier, the best solution reported to overcome this problem of redox interference is the use of a permselective membrane to cover the electrode[32,41]. The membrane is permselective to cations and therefore transport H^+ with no problems. It attenuates instead the effects of oxidising or reducing redox species that interfere with the response of an uncoated electrode. As previously mentioned, this method is also used to reduce the changes in the drift typical of these electrodes and its downside is that the response time is considerably increased.

1.3. Applications of iridium oxide electrodes

There exists a broad list of publications on the use of AIROF and thermal iridium oxide films (TIROF) in animal studies and in vivo applications[42]. The vast majority are biological applications such as pH measurements in biofilms[4], animal tissues[11,43,44], proteins[15] and in vivo measurements of gastric pH[36] and acidity of other human body fluids[45]. Iridium oxide sensors have also been used for CO_2 in medical applications[46]. However, no industrial scale uses for pH monitoring have been found to the best of the author's knowledge. The only application in quality control is pH monitoring of engine oil at high temperatures[47]. Therefore, the study of the

performance of the thermally grown electrodes in pH monitoring and control of pilot scale industrial processes will be the main aim in this project.

Most of the process used in this project are carried out in non-aqueous environments and, as mentioned above, not many studies of the response of iridium oxide electrodes have taken place in these type of systems. Therefore, in this research not only is there the challenge of testing these sensors for industrial monitoring and control purposes, but there is also the novelty of the study of the response of these electrodes in systems that have not been studied before.

1.4. Reference electrodes

Metal-metal oxide sensors require a reference electrode, which may be immersed directly in the test solution to form a cell without transfer, or in a separate reference solution connected to the test solution by a liquid junction, in which case it forms a cell with transfer. In both of the cases, the most frequently used reference electrode is the silver-silver chloride electrode although other types can be used in some occasions. Mercury-based electrodes require more care than the silver-silver chloride type and would not normally be favoured. It should also be recognised that, in the event of an accident, mercury-based electrodes create toxic hazards that could spread very quickly, especially at high temperatures[5]. However, Ag/AgCl reference electrodes specially adapted for high temperature conditions are commercially available[48]. The problems of Ag/AgCl reference electrode are that KCl in the electrolyte has a tendency to crystallize and reduce the potential at the junction altering the pH reading. Also, silver from the silver-silver chloride internal element gets into the KCl fill solution, reacts with sulphides and halides and clogs the junction[3].

The problem of the cells without transfer (apart from the error in measurement of pH due to the diffusion potential) is that there is a closer contact between the reference electrolyte and the solution. Therefore, the reference electrode is open to any interference coming from the presence of certain ions (e.g. Cl^-) in the test solution[5,49]. Because of these difficulties, cells without transfer are only applicable to specific and well-defined applications.

The cells with transfer used in pH measurements at high temperature can be divided into isothermal types, in which the sensing and reference electrode are at the same temperature, and thermal types, in which the reference electrode is maintained at or near room temperature[5]. Thermal cells are used to prevent the degradation of the reference electrode by hydrolysis or dissolution. The downside is that special equipment for cooling and equalizing the pressures on either side of the junction are needed. The liquid-junction potential also becomes more susceptible to errors related to differences in mobility on the two sides of the junction. This is due to the mass transfer from the reference electrode (usually with a higher static pressure) and because of the thermal liquid-junction potential in the reference electrode that is produced by the different tendencies of ions to move across a temperature gradient. Most of these sources of errors are avoided using isothermal cells (i.e. reference electrode kept at the temperature of the solution), provided the reference electrode withstands the high-temperature conditions of the test solution.

Sometimes, the problems of diffusion potential and stability of the electrolyte at high temperatures can be solved by using solid-state reference electrodes. In most of these systems, the internal silver-silver chloride element resides in wooden dowels or pieces of Teflon saturated with KCl. The main problem of this type of electrodes for on-line pH monitoring is their low response and need of frequent and accurate calibration[3]. Other common solid reference system such as Pt, Au or Mo wires are not valid as reference electrodes as their response is highly sensitive to the pH of the test solution[50].

1.5. Non-aqueous systems

The measurement of pH in non-aqueous solutions depends upon the definition of activity in non-aqueous solvents. This definition is normally referred to as the value of the activity of a particular substance in aqueous solution plus an activity change, which is associated with the change of medium from water to solvent[51]. Therefore, the pH values depend very much upon the solvent present in solution. In non-aqueous solutions, the solvent can be an acid, base, alcohol or hydrocarbon instead of water[3]. An acid solvent acts as a proton donor and the pH is shifted down with pH values lower than zero. A base solvent acts as a proton acceptor so the proton activity is

decreased and the scale is shifted up with pH values greater than 14. An alcoholic solvent acts as both a proton donor and acceptor like water, so that changes in proton activity are moderated. The pH scale occupies about the same region as water but may extend slightly further upscale and downscale. A hydrogen-containing solvent acts as neither a proton donor nor acceptor so that the solvent is passive to changes in proton activity. Consequently, in this type of solvents the pH scale upper and lower limits are usually much further apart than for water.

Liquid ammonia is the best investigated non-aqueous solvent. In this environment measurements of pH are carried out normally with common reference electrodes where ammonia is used as a reference electrolyte. Low-water electrolytes can also be used in these measurements[51]. For the measurement of pH in organic solvents, the correct procedure would be to set up a pH scale with primary pH standards for each solvent[3,51]. This is necessary due to the uncertainty in the determination of pH originating from the different diffusion potentials in different solvents and the phase boundary potential in the interphase aqueous-nonaqueous solution when using aqueous reference electrolytes[51]. Alcohols and alcohol-water mixtures have been the most extensively studied non-aqueous systems[50,51]. They also happen to be the simplest systems, as alcohols act as both a proton donor and acceptor similarly to water. They are also miscible with water with small values of phase boundary potentials. However, phase boundary potentials between water and a water-immiscible solvent are likely to be appreciably greater. In fact, large non-reproducible potentials have been observed at the reference electrode if the aqueous reference electrode comes into direct contact with a medium that is immiscible with water[51]. Therefore, for the purpose of pH measurements in non-aqueous solvents it is best to avoid phase boundaries between two immiscible solutions by incorporation of a bridge, whose electrolyte is miscible with both the reference electrolyte and the sample[3,51]. This is the reason why LiCl in methanol or ethanol is commonly used instead of the aqueous electrolyte in the reference electrode or the salt bridge for pH determinations in non-aqueous systems[51,52].

Normal calomel or Ag/AgCl reference electrodes with a salt bridge with a suitable solvent depending on the system being considered, are the most frequently used reference electrodes in electrochemical experiments with non-aqueous

solutions[50]. It is therefore recommended to change periodically both the aqueous electrolyte in the electrode and the solvent in the salt bridge to avoid contamination due to transfer from one solvent to the other.

Although the glass electrode has shown a Nernstian response in some non-aqueous systems, its response is very slow (with response times of around 1 hour) due to the formation of a hygroscopic gel layer at the glass surface[36]. Metal oxide sensors are a good alternative to the use of glass electrodes in non-aqueous systems. Not many studies have been found in the literature on the application of metal-metal oxide electrodes for pH measurement in non-aqueous environments. Bordi *et al.* studied the response of thermally grown iridium oxide electrodes in hydroorganic mixtures[53]. They found a good Nernstian response at 20, 0, and –20 C°, although response times and values of impedance were considerably larger than those detected using aqueous mixtures. Some other studies have also been carried out with pure organic mixtures obtaining a good Nernstian response. In fact, Izutsu *et al.* studied the response of commercial IrO_2 electrodes in different solvents and with different concentrations of picric acid[54]. Nernstian response was always obtained with much faster response than that of the standard glass electrodes.

2. Experimental Systems for the Study of Iridium Oxide pH Sensors

As has been explained before, there are three ways of preparing iridium oxide electrodes: anodic electrodeposition, plasma reactive sputtering and thermal oxidation. This latter method was the one of choice for the production of solid state sensors in this project. The reasons for this were its capacity of regeneration, simplicity of fabrication and good response. Furthermore, previous work with these sensors at Strathclyde University provided a valuable experience for the project. In this section, the procedure used in the thermal oxidation of iridium metal to obtain the oxide coating is explained. The different designs of probes for the use in industrial pH monitoring are also discussed. Finally, the different ways to monitor the signals coming from the sensors are described in the last part of the section.

2.1. Production of the sensors

The starting point in this project was the study of the response obtained from old iridium oxide sensors used in previous research at Strathclyde. Several

electrodes were recovered from the studies carried out by Hitchman *et al.*[14] at the beginning of the nineties. The aim of these preliminary tests was to prove the long term stability of these sensors and encourage the work in this field in order to develop solid-state pH sensors for industrial monitoring. As the old electrodes were of uncertain age, and the exact parameters of construction and store conditions were not fully defined, a detailed analysis of the sensors was not possible. However, these electrodes were a reference point in the attempt of producing new electrodes with the same characteristics to be used in the project.

The old sensors were made from iridium wires of length 1 cm, diameter 0.5 mm and purity 99.9%. The electroactive coating was reported to be formed by soaking the wire in 2 M sodium hydroxide and then heating the wetted wire at 800°C in a furnace for 30 min. Hitchman *et al.* repeated this process three times in order to obtain a uniform coating[14]. At the end of this process, the electrodes were then cooled in air and immersed in distilled water for two days to ensure that the iridate coating formed during the thermal treatment was converted to iridium oxide. However, it should be highlighted that the old electrodes that Hitchman *et al.* produced were kept in a dry box for years before they were immersed again in distilled water and tested on the preliminary experiments mentioned above. The next section describes the key conclusions extracted from the production of new sensors following this method.

2.1.1. Importance of the temperature in the production of the sensors

Initially, the first electrodes were produced using exactly the same method as reported by Hitchman *et al.*[14] However, as they were to be tested in hot toluene and other non-aqueous solution, glass was preferred to plastic as the support for the pH probe. This way of growing the oxide layer seemed to be the easiest method of preparation and have been followed by other researchers[15,36], although other methods to thermally fabricate sensors have also been described in literature[13,17,22,23,35,53]. In most of them a piece of Ti was used as a support, impregnated in a paste obtained by dissolving $IrCl_3$ in water (although isopropanol can also be used as a solvent)[22]. The thermal oxidation was achieved by keeping the impregnated piece of Ti in a furnace at a constant temperature normally within the range of 400-450°C.

In the first batch of sensors, the oxidised iridium wires were between 8 and 10 mm long and 99.9% pure (Goodfellow IR005150/2). These small electrodes were brazed to copper wire and covered in glass half of the size of the electrode. Due to the small size of the electrodes and the relatively high temperature used during the glass sealing process, part of the iridium oxide coating was likely to have been damaged. In fact, different colour spots were clearly observed on the electrodes, close to the glass sealing point showing damage in the coating. These parts with different oxidised state for iridium species have been shown to affect the overall response for the electrodes causing drifts in the measured potential[16].

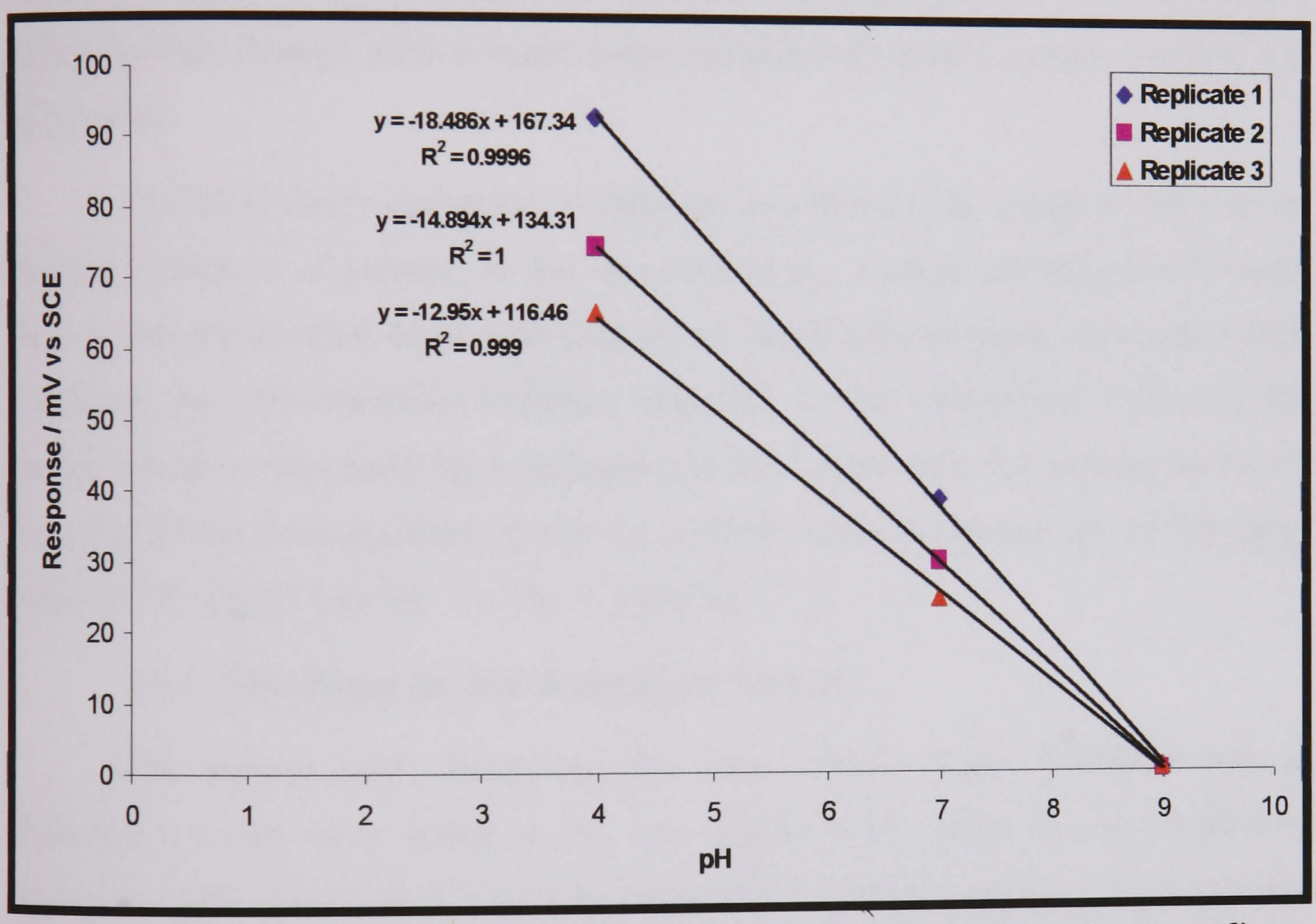

Figure 5.1. Change in the response with pH obtained in three replicate measurements with one of the sensors produced in the second batch of electrodes

In a second batch of electrodes, the stage of covering the electrodes in glass was carried out prior to the oxidation step. This was necessary as the flame used during the sealing affected the oxide layer produced during the thermal oxidation[15,23]. Quartz was used instead of standard Pyrex glass due to the high temperatures used during the thermal oxidation process[55]. The oxide coating was formed by heating the wire (sealed in quartz), which had previously been soaked in 2 M NaOH, at 800°C

in a furnace for 30 minutes. This process was repeated three times in order to obtain a uniform blue-black oxide layer as Hitchman *et al.* reported[14]. After this process, the electrodes were kept in distilled water for at least two days. When not in use the electrodes were always kept in distilled water. In the experiments performed with this second batch of sensors, a linear change in the response with pH was observed in all of the cases. However, the signals were neither Nernstian, nor reproducible, as is shown in *Figure 5.1*. The explanation for this was not clear at the time. However, it was suspected that the lack of a good temperature control in the oven where the oxidation took place would have produced faulty electrodes. The fact that a good Nernstian response was observed on a third batch of electrodes that were constructed using another furnace with a much better temperature control system verified this hypothesis. .

Therefore, the temperature of oxidation was found to be a crucial factor in the thermal oxidation of iridium. In the case of iridium, a value less than 800°C could have produced an oxide layer with iridium not completely oxidised. This could have produced the non-Nernstian response observed in the experiment. However, the Redox reactions that could have undergone in the system were not clear as the theory says that all the three equilibria involving iridium oxides in solution give a Nernstian slope of 59 mV/pH (see Eq. 5.1, Eq. 5.2 and Eq. 5.3).

2.1.2. New design for use in chemical reactors

The iridium oxide electrodes that were initially made of iridium wire of diameter 0.5 mm were found to be very fragile under rapid stirring conditions. Therefore, after some initial tests were performed with these sensors, new electrodes were produced using iridium rod with a diameter of 2 mm (Goodfellow IR005150/5). This change in diameter made the electrodes more robust for use in the 5-L reactor systems where the stirring conditions were relatively severe.

The oxide coating was formed following exactly the same procedure as for the thinner electrodes. *Figure 5.2* shows how with this design the iridium rod was easily removable for regeneration of the coating. Therefore, only the iridium rod was introduced into the furnace for the thermal oxidation as no sealing in glass or quartz was needed in this design. In this probe, a screw-on a PTFE fitting compressed

another PTFE holder that sealed the thermally oxidised iridium rod and avoided any liquid entering the probe and touching the electrical contacts. The use of PTFE components is becoming very common in pH probe design to avoid corrosion problems[56]. A simple stainless steel screw welded to a piece of 0.56 OD Nickel-Chrome wire (BDH 277/0030/03) served as the electrical contact between the iridium wire and the cable[57]. The thermally oxidised coating in one of the ends of the wire was removed using sand paper to improve the quality of the electrical contact. Finally, the PTFE fittings were enclosed into a 360 mm long glass tube with an inside diameter of 10 mm.

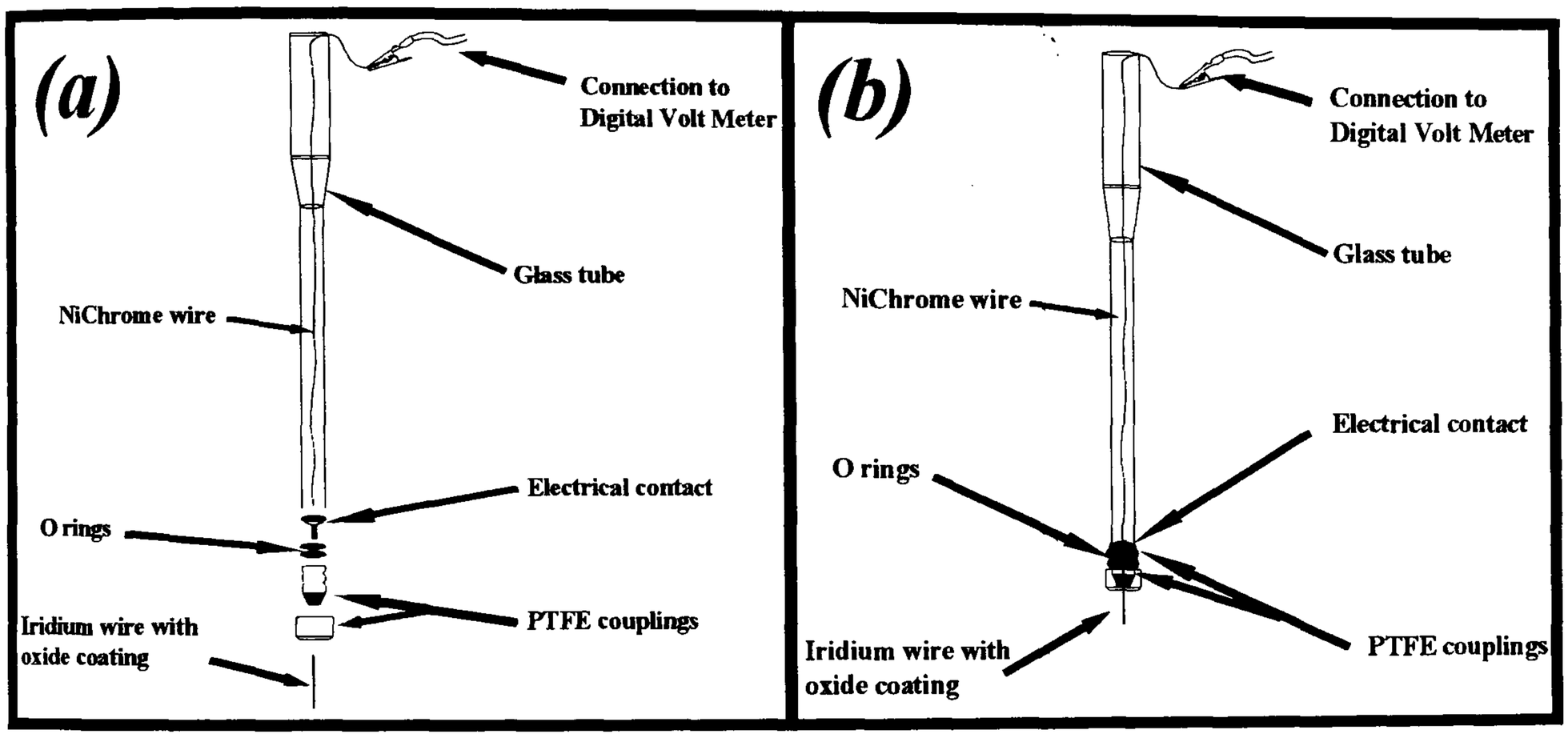

Figure 5.2. Sketch of the components of the new design for a (a) non-assembled and (b) assembled iridium oxide pH probe

2.2. Monitoring systems and problems with noise

Initially, the acquisition software Labview from National Instruments was used to measure the signals from the solid-state sensors and glass electrodes used in the project. M. Weerasinghe, a control engineer working for CPACT, developed the Labview screen in which the response could be monitored in time[58]. Other authors had previously used Labview in the production and monitoring of the response with AIROF sensors[27,44]. After some capacitors (0.1 μF RS 264-5015) were used in the connections to the signal conditioning box[58], a noise of ±5 mV was observed in most of the experiments. This level of noise was accepted in the experiments with aqueous systems, although it meant a maximum error of ±0.1 pH units in the acidity measurements. When the experiments with low conductivity non-aqueous systems

were initiated, the level of noise got too high, specially considering the small changes in potential observed with the change in acidity. This noise, according to the Johnson equation[51], depends upon the temperature and the resistance of the system:

$$U_R = (4kT)^{1/2}(R_m B_b)^{1/2} \qquad \text{Eq. 5.5}$$

where:

U_R = *Level of noise (V)*
k = *Boltzman constant (1.381×10^{-23} J K^{-1})*
T = *Temperature (K)*
R_m = *Membrane resistance (Ω)*
B_b = *Band width of the transmitted signal (Hz)*

Both the use of low conductivity solvents and high resistance glass pH membranes increased the level of noise observed in the measurements. In some cases, no signal was observed from the glass electrode, which had a characteristic impedance of about 10^8 ohms[59]. Due to the high impedance typical of glass electrodes, the amplifier which detects the potential between the glass electrode and the reference system must have an impedance of at least 10^{-11} ohms because all current drawn must pass through the glass bulb[51,59]. This impedance must be even lower when low conductivity solvents are used. Therefore, the low power output of the glass pH sensor and use of non-aqueous solvents impose severe design and installation restrictions where high impedance circuitry must be compact and well shielded to avoid interference from electrical noise. Also, the system must be well insulated to avoid losing the signal by leakage to ground[59,60]. Although different types of cabling were tested in the non-aqueous experiments, the intensity to noise ratio could not be improved by the use of low-noise shielded cable (RS 367-280) with the Labview system. Therefore, a Solomat 520C system was used to monitor the signals coming from the electrodes for non-aqueous systems. The Solomat system is a portable device provided with the special filtering circuitry and amplifiers needed for the measurement of signals from high impedance electrodes[61]. It was observed that the noise detected with the Solomat system in aqueous system was reduced to ±0.1mV (i.e. ±0.002 units of pH) with iridium oxide sensors and ±1mV (i.e. ±0.02 units of pH) with glass electrodes.

3. Testing and Development of Iridium Oxide Solid State pH Sensors

It has been already mentioned in Chapter 1 why the interest in solid-state pH sensors started in this project. A pH glass electrode failed to monitor the acidity during the esterification of crotonic acid. In *Figure 1.4* it has been shown how the pH probe failed after holding at a high temperature of 105°C in the process for more than 155 minutes. Initially, this failure was believed to be due to the high temperatures used in the process. Therefore, the ultimate aim in the work with the iridium sensors was the development of pH sensors for high temperature conditions. As will be seen later, the pH experiments in this project discovered that the failure of the pH probe was more related with the damage of the reference system in the electrode due to the presence of toluene in the system. The effect of the high temperature did also contribute to a more likely failure of the pH glass electrode. Thus, as the project progressed, the aim of the project become the development of pH iridium oxide sensors capable to overcome these problems observed for combination glass electrodes in non-aqueous systems and at high temperatures.

Initially and after some preliminary tests were carried out, the thermal oxidation method reported by Hitchman *et al.*[14] was repeated to produce iridium oxide sensors. After this, the electrodes were tested in water and their response was compared with that obtained using standard glass electrodes. The experiments in aqueous solutions were aimed at the development of the sensors in simple systems before moving on to more complicated non-aqueous processes where the monitoring of the acidity is less defined. Furthermore, the tests in aqueous environment also looked for advantages and disadvantages of the iridium oxide sensors with respect to the glass electrode in aqueous systems.

3.1. pH measurements in aqueous systems

Although some preliminary tests were performed in beakers without any temperature control, most of the experiments were carried out in the 1-L jacketed reactor. The monitoring of the signals was mainly done using the Solomat system and Hyperterminal software under Windows for the data acquisition, although the Labview system was also used in some initial experiments. In the preliminary tests, a combination glass electrode with a built-in reference system was used for comparison.

However, some experiments with non-aqueous systems showed that the reference part of the glass electrode was the source of its failure in organic solvents. It was observed that toluene was penetrating into the cavity where the reference electrode was immersed and getting mixed with the electrolyte there. This affected the response of the combination glass electrode producing the eventual failure of the probe. Therefore, a glass only reference electrode was used in the tests. This allowed a fair comparison between the responses for the solid-state sensors and the glass electrodes, as the two signals were measured with respect to the same reference system[62].

A double-junction saturated calomel electrode (SCE) was initially used as the reference system. However, it soon was replaced by a double-junction Ag/AgCl electrode, which is safer in experiments at high temperatures[63]. A salt bridge with 1.0 M KNO_3 as the electrolyte solution was used in most of the experiments to put the reference electrode in contact with the test solution. This attempted to avoid any problems of corrosion of the sensors and redox interference with the Cl^- ions in the electrolyte of the reference system[14]. The length of the salt bridge (30 cm) guaranteed a constant over pressure and provided a small and constant liquid junction potential[64]. Some preliminary tests were also performed changing the electrolyte solution in the salt bridge but no effect on the signals in aqueous systems was noticed after this change.

3.1.1 Change of the response with pH

For calibration and testing of the performance of the electrodes in water, the response of the sensors in three buffer solutions was monitored. The pH 4, 7 and 9 buffer solutions used (BDH 33156 and 816-004, 007 and 008 by Electronic Temperature Instruments) were prepared by adding one of the commercial buffer tablets to 100 ml of distilled water. Initially, a combination glass electrode (BDH 309/1070/12) and a pH-meter (Hanna Instruments HI 8424) were used in the experiments. This was later replaced by a glass only electrode (BDH 309-1015-02) in order to achieve a fair comparison between the iridium oxide and glass electrode responses.

Both electrodes made with thin 0.5 mm OD wire and thick 2 mm iridium rod were used in the calibration of the response in aqueous buffers. A typical calibration

plot is shown in *Figure 5.3*, where the signals obtained for the iridium oxide sensors were compared with that from the glass only electrode. In the figure it is observed that the responses were very linear in all of the cases. Although they all agreed quite well with the prediction made using the Nernst equation, the slope of the calibration lines was slightly super-Nernstian for the solid-state sensors. The response for the glass electrode provided a slope slightly smaller than expected by the Nernst equation at 20°C, the temperature at which the experiments were carried out. However, absolute values lower than the theoretical Nernstian slope are normally expected in glass

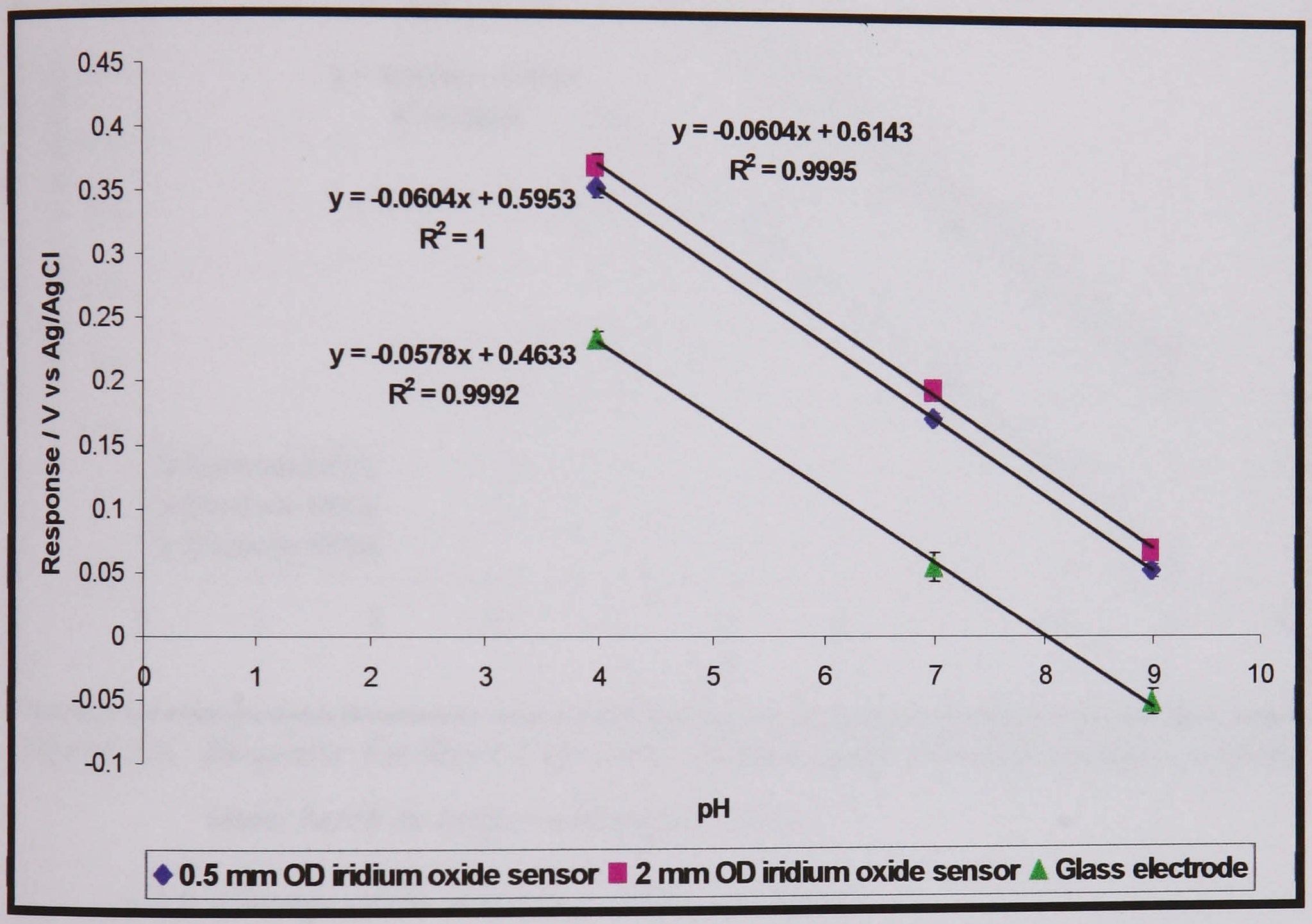

Figure 5.3. Response for two types of iridium oxide sensors and a glass electrode in buffer solutions at 20°C

electrodes[65]. Moreover, experimental determinations of the Nernstian slope in the range 96-102% of the theoretical value are accepted as good[66]. *Figure 5.4* shows how straight lines with similar slopes were also obtained in measurements with other iridium oxide electrodes produced in the same batch. However, there was always a variation in the response or difference in the $E^{o'}$ value between the electrodes that made impossible the definition of a universal calibration equation for the thermal oxidised iridium oxide electrodes. Kinlen *et al.* also encountered a significant lack of batch to batch repeatability in terms of oxide adhesion and pH response[26]. Some

producers of sensors[67] have reported a reproducibility of 1 mV within a batch although the batch to batch variance was about 100 mV. Formal potentials $E^{o'}$ ranging from 0.63 to 0.82 V vs. Ag/AgCl have been reported for thermally grown and sputtered iridium oxide sensors and from 0.7 to 1 V in AIROF sensors[26]. These values agree with the results obtained in the calibration experiments reported here.

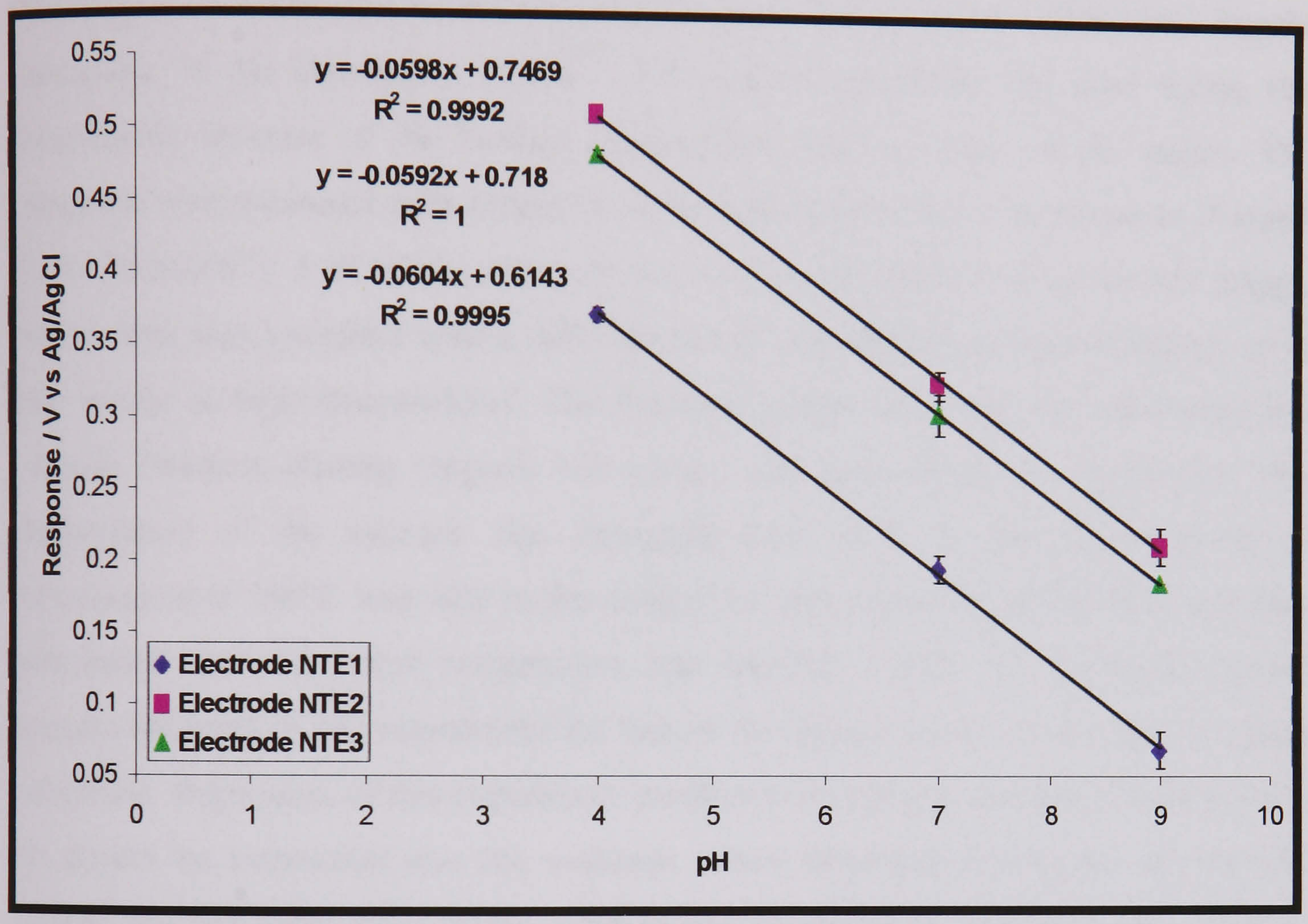

Figure 5.4. Response for three 2 mm OD iridium oxide electrodes produced in the same batch in buffer solutions at 20°C

3.1.2. Change of the response with temperature

According to the Nernst equation described in the introduction of this chapter, the response obtained in a redox process depends upon the temperature at which the process is carried out. Equation Eq. 5.6 presents this dependence for the case of the redox process involving the species IrO_2 and Ir_2O_3. Equation Eq. 5.7 introduces a similar relationship for the change of the redox potentials observed when a glass electrode is used.

$$E = E^{o} + [\frac{2.303R}{2F} \log \frac{[IrO_2]^2}{[Ir_2O_3]} - 1.98 \cdot 10^{-4}\ pH]T \qquad \text{Eq. 5.6}$$

$$E = E^{o}_{Glass} - 1.98 \cdot 10^{-4}\ T\ pH \qquad \text{Eq. 5.7}$$

A comparison experiment to analyse the temperature effect in both the iridium sensors and the glass electrode was performed. In this test, the response of the 2 mm OD sensors (more resistant to stirring) was tested in the 1-L reactor system. 1 L of pH 3 HNO_3 (Aldrich 25,811-3) solution and 1 M KNO_3 (Aldrich 22,129-5) were used in the experiment. The KNO_3 was used to increase the ionic strength of the solution and therefore avoid diffusion potential in the junctions that could have altered the signals according to the Henderson theory[51]. The reactor condenser was used during the experiment because of the boiling temperatures used in some of the stages. The response was measured with respect to a Ag/AgCl double junction electrode (Russell CRL/DJ/AG/S7). 1 M KNO_3 solution was used as the electrolyte in the salt bridge, which was also provided with a little condenser to avoid the pressure building up in the bridge at high temperatures. The Solomat system was used for monitoring the signals. Medium stirring (approx. 125 r.p.m.) was used during the experiment. The temperature of the mixture was increased from 30°C to the boiling point. A temperature of 100°C was held in the system for approximately half an hour and then decreased until the initial temperature was reached. *Figure 5.5* shows the typical results obtained in this experiment for one of the iridium oxide sensors and the glass electrode. Replicates of this experiment confirmed the reproducibility of these results. It should be mentioned that the response values observed in the plot are the real values for the solid-state sensor used in the experiments. However, the response values for the glass electrode were shifted 770 mV before plotting in order to compare more clearly in the graph the results obtained.

In *Figure 5.5* it is observed how the response for the glass electrode became unstable at high temperatures. In fact, the repetition of the experiments with this electrode produced a progressive deterioration of its response that eventually caused the breakage of the electrode. Although some glasses are specially built for high temperature applications and have been successfully used at 104°C, the usual temperature limit for the glass electrodes[64] is in the range 80 or 90°C. This damage was not observed with the iridium oxide electrodes that were more stable at high temperatures. However, it is seen how the signal from the solid-state sensors drifted significantly when the temperature was high. There was also a drift at low temperatures that was observed when the initial temperature was recovered after the

experiment. This was not observed at the beginning of the test as the sensors were stabilised in the solution for at least 12 hours before the experiment was started. These results caused a great concern in the project about the stability in the response obtained from the iridium oxide sensors, which drifted more than expected and with variations that depended on the temperature. More about the analysis of the stability in the response of these sensors is discussed later on this chapter (section *3.1.5*).

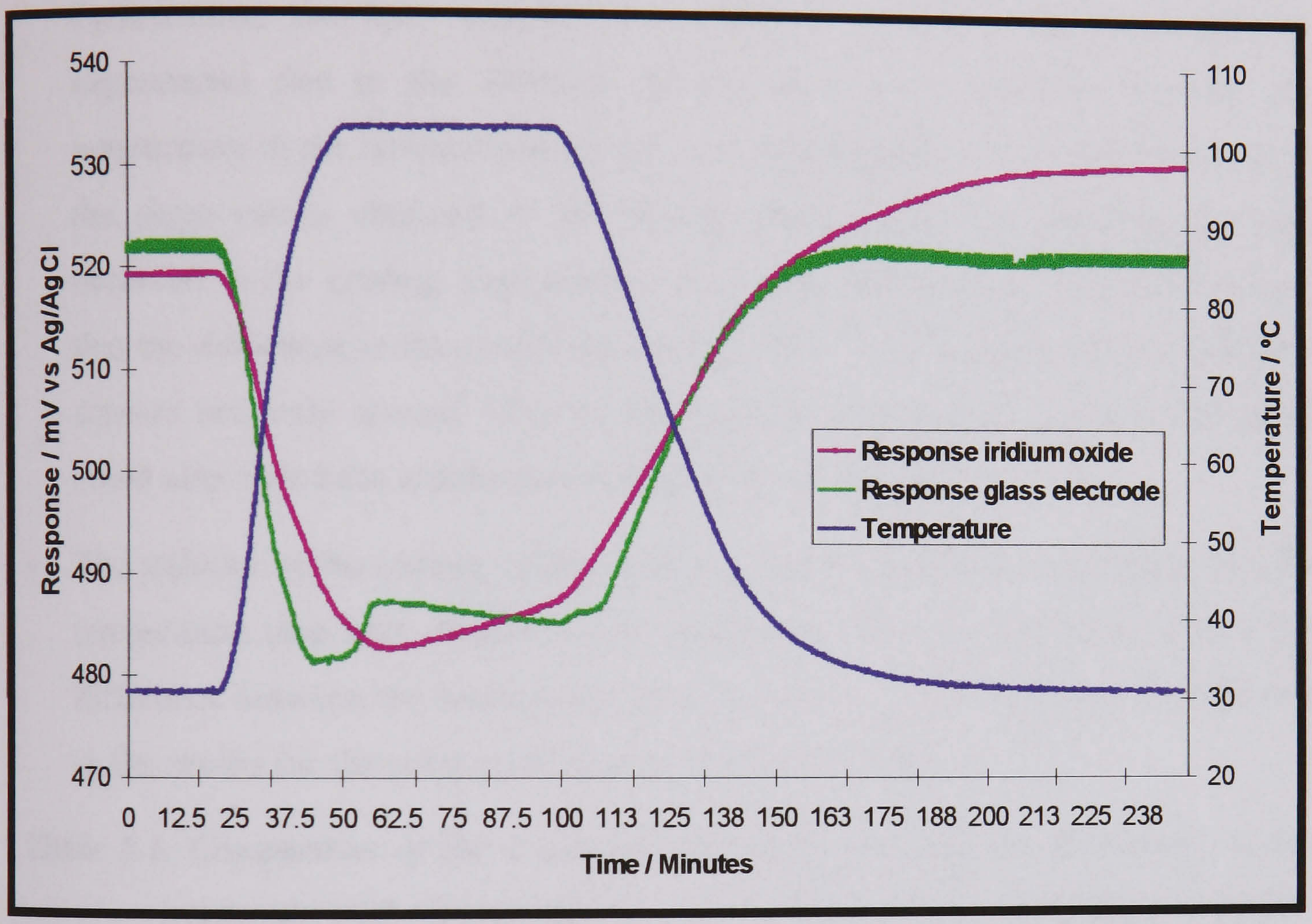

Figure 5.5. Change in the response for a 2 mm OD iridium oxide electrode and a glass electrode when the temperature was varied

Despite the drifts observed in the response, the signals were found to vary linearly with the temperature for both the heating and cooling stages of the experiment. Regression coefficients of at least 0.998 were found in the analysis. This was also observed for the glass electrode before the irreversible failure occurred. *Table 5.1* summarises the results obtained in this experiment for a glass electrode and two iridium oxide sensors. The precision detected in the results and the theoretical slopes obtained from the Nernst equation are also shown in the table. In the case of the solid-state electrodes this theoretical calculation was not possible as the ratio of concentrations for the oxidised species needed in equation Eq. 5.6 was unknown. This undetermined value is the reason why the calibration of the temperature effect in a

new batch of electrodes must be determined. This procedure would be needed after every batch of sensors if the ratio of oxidised species is found to vary from batch to batch. The results in *Table 5.1* show how the values obtained in the heating and cooling experiments were different for the three electrodes. There are two possible reasons to explain this:

- The salt bridge and reference system could have been badly insulated. Furthermore, the heat transfer was different for the cooling and heating experiments due to the different driving force (i.e. difference between the temperature in the mixture and the ambient temperature). This could have caused the slope values obtained in the heating experiment to be different to those observed in the cooling experiment, which also took longer. However, the fact that the difference in the results varied from 34-50% in the case of the solid-state sensors and only around 12% for the glass electrode made us think that there could also have been another reason behind these changes.

- The stability of the iridium oxide sensors, which was observed to change with the temperature (see later, section *3.1.5*), could have been the reason for such a big difference between the heating and cooling results. The lower precision obtained in the results for the solid-state sensors supports this theory.

Table 5.1. Comparison of the slopes obtained and predicted for the change in the response with temperature in cooling and heating experiments using two iridium oxide sensors and one glass electrode

Electrode	*NTE2*	*NTE3*	*Glass*
Experimental heating slope (mV/°C)	-0.377	-0.396	-0.681
Precision in the heating results (%RSD)	6.41	2.45	1.01
Experimental cooling slope (mV/°C)	-0.561	-0.530	-0.610
Precision in the cooling results (%RSD)	3.48	4.19	0.69
Theoretical slope (mV/°C)	NA	NA	-0.594

Finally, the same experiment was repeated using commercial buffers and distilled water and giving similar profiles and results. However, the use of these systems did not provide as good conditions for the analysis of the temperature effect. The use of distilled water, with no buffer control of the pH and very low ionic strength, provided more noisy measurements with a much lower precision in the

results. On the other hand, the use of commercial buffers in experiments where the temperature was varied produced a change in the equilibrium constant for the buffer reaction that was believed to affect the results and therefore the values of the slope obtained in the tests[52,63].

3.1.3. Analysis of the response time

The response time is the time required by the measuring sensor to reach its final value after a sudden change in the pH of the sample. There are different parameters that are used for the quantification of the analysis time. In this work, the T_{90}, which is the 90% of the total response time as defined above, was the parameter studied in the tests. For the analysis of the response time, titration experiments or the replacement of a certain solution by another with different acidity in a flowing system are normally used. The method of transferring the electrodes between vessels with different pH solutions is not recommended, as there can be an interference current from the measuring system causing the glass electrodes to acquire a static charge when removed from the solution[51].

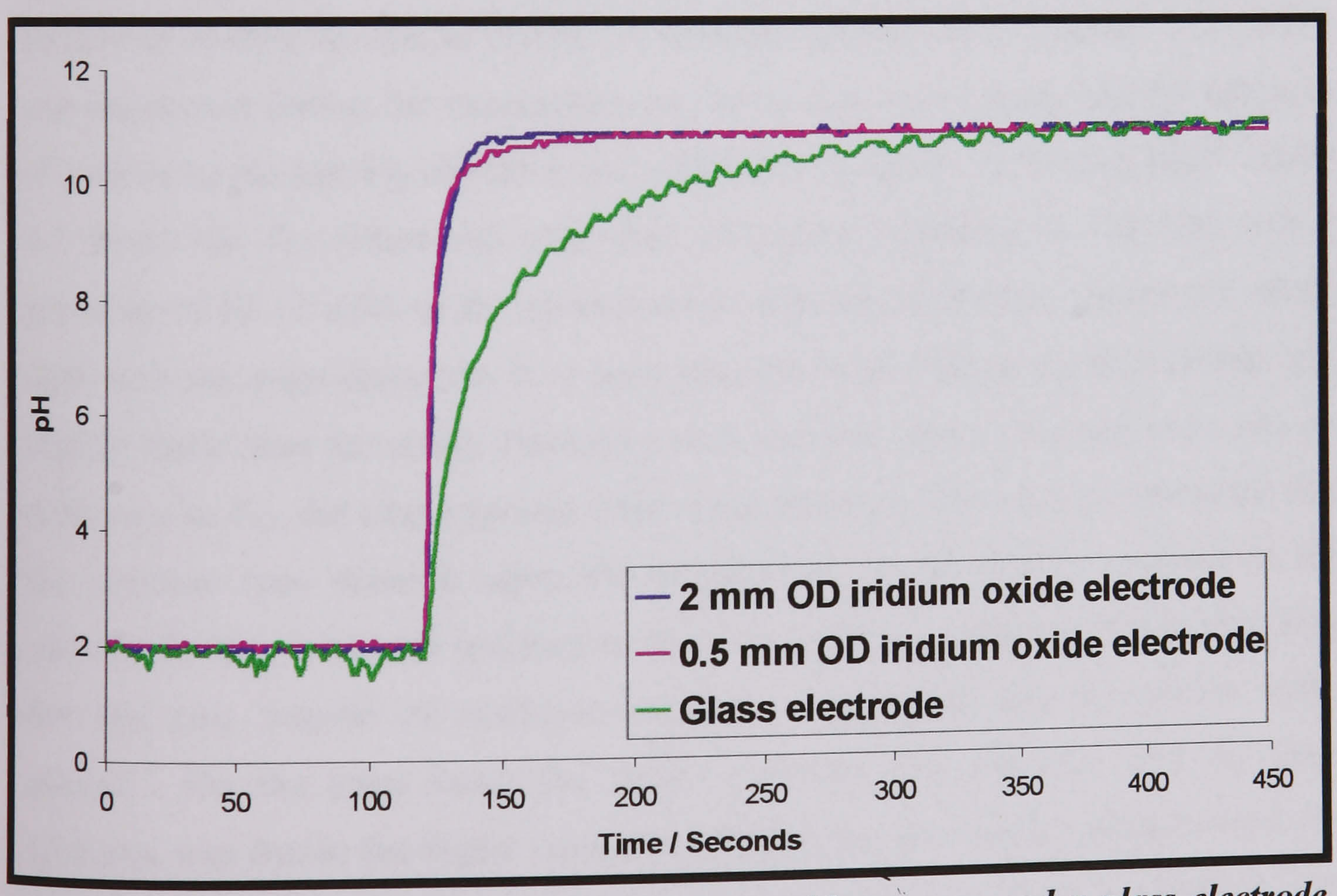

Figure 5.6. Response for two types of iridium oxide sensors and a glass electrode when the pH was suddenly changed at room temperature

In this work, the response time in a step change of pH in a titration process was analysed and a comparison between the solid-state sensors and the glass electrode was made. Walker carried out similar neutralisation tests to define the dynamics of pH sensors[68]. *Figure 5.6* shows the response for two types of solid-state sensor and a glass electrode obtained when the pH of 100 ml of a 0.01 M HNO_3 (Aldrich 25,811-3) solution was changed by the addition of 100 ml of 0.015 NaOH (Aldrich 22,146-5) solution at approximately t= 120 seconds. The use of strong acids and bases minimised the effect of the kinetics of the neutralisation reaction in the dynamics of the process. However, in most of the cases the neutralisation reactions are so fast that the lags in the response due to the reaction kinetics can be ignored [68].

The same reference and salt bridge systems as in the calibration tests with buffers were used in this experiment. The figure shows how the response obtained from the iridium oxide sensors, regardless of the thickness, was much faster than that obtained with a new clean glass electrode (BDH 309-1015-02). Replicate experiments using different iridium oxide sensors and glass electrodes confirmed these results. Also, a similar experiment but with a step decrease in pH instead of increase was performed leading to similar results. A constant stirring speed (approx. 125 r.p.m.) was maintained during the experiments as the mixing of chemicals and the diffusion of protons to the sensing electrode also affect the dynamics of the response[68]. *Table 5.2* shows the T_{90} values and total time of response obtained in the tests with a precision of ±0.12 s/pH in the measurement with the solid-state sensors and ±0.60 s/pH with the glass electrode. It is seen how the thick iridium oxide electrode was slightly faster than the sensor fabricated with a thinner wire. Although there was no difference in T_{90}, the total response times were different. This was an indication that the response time depends upon the morphology of the surface exposed to the solution. In fact, a smooth polished surface is considered indispensable in providing fast and easy transfer of electrons between the electrode and the analyte redox species[69]. On the other hand, the longer response time detected with the glass electrode was due to the higher resistance of the glass membrane compared with the metallic iridium oxide layer. The higher the resistance, which increases at low temperatures, the more time it takes for the reading to stabilise[70]. In addition to this, the glass membrane can get easily dirty and is subject to blockages that increase

considerably the response time of the electrode[68]. This does not happen with the iridium oxide solid-state sensors, which exhibit low impedance and therefore fast response time to changes in pH[12,14].

Table 5.2. Results obtained in the response time studies for the iridium oxide and glass electrodes

Electrode	T_{90} *(s pH^{-1})*	*Response time (s pH^{-1})*
2 mm OD iridium oxide	1.48	3.01
0.5 mm OD iridium oxide	1.48	7.5
Glass	12.5	26.48

Although lower response times (between 0.1 and 1s) have been reported in literature for some glass electrodes, these values were never reached with the electrodes and experimental set-up used in this work. For the case of the iridium oxide sensors, some of the variable response times obtained by other researches are shown in *Table 5.3*. However, as the response time depends very much on the step change on pH and the type of glass in the electrode, a fair comparison with the data published in the literature was not possible. Moreover, none of the studies found in the literature were performed with thermally grown iridium oxide electrodes, that were only used in qualitative studies of the response time[14,36].

Table 5.3. Values of the response time obtained in other studies for different types of iridium oxide glass electrodes

Authors	*Type of sensor*	*Metallic sensing layer*	*Support*	*Response time(s pH^{-1})*
Mihell *et al.*[10]	Planar thick	Ruthenium oxide	Polymer paste	1.52
Pásztor *et al.*[31]	AIROF	Iridium oxide	Au wire	8.16
Olthuis *et al.*[16]	AIROF	Iridium oxide	Ir wire	0.035
Kinlen *et al.*[32]	Sputtered	Iridium oxide	Alumina	4.05

3.1.4. Acid and alkaline error

The acid and alkaline errors refer to the non-linearity observed in the calibration of the response of the glass electrode at very low and very high values of pH respectively. They are related to the presence of certain anions (acid error) and cations (alkaline error) that are normally present at high concentration in aqueous solutions at extreme pH conditions[51]. The error in the pH measurement is produced due to the reaction of the cations and anions with some groups in the glass membrane

of the electrode[71]. Therefore, as this reactive process is affected by the concentration of protons, the measurement of the actual pH value in the test solution can be altered by these processes in the glass membrane. The acid error is observed by an increase in the proton activity in the outer swelling layer of the glass electrode at low pH values[72]. It is normally observed at pH values lower[73,74] than 1.5. However, the acid error is normally lower than the alkaline error and does not have the same importance for practical measurement techniques[51]. Therefore, the analysis of the performance of the iridium oxide sensors at high pH values is considered here and compared with that for the glass electrode. The aim was to prove that the absence of alkali error in the solid-state electrodes constitutes an advantage in the use of these sensors. As the pH glass electrode tends to fail in hot alkaline solutions[64], in some applications the measurement of conductivity can be more accurate than pH measurements to determine the acidity of solutions[74].

Since alkali errors are mainly observed in the presence of sodium, they are usually referred to as sodium errors[51]. Therefore, sodium hydroxide was used in the studies for the alkaline error, although some preliminary tests with potassium hydroxide were also performed. In the experiments, the response of a glass electrode and two iridium oxide sensors were measured with respect to a Ag/AgCl double junction electrode (Russell CRL/DJ/AG/S7). 1 M KNO_3 (Aldrich 22,129-5) was used as the electrolyte in the salt bridge. Two Solomat systems were used for monitoring the signals. The experiments were carried out in the 1-L reactor system at a constant jacket temperature of 30°C. The electrodes were immersed in 1 L of 1 M $NaNO_3$ (Aldrich 22,134-1) solution for at least 12 hours before the start of the test in order to stabilise the sensors and reach a constant temperature in the system. Other authors have used NaCl instead of $NaNO_3$ for the analysis of the alkaline error[64]. However, in this work, the use of NaCl was avoided as Cl^- can lead to problems of corrosion with metal oxide sensors[14].

Several additions of NaOH (Aldrich 22,146-5) solutions were performed for increasing both the sodium concentration and the pH. Medium stirring (approx. 125 r.p.m.) was used during the experiment. Replicates of these experiments were performed and confirmed the good reproducibility in the results obtained in the tests. In preliminary tests, nitrogen gas was bubbled during the experiment to avoid the

absorption of CO_2 and thus the incontrollable change in the pH of the test solution. However, this produced changes in the temperature of the solution that caused important drifts in the response of the solid-state electrodes. Also, as the experiments aimed at a comparison between the performances of the two type of electrodes at high pH values, the small influence of the CO_2 dissolved in the solution was not expected to affect the final conclusions extracted from the tests. Therefore, because all of these reasons, it was decided not to use nitrogen gas in the comparative studies of the alkaline error. Finally, at the end of each replicate of the experiment, the response of the iridium oxide sensors and the glass electrode were calibrated in buffer solutions. This attempted to avoid any drifts in the response that could affect the final results, which can be specially important for the solid-state sensors.

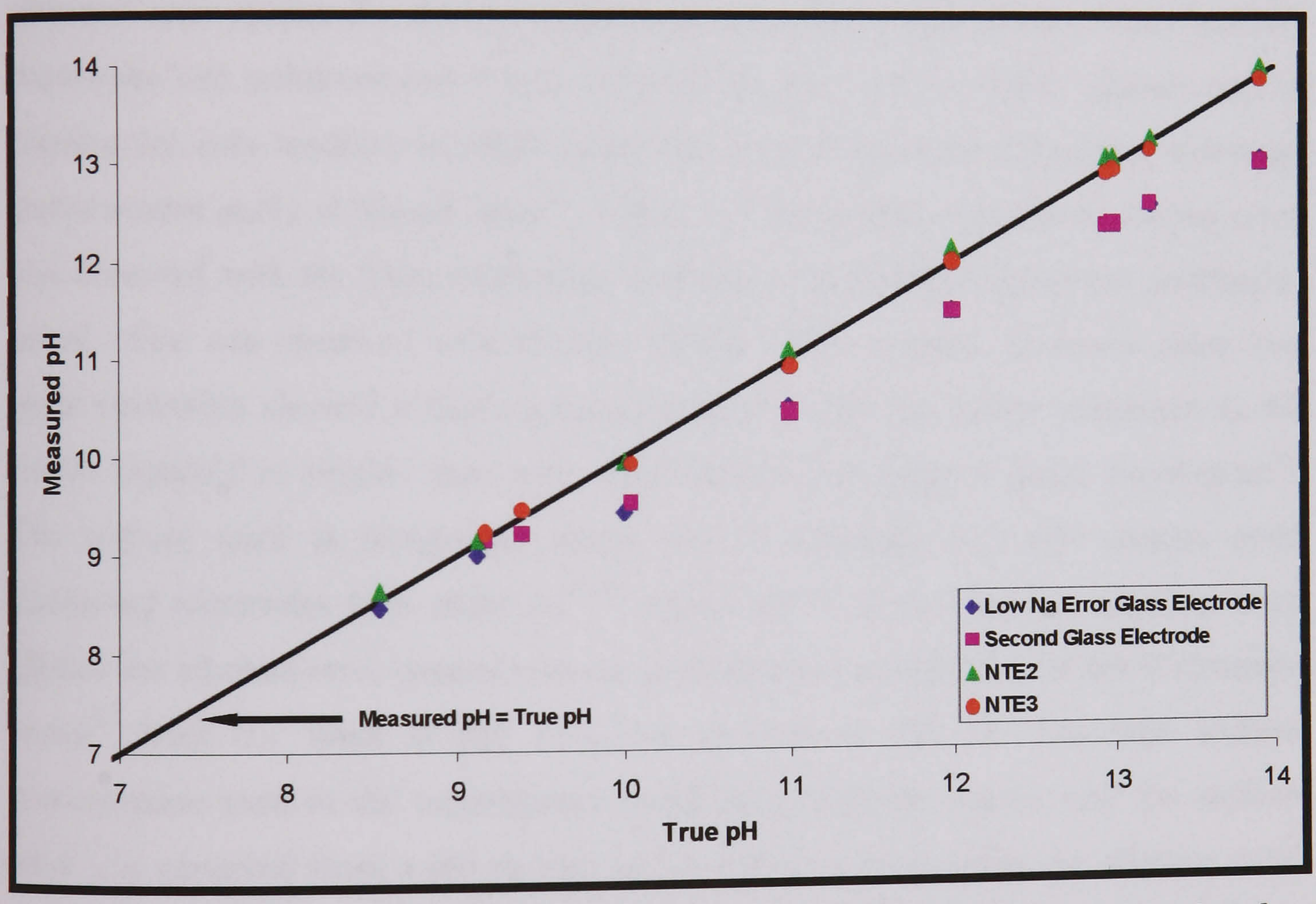

Figure 5.7. Comparison between the predicted value of pH and the real value for two glass electrodes and two iridium oxide sensors at high pH conditions

Figure 5.7 shows the results obtained for the two iridium oxide sensors and the glass electrode. The figure represents the measured value of pH versus the predicted value. The measured value was calculated by applying the calibration equation (obtained at the end of the experiments using buffer solutions) to the

response measured with the sensors during the tests. The predicted value of pH was theoretically obtained by using the pH data at the start of the experiment (measured with the glass electrode) and considering the sodium hydroxide that is added to the mixture. As the initial pH varied slightly with the experiment, it was not possible to plot the error bars that would show the good reproducibility obtained in the replicate experiments. However, it should be mentioned that all of the replicate experiments showed the typical trends shown in *Figure 5.7*.

Two glass electrodes were used in the tests; one that was catalogued as made of special glass with a low alkaline error (BDH 309-1015-02). The other was a more common glass electrode (Russell PHM-100-011-N), with no special indications regarding the intensity of the alkaline error in its measurements, although the results obtained were similar for the two glass electrodes. The composition of the electrode membrane was unknown but it was believed not very rich in Al_2O_3. Glasses rich in alumina are very sensitive to alkali metal ions even at moderate pH as they exchange protons more easily in the gel layer[41]. *Figure 5.7* shows that a degree of alkaline error was observed with the glass electrodes, whereas a much better agreement prediction-actual value was observed with the two iridium oxide sensors. However, these two glass electrodes showed a fairly good response at high pH values compared to the results reported in similar tests with other commercial types of glass membranes[75]. The sodium error is recognised above pH 10 although with low sodium error measuring electrodes it is observed[73,74] above pH 12.5-13.0. In low alkaline error glasses the alkaline error depends on the concentration of alkaline ion but it normally varies[70] from 0.1 units at pH 12.5-13.0 to 0.40 at pH 14. The high sodium concentration used in the experiments could have been the reason why the sodium error was observed from a pH as low as 9.5 with our supposedly low alkaline error glass electrodes. Also it could have been due to a second source of error at high pH values that is produced with glass electrodes when concentrated caustic solutions begin to etch the sensitive measuring glass surface, reducing the sensitivity of the glass membrane[74]. The results proved that the absence of the sodium error makes the use of solid-state sensors preferable to the glass electrodes at high pH conditions. Finally, when the experiments were repeated with KNO_3 (Aldrich 22,129-5) and KOH (Aldrich 22,147-3) a smaller difference in the results was obtained between the

glass and the solid-state sensors for measurements at high pH. In fact, it was not clear the presence of alkaline error in the glass electrode when KNO_3 and KOH were used.

3.1.5. Stability measurements

As mentioned, the drift in the response monitored with the iridium oxide sensors appears to be the major downside in their use for industrial pH monitoring. In this section, a set of experiments and tests were performed to study the stability in the response of the thermally grown iridium oxide sensors used in this project. *Table 5.4* shows the parameters obtained in several calibration experiments using one 0.5 mm OD iridium oxide sensor over a 12 month period. These results gave an idea of the drift in the response of the sensors. Changes of up to 5.2% in the slope and 44% in the offset were observed. Similar results were obtained with other iridium oxide electrodes with the same characteristics, but thicker in diameter (2 mm OD iridium rod). It should be mentioned that all of the electrodes were kept in distilled water when not in use, as suggested by Hitchman *et al.*[14]

Table 5.4. Calibration parameters obtained in five different calibrations over a 12 months period for a 0.5 mm OD iridium oxide sensor in buffers at 18°C

	Slope ($V\ pH^{-1}$)	***Offset (V)***
Initial response	-0.0571	0.7636
Response after 4 months	-0.0586	0.6513
Response after 8 months	-0.0557	0.5321
Response after 10 months	-0.0574	0.6315
Response after 12 months	-0.0574	0.6428

The changes observed in the slope were within the expected variability in the results and a similar variation was observed with commercial glass electrodes. However, the changes observed in the offset were very high and showed drifts that did not allow for the definition of a reliable pH-response calibration. Moreover, this drift was found to be variable with time and the temperature of the solution, with a very long conditioning before stable readings could be measured. *Figure 5.8* shows a typical response-time curve obtained for two iridium oxide sensors and a glass electrode immersed in a pH 4 buffer solution kept at a constant temperature of 80°C. A similar trend but with lower drifts and slower changes in time was observed with

the same sensors in a solution at 30°C. This indicated that the iridium oxide sensors undergo a slow process of conditioning with the kinetics highly dependent on the temperature.

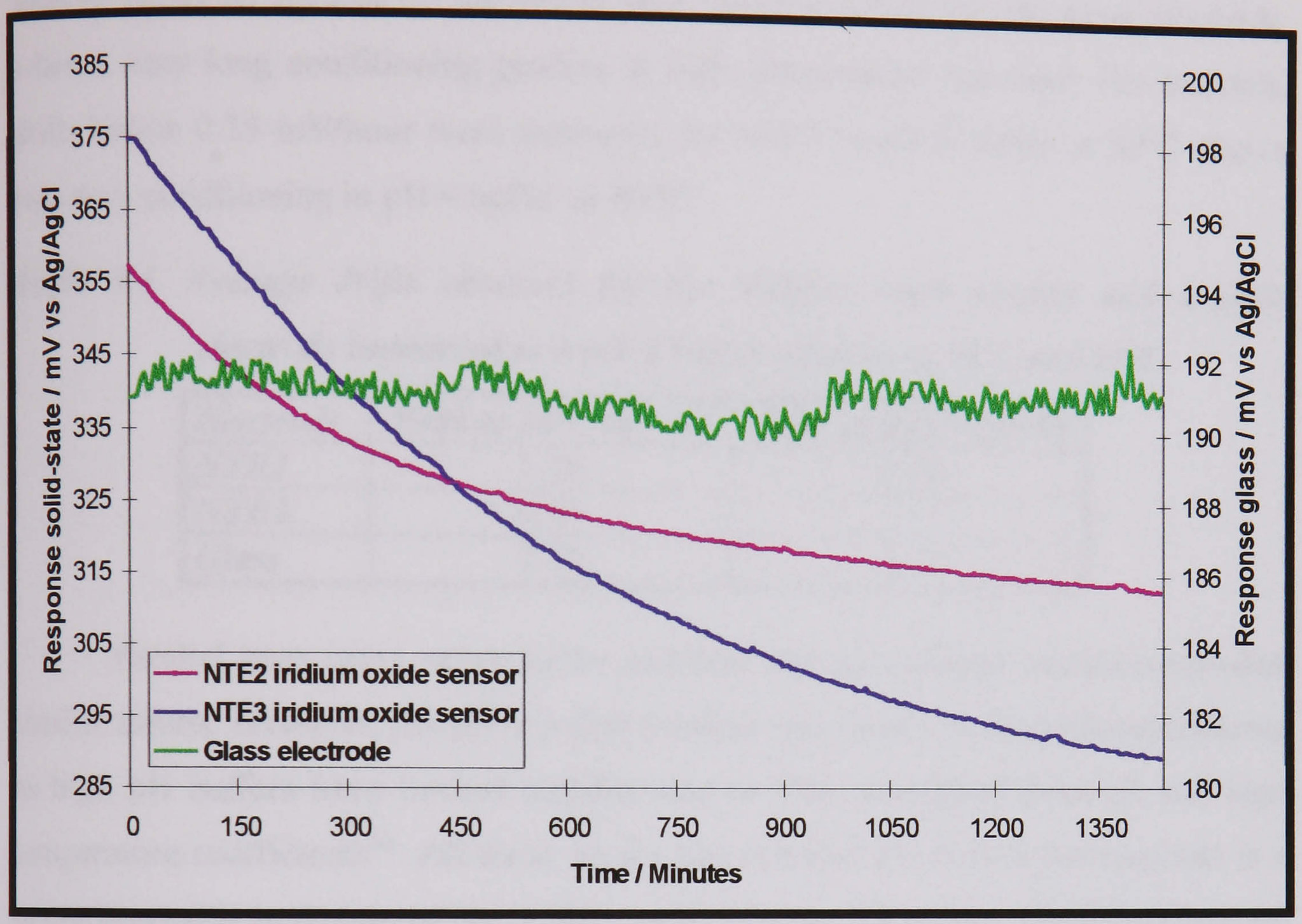

Figure 5.8. Change of the response with time in a pH 4 buffer solution at 80°C

Table 5.5 summarises the average drifts observed in three replicate experiments with the two solid-state sensors and the glass electrode. The values in the table are the average of three measurements and were monitored for a period of 24 hours and after 12 hours of temperature conditioning by immersing the electrodes in the solution. It was noticed that the precision in the results was within reasonable figures (i.e. <5% RSD) if the electrodes were immersed in distilled water for at least two days before the replicate was performed. Otherwise, the drift was very variable as it depended on the stage of the electrode within the conditioning process. NTE3 showed slower conditioning kinetics that made its drift at 80°C higher than at 30°C when the electrodes were immersed for 12 hours in the solution before the measurements. On the other hand, the different kinetics for the conditioning process can be the reason why NTE2 showed a lower drift at 30°C than at 80°C after 12 h of conditioning. The drift observed for the glass electrode was measured as the difference between the maximum and minimum values for the response. This was

due to the fact that a continuing decrease or increase in the response was not observed as for the solid state sensors, and the drift was only associated with the noise observed in the signals. Finally, it was noticed that the drift observed in the iridium oxide sensors could be reduced to the levels near those observed for the glass electrode, when a very long conditioning process at high temperature was used. For example, drifts below 0.25 mV/hour were measured for NTE3 in pH 4 buffer at 30°C after a two days conditioning in pH 4 buffer at 80°C.

Table 5.5. Average drifts observed for the iridium oxide sensors and a glass electrode immersed in a pH 4 buffer solution at 30°C and 80°C

Electrode	*Drift at 30°C (mV/h)*	*Drift at 80°C (mV/h)*
NTE2	1.20	0.76
NTE3	0.95	1.77
Glass	0.17	0.13

Parallel tests using other buffer solution and un-buffered mixtures provided similar results. However, the pH 4 buffer solution was finally used in the experiments as high pH buffers have limited stability due to CO_2 absorption from air and high temperature coefficients[60]. All these results showed that the drift in the response is a major downside in the use of the iridium oxide sensors. Moreover, the drifts observed were variable with time, with the conditioning process and with the sensor, which made difficult to model the variation of the offset detected in the response. Further research could be aimed in the study of the kinetics of the long conditioning process needed for the solid-state sensors. The definition of these kinetic parameters could lead to a clearer idea about the mechanism of the process responsible for the drift in the response of the iridium oxide sensors.

Other authors have noticed and measured this drift problem in the response of solid-state sensors, although a comparison with our results was not possible due to the high variability observed in the results and dependence on the conditioning process. Kinoshita *et al.* observed drifts of up to 80 mV in the offset measured in the calibration parameters[13] using iridium oxide electrodes obtained by deposition of iridium on a titanium coupon with a solution of $IrCl_3$ in water. Tarlov *et al.* also noticed a very big change in the response of sputtered iridium oxide sensors[12]. They measured drifts of up to 60 mV in the offset for the calibration parameters and 4 mV/h

in buffers in the range pH 4 to pH 7. On the other hand, Olthuis *et al.* measured a variability of below 0.3 mV/h with AIROF electrodes in pH 4 buffer solutions[16]. Hitchman *et al.* noticed drifts of 2 mV/h in pH 2-8 buffers, 6 mV/h in pH 10 buffers and 47 mV/h in pH 12 buffers using iridium sensors formed by potential cycling[6]. The same authors measured[14] maximum drifts of 16.2 mV/h in pH 4 buffers, 27 mV/h in pH 7 buffers and 18.6 mV/h in pH 9 buffers using thermally oxidised iridium electrodes in solutions at 95°C. They also obtained very variable results depending on the solid-state sensor used in the experiment. Only for some of the signals, from some of the sensors, were the drifts comparable to those obtained with glass electrodes, which were unusually high. However, this comparison was performed in short term experiments (<20 minutes) and no information of a comparative long term performance between the electrodes was given. Moreover, the comparison was made between iridium sensors that underwent different conditioning processes. Hitchman *et al.* proposed a poisoning technique to overcome the problem of drifting response observed in thermally oxidised sensors[30]. They proposed a field induced poising technique by which they reached the equilibrium relative mole fraction of Ir(IV) and Ir(III) oxides in the sensors by using a charge injection/ejection procedure. If the equilibrium mole fraction for those species was reached, the potential of the redox process should stay constant and smaller drifts would be observed. In fact, they measured drifts in the range 0.08-0.13 mV/h after this poisoning method was applied. This technique could be suggested for further work in the development of the iridium oxide sensors. Finally, Katsube *et al.* also observed that the ageing process of iridium oxide electrodes may be accelerated by heating in water at elevated temperature and pressure[32], in agreement with our results.

As the drift varied with the time that the electrode was immersed in the solution, it was believed that the conditioning process was taking place in the surface of the sensor. In fact, previous studies have shown that the performance of the iridium oxide sensors was very dependent on the morphology and the microstructure of the oxide film[76]. The film must be dense, uniform and with no impurities in order to reduce the drift in the pH sensitivity. This dependence on the surface properties suggested that the drift in the response could also be affected by the stirring, which contradicts the observation of other authors by which the iridium oxide electrodes

were found to be insensitive to stirring[11,15]. Several test such as those shown in *Figure 5.9* showed the effect of stirring on the conditioning of the electrodes and therefore the drift in the response. In this experiment, the response of two 2 mm OD iridium oxide sensors and a glass electrode (BDH 309-1015-02) were monitored in a pH 4 buffer solution at 30°C. The response was measured with respect to a Ag/AgCl double junction electrode (Russell CRL/DJ/AG/S7). 1 M KNO_3 (Aldrich 22,129-5) was used as the electrolyte in the salt bridge between the reference system and the buffer solution. Medium stirring (approx. 125 r.p.m.) was initiated at t = 20 minutes to study the effect of stirring on the response of the sensors. No stirring effect was observed for the glass electrode, which showed a constant response with a noise of ± 1 mV. The iridium oxide electrodes showed a variable drift of response depending on whether stirring was used or not. It must be pointed out that the preconditioning undergone by each of the solid-state sensors was different in order to analyse its effect on the response. So NTE2 was immersed in the solution for 30 minutes with stirring and 60 more minutes without stirring before the experiment. NTE3 had a more severe conditioning with 24 hours in the pH 4 buffer solution at 80°C and five days in the same solution at 30°C. These differences in the preconditioning were responsible for the different curves observed in *Figure 5.9*. Whereas NTE2 showed a drift that was still decreasing after 40 minutes, NTE3 had stabilised in the solution, showing a very stable response after 30 minutes (i.e. 10 minutes with stirring). This shows how the temperature, time of conditioning and stirring affects the drift in the response obtained from the solid-state sensors. This was not observed for the glass electrode, which underwent a short preconditioning period at low temperature identical to that applied for NTE2. However, stirring has been reported to be a key role in glass electrode calibration, where the same stirring applied in the process is advised to be used in the calibration of the electrode[66].

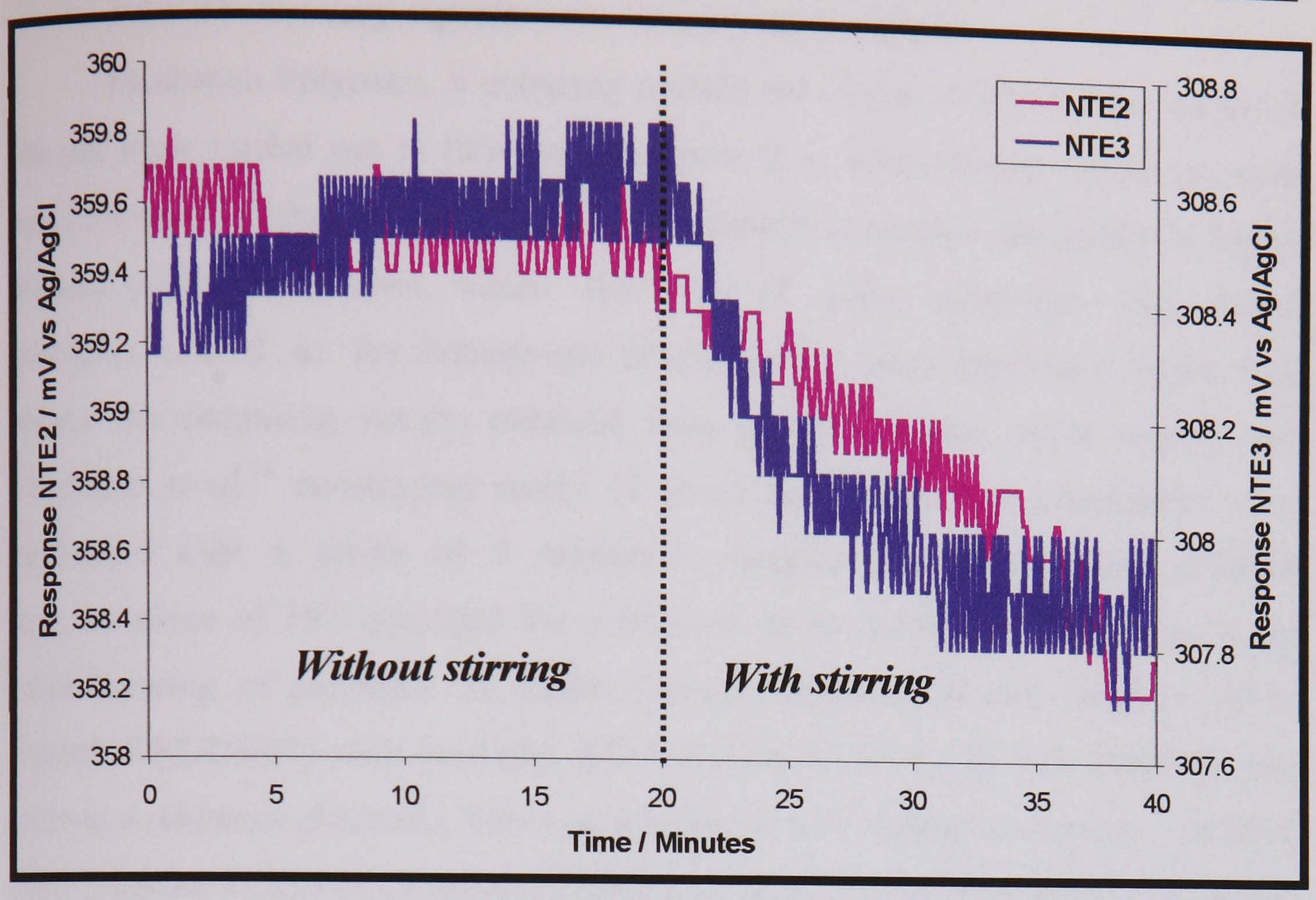

Figure 5.9. Analysis of the effect that the stirring had on the drift in the response monitored for two 2 mm OD iridium oxide sensors in a pH 4 buffer solution at 30°C

3.2. Measurements of acidity in non-aqueous systems

Various advantages and disadvantages in the use of the iridium oxide glass electrodes in aqueous systems have been shown above. Only at very high temperatures and high pH conditions have the solid-state sensors clearly proved to be superior to the glass electrode. As the glass pH probe failure that initiated the work in this project was observed in toluene, it was thought that the iridium oxide sensors could also be a better alternative to the use of glass electrodes in non-aqueous environments. Preliminary experiments in highly viscous polymeric samples showed promising results that encouraged the development of iridium oxide sensors for monitoring the acidity of processes carried out in non-aqueous solvents. However, it should always be borne in mind that the acidity measurements in non-aqueous systems have not been as extensively studied as the pH measurements in aqueous environments[51].

3.2.1. Preliminary experiments with polymeric samples

Huntsman Polymers, a company outside the circles of CPACT but aware of the pH work carried out in this project, showed a great interest in the potential applications of iridium oxide sensors. They needed to monitor the acidity in highly viscous polymeric samples, where the use of glass electrodes had shown problems related to the damage and dirtying of the glass membrane. *Figure 5.10* shows the promising results obtained with the old iridium oxide sensors that Hitchman *et al.*[14] constructed nearly 10 years ago. These first experiments were performed over a series of 5 polymeric samples (isocyanates) with different concentrations of HCl provided by a division of the company, specialised in the manufacturing of polymers. A double junction standard calomel electrode (SCE, Russell CRL/DJ/S7) with saturated KCl (Aldrich 20,800-0) in both chambers was used as a reference electrode. This was attached to a salt bridge containing[52] saturated LiCl (Aldrich 21,323-3) in ethanol (Aldrich 27,074-1) a common electrolyte used in acidity measurements in non-aqueous systems[77]. Further details about the composition of the samples and further experiments using these isocyanates are not covered here because of confidentiality issues. However, it was concluded that the sensors gave a non-linear response with the concentration of HCl, or close to linear with the pH, but in any case, were capable of distinguishing between samples of different HCl concentration. Repetition of these experiments showed identical trends but with drifts in the response of each electrode. The signals were found to vary greatly at low HCl concentrations, whereas at high values the variation was smaller following a polynomial trend. Also, the difference in the measurements between electrodes seemed to increase as the HCl concentration got higher. Despite these problems, the results obtained and a review of other published studies with iridium oxide sensors in non-aqueous systems[53,54] encouraged the development work using the sensors in non-aqueous environments.

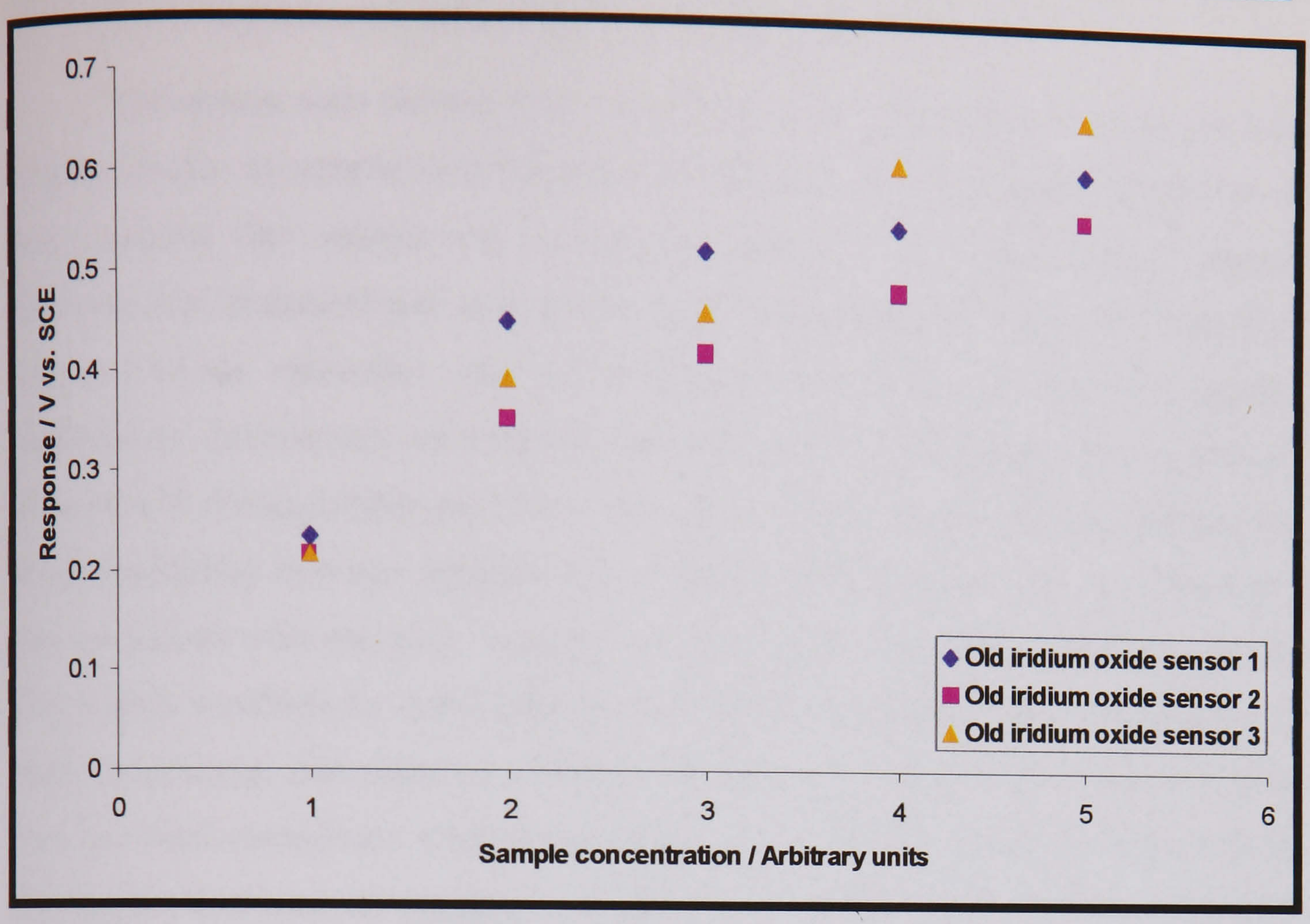

Figure 5.10. Response of old iridium oxide electrodes in highly viscous polymeric samples with different concentrations of HCl at room temperature

3.2.2. Acids used in the calibration samples

Initially, H_2SO_4 (Aldrich 25,810-5) a common catalyst in esterification reactions, was used as the acid to prepare samples with different proton concentrations. However, it was noticed than even small concentrations of this acid appeared to sulphonate the toluene when this was used as the solvent in the samples. Immiscible yellow droplets of a second phase were observed in mixtures of toluene with sulphuric acid. Paratoluenesulphonic acid (Aldrich 40,288-5) was also tried as it can also be used as a catalyst for the esterification of crotonic acid. This acid was not used either as it was found not to be very soluble in toluene at room temperature. Also, when heated, indications of a polymerisation process with the organic acid were observed as the viscosity of the mixture increased. Finally, dichloroacetic acid (Aldrich D5,470-2), a strong organic acid in liquid state and soluble in toluene was chosen for the experiments in non-aqueous environments.

3.2.3. Experiments with samples with alcohol as a solvent

Preliminary tests showed how combination glass electrodes were not useful to measure acidity in samples with toluene as the probes failed during the experiments. It was observed that toluene was penetrating into the cavity where the reference electrode was immersed and getting mixed with the electrolyte there. The Nernstian response of the electrodes was not maintained after the tests and they needed regeneration. Preliminary experiments with solid-state iridium oxide sensors did not show failure although other problems with noise in the response and the impossibility of distinguishing between samples with different acidity were observed. The noise was associated with the poor conductivity of toluene. Therefore, alcoholic solvents with higher conductivity were used in the initial experiments before moving on to more complicated non-aqueous systems. Alcohols and alcohol-water mixtures have been the most extensively studied non-aqueous systems[50,51]. They also happen to be the simplest non-aqueous systems, as alcohols act as both a proton donor and acceptor similarly to water. A glass electrode was used for comparison studies, using a Ag/AgCl electrode as the reference system in a configuration identical to that described before for the testing of the response of the electrodes in buffers. The standard electrolyte used for non-aqueous systems (ethanol saturated in LiCl) was employed in the initial experiments.

As has been mentioned before, the initial results using the iridium oxide sensors in toluene samples were not good and showed no stable readings. To explain this, the hypothesis of a problem with non-conductivity at the salt bridge was suggested. In fact, it was believed that a phase boundary potential between the ethanol in the salt bridge and the toluene could have caused the high level noise detected in the experiments and the incapability to distinguish between toluene samples with different acid concentration. This was supported by the large non-reproducible potentials that have been observed at the reference electrode by some authors when they put an aqueous reference electrode into direct contact with a medium that was immiscible with water[51].

When the experiments were repeated with ethanol as the solvent in both the samples and the salt bridge, this problem was not observed. In this case the noise

observed was reasonable and the electrodes were able to distinguish between samples with different concentrations of dichloroacetic acid. *Figure 5.11* shows how a very low change in the response was observed when the acidity was varied. This was noticed for various electrodes with different thickness and also for the glass electrode. However, the iridium oxide sensors showed a large drift in the response (larger than in aqueous solutions) that made it impossible to obtain a reliable calibration, especially considering the small variations of the response with the acidity. These changes in the response, depending on the conditioning, were not observed with the glass electrode. An advantage in the use of the solid-state was that the response time was shorter than for the glass electrode (T_{90} = 5 ± 0.33 seconds for the solid-state sensors vs. T_{90} = 20 ± 1.05 seconds for the glass electrode in a step change from 0 to 0.82 g dichloroacetic acid in 100 ml of ethanol).

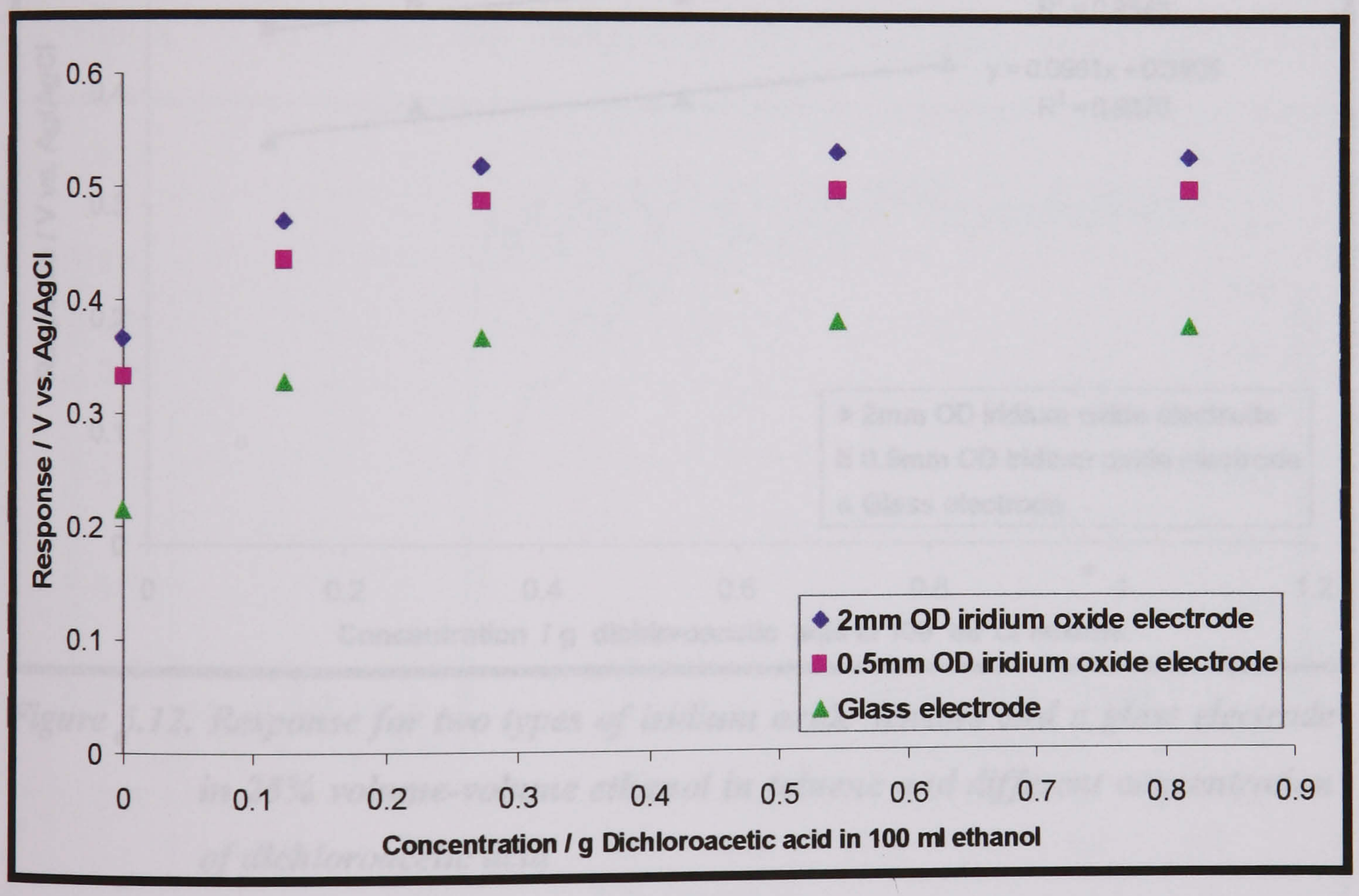

Figure 5.11. Response for two types of iridium oxide sensors and a glass electrode in ethanol with different concentration of dichloroacetic acid

3.2.4. Experiments with samples with toluene-alcohol mixtures as solvent

The results obtained with ethanol indicated that the problem of acidity measurements with toluene samples was probably related to the low conductivity of the solvent and the existence of phase boundaries between the samples and the

electrolyte in the salt bridge. New tests were performed using toluene-alcohol mixtures. The most interesting toluene-alcohol mixture was that with 25% volume-volume of alcohol, as this was the ratio used in the esterification reaction where the glass pH probe failed. In particular, during the esterification of crotonic acid, butanol was used as a reactant. When butanol was used as the alcohol in the mixture and dichloroacetic acid to vary the acidity in the samples, noisy signals with huge drifts for both the iridium oxide sensors and the glass electrode were observed. Different electrolyte mixtures (butanol-toluene and ethanol-toluene saturated in LiCl) were tried in the salt bridge without any improvement in the quality of the response.

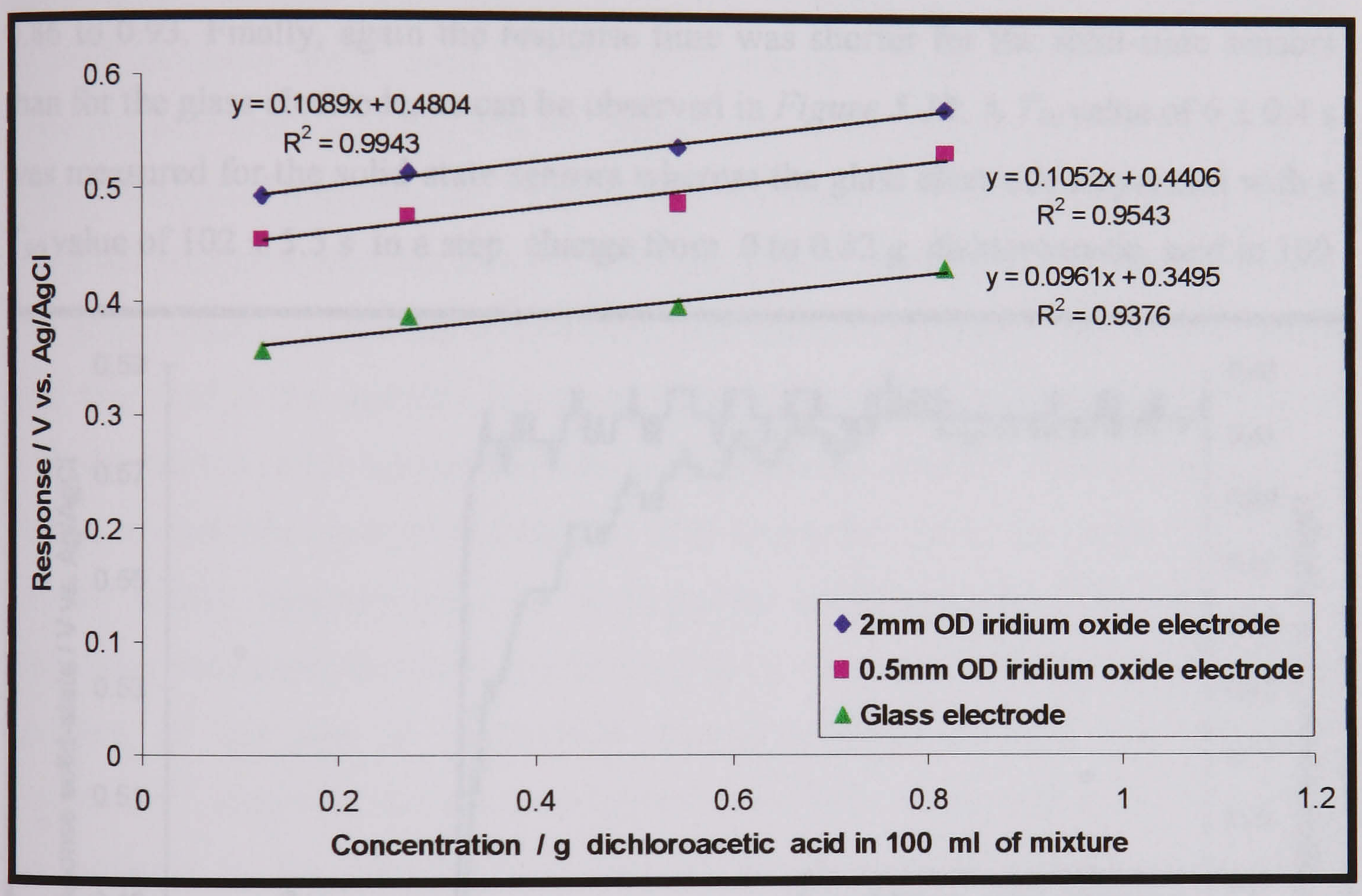

Figure 5.12. Response for two types of iridium oxide sensors and a glass electrode in 25% volume-volume ethanol in toluene and different concentration of dichloroacetic acid

When ethanol was used in the mixture, better responses were obtained that could be used to distinguish between samples with different acidity. *Figure 5.12* shows how a very low change in the response was observed when the acidity was varied for both the solid-state sensors and the glass electrode. Again, the iridium oxide sensors showed a large drift in the response (larger than in aqueous and ethanol solutions) that made it impossible to obtain a reliable calibration. Considerable drifts were also observed in the response from the glass electrode. However, this change

was always lower than for the case of iridium oxide sensors and was not affected by the conditioning of the electrode (i.e. time in solution before the measurement). Chernysheva *et al.* performed similar tests using HCl as an acid in 75% volume-volume ethanol in toluene mixtures[77]. They measured the response of a glass electrode with respect to a hydrogen electrode and observed a slope of approximately –56.70 mV/log(M) when plotting the signals vs. log(concentration of acid). In our case, slopes of -90.5, -85.5 and -81.8 mV/log(M) were observed in such a system for 2 mm OD iridium oxide, 0.5 mm OD iridium oxide and the glass electrode, respectively. However, quite poor regression coefficients were obtained, ranging from 0.86 to 0.93. Finally, again the response time was shorter for the solid-state sensors than for the glass electrode, as can be observed in *Figure 5.13*. A T_{90} value of 6 ± 0.4 s was measured for the solid-state sensors whereas the glass electrode responded with a T_{90} value of 102 ± 5.5 s in a step change from 0 to 0.82 g dichloroacetic acid in 100

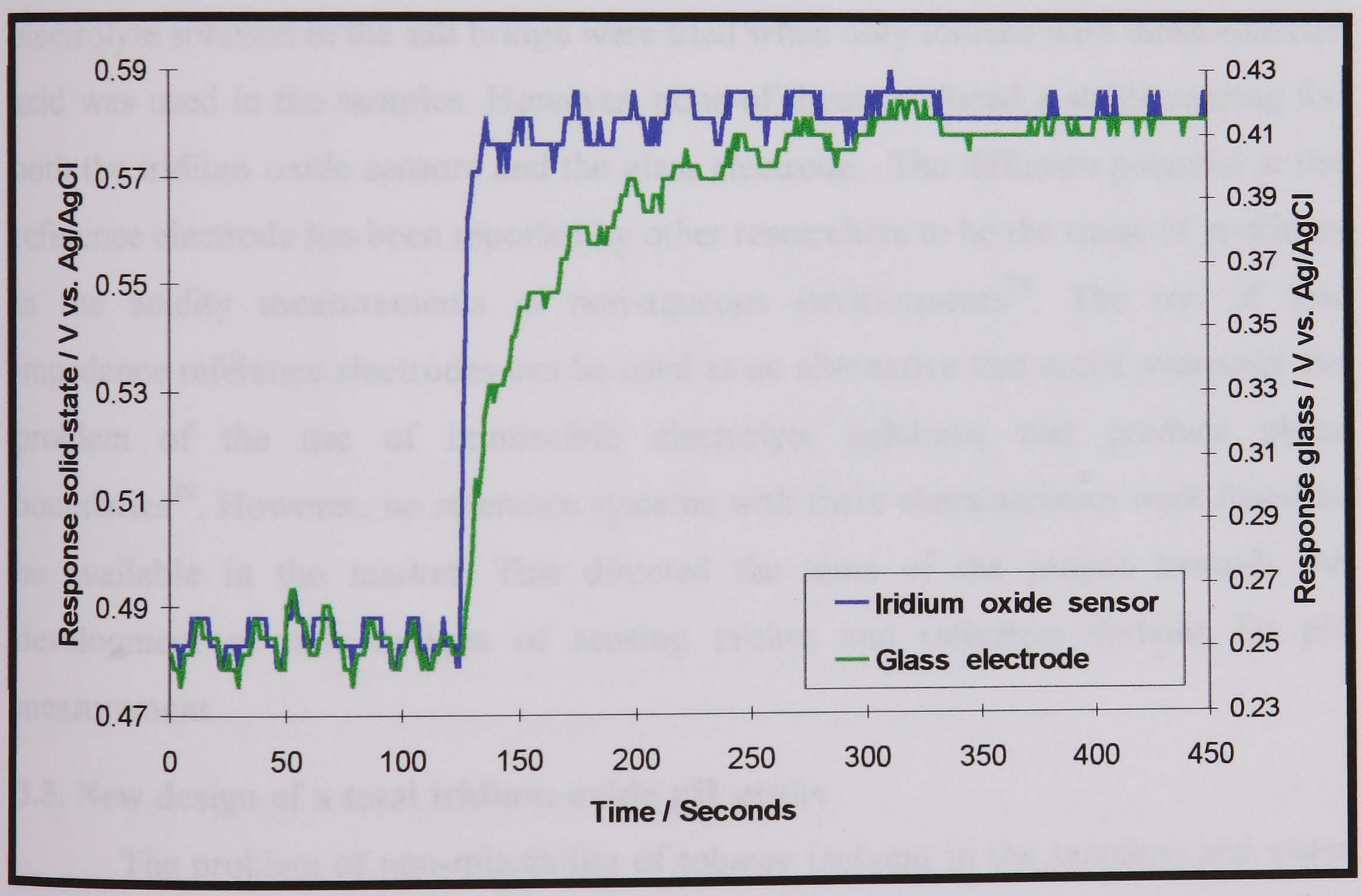

Figure 5.13. Response for a 2 mm OD iridium oxide sensor and a glass electrode in a step change in the acidity of a 25% volume-volume mixture of ethanol in toluene

ml of 25% volume-volume ethanol in toluene. These results showed how the response time increased considerably (specially for the glass electrode) when the conductivity

of the solution decreased, as the T_{90} values were larger than for the same experiments with only alcohol as a solvent. Moreover, the noise observed in the response also increased when the ratio of toluene increased in the mixtures. This was expected in non-aqueous environments where the use of highly resistive organic solvents as reference electrolytes raises the resistance of the reference electrode, producing noisy and slow responses[78].

3.2.5. Experiments with samples with toluene as a solvent

The measurements in samples with toluene were problematic since the start of the project. This was the reason why simpler systems with alcohols and toluene-alcohol mixtures were used in the development of the sensors. From these experiments it was concluded that the conductivity of the samples and the existence of phase boundaries between the samples and the electrolyte in the salt bridge could cause the problems with the measurements in toluene. Different compositions for the electrolyte solution in the salt bridge were tried when only toluene with dichloroacetic acid was used in the samples. However, none of them produced a stable reading for both the iridium oxide sensors and the glass electrode. The diffusion potential at the reference electrode has been reported by other researchers to be the cause of problems in the acidity measurements in non-aqueous environments[78]. The use of low impedance reference electrodes can be used as an alternative that could overcome the problem of the use of immiscible electrolyte solutions that produce phase boundaries[79]. However, no reference systems with these characteristics were found to be available in the market. This directed the aims of the project towards the development of new designs of sensing probes and reference systems for pH measurement.

3.3. New design of a total iridium-oxide pH probe

The problem of non-miscibility of toluene (solvent in the samples) and water (solvent in common reference electrodes) was initially solved using a salt bridge with ethanol, soluble in both solvents. Also, the electrolyte in the reference system was replaced by the standard saturated LiCl in ethanol, as advised by many manufacturers of pH electrodes[52]. None of these alternatives gave satisfactory results with toluene samples. Different alternatives to the use of wet reference systems in contact with the

test solution through a porous frit (typical of combination electrodes and reference systems) have been found in literature. Tedjar *et al.*[80] reported the use of a solid reference system formed with PbO_2. However, these designs are still not well established in terms of stability of the response, which showed sub-Nernstian behaviour in all of the experiments. Other authors have used solid proton-conducting electrolytes to develop all solid glass pH probes[81]. However, they showed poor stability as the electrolyte was drying out in the solid material, and also gave very sub-Nernstian responses. Also, Kinlen *et al.* developed an entirely solid-state pH sensor based on Nafion coated iridium oxide and a polymer modified solid Ag/AgCl electrode as a reference system[26]. Although they obtained good Nernstian responses, they experienced big problems with drifts and poor reproducibility in the results. Other authors[82] have proposed the use of ISFET technology for pH measurements with an internal reference system so that a separate reference electrode is not required. However, these systems do not withstand very high temperatures like glass electrodes[60].

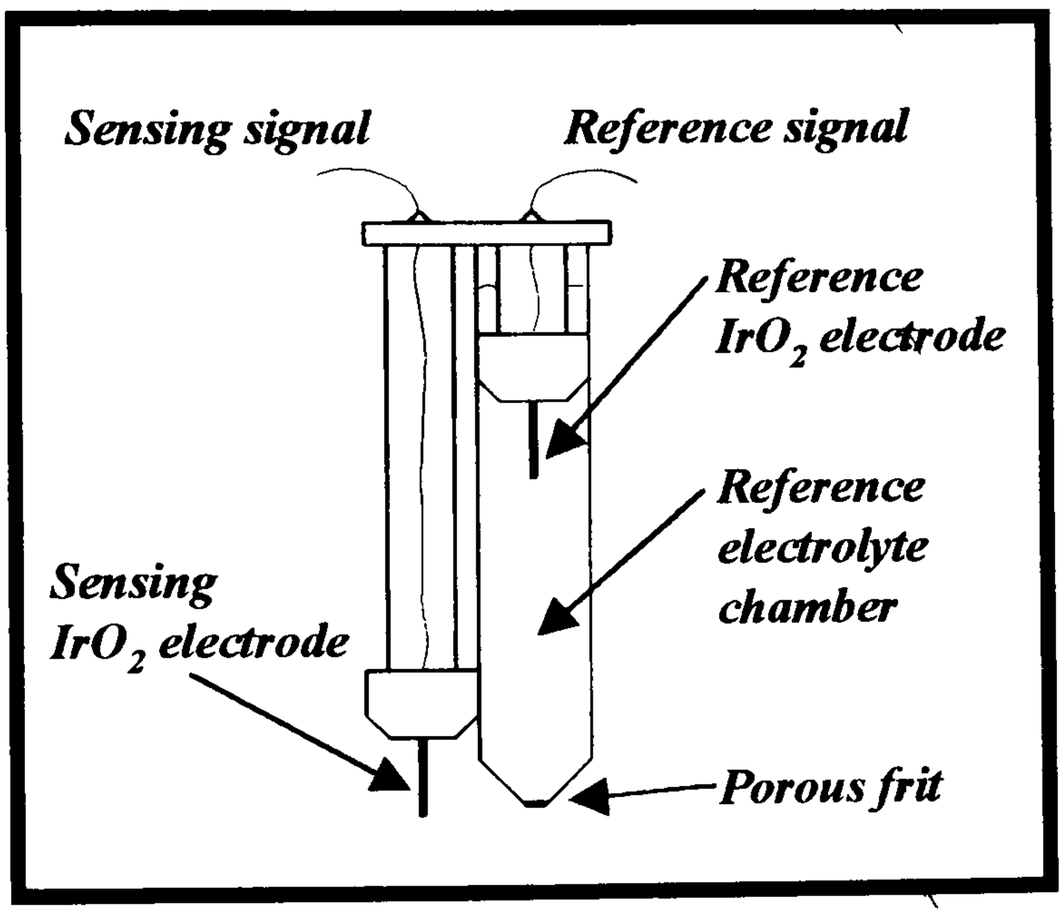

Figure 5.14. Sketch of the new design of total iridium oxide probe

The problems experienced in our experiments and in the designs reviewed in the literature contributed to the idea of using another iridium oxide electrode immersed in a salt bridge with a known acidity solution, as a reference system for another sensor that would be in direct contact with the sample solution. This design would constitute a total iridium oxide measuring system that would avoid phase boundaries between non-miscible solvents[63]. *Figure 5.14* shows a schematic drawing of such a configuration. This new design is similar to the differential electrode system

described by King, where the pH is related to the difference in signal monitored from two glasses electrodes[83]. In this design, one of the glass sensors is immersed in a chamber with pH 7 buffer solution and in contact with the test solution through a tight ceramic plug. King developed this system to overcome the errors in pH measurement produced by the dilution of the reference electrode.

3.3.1. Preliminary tests in water

This new configuration was initially tested in water. The salt bridge contained a solution with a known and constant concentration of protons, e.g. a pH 7 buffer solution. For calibration and testing of the performance of the system in water, the response of the sensors in pH 9, 7, and 4 buffer solutions (816-004, 007 and 008 by Electronic Temperature Instruments) was monitored. The response obtained was very linear, reproducible and slightly super-Nernstian, as is shown in *Figure 5.15*. This proved that another solid-state sensor immersed in a salt bridge with a buffer solution could be used as a reference system. It was therefore possible to build a single probe for pH monitoring that combined the sensing electrode and the reference system, both made of iridium rods coated in iridium oxide. This combination probe appeared to

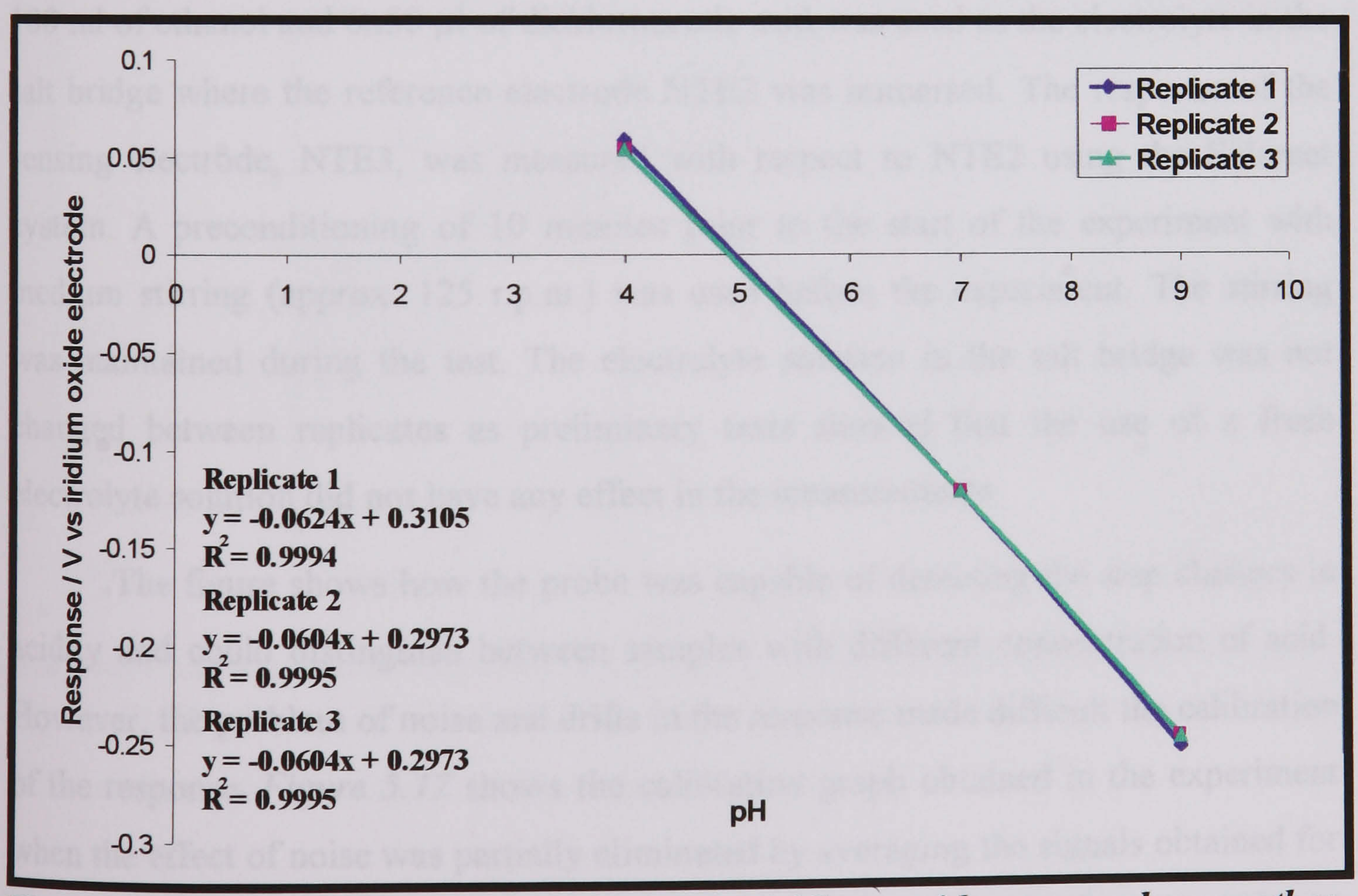

Figure 5.15. Change in response with pH for iridium oxide sensor when another iridium oxide electrode immersed in a salt bridge with pH 7 buffer solution is used as a reference system

be very attractive as it avoided the use of glass in the probe, and so the sensing and the reference system were more robust than that used with standard glass electrodes. Titration experiments and step changes in pH also showed a very fast response in aqueous solutions with $T_{90} = 0.33 \pm 0.07$ s pH^{-1} and response times of 0.44 ± 0.9 s pH^{-1}, much shorter than the values reported earlier (see section *3.1.3*) for similar experiments but using a Ag/AgCl reference electrode.

3.3.2. Tests in non-aqueous systems

This new design of probe allowed the use of a reference solution in the reference chamber of the same kind as the test sample. This would overcome the problem of phase boundary potentials between immiscible phases and typical of acidity measurements in non-aqueous environments. However, other problems with huge drifts and noise in the response were faced when the new total iridium oxide probe was tried in non-aqueous systems. *Figure 5.16* shows the results obtained with a step addition of dichloroacetic acid to ethanol. In this experiment 6 additions of 50 µl of dichloroacetic acid were made into 100 ml of ethanol in a temperature controlled reactor used to maintain a constant temperature of 20°C . A solution made up with 100 ml of ethanol and 6x50 µl of dichloroacetic acid was used as the electrolyte in the salt bridge where the reference electrode NTE2 was immersed. The response of the sensing electrode, NTE3, was measured with respect to NTE2 using the Solomat system. A preconditioning of 10 minutes prior to the start of the experiment with medium stirring (approx. 125 r.p.m.) was used before the experiment. The stirring was maintained during the test. The electrolyte solution in the salt bridge was not changed between replicates as preliminary tests showed that the use of a fresh electrolyte solution did not have any effect in the measurements.

The figure shows how the probe was capable of detecting the step changes in acidity and could distinguish between samples with different concentration of acid. However, the problem of noise and drifts in the response made difficult the calibration of the response. *Figure 5.17* shows the calibration graph obtained in the experiment when the effect of noise was partially eliminated by averaging the signals obtained for each step addition. Therefore, the large error bars observed in the figure are almost exclusively due to the drift in the response observed between replicates. The

magnitude of the error did not allow a good differentiation between samples with different acid concentration, especially at high concentration where the response varied very little with the acidity. Further tests in non-aqueous systems also showed similar trends to those of the glass electrode in step addition of acids in alcohol and alcohol-toluene mixtures. However, huge drifts in the response were observed for the total iridium oxide probe. The glass electrode also showed unstable responses and drifts when little acid was present in the non-aqueous solvent. When the acidity and conductivity in the solution were higher after further additions of dichloroacetic acid, the response was very reproducible for the glass electrode, although quite slow and noisy. These results made it necessary to perform further studies on the stability of the signal coming from the new probe before doing more experiments in non-aqueous systems.

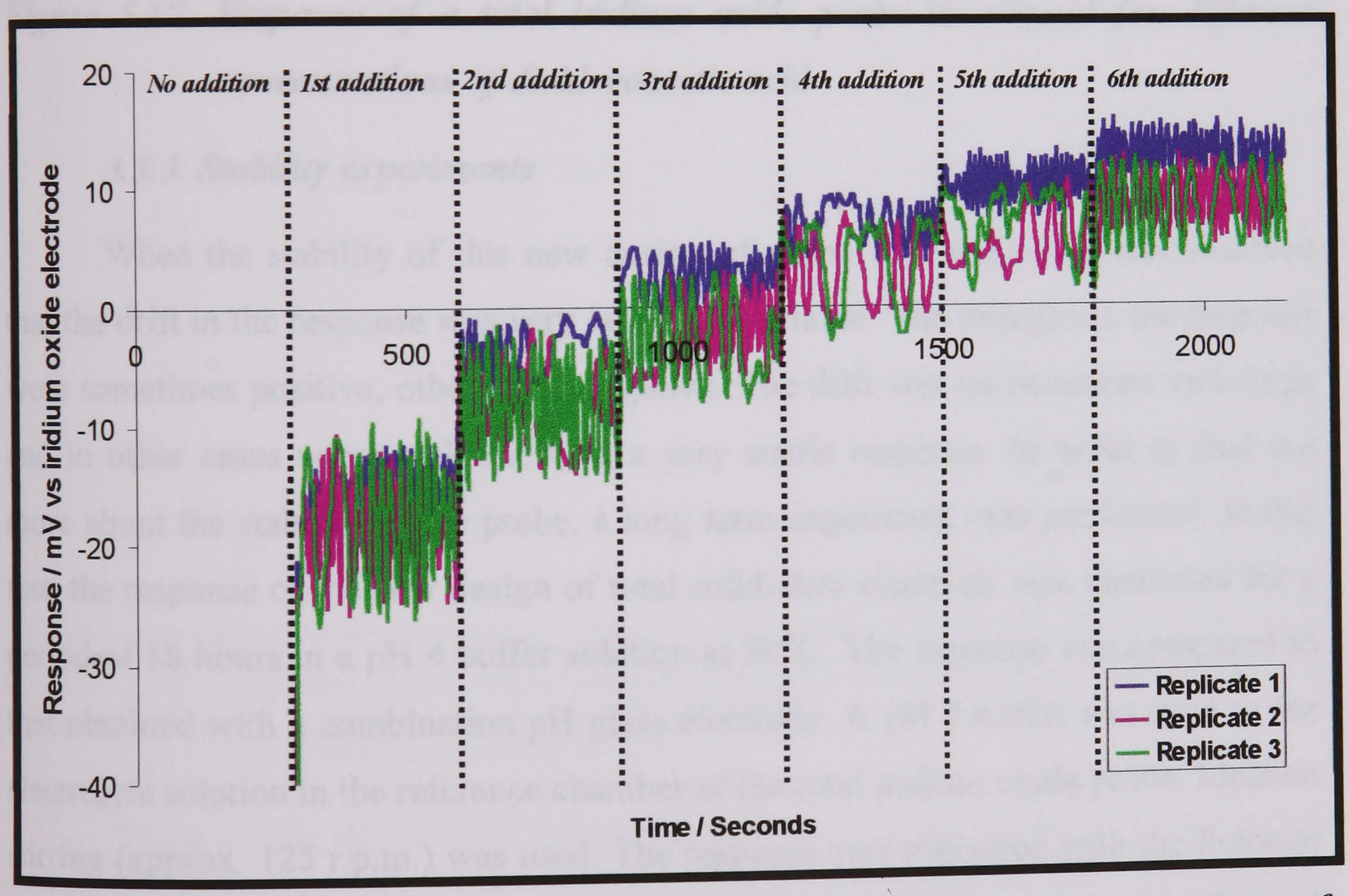

Figure 5.16. Response of a total iridium oxide probe to step additions of dichloroacetic acid to ethanol at 20°C

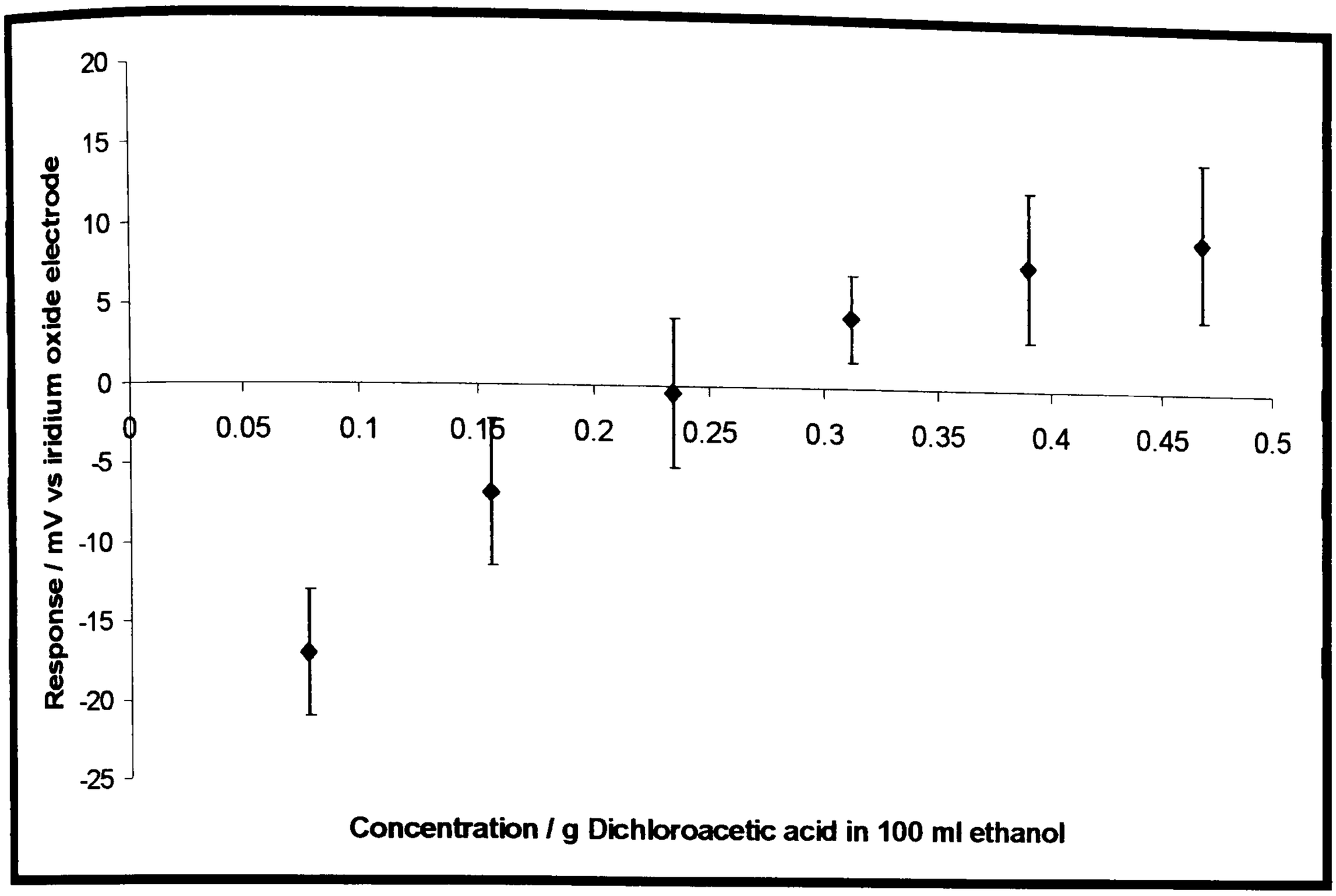

Figure 5.17. Response of a total iridium oxide probe in ethanol for different concentrations of dichloroacetic acid

3.3.3. Stability experiments

When the stability of this new design of probe was studied, it was observed that the drift in the response was very large and variable. The changes in the response were sometimes positive, other times negative. The drift was on occasions very large and in other cases very small showing a very stable response. In order to find out more about the stability of the probe, a long term experiment was performed. In this test, the response of the new design of total solid-state electrode was monitored for a period of 18 hours in a pH 4 buffer solution at 30°C. The response was compared to that obtained with a combination pH glass electrode. A pH 7 buffer was used as the electrolyte solution in the reference chamber of the total iridium oxide probe. Medium stirring (approx. 125 r.p.m.) was used. The response was measured with the Solomat system with a sampling acquisition time of 5 min. The sensors were preconditioned in the solution at 30°C for at least 12 hours before the start of the experiment.

Figure 5.18 shows the results obtained in one of the replicate experiments of the test. It is observed how the response drifted significantly describing a cycle between –100 and 100 mV (potential versus the iridium oxide electrode used as a

reference). On the other hand, the glass electrode produced a constant reading of pH 3.89 ± 0.02 during the whole experiment. The variable drift in the response of the total iridium oxide probe explained why in some experiments little variations of the response were observed whereas in other tests large drifts were seen. It also proved why, in experiments involving a change in the temperature, poor precision in the results was obtained due to big drifts in the response, especially at high temperatures. When the experiment was repeated the results showed the same variable drift with an increasing and decreasing response around the same limits. However, the kinetics of the process were different and the cycle normally took longer than 18 hours with long flat areas alternating big changes in the response.

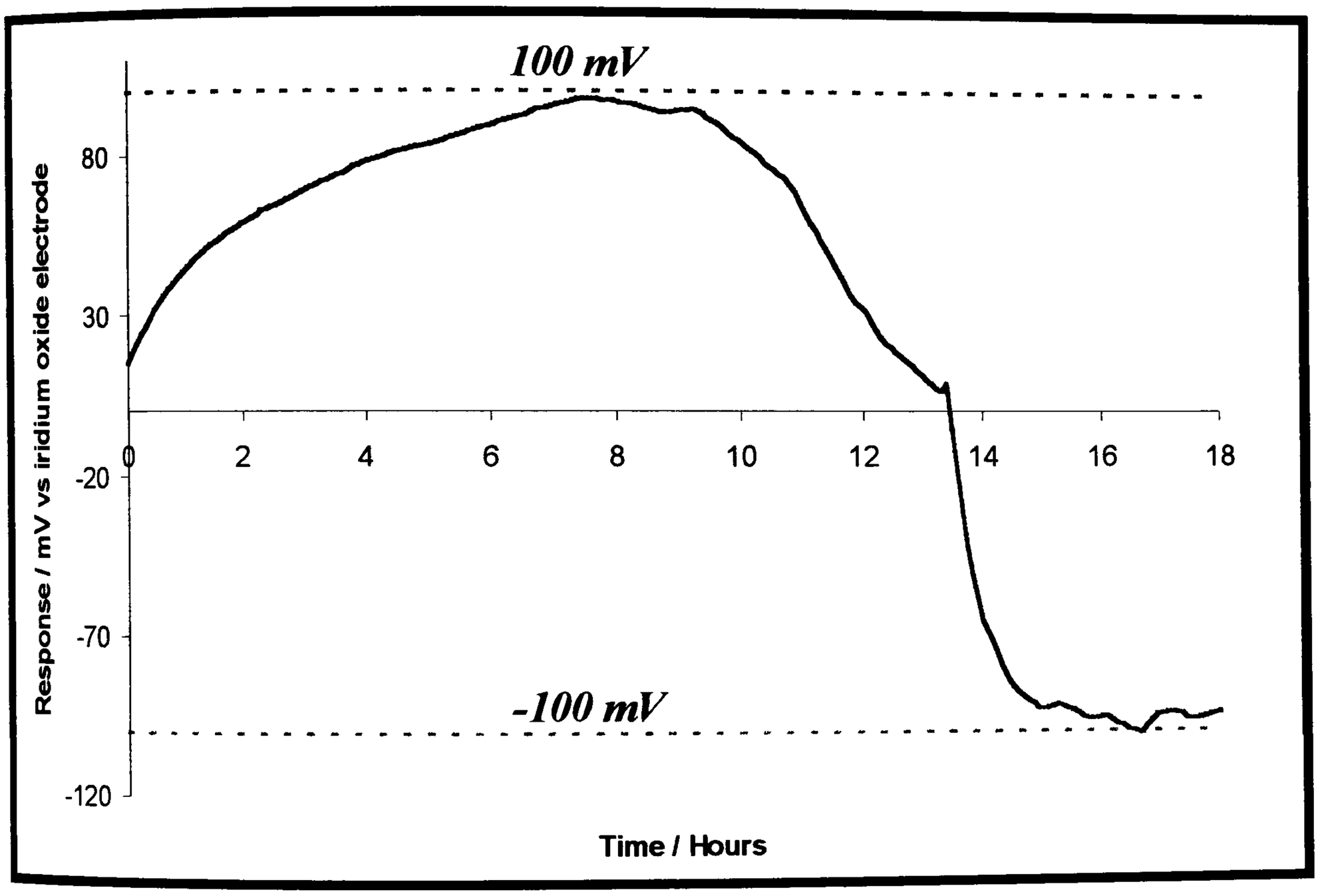

Figure 5.18. Change of the response with time for a total iridium oxide probe in a pH 4 buffer solution at 30°C

These results showed that further development work needs to be carried out to overcome the problems of instability observed in this design of total iridium oxide probe. As the potential[84] for the couple Ir_2O_3/Ir is 0.1 V, it seems as if in the new design of a total iridium oxide probe both the sensing and the reference electrodes are charged and discharged in cycles. This problem needs to be solved before the probes are developed for industrial applications.

3.4. Advantages in the use of solid state sensors

In conclusion, the tests performed with the iridium oxide sensors showed how the drift in the response is still the largest problem to overcome in the development of these electrodes. This problem was especially important in the new design of a total iridium oxide probe presented in this chapter. However, the results obtained encouraged further development work in this area as they had a number of interesting features:

- Iridium oxide sensors allow the measurement of pH in high temperature conditions where glass electrodes cannot be used.
- The solid-state sensors showed a faster and less noisy response than the glass electrode, which could be very interesting in analysis and control of very fast processes involving changes in the acidity.
- At high pH conditions the iridium oxide sensors behave well and do not produce the alkaline errors typical of the glass electrodes.
- In non-aqueous systems, the iridium oxide electrodes have shown similar characteristics to the glass electrode for responses to changes of acidity. They have also proved to be superior to the extensively used combination glass electrode, whose reference system gets easily damaged in non-aqueous environments.
- Finally, preliminary tests with a new design of total iridium oxide probe showed promising results. Provided the problem of the drift is solved, this new probe could be very useful in conditions of temperature and pressure where other reference systems cannot be used.

In addition to these advantages, solid-state iridium oxide electrodes can be miniaturised and used in conjunction with reduced reference systems to fabricate microsensors[9,43]. Some authors[85] have produced AIROF iridium oxide electrodes with diameters lower than 25 μm. On the other hand, the glass electrode is difficult to miniaturise[8] although some micro glass electrodes have been constructed and tested[86], but with non-Nernstian and non-linear response to changes with pH.

These possibilities have produced new trends on the development of pH probes. Now, the sensor industry has started focussing in the development of metal oxide pH sensors based on iridium that could outperform glass and other metal oxide electrodes in the market[67]. Even in the design of new pH transmitters and displays new trends in pH sensing are being considered as they are now constructed to be compatible for both glass electrodes and solid-state iridium oxide sensors[87].

4. References

1. M. J. Tarlov, K. G. Kreider, S. Semancik and P. Huang, *pH sensors based on iridium oxide,* AIChE Symposium Series No. 267, 85, 36-41.
2. K. Kreider, 1991, *Iridium oxide thin-film stability in high-temperature corrosive solutions,* Sensors and Actuators B, 5, 165-169.
3. B. G. Lipták, 1994, *Analytical Instrumentation*, Chilton Book Company, Pennsylvania, USA.
4. P. VanHoudt, Z. Lewandowski and B. Little, 1992, *Iridium oxide pH microelectrode*, Biotechnology and Bioengineering, 5, 601-608.
5. D. Midgley, 1990, *A review of pH measurement at high temperatures,* Talanta, 37, 767-781.
6. M. Hitchman and S. Ramanatham, 1988, *Evaluation of iridium Oxide electrodes formed by potential cycling as pH probes,* Analyst, 113, 35-39.
7. K. G. Kreider, M. J. Tarlov and J. P. Cline, 1995, *Sputtered thin-film pH electrodes of platinum, palladium, ruthenium, and iridium oxides*, Sensors and Actuators B, 28, 167-172.
8. M. F. Teixeira, F. C. Moraes, O. Fatibello-Filho, L. C. Ferracin, R. C. Rocha-Filho, and N. Bocchi, 1999, *A novel λ-MnO_2-based graphite-epoxy electrode for potentiometric determination of acid and bases,* Sensors and Actuators B, 56, 169-174.
9. Diamond General development Corporation, Internet web page, 2001, *Diamond General Catalogue*, http://www.diamondgeneral.com/pdf/catalog/page20.pdf
10. J. A. Mihell and J. K. Atkinson, 1998, *Planar thick-film pH electrodes based on ruthenium dioxide hydrate*, Sensors and Actuators B, 48, 505-511.
11. S. A. M. Marzouk, S. Ufer, R. P. Buck, T. A. Johnson, L. A. Dunlap and W. E. Cascio, 1998, *Electrodeposited iridium oxide pH electrode for measurement of extracellular myocardial acidosis during acute ischemia*, Analytical Chemistry, 70, 5054-5061.
12. M. J. Tarlov, S. Semancik and K. G. Kreider, 1990, *Mechanistic and response studies of iridium oxide pH sensors*, Sensors and Actuators B, 1, 293-297.
13. K. Kinoshita and M. J. Madou, 1984, *Electrochemical measurements on Pt, Ir, and Ti oxides as pH probes,* Journal of The Electrochemical Society, 131, 1089-

1094.

14. M. L. Hitchman and S. Ramanathan, 1992, *Thermally grown iridium oxide electrodes for pH sensing in aqueous environments at 0 and 95° C*, Analytica Chimica Acta, 263, 53-61.

15. G. Papeschi, S. Bordi, C. Beni and L. Ventura, 1976, *Use of an iridium electrode for direct measurement of pH of proteins after isoelectric focusing in polyacrylamide gel,* Biochimica et Biophysica Acta, 453, 192-199.

16. W. Olthuis, M. A. M. Robben, P. Bergveld, M. Bos and W. E. Van der Linden, *pH sensor properties of electrochemically grown iridium oxide*, Sensors and Actuators B, 2, 247-256.

17. L. D. Burke, J. K. Mulcathy and D. P. Whelan, 1984, *Preparation of an oxidised iridium electrode and the variation of its potential with pH,* Journal of Electroanalytical Chemistry, 163, 117-128.

18. B. E. Conway and J. Mozota, 1983, *Surface and bulk processes at oxidised iridium electrodes I,* Electrochimica Acta, 28, 1-8.

19. K. Kreider, 1986, *Summary abstract: IrO_2 radio frequency sputtered thin film properties,* Journal of Vacuum Science and Technology A, 4, 606-607.

20. L. M. Schiavone, W. C. Dautremont-Smith, G. Beni and J. L. Shay, 1979, *Electrochromic iridium oxide films prepared by reactive sputtering,* Applied Physics Letters, 35, 823-825.

21. R. Sanjinés, A. Aruchamy and F. Lévy, 1989, *Thermal stability of sputtered iridium oxide films,* Journal of The Electrochemical Society, 136, 1740-1743.

22. S. Ardizzone, A. Carugati and S. Trasatti, 1981, *Properties of thermally prepared iridium dioxide electrodes,* Journal of Electroanalytical Chemistry, 126, 287-292.

23. J. Augustynski, M. Koudelka, J. Sanchez and B.E. Conway, 1984, *ESCA study of the state of iridium and oxygen in electrochemically and thermally formed iridium oxide films,* Journal of Electroanalytical Chemistry, 160, 233-248.

24. B. E. Conway and J. Mozota, 1983, *Surface and bulk processes at oxidised iridium electrodes II,* Electrochimica Acta, 28, 9-16.

25. V. Birss, R. Myers, H. Angerstein-Kozlowska and B. E. Conway, 1984, *Electron microscopy study of formation of thick oxide films on Ir and Ru electrodes,* Journal of The Electrochemical Society, 131, 1502-1510.

26. P. J. Kinlen, J. E. Heider, and D. E. Hubbard, 1994, *A solid-state pH sensor based on a Nafion-coated iridium oxide indicator electrode and a polymer-based silver chloride reference electrode,* Sensors and actuators B, 22, 13-25.

27. Centre for Neural Communication Technology, Internet web page, 2000, *Iridium activation*, http://www.engin.umich.edu/facility/cnct/activ.html

28. P. Häring, R. Kötz, G. Repphun, O. Haas and H. Siegenthaler, 1998, *In situ scanning probe microscopy investigations of electroactive films*, Applied Physics A, 66, S481-S-486.

29. M. Pourbaix, 1966, *Atlas of electrochemical equilibria in aqueous solutions*, Pergamon Press, Oxford, UK.

30. M. Hitchman and S. Ramanatham, 1992, *A field-induced poising technique for promoting convergence of standard electrode potential values of thermally oxidised iridium pH sensors,* Talanta, 39, 137-144.

31. K. Pásztor, A. Sekiguchi, N. Shimo, N. Kitamura and H. Masuhara, 1993, *Iridium oxide-based microelectrochemical transistors for pH sensing*, Sensors and Actuators B, 12, 225-230.

32. P. J. Kinlen, J. E. Heider and D. E. Hubbard, 1994, *A solid-state pH sensor based on a Nafion-coated iridium oxide indicator electrode and a polymer-based silver chloride reference electrode*, Sensors and Actuators B, 22, 13-25.

33. Hendrikse, W. Olthuis and P. Bergveld, 1998, *A method of reducing oxygen induced drift in iridium oxide pH sensors*, Sensors and Actuators B, 53, 97-103.

34. M. Hitchman, 1977, *Analysis of equilibrium potentials of hydrogen tungsten bronzes,* Journal of Electroanalytical Chemistry, 85, 135-144.

35. G. K. Wertheim and H. J. Guggenheim, 1980, *Conduction-electron screening in metallic oxides: IrO_2,* Physical Review B, 22, 4680-4683.

36. G. Papeschi, S. Mergliano, G. Zaninotto, M. Baessato, E. Ancona and M. Larini, 1984, *The iridium/iridium oxide electrode for in vivo measurement of oesophageal and gastric pH,* Journal of Medical Engineering and Technology, 8, 221-223.

37. S. Gosttesfeld and J. D. E. McIntyre, 1979, *Electrochromism in anodic Iridium oxide films,* Journal of The Electrochemical Society, 131, 742-750.

38. M. L. Hitchman and S. Ramanathan, 1991, *Potentiometric determination of proton activities in solutions containing hydrofluoric-acid using thermally*

oxidised iridium electrodes, Analyst, 116, 1131-1133.

39. E. Kinoshita, F. Ingman, G. Edwall and S. Thulin, 1986, *Polycrystalline and monocrystalline antimony, iridium and palladium as electrode material for pH-sensing electrodes,* Talanta, 33, 125-134.

40. PDII-LIPI Indonesia, Internet web page, 2001, *Corrosion 54: 1 (JAN 1998) Materials Science & Engineering*, http://www.pdii.lipi.go.id/ weblm/pdii-lipi/milne1/ cor2.htm

41. Utah State University, Internet web page, 2001, *The combination pH electrode*, http://www.chem.usu.edu/faculty/sbialkow/Classes/3600/Overheads/pH/ionselctive.html

42. EIC laboratories Ltd. Internet web page, 2001, *Activated iridium oxide and thermal iridium oxide: use in animal studies and in vivo stability*, http://www.eiclabs.com/Iridium%20Oxide%20Medical%20Electrode%20Literature.pdf

43. H. Suzuki, T. Hirakawa, S. Sasaki and I. Karube, 1998, *Micromachined liquid-junction Ag/AgCl reference electrode,* Sensors and Actuators B, 46, 146-154.

44. Southern biochemical engineering conference,Internet web page,2001, *S. A Grant et al. Development of fiber optic and electrochemical pH sensors to monitor brain tissue*, http://sbec.abe.msstate.edu/1999/abstracts/077.html

45. The University of North Carolina, Internet web page, 2001, *UNC scientists invent new way to measure acid level of body fluids*, http://www.unc.edu/news/ newsserv/research/acid.htm

46. Electrosynthesis company incorporated, Internet web page, 2001, *The electrochemistry of gases: New sensing opportunities*, http://www.electrosynthesis. com/news/ w2content.html

47. Mechanical engineering magazine, Internet web page, 2001, *Recording oil's vital signs*,
http://www.memagazine.org/backissues/may99/features/vitalsigns/vitalsigns.html

48. Cormet testing systems, Internet Web Page, 2000, *High temperature electrodes*, http://www.cormet.fi/trend/hightemp.html

49. W. Olthuis, J. C. Van Kerkhof, P. Bergveld, M. Bos and W. E. Van der Linden, 1991, *Preparation of iridium oxide and its application in sensor-actuator systems*,

Sensors and Actuators B, 4, 151-156.

50. D. J. G. Ives and G. J. Janz, 1961, *Reference electrodes: theory and practice,* Academic Press, London, UK.

51. H. Galster, 1991, *pH measurement: fundamentals, methods, applications, instrumentation,* VCH Publishers, New York, USA.

52. Complete catalogue Metrosensor electrodes, 1999, Metronhm U.K., Switzerland.

53. S. Bordi, M. Carlà and G. Papeschi, 1984, *Iridium/iridium oxide electrode for potentiometric determination of proton activity in hydroorganic solutions at sub-zero temperatures,* Analytical Chemistry, 56, 317-319.

54. K. Izutsu and H. Yamamoto, 1996, *Response of an iridium oxide pH-sensor in nonaqueous solutions. Comparison with other pH sensors,* Analytical Sciences, 12, 905-909.

55. D. Mamman, 1999, *Personal communications* (development of iridium oxide solid-state sensors), Department of Pure and Applied Chemistry, University of Strathclyde, Glasgow, UK.

56. Sermatech-Ethylene corporation, Internet web page, 2001, *Ethylamor in-line pH probe*, http://www.ethylenecorp.com/inline_probe.htm

57. A. Kennedy, 2001, *Personal communications* (design and construction of a new total iridium oxide pH probe), Department of Pure and Applied Chemistry, University of Strathclyde, Glasgow, UK.

58. M. Weerasinghe, 2000, *Personal communications* (use of Labview for monitoring the response of iridium oxide sensors), Industrial Control Centre, University of Strathclyde, Glasgow, UK.

59. T. R. Barben, 1969, *Industrial pH measurement,* Instruments and control systems, 41, 85-86.

60. D. May and G. Kalis, 1987, *Practical points for pH and redox monitoring,* Chemistry and Industry, 1, 77-78.

61. M. Park, 2001, *Personal communications* (use of the Solomat system to monitor the signal from glass and solid-state electrodes), Department of Pure and Applied Chemistry, University of Strathclyde, Glasgow, UK.

62. D. Littlejohn, 2000, *Personal communications* (development of iridium oxide solid-state sensors), Department of Pure and Applied Chemistry, University of

Strathclyde, Glasgow, UK.

63. M. L. Hitchman, 2000, *Personal communications* (development of iridium oxide solid-state sensors), Department of Pure and Applied Chemistry, University of Strathclyde, Glasgow, UK.
64. G. Tauber, 1984, *pH glass electrodes for high temperature and high pH applications,* Process automation, 51-58.
65. G. Meinrath, and P. Spitzer, 2000, *Uncertainties in determination of pH,* Mikrochimica acta, 135, 155-168.
66. Brinkmann group, Internet web page, 2001, *The background of pH measurement and hints for your daily work,* http://www.brinkmann.com/brink2001/pdf/pH-background.pdf
67. Sensors, Internet web page, 2001, *Sensor industry developments and trends,* http://www.sensorsmag.com/resources/businessdigest/sbd0900.shtml
68. W. A. Walker, 1979, *Preliminary studies in dynamics of pH electrodes in neutralisation vessels,* Australian conference on control engineering, 98-102.
69. R. Feeney and S. P. Kounaves, 1999, *Determination of heterogeneous electron transfer rate constants at microfabricated iridium electrodes,* Electrochemistry Communications 1, 453-458.
70. HANNA instruments, Internet web page, 2001, *Temperature-resistance correlation for HANNA pH sensitive glass,* http://www.hannainst.com/products/electro/techover.htm
71. Notes in chemistry, Internet web page, 2001, *The Nernst equation and electrode function,* http://www.sensorsmag.com/resources/businessdigest/sbd0900.shtml
72. K. Schwabe, 1979, *Behaviour of pH-glass electrodes in strongly acid and non-aqueous solutions,* Acta IMEKO, 529-534.
73. bat4pH downloads, Internet web page, 2001, *pH frequent asked questions,* http://www.bat4ph.com/images/faqs.pdf
74. L. MacPherson, 1995, *Properly measure ions in solution,* Chemical Engineering Progress, February, 54-57.
75. A. Beliustin, A. M. Pisarevsky, G. P. Lepnev, A. S. Sergeyev and M. M. Shultz, 1992, *Glass electrodes: a new generation,* Sensors and Actuators B, 10, 61-66.
76. The minerals, metals & materials society, Internet web page, 2001, *P. I. Gouma et*

al. Microstructural characterization of sensors based on electronic ceramic materials, http:/www.tms.org/pubs/journals/ JOM/9811/Gouma/Gouma9811.html

77. G. M. Chernysheva, I. M. Kutyrev and N. N. Basargin, 1997, *Buffer solutions for a standard scale of acidity in toluene-ethanol media,* Journal of Analytical Chemistry, 52, 730-735.

78. Mailgate newsgroup, Internet web page, 2001, *pH in non-aqueous media,* http://www.mailgate.org/sci/sci.chem.electrochem/msg00703.html and http://www.mail gate.org/sci/sci.chem.electrochem/msg00704.html

79. D. J. Clarke, D. J. Schiffrin and M. C. Wiles, 1989, *A tetraphenylborate internal reference electrode for immiscible electrolyte solutions and ion selective electrodes,* Electrochimica Acta, Vol. 34 No. 6, 767-769.

80. F. Tedjar, and L. Zerroual, 1990, *"All solid" pH sensor,* Sensors and Actuators B, 2, 215-217.

81. L. Zerroual and L. Telli, 1995, *Application of a proton-conducting electrolyte for a pH sensor,* Sensors and Actuators B, 24-25, 741-743.

82. P. Bergveld, 1972, *Development, operation, and application of the Ion-Sensitive Field-Effect Transistor as a tool for electrophysiology,* IEEE Transactions on Biomedical Engineering, Vol. BME-19 No. 5, 342-351.

83. K. L. King, 1974, *Electrode systems pass the acid test,* Instruments and Control Systems, 47, 69-70.

84. R. C. Weast, 1982, *CRC Handbook of Chemistry and Physics*, CRC Press Inc. Florida, USA.

85. Pittcon conference 2001, Internet web page, 2001, *A microparticle iridium oxide pH microelectrode for SECM*, http://pittcon.omnibooksonline.com/2001/papers /1624P.pdf

86. H. Suzuki and A. Sugama, 1994, *Micromachined glass electrode*, Sensors and Actuators B, 20, 27-32.

87. TBI-Bailey group, Internet web page, 2001, *Advantage series two-wire pH/ORP/plon transmitter*, http://www.tbi-bailey.com/ph_analyzer/pdf/S_tb82.pdf

CHAPTER 6

CONCLUSIONS AND FURTHER WORK

1. Sampling studies: fast loops for on-line NMR

1.1. Conclusions

A literature review was carried out to determine the factors that determine the sample collection from stirred vessels. It was found that good selection of the sampling velocity and the dimensions and orientation of the sampling probe are crucial to achieve representative sampling. Also, the flow-patterns and stirring conditions inside the vessel need to be studied in order to optimise the orientation of the sampling probe and improve mixing. Attending to all these considerations, a fast sampling loop system was designed and built. The device was intended to provide a continuous flow of adequately representative heterogeneous samples needed for the on-line implementation of a low-field NMR spectrometer.

In the fast sampling system the probe was placed horizontally at the stirrer plane between the wall and the stirrer blades. The number of fittings and changes of direction in the sampling lines were kept to a minimum in order to increase representativeness in the sample collection. Physical modelling studies in the system investigated how the physical variables affected the sample collection using the fast sampling loop. It was found that the stirring conditions in the vessel were the most important physical variable affecting sampling. It is therefore important to ensure good mixing conditions in the reactor with a suitable choice of stirrer and baffle configurations. Once the optimum conditions are assured, a detailed study of the flow patterns inside the vessel is needed in order to choose the optimum orientation for the sampling probe, which should be parallel to the flow streamlines. In this work, the study of the flow-patterns was based on published information and measurements of pressure at different points. The results obtained confirmed both that the stirrer plane is the optimum sampling location and that the best orientation of the probe is horizontally. The sampling velocity was not found to be as a important variable affecting the sample collection as the mixing conditions, position and orientation of the sampling probe. It was concluded that superisokinetic sampling conditions offer the best compromise between adequately representative sampling and small dead times in the sample collection. Therefore, a fast sampling flow-rate was used in the final version of the loop, avoiding the use of flow-meters in the lines that could be

likely blockage points when working with heterogeneous systems.

The sampling device was successfully tested and calibrated with heterogeneous mixtures of glass beads in water and heating oil in water. The systems with particles in suspension were found to be more challenging from the sampling point of view as the sample collection depended more on variables such as the location of the probe and the stirring conditions. Finally, the use of the sampling loop produced considerable heat losses in tests at high temperatures and also a release of heat due to friction observed in experiments at low temperatures.

In the chemical modelling experiments with the loop the homogeneous process of esterification of crotonic acid was used. It was found that the effect of the loop on the chemistry of the process can be easily modelled by defining the new kinetic conditions with the use of the sampling system. It was also concluded that this effect is normally associated with an increase in the rate of the reaction produced by an enhancement of the mixing conditions in the system, mainly due to the use of a pumping device. In addition to these findings, the kinetic model and thermodynamic parameters for the crotonic acid esterification reaction and the heat exchange properties of the reactor system were determined. Therefore, the chemical study of the esterification process also assisted the control engineering work carried out in the CPACT projects.

A low-field NMR instrument was successfully implemented in a secondary loop that conditioned the sample to render it to the spectrometer at appropriate flow conditions. Tests with challenging heterogeneous systems (e.g. toluene-water mixtures) showed that the secondary line delivered adequately representative samples to the NMR instrument provide the flow-rate in the line was higher than 50 ml/min. Lower flow-rates allowed for the separation of the phases inside the NMR line. In addition to this, the NMR analysis of different mixtures of toluene and water showed reproducible results that could be calibrated provided the concentration of toluene in the mixture was high enough to overcome the detection limits of the instrument.

In summary, based on a literature survey and empirical tests, the procedures needed for an optimum design and modelling of sampling systems for stirred vessels were defined. This methodology was not fulfilled by any of the prototypes of

sampling systems for reactor vessels that were found in the market. Moreover, the procedure was successfully used for the optimum design of a fast sampling loop towards the on-line implementation of a low-field NMR spectrometer.

1.2. Further work

Following the procedure to design, test and develop sampling systems described in this thesis, the performance of any sampling device for chemical reactors can be assessed and improved. In addition to this, if the sample collection in the 5-L reactor needs to be improved, the mixing conditions in the system have to be enhanced. This could be done by implementing baffles and new stirrer designs into the reactor vessel. If possible, the use of modern laser doppler anemometry (LDA) techniques[1] and computational fluid dynamics (CFD) predictions[2] should be used to asses the quality of the stirring. LDA and CFD could also be used to study the flow-streamlines in the system and therefore define the best position and orientation for the sampling probes[3].

As every system is different in terms of heterogeneity and mixing properties, the physical modelling experiments covered in this work could also be performed in other heterogeneous mixtures of interest. Also, the effect of a particular sampling system on the chemical evolution of a particular process could be evaluated following the guidelines outlined in this thesis. Again, CFD simulations could be used to predict the effect of mixing on the kinetics of the process and compare the values obtained with the empirical kinetic model[4]. For this, it would be necessary to use a better established processes than the esterification of itaconic acid reaction. Unfortunately, this esterification reaction was not well established, especially from the analytical point of view. With the use of well established processes the published information about the reaction could be compared with the experimental findings.

The fast sampling loop could be used for further studies on the on-line implementation of a low-field NMR spectrometer[5]. Although from the sampling point of view the performance of the NMR sampling line was proved to be satisfactory, no experiments involving reactive systems were performed with the NMR instrument on-line because of lack of time. However, the use of reactive processes would have only been of interest from the sampling and engineering point of view if the reaction was

heterogeneous. As the crotonic acid esterification was homogeneous and the itaconic acid esterification was analytically not well established, the on-line NMR monitoring tests with heterogeneous reactions were left out for further work.

The use of the fast sampling loop for adequately representative sample collection from stirred vessels could also be of interest for the on-line use of other analytical techniques with heterogeneous processes[6]. This interest comes from the fact that the fast loop transfers a mixture from a chaotic turbulent system where the flow patterns are not well defined and vary with time, to a straight pipe where the flow streamlines usually have simple and steady patterns. This could therefore be beneficial with heterogeneous systems as different on-line probes could be immersed in the loop instead of inside the reactor, providing more reproducible results and enhancing the performance of a particular analytical technique. Hence, in future work the use of NIR, MIR, Raman and U.V. probes inside the loop and with heterogeneous processes could be assessed and compared with the measurements acquired with the probes inside the reactor.

Finally, all the physical and chemical modelling studies reported in this report could be repeated in the development of sampling systems for other types of systems different to batch reactors. Hence, continuous stirred tank reactors (CSTR), plug flow reactors (PFR) and associations of CSTR and/or PFR could be studied and the effect of, for example, fast sampling loops on kinetics and mixing conditions could be assessed.

2. Discrete samplers: sampling probes for on-line HPLC

2.1. Conclusions

The problem of sampling was presented as the most important obstacle for the reliable on-line use of liquid chromatography. Different designs of automated sampling systems were presented to deliver adequately representative samples from a reactor to, for example, an HPLC system or other on-line analysers where sampling, reaction quenching and dilution are required. The work focussed on the development of the Mark IV probe, which was designed to overcome the size and sealing problems observed in previous prototypes.

An acceptable performance of the probe with %RSD values lower than 5% was achieved when a dead time was implemented in the sequence of events programmed in the system, between the sampling and mixing stages. Problems with diffusion of chemicals were observed when the lines were filled with diluent before sampling. Further changes such as the use of non-return valves and air-flow restrictors did not show any improvements in the performance of the probe when the lines where empty, properly cleaned and flushed before sampling. Finally, it was found that a smaller volume than expected was collected using the Mark IV design. This led us to work in a non-linear range of U.V. absorbances with the diluted samples. Future work should therefore use either more concentrated test solutions or less dilution in the samples in order to overcome this problem.

2.2. Further work

Further work with the sampler prototypes should include the construction and performance of development tests with the Mark III sampler[7]. Also, further tests could be carried out with the Mark IV sampler in order to analyse its performance in heterogeneous systems[8,9]. These experiments would have to be carried out either using solvents that convert almost instantly the sample from a heterogeneous mixture to a homogeneous solution or with disconnecting the probe from the control unit to asses only the collection using the probe. Otherwise, problems with blocking of the lines and separation of phases in the mixing chamber inside the control unit would have to be faced.

The review on sampling included in this report and the experience obtained in the design and development of the fast sampling loop could be used in future designs of better probes. Important factors such as the orientation of the probe, the sampling velocity and the dimensions of the lines were not considered in the design of any of the Mark prototypes. This would give rise to serious difficulties when the samplers needd to be used with heterogeneous processes. In future designs those considerations must be taken into account using similar approaches to that reported by Freitas *et al.*[10]. They considered all the main factors affecting sample collection and developed an isokinetic sampler which was orientated parallel to the flow-streamlines in the process. However, their design was used to measure solids-hold-up in fluidised three-

phase reactors and was not automated or adapted for industrial applications.

Finally, the future trends in industry also have to be considered in the design of new probes and implementation of analytical systems for on-line analysis. In fact, approaches like NeSSI (New Sampling and Sensor Initiative) are becoming of a great interest where it is intended to develop modular process analysers with sampling system components[11,12].

3. Iridium-oxide sensors for pH measurements

3.1. Conclusions

A literature review of the development of solid-state sensors for pH measurements showed that iridium-oxide sensors are one of the most promising alternatives to the use of glass electrodes. Furthermore, previous research in the Chemistry department at Strathclyde showed that thermally grown iridium-oxide sensors offered a good balance between ease of construction and regeneration, and good quality and stability of the response[13].

Based on the good results obtained in previous research in the department and their promising features for pH measurement, new thermally grown iridium oxide electrodes were built and tested. The oven temperature used during the thermal oxidation process was found to be crucial in the construction of the sensors. Two types of iridium-oxide electrodes were constructed and tested using different thickness of iridium wire. Their response was compared to that of a glass electrode, measured with respect to the same reference system. Both types of solid-state sensors showed a good Nernstian response when calibrated in aqueous buffers. Furthermore, their response was faster and less noisy than that of the glass electrode. Also, their use at high temperature did not damage the sensors, overcoming the fragility problems observed with the glass electrodes. In addition to this, the iridium-oxide sensors did not show the alkaline error typically observed with glass electrodes at high pH conditions. Despite all these advantages, the solid-state sensors showed an significant drift in their response unless very long conditioning of the electrodes in the test solution was applied. This drift in the response during the conditioning process was found to be dependent on the temperature and stirring conditions used during the measurements.

In non-aqueous solutions, the iridium oxide sensors showed similar characteristics to the glass electrode with small changes in the response when the acidity was varied. However, the response were again faster for the solid-state sensors, which is a clear advantage in control applications with short time-scale processes. Both the iridium-oxide sensors and the glass electrodes, using a separate reference system and a salt bridge, overcame the problems observed with a combination electrode. However, they also presented difficulties due to phase boundary potentials between the solution and the reference system. To overcome this, a new design of total iridium-oxide probe was presented and successfully tested in aqueous solutions, where it showed a good Nernstian response. However, again the large drifts in the response showed the limitations of the design, especially in non-aqueous systems where the signals varied only slightly with changes in the acidity.

In summary, there are advantages in the use of iridium-oxide sensors that encourage their development. Unfortunately, there also exist disadvantages that indicate that further improvements need to be made before they could be reliably used in industrial applications. The future development work to be carried out with the sensors should be focussed on improving the stability of their response and reducing the conditioning time needed by the iridium-oxide electrodes.

3.2. Further work

As mentioned earlier, the stability measurements performed in this work did not give the expected good results according to the findings obtained by other researchers in this department[13]. Therefore, any further work in the development of the iridium-oxide sensors must be focussed on improving the stability of their response and reducing their time of conditioning. A strategy similar to that described by Hitchman *et al.*[14] could be used to avoid the drift in the signals. They proposed a field induced poising technique by which the equilibrium mole fraction of Ir(IV) and Ir(III) oxides is reached in the sensors with the use of a charge injection procedure. Another alternative such as the formation of complex compounds with the iridium species were analysed in order to achieve a constant mole fraction of the two oxides. However, no information was found in the literature on any substances that could lead to the formation of stable complex compounds with the iridium species when in

contact with the iridium-oxide coating.

Other authors blamed the large variations in the response on the redox interferences that the iridium-oxide sensors can experience[15]. They proposed the use of permselective membranes to coat the electrodes and overcome the problem of the drift in the response. However, this improvement in the stability with the use of the membrane is normally associated with an increase of the response time, which can be a problem in the monitoring of fast processes.

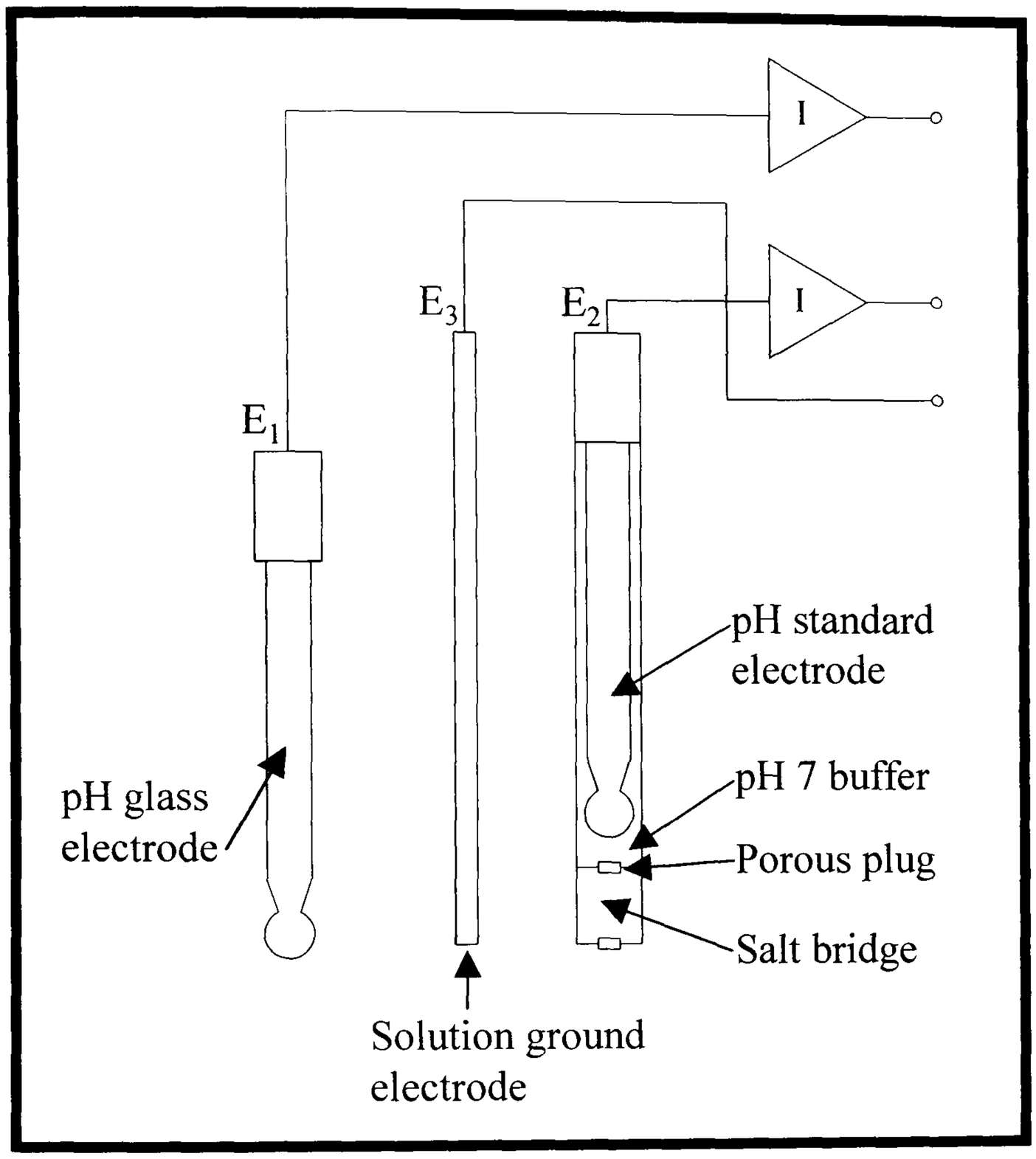

Figure 6.1. Differential electrode system designed by K. L. King[17]

The performance of the total iridium-oxide probe could also be improved by the use of a solution ground electrode. A solution ground is a corrosive resistant conductive material in contact with the specimen fluid to provide a ground path to the indicator/transmitter, usually through the sensor and by wire through the sensors cable[16]. In the differential electrode described by K. L. Kings, a third metallic solution ground electrode was also used in conjunction with the two glass electrodes[17]. The pH in the system was a function of the difference in the signals between the glass electrodes, which were measured with respect to this electrode. In other words:

$pH = f[(E_1-E_3)-(E_2-E_3)] = f(E_1-E_2)$ where E_1, E_2 were the signals coming from the glass electrodes and E_3 was the voltage coming from the solution ground electrode (see *Figure 6.1*). A similar ground system in the total iridium-oxide probe could be a way to sort out the stability problems observed in their response as the ground electrode would experience interfering redox reactions. This would improve the stability of the sensors avoiding the huge drifts that otherwise are normally observed in the signals.

Another interesting use of the solid-state sensors could be in the pH monitoring of high-purity water[18]. This is of great importance in industry to prevent corrosion of extremely expensive components. The pH measurement of high-purity water can be very difficult due to its high specific resistance. The low conductivity of the water produces a high electrical resistance between electrodes. As a consequence the measurement is more sensitive to electrical noise and static electric pickup. In addition, the flow of high-purity water through plastic tubes can generate its own static charge. Any of these effects produce a voltage gradient between the measurement and reference electrodes that affects the reading of pH[19]. As plastic and glass are insulators, the electrode materials and geometry of the pH probe also have an effect on these voltage gradients. The use of iridium-oxide sensors could improve pH measurement in high-purity water as they have lower impedance than glass electrodes and the metallic surfaces produce very little static charge[20].

4. References

1. P. Mavros, C. Xuereb and J. Bertrand, 1996, *Determination of 3-D flow fields in agitated vessels by Laser-Doppler Velocimetry: Effect of impeller type and liquid viscosity on liquid flow patterns*, Trans. IChemE. Part A, 74, 658-668.
2. Y. Xu and G. McGrath, 1996, *CFD predictions of stirred tank flows*, Trans. IChemE., 74a, 471-475.
3. A. Bakker, J. B. Fasano and K. J. Myers, 2000, *Effects of flow pattern on the solids distribution in a stirrer tank*, http:www.bakker.org/cfmbook/solids.pdf
4. A. Bakker and J. B. Fasano, 2000, *Turbulent mixing and chemical reaction in stirred tanks*, http:www.bakker.org/cfmbook/reaction.pdf
5. A. Nordon, 2001, *Personal Communications (future work in the area of on-line NMR)*, Department of Pure and Applied Chemistry, University of Strathclyde, Glasgow, UK.
6. D. Littlejohn, 2001, *Personal communications*, (*future applications of the fast sampling loop*), Department of Pure and Applied Chemistry, University of Strathclyde, Glasgow, UK.
7. N. Holmes, 2001, *Personal communications*, (*construction and future work with the Mark III probe*), BP Chemicals, Grangemouth, UK.
8. K. Meney, 2001, *Personal communications*, (*future work testing the Mark prototypes in heterogeneous systems*), Avecia, Grangemouth, UK.
9. B. Grieve, 2001, *Personal communications*, (*industrial interest in the development of automated discrete samplers*), Syngenta, Grangemouth, UK.
10. C. Freitas, A. A. Vicente, M. Mota and J. A. Teixeira, 1997, *A new sampling device for measuring solids hold-up in a three-phase system,* Biotechnology Techniques, Vol. 11 No. 7, 489-492.
11. R. Dubois, F. Saskatchewan, and P. van Vuuren, 2001, *Citius, Altius, Fortius: A new sampling/sensor initiative (NeSSI)*, Oral presentation at the fifteenth international forum of process analytical chemistry IFPAC-2001, Amelia Island, Florida, USA.
12. J. Gunnell, 2001, *New sensor/sampling initiative*, Oral presentation at the CPACT conference in advances in process analytics and control, Glasgow, UK.
13. M. L. Hitchman and S. Ramanathan, 1992, *Thermally grown iridium oxide*

electrodes for pH sensing in aqueous environments at 0 and 95° C, Analytica Chimica Acta, 263, 53-61.

14. M. Hitchman and S. Ramanatham, 1992, *A field-induced poising technique for promoting convergence of standard electrode potential values of thermally oxidised iridium pH sensors,* Talanta, 39, 137-144.
15. P. J. Kinlen, J. E. Heider and D. E. Hubbard, 1994, *A solid-state pH sensor based on a Nafion-coated iridium oxide indicator electrode and a polymer-based silver chloride reference electrode*, Sensors and Actuators B, 22, 13-25.
16. bat4pH downloads, Internet web page, 2001, *pH frequent asked questions*, http://www.bat4ph.com/images/faqs.pdf
17. K. L. King, 1974, *Electrode systems pass the acid test,* Instruments and Control Systems, 47, 69-70.
18. J. Gunnell, 2001, *Personal communications*, *(use of iridium-oxide sensors for pH monitoring of high-purity water)*, Exxon Mobil Corporation, Fife, UK.
19. D. M. Gray, 1985, *Upgrade your pH measurement in high purity water,* Power, 129, 95-96.
20. M. L. Hitchman, 2001, *Personal communications (use of iridium-oxide sensors for pH monitoring of high-purity water)*, Department of Pure and Applied Chemistry, University of Strathclyde, Glasgow, UK.

APPENDIX 1

PUMP SPECIFICATIONS

As covered in Chapter 2, isokinetic conditions are recommended in order to get representative samples from heterogeneous processes. The expression for the isokinetic velocity at the stirrer plane has been defined as:

$$U_0 = \frac{B_1 N D^2}{r} \qquad \text{Eq. A1.1}$$

where:

U_0 = *Sampling velocity (ft/s)*
B_1 = *Constant dependent upon the number of impeller blades and the ratio of the impeller to tank diameter (1/rev)*
N = *Impeller rotational speed (rev/s.)*
D = *Impeller diameter (ft)*
r = *Radial distance measured from the centre of the impeller (ft)*

If the magnitudes are in metric units then Eq. A1.1 becomes:

$$U_0 = 0.3280 \frac{B_1 N D^2}{r} \qquad \text{Eq. A1.2}$$

The values for B_1 can be extracted from the following table[1]

Table A1.1. B values to work out the velocity of flow

	B	B
D/T	**4 blades**	**6 blades**
0.40	0.967	1.15
0.33	0.952	1.13
0.25	0.928	1.10
0.20	0.910	1.08

In *Table A1.1* D/T is the ratio of impeller diameter to tank diameter

In our design:

- $\frac{D}{T} = \frac{0.166m}{0.364m} = 0.46$ and there were 3 blades. Therefore $B_1 \approx 0.89$. This approximate value was obtained by extrapolation using the data shown in *Table A1.1*. It should be noticed that our value lied outside the range of data shown in this table. However, the aim was to obtain an estimation of the power of the pump needed for the design.

- R = Impeller radius + half the distance from impeller blade to the wall $= 0.083 + \frac{0.091 - 0.083}{2} = 0.087\ m.$
- D = 0.166 m.
- The usual operating conditions for the stirrer speed in the 5-L reactor were within the range N=100 r.p.m. to N= 400 r.p.m.

Therefore, using Eq. A1.2 the pump needed in the sampling system had to be capable of delivering a sampling velocity within the range U_0= 0.15-0.62 m/s depending on the stirring speed that was used. Therefore, when a 8 mm ID pipe was used, the volumetric flow range had to be within the range 1.8-7.5 l/min.

The range for the head of the pump was calculated by applying a mechanical energy balance to the system between the sampling and returning point[2]:

$$H_{tot} = H_{stat} + h_s + H_f + \frac{v_2^2 - v_1^2}{2g} \qquad \text{Eq. A1.3}$$

where:

H_{tot} = *Total head that the pump must be capable to deliver (m)*
H_{stat} = *Static head that the pump must overcome (measured as the difference between the level of liquid at the sampling point and the level of liquid in the returning point (m)*
h_s = *Head associated to the difference in pressure between the sampling point (atmospheric + hydrostatic) and the returning point (atmospheric) (m)*
H_f = *Friction loss (sum of all losses in head in pipes, bends, valves, instruments for measuring the flow, filters, etc.)*
v_1 = *Sampling velocity at the sampling point (m/s)*
v_2 = *Sampling velocity at the returning point (m/s)*
g = *Gravitational constant (m/s^2)*

In addition, the following considerations had to be borne in mind:

- The fluid velocity through the loop had to be the isokinetic sampling velocity (U_0)
- In the most unfavourable case the isokinetic velocity had to be maintained throughout the loop. Therefore, $v_1 = v_2 = U_0$ and $\frac{v_2^2 - v_1^2}{2g} = 0$.

- The hydrostatic pressure (between the sampling point and the level of liquid in the tank) compensated the static pressure (as the returning point was located more or less at the level of liquid in the tank). Therefore $H_{stat} + h_s = 0$.
- To work out the friction losses in the loop, an equivalence longitude of L_e=1.032 m was considered (considering 4 standard elbows 90°, 1 standard elbow 45°, and 1 3-way valve flow straight through)[3]. The Nikuradse equation[4] was used to work out the friction loss coefficient (f):

$$\frac{1}{f^{1/2}} = 4\log(\mathrm{Re} f^{1/2}) - 0.4 \qquad \text{Eq. A1.4}$$

where Re is the dimensionless Reynolds number.

Therefore:

$$H_{tot} = H_f = 2 f U_0^2 \frac{L + L_e}{gd} \qquad \text{Eq. A1.5}$$

where L is the longitude of the loop, g is the gravitational constant and d is the inside diameter of the pipe. Therefore, doing the appropiate calculations it was concluded that the pump had to deliver a head at least within the range H_{total}= 0.33 m (using minimum value for U_0) and H_{total}= 0.83 m (using maximum value for U_0).

Therefore, the pump specifications can be summarised as:

- Sampling velocity: 0.15 - 0.62 m/s
- Flow-rate: 1.5 – 7.5 l/min (using a 8 mm ID pipeline)
- Head: 0.33 – 0.83 m
- Tolerate corrosive materials and high temperature (around 110 – 120°C)
- Inlet/Outlet diameter > 8 mm. (0.315 in.)
- Optional speed control for varying the flow-rate

Finally, the $NPSH_a$ (Net Positive Suction Head Available) requirement had to be considered and met by the designed pump[5]. This is determined by the pipe system on the suction (inlet) side of the pump. It is therefore, the part of the mechanical balance (and therefore H_{tot}) from the suction point to the pump. Hence:

$$NPSH_a = H_a + H_{stat1} + H_v + H_f \qquad \text{Eq. A1.6}$$

where:

H_a = *Pressure of the liquid surface in the supply tank (m)*
H_{stat} = *Difference of level between the suction point and the pump (m)*
H_v = *Vapour pressure of the liquid being pumped (m)*
H_f = *Friction loss in the suction piping (m)*

On the other hand, $NPSH_r$ (Net Positive Suction Head Required) determines the required suction head (maximum suction lift). It is inherent to the design of the pump. The manufacturer provides the plots of $NPSH_r$ versus capacity for a certain pump.

The pumping system had to be chosen so $NPSH_a \geq NPSH_r$ (i.e. the head available from the system was greater than the head the pump required). Basically, this condition means that the designed pump must not generate a vacuum at the suction point (taking into account the head that the system itself creates over the suction point) that makes the liquid evaporate. Failure to meet this requirement would cause reduced flow rate, cavitation, and vibration of the pump.

It should be noticed that this pump design has been illustrated using the model system of the 5-L reactor. Similarly, the same guidelines of design could be followed for the design of the pump required for a sampling loop in any other type of system. In this case, new values for D/T, number of blades, N, D, r, L, L_e and d must be used.

- **References**

1. J. H. Rushton, 1965, *The continuous removal of mixed phases from a mixing tank.* A.I.Ch.E.-I.Chem.E. Symposium Series, 10, 3-7.
2. A. Diez-Lázaro, 2000, *Design of a Fast Sampling Loop,* CPACT IMB Internal report (Ref: 00/P1/4), Centre for Process Analytics and Control Technology, CPACT/University of Strathclyde, Glasgow, UK.
3. Engineering Equipment and Materials Users Association, 1988, EEMUA 138: *Design and installation of on-line analysers,*
4. R. H. Perry and C. H. Chilton, 1973, *Chemical Engineers' Handbook,* McGraw-Hill, New York, USA.
5. South African Pump Manufactures Association (SAPMA), 1991, *Pumps: Principles & Practice,* K. Myles and Associates, Northcliff, South Africa.

APPENDIX 2

DESIGN OF INSULATION

With a simple energy balance it could be worked out that the heat losses in the sampling loop produced a decrease in the temperature in the fluid flowing through the pipe[1]. Therefore:

$$mc_p(T_1 - T_2) = UA\Delta T_{m\log} \qquad \text{Eq. A2.1}$$

where:

m = *Mass flow through the pipe = volumetric flow-rate × density = $F \times \rho$ (kg/s)*
c_p = *Specific heat of the fluid flowing through the pipe (J/kg°C)*
ΔT_{mlog} = *Log mean temperature difference (°C), and it is expressed as:*

$$\frac{\Delta T_1 - \Delta T_2}{\ln\left(\frac{\Delta T_1}{\Delta T_2}\right)} = \frac{T_1 - T_2}{\ln\left(\frac{T_1 - T_{ext}}{T_2 - T_{ext}}\right)} \qquad \text{Eq A2.2}$$

T_{ext} = *External temperature, temperature of the air surrounding the system (room temperature) (°C)*
T_1 = *Temperature at the sampling point, equal to the temperature of reaction (°C)*
T_2 = *Temperature at the returning point (°C)*
U = *Overall heat transfer coefficient ($J\,m^{-2}\,s^{-1}\,{}^{o}C^{-1}$) which is defined by:*

$$UA = \frac{1}{\frac{1}{r_i h_i} + \frac{\ln(r_{\text{int } er}/r_i)}{k_{tube}} + \frac{\ln(r_0/r_{\text{int } eri})}{k_{insul}} + \frac{1}{r_0 h_0}} \qquad \text{Eq. A2.3}$$

where:

r_i = *Inner radius, internal radius of the tube (m)*
r_{inter} = *Intermediate radius, external radius of the tube and internal of the insulator (m)*
r_0 = *Outer radius, external radius of the insulator (m)*
k_{tube} = *Thermal conductivity of the tube ($J\,s^{-1}\,{}^{o}C^{-1}$)*
k_{insul} = *Thermal conductivity of the insulator ($J\,s^{-1}\,{}^{o}C^{-1}$)*
h_i = *Heat transfer coefficient of the fluid inside the tube ($J\,m^{-1}\,s^{-1}\,{}^{o}C^{-1}$)*
h_o = *Heat transfer coefficient of steady air at room temperature ($J\,m^{-1}\,s^{-1}\,{}^{o}C^{-1}$)*

In order to design an effective insulation for all the operating conditions, the least favourable parameters had to be used in the calculations. Therefore, the following values were used:

- F = 8 l/min (maximum F implied maximum heat loss and therefore, least favourable conditions)
- ρ (toluene) = 865 kg/m^3 (solvent used in the esterification reactions)
- m = F × ρ = 0.12 kg/s
- c_p (toluene) = 1839.2 J kg^{-1} °C^{-1}
- $T_{ext} \approx 20$ °C (room temperature)
- $T_1 = 110$ °C (least favourable conditions since that is the boiling point of toluene).
- $r_i = 3.4$ mm.
- $r_{inter} = 4$ mm.
- k_{tube} (Stainless steel 316 L) = 5.03 J m^{-1} s^{-1} K^{-1} (the heat losses in stainless steel (first version of the sampling loop) were higher (i.e. least favourable conditions) than for other materials used in posterior versions of the loop)
- k_{insul} (RS components, 797-990) = 0.035 J m^{-1} s^{-1} K^{-1}
- h_i (toluene) = 5183.17 J s^{-1} m^{-2}, worked out using the Sieder-Tate equation[2]:

$$h_i = \frac{k}{D} 0.023 \mathrm{Re}^{0.8} \mathrm{Pr}^{0.33} \qquad \text{Eq. A2.4}$$

where:

k (toluene) = *0.1056 J m^{-1} s^{-1} K^{-1}*
D = *2 r_I = 6.8 mm.*
Re = *Reynolds number, described by the equation:*

$$\frac{\rho D v}{\mu} \qquad \text{Eq. A2.5}$$

v = *0.62 m/s (fluid velocity through the pipe = greatest sampling velocity for least favourable conditions).*
μ = *(viscosity for toluene at 110 ° C) = 0.23 × 10^{-3} kg m^{-1} s^{-1}.*
Pr = *Prandl number, described by the equation:*

$$\frac{c_p \mu}{k} \qquad \text{Eq. A2.6}$$

h_o = *7.89 J s^{-1} m^{-2} (from reference 2)*

At this stage, calculations could be performed for the different thickness of insulator available in the market (RS components, 797-990). When the value for the thickness, together with the constants values quantified above, was introduced into the design equation, the temperature T_2 for the returning point could be obtained for different values of T_1. Therefore, the analysis of T_2 was used to analyse whether or not this value was acceptable and the control system could compensate the decrease in the temperature of the circulating sample. In fact, it was seen that even with the smallest thickness (13 mm, i.e. $r_o = 20.5$ mm) T_2 resulted in an acceptable value and

$T_2 = 109.99\ ^0C$ for a $T_1 = 110\ ^0C$ (i.e. $T_2 = 99.99\%$ of the value at the sampling point, T_1).

With cylindrical geometries an increase in the thickness of the insulator (r_0) produces an obvious decrease in the heat transfer rate. However, the transversal area also increases and it sometimes makes the absolute heat lost (i.e. heat transfer rate multiplied by the transversal area) increase as well. In other words, there exists a critical value for the insulator radius (r_{crit}) such that if $r_0 < r_{crit}$ the heat losses increase with the use of the insulator. Therefore, the only consideration left in the design was to ensure that $r_0 > r_{crit}$. The critical radius is given by the expression[3]:

$$r_{crit} = \frac{k_{insul}}{h_0} \qquad \text{Eq. A2.7}$$

that in our case took the value of $r_{crit} = \frac{0.035}{7.89} = 0.00444m = 4.44mm$. Therefore, the condition $r_0 > r_{crit}$ was verified.

It should be noticed that the considerations for the design of the insulation outlined above were made in particular conditions. This was in the case of the first version of the sampling system designed for the 5-L reactor (made of stainless steel) and for the particular example of the insulator chosen for the system (RS components, 797-990). Similarly, the same guidelines of design can be followed for the design of the insulation required for a similar sampling loop for use in another type of reactive system and with another insulation material. In this case, new values for ρ, c_p, T_{ext}, T_1, r_i, r_{inter}, k_{tube}, k_{insul}, h_i, k, v, μ, and h_o must be used.

• References

1. A. Diez-Lázaro, 2000, *Design of a Fast Sampling Loop,* CPACT IMB Internal report (Ref: 00/P1/4), Centre for Process Analytics and Control Technology, CPACT/University of Strathclyde, Glasgow, UK.
2. R. H. Perry and C. H. Chilton, 1973, *Chemical Engineers' Handbook,* McGraw-Hill, New York, USA.
3. F. M. White, 1984, *Heat Transfer*, Addison-Wesley, London, UK.

APPENDIX 3

SPECIFICATIONS OF THE SAMPLING LOOP

- *Main sampling loop*

As required in the design, the sampling device had to be capable of providing representative off-line samples as well as delivering samples for the implementation of on-line analysers. A low-field NMR sprectrometer was the example of interest for the on-line implementation in this project. The designed sampling loop system took the sample from the reactor stirrer plane and in a parallel direction to the flow streamlines (i.e. horizontal direction). The inside diameter of the sampling probe was 8 mm, although different designs and dimensions of the probe can be analysed by changing the configuration of the sample tip. Initially, the loop was made of 316 stainless steel, but problems of corrosion were detected with this material in some of the processes used in this project. PTFE tube and quick-fit glass fittings replaced stainless steel in a second version of the loop. Concerns about safety and fittings popping out in case of pressure build-up, led to the construction of the whole of the loop in PTFE with compression ferrule-type connections that withstood pressure conditions of 100 psig (impossible to be reached in this system). The specifications of the pump and type of fittings used in the loop are summarised in *Table A3.1*.

Table A3.1. Specifications of the different components in the loop

COMPONENT	*UNITS IN THE LOOP*	*MAIN FEATURES*
Self priming centrifugal pump	1	-Total head: 1.5 m. -Capacity: 1 to 8 l/min
Equal elbow coupling	3	-12 mm O/D -One turns the line from the reactor port towards the pump -One at the inlet of the pump -One turns the line towards the off-line sampling port
Equal T coupling	1	-12 mm O/D - Opens a line for off-line sampling
BSPT male stud coupling	1	-12 mm O/D and 1/2" stud thread (BSPT) -Connects the port valve for isolating the loop with the main line
Port ball valve	2	-12 mm O/D -One for insulating the loop from the reactor system -One for manual off-line sampling
Coarse control needle valve	1	-Thread size 3/8" NPT -For flow control in the loop
Reduction straight coupling	1	-Adapts tube sizes from 8 mm O/D (reactor port) to 12 mm (main line in the loop)

Apart from those fittings, a glass rotameter with stainless steel float and connections was used for measuring the flow-rate in the sampling loop. Later on in the project, the stainless steel float and connections in the flow-meter were replaced by a PTFE float and PTFE home-made fittings to avoid corrosion problems. The new PTFE float was constructed with the faces well machined to avoid air bubbles getting attached to the float and modify the reading obtained in the meter. Also, the symmetry of the float was found to be very important as the smaller diameter PTFE float oscillated too much affecting the reading. An alternative to the use of a float made entirely of PTFE would be the construction of a heavier float with a larger diameter and heavier by using a steel float covered in PTFE.

The different fittings summarised above had to be assembled in such a way that the off-line sample was obtained via sampling in the direction of the flow. Therefore, from the different dispositions represented in *Figure A3.1, (b)* was preferred to *(a)*. After some test experiments were performed in the system, the use of unnecessary fittings was avoided as they were found to cause problems with heterogeneous processes. Therefore, disposition *(c)* was adopted where the rotameter, two elbows and the control valve were removed.

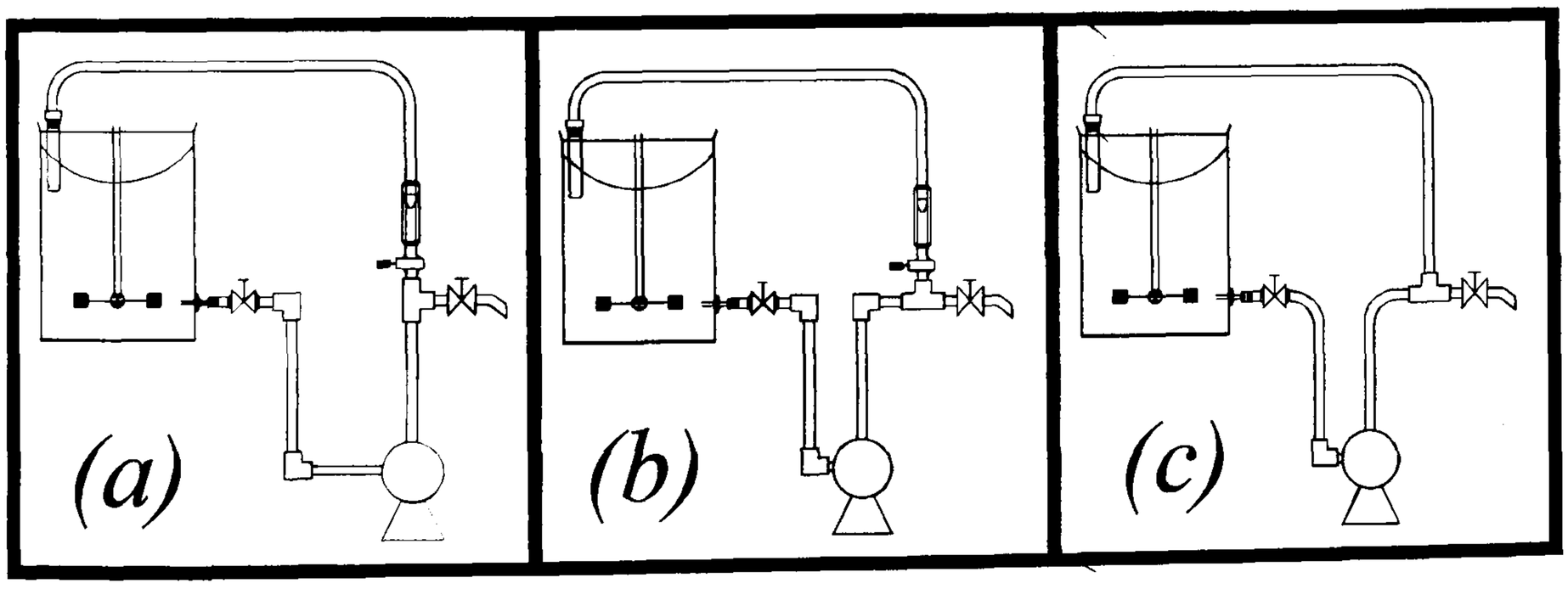

Figure A3.1. Different dispositions of the fittings in the sampling port

As described in Chapter 2, the return point was placed on the side of the reactor opposite to the sampling point and pointing the stream to the wall of the reactor so that the fluid lost its energy and the return jet did not modify the flow patterns in the system, especially at the sampling point (see *Figure A3.2*).

Finally, the high quality of the PTFE connections and their capacity to withstand relatively high pressure conditions led to the decision of not using the high pressure relief valve initially planned. The high cost of this element also contributed to taking this decision of not building the pressure relief line.

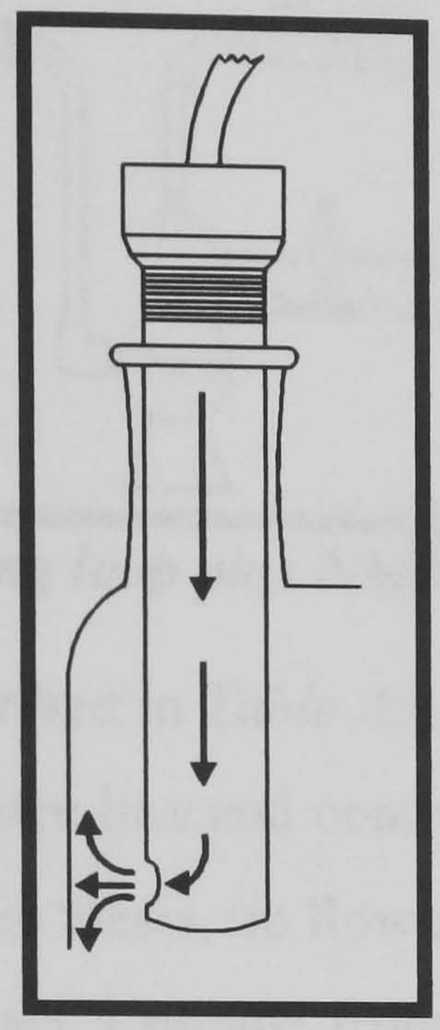

Figure A3.2. Detail of the return point configuration

- *Implementation of the NMR system in the main sampling loop*

A sketch of the designed sampling loop + NMR line is shown in *Figure A3.3*. The main sampling loop system verified the specifications pointed out in the previous section in terms of location of the sampling point, dimensions of the loop and design of the pump. The NMR line was made of viton (I.D. 2.794 mm.). The use of a pressure indicator and a rotameter were omitted to reduce the number of fittings in the lines as explained in Chapter 2. A Teflon needle valve was implemented to regulate the flow within the rage 0-100 ml/min. In the future, an air shut-off valve could be implemented to close this line when NMR on-line analysis is not needed.

As has been mentioned in Chapter 2, the temperature conditioning of the sample was not covered as the effect that the temperature had on the NMR signals was a matter of study in another project. However, it must be highlighted that in cases when the temperature of reaction is too high it may be that the temperature of the sample delivered to the analyser is higher than desired. In these cases, a cooling system would have to be developed and implemented in the system.

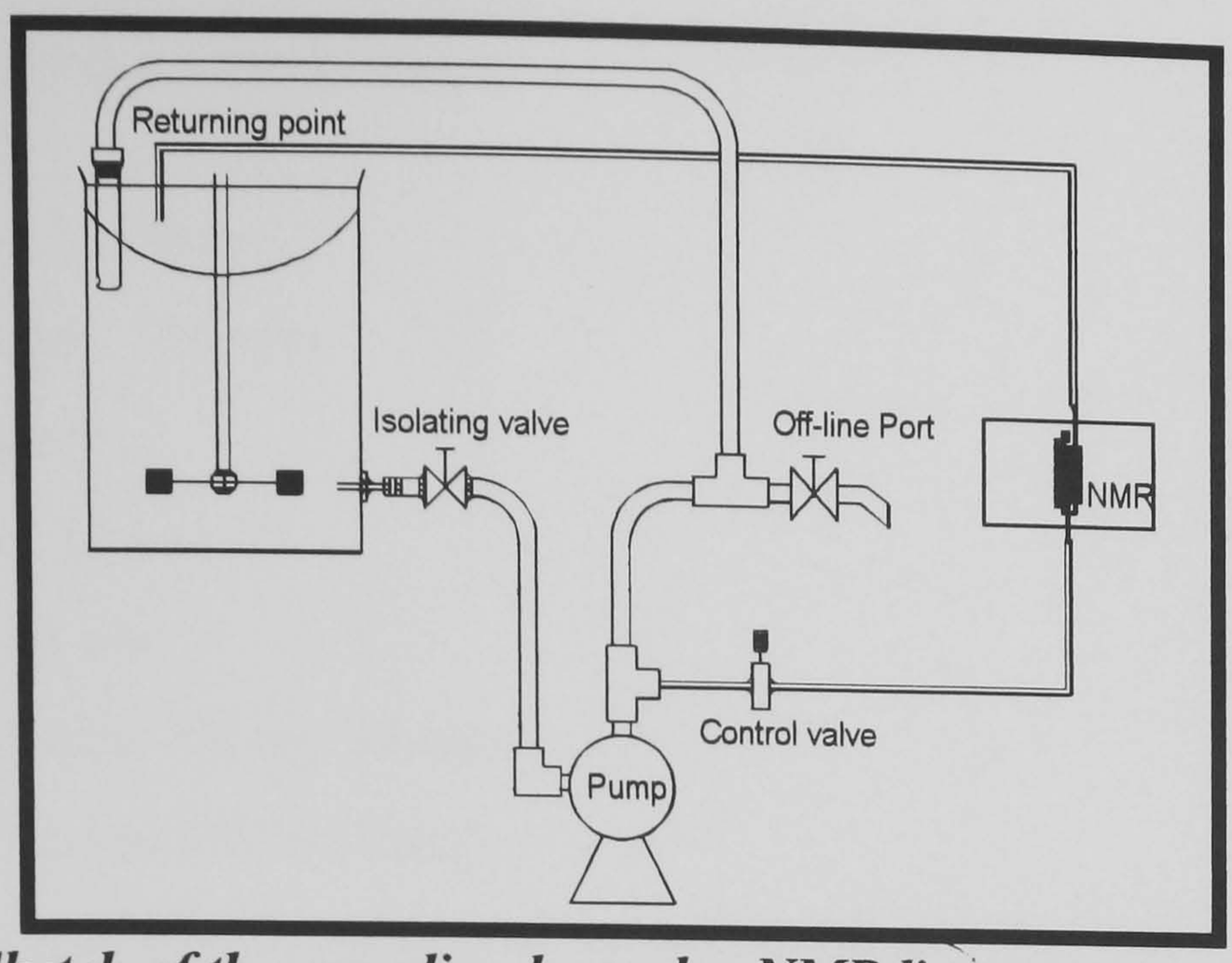

Figure A3.3. Sketch of the sampling loop plus NMR line system

The additional fittings described in *Table A3.2* were implemented in the NMR line to extract a sample from the main line and control the flow-rate in the NMR line. In the experiments performed in this thesis, no flow-meter was used in the NMR line. Also, no connection fitting to extract a sample from a direction parallel to the flow-streamlines (see *Figure A3.4*) was implemented in the T coupling that was used to extract the sample from the main line.

Table A3.2. Specifications of the additional components used in the NMR line

COMPONENT	*UNITS IN THE LOOP*	*MAIN FEATURES*
Equal T coupling	1	-12 mm O/D - It opens a secondary loop for the NMR at the outlet of the pump
Fine control needle valve	1	-8 mm O/D -For fine flow control in the NMR loop

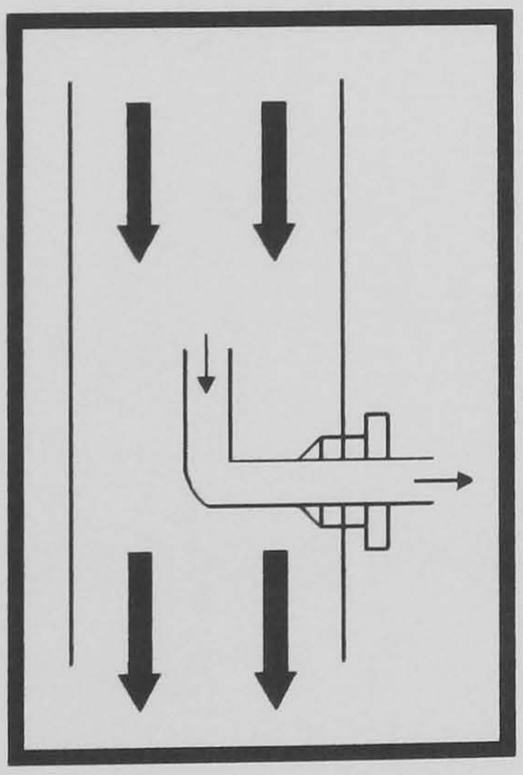

Figure A3.4. Connection fitting to extract a representative sample from a straight pipe-line in a direction parallel to the flow-streamlines

APPENDIX 4

SPECIFICATIONS OF THE 5-L BEAKER SYSTEM FOR SAMPLING STUDIES

- Characteristics of the beaker:

Beaker:

Diameter: 165 mm

Total Height: 226 mm

Ports in the Beaker:

Diameter: 18 mm ID

Length: 65 mm

Height (Stirrer Plane): 38 mm

Height (Above Stirrer Plane): 121 mm

(Heights measured from bottom up to the centre of the port)

- Characteristics of the stirrer motor:

Heidolph RZR1 stirrer 50 Hz. motor with variable speed control (35-2200 r.p.m.)

- Characteristics of the sampling probe:

Tube: Glass tapered at the sampling side

Diameter (at sampling point): 6 mm ID

Diameter (at connection with tubing): 9 mm ID

Length: 150 mm

Exposure (i.e. distance wall-sampling point): 10 mm approx.

- Characteristics of the sampling line:

Centrifugal Pump:

Totton NDP 25/4 Pump; 220-240 V, 1 PH, 50 Hz, 0.5 Amps., 18 Watts; Max. Flow 22 L/min.; Max. Head 4 m.

Tubing used with the centrifugal pump:

Material: Rubber

Length: 1160 mm

Diameter: 6 mm ID, 12.5 OD

Peristaltic Pump:

Watson Marlow Peristaltic Pump with variable speed control

Tubing used with the peristaltic pump:

Material: Silicone

Length: 850 mm

Diameter: 6 mm ID, 10 mm OD.

APPENDIX 5

CODE FOR THE PLC PROGRAMS IN THE CONTROL UNIT USED IN THE HPLC SAMPLER

• PLC original programming code

```
0    LD   M8002
1    SET  M8028
3    LDI  M0
4    ANI  M10
5    ANI  M20
6    ANI  M30
7    MPS
8    AND  X000
9    SET  S0
10   MRD
11   A0ND X001
12   SET  M10
13   MRD
14   AND  X002
15   SET  M20
16   MPP
17   LD   X000
18   OR   X001
19   OR   X002
20   ANB
21   RST  C0
23   RST  C0
24   OR   M30
25   LD   M10
26   LDI  M2
27   OR   M12
28   ANB
29   ORB
30   LD   M20
31   LDI  M2
32   ANI  M12
33   OR   M22
34   ANB
35   ORB
36   PLS  M1
38   LD   M1
39   SET  S0
41   RST  M2
42   RST  M12
43   RST  M22
44   STL  S0
45   OUT  T0
          K200
48   LD   T0
49   SET  S1
51   STL  S1
52   OUT  T1
          K400
55   LD   T1
56   SET  S2
58   STL  S2
59   OUT  T2
          K200
62   LD   T2
63   SET  S3
65   STL  S3
66   OUT  T3
          K150
69   LD   T3
70   SET  S4
72   STL  S4
73   OUT  T4
          K150
76   LD   T4
77   RST  S4
79   RST  M0
80   RST  M30
81   SET  S2
82   RET
83   LD   M10
84   OR   M20
85   AND  M2
86   ANI  M12
87   PLS  M11
89   LD   M11
90   SET  S10
92   STL  S10
93   OUT  T10
          K50
96   LD   T10
97   SET  S11
99   STL  S11
100  OUT  T11
          K50
103  LD   T11
104  SET  S12
106  STL  S12
107  OUT  T12
          K750
110  LD   T12
111  SET  S13
113  STL  S13
114  OUT  T13
          K3000
117  LD   T13
118  RST  S13
120  RST  M10
121  SET  M12
122  RET
123  LD   M20
124  AND  M2
125  AND  M12
126  ANI  M22
127  PLS  M21
129  LD   M21
130  SET  S20
132  STL  S20
133  OUT  T20
          K150
136  LD   T20
137  SET  S21
139  STL  S21
140  OUT  T21
          K200
143  LD   T21
144  SET  S22
146  STL  S22
147  OUT  T22
          K300
150  LD   T22
151  SET  S23
153  STL  S23
154  OUT  T23
          K10
157  LD   T23
158  SET  S24
160  STL  S24
161  OUT  T24
          K400
164  LD   T24
165  SET  S25
167  STL  S25
168  OUT  T25
          K10
171  LD   T25
172  RST  S25
174  RST  M20
175  SET  M22
176  RET
177  LD   M22
178  OUT  C0
178  OUT  C0
          K0
181  MPS
```

```
182  ANI  C0
183  SET  M20
184  MPP
185  AND  C0
186  OUT  T30
          K6000
189  AND  T30
190  SET  M30
191  LD   S1
192  OR   S12
193  OR   S24
194  OUT  Y002
195  LD   S0
196  OR   S3
197  OR   S4
198  OR   S21
199  OR   S22
200  OR   S23
201  OR   S25
202  OUT  Y003
203  LD   S10
204  OR   M41
205  OUT  Y004
206  LD   S11
207  MPS
208  ANI  T36
209  OUT  M41
210  MRD
211  ANI  T37
212  OUT  T36
          K15
215  MPP
216  AND  T36
217  OUT  T37
          K5
220  LD   S2
221  OR   S13
222  OR   S20
223  OUT  Y005
224  LD   S20
225  OR   S23
226  OR   S24
227  OR   S25
228  OUT  Y006
229  LD   S0
230  OR   S2
231  OR   S3
232  OR   S4
233  OR   S21
234  OR   S22
235  OUT  Y007
236  LD   S0
237  OR   S1
238  OR   S4
239  OR   S21
240  OR   S23
241  OR   S25
242  OUT  Y010
243  LD   S3
244  OR   S12
245  OR   S13
246  OR   S22
247  OUT  Y011
248  LD   S1
249  OR   S2
250  OR   S12
251  OR   S13
252  OR   S20
253  OR   S24
254  MPS
255  ANI  T34
256  OUT  Y012
257  MRD
258  ANI  T35
259  OUT  T34
          K10
262  MPP
263  AND  T34
264  OUT  T35
          K40
267  LD   M0
268  OR   M30
269  AND  M40
270  OR   M2
271  OUT  Y013
272  LD   M10
273  OR   M30
274  AND  M40
275  OR   M12
276  OUT  Y014
277  LD   M20
278  OR   M30
279  AND  M40
280  OR   M22
281  OUT  Y015
282  LDI  T32
283  OUT  T33
          K25
286  LD   T33
287  OUT  T32
          K25
290  OUT  M40
291  END
292  NOP
     .
     .
     .
```

- **PLC programming code to fill the lines with diluent before sampling**

```
0    LD   M8002
1    SET  M8028
3    LDI  M0
4    ANI  M10
5    ANI  M20
6    ANI  M30
7    MPS
8    AND  X000
9    SET  S0
10   MRD
11   A0ND X001
12   SET  M10
13   MRD
14   AND  X002
15   SET  M20
16   MPP
17   LD   X000
18   OR   X001
19   OR   X002
20   ANB
21   RST  C0
23   RST  C0
24   OR   M30
25   LD   M10
26   LDI  M2
27   OR   M12
28   ANB
29   ORB
30   LD   M20
31   LDI  M2
32   ANI  M12
33   OR   M22
34   ANB
35   ORB
36   PLS  M1
38   LD   M1
39   SET  S0
41   RST  M2
42   RST  M12
43   RST  M22
44   STL  S0
45   OUT  T0
          K200
48   LD   T0
49   SET  S1
51   STL  S1
52   OUT  T1
          K400
55   LD   T1
56   SET  S2
58   STL  S2
59   OUT  T2
          K200
62   LD   T2
63   SET  S3
65   STL  S3
66   OUT  T3
          K150
69   LD   T3
70   SET  S4
72   STL  S4
73   OUT  T4
          K150
76   LD   T4
77   SET  S12
79   STL  S12
80   OUT  T5
          K750
83   LD   T5
84   RST  S12
86   RST  M0
87   RST  M30
88   SET  M2
89   RET
90   LD   M10
91   OR   M20
92   AND  M2
93   ANI  M12
94   PLS  M11
96   LD   M11
97   SET  S10
99   STL  S10
100  OUT  T10
          K50
103  LD   T10
104  SET  S11
106  STL  S11
107  OUT  T11
          K50
110  LD   T11
111  SET  S13
113  STL  S13
114  OUT  T13
          K3000
117  LD   T13
118  RST  S13
120  RST  M10
121  SET  M12
122  RET
123  LD   M20
124  AND  M2
125  AND  M12
126  ANI  M22
127  PLS  M21
129  LD   M21
130  SET  S20
132  STL  S20
133  OUT  T20
          K150
136  LD   T20
137  SET  S21
139  STL  S21
140  OUT  T21
          K200
143  LD   T21
144  SET  S22
146  STL  S22
147  OUT  T22
          K300
150  LD   T22
151  SET  S23
153  STL  S23
154  OUT  T23
          K10
157  LD   T23
158  SET  S24
160  STL  S24
161  OUT  T24
          K400
164  LD   T24
165  SET  S25
167  STL  S25
168  OUT  T25
          K10
171  LD   T25
172  RST  S25
174  RST  M20
175  SET  M22
176  RET
```

```
177  LD   M22
178  OUT  C0
178  OUT  C0
          K0
181  MPS
182  ANI  C0
183  SET  M20
184  MPP
185  AND  C0
186  OUT  T30
          K6000
189  AND  T30
190  SET  M30
191  LD   S1
192  OR   S12
193  OR   S24
194  OUT  Y002
195  LD   S0
196  OR   S3
197  OR   S4
198  OR   S21
199  OR   S22
200  OR   S23
201  OR   S25
202  OUT  Y003
203  LD   S10
204  OR   M41
205  OUT  Y004
206  LD   S11
207  MPS
208  ANI  T36
209  OUT  M41
210  MRD
211  ANI  T37
212  OUT  T36
          K15
215  MPP
216  AND  T36
217  OUT  T37
          K5
220  LD   S2
221  OR   S13
222  OR   S20
223  OUT  Y005
224  LD   S20
225  OR   S23
226  OR   S24
227  OR   S25
228  OUT  Y006
229  LD   S0
230  OR   S2
231  OR   S3
232  OR   S4
233  OR   S21
234  OR   S22
235  OUT  Y007
236  LD   S0
237  OR   S1
238  OR   S4
239  OR   S21
240  OR   S23
241  OR   S25
242  OUT  Y010
243  LD   S3
244  OR   S12
245  OR   S13
246  OR   S22
247  OUT  Y011
248  LD   S1
249  OR   S2
250  OR   S12
251  OR   S13
252  OR   S20
253  OR   S24
254  MPS
255  ANI  T34
256  OUT  Y012
257  MRD
258  ANI  T35
259  OUT  T34
          K10
262  MPP
263  AND  T34
264  OUT  T35
          K40
267  LD   M0
268  OR   M30
269  AND  M40
270  OR   M2
271  OUT  Y013
272  LD   M10
273  OR   M30
274  AND  M40
275  OR   M12
276  OUT  Y014
277  LD   M20
278  OR   M30
279  AND  M40
280  OR   M22
281  OUT  Y015
282  LDI  T32
283  OUT  T33
          K25
286  LD   T33
287  OUT  T32
          K25
290  OUT  M40
291  END
292  NOP
      .
      .
      .
```

Note: Red colour highlights the differences between this and the original codes

- **PLC programming code with a dead time between sampling and mixing**

The PLC programming code used to apply a dead time between the stages of sampling and mixing was the same as the original programming code but without the ten lines in between lines 206-217.

0	LD	M8002	45	OUT	T0	100	OUT	T11
1	SET	M8028			K200			K50
3	LDI	M0	48	LD	T0	103	LD	T11
4	ANI	M10	49	SET	S1	104	SET	S12
5	ANI	M20	51	STL	S1	106	STL	S12
6	ANI	M30	52	OUT	T1	107	OUT	T12
7	MPS				K400			K750
8	AND	X000	55	LD	T1	110	LD	T12
9	SET	S0	56	SET	S2	111	SET	S13
10	MRD		58	STL	S2	113	STL	S13
11	A0ND	X001	59	OUT	T2	114	OUT	T13
12	SET	M10			K200			K3000
13	MRD		62	LD	T2	117	LD	T13
14	AND	X002	63	SET	S3	118	RST	S13
15	SET	M20	65	STL	S3	120	RST	M10
16	MPP		66	OUT	T3	121	SET	M12
17	LD	X000			K150	122	RET	
18	OR	X001	69	LD	T3	123	LD	M20
19	OR	X002	70	SET	S4	124	AND	M2
20	ANB		72	STL	S4	125	AND	M12
21	RST	C0	73	OUT	T4	126	ANI	M22
23	RST	C0			K150	127	PLS	M21
24	OR	M30	76	LD	T4	129	LD	M21
25	LD	M10	77	RST	S4	130	SET	S20
26	LDI	M2	79	RST	M0	132	STL	S20
27	OR	M12	80	RST	M30	133	OUT	T20
28	ANB		81	SET	S2			K150
29	ORB		82	RET		136	LD	T20
30	LD	M20	83	LD	M10	137	SET	S21
31	LDI	M2	84	OR	M20	139	STL	S21
32	ANI	M12	85	AND	M2	140	OUT	T21
33	OR	M22	86	ANI	M12			K200
34	ANB		87	PLS	M11	143	LD	T21
35	ORB		89	LD	M11	144	SET	S22
36	PLS	M1	90	SET	S10	146	STL	S22
38	LD	M1	92	STL	S10	147	OUT	T22
39	SET	S0	93	OUT	T10			K300
41	RST	M2			K50	150	LD	T22
42	RST	M12	96	LD	T10	151	SET	S23
43	RST	M22	97	SET	S11	153	STL	S23
44	STL	S0	99	STL	S11	154	OUT	T23

```
        K10
157 LD  T23
158 SET S24
160 STL S24
161 OUT T24
        K400
164 LD  T24
165 SET S25
167 STL S25
168 OUT T25
        K10
171 LD  T25
172 RST S25
174 RST M20
175 SET M22
176 RET
177 LD  M22
178 OUT C0
178 OUT C0
        K0
181 MPS
182 ANI C0
183 SET M20
184 MPP
185 AND C0
186 OUT T30
        K6000
189 AND T30
190 SET M30
191 LD  S1
192 OR  S12
193 OR  S24
194 OUT Y002
195 LD  S0
196 OR  S3
197 OR  S4
198 OR  S21
199 OR  S22
200 OR  S23
201 OR  S25
202 OUT Y003
203 LD  S10
204 OR  M41
205 OUT Y004
206 LD  S2
207 OR  S13
208 OR  S20
209 OUT Y005
210 LD  S20
211 OR  S23
212 OR  S24
213 OR  S25
214 OUT Y006
215 LD  S0
216 OR  S2
217 OR  S3
218 OR  S4
219 OR  S21
220 OR  S22
221 OUT Y007
222 LD  S0
223 OR  S1
224 OR  S4
225 OR  S21
226 OR  S23
227 OR  S25
228 OUT Y010
229 LD  S3
230 OR  S12
231 OR  S13
232 OR  S22
233 OUT Y011
234 LD  S1
235 OR  S2
236 OR  S12
237 OR  S13
238 OR  S20
239 OR  S24
240 MPS
241 ANI T34
242 OUT Y012
243 MRD
244 ANI T35
245 OUT T34
        K10
248 MPP
249 AND T34
250 OUT T35
        K40
253 LD  M0
254 OR  M30
255 AND M40
256 OR  M2
257 OUT Y013
258 LD  M10
259 OR  M30
260 AND M40
261 OR  M12
262 OUT Y014
263 LD  M20
264 OR  M30
265 AND M40
266 OR  M22
267 OUT Y015
268 LDI T32
269 OUT T33
        K25
272 LD  T33
273 OUT T32
        K25
276 OUT M40
277 END
278 NOP
    .
    .
    .
```